

**Potential for Natural Flood Management and land  
management practices to mitigate flooding in upland  
catchments**

**Gareth John Owen, B.Sc., M.Sc.**

A thesis submitted for the degree of Doctor of Philosophy (Ph.D) to the  
School of Civil Engineering and Geosciences at Newcastle University

September 2016

## **Declaration**

I certify that no part of the material offered in this thesis has been previously submitted by me for a degree or other qualification in this or any other University.

Signed

Gareth Owen

## Abstract

There is an increasing uptake of Natural Flood Management (NFM) and land use management (LUM) schemes to tackle excessive, rapid runoff in rural catchments. At the local scale, there is a growing knowledge base regarding the impacts of NFM and LUM. However, evidence and understanding of how these local impacts manifest at a larger catchment scale is less well understood.

There are many types of model that have been used for investigating NFM and LUM impacts at larger scales ( $>10 \text{ km}^2$ ), ranging from the comparatively simple lumped conceptual approaches to more complex, physically-based, distributed models. How best to represent NFM and LUM impacts in models is ambiguous. This thesis presents research into impact modelling of flood mitigation measures from the hillslope to the catchment scale, using the lumped FEH rainfall-runoff model and a novel physically-based, distributed model, Juke. A Flood Impact Modelling (FIM) methodology is proposed for rapid impact assessment using the FEH approach; FEH hydrographs are generated for sub-catchments and routed to the outlet. The impact of changes in timing and runoff generation in specific sub-catchments on the downstream hydrograph can be investigated to inform catchment planning. The Juke methodology is designed to make best use of field observations and existing GIS datasets for parameterising the runoff and routing components. Juke uses some of the knowledge embedded in the FEH approach regarding the timing and runoff generation and applies it spatially. Juke is capable of emulating the FEH, but also allows consideration of spatial changes in LUM.

Two catchments in the north of England have been instrumented to characterise the rainfall-runoff behaviour and understand what causes the largest flood events, where NFM and LUM have taken place. This knowledge informs the LUM and NFM scenarios explored as well as for model parametrisation. Results from the lumped FEH modelling suggest that the mitigation of flood flow by managing the volume and timing of fast runoff will have the greatest impact on floods caused by short duration, high intensity rainfall events. The Juke modelling also suggests that the impact of NFM and LUM is likely to be minimal ( $<10 \%$  flood peak reduction for  $12 \%$  coverage of riparian woodland) and depends on the duration and intensity of rainfall events and the internal synchronisation of the component sub-catchments. The flood peaks for some events

may increase due to the effects of timing and synchronisation of flows from the landscape elements.

The outcomes of this thesis recommends flood managers make field observations to better understand the causes of flooding within a catchment. Schemes using NFM and LUM are likely to be most beneficial for comparatively small catchments (<10 km<sup>2</sup>) that suffer from frequent flooding from short duration, high intensity rainfall.

## **Acknowledgements**

I would like to thank my first supervisor Dr Paul Quinn for his boundless ideas and enthusiasm for his work, as well as the feedback and comments on the draft of the manuscript.

I cannot thank my second supervisor Dr Greg O'Donnell enough for his feedback and comments on the manuscript. Almost as significant was his encouragement and tutoring of me to programme in Python. Greg invested a lot of time in getting me off the ground; it certainly made data analysis and plotting, quicker, easier and possibly more sophisticated and attractive than possible with Excel.

I am also very grateful to Dr. Nick Barber for his comments and feedback on several of my chapters, a true friend. Thanks also to Dr. Josie Geris, Dr. Matt Perks, Mr. Luke Smith, Dr. Jennine Jonczyk, Miss Mhari Barnes, Miss Eleanor Starkey and Dr. Mark Wilkinson for their assistance with field work and numerous other tasks.

This work has been funded by a combination of Defra, through the Demonstration Test Catchments (DTC) and the Environment Agency (EA: Great Ayton Flood mitigation). Particular thanks go to the Eden DTC consortium, Mr. Bob Carrick (EA) and Mr. Peter Kerr (EA).

My Mum, Dad and Sister have been very supportive and always there with a kind word. Thanks especially to my Mum and Father-in-law for their efforts looking after Rhys whilst me and Tracey are at work. Without their generous free help I could not financially have afforded to complete the thesis.

Finally, I would like to thank my wife Tracey for her endless love, support and encouragement; and for bringing Rhys and Dylan into our lives, who have certainly made the task more tiring but also more worthwhile and enjoyable. The next chapter in our lives is about to begin.

# Contents

	<b>Page</b>
Abstract	i
Acknowledgements	iii
List of Figures	xi
List of Tables	xix
List of Abbreviations	xxii
<b>Chapter 1: Introduction</b>	
1.1 Background	1
1.2 Aim	3
1.2.1 Objectives	3
1.3 Thesis outline	4
<b>Chapter 2. Literature review</b>	
2.1 Introduction	6
2.2 Hillslope scale flood generation and routing	7
2.2.1 Local scale runoff generation - storage	7
2.2.2 Local scale routing and connectivity	7
2.2.3 Scaling up	8
2.3 Land Use Management and flood hazard	8
2.3.1 Policy	10
2.3.2 Livestock farming	11
2.3.3 Arable farming	13
2.3.4 Forest/woodland	14
2.3.5 Drainage	16
2.3.6 Summary	17
2.4 Novel flood hazard mitigation methods	20
2.5 Detecting land use change signals	23

2.5.1	Paired catchment studies	23
2.5.2	Analysis of historical datasets	24
2.5.3	Detection methods summary	25
2.6	Modelling land use change and flood mitigation	25
2.6.1	Statistical modelling (Metric)	26
2.6.2	Spatially distributed-physically and semi-physical models	31
2.6.3	Meta-modelling	34
2.6.4	Conceptual modelling	38
2.6.5	Hydro-dynamic modelling	39
2.6.6	A true (verified) model versus an acceptable (confirmed/validated) model	42
2.7	Communicating flood risk	43
2.8	Summary	46
<b>Chapter 3. Methodology</b>		
3.1	Introduction	49
3.2	Research catchments	49
3.2.1	Great Ayton	50
3.2.2	Morland	51
3.2.3	Catchment summaries	51
3.3	Experimental design	53
3.4	Instrumentation	54
3.4.1	Automatic Weather Station (AWS)	54
3.4.2	Rainfall	54
3.4.3	Stage	55
3.4.4	Morland instrument locations and data availability	57
3.4.5	Great Ayton instrument locations and data availability	58
3.5	Rating curve development	61
3.5.1	Flow gauging	61

3.5.2	Modelling Flow	62
3.6	Storm analysis	63
3.6.1	Rainfall runoff	63
3.6.2	Celerity	64
3.7	Flood Impact Modelling (FIM)	65
3.7.1	FEH rainfall-runoff model	68
3.7.2	Juke rainfall-runoff model	68
3.8	Decision support tool	76
3.9	Summary	78
3.9.1	Catchments and data	78
3.9.2	Rainfall-runoff modelling	79
<b>Chapter 4. Morland catchment characterisation</b>		
4.1	Introduction	80
4.2	Catchment overview	80
4.2.1	General hydrological statistics	81
4.2.2	Flood risk	82
4.3	Physical catchment characterisation	83
4.3.1	Geology and Soils	83
4.3.2	Land use and vegetation	85
4.4	Hydrological characterisation	88
4.4.1	Rating curve development	88
4.4.2	Rainfall runoff	90
4.5	Mitigation approaches	98
4.5.1	Runoff Attenuation Features (RAFs)	99
4.5.2	Sward lifting (aeration) - Land use management	101
4.6	Discussion	102
4.6.1	Rainfall-runoff response	102
4.6.2	Flood risk	103



4.7	What next?	103
-----	------------	-----

## **Chapter 5. Great Ayton catchment characterisation**

5.1	Introduction	104
5.2	Catchment overview	104
5.2.1	General hydrology statistics	105
5.2.2	Flood risk	106
5.3	Physical catchment characterisation	107
5.3.1	Geology	107
5.3.2	Soils	109
5.3.3	Land use and vegetation	112
5.4	Hydrological characterisation	116
5.4.1	Rating curve development	116
5.4.2	Flood frequency	117
5.4.3	Rainfall runoff	119
5.5	Flood mitigation approaches	128
5.5.1	Property level protection	129
5.5.2	Online - Woody debris features	130
5.5.3	Offline - Wooden attenuation features	131
5.5.4	Offline storage feature	131
5.5.5	Potential additional features	133
5.6	Discussion	133
5.6.1	Catchment characteristics and data	133
5.6.2	Rainfall-runoff response and flood risk	134
5.6.3	Mitigating flood hazard	134
5.6.4	What next?	134

## **Chapter 6. Lumped Conceptual Modelling - FEH**

6.1	Introduction	136
-----	--------------	-----

6.2	Modelling approaches	136
6.2.1	FEH	137
6.2.2	ReFH modelling	137
6.2.3	Model parameterisation- Great Ayton	138
6.2.4	FARM decision support tool	139
6.2.1	Land use change	140
6.2.2	FEH or ReFH	143
6.3	FEH modelling to Great Ayton	145
6.3.1	Impact of change on different return interval floods	145
6.3.2	Impact of storm duration	146
6.3.3	Spatial scale and LUM scenario impacts	148
6.3.4	Knowledge gained from Great Ayton and application to Morland	149
6.4	Flood Impact Modelling tool (FIM)	151
6.4.1	FIM description	152
6.4.2	Scenarios of changes modelled	153
6.5	Discussion	157
6.5.1	FEH rainfall-runoff	158
6.5.1	What has Morland shown?	160
6.5.2	FIM tool	160
6.5.3	What next?	161

## **Chapter 7. Introduction to Juke**

7.1	Introduction	163
7.2	Juke parameterisation and testing	164
7.2.1	FEH input data	165
7.2.2	Runoff generation	167
7.3	Celerity – flow routing	171
7.4	Conclusions	178

## **Chapter 8. Juke: Impact Scenarios**

8.1	Introduction	180
8.2	Flood mitigation scenarios	180
	8.2.1 Scenarios	180
8.3	Great Ayton scenario results	185
	8.3.1 Scenario 0 – Baseline Parameterisation	185
	8.3.2 Scenario 1 – Degraded catchment	187
	8.3.3 Scenario 2 - Riparian woodland	190
	8.3.4 Scenario 3 – NFM	198
	8.3.5 Scenario 4 - Sub catchment suitability	200
	8.3.6 Scenario 5 – Scale effects	204
	8.3.7 Morland	207
8.4	Measurement errors and model parametrisation uncertainty on Qp impacts	212
8.5	FARM tool	214
	8.5.1 Catchment wide - $\gamma$ (SPR) modification	215
	8.5.2 LUM and NFM scenarios	217
	8.5.3 Scale effects	218
8.6	Discussion and conclusions	218
	8.6.1 Degradation impacts	219
	8.6.2 Flood mitigation	219
	8.6.3 FARM tool	220
	8.6.4 Model and data uncertainty	221
	8.6.5 Juke - Flood Impact Modelling	221

## **Chapter 9. Conclusions and recommendations**

9.1	Introduction	223
9.2	Research summary	223
9.3	Conclusions	224
9.4	Recommendations and future work	230

9.4.1	Catchment observations	231
9.4.2	Modelling	231
9.4.3	What next for policy?	232
	<b>References</b>	234
	<b>Appendix</b>	247

## List of Figures

	<b>Page</b>
 <b>Chapter 2</b>	
Figure 2-1	Pre-war (a) and recent (b) agricultural landscapes at the hillslope scale (O'Connell et al., 2007) <span style="float: right;">9</span>
Figure 2-2	Catchment-scale classification of NFM strategies (Pescott and Wentworth, 2011) <span style="float: right;">20</span>
Figure 2-3	Hypothetical design of a RAF/NFM network (Quinn et al., 2013) <span style="float: right;">22</span>
Figure 2-4	Meta-modelling: changing complex small-scale models into field-scale simple models (Wheater et al., 2008) <span style="float: right;">34</span>
Figure 2-5	Model output from JFLOW of floodplain inundation; taken from (Rose et al., No date) <span style="float: right;">40</span>
Figure 2-6	MIRSED matrix for soils in the Great Ouse catchment (taken from (Brazier et al., 2001)) <span style="float: right;">44</span>
Figure 2-7	The FARM tool – Highest risk of flooding, top right (taken from Wilkinson et al., 2013) <span style="float: right;">46</span>
 <b>Chapter 3</b>	
Figure 3-1	Monitoring locations in Great Ayton Map <span style="float: right;">50</span>
Figure 3-2	Monitoring locations in Morland <span style="float: right;">51</span>
Figure 3-3	Schematic of monitoring network design for Great Ayton <span style="float: right;">53</span>
Figure 3-4	Casella tipping bucket rain gauge <span style="float: right;">55</span>
Figure 3-5	Weir at EA Easby level monitoring location <span style="float: right;">55</span>
Figure 3-6	Comparison of water levels recorded by 'vented' and 'compensated' pressure transducers at Little Ayton in the Great Ayton catchment <span style="float: right;">56</span>
Figure 3-7	Theissen polygons for Morland rainfall weightings used in modelling <span style="float: right;">58</span>
Figure 3-8	VARE output showing stage-discharge curve (blue), gauged data (blue dots) and stage-velocity curve (red) <span style="float: right;">63</span>
Figure 3-9	Schematic illustrating the desired impact of increasing the time to peak of a catchment <span style="float: right;">65</span>
Figure 3-10	Illustrating shift in HOST model from A to E for change in class 5 to 7 (Boorman et al., 1995) <span style="float: right;">68</span>
Figure 3-11	Schematic of the Juke model processes (Beven et al., 2008) <span style="float: right;">71</span>

Figure 3-12	Great Ayton hydrograph illustrating the task of the matching element (Observed hydrograph in black, qfastsim in red and the matching gain in blue)	72
Figure 3-13	Showing the actual (points) and estimated (line) for three spatial scales; BLUE are results of the travel time from the nested flow gauge to the outlet, RED are the travel times calculated for the average flow path length from the cell to the nested gauge and GREEN from the cell to the outlet	73
Figure 3-14	A. gam as calculated from HOST (Equation 3 4). B. Modified pattern of gam, where SPR/gam has been reduced for areas within the improved grassland pattern (Equation 3 5)	75
Figure 3-15	Schematic of Juke	76
Figure 3-16	FARM tool illustration, lowest flood risk bottom left (green), highest flood risk top right (red)	78
<b>Chapter 4</b>		
Figure 4-1	Morland catchment elevations with the outlet and substation locations identified	81
Figure 4-2	The EA risk of flooding from rivers and sea map for the Morland catchment outlet (EA, 2014). (Red dot indicates Morland outlet location)	83
Figure 4-3	Morland bedrock geology	84
Figure 4-4	Morland superficial deposits	85
Figure 4-5	Land cover map (derived from the LCM2007 (Centre for Ecology and Hydrology, 2007))	86
Figure 4-6	Evidence of poaching cause by dairy cattle in the Morland catchment	87
Figure 4-7	Increased catchment connectivity with flow on tracks	87
Figure 4-8	Morland outlet rating curve plotted against the cross section	89
Figure 4-9	Flow exceedance curves for the three Morland gauges	90
Figure 4-10	Cumulative rainfall and runoff from Morland outlet plots for three hydrological years	91
Figure 4-11	Rainfall-runoff relationship, blue indicates winter events whilst the red are summer. Circle size (bottom right) indicates the relative size of the flood peak (qp)	93
Figure 4-12	Percentage rainfall as runoff for events to Morland outlet, blue indicates winter events whilst the red are summer	94
Figure 4-13	Flood peaks versus the API5, antecedent index, for Morland outlet	94

Figure 4-14	A set of hydrographs for the three monitoring points in Morland illustrating the difference in response with spatial scale	95
Figure 4-15	A summer (18/05/2012) and winter (20/12/2012) event, illustrating the difference in rainfall duration and intensity and what effect this has on the corresponding time to peak and flood hydrograph	96
Figure 4-16	Storm peak against the lag from rainfall to flood peak; red dots are spring/summer, blue dot autumn/winter	97
Figure 4-17	Celerity relationships between the two Morland sub-catchments and Morland outlet	97
Figure 4-18	Ranking of sub-catchment peak magnitudes against the outlet ranking	98
Figure 4-19	Photo of track runoff diversion in to a RAF	99
Figure 4-20	Photo of a RAF capturing overland flow	100
Figure 4-21	Morland mitigation features plotted on the topographic wetness index map (The higher the TWI the greater the concentration of upstream flows).	100
Figure 4-22	Photo of the sward lifting hardware used on the Morland catchment	101
 <b>Chapter 5</b>		
Figure 5-1	Elevation map for the Leven catchment to Great Ayton (© Crown Copyright/database right 2016. An Ordnance Survey/EDINA supplied service)	105
Figure 5-2	EA Flood Map for the Leven at Great Ayton (Contains public sector information licensed under the Open Government Licence v3.0; © Crown Copyright/database right 2016. An Ordnance Survey/EDINA supplied service)	107
Figure 5-3	Geology of the Great Ayton catchment (Crown Copyright/database right 2016. A British Geological Survey/EDINA supplied service)	108
Figure 5-4	Superficial deposits (Crown Copyright/database right 2016. A British Geological Survey/EDINA supplied service)	109
Figure 5-5	Soil Associations (Soil data © Cranfield University (NSRI) and for the Controller of HMSO 2013)	110
Figure 5-6	Land Cover Map 2007 (Centre for Ecology and Hydrology, 2007)	112
Figure 5-7	Improved grassland adjacent to heather grassland (potentially under-drained)	114
Figure 5-8	Evidence of soil degradation on the Dunkeswick soils, with wheelings and erosion at gateways	114

Figure 5-9	Wheelings delivering sediment rich overland flow directly to the stream (taken 26/11/2012)	115
Figure 5-10	Topographic wetness index map showing the locations of the photographic evidence of degradation	115
Figure 5-11	Flow exceedance curves for both the EA and Newcastle gauges in Great Ayton	117
Figure 5-12	Flood frequency curve developed using FEH pooled analysis	119
Figure 5-13	Analysis of flood peaks and the rainfall that generates them for Great Ayton; circle size (bottom right), indicates qp magnitude. Red = summer event (April to September), Blue = winter (October to March)	121
Figure 5-14	Hydrographs and corresponding event rainfall for a summer (17/07/2009) and a winter event (16/01/2010)	122
Figure 5-15	Runoff as a percentage of rainfall for a range of flood peaks. Red = summer event (April to September), Blue = winter (October to March) Timing and celerity	122
Figure 5-16	Lag time analysis for the Great Ayton catchment. Red = summer event (April to September), Blue = winter (October to March)	123
Figure 5-17	Travel time plot the catchments upstream of Easby to Great Ayton	124
Figure 5-18	Celerity plot for the catchments upstream of Easby to Great Ayton	125
Figure 5-19	Celerity plot the catchments downstream of Easby to Great Ayton	125
Figure 5-20	Comparison of peak discharges at Foxton Bridge and Easby as specific discharges (mm/hr)	126
Figure 5-21	Leven event of November 2009. Foxton at 168 km <sup>2</sup> , Great Ayton at 30 km <sup>2</sup> and Easby at 15 km <sup>2</sup>	127
Figure 5-22	Peak event rankings for Foxton and Great Ayton (RED) and Great Ayton and Easby (GREEN) (High rank equals high flow)	128
Figure 5-23	Catchment map and mitigation features are numbered for the following discussion (© Crown Copyright/database right 2016. An Ordnance Survey/EDINA supplied service)	129
Figure 5-24	Flood proofing locations within Great Ayton highlighted by red squares (© Crown Copyright/database right 2016. An Ordnance Survey/EDINA supplied service)	130
Figure 5-25	Woody debris features in Leven Vale (Site 1)	130
Figure 5-26	Looking upslope at a wooden barrier feature at site 4 for attenuating overland flows	131



Figure 5-27	Little Ayton offline storage pond and oxbow feature; a. concrete inlet pipe to the offline storage pond; b. view of offline storage pond and oxbow in the background	132
Figure 5-28	Old Mill pond playing field feature upstream of Great Ayton	132
<b>Chapter 6</b>		
Figure 6-1	FEH and ReFH for the 100-year, 12 hour design storm to Great Ayton	138
Figure 6-2	Matrices produced for Great Ayton using the (a) FEH and (b) ReFH models for the 100-year, 12 hour event	144
Figure 6-3	Peak discharge values for the 100-year flood for multiple SPR and $T_p$ scenarios as modelled with FEH (Solid line) and ReFH (Broken line)	145
Figure 6-4	Risk matrix for the 25-year, 12 hour FEH model run to Great Ayton	146
Figure 6-5	Risk matrices for FEH model runs to Great Ayton using different storm durations. a) 2.75hrs, b) 23.75hrs	148
Figure 6-6	Peak discharge values for the 100-year flood for multiple SPR (colour of line) and $T_p$ scenarios (x-axis).	150
Figure 6-7	Completed $Q_p$ matrix using interpolation and verified values in red, for the 100-year, 8 hour event to Morland	151
Figure 6-8	The FIM tool interface for the Great Ayton Catchment (parameter manipulations can be made to sub-catchments and the impact at the outlet immediately observed).	154
Figure 6-9	Results of increasing the TP and reducing the runoff (through $Q_p$ ) for the Dikes Beck catchment within the FIM tool.	155
Figure 6-10	Results of increasing the TP and reducing the runoff (through $Q_p$ ) for the Dikes Beck and Kildale catchments within the FIM tool.	156
Figure 6-11	The 2.75 hours and 23.75 hours hydrograph and hyetographs generated using the FEH model	159
<b>Chapter 7</b>		
Figure 7-1	The 8 hour, 100 and 50 year return interval events for Great Ayton and Easby	166
Figure 7-2	Flood frequency curves for Great Ayton generated from the flood peaks for different storm durations by the FEH rainfall-runoff model	167
Figure 7-3	Illustration of the behaviour of the matching gain ( $L_{gam}$ ; red) for an FEH 100 year calibrated event (black)	168

Figure 7-4	Soils map for Great Ayton showing the HOST attributes (Soil data © Cranfield University (NSRI) and for the Controller of HMSO 2015)	170
Figure 7-5	Results illustrating the changes in $Q_p$ when manipulating uniform and distributed patterns of $\gamma$	171
Figure 7-6	Celerity function plotted for three different scales, where $q^*$ is the flow at a particular scale	173
Figure 7-7	Illustration of the number of cells with a given upstream area	174
Figure 7-8	Impact of manipulating $\delta$ plots; a. Change in $T_p$ (positive $t$ = increase) b. Change in $Q_p$ form the modelled FEH hydrographs	175
Figure 7-9	Impact of changing $\delta$ on the FEH 100-year, 8 hours duration event	175
Figure 7-10	Impact of manipulating $\phi$ plots; a. Change in $T_p$ (positive $t$ = increase) b. Change in $Q_p$ form the modelled FEH hydrographs	176
Figure 7-11	Impact of changing $\phi$ on the FEH 100-year, 8 hours duration event	176
Figure 7-12	Impact of manipulating $\eta$ plots; a. Change in $T_p$ (positive $t$ = increase) b. Change in $Q_p$ form observed	177
Figure 7-13	Impact of changing $\eta$ on the FEH 100-year, 8 hours duration event	177
Figure 7-14	Observed and modified hydrographs with their corresponding outlet celerity plots	178
<b>Chapter 8</b>		
Figure 8-1	Relative effects of LUM and NFM on flood flows	183
Figure 8-2	Great Ayton observed hydrograph, highlighting the four largest modelled events	185
Figure 8-3	Hydrograph for a large event in November 2012 and the corresponding $L_{gam}$	187
Figure 8-4	Map of the areas where SPRs are changed to an alternate, grey, and remain the same, black	189
Figure 8-5	Result for worst-case scenario showing change in peak magnitude	189
Figure 8-6	Plots of the observed versus the modelled hydrograph for scenario 1 for the rank 3 event	190
Figure 8-7	The effect of reducing $\delta$ by half on the celerity function; broken line modified	193
Figure 8-8	Pattern showing areas suitable for wet woodland identified in grey	194
Figure 8-9	Riparian woodland results; change in $T_p$ and % change in $Q_p$	195

Figure 8-10	Hydrographs of wet woodland having beneficial impact on the downstream hydrograph	196
Figure 8-11	Hydrographs of riparian woodland having a negative impact on the downstream hydrograph	196
Figure 8-12	Riparian woodland scenarios; $\delta$ reduced by 50 %, * indicates SPR reduced by 20 %	197
Figure 8-13	Riparian woodland results for sub catchment mitigation (Scenario 2.1; triangles) and main channel sub catchment mitigation (Scenario 2.3; circle; *)	198
Figure 8-14	Hydrographs of NFM scenario where $\delta$ is reduced by 75 %	199
Figure 8-15	Wet woodland scenarios; $\delta$ reduced by 50 % and 75 %	200
Figure 8-16	Patterns used in Scenario 4; Grey indicate cells within the pattern, Black are not.	202
Figure 8-17	Sub-catchment investigation results; change in $T_p$ and percentage $Q_p$ change	203
Figure 8-18	Event with the greatest reduction in $Q_p$ for each version of the scenario	203
Figure 8-19	Results of changing SPR and Celerity independently and together (both) for Lonsdale	204
Figure 8-20	Pattern of the two sub-catchments being used in this scenario, Leven Vale (green) and Lonsdale (grey)	205
Figure 8-21	Impact of reducing SPR in both Leven Vale and Lonsdale at Easby and Great Ayton	206
Figure 8-22	Impact as the average percentage reduction on local $Q_p$ , at Great Ayton (broken line) and Easby (Solid line) for the two SPR reduction scenarios of 10 % (blue) and 20 % (red)	207
Figure 8-23	Patterns used for the Morland scenarios (Scenario 1: Grey area in the mitigation pattern, black and green not in the pattern, green indicates the mitigation catchment. Scenario 2: Grey area in the mitigation pattern, black excluded)	209
Figure 8-24	Morland Scenario 1 results showing change to $T_p$ and $Q_p$	209
Figure 8-25	Noisy in the hydrograph peak (Rank 4 event) makes it appear the that $T_p$ has been reduced under mitigation	210
Figure 8-26	Increased $Q_p$ due to attenuation of flows but cause coincidence with the peak (Rank 2)	211
Figure 8-27	Impact on flood peaks for the Morland and Great Ayton catchments with catchment wide riparian woodland implemented	211

Figure 8-28	Rating curve uncertainty impact on the modelled flood peaks for the degradation scenario	213
Figure 8-29	Modelling results for the experiment to investigate the uncertainties associated with the rating curves and runoff parameterisation.	214
Figure 8-30	Modelling results showing the changes in $Q_p$ and $T_p$ for a range of $\gamma$ manipulation scenarios	215
Figure 8-31	A farm matrix showing the percentage change in $Q_p$ and change in $T_p$ for the rank 1 event	216
Figure 8-32	Multiple peaked, rank 2 event, with a reduced $T_p$ for less runoff	216
Figure 8-33	FARM matrix showing the results for the rank 1 event for the scenarios modelled	217
Figure 8-34	FARM matrix illustrating the effects of the spatial extent of mitigation and the scatter/uncertainty in the magnitude of reduction magnitude	218

## List of Tables

	<b>Page</b>
<b>Chapter 2</b>	
Table 2-1	Summary table of land use /NFM studies investigating flood hazard and mitigation 19
Table 2-2	NFM studies and results 23
Table 2-3	Summary of statistical modelling project investigating potential land use change impact 28
Table 2-4	HOST classification numbers. Numbers in brackets are HOST SPR values (* IAC used to index lateral saturated conductivity) (Boorman et al., 1995) 29
Table 2-5	Excerpt from a USDA curve number table for land use and hydrologic soil groups (USDA, 1986) 30
Table 2-6	Mappings of U.S Department of Agriculture (USDA) and Hydrology of Soil Types (HOST) soil classifications (Bulygina et al., 2011a) 31
Table 2-7	Summary of modelling projects investigating potential land use change impacts using distributed physical models [Spatial resolution of model in square brackets] 32
Table 2-8	Summary of some meta-modelling approaches used for land use change impact assessment 37
Table 2-9	Summary of conceptual rainfall-runoff models used for modelling land use change impacts 38
Table 2-10	Examples of NFM and land use scenarios modelled using hydrodynamic models 41
<b>Chapter 3</b>	
Table 3-1	Summary of land use, land management and climate of the two research catchments 52
Table 3-2	Morland catchment and sub-catchment instrumentation summary 57
Table 3-3	Morland data availability 57
Table 3-4	The EA instrumentation being used in the Great Ayton analysis and modelling 59
Table 3-5	Newcastle university installed gauges data availability 60
Table 3-6	Location and other attributes of the Newcastle university sites 61
Table 3-7	HOST classes and their revised, degraded reclassification (* indicates some uncertainty in the reclassification; Lettering next to class number

signifies the catchment in which they are found M = Morland, G= Great Ayton; Packman et al. (2004) 67

#### **Chapter 4**

Table 4-1	FEH statistics for Morland	82
Table 4-2	Morland land cover 2007 breakdown	86
Table 4-3	Summary of rating curve quality	88
Table 4-4	Rainfall-runoff statistics for Morland outlet for the three hydrological years 2011-2014	91

#### **Chapter 5**

Table 5-1	FEH statistics for Great Ayton	106
Table 5-2	Soil type descriptions provide by national soil dataset (Soil data © Cranfield University (NSRI) and for the Controller of HMSO 2013)	111
Table 5-3	Great Ayton land cover 2007 breakdown	113
Table 5-4	Great Ayton flow record information	116
Table 5-5	Relative ranking of events at Great Ayton and Easby	118
Table 5-6	Relative distance of the Great Ayton sub-catchment gauges to the outlet	123

#### **Chapter 6**

Table 6-1	Changes in SPR suggested by Packman et.al (2004) for the soil types found in the Leven catchment	141
Table 6-2	Tp and SPR values modelled by Packman et al. (2004)	141
Table 6-3	Percentage change in Qp taken from Packman et al. (2004) for a range of different return interval events	142
Table 6-4	Flood peak discharges for different magnitude storms under different catchment conditions	146
Table 6-5	Rainfall characteristics for different duration storms that produce a 1-in100-year flood	147
Table 6-6	The impact on QP for each of the sub catchments of applying the degradation and improved catchment scenarios outlined in the FEH improvements study.	149
Table 6-7	FIM scenario results	157

## **Chapter 7**

Table 7-1	Summary table of the FEH rainfall event characteristics used to generate the design hydrographs	165
Table 7-2	Percentage change in $Q_p$ for range of design storms modelled with Juke and the FEH	168
Table 7-3	Peak scaling parameters	172

## **Chapter 8**

Table 8-1	Overview of LUMC and NFM scenarios	182
Table 8-2	Hydrological characteristics of the four largest flood peaks modelled to Great Ayton	184
Table 8-3	Celerity parameters for the Leven to Great Ayton	186
Table 8-4	HOST classification and alternate SPRs as recommended by (Packman et al., 2004)	188
Table 8-5	Areas of the component catchments and the proportion of total catchment they represent undergoing modification	205
Table 8-6	Scenarios modelled for Morland	207
Table 8-7	Rainfall characteristic of the four largest flood peaks modelled to Morland	208
Table 8-8	Rainfall-runoff totals for the three derivations of the Morland outlet rating curves (The values in brackets are the percentage equivalent of the original, two year period.	212
Table 8-9	Summary of the scenarios, parameter manipulation made and the percentage of catchment affected	217
Table 8-10	Summary statistics of the scenario impacts on $Q_p$ and $T_p$	221

## **List of Abbreviations**

ADCP	Acoustic Doppler Current Profiler
AMAX	Annual maximum flow
AWS	Automatic Weather Station
BFI	Baseflow Index
CEDA	Central for Environmental Data Archive
CEH	Centre of Ecology and Hydrology
CFMP	Catchment flood management plans
CPD	Continuing Professional Development
DBM	Data Based Mechanistic
Defra	Department for Environment, Food and Rural Affairs
DEM	Digital Elevation Model
DTC	Demonstration Test Catchments
EA	Environment Agency
EU	European Union
EVO	Environmental Virtual Observatory
FEH	Flood Estimation Handbook
FIM	Flood Impact Model
FRMRC	Flood Risk Management Research Consortium
GLUE	Generalized Likelihood Uncertainty Estimation
gam	Distributed rainfall partitioning factor
HOST	Hydrology of Soil Types
IAC	Integrated Air Capacity (downward percolation)



Lgam	Time varying lumped partition
LUM	Land Use Management
LUMC	Land Use Management Change
m.a.o.d	metres above ordnance datum
NFM	Natural Flood Management
NGO	Non-Governmental Organisations
PDM	Probability Distributed Model
PIF	Permanently Ineligible Feature
Qp	Flood peak discharge.
RAF	Runoff Attenuation Feature
ReFH	Revitalised Flood Hydrograph model
SCS-CN	Soil Conservation Service runoff Curve Number
SEPA	Scottish Environment Protection Agency
SAAR	Standard Average Annual Rainfall
SPR	Standard Percentage Runoff
SPRHOST	Standard Percentage Runoff derived from Hydrology of Soil Type
tix	Asymptotic time limit for fast discharge (h)
Tp	Time-to-peak
TWI	Topographic Wetness Index
UH	Unit Hydrograph
USDA	United States Department of Agriculture.
VARE	Velocity Area Rating Extension

# Chapter 1. Introduction

## 1.1 Background

Recent flooding in the UK has brought to the fore a debate about the way in which flood hazard is managed. There is a growing interest, especially within the media, for greener, nature-based solutions as an alternative to the traditional use of hard-engineered walls and embankments (Monbiot, 2015a; Monbiot, 2015c). Interest in alternative methods had been roused prior to this as a result of many locations, such as Keswick and Carlisle in Cumbria, having had formal engineered defences overwhelmed in December 2015 (BBC, 2014; BBC, 2015; Monbiot, 2015b). There is also a growing appreciation from Government Agencies (e.g. EA) that they cannot keep building ever bigger defences. Nature-based flood management options include Land Use Management Change (LUMC) and the use of landscape interventions termed Runoff Attenuation Features (RAFs), both of which fall under the wider banner of Natural Flood Management (NFM). It is widely accepted that increased agricultural intensity in the UK has led to increased volumes of fast flows contributing to flooding (O'Connell *et al.*, 2004; O'Connell *et al.*, 2007). Flood risk and catchment managers also have to contend with the potential for flood risk increasing in the future due to climate change (Kendon *et al.*, 2014).

The potential for land use impacts to increase flood hazard has been demonstrated through numerous plot and field scale studies. Soil compaction due to heavy machinery and repeat trafficking, as well as heavier and greater stocking densities of livestock, have been demonstrated to reduce infiltration and increase soil bulk density (Bilotta *et al.*, 2007). As the dominant land use in the UK, agriculture (accounting for c.a. 70 % of the land cover) has the potential to play a significant role in the mitigation of flood hazard. This could be through more hydrologically sensitive farming, for example reducing compaction and providing cover crops over winter. These types of intervention have been proven to increase the infiltration and storage capacity of the soil, therefore potentially reducing the volumes of both saturation and infiltration excess runoff.

Detecting and identifying land use impacts in historic runoff records has not been possible for numerous reasons, including; (1) non-stationarity of the climate and antecedent conditions; (2) data errors and uncertainty due to the limited length of

observed records; (3) additional unknown and uncontrollable factors within the catchment (e.g. dredging, straightening or construction and urbanisation). Each of these factors makes attributing any changes in the hydrological response to LUMC very difficult.

One method for investigating how LUMC impacts on flood risk at larger scales is to make use of computational models, where the modeller has direct influence over the changes made, thus making the link between cause and effect more transparent. There are numerous considerations to be made, however, when selecting the use of models. For example, what complexity of model to use? Comparatively simple, lumped rainfall runoff models, with a limited number of parameters or more complex, distributed physics-based models. There is limited evidence regarding LUMC impacts at spatial scales larger than field or plot, so there is significant uncertainty as to what level of manipulation to apply to lumped catchment scale models. Distributed, physics-based models may be more appropriate as the parameter manipulations applied to reflect LUMC impacts can be undertaken at scales closer to the field observations. Distributed physics-based models, however, have a large number of parameters. This can lead to the potential for multiple acceptable parameter sets in calibration. The uncertainty in the most appropriate parameter set means there is uncertainty in the modelled output and therefore impacts (Brazier *et al.*, 2000; Beven and Freer, 2001; Ewen *et al.*, 2006).

This thesis will make use of two modelling approaches to investigate the potential for LUMC and NFM approaches for mitigating flood hazard. The first modelling approach is the lumped Flood Estimation Handbook (FEH) rainfall-runoff model. The FEH model has previously been used to investigate LUMC scenarios and provides a knowledge base derived from expert opinion as to the likely catchment scale, hydrological impacts of soil degradation (Packman *et al.*, 2004). The second model used is a novel, distributed model, Juke (Beven *et al.*, 2008), which has been specifically developed for investigating LUMC and NFM impacts. Juke makes use of available GIS datasets and observed hydrological data to parametrise the runoff generation and routing components of the model in a transparent and physically reasonable way. The physically based parametrisation of Juke enables LUMC and NFM impacts to be applied in a transparent and unambiguous way. As Juke is distributed it enables the investigation of routing effects on the field scale impacts and how they manifest at a larger catchment scale.

The modelling results are used to populate the Floods and Agriculture Risk Matrix (FARM) tool (Wilkinson *et al.* (2013)). The FARM tool has previously been used as a means of communicating the likely flood hazard impacts of LUMC decisions, however, with no quantification as to the level of LUMC and associated hazard. The outputs from this thesis aim to provide some level of quantification of the potential flood hazard reductions. This is being done to address several questions commonly asked by stakeholders and policy makers including: how much intervention of a given type is required and where are they best located? What are the potential downstream impacts of changing the synchronicity of flows from multiple sub catchments?

The thesis will make use of the latest expert knowledge and opinion combined with field observations to achieve the following aim, by fulfilling seven objectives, as described in section 1.2

## **1.2 Aim**

The aim of this thesis is to demonstrate the potential effectiveness of NFM interventions in reducing flood hazard at the small catchment scale ( $\leq 30 \text{ km}^2$ ) using modelling techniques of increasing complexity supported by field observations.

### **1.2.1 Objectives**

1. Carry out a comprehensive literature review of the current understanding and quantification of the impacts of NFM interventions and agricultural practices on flood generation. This will support objectives 4 and 6.
2. Collect high quality hydrological data from two catchments in which NFM interventions are either planned or have been implemented. Great Ayton (River Leven) and Morland (Newby Beck) have been chosen as the study catchments, as these provide a good contrast in term of spatial scale and interventions proposed.
3. Characterise the study catchments to understand how floods develop and along which hydrological pathways the water is being transferred.
4. Develop suitable scenarios for potential LUMC and NFM adoption, designed to reduce flood hazard within catchments, based on expert knowledge and field data.
5. Explore the limitations of a widely used ‘traditional’ modelling approach, the FEH method, which is widely used by practitioners.

6. Use a novel modelling technique (Juke) to test potential catchment management scenarios including land use change and NFM on the catchment flood response. This approach differs from the FEH, in that expert knowledge can be directly used to change the catchment functioning in a transparent fashion.
7. The outcomes of 5 and 6 will be used to populate a series of risk matrices based on the Floods and Agriculture Risk Matrix (FARM) tool (Wilkinson et al., 2013). The tool helps to synthesise and convey both the limitations of traditional modelling structures for land use change scenario modelling and the implications of land use management decisions on flood risk. The results will provide guidance to practitioners, the scientific community and others with an interest in NFM and land use management as a means of reducing flood risk.

### **1.3 Thesis outline**

**Chapter 2 (Objective 1)** – Provides an overview of the literature relevant to this thesis, including a description of the hydrological processes that control the generation and routing of flood flows. The impact that agricultural practices can have on these hydrological processes is then investigated along with the role of government policy in managing this impact. An overview is then provided of the different modelling approaches used within flood impact studies and an assessment of their strengths and weaknesses is provided.

**Chapter 3** – Outlines the methodological approaches used to achieve the objectives of this thesis. The research catchments and their experimental design are described along with the hydrometeorological instruments used. The way in which the rainfall-runoff data are analysed and used to inform the modelling is then discussed; two modelling approaches are used to investigate land use impacts; (1) the widely used, lumped, FEH rainfall-runoff model; and (2) the novel, distributed, Juke rainfall-runoff model.

**Chapter 4 (Objective 2 & 3)** – Presents the characterisation of the Morland catchment (12.5 km<sup>2</sup>) including the physical and hydrological characteristics. The physical characterisation provides an overview of the flood risk, the soils, geology and land cover. The hydrological characterisation details the hydrometeorological data including the development of the stage-discharge rating curves, followed by an analysis of the rainfall-runoff dynamics of the catchment and how these may be of use in modelling the catchment.

**Chapter 5 (Objective 2 & 3)** – Provides a hydrological and physical characterisation of the Great Ayton catchment (30 km<sup>2</sup>), North Yorkshire. As in Chapter 4 this is to help understand the hydrological characteristics that cause the largest flood peaks. Understanding the physical characteristics, such as soils, that are susceptible to land use change is important when considering potential mitigation measures.

**Chapter 6 (Objective 5 & 7)** – Uses the lumped FEH rainfall-runoff model to investigate land use impacts on flood peaks. This chapter explores how the impacts affect different magnitude and duration storms, as well as investigating how the impacts change with spatial scale. The development of a simple Flood Impact Model is discussed and a series of potential mitigation scenarios are considered and mapped to the FARM tool.

**Chapter 7 (Objective 5)** – Describes the validation of the Juke model to show that it is consistent with the FEH rainfall-runoff model and therefore a sufficient emulator. This is important as the FEH and Hydrology Of Soil Types (HOST) provides a well-established and accepted level of expert knowledge, including methods that can be used for exploring LUMC impacts. The parameters associated with runoff generation and routing are sensitivity tested to examine their likely impact in mitigation scenarios.

**Chapter 8 (Objective 4, 6 & 7)** – Explores a number of future potential LUMC and NFM scenarios, using Juke, that could be adopted in the Great Ayton and Morland catchments. Where possible the scenarios used knowledge of land use impacts from the literature to investigate where in each catchment was best suited for intervention as well as what proportion of each catchment needs to undergo mitigation to have a meaningful impact at the downstream point of interest.

**Chapter 9** – The final chapter concludes the thesis by evaluating the findings against the aims and objectives set out in section 1.2 and provides recommendations for further work.

## Chapter 2. Literature review

### 2.1 Introduction

In recent decades there have been numerous significant flood events across northern and central Europe (Barredo, 2007; Barredo, 2009). In the UK large-scale flooding has been experienced across many parts of the country; North Yorkshire in 2000 (Marsh, 2001), River Eden, Cumbria in 2005 and 2015 (Roberts *et al.*, 2009), Yorkshire in 2007 (Blackburn *et al.*, 2008), Cumbria (R. Derwent) in 2009 (Met-Office, 2009), many parts of the UK in 2012, and Somerset in early 2014.

The costs associated with flooding are increasing. Insurance companies spent £4.5 billion on flood damage to households and businesses from 2000 – 2010, 200 % more than the £1.5 billion spent in the previous decade (ABI, 2010). This trend has been observed across much of Europe with the increase partially attributed to upstream land use change and loss of natural attenuation, as well as increased populations and wealth in flood prone areas (Barredo, 2009; Feyen *et al.*, 2012). Notwithstanding changes in land use, many experts predict that the impacts of climate change will lead to increased flood risk both in the UK and across Europe (Hall *et al.*, 2005; Feyen *et al.*, 2012). Moreover, Kendon *et al.* (2014) suggests that an increase in high intensity summer events will have greatest effects on smaller catchments (<35 km<sup>2</sup>).

This chapter provides an overview of the literature relevant to this thesis, specifically with regard to the evidence base and modelling of the impacts of rural land management on flooding. The first section describes the dominant hydrological processes that generate local flood flows. Next the implications of rural land use management practices are considered, particularly how practices impact on catchment hydrological functioning and how they can increase the flood hazard at the larger catchment scale. Spatial and temporal scales are then considered. Understanding the role of spatial scale, such as the impact of local-scale overland flow generation downstream at the larger catchment scale, is necessary to underpin effective catchment planning and policy. Natural flood management as a means of reducing flood risk is then introduced, with examples of the different approaches given. The next section provides a synthesis of relevant modelling approaches and examples in which they have been used for land use management change impact studies. Finally, the questions that need to be addressed with regards to policy are considered.

## **2.2 Hillslope scale flood generation and routing**

The following sections consider what is known about land use impacts on flood generation and routing. The rationale is that there is understanding of the impacts at the small, 'local', i.e. the point or hillslope/field scale but how these manifest at a larger scale is unclear.

### ***2.2.1 Local scale runoff generation - storage***

Rainfall has a number of potential flow paths when it hits the ground. It can infiltrate into the soil and be taken up by plants, infiltrate to become groundwater, or it can follow a hydraulic gradient, generally in a downslope direction, as subsurface flow. Rainfall can also move across the land surface as overland flow, which is generated by two principal mechanisms: Saturation excess, where the soil matrix is full and cannot store any additional water (Dunne and Black, 1970), or infiltration excess (also known as Hortonian overland flow), where the rainfall rate exceeds the infiltration capacity of the soil (Horton, 1933). The storage and infiltration capacity of the soil is determined by its physical characteristics including the pore space and size. The total pore space available will affect the amount of water a soil can hold whilst the pore size affects the rate at which water can move through and into the soil, the conductivity (Mualem, 1976), all of which are sensitive to land use change and land management.

### ***2.2.2 Local scale routing and connectivity***

An important controlling factor in the generation of flood flows is the speed at which water moves through or across the landscape to the stream network. At the small spatial scale, soil storage and infiltration are important, with increasing scale the connectivity and routing of flows becomes more important. Different soil types have different structures, hence different capacities for storing and conducting water. For example, a clay soil has a relatively large (total) pore space but has very small pores, resulting in a low conductivity, while a sandy soil has larger pores allowing water to move more readily into and through its matrix (Van Genuchten, 1980). This is of significance when studying flooding within a catchment, as different areas underlain by different soils will have different propensities to propagate subsurface flow and generate overland flow. Topography and land cover also play important roles, particularly for overland flow as they can directly affect the speed at which water can move. Hence, the soil plays a crucial role in generating runoff and is sensitive to degradation (Heathwaite and Dils, 2000).



The rate at which flows reach the main channel also affects the propagation of a flood. Subsurface and overland flows that can readily enter the channel network to contribute to the flood hydrograph are said to have a high level of ‘connectivity’ (Bracken and Croke, 2007). The connectivity of the landscape has been enhanced in most anthropogenic landscapes, particularly for agriculture, where subsurface drains and field boundary ditches have been incorporated. Conversely, landscapes with soils of high infiltration and storage capacity, low relief and obstructions to flow are described as having a low level of connectivity. Generally there has been a loss of natural saturated zones and straightening of channels which increases connectivity in agricultural landscapes (O’Connell *et al.*, 2007)

### **2.2.3 Scaling up**

Generally, the hydrological processes at the point scale are well understood due to the ease at which the measurements can be made; it must be noted that agriculturalists have long studied point scale processes in a quest to increase agricultural productivity. Our understanding of how changes to these small scale processes propagate to the catchment scale to impact on downstream flood hazard is less well known. The implications of temporal and spatial scale effects on routing and travel times is less well known (Blöschl *et al.*, 2007).

When considering flooding it is important to have an understanding of both the spatial and temporal scales that operate within a catchment. At the small scale (0.01 m – 100 m), infiltration or saturation excess overland flow can take minutes; at the very large scale (tens of thousands of square kilometres) flood flows can take days and weeks to develop. Solving the flooding issues at these varying scales will require different approaches because of the relevance of different processes, i.e. the relative importance of the hillslope and channel network. The variability in response at the small scale is driven by variable topography and soil type whilst rainfall patterns and river processes are more important at large catchment scales (Mesa and Mifflin, 1986; Blöschl *et al.*, 1995).

## **2.3 Land Use Management and flood hazard**

In the UK 17.19 million hectares of land was in use for agricultural production in 2012 (Defra, 2013). Of that 6.26 million ha was under crop, 9.73 million ha was under permanent grass (incl. rough grazing) and the remaining 1.17 million ha is of other use

such as woodland or outdoor pigs (Defra, 2013). The post-World War Two (WWII) intensification of agricultural practices led to dramatic changes in the landscape, as summarised by O’Connell *et al.* (2007) (Figure 2-1) :

- *accelerated loss of hedgerows and subsequent creation of larger fields;*
- *cultivation practises causing deeper compacted soils;*
- *land drains connecting the hill to the channel;*
- *cracks and mole drains feeding overland flow to drains and ditches;*
- *unchecked wash-off from bare soil, due to loss of field boundaries as mentioned above and the sowing of winter crops leaving limited canopy coverage over the wettest time of the year;*
- *plough lines, ditches and tyre tracks concentrating overland flow;*
- *tramlines and farm tracks increasing hydrologic connectivity and compacting soil;*
- *channelised river with no riparian buffer zone.*

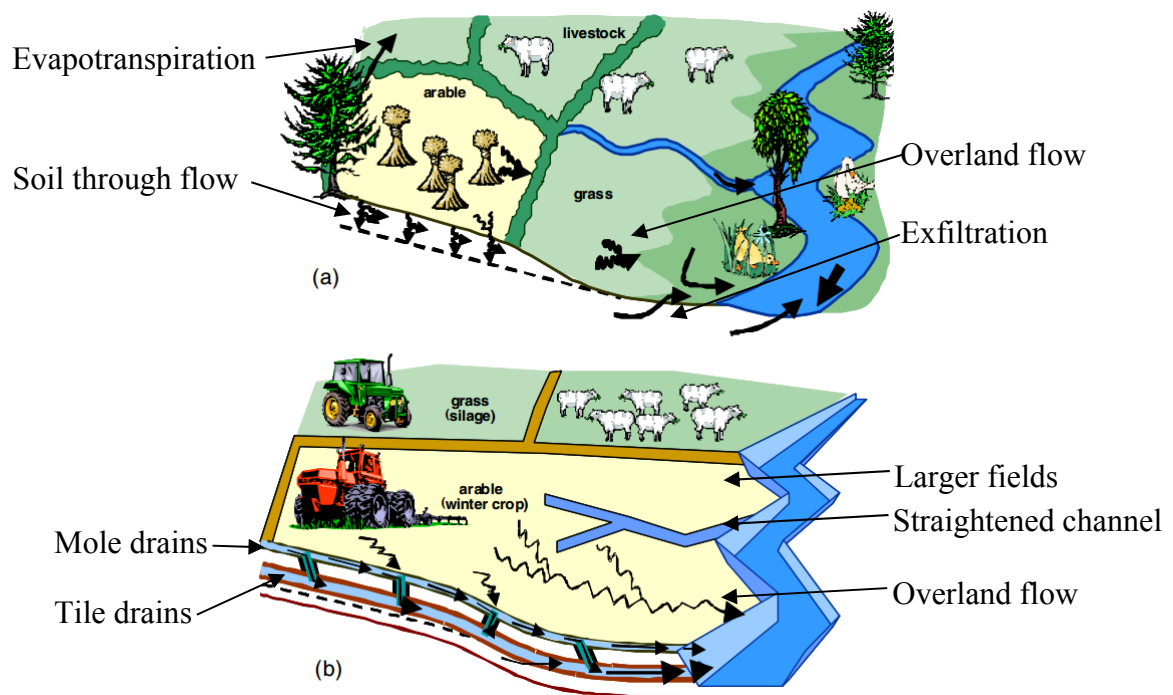


Figure 2-1 Pre-war (a) and recent (b) agricultural landscapes at the hillslope scale (O’Connell *et al.*, 2007)

The following section discusses national and European policies that have influenced land use management decisions in the UK. The hydrological impact of different land use management approaches is then discussed with an overview of case studies and experiments.

### **2.3.1 Policy**

Much of the rural landscape of the UK is heavily managed, with just over 70 % used for agriculture (Defra, 2013). There is growing concern that land management practices may impact on flood hazard through the deterioration of soil structure and loss of natural buffers (O'Connell *et al.*, 2004; O'Connell *et al.*, 2007; Hannaford and Marsh, 2008).

Post-war government policy at the national level through the 1947 Agriculture Act and the Common Agricultural Policy (CAP) at the European level supported the intensification of agriculture to ensure self-sufficiency in food production (Robinson and Sutherland, 2002; O'Connell *et al.*, 2007). To increase the availability of productive agricultural land, drainage was subsidised through policy and was ongoing until the late 1970s (Tunstall *et al.*, 2004; Penning-Rowsell *et al.*, 2006). Land drainage policy encouraged draining less favourable land such as coastal and river wetlands and the straightening and dredging of rivers, the aim being to remove water as fast as possible (Tunstall *et al.*, 2004; Penning-Rowsell *et al.*, 2006). Arable land cover rose by 50 % over 5 years from the beginning to the end of the Second World War, from its lowest recorded coverage of 5.8 million hectares to its largest at 7.8 million hectares (Keep, 2009), thereafter there has been a steady decline to 6.26 million hectares in 2012 (Defra, 2013), still 8 % greater than the pre-war coverage. The decrease in area has also coincided with a shift to both autumn and spring sown crops rather than just traditional spring sown. This has largely been made possible through technological advancement and heavier, more powerful, machinery.

There has also been a significant increase in the livestock densities reared on British farms. There was a significant increase in cattle numbers from 6 million cattle in 1864 to 15.2 million in 1974 (Keep, 2009). A number of factors have led to a steady decline since the peak in the 1970s including the European Union (EU) milk quota introduction and some effect from BSE (late 1980s early 1990s) and foot and mouth disease (2007) (Keep, 2009).

It is now argued that land use management practices could, and should, play a role in flood hazard reduction planning, as part of the solution and not simply the problem. The Pitt Review (Pitt, 2008) of the summer 2007 flood events notes:

*'It is now widely accepted that flood risk cannot be managed by simply building ever bigger hard defences. Softer approaches, such as flood storage and land management, can offer more sustainable ways of managing the risk, and can complement and extend the lifetime of more traditional defences.'*

This recommendation can be seen as being especially pertinent now, considering the economic constraints being placed upon many government departments. Making use of agri-environment schemes (e.g., Countryside Stewardship, Catchment Sensitive Farming) where there is a monetary incentive for farmers to adopt certain management regimes may prove a plausible flood mitigation option but there are long-term management issues. Currently, however, any features built on productive land that take that land out of production would have to be designated as Permanently Ineligible Features (PIF) which cannot be claimed for. The most recent legislation are promoting more holistic approaches to tackle excess runoff, for example the European Flood Directive (2007/60/EC) and in the UK the Flood and Water Management Act (2010) as well as the Catchment Based Approach (CaBA; 2013).

### **2.3.2 Livestock farming**

#### ***Implications for runoff generation***

Pastoral livestock rearing degrades the soil structure, often referred to as poaching, with increased bulk density (soil mass per unit volume) and decreased macroporosity (loss of soil structure and pore space) (Houlbrooke *et al.*, 2011). This leads to a reduction in infiltration rate and consequently an increased tendency to produce overland flow (Sansom, 1999; Carroll *et al.*, 2004; Wheeler *et al.*, 2008). The impact of heavy animals on soils especially when wet is detrimental to soil structure (Bilotta *et al.*, 2007; Bilotta *et al.*, 2008).

#### ***Field evidence***

A number of national and international studies have investigated the impact of livestock rearing and its hydrological impact on soil in temperate climates, relevant to the UK. Sansom (1999) argues that the incentivisation of sheep rearing has led to less desirable

land being farmed. This includes upland areas with poor soils and high rainfall, which has led to increased runoff, soil erosion and river bank erosion rates (Sansom, 1999). The Pontbren catchment located in the headwaters of the River Severn catchment, mid-Wales, has been studied to investigate the impact of upland management on flood risk by the Flood Risk Management Research Consortium (FRMRC Wheater *et al.* (2008)). Infiltration rates of ~0-30 cm/h for grazed improved pasture, compared with ~60-70 cm/h for adjacent areas under trees with the same soil type, are reported (Carroll *et al.*, 2004).

Studies in New Zealand have shown the hydrological impact of farming dairy cattle to be significantly greater than for sheep grazing. Drewry *et al.* (2000) measured saturated hydraulic conductivities of 1 to 3.2 cm/h for soil under dairy cattle compared to 2.6 to 8.6 cm/h for the same soil type under sheep. Drewry *et al.* (2000) also note that macroporosity was higher and bulk density lower under sheep. It was also demonstrated that the impacts are not uniform over the landscape as cattle tend to congregate in certain areas causing localised poaching and degradation. Pathways developed by livestock movement create preferential flow pathways and increased soil erosion (Pietola *et al.*, 2005; Drewry, 2006). Pietola *et al.* (2005) observed that infiltration rates at livestock drinking sites were 20 % lower than those at un-trampled pasture, and tended to be worse on soils with high clay content with infiltration rates at 10-15 % of adjacent pasture. The practice of sheep fattening, where sheep are put out onto bare soil in Autumn and early Winter to feed on the greens left after beet harvesting, can have a significant impact on soil structure and exposure (Holman *et al.*, 2003).

### ***Management options***

The effects of soil compaction can be reversed or partly mitigated for using mechanical, aeration/loosening techniques (Burgess *et al.*, 2000). Aeration of the soil is performed by dragging a sled fitted with a series of cutters/spikes behind a tractor to break up the compacted layer. Natural processes can also improve soil compaction if allowed through reduced stocking for example, through earthworm and root activity, freeze thaw heave and wetting and drying cycles (Dexter, 1991; Whalley *et al.*, 1995; Drewry and Paton, 2000).

### **2.3.3 Arable farming**

#### ***Implications for runoff generation***

Arable farming practices can lead to increased surface and near-surface (fast) runoff generation which coupled with activities that have increased levels of landscape connectivity can ultimately lead to greater flood hazard. Such practices include:

- Moving from spring to winter sown cereal to increase yields, creating extended periods of bare or near bare soil (Boardman, 1995).
- Late harvesting of crops such as maize, sugar beet and main crop potatoes, during Autumn and early Winter (Holman *et al.*, 2002).
- Use of heavier machinery, as well as machinery accessing land at sub-optimum times of the year, compacting the soil.
- Removal of hedgerows, which inhibited overland flows and encouraged infiltration.
- The introduction of under drainage and field perimeter ditching to rapidly remove water from cultivated land.
- Introduction of wheeling's (Silgram *et al.*, 2010).

#### ***Field evidence***

Localised surface water floods associated with arable land are often known as 'muddy floods' and are experienced in many regions of north western Europe; including Belgium (Verstraeten and Poesen, 1999), the Netherlands, France and the South Downs in England (Boardman *et al.*, 1994). The term 'muddy' is due to the significant volumes of soil that can be transported in the overland flows. Over time this surface runoff can concentrate into gullies as opposed to sheet wash, which can exacerbate the problem as water velocity increases along with the potential for soil erosion (Poesen *et al.*, 2003). Vehicle tracks, or 'wheelings' can also act as preferential flow pathways that can connect distant parts of the catchment to the watercourse (Boardman *et al.*, 1994). Wheelings have also been shown to have a significant impact on the compaction of soils, reducing the structure and increasing the bulk density by up to 28 % to depths of ~40 cm (Horn *et al.*, 2003; Pereira *et al.*, 2007).

There is evidence that at the larger scale, significant increases in the sediment yield of a river can reduce the conveyance of channels and flood plains by 40 %, potentially exacerbating floods (Walling, 1999). Increased sediment yields can also have

undesirable ecological impacts through eutrophication and clogging of gravel beds used by spawning fish (Greig *et al.*, 2005; Owen *et al.*, 2012).

### ***Management options***

Potential management options include: ensuring that there are over winter cover crops would likely reduce the volume of soil eroded (Boardman, 1995); not maintaining the drainage and ditch network is likely to lead to them accumulating sediment and reducing the rate at which the water leaves the land, therefore reintroducing some of the lost attenuation; and not using heavy machinery during unfavourable wet conditions will also reduce levels of compaction and wheeling's (Silgram *et al.*, 2010). Sedimentation ponds can be strategically placed to capture sediment rich overland flows to reduce the energy within flow and encourage sediment deposition (Deasy *et al.*, 2010; Barber and Quinn, 2012).

### ***2.3.4 Forest/woodland***

#### ***Implications for runoff generation***

Forestry and woodland is viewed as having a largely beneficial impact on flood hydrology as evidence shows that there is increased levels of infiltration, brought about through improved soil structure, e.g. through reduced bulk density (Wheater *et al.*, 2008). There are also greater rates of evapotranspiration and interception losses associated with woodland through increased biomass and landscape roughness when compared to open moorland and grazed pasture, hence lowering the water table. The additional storage will reduce the flood hazard for catchments where antecedent conditions are important, especially where a storage deficit must be satisfied before flooding can occur.

#### ***Field evidence***

Woodlands and forests have long been the subject of investigations into their influence on the hydrological response of catchments. One of the longest running studies is the Coalburn catchment in Northumberland (Robinson, 1986; Robinson and Sutherland, 2002). The study was set up to investigate the effects of afforestation on the hydrological response, however, the instrumentation has remained in place to monitor the catchment response from young growth right through to fully grown and subsequent harvesting. The Coalburn study showed that for the first five years post tree planting, flood peaks increased by 18 % and time to peak decreased (Robinson, 1986). This

counterintuitive finding was attributed to the effect of new forest roads and drainage ditches (McCulloch and Robinson, 1993). However, within 20 years peak discharge had decreased by 5 % and the time to peak was returning to the pre-afforestation rates. The methods of draining and ditching for afforestation used in the Coalburn are no longer representative of modern practices (Nisbet, 2015, per. comm.)

The impacts of ‘shelter belts’ on catchment hydrological response were studied as part of the Pontbren Flood Risk Management Research Consortium (FRMRC) study (Wheater *et al.*, 2008). Shelter belts are strips of land that are fenced off and planted with trees to provide a form of wind protection for livestock (Wheater *et al.*, 2008). Soil infiltration rates were found to be up to 60 times greater under wooded areas than open grazed pasture (Carroll *et al.*, 2004). Grazed land within close proximity (<5 m) to the woodland also demonstrated increased infiltration rates but the effect diminished with distance (Carroll *et al.*, 2004; Marshall *et al.*, 2009). The increase in infiltration was found to occur within 2 years of the conversion of pasture to trees with a continued increase in infiltration rates to around 6-7 years when it then began to stabilise.

Woodland is also seen as having higher losses through evapotranspiration and interception losses than moorland and grassland as it has a greater surface area and increases the roughness of the landscape it therefore dries out quicker building up the potential soil storage (Calder, 1990).

Riparian tree planting and in channel leaky barriers can be used to increase roughness and attenuate the flood flows.

### ***Management Options***

The effects of woodland have been shown to be beneficial in reducing runoff generation in a number of ways and may prove useful if used in a strategic approach such as shelter belts rather than blanket coverage of trees which would take land out of farming. The positive effects of shelter belts are:

- Increased infiltration rates within forested areas as well as locally within grazed areas.
- Many shelter belts distributed in the landscape, including on or at the foot of slopes, could potentially reduce the rate at which overland flow generated upslope on grazed areas can travel.



Issues that must be considered are for upland areas plant tree species must be appropriate for the soil type and require little drainage; they must also prove to be economically viable, not taking too much agricultural land out of production. Forest can also lower the total runoff yield which may have impacts on water resources (Robinson, 1998).

Increased channel and riparian roughness can be used to attenuate flood flows as has been demonstrated in the Pickering ‘Slowing the flow’ project and for the river Parrett. (Thomas and Nisbet, 2012; Nisbet *et al.*, 2015).

### **2.3.5 Drainage**

#### ***Implications for runoff generation***

A common method for increasing the agricultural potential of land is to artificially drain it. The aim is to allow animals and heavy machinery to use the land for longer periods of the year and prevents crops from being water logged (Robinson and Armstrong, 1988). Drainage is undertaken through a number of different ways, including ‘mole’ and ‘tile’ drains under arable and pastoral land, and open drainage ditches along field boundaries (Armstrong and Garwood, 1991; Bilotta *et al.*, 2008). These open drains often collect the discharge from a number of drains and transport runoff to the existing stream network. The ultimate effect is that of increased connectivity and bypassing of the soils’ natural buffering capacity (O’Connell *et al.*, 2007).

Artificial drainage is not restricted to lowland agriculture - significant peat areas of the British uplands have been drained using open ditches known as ‘grips’. This has been carried out for a number of reasons including afforestation of the uplands, expanding sheep grazing in the uplands, freeing up land in the lowlands and the rearing of game birds (Holden *et al.*, 2004; Lane and Milledge, 2013).

#### ***Field evidence***

Robinson (1990) carried out a detailed investigation of a number of plot sites before and after the introduction of underdrainage. The results were shown to be slightly mixed with peak flows for most sites being reduced, but the overall flow volumes appearing largely unchanged. It was shown for most sites the time-to-peak reduced, however this varied depending on the type of soil drained. The ‘peakyness’ of mineral soils such as

clays, was shown to have been reduced, whilst organic, peaty, soils were made peakier, with larger peaks occurring faster.

As the experiment was performed at a very small spatial scale there is limited understanding of downstream impacts at the larger catchment scale. It is largely accepted though that by increasing the rate at which water can reach the main channel should increase the flood peaks and reduce the time to peak at the larger scale (O'Connell *et al.*, 2007).

### ***Management Options***

If it is generally accepted that reducing local time-to-peak is a negative thing then an obvious option would be not to clear or maintain drainage and ditch networks but this may not be realistic in intense agricultural areas. Another option may be to consider methods for reintroducing attenuation, discussed below under novel methods.

### ***2.3.6 Summary***

The sections above have provided an overview of the multiple factors affecting catchments and the way in which land use impacts upon flood hazard.

The table below (Table 2-1) summarises a number of research studies that have examined the impacts of land use on flood hazard. The studies provide both direct evidence, observations in the field, and indirect evidence gleaned from modelling. They have also provide an evidence base for modelling land use impacts on flood generation.

<b>Catchment/NFM approach</b>	<b>Evidence type</b>	<b>Results and comments</b>	<b>References</b>
<b>Pastoral farming</b>			
Multiple catchments, New Zealand	Monitoring	Animal trampling reduced soil structure, increasing the bulk density and reduced infiltration.	(Drewry <i>et al.</i> , 2000; Drewry and Paton, 2000; Pietola <i>et al.</i> , 2005; Drewry, 2006)
Field scale (x4), Ireland	Monitoring	Presence of cattle changed physical properties of soil, leading to increased overland flow and reduced water quality with increases in nutrients.	(Kurz <i>et al.</i> , 2006)
<b>Forestry</b>			
Plynlimon, Wales. (37.5 km <sup>2</sup> and 10 km <sup>2</sup> )	Monitoring	Paired catchment experiment examining the hydrological differences of forested and rough pasture catchments. Concluded that a fully forested, 37.5 km <sup>2</sup> , catchment would reduce water yield by 42 %. No mention of effects on flood peaks (Q <sub>p</sub> ).	(Kirby <i>et al.</i> , 1991)
Coalburn, England. (1.5 km <sup>2</sup> )	Monitoring	Frequency of smaller peak flows increased, linked to land drainage for forestry, the effect diminished over time. Annual maximum flood increased by 15 % but due to annual variations was statistically insignificant. Catchment response time was quicker, again linked to drainage and diminished over time.	(Robinson, 1998; Archer <i>et al.</i> , 2010)
Pontbren, Wales. (10 km <sup>2</sup> )	Monitoring/ Modelling	Infiltration rates of grazed areas found to be ~0-30cm/h compared to ~60-70cm/h under adjacent treed shelter belts. No catchment scale change to runoff detectable. Modelling suggested a 60 % reduction in Q <sub>p</sub> for a fully forested catchment against a baseline for low return interval storms but reduced impact with increased return interval.	(Carroll <i>et al.</i> , 2004; Wheater <i>et al.</i> , 2008)

Balquhiddy, Scotland.	Monitoring	Paired catchment study comparing forested and moorland catchments and the effects of afforestation. No effect on annual water balance detectable, no mention of effect on $Q_p$ .	(Gustard and Wesselink, 1993; Jakeman <i>et al.</i> , 1993)
River Cary, England. (82 km <sup>2</sup> )	Modelled	Modelling outputs showed positive effects in using floodplain tree planting for attenuating flood flows. Increased local storage, no quantification of reduced downstream $Q_p$ .	(Thomas and Nisbet, 2007)
<b>Multiple Options</b>			
Hodder, England. (260 km <sup>2</sup> )	Monitoring	Results from a short term study identified the impact of grip blocking at the micro-scale (0.5 km <sup>2</sup> ) on the rate of hydrograph response. However, no impact could be detected at any catchment larger where grip blocking, tree planting and reduced stocking densities were used alone or together. The total area of land undergoing management change was 28 km <sup>2</sup> .	(Ewen <i>et al.</i> , 2010; Geris, 2012)
<b>Drainage</b>			
Moor House, England. (>20 km <sup>2</sup> )	Monitoring	Compared intact and drained peat; found <1 % of runoff from undrained peat was matrix through flow, but was about 23 % in drained peat. No mention of effect on $Q_p$ .	(Conway and Millar, 1960; Robinson, 1985; Holden <i>et al.</i> , 2006)
6 UK plot scale sites (0.00005 – 0.135 km <sup>2</sup> )	Monitoring and modelling	$Q_p$ for drained loamy soil was increased but not clay soils. Plot experiments of drained against non-drained soils showed antecedent conditions were important. When dry, $Q_p$ was higher in drained soils but the recession was longer; the reverse was true when the plot was wet (autumn/winter).	(Robinson, 1990)

Table 2-1 Summary table of land use /NFM studies investigating flood hazard and mitigation

## 2.4 Novel flood hazard mitigation methods

A number of different novel flood mitigation methods have been trialled by research projects across the UK. They are often termed as Natural Flood Management (NFM) schemes, which was defined in a Parliamentary Office of Science and Technology note (Pescott and Wentworth, 2011) as:

*‘alteration, restoration or use of landscape features ... as a novel way of reducing flood risk.’*

The relative scale at which different NFM options are implemented and an assessment of their known effectiveness is succinctly captured in Figure 2-2. Different flood mitigation options are categorised along two axes in Figure 2-2; the y-axis being where in the catchment they are generally located, from source to downstream; the x-axis describing the spatial concentration from spatially distributed, meaning there are likely to be many features, to the spatially concentrated. Figure 2-2 also indicates that there is increasing scientific certainty and response reliability for options that are further downstream and spatially concentrated. It is easier to monitor the local impact of spatially concentrated features compared to distributed changes which require consideration of how the distributed impacts propagate and aggregate with scale.

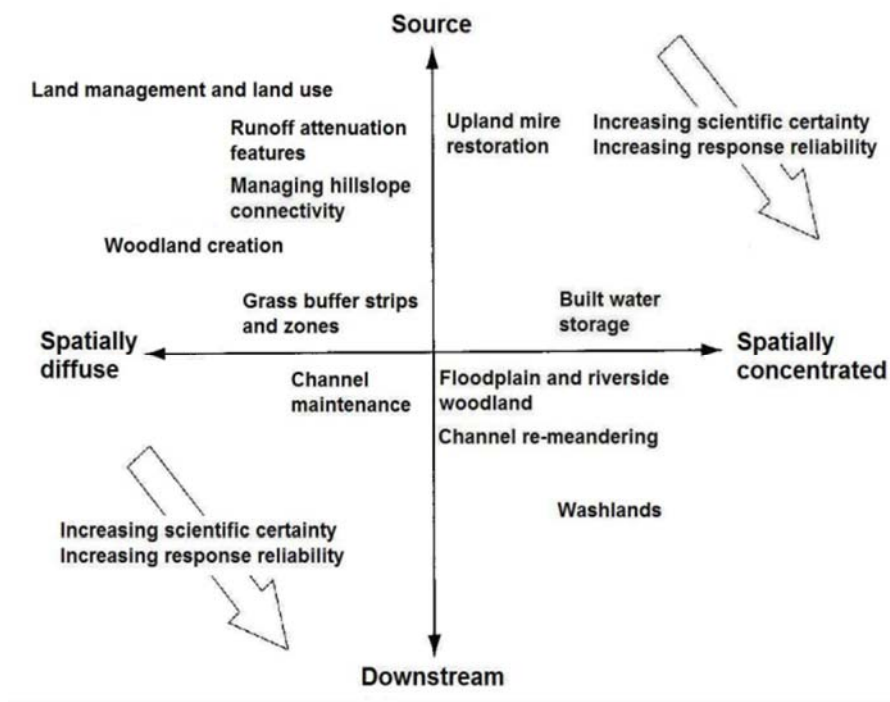


Figure 2-2 Catchment-scale classification of NFM strategies (Pescott and Wentworth, 2011)

The ‘Proactive’ group at Newcastle University pioneered the use of Runoff Attenuation Features (RAFs), soft engineered features designed to intercept and attenuate fast flows (Wilkinson and Quinn, 2010; Nicholson *et al.*, 2012; Quinn *et al.*, 2013). The key concept of RAFs is to slow the rate at which overland flow reaches and travels along the watercourse in order to reduce the downstream peak magnitude as well as increasing the time to peak (Wilkinson and Quinn, 2010).

There are three types of RAF; (1) those intercepting surface runoff before it reaches the channel (known as offline features); (2) In-channel features such as woody debris dams are designed to impede the flows and increase the interaction between the channel and flood plain during high flow events (online features); (3) Offline storage on floodplains of flows diverted from the channel. Other research groups and environmental bodies have used similar concepts for mitigating flood hazard (See Table 2-2). Landscape interventions including RAFs have also been used to improve water quality by reducing losses of suspended sediment and nutrients, such as phosphorus and nitrate (Deasy *et al.*, 2010; Barber and Quinn, 2012; Ockenden *et al.*, 2014).

### ***Hydrological impact***

- Offline features attenuate overland flows, increasing the time taken for flows generated on land to reach the channel.
- Online pond features attenuate flows and have the potential to remove sediments and their associated nutrient load.
- Woody debris dams can retard the in-stream channel velocities, increasing the water levels locally and more readily connect the channel to the flood plain.

### ***Management considerations***

- Each feature has a relatively local effect. There would need to be a significant number installed as a network to alter the hydrological regime at a larger scale as demonstrated in Figure 2-3.
- Best suited for targeting specific issues regarding overland flows with the added benefit of sediment removal and habitat creation.
- Potentially suitable as a means of future proofing existing schemes and mitigating for potential climate change impacts.
- There are wider issues regarding ownership and maintenance.

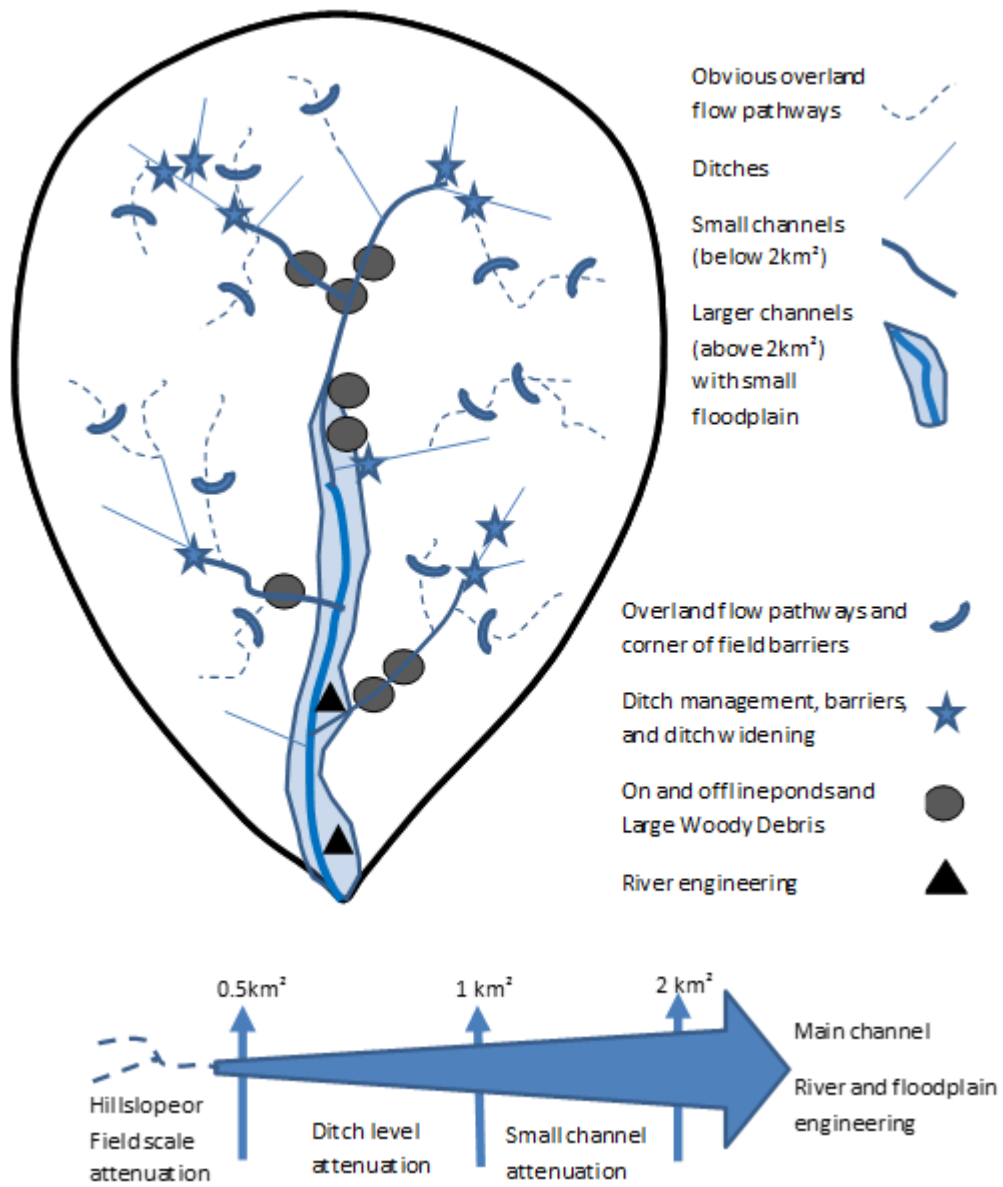


Figure 2-3 Hypothetical design of a RAF/NFM network (Quinn *et al.*, 2013)

Table 2-2 NFM studies and results

Study location	Mitigation and results	Reference
Belford, England. (6 km <sup>2</sup> )	Evidence of impact on Qp and Tp caused by attenuating overland flows in leaky dams. Scaled using models. Estimated reduction in Qp of 8 % for 1 in 5 year event.	(Wilkinson <i>et al.</i> , 2010; Nicholson <i>et al.</i> , 2012)
Holnicote, England (22 km <sup>2</sup> )	Wide range of options adopted, including: - Moorland restoration - Woody debris dams - Flood meadows Modelling indicates a 7 % reduction in Qp, with 1 hour increase in Tp locally for a 1.5 km stretch of river and adjacent flood meadows.	(Rose <i>et al.</i> , 2010; Rose <i>et al.</i> , 2011)
Pickering, England. (69 km <sup>2</sup> )	Modelled reduction in Qp of up to 8 %, locally, through use of in-stream wooden debris dams and riparian tree planting.	(Odoni and Lane, 2010)

## 2.5 Detecting land use change signals

A number of methodologies have been used to investigate if the impacts of land use management change can be detected at catchment scales including paired catchment studies and statistically identify trends and changes within historical data.

There are differences in the hydrological feature of interest and the methodology by which the data are analysed. There are those that investigate the impacts on water yield from a resource point of view, whilst others are specifically interested in flood peaks and the trends (Robson *et al.*, 1998).

### 2.5.1 Paired catchment studies

Studies examining the impact of land use change have traditionally used paired catchments, some of which have been discussed above e.g. Coalburn (Robinson, 1986) and Plynlimon (Robinson *et al.*, 2013). Typically two hydrologically similar catchments or plots in close proximity are monitored, with the assumption being that if treated the same they would behave in a hydrologically similar fashion. One of the catchments then typically undergoes change such as underdrainage or land cover from grass to forestry for



example and the change in runoff response are compared to the control catchment that has not undergone any change. Land use impacts have been identified from these types of experiments, particularly those concerned with water yield. Typically at least 20 % of a catchment must undergo land use change such as afforestation to have any discernible effect on yield (Bosch and Hewlett, 1982).

These studies are obviously useful, however, they are usually implemented in relatively small catchments (<40 km<sup>2</sup>) with typically less than 10 years' worth of data (Brown *et al.*, 2005). How larger catchments respond, where the vegetation change is distributed and generally less than the 20 % of total catchment area is unclear (Brown *et al.*, 2005). There is limited evidence from paired catchment studies of the effect on peak flows as the studies have largely concentrated on the effect of woodland on water yield.

### **2.5.2 Analysis of historical datasets**

Historical data sets have been used in two key ways, one is statistical approach to identify changes or trends in flow records that can be attributed to land use management practices as explanation. Secondly through modelling to identify whether a suitable parameter sets exist for pre- and post- land use change and again if any differences can be attributed to the land use (Beven *et al.*, 2008; Birkinshaw *et al.*, 2014). If this change in parameterisation can be linked conceptually to change in the catchment this may provide an evidence base.

#### **Statistical approach**

Kundzewicz and Robson (2004) provide a thorough review of statistical methodologies available for identifying step changes and '*gradual*' trends. One of the most significant factors that needs to be considered is the length of data records available for analysis and modelling. It is possible in short records for climate variability to appear as a trend, however, due to more variability these trends are less obvious as more data are collected (Kundzewicz and Robson, 2004). It has also been argued that to truly understand if the catchment hydrology has been changed a shift in the flood frequency curve must be shown rather than just large events (O'Connell *et al.*, 2004). This is ideally how change would be demonstrated and quantified, however, a more pragmatic approach would be to monitor for decades to build the evidence base.

### ***Modelling approach***

Models have been used to study whether changes in response can be identified from historic datasets. The methodology used by Beven *et al.* (2008) involved using a Data-Based Mechanistic (DBM) modelling approach to identify change in hydrographs. Firstly, this approach looked for steady change in parametrisation over time. The second approach split the series by event type based on antecedent rainfall and flow peak magnitude. Some relationships were identified, however, due to inconsistencies in the data these were discounted. A similar investigation for the Pontbren study in which the DBM model was used failed to find any trends over time, however, changes linked to seasonality were found (McIntyre and Marshall, 2010).

#### ***2.5.3 Detection methods summary***

As discussed in the preceding sections, using observed catchment records to identify direct cause and effects between land management and flood hazard is problematic due to the underlying uncertainties and non-stationarity of land use, climate, antecedent conditions and data errors (Burt and Slattery, 1996; Beven *et al.*, 2008)

To do any form of meaningful statistical analysis requires significant amounts of data or the use of statistical methods such as the Flood Estimation Handbook (FEH), which have significant uncertainties (O'Connell *et al.*, 2004). The FEH methodology for estimating an event with an N-year return interval requires at least 5 x N-years of data; which means only a limited assessment can be made using data at a single site due to record lengths. The peaks available for a single site can be complemented by peaks from other similar sites to create a pooled group of peaks, as recommended by FEH for short records. However, this introduces significant uncertainties associated with regionalisation, specifically extrapolating data from other catchments.

### **2.6 Modelling land use change and flood mitigation**

Models offer a means of studying land use management change and NFM scenarios with a clearer identification of cause and effect. They can also be used in an attempt to scale the known local scale impacts to the larger catchment, as will be discussed in the following sections. However, there are significant issues regarding what structure should they take; e.g. are lumped rainfall-runoff models adequate or are fully physical, distributed approaches more appropriate? The strengths and weaknesses of different model types and structures will be discussed below. As well as considering some of the

modelling parameter and input data uncertainty (Brazier *et al.*, 2000; Vázquez *et al.*, 2008).

There are a number of model types, each with their own strengths and weaknesses for certain applications. Wheater *et al.* (2012) provide a useful classification of hydrological (rainfall-runoff) models using three broad groups: 1. Metric models are simple models, calibrated to optimise statistical relationships between input (rainfall) and outflow (Q), an example of which includes the widely used unit hydrograph as used within the Flood Estimation Handbook (FEH) (Houghton-Carr, 1999); 2. Physics-Based models where the physical processes are explicitly defined using point scale physics equations such as SHETRAN (Ewen *et al.*, 2000); 3. Conceptual models, where representations have been made for the perceived key hydrological storages, losses and routing components of the hydrological cycle, for example the Probability Distributed Model (PDM) model (Moore, 2007). A fourth type is considered here, the hydrodynamic models; which can be used to understand how water moves in a more detailed way than hydrological models. Traditionally they are used for inundation modelling and flood mapping but have also been used in flood mitigation studies.

The sections below summarise some of these models and case studies where they have been used. It also highlights some of the strengths and weaknesses of these approaches.

### **2.6.1 Statistical modelling (Metric)**

Metric models are largely event based and used for examining the direct impacts on Qp caused by change rather than modelling a time-series of data. One such model that is widely used is the FEH rainfall-runoff model which is a simple event based model. Two principal components of the FEH model are the Unit-Hydrograph (UH) and the loss model; The UH hydrograph determines the shape of the resulting hydrograph where the loss model provides the effective rainfall. From the Hydrology Of Soil Type (HOST) classification and the FEH catchment descriptors the Standard Percentage Runoff (SPR) and time-to-peak (Tp) parameters are used to calculate the shape of the unit hydrograph in the FEH approach. The Tp parameter is calculated from the catchment descriptors provided with the FEH CD-ROM and provides the time base of the unit hydrograph. The FEH CD-ROM provides catchment descriptors for any catchment in the UK (>0.5 km<sup>2</sup>) through a regionalisation approach. The HOST dataset was designed to provide the parameters for the FEH rainfall-runoff model.

Within the UK the FEH rainfall runoff model has been proposed and used for investigating land use change impacts on Qp (Packman *et al.*, 2004). A methodology was developed making best use expert knowledge and widely available datasets. The process provided a methodology for using the national HOST dataset, which categorises the soils of the UK into 29 classes that are based on the physical descriptions of the soil profile (Boorman *et al.*, 1995). This means that a model can be set up and land use change impacts be investigated for ungauged catchments.

The HOST classification is based upon 11 conceptual models (A – K) that describe the dominant flow pathways through the soil and subsurface (Boorman *et al.*, 1995). There are three key base models that form the physical settings from which the others are derived; these are highlighted in green in Table 2-4 and are associated with absence or presence of and depth of groundwater. The additional columns within Table 2-4 represent the different depth at which the gleyed layer can be found and the rows are related to infiltration. The values in the table cells refer to the classes and the number in the brackets are the SPR values which is an event based statistic that provides the typical runoff as a percentage of rainfall.

A method for moving from one HOST class to an alternate, to reflect changes in SPR, based on expert opinion of soil degradation has been provided by Packman *et al.* (2004) as well as proposing changes to Tp of:

- *Forest drainage could reduce local Tp by 2-3 hours;*
- *Agricultural drainage in low SPR soils could reduce local Tp by 1-2 hours, but in high SPR soils increase Tp by 1-2hours.*

How applicable these adjustments are at all spatial scales and for all catchments is a matter of debate. For example, is the 2-3 hour delay in Tp for a forested catchment true at both the 10 km<sup>2</sup> and 100 km<sup>2</sup> scales? This seems a considerable delay and much larger than those described in the literature. The longest delay found in the literature is from the modelling work of Thomas and Nisbet (2007) who suggested that the introduction of a 2.2 km reach of riparian woodland to a tributary of the River Parrett could increase the Tp by 2.3 hours. How representative this catchment/river and associated result is in a wider UK context is debateable.

**Table 2-3 Summary of statistical modelling project investigating potential land use change impact**

<b>Catchment</b>	<b>Model</b>	<b>Modelled results</b>	<b>Reference</b>
4 UK Catchments (4 -72 km <sup>2</sup> )	FEH Rainfall-runoff	Modelled a number of scenarios for 2-100 year return interval floods. Moving from the original catchment SPRHOST and reducing Tp by 1 hour to the alternate discussed above led 23-28 % increase for all events across all catchments. Manipulating SPR led to a percentage change in Qp very close to the manipulation of SPR applied.	(Packman <i>et al.</i> , 2004)

SUBSTRATE HYDROGEOLOGY	MINERAL SOILS					PEAT SOILS		
	Groundwater or aquifer	No impermeable/ gleyed layer within 1m	Impermeable layer within 1m or gleyed layer at 0.4 to 1m		Gleyed layer within 0.4m			
Weakly consolidated, microporous, by-pass flow uncommon (Chalk)	Normally present and at >2m	1 (2)	13 (3)		14 (25)		15 (48)	
Weakly consolidated, microporous, by-pass flow uncommon (Limestone)		2 (2)						
Weakly consolidated, microporous, by-pass flow uncommon		3 (15)						
Strongly consolidated, non/ slightly porous, by-pass flow common		4 (2)						
Unconsolidated, macroporous, by-pass flow very uncommon		5 (15)						
Unconsolidated, macroporous, by-pass flow very common		6 (34)						
Unconsolidated, macroporous, by-pass flow very uncommon	Normally present and at ≤2m	7 (44)			IAC* <12.5 [ $<1\text{m day}^{-1}$ ]	IAC* ≥12.5 [ $\geq 1\text{m day}^{-1}$ ]	Drained	Undrained
Unconsolidated, macroporous, by-pass flow very common		8 (44)			9 (25)	10 (25)	11 (2)	12 (60)
Slowly permeable	No significant groundwater or aquifer	16 (29)	IAC* > 7.5	IAC* ≤ 7.5	24 (40)		26 (59)	
Impermeable (hard)			18 (47)	21 (47)				
Impermeable (soft)		17 (29)	19 (60)	22 (60)	25 (50)		27 (60)	
Eroded Peat			20 (60)	23 (60)				
Raw Peat								28 (60)

Table 2-4 HOST classification numbers. Numbers in brackets are HOST SPR values (\* IAC used to index lateral saturated conductivity) (Boorman *et al.*, 1995)

### **Soil Conservation Service Curve Number**

An alternative regionalised dataset to the FEH that has been used for land use change modelling is the Soil Conservation Service Curve Number (SCS-CN) (USDA, 1986). The SCS-CN approach categorises soils into 4 broad hydrological soil groups (A, B, C, D) that can then be further tailored to reflect the dominant land cover and the soil condition (Table 2-5). The equations used to calculate discharge using the SCS-CN methodology are described in Equation 2-1 and Equation 2-2 below.

**Equation 2-1**

$$Q = \frac{(P - 0.2S)^2}{(P - 0.8S)}$$

where S is calculated from Equation 2-2, Q is event runoff, P is event rainfall (mm).

**Equation 2-2**

$$S = \frac{1000}{CN} - 10$$

**Table 2-5 Excerpt from a USDA curve number table for land use and hydrologic soil groups (USDA, 1986)**

Cover description		CN for hydrologic soil group			
Cover type	Hydrologic condition	A	B	C	D
Pasture, grassland, or range—continuous forage for grazing.	Poor	68	79	86	89
	Fair	49	69	79	84
	Good	39	61	74	80
Meadow—continuous grass, protected from grazing and generally mowed for hay.	—	30	58	71	78
Brush—brush-weed-grass mixture with brush the major element.	Poor	48	67	77	83
	Fair	35	56	70	77
	Good	30	48	65	73

Although developed from a database of American soils, a number of British studies provide a method categorising British soils onto the curve numbers. The method for mapping HOST classes on to the SCS-CN classification was used by Bulygina *et al.* (2011) and is shown in Table 2-6; it was used within a meta-modelling study described in section 2.6.3.

**Table 2-6 Mappings of U.S Department of Agriculture (USDA) and Hydrology of Soil Types (HOST) soil classifications (Bulygina *et al.*, 2011a)**

USDA Hydrologic soil group	HOST Class
A	1, 2, 3, 5, 11, 13
A, B	4, 7
B	6, 8, 9, 10, 16
B, C	17
C	18, 19, 20
C,D	14, 15, 18
D	12, 21 – 27, 29

### ***Strengths***

- The model is simple and easy to understand.
- Expert knowledge of hydrological impact of soils can be incorporated transparently.

### ***Weaknesses***

- The lumped structure may possibly mean the model is too simple for such a complicated, distributed problem.
- As it is not distributed it cannot account for the location and travel time of likely impact.
- Not enough observed evidence of catchment scale impacts to make sound catchment scale, lumped changes to Tp. Tp changes may be scale dependant.

### ***2.6.2 Spatially distributed-physically and semi-physical models***

Physically based model use small scale physics based mathematical equations to describe the processes that occur on and within the land surface. These include processes such as infiltration (described using the Richard’s equation), overland flow (Manning’s equation), and interception loses, amongst many others – all accounting for the movement and loss of water across a land unit. Theoretically as the equations used are point scale, model parameters could be measured in the field, but as the parameters are applied to grid cells, they tend to be scale dependant with models requiring effective parameters as they reflect a different scale. Due to the significant number of processes involved in physically based modelling and the detailed spatial description the associated number of parameters can introduce equally significant amounts of



uncertainty, and the possibility of multiple optimal parameter sets in calibration, i.e. many parameter sets can achieve an adequate objective function such as Nash-Sutcliffe efficiencies (NSE); a phenomena described as equifinality (Beven, 2011). A key limiting factor in the evaluation of models for performance in modelling land use and NFM scenarios is a lack of reliable distributed validation data for catchments that have undergone change. This needs to be addressed through long field campaigns and the establishment of catchment laboratories. However, O’Connell *et al.* (2004), recommended that spatially distributed and at least partially physical models are necessary for modelling land use management change.

*‘so that the physical properties of local landscapes, soils and vegetation can be represented, and it should include detailed modelling of surface water flow so that the effects of changes can be tracked downstream. A considerable amount of high-quality field data on impacts will be needed to support the development of robust methods for predicting impacts’*

O’Connell *et al.* (2004) also provide a comprehensive list of models used in investigating land use change impacts. Some of these models and a summary of the results are shown below in Table 2-7

**Table 2-7 Summary of modelling projects investigating potential land use change impacts using distributed physical models [Spatial resolution of model in square brackets]**

<b>Catchment</b>	<b>Model</b>	<b>Modelled results</b>	<b>Reference</b>
Draix (0.86 km <sup>2</sup> )	SHETRAN [50m]	Model blind calibrated (i.e. without knowledge of hydrological response data), with significant uncertainty in final parameterisation. Fully forested catchment reduced annual runoff by 36 %, no mention of impact on flood peaks.	Lukey <i>et al.</i> (2000)
Meuse and Oder (32457 km <sup>2</sup> , 59162 km <sup>2</sup> )	LISFLOOD [1 km]	For both catchments land cover information for 1975 and 1992 were used to parameterise the models and compare the hydrologic response for each period. For the Oder there were no significant land cover changes no change in hydrological response. The Meuse showed some increase in flood peaks linked to urbanisation, however, parameter uncertainty gives limited weight to results.	(De Roo <i>et al.</i> , 2001)

Dietzhölze (82 km <sup>2</sup> )	SWATmod [N/A]	A 9 % increase in water yield was modelled for a 35 % increase in grassland. It is noted that flood peaks increased but was not quantified.	(Fohrer <i>et al.</i> , 2001)
Thames to Kingston (10000 km <sup>2</sup> )	CLASSIC [20 km]	A small change in flood frequency was mentioned but not quantified for the 30 year modelling period, 1961-1930.	(Crooks and Davies, 2001)
Coalburn (1.5 km <sup>2</sup> )	SHETRAN [50m]	Reduced annual yield from catchment due to increased interception and evaporative losses. Some discussion of increased Qp for young trees, however, this was linked to outdated planting procedures. Impact of forestry on Qp reduces with increasing flood magnitude.	(Birkinshaw <i>et al.</i> , 2014)

### **Strengths**

- The model can theoretically be parametrised from field measured values.
- There is a strong scientific understanding of land use change impacts at the plot scale and field; a scale at which they can be modelled.
- The models are distributed so the change in land use can be applied in a distributed way and then routed to understand the impact at a larger scale.

### **Weaknesses**

- The large number of parameters always leads to multiple suitable parameter sets
- Although measurements of model parameters can be taken in the field, there is difference between the scale of measurement and the modelling resolution. Typically to account for the heterogeneity within a given cell a scale dependant ‘*effective parameter*’ will be calibrated (Vázquez *et al.*, 2002).
- Can be computationally demanding depending on size of area modelled, resolution of model and the number of scenarios to be modelled.
- Formal uncertainty analysis such a Generalized Likelihood Uncertainty Estimation (GLUE) particularly shows the problems of reliance on physically-based distributed modelling and the dangers of calibration to observations such as flow time series (Brazier *et al.*, 2000; Ewen *et al.*, 2006; Vázquez *et al.*, 2008).

### 2.6.3 Meta-modelling

Meta-models are simplified versions of a more complex model, trained to mimic the behaviour of the more complex model. Due to their relative computational efficiency they can be favoured for allowing more scenarios and greater uncertainty testing to be carried out within a given time frame (Barton, 1998; Fraser *et al.*, 2013).

The Pontbren study used a meta-modelling approach to extrapolate from local-scale effects to the larger catchment scale. Physically based distributed, Soil-Plant-Water (SPW; Jackson *et al.* (2008)), models were created and calibrated for a number of different hillslopes to capture the heterogeneity in both soil and land use. The catchment scale model was ‘trained’ using the detailed physics-based simulations, so that it encapsulated the dominant responses of the more detailed model (Wheater *et al.*, 2008). This was achieved by linking the model parameters in a consistent manner.

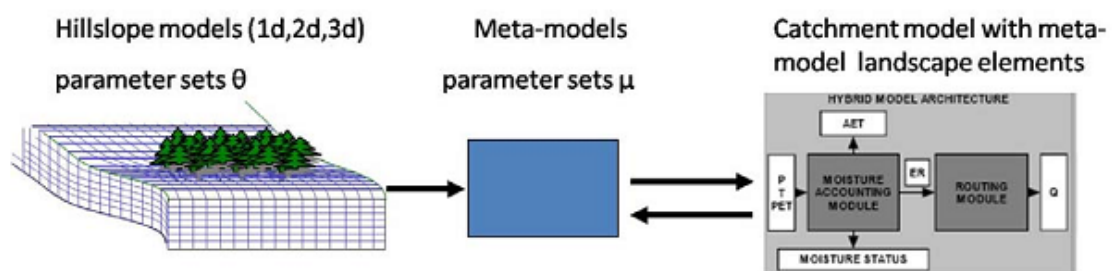


Figure 2-4 Meta-modelling: changing complex small-scale models into field-scale simple models (Wheater *et al.*, 2008)

A summary of some modelling methodologies that have been adopted for investigating land use change impacts are summarised in Table 2-8.

#### Strengths

- Theoretically behave like physically based models meaning parameter changes made to reflect land use change is transparent; i.e. there is a link between the simple conceptual parameters and physical attributes, as represented in the physically based models.
- Are simpler and faster to run than fully physical, distributed models, meaning more scenarios sensitivity and uncertainty studies could be done in a given time frame.

### ***Weaknesses***

- Moving from one model to another may be cumulatively increasing the uncertainties in the outputs.
- Over simplified hydrology.

<b>Catchment</b>	<b>Model</b>	<b>Model results</b>	<b>Reference</b>
Pontbren (10 km <sup>2</sup> )	Modular RRMTSD	Fully wooded catchment increased Tp by 45mins, median reduction in Qp of 50 %. Strategically placed shelter belts increased Tp by 15mins, median reduction in Qp of 30 %. Significant uncertainties noted.	(Wheater <i>et al.</i> , 2008)
Oughtershaw Beck (13.8 km <sup>2</sup> )	(?)	Coupled 4, 1D models to represent hillslope flow in 3D using a simplified physical approach. Developed to model the water table and drain flow interaction in blanket peats. No land use scenarios modelled as such but channel and surface roughness found to be important factors in controlling peak flows.	(Ballard <i>et al.</i> , 2011)
Plynlimon	PDM	Developed a method for calibrating a Probability Distributed Model (PDM) for ungauged catchments using a Bayesian approach. The regionalised BFIHOST and the curve number (CN) of the U.S. Department of Agriculture's Soil Conservation Service classification were used to provide information regarding the soil type and land use effects. The approach was tested on the paired catchments at Plynlimon with uncertainty reduced in results when compared to only using only BFIHOST conditioning. The CN incorporation provides a methodology for investigating land use and soil condition change.	(Bulygina <i>et al.</i> , 2009; Bulygina <i>et al.</i> , 2011b)
Hodder (261 km <sup>2</sup> )	Catchment Moisture Deficit model	The physical model is based on 200 x 200 m square runoff response units that capture HOST soil type, land use, soil condition, and flow direction and are used to condition the conceptual model using a Bayesian approach as mentioned above. Four scenarios tested to upscale known local scale impacts for tree planting and pastoral farming. Both tree planting scenarios (plantation and riparian woodland) both reduced flood peaks. Generally it was found that land use effects reduced with increasing flood peak magnitude.	(Bulygina <i>et al.</i> , 2012)

Hodder sub-catchment (25 km <sup>2</sup> )	Catchment Moisture Deficit model	Similar to above, smaller area modelled but it was deemed that the metamodeling procedure adopted introduced significant modelling uncertainties, with 60 % of the uncertainty in land use change scenarios deemed to have come from the meta-modelling procedure when compared to the same scenario modelled with the original physical model.	(Fraser <i>et al.</i> , 2013)
--	---	---	-------------------------------

**Table 2-8 Summary of some meta-modelling approaches used for land use change impact assessment**

### 2.6.4 Conceptual modelling

Conceptual hydrological models are widely used within hydrology for a number of different purposes. Principally they are designed to quantify runoff from rainfall using representations of the process deemed important from the modellers conceptual understanding of the catchments behaviour. An example of a conceptual model is the PDM model which is widely used within the UK and Europe (Cabus, 2008; Poelmans *et al.*, 2011). The range of soil depths within a catchment are represented as a probability distribution function (i.e. a range of potential soil depths and the likely distribution of the depths) which can be calibrated. The rainfall is then applied to the statistical distribution of stores, the losses such as evaporation, subsurface flow, are accounted for and the excess water is then routed as fast flow. The combined fast and slow flows produce the modelled output. Table 2-9 provides examples of conceptual models used for land use impact assessment.

Table 2-9 Summary of conceptual rainfall-runoff models used for modelling land use change impacts

Catchment	Model	Modelled results	Reference
Molenbeek, Belgium. (48 km <sup>2</sup> )	PDM	Modelled the likely impacts of climate change and urban expansion for 2050 high and low emissions scenarios. Found the climate change scenarios to be of more significance than likely land use impacts with peaks increasing by 30 % in a wet scenario and reducing by 18 % for drier scenario (developed from IPCC AR4 database) with an increase in urban area of 70–200 %, from 19 %, increasing peak flows by 6–16 %.	(Poelmans <i>et al.</i> , 2011)
Kishwaukee, USA (3258 km <sup>2</sup> )	HSPF	Investigated impacts of urbanisation on the flow regime of a catchment. No significant changes to the flood frequency curve were detected.	(Choi and Deal, 2008)

### Strengths

- The expert knowledge based on impacts to soil response to land use has been incorporated through statistical approaches.
- The models are relatively simple and easy to understand.

## ***Weaknesses***

- Known local land use change impacts can't be applied in a clear and unambiguous way at the lumped catchment scale.
- The models are lumped so the distributed nature of change is not accounted for.
- There are potentially numerous suitable parameter combinations, due to the interaction of parameters in calibration, the more parameters there are, potentially the greater the uncertainty. Therefore uncertainty in the potential impacts.
- Developed for purposes other than modelling land use change impacts.

### ***2.6.5 Hydro-dynamic modelling***

Hydrodynamic modelling is used to simulate in more detail the local physical effects as well as downstream impacts caused by physical features such as riparian woodland planting, debris dams and both on- or off-line ponds. This type of modelling is widely used in UK consultancies for inundation and flood mapping. One-dimensional models enable likely flood extents to be mapped whilst the two-dimensional approach enables the complexity of floodplains to be better accounted for by having features and buildings explicitly represented in the model where, in the 1D model this would have to be accounted for by changing a roughness parameter. The approach of modifying overbank roughness values has been used to investigate the impact of riparian woodland on flood wave propagation (Thomas and Nisbet, 2007).

A Multi-objective flood management demonstration project based in the Holnicote catchment, Exmoor, England, used a coupled 1D-2D hydrodynamic model (JFLOW) to investigate the potential for enhancing floodplain inundation through the construction of levees on a floodplain, perpendicular to the channel (Figure 2-5; (Rose *et al.*, 2011). For the 2 km length of reach modelled in Figure 2-5, the flood peaks for the 5 and 20 year return interval floods were locally reduced by 7 % and 2.5 % and delayed by 1 and 0.8 hours, respectively (Rose *et al.*, No date).



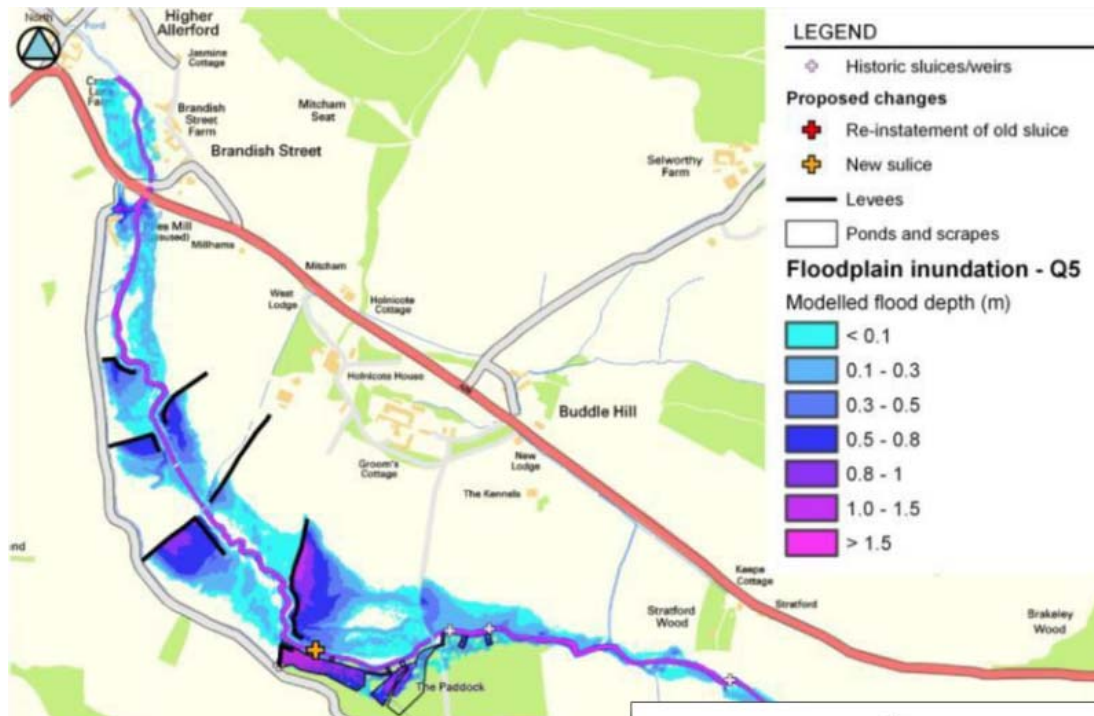


Figure 2-5 Model output from JFLOW of floodplain inundation; taken from (Rose *et al.*, No date)

There are still difficulties, however, in capturing the complexities and impacts of NFM approaches such as woody debris dams in hydraulic models. These currently have to be included in the model by increasing roughness or adding a weir feature.

Some examples of hydrodynamic models being used for studying impact of flood mitigation options are shown in Table 2-10.

**Table 2-10 Examples of NFM and land use scenarios modelled using hydrodynamic models**

<b>Catchment</b>	<b>Model</b>	<b>Modelled results</b>	<b>Reference</b>
Belford (6 km <sup>2</sup> )	Pond model (1D)	Used observed water level data to forensically understand the local impact of a storage pond (RAF) with a maximum volume of 550m <sup>3</sup> . The result was then extrapolated using simple hydraulic based approach to represent a network of ponds in series. It was found that the peak of discharge attenuated to by 5, 10 and 20 RAFs; approximately 10 %, 15 % and 25 %, respectively	(Nicholson <i>et al.</i> , 2012; Nicholson, 2014)
River Cary, England. (82 km <sup>2</sup> )	1D-2D coupled HECRAS- River2D	Show the positive effects of using floodplain tree planting for attenuating flood flows, which was modelled by increasing floodplain roughness. Increased local storage, no quantification of reduced downstream Qp. Significant increase in Tp.	(Thomas and Nisbet, 2007)
Pickering, England. (69 km <sup>2</sup> )	Overflow	Roughness of flood plains increased using Manning's 'n' to represent riparian woodland as was done to represent in stream debris dams. Reduction in Qp of up to 11 %, at the catchment outlet, through use of in-stream wooden debris dams and riparian tree planting. Found that mitigating in the sub-catchments with the greatest travel distance to the outlet had the greatest impact on the outlet flood hydrograph.	(Odoni and Lane, 2010)
Holnicote, England. (22 km <sup>2</sup> )	JFLOW 1D-2D coupled	Multiple options for flood hazard reduction implemented including moorland drainage management and attenuation features. Qp for the 5 and 20 year return interval floods were locally reduced by 7 % and 2.5 % and delayed by 1 and 0.8 hours, respectively	(Rose <i>et al.</i> , 2011; Rose <i>et al.</i> , No date)

### ***Strengths***

- Model features such as attenuation ponds and riparian features designed for attenuating overbank flows in a more robust way than rainfall runoff models.
- Structures and NFM features can be modelled as part of a network, therefore the effects happen in a distributed manner with the upstream effect routed downstream to investigate the impact at a larger scale.
- Structures such as bridges, culverts or pipes can be represented in detail and the impact locally and downstream of trash build up at the entrances to bridges and culverts can be investigated.

### ***Weaknesses***

- Do not have a runoff generation or infiltration component so are only useful for modelling instream or riparian mitigation options.
- Riparian features such as woodland are represented by manipulating a roughness coefficient such as Manning's 'n'.
- Cannot explicitly represent woody debris and leaky features.

#### ***2.6.6 A true (verified) model versus an acceptable (confirmed/validated) model***

Models will always be simplifications of the natural environment and the processes that occur within. The philosophical argument is that it is not, and never will be possible to demonstrate that a model is 'verified', i.e. representative of the 'truth' (Oreskes *et al.*, 1994). Validation is used to affirm the acceptability of a model's performance and behaviour. Model validation is performed in a number of ways, including split and blind testing. Split testing involves splitting an observed series in two, one part is used for calibration whilst the second part is used to validate the model parameterisation by checking the model still provides an adequate fit. It has been argued, however, that this process leads to adjustments being made to the parameterisation to make sure a better fit to both the calibration and validation period; it is therefore just an extension of the calibration process and in no way is the model validated (Oreskes *et al.*, 1994; Beven, 2001). However, Beven (2001) argues that this is inappropriate as no real complex system can be expected to be fully represented by a model in its totality, but it could be argued that the key features can be adequately included in modelling at larger scales.

In a review of testing methods Klemes (1986), found the split testing approach to be weak, an alternative was proposed, '*the differential split test*', and identified as particularly important if a model is to be used for predicting future climate scenarios. The model is calibrated against a dry period and tested against a wet period or vice-versa, to test how well it performs for conditions it was not calibrated against. It has been argued, however, that that calibrating to the extremes of a series does not mean the model will adequately capture the future stable wetter or drier behaviour (Ewen and Parkin, 1996). Ewen and Parkin (1996) suggest that blind validation may be more suitable particularly for physically based models. In this method the modeller does not have access to any observed hydrological flux time series; as the test is to investigate whether available data regarding soil and vegetation can parameterise a model adequately to reproduce observed hydrological fluxes. It can then be tested against the observed flow for a number of pre-defined conditions depending on the purpose of model. For example for water resources purposes it may be important that annual yield is successfully modelled or storm hydrographs that the modelled output is within 90 % confidence intervals (Ewen and Parkin, 1996). To truly validate a model, reliable, high quality hydrological data at multiple spatial scales will be required to provide the evidence against which the models can be fully evaluated. There are also questions regarding how distributed information can be directly used to parameterise models, especially those with a physical basis (e.g. the effective parameter problem, in which the field measurement scale differs from the model grid scale). Lamb *et al.* (1998) demonstrate the usefulness of distributed data, including water tables, in improving simulation for discharges.

## **2.7 Communicating flood risk**

There is a need to communicate flood risk effectively to stakeholder and decision makers, especially when considering the uncertainty and complications of heterogeneous catchments (Wilkinson *et al.*, 2013; Wilkinson *et al.*, 2015). Being able to illustrate how land use management options have the potential to affect flood risk may help stakeholders consider the potential impacts of their actions. It is argued that managing flood risk will often require a number of different solutions and increasingly require a '*portfolio of flood risk management measures*' (Hall and Solomatine, 2008). Hall and Solomatine (2008) go on to show that it is likely to require action by a number of governmental and non-governmental stakeholders. '*This places an increasing*

*emphasis upon effective communication and mechanisms to reach consensus.*' (Hall and Solomatine, 2008).

A tool for communicating the LUM hazards and risks, is the Floods and Agriculture Risk Matrix (FARM) tool (Packman *et al.*, 2004; Wilkinson *et al.*, 2013). The tool was originally developed for a Defra study, FD2114, investigating land use impacts on flood risk (Packman *et al.*, 2004). The approach was originally inspired by the work of (Brazier *et al.*, 2001) who showed the power of visualising sediment loss rates when mapped against key model parameters. Brazier *et al.* (2001) proposed a methodology using a Minimum Information Requirement model (MIRSED), which was based upon a more physical model that enabled a soil erodibility index to be derived that could be mapped against the soil properties such as percentage sand and clay content (Figure 2-6, the greater the sand content the higher the erodibility).

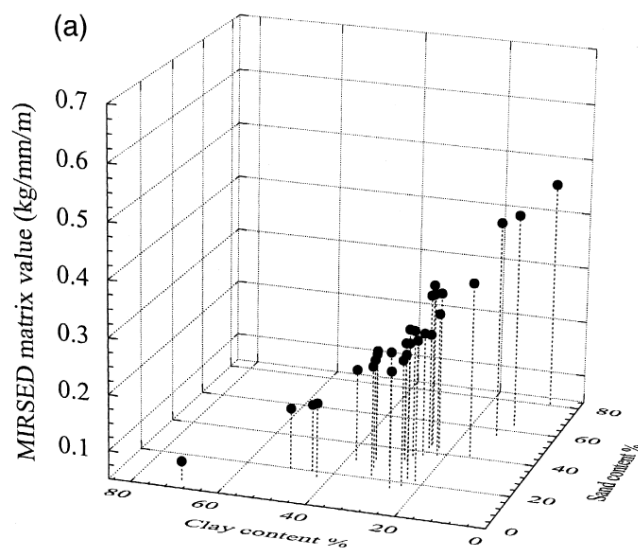


**Figure 2-6 MIRSED matrix for soils in the Great Ouse catchment (taken from (Brazier *et al.*, 2001))**

This gave rise to the concept of a Decision support matrix where nutrient losses were mapped against key underlying drivers (Hewett *et al.*, 2004). The current version of the FARM tool was developed for the Environment Agency (EA) as part of the Making Space for Water project (Wilkinson *et al.*, 2013).

The FARM tool has two key factors that represent runoff rates, firstly, the loss of storage in catchment brought about by the degradation of the soil; secondly, increased connectivity through artificial drainage and channel straightening. Thus the FARM tool has two axes: soil condition (infiltration, storage and tillage regime) and flow

connectivity (Figure 2-7). This complements the hydrological concepts of SPR and Tp; SPR can be used to reflect changes in soil condition and a change in connectivity will become evident in Tp (where high connectivity equates to lower Tp). The stakeholder, in this case a farmer, answers a series of questions, from drop down menus. The questions cover:

1. Increased runoff due to reduced soil infiltration, storage and tillage. i.e. the key attributes relating to:
  - Soil exposure
  - Slope of field
  - Soil degradation
  - Crop and tillage regime
  - Soil management practices
2. Risk of increased runoff due to flow connectivity
  - Land drains and ditches
  - Hillslope form
  - Tramlines, tyre tracks, roads and trafficking
  - Presence of hedgerows, buffer zones, wetlands and water-logged zones, ponds and flood storage ponds

As the stakeholder provides information for each of the above, the highlighted square in Figure 2-7 moves around the matrix so that an understanding of factors and corresponding risk or hazard is established. Once the questions are complete and the risk score for a farm is plotted, the stakeholder is asked to go back through the questions to see what could feasibly be done to reduce the risk score of the farm.

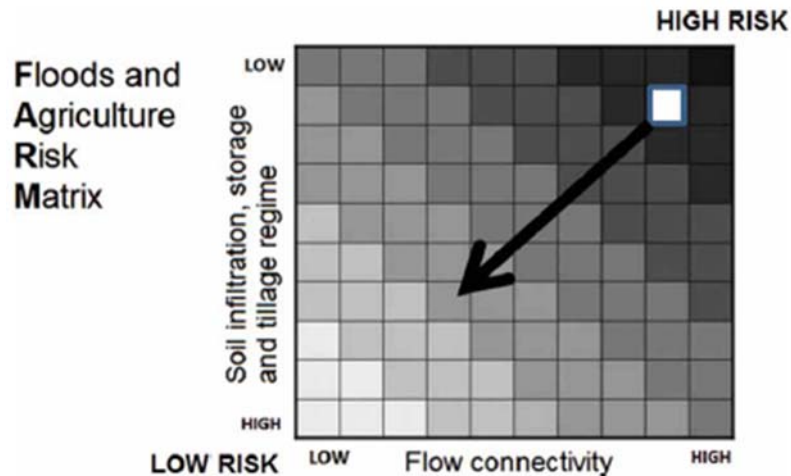


Figure 2-7 The FARM tool – Highest risk of flooding, top right (taken from Wilkinson *et al.*, 2013)

The tool is purely qualitative, with no quantification to help the stakeholder understand what would be required to achieve the outcomes. The scale at which the tool applies is quite generalised, with examples provided at the field-scale.

The FARM tool has recently been demonstrated to stakeholders in the Morland catchment, Cumbria, and the Belford catchment in Northumberland, through a series of public and farmer meetings (Wilkinson *et al.*, 2013). It is noted that the FARM tool has helped stakeholders understand runoff generation problems (Wilkinson *et al.*, 2013). Using the FARM tool with a farmer led to the construction of two overland flow attenuation features. The tool was also used in the NERC pilot Environmental Virtual Observatory (EVO) project which was reported in Wilkinson *et al.* (2015).

## 2.8 Summary

There is a significant and growing wealth of information from field experiments that land use management decisions have potentially significant hydrological consequences. Examples in the literature provide strong field based evidence of the effects of compaction due to cattle on soil bulk density and conductivity as well as the increased infiltration rates under woodland versus pasture (Wheater *et al.*, 2008). The observations of hydrological impact are however, only well understood at the point of observation, generally the point or plot scale. From a catchment management and flood prevention point of view an understanding of how these land use impacts affect flood hazard at the larger, catchment scale is needed, and this however, is not well understood. It has proved difficult to detect the impacts of land use change within

historical data sets due to a number of complicating factors such as climate variability, data errors and the limited length of data records.

Modelling offers the potential for scaling local impacts to the catchment scale. There are, however, a number of implications with regards to the suitability of different models for investigating land use management impacts. These implications include the level of complexity and structure required for adequately capturing the observed land use impacts. Intuitively it would seem the most practical model for investigating land use impacts would be the distributed, physically based models, in which the hydrological and hydraulic behaviour of the landscape are parameterised in great detail using mathematical, physics based equations. Theoretically these models can be parameterised from field measurements such as infiltration and conductivity. However, the scale of measurement is often much smaller than the scale at which distributed models run. They therefore require calibrating to find an effective parameter set that adequately reproduces the catchment outflow and with the large number of parameters there may be more than one suitable parameter set (Vázquez *et al.*, 2002).

Simply using field based measurements or best available information regarding soil and land cover to parameterise the SHETRAN model during a blind validation test was found to be inadequate at recreating the catchment outflow (Ewen and Parkin, 1996). Even when an upper and lower bound of acceptable values was placed on the observed values the range of model outputs still did not adequately capture the catchment response.

The implication of calibrating effective parameter values for physically based models is that attempting to apply any field based observations of land use impacts may be invalid as the sensitivities of the model may differ from the point at which the observation was made.

Alternative methods have used expert knowledge regarding the impact on the hydrological response of soil due land use impact. These methods include the use of regionalised datasets such as HOST or Curve Numbers where parameters regarding soil rainfall-runoff response are changed to reflect likely increased runoff due to soil degradation (Packman *et al.*, 2004).



This leads to the need of this thesis to address these key points. This thesis will make best use of existing data and observations. To produce model structures that are sensitive to uncertainties and to make the most of process understanding but not to over use that understanding so that models become too complex. It is also important that any suggested model structure can be used by end users to assess the potential of land use management change and NFM on  $Q_p$  and  $T_p$  across scale. Hence, how the likely impact of any decisions are communicated regarding flood impact is important.

## **Chapter 3. Methodology**

### **3.1 Introduction**

This chapter describes the methodological approaches adopted in this thesis. Two catchment-based field experiments are introduced and described, followed by a discussion of the experimental design and instrumentation used therein. The two catchments are in the north of England and are undergoing land management changes related to modifying hydrological flow pathways in order to mitigate for flood flows and address water quality issues; the River Leven catchment to Great Ayton (30 km<sup>2</sup>), North Yorkshire, and the River Morland Demonstration Test catchment (12.5 km<sup>2</sup>) in Cumbria.

The analysis methods used in characterising the catchment and understanding the rainfall-runoff response are then described. Of particular interest are the rainfall characteristics that lead to the largest flood peaks, the rate of response of different sub-catchments, and the synchronisation of sub-catchment contributions.

This study will compare two different modelling approaches. The first is the FEH rainfall-runoff model, which uses an event based unit hydrograph approach. The second, a novel model named Juke, uses a distributed, semi-physical approach, designed specifically for land use management (LUM) impact investigation. The conceptual design of Juke is presented to familiarise the reader with its novel design aspects, while a detailed breakdown of its parameterisation is covered in Chapter 7.

Finally, the Floods and Agriculture Risk Matrix (FARM) tool is discussed. The matrix will be populated with the simulated results from the two models to help stakeholders understand in an intuitive way the potential impacts of LUM practises and mitigation methods.

### **3.2 Research catchments**

The Great Ayton catchment forms the core of the data analysis and modelling for this study, as it has the longest available data sets and is a larger spatial scale. The Morland catchment is used to compare the impacts from the modelling of the Great Ayton catchment for a catchment of a smaller spatial scale.

### 3.2.1 Great Ayton

The Environment Agency (EA) has undertaken a flood management scheme in the Leven catchment, to Great Ayton (30 km<sup>2</sup>; Figure 3-1), using two approaches: (1) the flood proofing of at-risk properties; (2) upstream works in the catchment designed to attenuate flood flows. The upstream features include woody debris in the headwaters and offline storage ponds (which receive water from the stream in high flow events); a detailed summary of the features is provided in Chapter 5.

Newcastle University were commissioned by the EA to carry out stream monitoring for the period January 2012 to December 2014. Seven water-level gauges were installed in the catchment - six in the stream network and an additional one within an offline storage feature located at Little Ayton. This augments the EA's current hydrometric monitoring network, which comprises two stream gauges, an event (tipping bucket) rain gauge and a daily rain gauge.

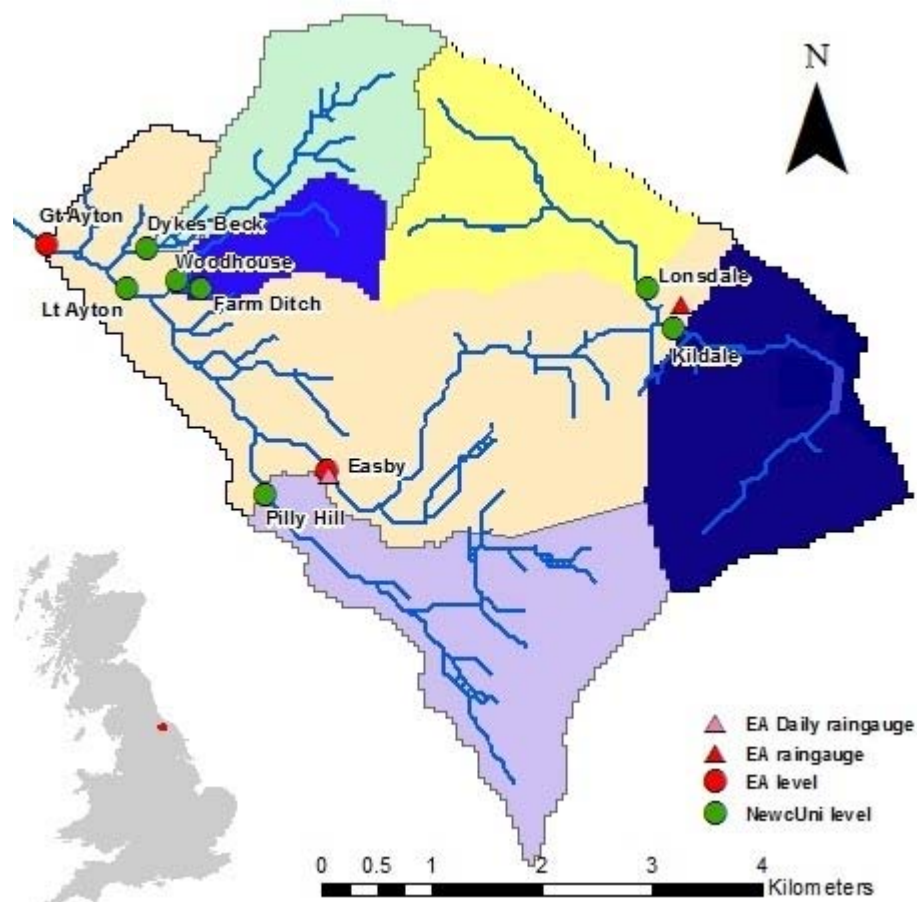


Figure 3-1 Monitoring locations in Great Ayton Map

### 3.2.2 Morland

The Demonstration Test Catchments (DTC) programme aims to test and monitor a multitude of methods for mitigating Diffuse Water Pollution from Agricultural (DWPA) (Owen *et al.*, 2012). It is jointly funded by the Department for Environment, Food and Rural Affairs (Defra), the EA and the Welsh Assembly Government (WAG).

The Eden DTC, based in the River Eden catchment (2288 km<sup>2</sup>) in Cumbria, northwest England, is one of three national demonstration catchments, along with the Avon in Hampshire and the Wensum in Norfolk. The Eden DTC is monitoring three tributaries of the Eden (~10 km<sup>2</sup> sub-catchments), chosen to represent the different farming practices and land uses found in upland areas of Northern England. This study will focus on the Morland catchment (Figure 3-2; 12.5 km<sup>2</sup>).

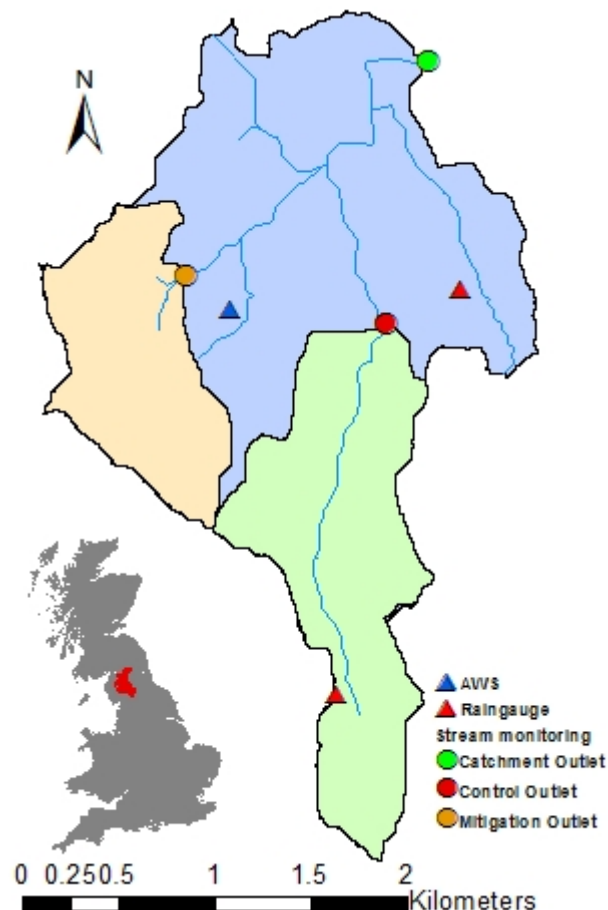


Figure 3-2 Monitoring locations in Morland

### 3.2.3 Catchment summaries

A summary of the land use and management found in the 2 research catchments, as well as the local flooding issues is provided in Table 3-1.

Table 3-1 Summary of land use, land management and climate of the two research catchments

	<b>Great Ayton</b>	<b>Morland</b>
<b>Region</b>	North Yorkshire, north-east England	Cumbria, north-west England
<b>Watercourse</b>	River Leven	Newby Beck
<b>Major catchment</b>	Tees	Eden
<b>Area</b>	30 km <sup>2</sup>	12.5 km <sup>2</sup>
<b>Elevation (AOD) range</b>	84 m to 395 m	144 m to 348 m
<b>Annual average rainfall</b>	805 mm	1167 mm
<b>Soils</b>	Predominantly slowly permeable and seasonally wet clayey soils. Peats in the upper areas.	Dominated by slowly permeable and seasonally wet glacial tills.
<b>Geology</b>	Predominantly mudstone, sandstone and siltstone. Steeper hillslope faces interbedded Sandstone and Ironstone	Interbedded limestone, mudstone and sandstone of the Carboniferous Yoredale group
<b>Hydrology and geomorphology</b>	The catchment can be sluggish to respond after a prolonged dry period. Antecedent conditions important must be saturated to generate medium to events.	Flashy response to rainfall. The headwaters can become very dry during the summer months due to losses to limestone.
<b>Land cover and use</b>	Predominantly pasture for sheep and cattle. Game rearing on the upland moors with some arable. Some woodland on slopes.	Predominantly pasture for sheep and cattle with some arable.
<b>Land management</b>	Almost half the catchment is improved grassland for livestock. The upper catchment is moorland with sheep and game rearing.	Significantly improved (70 %) for animal rearing. Small amount of arable and woodland.
<b>Local land management and flooding issues</b>	Number of locations prone to flooding. Exacerbated by local constrictions such bridges and culverts. NFM uptake to attenuate flows.	Local flooding to farmland and roads and a small caravan park. Water quality an issue which is being mitigated for with attenuation features.

### 3.3 Experimental design

The monitoring network in each of the two research catchments uses a nested structure with an outlet gauge and internally located gauges. The nested approach is taken to understand how each catchment responds to rainfall, not only at the outlet but at multiple scales, to better understand how floods develop. Of most interest are the factors that drive the largest events; which areas contribute to flood peaks? What is the role of rainfall intensity and duration in generating the largest peaks? What is the importance of seasonality and antecedent conditions? And then, how does the flood wave propagate through the system? These questions will be answered through achieving objective three, catchment characterisation, and will contribute to parameterising the models used to achieve objectives five and six (lumped and distributed modelling, respectively).

Despite both employing a nested monitoring structure, the design of the networks differs between the two catchments. The DTC Morland catchment uses a paired catchment approach, with a gauge at the outlet and two separate sub-catchment outlets; one sub-catchment is being mitigated with features for reducing DWPA, whilst the other is a control catchment. The Great Ayton network was designed more specifically for the spatial understanding of flood generation. Figure 3-3 is a schematic of the Great Ayton monitoring network which illustrates the data observations that enables sub-catchment synchronisation and flow contributions to be quantified. The detailed design specific to each catchment is described in more detail in their respective characterisation chapters (4 and 5).

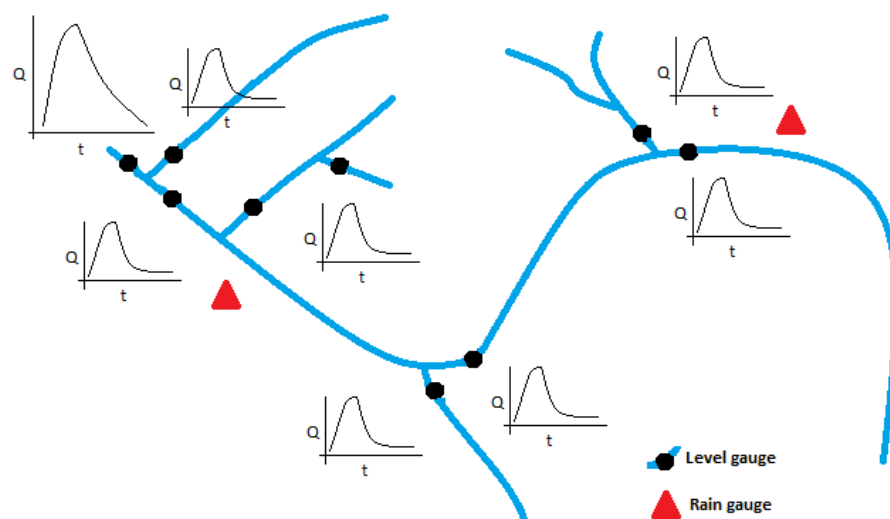


Figure 3-3 Schematic of monitoring network design for Great Ayton

### **3.4 Instrumentation**

This section describes the instruments used in the experimental catchments for monitoring hydrometeorological parameters (rainfall, flow and evaporation) needed to quantify various parts of the water cycle and to calculate a water balance. The author of this thesis was responsible for all hydrometeorological instrumentation, specifically, installation, maintenance, data collection and quality control thereof on behalf of Newcastle University and the DTC programme.

#### ***3.4.1 Automatic Weather Station (AWS)***

The AWS used in the Morland catchment is manufactured by Environmental Measurements Limited and consists of multiple instruments for monitoring the parameters required to calculate potential evaporation on a 15 minute time step (EML, 2015), including:

- Air temperature (°C)
- Humidity (%)
- Net radiation (Watts/m<sup>2</sup>)
- Wind speed (average, minimum and maximum; m/s)
- Wind direction (°)
- Rainfall (mm)

AWS data for the Great Ayton catchment are collected at RAF Fylingdales, in an adjacent catchment (Centre for Environmental Data Archive; Station 358).

#### ***3.4.2 Rainfall***

Rainfall data are collected using 0.2 mm tipping bucket rain gauges (Figure 3-4). The gauges record on an event basis which means they record a timestamp for every tip. The logged tips can then be resampled to produce a cumulative rainfall record for any time step, which in this study is 15 minutes.



**Figure 3-4 Casella tipping bucket rain gauge**

### ***3.4.3 Stage***

Three different methods are used for monitoring stream stage data in these studies. The method employed at the two EA sites in the Great Ayton catchment uses a weir with a stilling well and float system as shown in Figure 3-5.



**Figure 3-5 Weir at EA Easby level monitoring location**

Sites monitored by the author in Morland and Great Ayton use two types of pressure transducer located in natural channels. Pressure transducers record the head above the instrument. This can be done in two ways: (1) by measuring the ‘raw’ pressure, which is both the pressure of the water head and the ambient atmospheric pressure. This requires the additional measurement of atmospheric pressure by a barometer against which the raw, instream pressure can be compensated. (2) Using a ‘vented’ pressure



transducer; automatically accounts for the atmospheric pressure by having a tube that runs from the device to the atmosphere, therefore only affected by the head of water.

Each of the methods has their own merits. A weir with a stilling well is a highly accurate method of measuring river stage, especially at low flows. For water resource projects where accounting for low flows is important the use of a control structure is recommended. However, structures are expensive to install and cannot be economically justified. If the study is not concerned with the accurate quantification of low flows then pressure transducers offer a rapid to install and comparatively cheap method of monitoring stream stage.

It has been observed that the pressure transducers that require compensating can be affected by temperature, especially where there is a difference in temperature between the instream instrument and the barometer (Ewen *et al.*, 2010). The effect is most noticeable during warm periods when there is little flow. A method was developed by Ewen *et al.* (2010) that involves taking manual stage measurements at the instrument for a range of temperatures and depths. A relationship is established for the temperature dependency of stage that is then applied to the compensated level series as a multiplier for the observed temperature at the instream gauge. The corrected water level series provides an accurate record of level as is shown in Figure 3-6, where a vented pressure was situated alongside a non-vented gauge to confirm their accuracy.

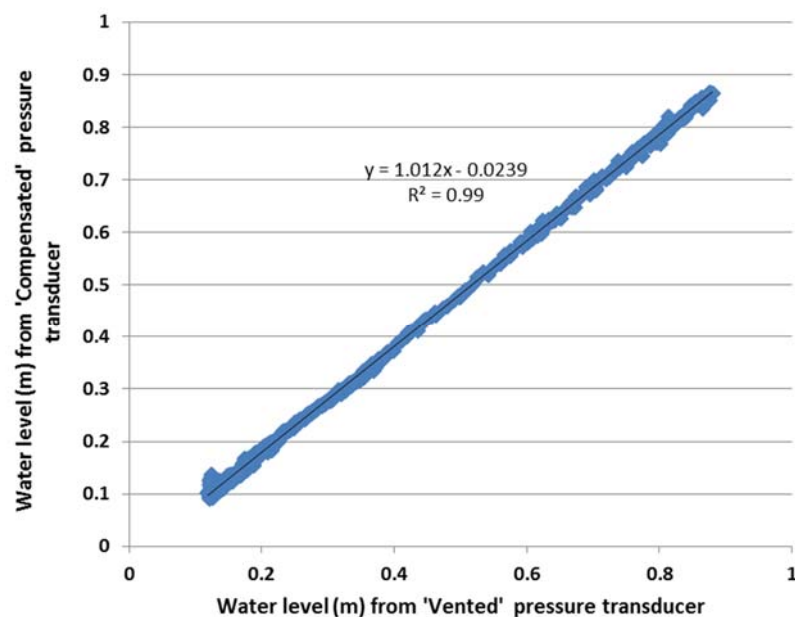


Figure 3-6 Comparison of water levels recorded by 'vented' and 'compensated' pressure transducers at Little Ayton in the Great Ayton catchment

### 3.4.4 Morland instrument locations and data availability

The locations of each of the monitoring instruments can be seen in Figure 3-2, with the location details summarised in Table 3-2.

Table 3-2 Morland catchment and sub-catchment instrumentation summary

Site	Easting	Northing	Elevation (m.a.o.d)	Area (km <sup>2</sup> )	% of catchment
<i>Water level</i>					
Mor_out	360057	521315	144	12.51	100
Mor_subM	358127	519614	209	1.55	12.4
Mor_subC	359719	519221	195	3.64	29
<i>Meteorological</i>				<i>Thiessen area</i>	<i>Thiessen weight (%)</i>
AWS	358482	519341	216	3.43	27.4
Telemetered	359317	516289	288	6.72	53.7
Non-telemetered	360310	519499	192	2.37	18.9

The analysis for Morland makes use of data for the three hydrological years from October 2011 to September 2014. This period contains events of varying magnitude with a mixture of antecedent conditions, as will be analysed and discussed in this chapter. Dataset completeness is summarised in Table 3-3 - short gaps in some of the records are due to logger failure and/or rain gauge blockage.

Table 3-3 Morland data availability

	2011			2012												2013												2014											
<i>Water level</i>	Oct	Nov	Dec	Jan	Feb	Mar	Apr	May	Jun	Jul	Aug	Sep	Oct	Nov	Dec	Jan	Feb	Mar	Apr	May	Jun	Jul	Aug	Sep	Oct	Nov	Dec	Jan	Feb	Mar	Apr	May	Jun	Jul	Aug	Sep			
Mor_out																																							
Mor_subM																																							
Mor_subC																																							
<i>Hydro-Met</i>																																							
AWS																																							
Tel_TBR																																							
NTel_TBR																																							

The analysis in Chapter 4 uses an aerially weighted, composite rain series created using Thiessen polygons, clipped to the catchment boundary (Figure 3-7). The Thiessen weights reflect the proportion of the catchment that lies closest to a particular rain gauge.



Figure 3-7 Theissen polygons for Morland rainfall weightings used in modelling

### ***3.4.5 Great Ayton instrument locations and data availability***

A nested, multi-scale, monitoring network consisting of eight level gauges has been implemented by the author across the stream network, supplementing the two existing EA flood warning level gauges. There is an additional level gauge within an offline flood storage pond that has been used to monitor its response and behaviour.

#### ***Environment Agency gauge***

The Environment Agency has a several level gauges along the River Leven for use in flood forecasting and warning, three of which are being used in the data analysis in Chapter 5 (Table 3-4). They are located Easby (15 km<sup>2</sup>), Great Ayton (30 km<sup>2</sup>), and Foxton Bridge (168 km<sup>2</sup>), which will allow analysis of catchment response at a range of spatial scales. Data from Foxton Bridge are being used to examine the effect of spatial and temporal scale on the hydrograph. Spatial and travel time analyses are being carried out to provide an understanding of the formation of floods; the attributes of the locations to be used in the scaling and analyses of travel time are listed in Table 3-4.

**Table 3-4 The EA instrumentation being used in the Great Ayton analysis and modelling**

<b>Gauge</b>	<b>Easting</b>	<b>Northing</b>	<b>Elevation (m.a.o.d)</b>	<b>Distance to Foxton (km)</b>
<i><b>Water Level</b></i>				
Easby	458503	508660	110	25.3
Great Ayton	455952	510723	84	20.0
Foxton Bridge	445578	509372	18	-
<i><b>Rain gauge</b></i>				
Easby	461724	510188	174	-

**Newcastle University gauges**

The availability of data from the eight level gauges installed by the university are listed in Table 3-5 below.

**Table 3-5 Newcastle university installed gauges data availability**

Water level	2012												2013												2014												2015											
	Jan	Feb	Mar	Apr	May	Jun	Jul	Aug	Sep	Oct	Nov	Dec	Jan	Feb	Mar	Apr	May	Jun	Jul	Aug	Sep	Oct	Nov	Dec	Jan	Feb	Mar	Apr	May	Jun	Jul	Aug	Sep	Oct	Nov	Dec	Jan	Feb	Mar	Apr	May	Jun	Jul	Aug	Sep			
Lonsdale																																																
Leven Vale																																																
Farm ditch																																																
Lt. Ayton																																																
Lt. AytonP1																																																
Woodhouse																																																
Dikes Beck																																																
Pilly Hill																																																

Grey - Data available

White - Data unavailable

Black - Data-logger corrupted/no data

**Table 3-6 Location and other attributes of the Newcastle university sites**

<b>Site</b>	<b>Easting</b>	<b>Northing</b>	<b>Elevation (m.a.o.d)</b>	<b>Area (km<sup>2</sup>)</b>	<b>% of catchment</b>
Lt Ayton	456686	510331	89	25.9	86
Lt Ayton P	456820	510259	90	-	-
Leven vale	461656	509963	169	5.0	17
Lonsdale	461409	510321	168	4.0	13
Pilly Hill	457930	508458	110	5.2	17
Woodhouse	457125	510401	95	1.4	5
Dikes Beck	456852	510682	94	2.9	10
Farm Ditch	457345	510335	99	0.5	1.7

### **3.5 Rating curve development**

A rating curve or a stage-discharge relationship is required to convert the recorded stage to a discharge. The traditional approach is to measure the velocity and cross sectional area that correspond to a range of the depths, often referred to as ‘gaugings’ or ‘flow gaugings’. There are methods for in-situ discharge monitoring, on a continuous basis, by measuring the velocity (e.g. using an Acoustic Doppler system) and the water level, which is used to lookup a cross-sectional area from a stage-area curve. However, Doppler systems are expensive and are difficult to operate in natural, non-geometrical channels that are prone to changes in cross-sectional area. No formal uncertainty assessment has been made however, the field observations are taken as the best information available. The major source of the uncertainty lies in extrapolating the ratings beyond the highest gauged flows. Using hydrological judgement rating curves have been extrapolated to ensure they are physically reasonable, through consideration of the long term water balance. The volume of water leaving the catchment, derived from the flow data obtained from the stage measurements and rating curve, was compared to the rainfall and evaporation over the period of interest. GLUE analysis of the Morland outlet rating curve showed it to be a robust relationship (Beven *et al.*, 2015).

#### **3.5.1 Flow gauging**

The manual gauged flows were collected using a number of different instruments. In medium to low flows where it was safe to enter the stream a Valeport model 801 electromagnetic flow (EM) gauge was used to take point velocity measurements

(Valeport, 2011). The velocity-area method (Shaw *et al.*, 2010) was used to attain the cross sectional discharge, by splitting the channel in to at least 10 panels, with no panels having a width greater than 0.3 m; the velocity was measured at 0.6 of the depth for each point. The EM gauge has a stated velocity measurement accuracy of  $\pm 0.5\%$ . Each velocity measurement is taken as the average over a 40 second recording interval and is only accepted if the standard deviation in the measurement interval is less than 10 % of the final value to eliminate erroneous values caused by turbulence.

Gaugings made during higher flows used the Teledyne ‘StreamPro’ Acoustic Doppler Channel Profiler (ADCP) (Teledyne, 2013). This method requires two operators to pull a float across the channel to record the required area and velocity measurements. The system builds a picture of the channel and avoids double counting by tracking its progress against fixed objects in the bed. It automatically adjusts the resolution at which it scans the channel from 2-20 cm depending on the depth and complexity of the flow regime. The ADCP has a stated accuracy  $\pm 1\%$  of water velocity relative to the ADCP and measurement accuracy of  $\pm 2$  mm/s. The discharge recorded is an average of at least three measurements taken on separate tracks across the channel, where each measurement is within 5 % of the average discharge.

### **3.5.2 Modelling Flow**

Opportunities to gauge the largest flows are infrequent and often missed due to their limit length. As a means of producing stage-discharge rating curves with limited gauged data, a method is proposed for modelling a rating curve using a surveyed channel cross-section, observed water levels and the available flow measurements. Beven (1979), found that in a river system the stream velocities asymptote to a maximum value with increasing discharge and it is this understanding that underpins the Velocity-Area Rating Extension (VARE) model, where the stage-velocity relationship is fitted by a sigmoid function, Figure 3-8 (Ewen *et al.*, 2010); every stage height is associated with a cross-sectional area, derived from field survey. The velocity value is applied to the stage-area relationship to derive discharge. VARE is used to produce rating curves that can be constrained in two ways. Firstly, the maximum in-channel velocity can be limited, meaning the extrapolation of the rating curve is likely to be physically realistic (Illustrated in Figure 3-8). Secondly, and in combination with the velocity capping, is the ability to calibrate the rating curve over a long period to achieve a physically realistic water balance. This is done by treating the hydrological cycle as a closed

system in which the flow record, the output, can be calibrated against the known input, rainfall and calculated potential evaporative losses from the weather station data. There may be additional losses from the system via abstraction and to groundwater, which can also be accounted for if quantities are known.

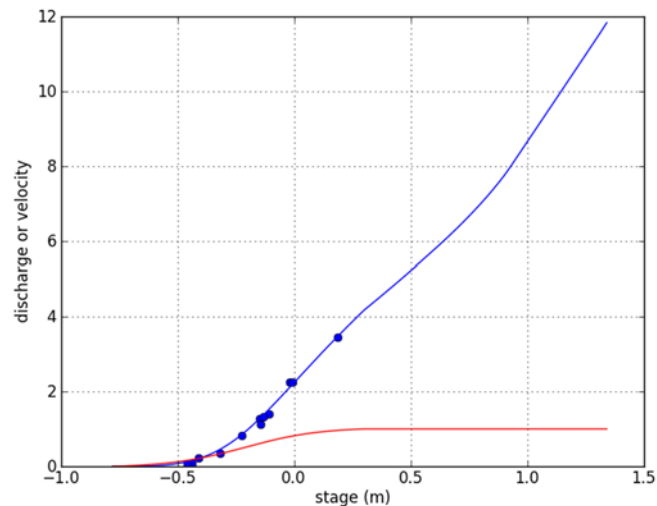


**Figure 3-8 VARE output showing stage-discharge curve (blue), gauged data (blue dots) and stage-velocity curve (red)**

VARE has been used in a number research projects at Newcastle University to generate rating curves, including the Hodder project studying the effects of the Sustainable Catchment Management Programme (SCaMP) (Ewen *et al.*, 2010; Geris, 2012), and the PhD work carried out in Belford (Nicholson *et al.*, 2012). A detailed description of the model can be found in the Hodder project reports (Ewen *et al.*, 2010; Geris, 2012).

### **3.6 Storm analysis**

To fully understand how a catchment behaves, the hydrometeorological parameters need to be quantitatively analysed against each other to understand how the catchment responds to rainfall, especially what causes the largest events. This analysis is discussed below.

#### **3.6.1 Rainfall runoff**

There are a number of factors that contribute to flood peak magnitude, including catchment antecedent wetness conditions and the space-time characteristics of the rainfall event driving it. In order to understand the conditions that cause the largest flow peaks in the catchment a number of algorithms have been developed to compare flood peaks against a number of rainfall statistics (total storm rainfall, mean storm intensity, maximum storm intensity and storm rainfall Duration). The start and end of the rainfall



event is selected for each discharge peak by identifying a window of 4 hours in which there was no rainfall at the beginning and end of the rainfall event. This simple approach has been used in numerous published papers as summarised in Dunkerley (2008). The 4 hour window provided a good selection of peaks of differing magnitudes, with few double peaked events. The events selected have also been split into two seasonal categories of 'autumn/winter' and 'spring/summer' to give an indication as to the likely antecedent conditions, i.e. wet and dry, respectively.

### **3.6.2 Celerity**

Celerity relates to the flood wave speed which is the catchment response to rainfall, including the hillslope and channel network. The interaction of different sub-catchments, and their relative timings are highly significant factors as they may influence the management options considered when designing a flood mitigation scheme. One specific goal of such schemes is to attenuate the flood peak, i.e. increase the time-to-peak ( $T_p$ ) and lower the flood peak and rate of recession as demonstrated in Figure 3-9. Understanding a catchment's response can be performed in a number of ways, including analysing the lag time between the centroid of rainfall events and the corresponding flood peaks in the river. An alternative approach is to examine the flood wave celerity - how the flood propagates through the river network by comparing the timing of flood peaks for gauges within a nested catchment.

Celerity is calculated using the distance between two monitoring points on a river and the lag time of peak values between those points. A relationship can be established between  $Q_p$  and celerity by analysing the celerity for a range of flood peak magnitudes. This is crucial to understanding the flood response for the current catchment being studied

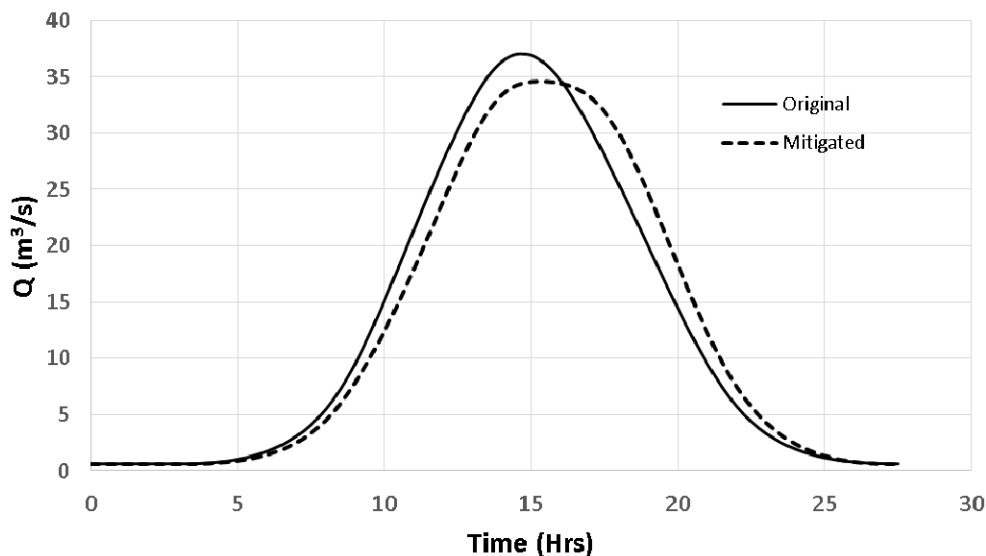


Figure 3-9 Schematic illustrating the desired impact of increasing the time to peak of a catchment

### 3.7 Flood Impact Modelling (FIM)

To illustrate the potential for LUM as a means of mitigating flood flows, two models with different structures are to be used for mitigation impact assessment. The models have both been selected as they are relatively simple to understand and the changes made to model parametrisation to reflect LUM impacts can be done in a transparent fashion. The first model is based on the FEH rainfall runoff model; widely used by UK consultancies for generating design flood events for flood risk assessment. The second is the Juke model, developed as a novel approach specifically for modelling LUM impacts based on physically based assumptions.

The modelling approaches adopted in this study aim to make best use of expert knowledge regarding LUM impacts on the generation and propagation of flood flows and apply them in a transparent and physically unambiguous way. This is done by making best use of:

- **Expert knowledge** and judgement of likely changes based on the findings and observations from field and modelling work as discussed in the literature review, Chapter 2.
- Take as much value as possible from **field measurements** for example analysing local measurements of flow propagation to the local catchment outfall and throughout the flow network
- Spatial **catchment data** from GIS including DEM, HOST and land cover. As was highlighted by O'Connell *et al.* (2007) '*Risk is likely to be catchment*

*specific, and dependent upon the natural catchment characteristics (topography, soils, etc.) as well as on land management practices.'*

### ***Expert Knowledge - How do landscapes respond to change?***

It has been illustrated in Chapter 2 that there are numerous plot and hillslope scale studies that have determined the impact of different land uses on runoff generation. Much of the existing evidence on the impacts of LUM has concerned detailed measurement of soil properties, for example reduced 1D infiltration rates through compaction brought about by increased bulk density and reduced pore space, leading to both infiltration excess and storage excess overland flow (Sansom, 1999; Carroll *et al.*, 2004; Wheeler *et al.*, 2008). Typically the spatio-temporal resolution at which rainfall-runoff models operate is greater than the resolution of the parameter measurement, therefore the model needs to be calibrated to find an '*effective parameter*' (Vázquez *et al.*, 2002). This makes the model sensitivities uncertain when trying to implement LUM impact changes to parameter values based on field observations.

### ***Field measurements***

Aim to use the observed rainfall and runoff records to understand as fully as possible the factors that contribute to the largest flood peaks and how large events propagate through the catchment network. Then use this data and understanding from observations to parameterise the impact model.

### ***Catchment data***

The most significant regionalised, spatial hydrological dataset available in the UK is the Hydrology of Soil Types (HOST). The dataset provides a GIS of the Baseflow Index (BFI) and Standard Percentage Runoff (SPR) values for 29 soil classes. The data set was classified based upon the physical characteristics of the soil and regression analysis of rainfall-runoff records for a number of catchments (Boorman *et al.*, 1995). The data and results from these catchments were then extrapolated to provide a regionalised, national dataset of the hydrological properties of soil. HOST therefore provides a dataset based on observed data that is representative of catchment response at larger scale. This dataset has been used in a number of hydrological modelling projects, including LUM change scenarios.

The SPR associated with each of the HOST classes are provided in Table 3-7. The SPR values represent the standard lumped catchment rainfall-runoff response and we use it

to parametrise information for historical data sets; then make changes to the SPR values to represent a proposed impact due to LUM change. The Defra funded FD2114 proposed such a methodology for switching from a current HOST class to a revised class based on the potential effect of soil degradation caused through intensive land management practises. These ‘revised’ worst case classes for the soils found in Morland and Great Ayton are shown in Table 3-7 (Packman *et al.*, 2004).

**Table 3-7 HOST classes and their revised, degraded reclassification (\* indicates some uncertainty in the reclassification; Lettering next to class number signifies the catchment in which they are found M = Morland, G= Great Ayton; Packman *et al.* (2004)**

Class	Description	Revised Class	Original SPR	Revised SPR
4 <sup>M</sup>	Free draining permeable soils on hard but fissured rocks with high permeability but low to moderate storage capacity	6*	2	15
5 <sup>G</sup>	Free draining permeable soils in unconsolidated sands or gravels with relatively high permeability and high storage capacity	7*	15	27
6	Free draining permeable soils in unconsolidated loams or clays with low permeability and storage capacity	8	34	44
7	Free draining permeable soils in unconsolidated sands or gravels with groundwater at less than 2m from the surface	7*	44	44
15 <sup>G</sup>	Permanently wet, peaty topped upland soils over relatively free draining permeable rocks	15	48	48
20 <sup>G</sup>	Slowly permeable soils with slight seasonal waterlogging and moderate storage capacity over impermeable clay substrates with no storage capacity	20	60	60
24 <sup>M,G</sup>	Slowly permeable, seasonally waterlogged soils over slowly permeable substrates with negligible storage capacity	25	40	49
25	Slowly permeable, seasonally waterlogged soils over impermeable clay substrates with no storage capacity	25*	50	60
26	Permanently wet, peaty topped upland soils over slowly permeable substrates with negligible storage capacity	26	59	59

To illustrate the revision of HOST classes and emphasise the change in flow pathway and the increased runoff rate, consider the soil originally classified as belonging to HOST class 5, being reclassified to the alternate class 7. This requires a shift in the original base model from that of the aquifer or groundwater being found at greater than 2 m, to being found within 2 m (Figure 3-10). This may be due to the development of a plough layer in the upper layers of the soil which impedes the vertical flow of water; it

may also be that some of the macro-porosity is lost through compaction. The key difference in response between the two models is that there is reduced storage within the soil profile; it will therefore reach saturation and the onset of overland flow more rapidly.

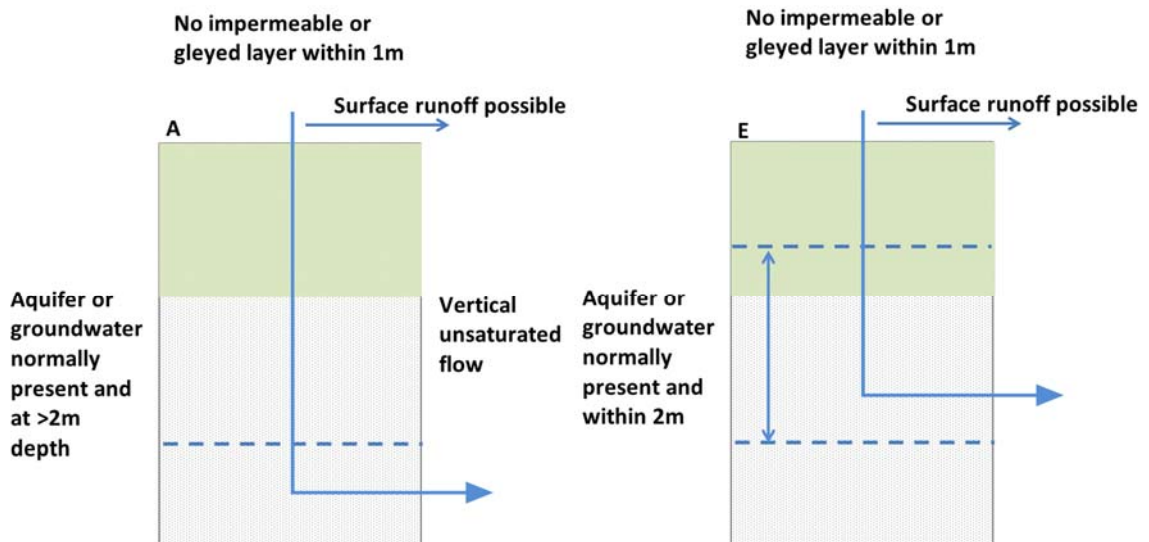


Figure 3-10 Illustrating shift in HOST model from A to E for change in class 5 to 7 (Boorman *et al.*, 1995)

### 3.7.1 FEH rainfall-runoff model

The FEH rainfall-runoff model is a widely used UK industry standard model. The rainfall-runoff model is based on the unit hydrograph. It is predominantly used for generating specific design flood hydrographs using regionalised statistics, including HOST, and more specifically SPR, which controls the magnitude of the unit hydrograph. The model design and parametrisation will not be discussed in significant detail here (please refer to Chapter 6, where the parameters are discussed and tested in full). The model is being used in this study due to its wide use and the fact that the SPRHOST value is integral to the model's design; the aforementioned reclassification of HOST by Packman *et al.* (2004) to represent soil degradation can be done in clear and intuitive way.

### 3.7.2 Juke rainfall-runoff model

The Juke model is a distributed conceptual rainfall-runoff model, specifically designed for modelling the local impacts of LUM and NFM and how these impacts propagate to a downstream point of interest. The model is novel in that the modeller has full control of mathematical structure of the model. The mathematical structure is defined through a set of "pattern equations" which describe the runoff generation and routing processes in

a spatial manner. These equations are defined in a model script which is a model input, the control file. This mathematical capability enables patterns of LUM flood mitigation scenarios to be created without the need to pre-process the patterns in traditional GIS packages.

Impact here is defined as the difference between two modelled hydrographs, for example, pre and post change. Structural errors in the process representation within traditional rainfall runoff models that lead to consistent errors in the modelled response, such as the recession rates, or the over or underestimation of peaks, etcetera, are carried forward into the impact assessment. An additional form of error incurred in rainfall runoff modelling is associated with the observed data and the variability and inconsistencies that lie within. One way to overcome these modelling errors is to force the modelled calibration (M) to match the observed hydrograph (O), i.e. achieve the perfect calibration in which the residuals are zero (Equation 3-1).

**Equation 3-1**

$$M(t) = O(t)$$

Therefore, any modifications made to the model parametrisation to reflect a LUM or NFM scenarios can be directly ‘injected’ into the hydrograph. Any impact is then a direct directly attributed to the modification ( $\delta$ ; Equation 3-2).

**Equation 3-2**

$$M(t) = O(t) + \delta(t,O)$$

The model design is discussed in some detail here as the approach taken is quite different from traditional rainfall-runoff models. However, the Juke model does have a number of features in common with many traditional rainfall-runoff models including lumped and distributed elements; the use of gridded maps to provide distributed information regarding topography, soil type and land use, as well as the conceptualisation of fast and slow flow pathways. The specific details regarding parameterisation are discussed in Chapter 7, together with sensitivity testing.

Key aspects of the model to highlight are:

1. The model has been specifically designed for modelling flood events and changes to event runoff due to distributed changes in local runoff generation.

2. The model is distributed, using GIS datasets regarding topography, land use and soil type that are used in customising how runoff is generated across the catchment.
3. The model is programmable, with a GIS based language allowing the definition of the mathematical structure generation. Distributed modifications in runoff generation delta, resulting from changes in the landscape
4. The model is forced by the observed hydrograph  $O$  to create a “perfect” calibration for pre-change conditions (i.e. zero residuals)  $M$ .
5. Routing is based on information obtained from the observed flow records.
6. There is no explicit representation of evaporation losses. The matching element, as will be described takes care of this, however it is assumed that event based evaporative losses are negligible.
7. The model is simple and physically interpretable with elements based upon runoff generation and propagation with units that are easily understood.

Juke is depicted in Figure 3-11, with the gridded and lumped elements highlighted by the boxes. The thin arrows represent the ‘fast information flows’ during the calibration process, whilst the larger arrows are the fast information flows during the modified (post-change) model run. The fast information flows are associated with the passage of information in attaining the observed hydrograph in calibration and then any information regarding change in a modelled scenario. The model is run twice, firstly a calibration process in which the scripts and data provided recreate the observed hydrograph. The second run of the model applies the modifications incorporated in scripts to reflect LUM options. The dotted lines indicate where the observed hydrograph is used within the model during the calibration process, specifically the modelling elements associated with network routing, latching and matching.

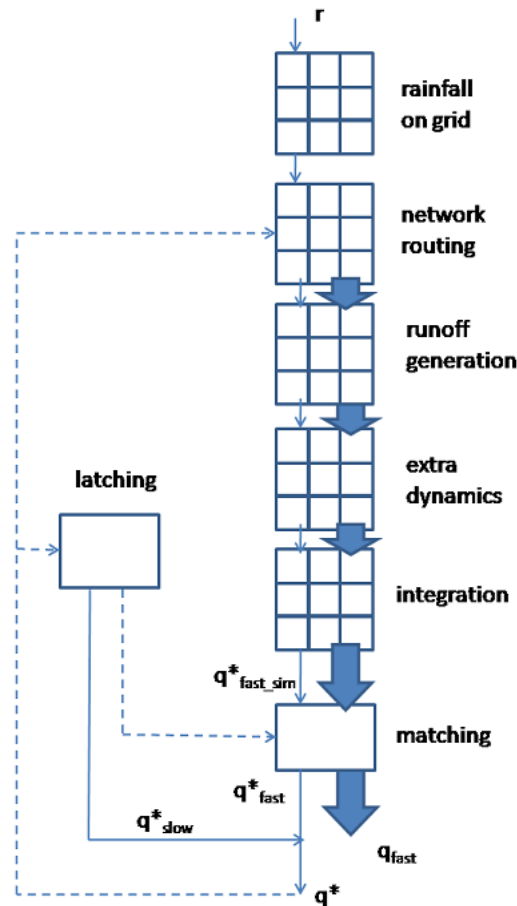


Figure 3-11 Schematic of the Juke model processes (Beven *et al.*, 2008)

The observed rainfall time series are used to create a distributed rainfall grid, with the grid squares receiving the rainfall value from the nearest gauge. The outlet hydrograph,  $q^{*}$  is assumed to have a fast ( $q^{*}_{fast}$ ) and slow ( $q^{*}_{slow}$ ) component, which sum to give the observed outlet hydrograph; a concept widely used in hydrological models. This study is looking at changes in flashy event runoff so any change will come from the distributed modelling and will be seen in  $q_{fast}$ .

### **How a perfect calibration is achieved**

This section describes the two lumped components latching and matching and how they ensure that the perfect calibration is achieved.

#### ***Latching***

With Juke we are only concerned with modelling the flood hydrograph, i.e. the fast response and not the long term base flow. The term ‘latching’ refers to the process by which the model hydrograph matches the observed hydrograph during drier periods below a threshold ( $q_{threshold}$ ). Simply, the method for hydrograph separation is:



**Equation 3-3**

$$q_{\text{slow}} = \text{MIN}(q^*, q_{\text{threshold}})$$

***Matching***

The role of the matching element is to ensure that the integrated (combined flows from the distributed modelling components) modelled fast response  $q^*_{\text{fast\_sim}}$  from the distributed modelling matches and is equal to the observed hydrograph to produce the  $q^*_{\text{fast}}$  (Figure 3-11). The model achieves this during the calibration procedure by calculating a time series of the ratio  $q^*_{\text{fast}}/ q^*_{\text{fast\_sim}}$  called the matching gain (Lgam). The time varying matching gain is similar to a rainfall-runoff ratio. If no information is provided regarding the distributed nature of runoff generation and 100 % of rainfall is routed from the cell to the outlet for all storms and all antecedent conditions, there will be too much water to recreate the hydrograph. Therefore, the matching ratio can be interpreted as similar to a rainfall-runoff ratio. The matching gain (Lgam) is illustrated in Figure 3-12, this element behaves in a similar way to a rainfall-runoff ratio, i.e. runoff increases as a storm progresses. Matching is also carried out for the nested flow gauge to allow the impact at different scales to be assessed.

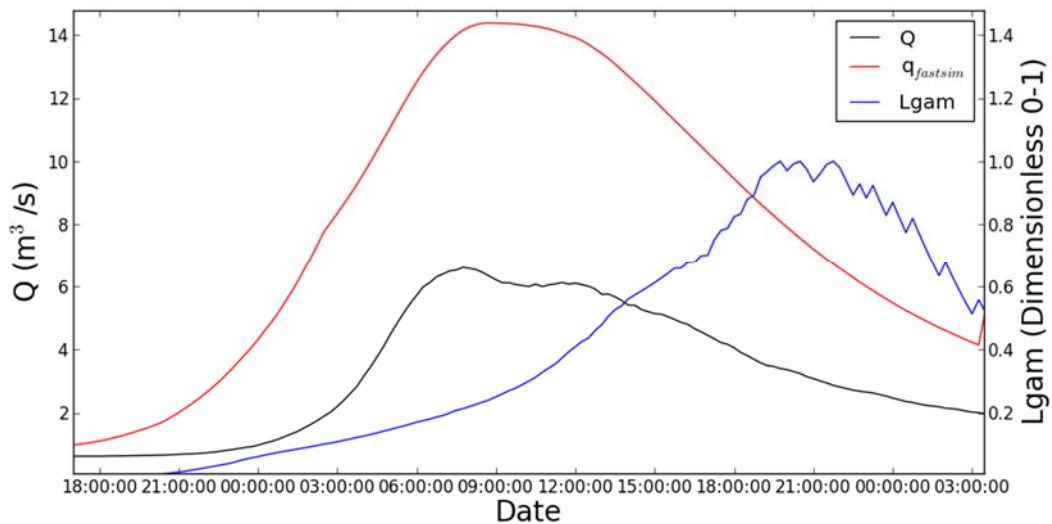


**Figure 3-12 Great Ayton hydrograph illustrating the task of the matching element (Observed hydrograph in black,  $q_{\text{fastsim}}$  in red and the matching gain in blue)**

**Distributed elements**

Traditionally in rainfall-runoff modelling the observed hydrograph is used for visual inspection of goodness of fit and quantitatively in an objective function. In the Juke calibration process, the observed hydrograph is used internally to achieve an exact match by disaggregating the outlet hydrograph in a physically reasonable way to

establish where the water came from and how fast it travelled from source. This is done by making use of the information in the observed rainfall and flow records, from different spatial scales, combined with distributed physical information regarding topography, soil type and land use.

### ***Network routing***

The observed hydrographs and rainfall, combined with a Digital Elevation Model (DEM), are used to parameterise the flow routing components. The DEM is used to create the network routing element, in which each cell is connected to the outlet. The celerity of the network is parameterised as a function of the outlet hydrograph to ensure that the travel times are correct. The function is parameterised through the travel time relationship for multiple storms between the rainfall grid and the nested gauges, of which there must be at least two to allow the tracking of flow peak timings (Figure 3-13). A detailed description of the parameterisation of this function is provided in Chapter 7, along with a description of how it can be manipulated to reflect LUM change. Figure 3-13 is an overview of the actual data used in the calibration of the celerity function for the Great Ayton model used in Chapter 8; the green and red data lines represent the average travel time from the individual cell to the flow gauges used in the model calibration. The scatter within the observed points is due to the space time patterns within the rainfall.

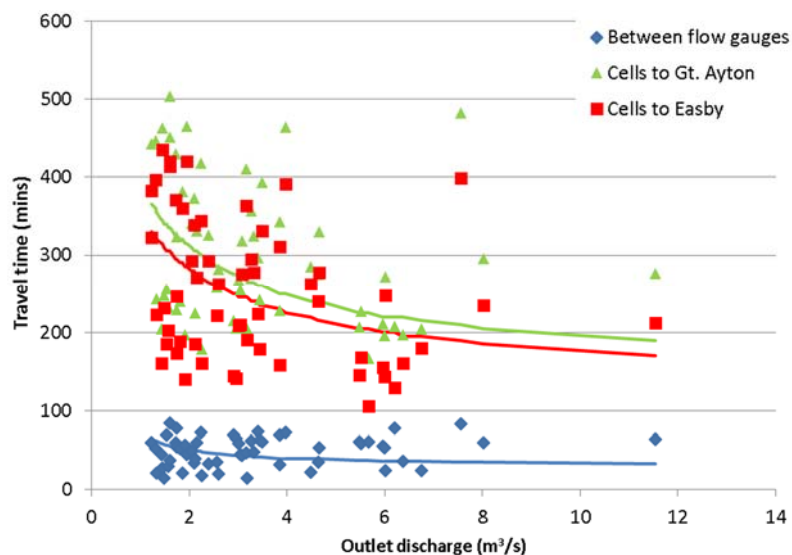


**Figure 3-13 Showing the actual (points) and estimated (line) for three spatial scales; BLUE are results of the travel time from the nested flow gauge to the outlet, RED are the travel times calculated for the average flow path length from the cell to the nested gauge and GREEN from the cell to the outlet**

### ***Runoff generation***

The modeller is able to control how the distributed runoff is generated, specifically how much rainfall is converted to fast runoff and how much goes into the slower storage. In this study the runoff generation element is given the distributed SPR data from HOST, which is based on the national soil maps and is calculated through Equation 3-4. This provides a scalar multiplier that can be applied to the rainfall. This distributed dataset provides the model with information regarding the propensity of different soils to generate different amounts of runoff. This is then routed to the matching element where the matching gain is applied to achieve the observed hydrograph.

As previously mentioned Juke has its own GIS based language which can be used to describe how runoff is generated in a distributed manner. A script for generating the rainfall partitioning factor ( $\gamma$ ) from a HOST GIS file, with each grid cell assigned a parameter as is shown in Equation 3-4. Equation 3-4 creates a distributed rainfall partitioning factor ( $\gamma$ ) by calling the 'host' GIS layer (grid) and populating the 'gam' layer with the appropriate 'spr' values (meta data for HOST). The resultant layer calculated from Equation 3-4 has an average cell value of 1 as it is divided by the average SPR value for the whole of the catchment domain (host . spr AV no\_c).

#### **Equation 3-4**

$$\gamma = (\text{host . spr}) / (\text{host . spr AV no\_c})$$

Changes to LUM or land cover can be applied in the runoff generation element to reflect a change in SPR based on expert knowledge (as in Packman *et al.* (2004). For example, the alternative HOST classes discussed in section 3.7 to reflect degradation can be applied through Equation 3-5. These changes are applied in a distributed way to affect runoff generation at the cell scale on the grid. The runoff is then routed and passed to the matching element where the calibrated matching gain is applied.

#### **Equation 3-5**

$$\gamma = (\text{host . spr} + \text{host . spr\_inc}) / (\text{host . spr AV no\_c})$$

This runoff element is illustrated in Figure 3-14 where the distributed rainfall multiplier calculated by Equation 3-4 in the calibration run is mapped (A) alongside a modified pattern of LUMC where areas under improved grassland have had runoff reduced by 20%. (B) The pattern of reduced runoff is produced using Equation 3-6, where

'improved\_grass' is a binary layer created from the land cover map containing a 1 where improved grassland is present.

Equation 3-6

$$\text{gam} = ((\text{host} . \text{spr}) - \text{gammod}) / ((\text{host} . \text{spr}) \text{AV no}_c)$$

**where:**  $\text{gammod} = (\text{host} . \text{spr}) \times \text{improved\_grass} \times 0.2$

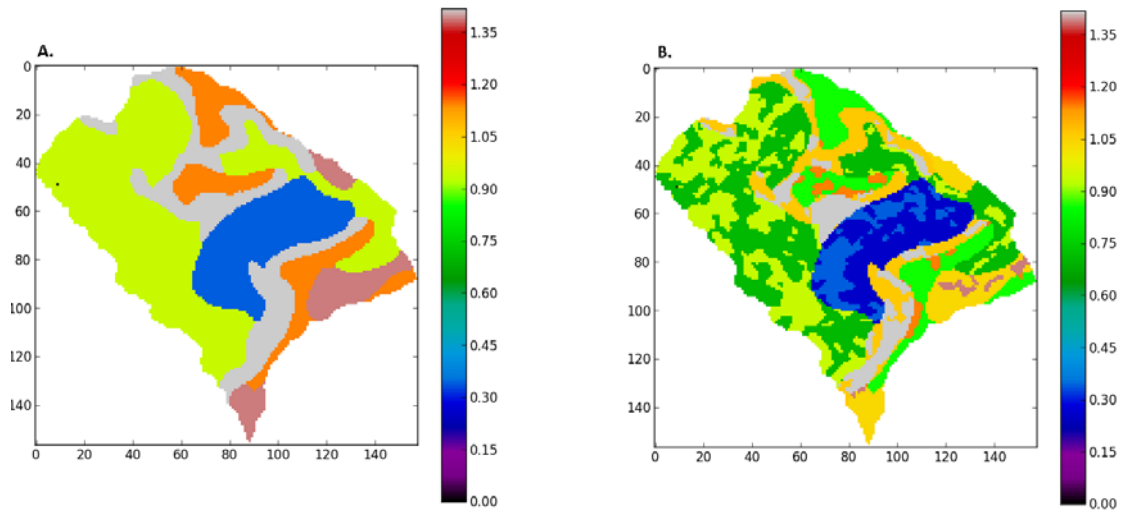


Figure 3-14 A. gam as calculated from HOST (Equation 3-4). B. Modified pattern of gam, where SPR/gam has been reduced for areas within the improved grassland pattern (Equation 3-5)

### ***Extra dynamics***

Storage effects must be accounted for somewhere in the model as the fast routing response alone would make the Juke estimation of fast runoff too responsive. For most storms, a surface storage deficit has to be satisfied when generating fast runoff and the shallow subsurface processes. Each cell on the grid has its own store with a constant linear parameter, *tix*, which controls the outflow. The role of *tix* is to provide the delay in the hydrograph response. Juke is provided with the rainfall (input) and calculates the network travel times from the observed flow records provided. Juke then uses both the input rainfall and travel time information to calculate the fast runoff. The fast runoff generated by the rainfall and travel time goes into a leaky bucket and the rate of discharge from the bucket depends on *tix* as illustrated in Figure 3-15. There is interplay between *tix* and the celerity function as they both affect the speed at which the flood wave reaches the outlet. The greater the *tix* value, the longer the water is held in storage and the faster the maximum celerity required to achieve the observed hydrograph ( $q^*$ ). Increasing *tix* dampens the flood wave response.

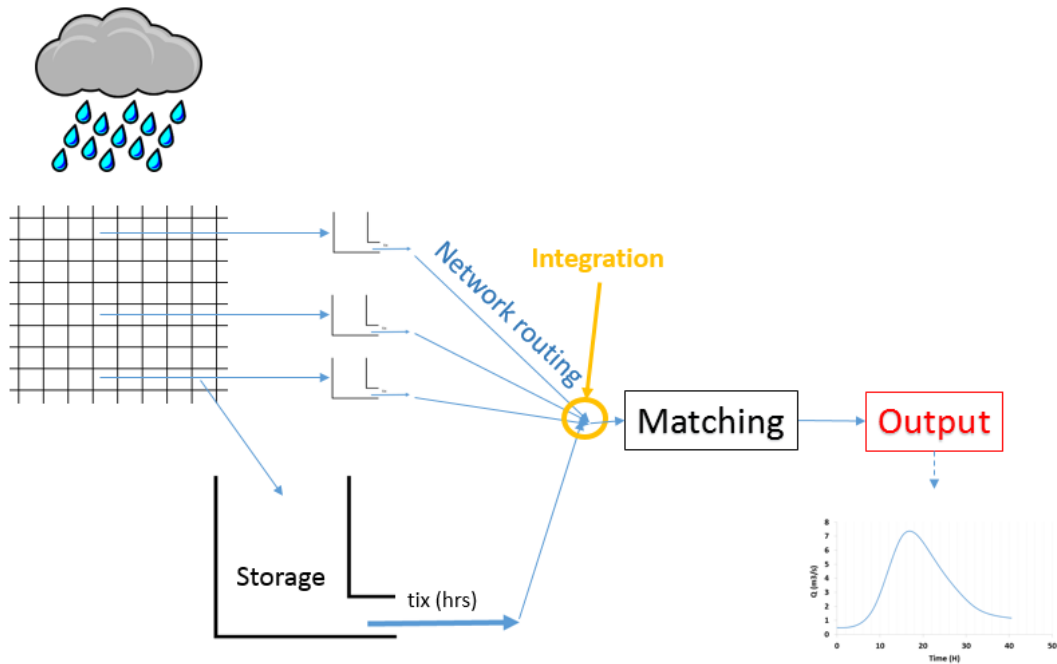


Figure 3-15 Schematic of Juke

### ***Integration***

This simply adds together the flows from each of the cells to produce the outlet hydrograph.

### ***Juke summary***

The lumped and distributed structure of Juke have been detailed and the way in which the observed data are used more directly in calibration than traditional rainfall-runoff models has been described to illustrate the novel aspects of Juke. The three key elements that allow LUM scenarios to be run in a transparent way are the runoff generation, extra dynamics and network routing. Once these have been calibrated using observed data, distributed changes can be applied in a physically reasonable way based upon expert knowledge and observations as highlighted in Chapter 2.

## **3.8 Decision support tool**

Decision support tools offer catchment managers the potential to make informed decisions on the most appropriate type of flood mitigation option to use, and where best in the catchment to focus efforts to gain maximum benefits, given limited resources. The decision makers may not necessarily be hydrologists with an understanding of hydrological processes and the complexities of catchments. However, it is possible to

get some of the key concepts across, for example, how management of soil can affect runoff volumes and the speed at which that runoff is propagated through the catchment.

One such way is through the FARM tool (Wilkinson *et al.*, 2013) which is illustrated in Figure 3-16. It is a risk matrix on to which differing LUM practices can be mapped to illustrate their potential impact on runoff generation, and hence flood risk. The axes have clear relationships with the key components of the FEH model. Soil condition is most appropriately linked with SPR, the assumption being that any improvement in soil condition will reduce SPR and vice versa. The connectivity axes relates to the  $T_p$ , the better connected the landscape is to the river network the lower the  $T_p$ .

The risk matrix will be populated with the percentage change in  $Q_p$  from the baseline, as now, SPR and  $T_p$  model result. The colours used in Figure 3-16 are to highlight the direction in which  $Q_p$  has changed, with green being a decrease, red an increase and yellow somewhere in the middle.

The modelling results of LUM and NFM scenarios will be mapped onto the FARM matrix to show end users what they can do to affect  $Q_p$ . The aim being to encourage the uptake of interventions in local areas that will have a catchment scale impact in reducing flood hazard.

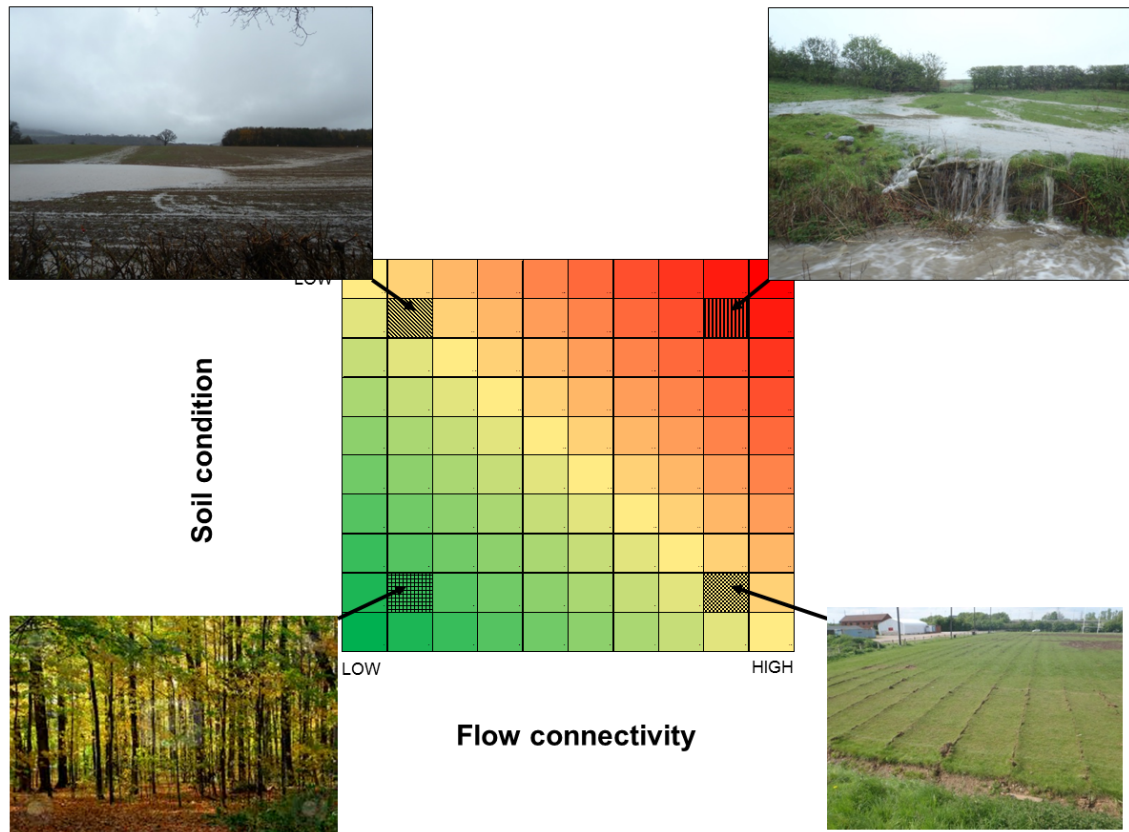


Figure 3-16 FARM tool illustration, lowest flood risk bottom left (green), highest flood risk top right (red)

### 3.9 Summary

#### 3.9.1 Catchments and data

Two catchments in the north of England have been instrumented in a nested structure to develop a distributed understanding of the generation and propagation of floods in the respective catchments. The catchments have been chosen as they are at different spatial scales, Great Ayton at 30 km<sup>2</sup> and Morland at 12.5 km<sup>2</sup> and have different physical and hydrological characteristics. Analysis of GIS data will provide an overview of the topography, soil, geology and land cover to establish an understanding of the hydrological regime and potential flood hazards.

The storm data for both catchments is to be analysed to investigate what rainfall characteristics lead to the largest flood peaks and how different magnitude storms develop. This will aid in suggesting potential mitigation measures that can be adopted in the catchment. The data will also form the parametrisation of the modelling approaches adopted.

### ***3.9.2 Rainfall-runoff modelling***

Two model types have been selected for investigating LUM and NFM impacts on catchment flood risk. One is the lumped FEH rainfall-runoff model and the second, Juke, is a physically based distributed GIS model. The two models have been chosen as they offer contrasting structures but can both make good use of available GIS and hydrometric data for parameterisation for flow generation and propagation. Parameterisation of the models in this way provides a more transparent and tangible link to the physical processes such as propagation of the flood wave and the generation of runoff. This provides a basis for studying flood management impacts despite the uncertainties regarding the parameterisation and in the data being modelled.



## **Chapter 4. Morland catchment characterisation**

### **4.1 Introduction**

This chapter provides an overview of the physical and hydrological characteristics of the Morland catchment. The physical assessment is performed by analysing the patterns of geology, soils, and land cover and is given to provide an understanding of the way in which the catchment is likely to respond to rainfall. The physical assessment also provides an insight into potential land use impacts on runoff generation. A hydrological assessment of observed rainfall and flows for three hydrological years (October 2011 - September 2014), which investigates the link between event rainfall characteristics and flood magnitude is performed. Understanding the rainfall runoff characteristics is of paramount importance for ensuring subsequent modelling is carried out in a suitable fashion as well as potentially identifying the mitigation strategies best suited to the catchment.

The Morland catchment has been instrumented as part of the Eden Demonstration Test Catchments (DTC) project (Owen *et al.*, 2012), a research platform for investigating strategies for mitigating Diffuse Water Pollution from Agricultural (DWPA). Many of the mitigation strategies being trialled will have benefits in terms of flood generation and propagation as they are largely associated with attenuation of overland flows to encourage the deposition of sediment and associated pollutants; including in ditches, on buffer strips and small flood plains.

### **4.2 Catchment overview**

The Morland catchment is located approximately 10 km south west of Penrith and is drained by Newby Beck. An outlet monitoring station (Mor\_out) with an upstream area of 12.5 km<sup>2</sup> is located next to a small caravan park, Figure 4-1. The catchment ultimately drains in to the River Eden, via the River Lyvennet and to the Irish Sea via the Solway Firth. The Eden catchment rainfall ranges from 650 mm in the lowland valleys to 2000 mm in the uplands (Mayes *et al.*, 2006). The long term Seasonal Annual Average Rainfall (SAAR) for Morland, according to the Flood Estimation Handbook (FEH), is 1167mm (see Table 4-1), towards the middle of the range for the Eden catchment.

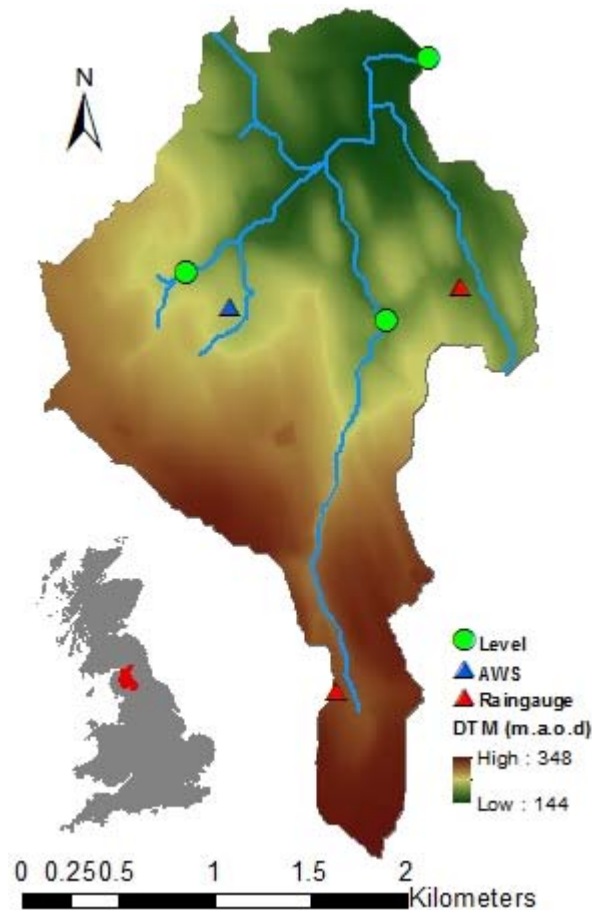


Figure 4-1 Morland catchment elevations with the outlet and substation locations identified

#### 4.2.1 General hydrological statistics

The FEH regionalised statistics provide a summary of both the physical and hydrological attributes of the catchment, Table 4-1. They show that the catchment is predominantly rural with only 0.38 % of the catchment classified as urban.

Standard Percentage Runoff (SPR) is an event-based statistic that describes the typical percentage of rainfall that directly contributes fast runoff to the hydrograph derived from historical events; with a value of 36 %, this is indicative of a high permeability catchment. BFI is a statistic calculated from long-term records and indicates the proportion of the total flow that is made up of baseflow (BFI); a BFI of 39 % suggests that groundwater is a significant hydrological component. Limestone underlies much of the catchment and in many reaches forms the bed of the river channel. The groundwater component is not well understood but hydrological analysis carried out below does provide some insight. The soils in the catchment are generally quite wet with PROPWET of 0.68 indicating that the soils have a low soil moisture deficit 68 % of the time.

Table 4-1 FEH statistics for Morland

<b>Parameter</b>	<b>Description</b>	<b>Value</b>
<b>AREA</b>	FEH catchment area (km <sup>2</sup> )	12.38
<b>ALTBAR</b>	Catchment average altitude (m)	233
<b>DPSBAR</b>	Catchment average slope (m/km)	69.1
<b>URBEXT2000</b>	Urbanised fraction of the catchment	0.0038
<b>FPEXT</b>	Fraction of catchment as floodplain	0.0471
<b>BFIHOST</b>	Baseflow index derived from HOST soil classifications	0.394
<b>PROPWET</b>	Proportion of time when soil moisture deficit is less than or equal to 6mm	0.68
<b>RMED-1H</b>	Median annual maximum 1 hour rainfall (mm)	10.7
<b>RMED-1D</b>	Median annual maximum 1 day rainfall (mm)	39.3
<b>RMED-2D</b>	Median annual maximum 2 day rainfall (mm)	53.1
<b>SAAR</b>	Seasonal annual average rainfall (mm)	1167
<b>SPRHOST</b>	Standard Percentage Runoff derived from HOST soil classifications (%)	35.72

#### **4.2.2 Flood risk**

There are no properties close to the catchment outlet at risk of flooding. However, the road can become impassable to most vehicles during moderate flows and the caravan park, situated on the right hand bank, is in the area with ‘medium flood risk’ (Extent of the 1:100-year event on the EA flood map).



Figure 4-2 The EA risk of flooding from rivers and sea map for the Morland catchment outlet (EA, 2014). (Red dot indicates Morland outlet location)

### 4.3 Physical catchment characterisation

The stream network is being monitored, under DTC, at three key locations, the outlet and two internal sub-catchments. One sub-catchment, the ‘mitigation’ sub-catchment (Mor\_subM - 1.55 km<sup>2</sup>), is undergoing land management changes and interventions to mitigate for diffuse pollution, with the other, (Mor\_subC - 3.4 km<sup>2</sup>) acting as a control, i.e. no intervention (Figure 4-1). This type of monitoring design is a traditional paired catchment approach, which has been discussed previously.

#### 4.3.1 Geology and Soils

At the commencement of the DTC project the British Geological Society (BGS) were commissioned to undertake an assessment of the geology and hydrogeology of all the DTC catchments. The aim of the assessment was to understand the groundwater flow paths and the potential transit times of these flow paths. This section provides an overview of their findings.

The bedrock of the catchment is predominantly interbedded limestone, mudstone and sandstone of the Carboniferous Yoredale group (Figure 4-3). The bedrock has a significant impact on the geomorphology as the bedrock dips to the northeast in the same

direction as drainage and there are a number of dip slopes and scarps created by the more resistant limestone (Allen *et al.*, 2010).

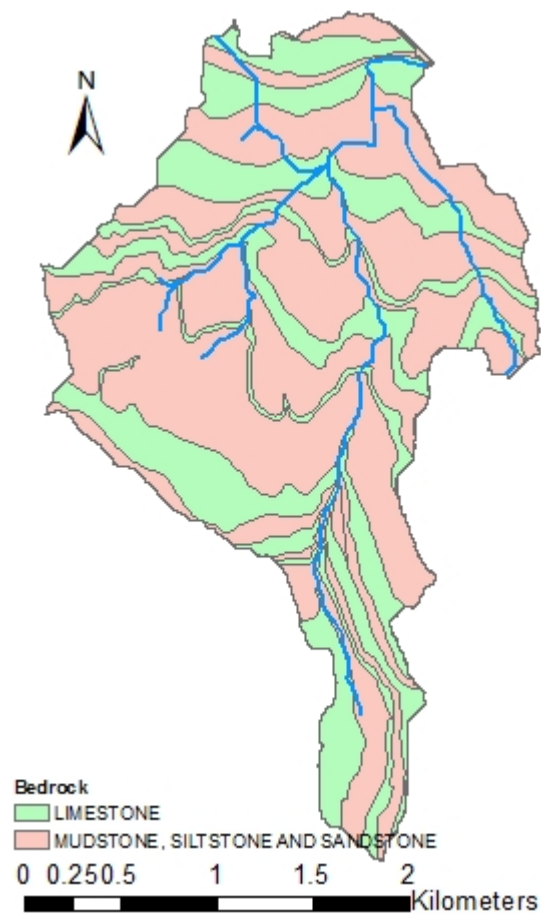


Figure 4-3 Morland bedrock geology

There is a near continuous covering of glacial till across the catchment (Diamicton; Figure 4-4), which is described as slowly permeable and seasonally wet, with the main risks from agriculture being compaction and poaching from machinery and livestock (Soilscapes, 2015). Whaleback drumlins are evident in the northeast of the catchment, just outside the control catchment (Allen *et al.*, 2010).

There are potentially aquifers in the more permeable bedrock units, although it is noted that they are likely to be local to the catchment and unlikely to be losses to regional aquifers.

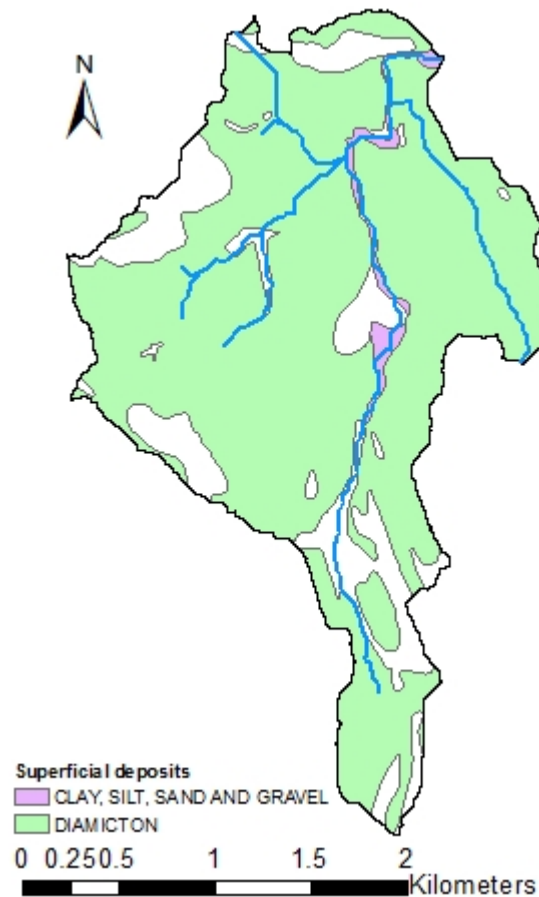


Figure 4-4 Morland superficial deposits

#### 4.3.2 Land use and vegetation

The dominant farming types in the catchment are pastoral with sheep and dairy cattle rearing. This is reflected in the land cover (Figure 4-5), with 87 % of the catchment being grassland of which 71 % is improved (Table 4-2). There is only a small amount of arable farming and woodland in the catchment, accounting for 6 % and 5 %, respectively. The mitigation catchment has a greater area of arable, which may mean more potential for fast runoff from bare soil, particularly if used for autumn sown crops.

Table 4-2 Morland land cover 2007 breakdown

Landover	Full catchment	Mitigation	Control
Improved grassland	70.7 %	65.4 %	82.9 %
Acid grassland	11.0 %	17.9 %	12.5 %
Rough low-productivity grassland	5.3 %		
Arable and horticulture	6.2 %	9.7 %	1.3 %
Woodland	4.7 %	4.7 %	2.7 %
Other	2.2 %		

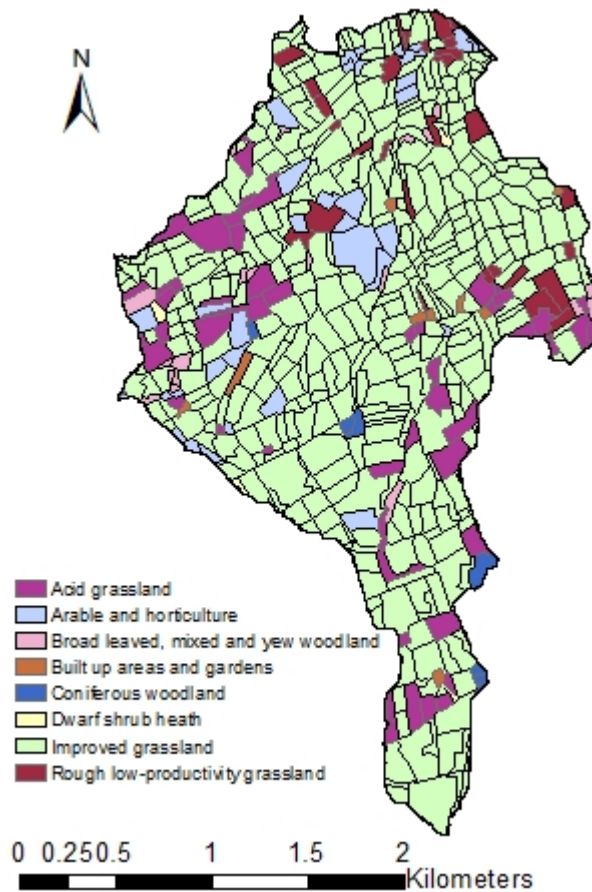


Figure 4-5 Land cover map (derived from the LCM2007 (Centre for Ecology and Hydrology, 2007))

As was discussed in Chapter 2 pastoral farming can potentially increase the onset of runoff generation through compaction and poaching by animals. There is evidence of soil degradation within the catchment (Figure 4-6), where seasonally waterlogged soils have been damaged by dairy cattle. This ‘soft’ data provided by the photographic evidence can be used to validate the behaviour of the distributed models, i.e. are the flow paths and wet areas represented in the right place at the right time (Seibert and McDonnell, 2002).



**Figure 4-6 Evidence of poaching cause by dairy cattle in the Morland catchment**



**Figure 4-7 Increased catchment connectivity with flow on tracks**



## 4.4 Hydrological characterisation

This section provides an overview of the hydrometeorological instrumentation installed and maintained in Morland and a hydrological assessment of the data collected. This is performed to provide an understanding of what rainfall characteristics drive floods and subsequently to provide an insight in to what mitigation methods may be best suited for reducing flood hazard. The installation, maintenance, data archiving and quality control of the hydrometeorological equipment and data was carried out by the author of this thesis as part of the DTC consortium.

### 4.4.1 Rating curve development

A rating curve is required to convert the observed water level series into flow. The rating curves have been developed through the collection of manual stream gauge measurements and the application of VARE (At one site a power function was used due to recording gaps at low flows preventing the required mass balance analysis). One site with no low flow data was fitted a power function. The VARE procedure converts the flows to a volume over the duration of the record (Ewen *et al.*, 2010; Geris, 2012). This volume is then used to evaluate the storage-discharge relationship i.e. whether a reasonable water balance has been achieved for a given timer period, normally a hydrological year. The VARE modelling methodology is used for Mor\_out and Mor\_subC.

The rating curve for Mor\_subM has been created by fitting a power function to the manually gauged flow points. During low flow periods the water level at this location is too low to be recorded by the Diver, hence a mass balance cannot be calculated and therefore a polynomial was fitted. There is a significant groundwater component to this sub-catchment. Only 47 % of the calculated flows for Mor\_subM are within the gauged range as shown in Table 4-3, 52 % of the time the flows are below the minimum gauged flow.

Table 4-3 Summary of rating curve quality

Site	No. of Gaugings	Min. gauged Flow (m <sup>3</sup> /s)	Max. gauged Flow (m <sup>3</sup> /s)	In gauged range (%)	Max. rated Flow (m <sup>3</sup> /s)
Mor_out	14	0.053	3.44	88 %	8.37
Mor_subM	9	0.0064	1.102	47 %	1.736
Mor_subC	7	0.026	1.025	98 %	4.58

The rating curve developed for the outlet is plotted in Figure 4-8; it shows the rating curve against the cross-section (XS) along with the gauged flows. The maximum observed water level is indicated by the solid blue line, whilst the broken blue line indicates the highest manually gauged flow.

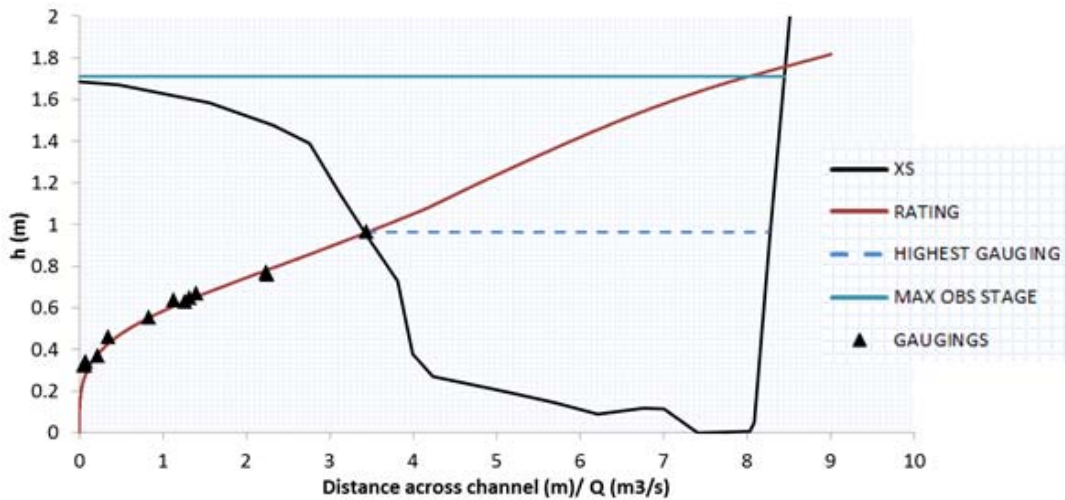


Figure 4-8 Morland outlet rating curve plotted against the cross section

The flow exceedance curves for the Morland gauges are plotted in Figure 4-9; data have been normalised by area to mm/hr to allow comparison between sites. The control catchment generates larger flows than the outlet and mitigation for the top 10 % of the exceedance curves. The outlet and control catchment exhibit similar trends, but the outlet has higher flows in the middle ranges, which may be an indication of the re-emergence of ground water flows. The mitigation catchment shows a much more rapid drop off in the middle ranges of flows and negligible if not zero flow for approximately 17 % of the time. During the driest parts of summer it has personally been observed that there is virtually no flow from the mitigation catchment.

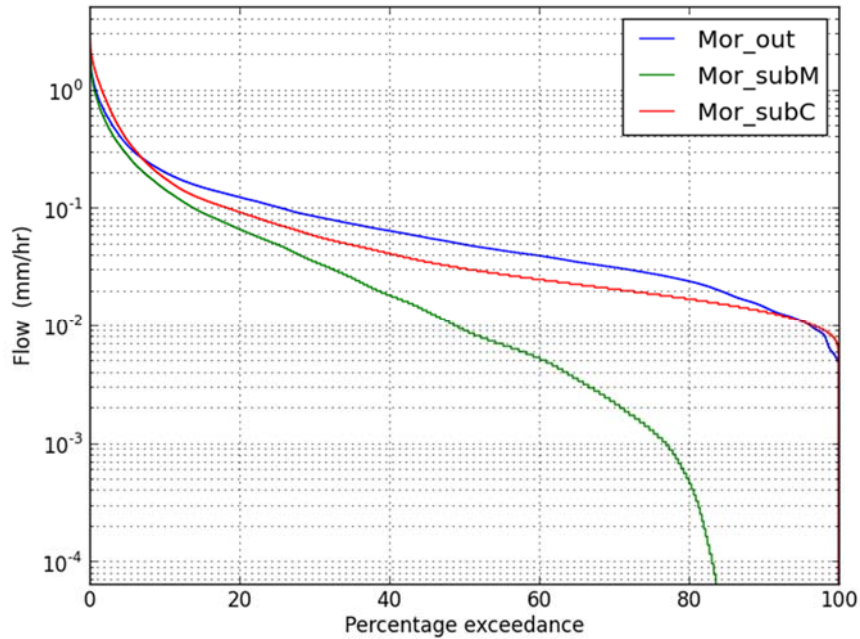


Figure 4-9 Flow exceedance curves for the three Morland gauges

#### 4.4.2 Rainfall runoff

The rating curves that have been developed were applied to the level time series to generate a time series of flows that can be used for rainfall-runoff analysis. Water balances are calculated for data quality assurance purposes and provide further validation of the rating curves. This is performed using Equation 4-1, where S is the catchment storage (mm), P is catchment rainfall total (mm) and E is the actual evaporation (mm). The potential evaporation series is calculated by the VARE model using the Penman-Monteith equation as defined in Food and Agriculture Organisation of the United Nations (FAO) guidelines of (Allen *et al.*, 1998). It is assumed that over a hydrological year the change in storage is low. The results of this analysis are shown in Table 4-4, and illustrate reasonable balance with 4-5 % losses compared to rainfall input in the final two years, with a good balance in the first year. The BFI calculated in the final column was performed using the Institute of Hydrology (IH (Gustard *et al.*, 1992) approach of finding the minimum daily mean flow in a 5 day window which are used to perform the base flow separation.

Equation 4-1

$$\Delta S = P - E - Q$$

where: S = storage, P = precipitation, E = evaporation and Q = discharge (all in mm)

Table 4-4 Rainfall-runoff statistics for Morland outlet for the three hydrological years 2011-2014

Year		P (mm)	Q (mm)	E (mm)	$\Delta S(\text{mm})$	rainfall:runoff	BFI
2011	-	1207.4	762.1	444.1	1.2	0.63	0.44
2012	-	1184.8	776.3	461.2	-52.7	0.66	0.39
2013	-	1468.7	1070.8	478.4	-80.5	0.73	0.40

The annual rainfall-runoff totals for the first two years of monitoring are very similar; however, the temporal distribution of rainfall differs. The cumulative annual total rainfall (solid line) and discharge (broken line) are illustrated in Figure 4-10. The winter of 2012/13 was wetter than that of 2011/12 while the 2011/12 summer (June-September) was wetter (Figure 4-10). The hydrological year 2013/14 was much wetter, largely due to a significant volume of rainfall at the beginning of 2014. Much of the UK experienced a wetter than average January and February in 2014 (Metoffice, 2015).

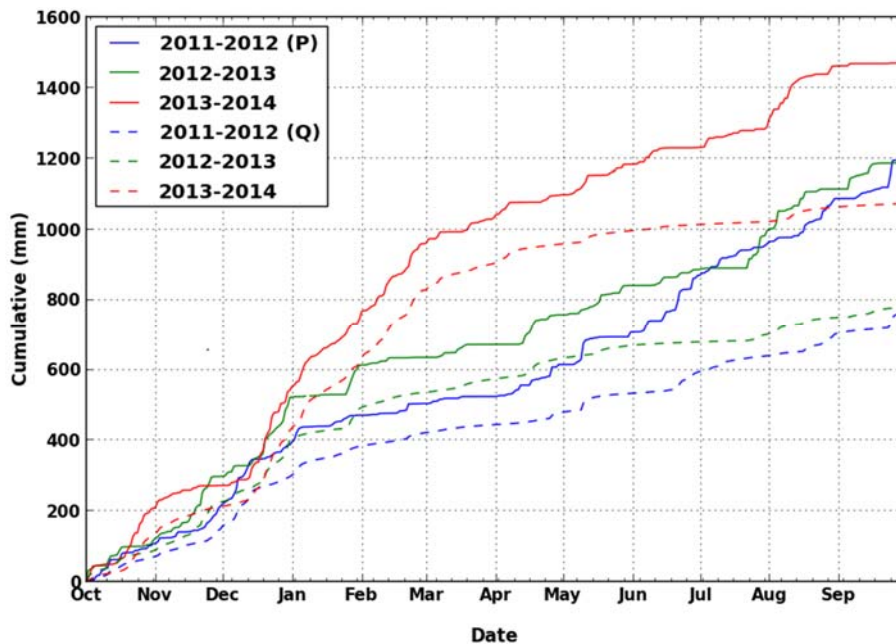


Figure 4-10 Cumulative rainfall and runoff from Morland outlet plots for three hydrological years

### ***Flood peaks and rainfall characteristics***

The following analyses examine how rainfall event characteristics affect the flood peak magnitude; it includes examining the relationships between flood peaks and total storm rainfall, mean storm intensity, maximum storm intensity and finally the storm duration

and total storm length with the circle size corresponding to flood peak magnitude (Figure 4-11).

An algorithm was developed to select event peaks for Morland outlet above a threshold of  $0.5\text{m}^3/\text{s}$ , as described in the methodology chapter. The start and end time of a rainfall event was selected by identifying a window of 4 hours in which there was no rainfall at the beginning and end of a rainfall period. The events selected have also been split into two seasonal categories of ‘autumn/winter’ (blue) and ‘spring/summer’ (red) to provide some indication as to the antecedent conditions. The algorithm selected 150 peaks, with 33 spring/summer and 117 autumn/winter events.

The first plot (top left panel in Figure 4-11) shows that higher storm rainfall leads to a greater flood peak (qp), as expected. The largest peaks coincide with rainfall totals greater than the RMED-1D total of 39.3 mm as detailed in Table 4-1. There does not appear to be any significant seasonal pattern in the plot. However, the role of antecedent conditions is evident with rainfall totals of 30 – 40 mm producing flood peaks between 0.8 mm and the largest event at 2.4 mm.

The top right plot depicts mean storm intensity against flood magnitude and shows that higher mean storm intensity leads to larger magnitude events. Generally, the maximum storm intensities are higher than the average intensity associated with the RMED-1D, 1.64 mm/hr.

In the bottom left plot there also appears to be some seasonal variation with the spring/summer events tending to be of greater intensity. However, there is a weak positive relationship between the peak storm intensity; some of the highest intensity events are of very short duration and therefore do not lead to significant increases in river flow. The rainfall associated with the largest summer runoff event of 2.3 mm/hr has an intensive rainfall component of 38.7 mm/hr (compared to RMED-1H 10.7 mm).

The bottom right plot shows the relationship between total storm rainfall and storm duration, with the circle size reflecting the peak flow magnitude. The pattern is very similar to the intensity versus qp plots, but the seasonal separation is slightly more distinguishable, with the winter events generally being of a longer duration at a lower intensity.

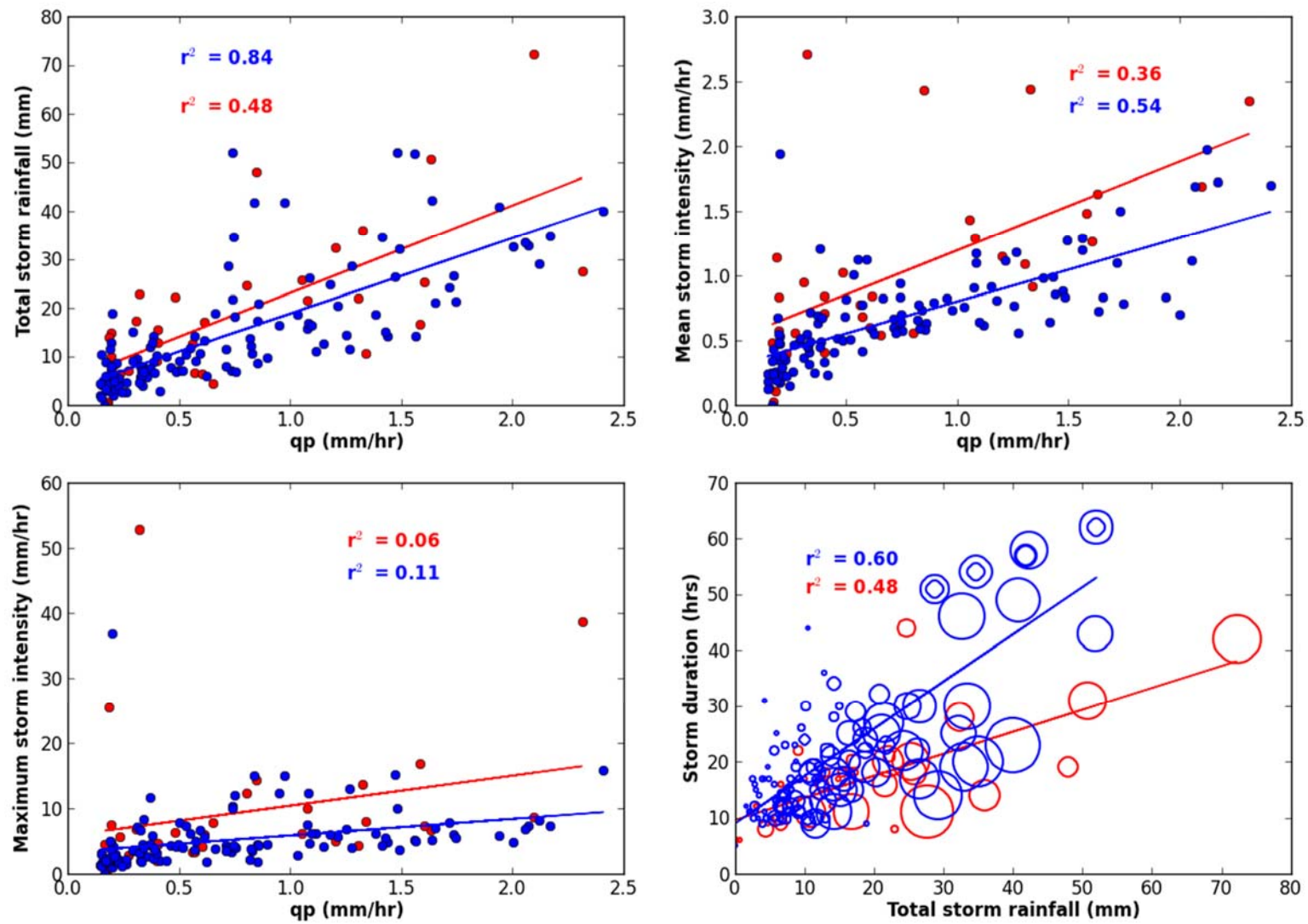


Figure 4-11 Rainfall-runoff relationship, blue indicates winter events whilst the red are summer. Circle size (bottom right) indicates the relative size of the flood peak (qp)

The data plotted in Figure 4-12 illustrates the relationship between runoff as percentage of rainfall against flood peaks. Generally, there is an increase in the amount of runoff as a percentage of rainfall with event magnitude but it is non-linear with the 5 largest events having runoff ratios of around 50 %. There is significant scatter in Figure 4-12, to some extent this is due to the rainfall measurement under estimating the catchment average rainfall for those above the general trend and over estimating for those below the trend; although antecedent conditions are highly likely to be a factor.

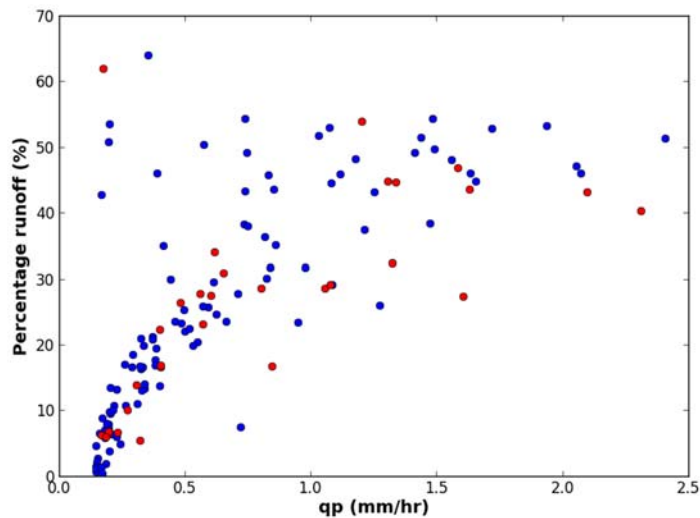


Figure 4-12 Percentage rainfall as runoff for events to Morland outlet, blue indicates winter events whilst the red are summer

To demonstrate the effect of antecedent conditions the API5 for each peak has been calculated and plotted in Figure 4-13. The scatter is considerable, especially for the smaller peaks where API5 values range from 4 to 22 mm can causing equal sized peaks.

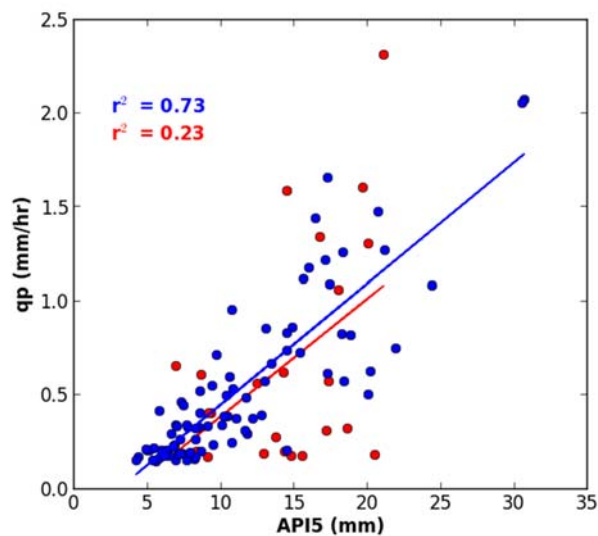


Figure 4-13 Flood peaks versus the API5, antecedent index, for Morland outlet

A set of hydrographs for a large autumn event are plotted in Figure 4-14. They illustrate that the smaller spatial scales have a higher propensity to generate runoff than the larger outlet, with the flood peaks at the sub catchments being close to the peak rainfall intensity of approximately 4 mm. The sub-catchments have peaks similar to the peak rainfall intensity, but the outlet is dampened.

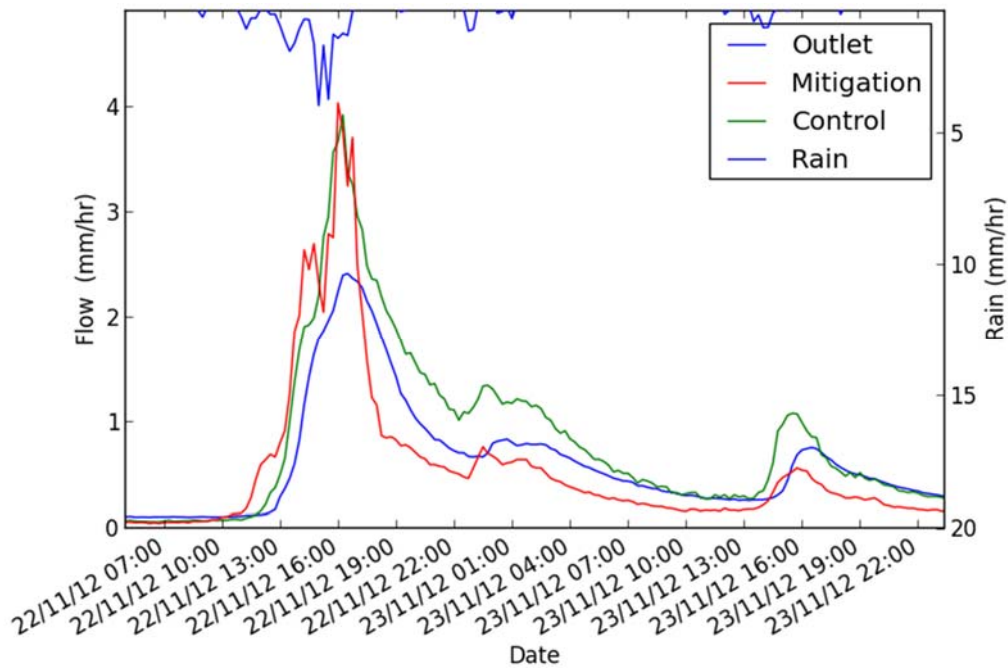


Figure 4-14 A set of hydrographs for the three monitoring points in Morland illustrating the difference in response with spatial scale

### ***Network routing – Travel time and celerity investigation***

There are a number of ways in which the speed of flood wave propagation in a catchment can be assessed. A common method is to investigate the catchment lag, which is the time between the centroid of the rainfall and the peak flow. The FEH method for estimating time-to-peak ( $T_p$ ), is performed by analysing the lag between the centroid of a rain event and the flood peak and calculated using Equation 4-2. This is being highlighted here as it will be used in later modelling chapters.

Equation 4-2

$$T_p(0) = 0.879 \text{ lag}^{0.951}$$

The analysis of lag times is shown in Figure 4-16. There is a difference in lag for summer and winter events, with the winter having a mean lag time of 6.25 hours and the summer being quicker at 4.8 hours. This is likely to be due to the longer duration rainfall events



observed during the winter as illustrated in Figure 4-15, where two events, a summer and winter have been plotted so that the rainfall starts at the same time. The different characteristics of the summer and winter rainfall are evident in the duration and maximum intensity and what effect this has on the corresponding time to peak. The overall average lag time is 6 hours which when calculated gives a time to peak of 4.75 hours. This analysis is useful in lumped modelling such as the FEH rainfall-runoff model which is used in chapter 5. The  $T_p$  of a catchment is an integral part of the unit hydrograph calculation.

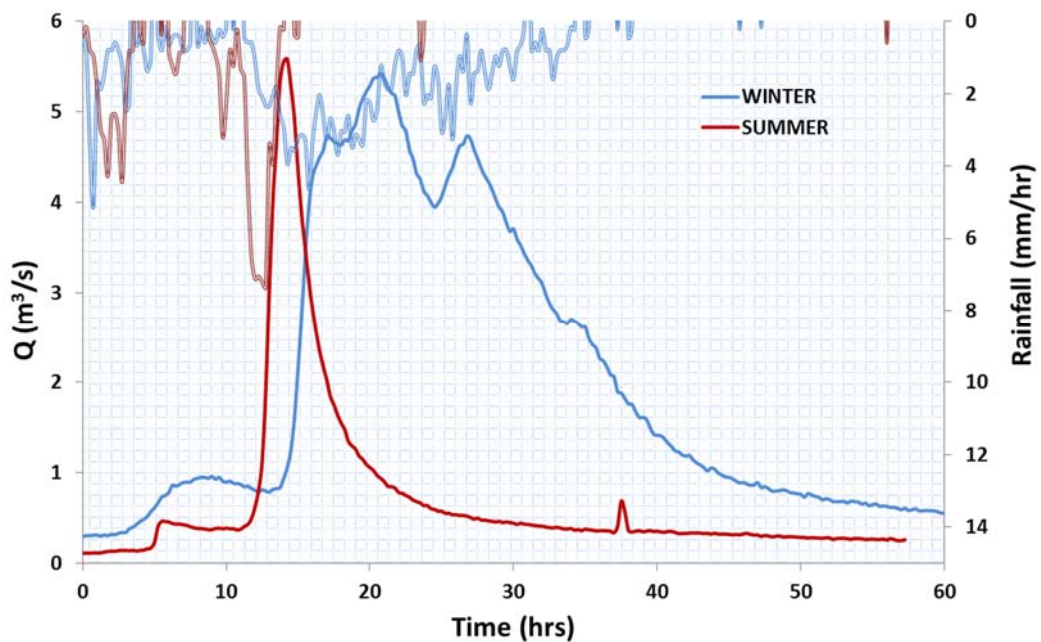


**Figure 4-15 A summer (18/05/2012) and winter (20/12/2012) event, illustrating the difference in rainfall duration and intensity and what effect this has on the corresponding time to peak and flood hydrograph**

The data in Figure 4-16 indicates that the catchment does not always respond in a synchronised manner. If the catchment were always well synchronised it would be expected that the lag time would be similar for events. However, as is indicated in Figure 4-18 not all regions of the catchment are equally as active in all storms, which is largely due to the spatial-temporal variability in the rainfall.

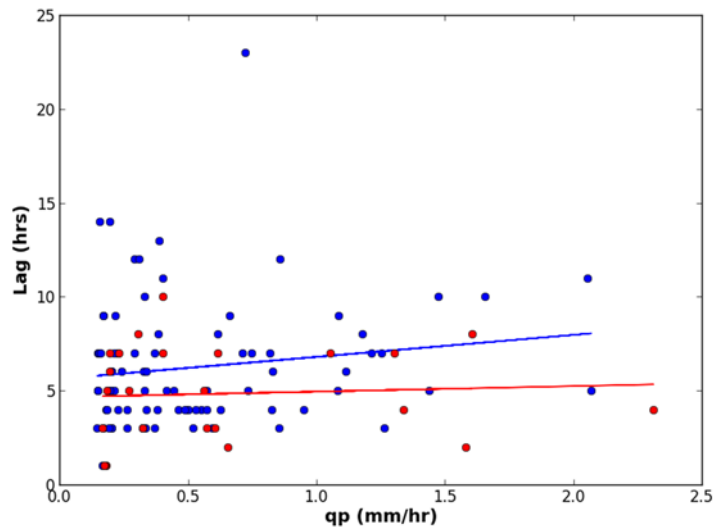


Figure 4-16 Storm peak against the lag from rainfall to flood peak; red dots are spring/summer, blue dot autumn/winter

For modelling floods in a distributed way it is important to understand how floods are generated and propagate through the stream network. Using observed data this can be performed by carrying out a peak-to-peak analysis of the outlet versus upstream gauges to understand the flood wave celerity for different magnitude storms. Celerity is the speed of the flood wave as it moves through the catchment and is not the same as the instream water velocity, meaning it cannot be measured at a single location; here it is inferred from peak to peak analysis between the outlet and nested gauges. The celerity relationships for the sub-catchments to Morland outlet are shown in Figure 4-17, with the larger events appearing to have similar celerities of between 1-2 m/s. These findings are similar to those found for other upland catchments in the UK of similar area where celerity was found to asymptote to 1-1.5m/s (Beven, 1979).

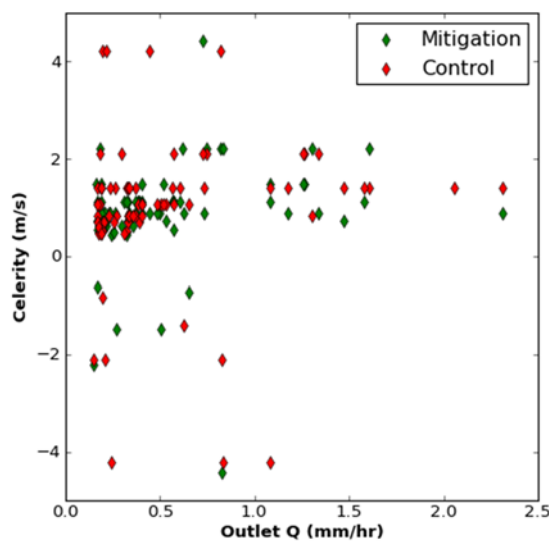


Figure 4-17 Celerity relationships between the two Morland sub-catchments and Morland outlet

Figure 4-17 displays considerable scatter, particularly for the smaller events, likely due to spatial and temporal distribution of the rainfall across the catchment. Events with a negative celerity are those where the outlet peaked before the sub-catchment. This result shows a low level of synchronisation between different parts of the catchment. This is illustrated in Figure 4-18, which shows the relative ranking of the sub-catchment peaks against the outlet and is a measurement of activity, with the dots above the 1:1 line indicating the sub-catchment was more active (wetter) than the catchment as a whole and below the line less so (drier). If the catchment behaved in a completely homogeneous way with all parts contributing the same amounts of flow at the same rate the relationship would be 1:1. However, this is not the case and spatial and temporal rainfall heterogeneity effects the sub-catchment contributions.

As event magnitude increases the rank of the sub-catchment peak magnitude matches much better with the outlet rank. This indicates that the two sub-catchments are behaving in a similar way. As discussed earlier (and shown by Figure 4-11), these larger events tend to be of longer duration with greater volumes of rainfall, the results in this section also indicate that they are catchment wide.

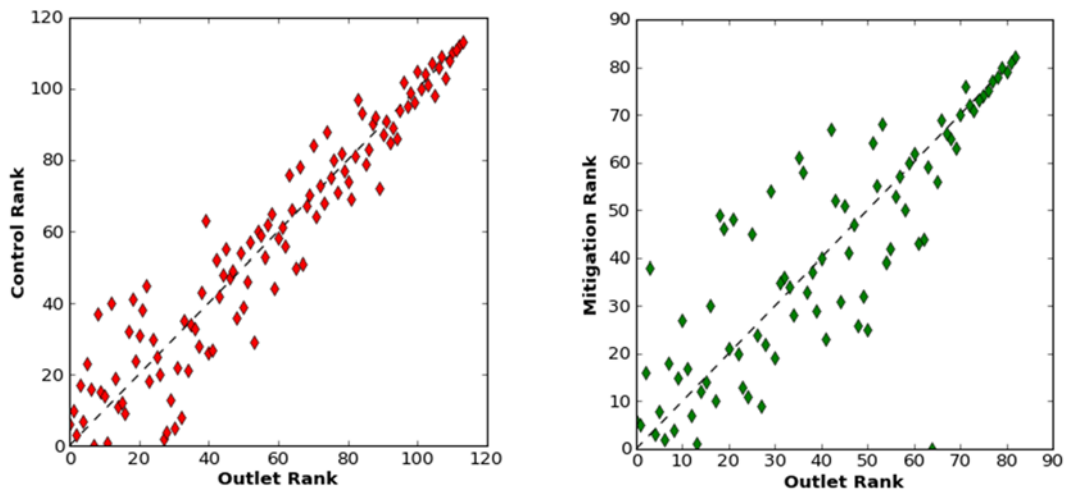


Figure 4-18 Ranking of sub-catchment peak magnitudes against the outlet ranking

#### 4.5 Mitigation approaches

The Eden DTC is predominantly concerned with reducing DWPA and the mitigation options adopted reflect that. This section discusses the mitigation features adopted in the catchment and some of the land management options being trialled. The mitigation options include:

1. Management of farm yard runoff to separate clean and dirty water (i.e. rainfall that falls on roofs compared to that, that falls on the yard.)
2. Runoff attenuation features as sediment traps
3. Aeration of the soil to improve the physical status of the soil and reduce compaction
4. Reduce connectivity by managing track flows

The options listed at 2 and 3 will be discussed below. The option of separating clean and dirty water is likely to have negligible effects on runoff volume and speed but point sources are important for tackling pollution. The clean water is routed directly to the channel via a land drain. The reduced runoff from the farmyard is routed to a ditch that joins the main channel but has an online barrier to encourage sedimentation, through attenuating the flow.

#### ***4.5.1 Runoff Attenuation Features (RAFs)***

As was discussed in Chapter 2, RAFs are designed to attenuate flows by either; storing water in channel (on line) or intercepting overland flows (off line) and reducing the connectivity to the channel. Examples of two different types of offline features are shown in Figure 4-19 and Figure 4-20. The feature shown in Figure 4-19 collects flow from an agricultural track, shown in Figure 4-7 and diverts it into an off line feature that consists of three consecutive retention ponds for sediment removal that eventually discharge to a ditch (Plotted as ‘a’ in Figure 4-21).



**Figure 4-19 Photo of track runoff diversion in to a RAF**

The feature in Figure 4-20 captures overland flow from several fields and attenuates the flow before discharging to a ditch (Plotted as 'b' in Figure 4-21).



**Figure 4-20 Photo of a RAF capturing overland flow**

These features have been constructed in the headwaters to deal with ephemeral, overland flows. The locations of the features are plotted in Figure 4-21 on the topographic wetness index (TWI) map which highlights the flow pathways.

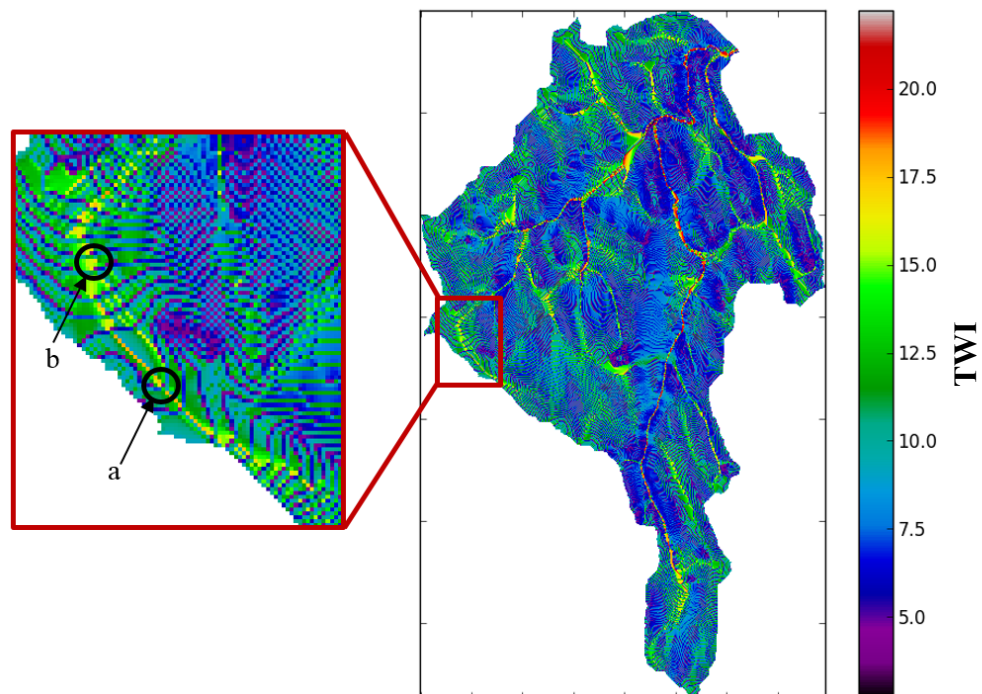


**Figure 4-21 Morland mitigation features plotted on the topographic wetness index map (The higher the TWI the greater the concentration of upstream flows).**

No data are yet available regarding the hydraulic behaviour of the ponds, however it will be in the near future as they being fitted with flumes at the inlets and outlets to quantify flow rates accurately.

There are a total of six offline leaky features in the mitigation catchment which provide an estimated total storage of 561 m<sup>3</sup>, which is equivalent to a rainfall depth of 0.04 mm when compared to the total catchment area. The dams are leaky in that water is discharged at a slower rate than it flows in from the stream during an event and they draw down once the event subsides..

#### ***4.5.2 Sward lifting (aeration) - Land use management***

A trial has been carried out to investigate the potential for reducing soil compaction through a soil aeration process called sward lifting Figure 4-22. The aim of this process is to improve the soil structure by reducing the bulk density (mass per unit volume) and therefore increase the pore space. The hydrological benefit of this process is increased storage within the soil and potentially improved infiltration, therefore less, fast overland flow generated. The process involves pulling the sward lifter behind a tractor which creates three incisions into the soil with the objective being to fracture the soil



**Figure 4-22 Photo of the sward lifting hardware used on the Morland catchment**

Two plots used for silage production were used in the DTC study, one underwent the sward lifting procedure and the other remained untreated to act as a control. The plots were assessed for the soil bulk density which showed a reduction of on average 1 g/cm<sup>3</sup> within the top 15 cm of the soil in the sward lifted areas but it was not deemed significant

when compared to a similar result in the control plot. Significantly greater yields of silage were, however, harvested from the plots that had undergone sward lifting. This may anecdotally indicate increased nutrient uptake due improved soil moisture conditions including larger and more connected pore spaces (Lipiec and Stpniewski, 1995; Hamza and Anderson, 2005).

## **4.6 Discussion**

The Morland catchment has been instrumented with a hydrometeorological monitoring network to understand the rainfall-runoff dynamics. This is required for the purpose of quantifying the potential change in the rainfall-runoff regime and the associated pollutants caused by mitigating for DWPA in the Morland catchment.

### ***4.6.1 Rainfall-runoff response***

The mitigation catchment has significant losses to ground water during the flow periods when compared to the outlet and control catchment as shown in the flow exceedance curves (Figure 4-9). The physical characterisation section highlighted that there is a considerable groundwater component to the hydrology of the catchment with a BFI of 0.39.

Analysis of the rainfall runoff records have shown that key drivers of the large flood events is the total rainfall volume and the mean storm intensity (Figure 4-11). The largest events tend to have a mean storm intensity of 1.5 to 2 mm/hr and the two largest events have a high maximum intensity above the annual average as estimated from the FEH of 10 mm/hr. The second largest summer event had a peak rainfall intensity of 72 mm/hr. The catchment has been shown to be flashy, i.e. there is a rapid runoff response, especially at the smaller sub catchment scale (Figure 4-14). As has been demonstrated the rainfall intensity is a key driving factor in the magnitude of the flood peaks.

There is evidence of seasonal effects, with winter events tending to be longer duration and less intense. This tends to mean that these events have longer lag to the flood peak (Figure 4-16). Higher mean rainfall intensities are observed for the larger events (Figure 4-11) and the summer tends to have more intense, shorter duration storms. The fact long duration, low intensity events are capable of producing the same magnitude flood peaks as high intensity, short duration events, fast, overland, runoff may be generated by both infiltration and saturation excess mechanisms.

It has been demonstrated that within even a modest sized catchment that there can be considerable variability in the generation of runoff, due to geology and soils. Figure 4-18 shows that the largest events happen when the whole of the catchment is similarly active, i.e. all parts of the catchment are generating equally large volumes of runoff, as the ranking of the flood events are increasingly similar at the outlet and nested gauges. The largest events at the outlet correspond to the largest events at both the sub-catchments. The scatter in the relative ranking of event between the sub catchments and the outlets can be linked to local antecedent conditions (ground water effects in the mitigation), and spatial and temporal patterns of the rainfall.

#### **4.6.2 Flood risk**

The caravan park on the right hand bank have not report issues of flooding, however, the road close to the park is impassable during moderate events ( $\sim 3 \text{ m}^3/\text{s}$ ) which can be an inconvenience. This type of event occurs several times a year and may benefit from NFM or LUMC in reducing the frequency.

#### **4.7 What next?**

The length of data records make statistical appraisal of change unfeasible. Understanding the likely impacts of any mitigation work will require modelling. Key modelling parameters such as the time to peak and flood wave celerity relationships have been derived from observed data and will be used to inform the modelling. The modelling to be undertaken will explore a number of potential future LUM and NFM scenarios including the use of RAFs and the management of track flows for attenuating overland flows.

Key data and results from this chapter that are used in the following chapters for model calibration and parametrisation are:

- Calculated time to peak value used to parametrise the FEH rainfall-runoff model in Chapter 6.
- Observed flow series for Morland outlet (Mor\_out) and the control catchment outlet (Mor\_subC) to be used in the calibration and parameterisation of the celerity function within the Juke rainfall-runoff model (Chapters 8).



## **Chapter 5. Great Ayton catchment characterisation**

### **5.1 Introduction**

The town of Great Ayton, North Yorkshire, has suffered a number of flood events from the River Leven in recent decades. Since 2012 the EA has implemented a flood mitigation scheme that involves a combination of flood proofing properties and constructing features within the upstream catchment, designed to attenuate and reduce peak flows. Newcastle University is monitoring the catchment at a number of locations, to characterise the catchment response and to understand the impact of small scale features at the catchment scale.

This chapter provides an overview of the physical and hydrological characteristics of the Great Ayton catchment. A description of the geology, soils, vegetation and land use is given to provide an understanding of the way in which the catchment is likely to respond to rainfall. This is supplemented by a hydrological assessment of observed rainfall and river flow, which examines the link between rainfall characteristics and flood magnitude. Rainfall-runoff data are available from two sources for this catchment. The EA have two river level gauges at Easby and Great Ayton, and two rain gauges used for flood warning and forecasting purposes (Figure 5-1). This is complemented by 7 in-stream level gauges, at various scales, maintained by Newcastle University. The EA also have data available for downstream locations which are used for a discussion regarding the effects on catchment scale and hydrological response.

### **5.2 Catchment overview**

Great Ayton lies within the River Leven catchment. The catchment to the EA level gauge in Great Ayton (henceforth referred to as the Great Ayton catchment) is 30 km<sup>2</sup>, which occupies approximately 18 % of the 168 km<sup>2</sup> Leven catchment. The river rises on Warren Moor to the south east of Kildale and enters the Tees between Yarm and Ingleby Barwick. The elevation of the Great Ayton catchment ranges from 395 m on Battersby Moor in the south, to 84 m at the outlet (Figure 5-1).

The catchment is naturally divided into two tiers with a step running through the middle where the relief is slightly steeper. This steeper section coincides with the interbedded sandstone and ironstone geology, whilst the flatter areas are largely mudstone (Figure 5-3).

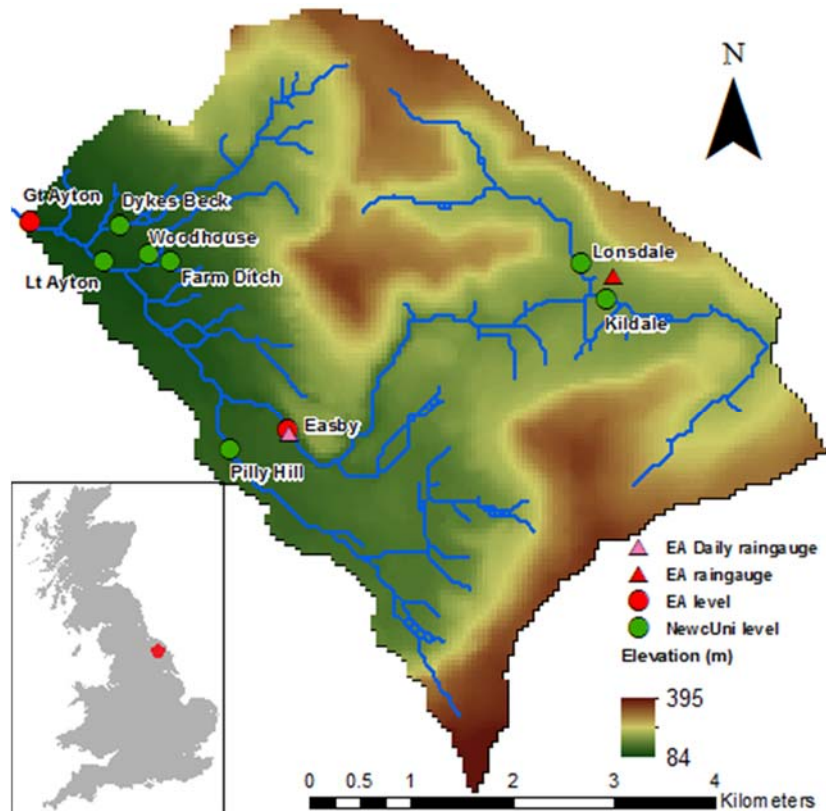


Figure 5-1 Elevation map for the Leven catchment to Great Ayton (© Crown Copyright/database right 2016. An Ordnance Survey/EDINA supplied service)

### 5.2.1 General hydrology statistics

The long term Seasonal Annual Average Rainfall (SAAR) for Great Ayton, according to the Flood Estimation Handbook (FEH), is 805 mm (Table 5-1). The majority of weather in the UK is driven by North Atlantic frontal depressions, with associated westerly and south-westerly winds, meaning that western parts of the country tend to receive greater rainfall totals, with less in the east due to a rain shadow effect caused by the Pennine Hills (Sweeney and O'Hare, 1992).

A Baseflow Index (BFI) of 44 % suggests that groundwater is a significant hydrological component of long term flows of the River Leven. The SPRHOST values are also relatively high, with a value of 41 %; 5 % greater than the Morland catchment (Chapter 4).

Table 5-1 FEH statistics for Great Ayton

<b>Parameter</b>	<b>Description</b>	<b>Value</b>
<b>AREA</b>	FEH catchment area (km <sup>2</sup> )	30.17
<b>ALTBAR</b>	Catchment average altitude (m)	195
<b>DPSBAR</b>	Catchment average slope (m/km)	123
<b>URBEXT2000</b>	Urbanised fraction of the catchment	0.0123
<b>FPEXT</b>	Fraction of catchment as floodplain	0.0301
<b>BFIHOST</b>	Baseflow index derived from HOST soil classifications (%)	0.443
<b>PROPWET</b>	Proportion of time when soil moisture deficit is less than or equal to 6mm (mm)	0.36
<b>RMED-1H</b>	Median annual maximum 1 hour rainfall (mm)	10.4
<b>RMED-1D</b>	Median annual maximum 1 day rainfall (mm)	37.2
<b>RMED-2D</b>	Median annual maximum 2 day rainfall (mm)	50.9
<b>SAAR</b>	Seasonal annual average rainfall (mm)	805
<b>SPRHOST</b>	Standard Percentage Runoff derived from HOST soil classifications (%)	40.68

### **5.2.2 Flood risk**

There are three main sources of flooding in Great Ayton (see Figure 5-2). Primarily the properties within the Great Ayton catchment affected by flooding are in the village itself. The other two sources are both tributaries that join the River Leven within the village of Great Ayton, which can also overtop and affect properties. Dikes Beck overtops and spills on to Station Road when the culvert is surcharged; the flood water runs down Station Road affecting properties at the bottom of the slope as well as School Lane and Old Mill Wynd. A second small stream just to the north affects properties on High Street, again due to the surcharging of a culvert.

Flooding in September 2000 affected 70 properties. The most recent flood event occurred on the 16<sup>th</sup> November 2009 when 5 properties were affected. From personal communication with consultants at Jeremy Benn Associates (JBA), it is suggested that the return interval of events that cause inundation to properties is between 5 and 10 years, estimated from an FEH, pooled, flood frequency analysis.

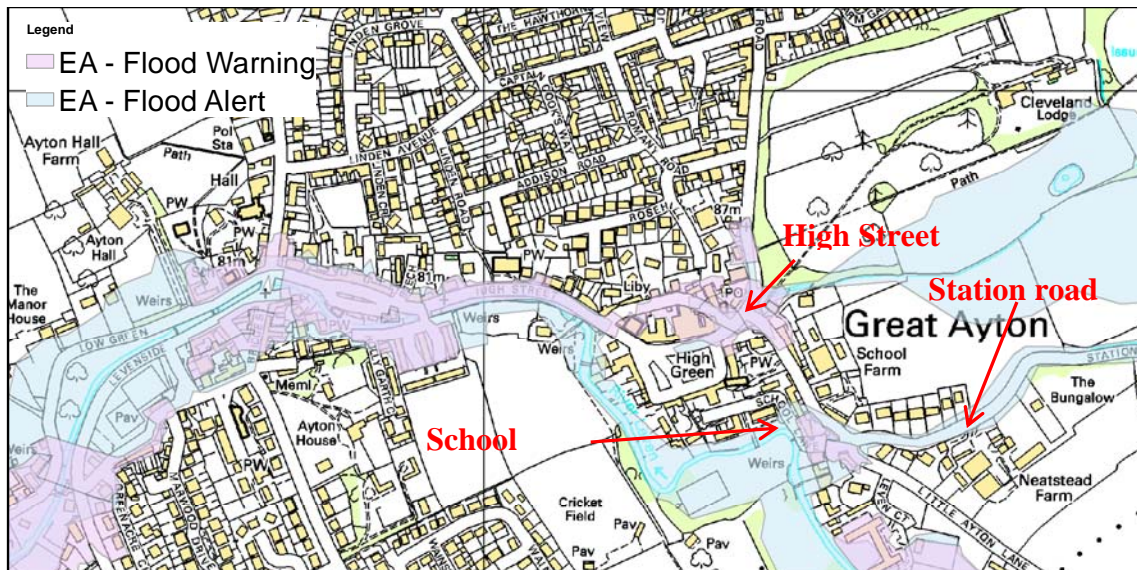


Figure 5-2 EA Flood Map for the Leven at Great Ayton (Contains public sector information licensed under the Open Government Licence v3.0; © Crown Copyright/database right 2016. An Ordnance Survey/EDINA supplied service)

### 5.3 Physical catchment characterisation

This Section provides an overview of the physical characteristics of the Great Ayton catchment, including the geology, soils and land covers.

#### 5.3.1 Geology

The geology of the Great Ayton catchment is shown in Figure 5-3. The upper part of the catchment is a mixture of mudstone, sandstone and siltstone, whilst the lower parts, and those of lower relief, are predominantly mudstone (green). The steeper, hillslope faces are interbedded sandstone and ironstone (orange and red). There is a small outcrop of the igneous, basaltic-andesite running from northwest to east (purple strip). The mudstones and ironstones are described as having some but not significant amounts of groundwater (Jones *et al.*, 2000). The sandstones, however, are described as having some potential as aquifers (Jones *et al.*, 2000).

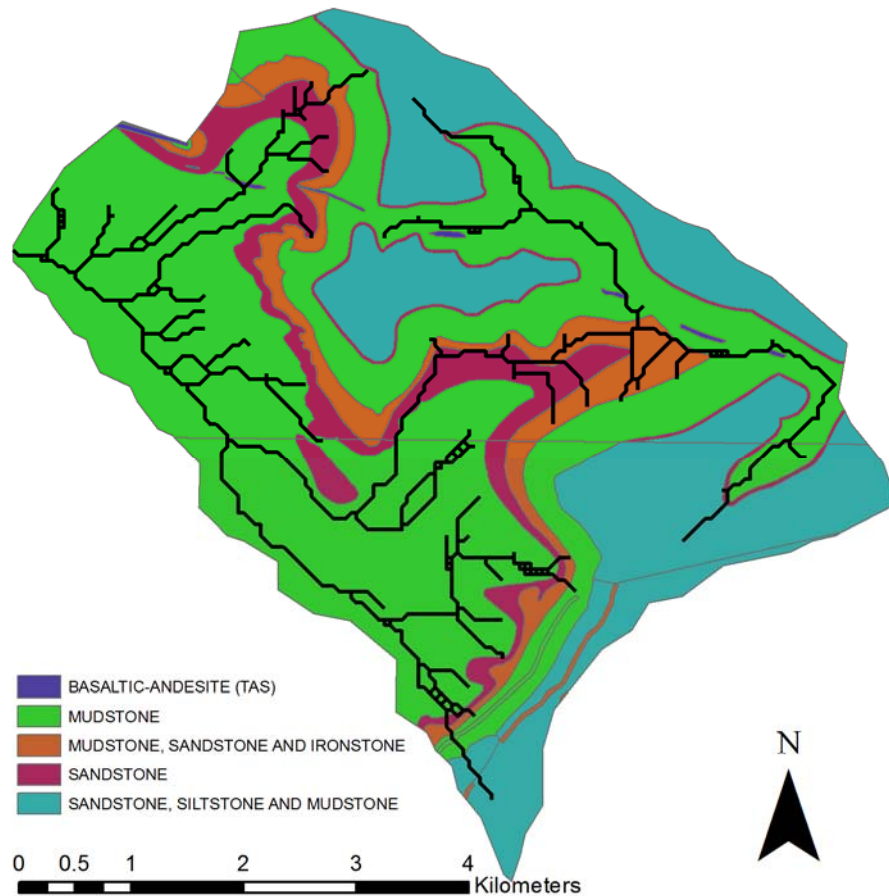


**Figure 5-3 Geology of the Great Ayton catchment (Crown Copyright/database right 2016. A British Geological Survey/EDINA supplied service)**

Superficial geology is shown in Figure 5-4, with Devensian glacial deposits accounting for the majority of the coverage, particularly in the valley bottoms and sides. There are also Alluvium deposits in the riparian zones of the lower half of the catchment (there are no superficial deposits in the white areas of Figure 5-15).

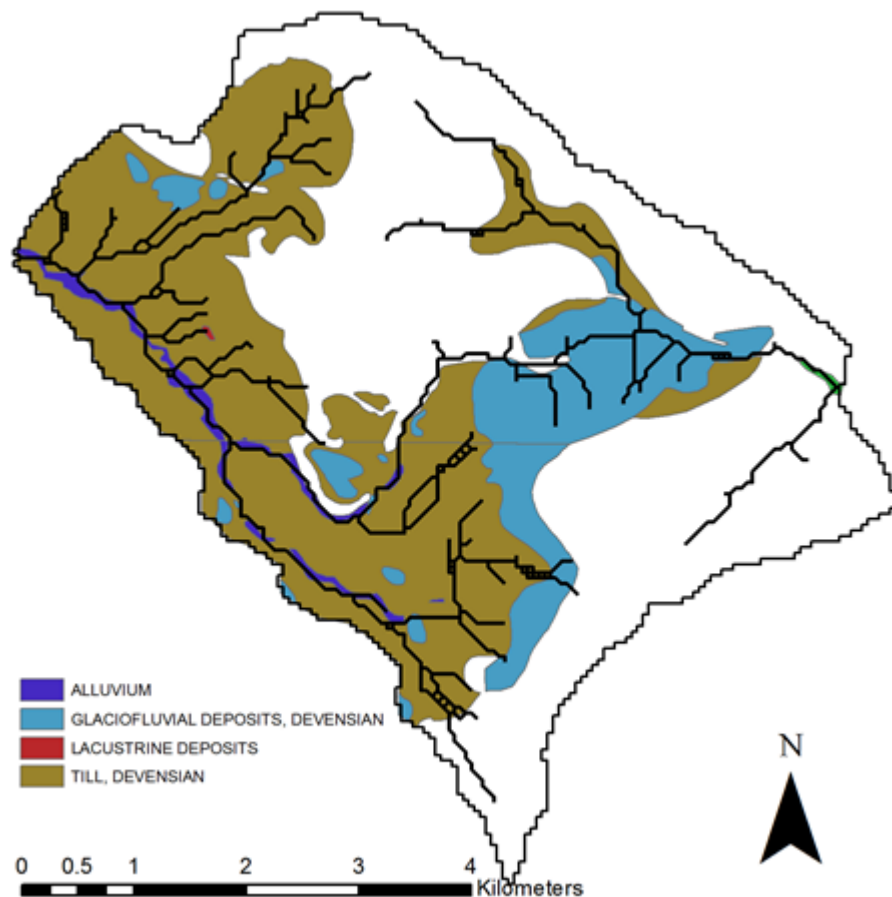


Figure 5-4 Superficial deposits (Crown Copyright/database right 2016. A British Geological Survey/EDINA supplied service)

### 5.3.2 Soils

A summary of the soil associations found in the Great Ayton catchment is provided in Figure 5-5 and Table 5-2. There is a marked difference in the soil found in the lower part of the catchment, predominantly Dunkeswick, which overlays much of the mudstone that lies beneath (Figure 5-3); whereas the upper parts of the catchment consist of a mixture of glaciofluvial deposits and organic peaty soil, which overlies the sandstone, mudstone and siltstone.

The information provided in Table 5-2 is taken directly from the National Soil Maps and associated data tables. There are 6 soil types that fall into two broad categories of slowly permeable clayey soils, making up 71% of the catchment. These clayey soils are found largely in the valley bottoms whilst the acidic organic soils, which make up the remaining 29 % are found on the higher and peripheral parts of the catchment. As a result of the slowly permeable nature of the soils, it is likely that land used for the rearing of livestock will require underdrainage or improving, this discussed further in this chapter.

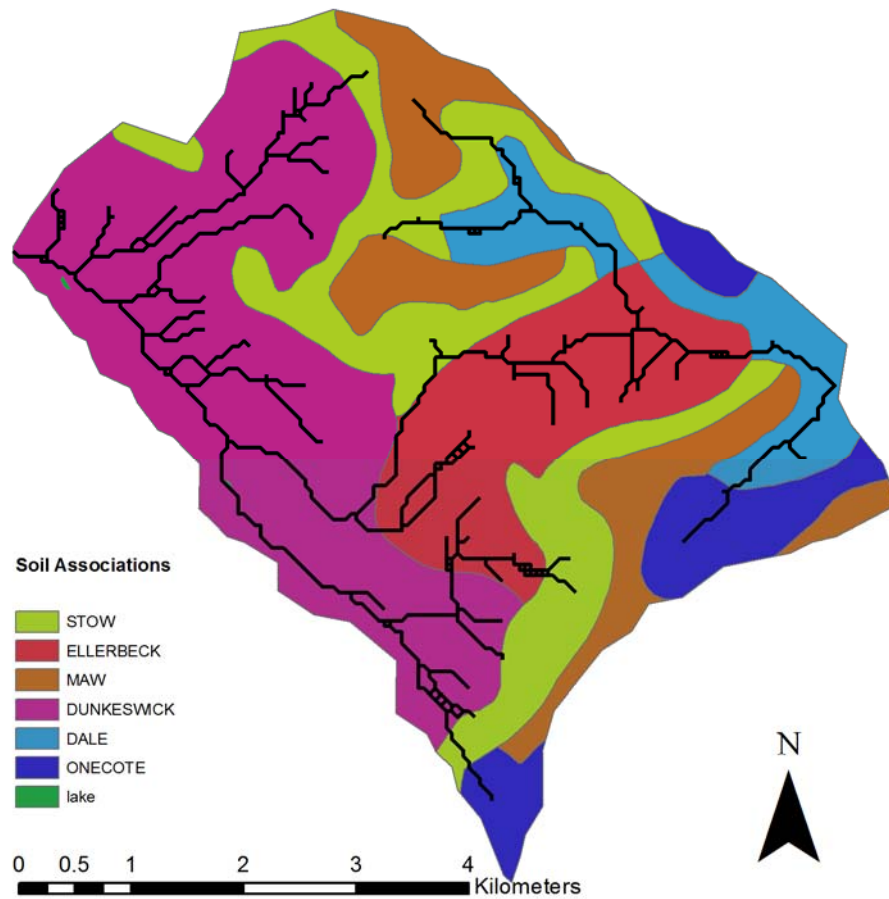


Figure 5-5 Soil Associations (Soil data © Cranfield University (NSRI) and for the Controller of HMSO 2013)

<b>Soil</b>	<b>Description</b>	<b>Geology</b>	<b>Hydrological description</b>	<b>Crop and Land use</b>	<b>% Area</b>	<b>HOST</b>
Ellerbeck	Stony loam over gravel	Glaciofluvial drift	Very stony well drained loamy soils locally on hummocky ground.	Stock rearing on permanent grassland in moist lowlands; some cereals, sugar beet in drier lowlands.	16 %	5
Maw	Peat to loam over sandstone	Carboniferous and Jurassic sandstone	Loamy very acid upland soils over sandstone with a wet peaty surface horizon, often with thin iron pan.	Wet moorland habitats of poor and moderate grazing value; stock rearing and dairying on improved ground; coniferous woodland.	13 %	15
Stow	Deep clay	Jurassic mudstone and siltstone	Slowly permeable clayey soils, mainly on steep slopes.	Permanent and short term grassland with dairying and stock rearing; some cereals; coniferous woodland.	19 %	20
Dale	Seasonally wet deep clay over shale	Carboniferous and Jurassic clay and shale	Slowly permeable seasonally waterlogged clayey, fine loamy over clayey and fine silty soils.	Dairying on permanent and short term grassland; some cereals; coniferous woodland.	8 %	24
Dunkeswick	Seasonally wet deep loam to clay	Till from Palaeozoic and Mesozoic sandstone and shale	Slowly permeable seasonally waterlogged fine loamy and fine loamy over clayey soils	Grassland in moist lowlands, some arable cropping in drier lowlands.	36 %	24
Onecote	Seasonally wet deep peat to loam over shale	Carboniferous and Jurassic mudstone	Slowly permeable seasonally waterlogged clayey and loamy upland soils with a peaty surface	Wet moorland habitats of poor and moderate grazing value; dairying on improved ground; coniferous woodland.	8 %	26

**Table 5-2 Soil type descriptions provide by national soil dataset (Soil data © Cranfield University (NSRI) and for the Controller of HMSO 2013)**



### 5.3.3 Land use and vegetation

The dominant land uses within the catchment are grazing for sheep and cattle on improved and rough pasture. The upper parts of the catchment are dominated by heather and heather grassland, mostly used for game bird rearing and sheep grazing. A full breakdown of the land cover types as categorised by the 2007 CEH land cover maps, can be seen in Table 5-3. The catchment is rural with only 1 % classified as suburban. Just under 15 % of the catchment is woodland, largely found on the steeper slopes and less desirable, waterlogged soils in the valley bottoms of the upper reaches of the catchment.

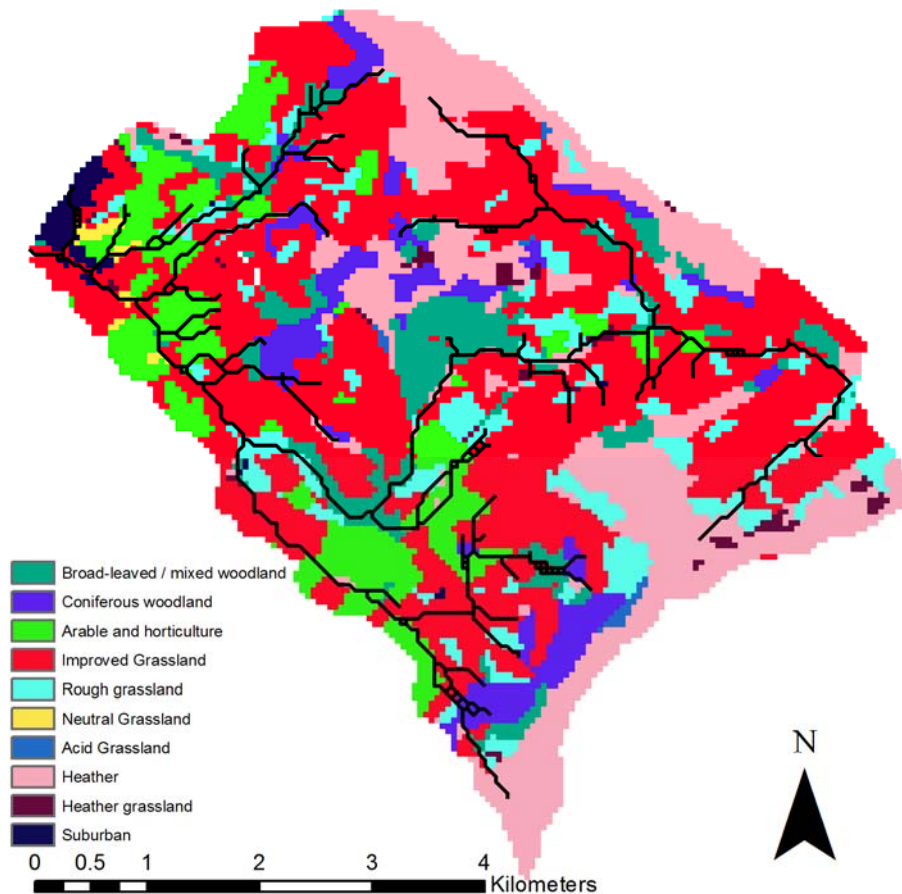


Figure 5-6 Land Cover Map 2007 (Centre for Ecology and Hydrology, 2007)

**Table 5-3 Great Ayton land cover 2007 breakdown**

<b>Landover</b>	<b>Percentage covered</b>
Broadleaved woodland	8 %
Coniferous woodland	6 %
Arable and Horticulture	11 %
Improved grassland	43 %
Rough Grassland	8 %
Acid or Neutral Grassland	2 %
Heather	21 %
Suburban	1 %

***Potential hydrological impacts of farming***

Many of the soils have been described as having low permeability (Table 5-2), meaning rapid runoff as overland flow is likely, especially during the largest and more intense rainfall events. This will only be exacerbated by the introduction of drainage for the improvement of soils for rearing of livestock as is evident in Figure 5-7 with improved grassland adjacent to heather and heather grassland. There is also evidence of soil degradation due to overuse with large stocks of sheep in fields (Figure 5-8) and wheelings caused by driving on the land in wet conditions (Figure 5-9). This can lead to both extensive and localised soil compaction along with the creation of preferential flow pathways that concentrate flows and can accelerate soil erosion.



**Figure 5-7 Improved grassland adjacent to heather grassland (potentially under-drained)**



**Figure 5-8 Evidence of soil degradation on the Dunkeswick soils, with wheelings and erosion at gateways**

The largest event observed during the monitoring period provided evidence of undesirable farming practices as shown in Figure 5-9. Bare soil during the wetter months is seen as both a water quality and flooding problem; ideally there would be a cover crop that reduces the losses of soil, which is a significant pollutant source and also impacts on the conveyance capacity of channels. The wheelings that are evident in Figure 5-9 are also undesirable as they act as conduits to rapidly move overland flow downstream which in turn exacerbates the erosion problem.



**Figure 5-9 Wheelings delivering sediment rich overland flow directly to the stream (taken 26/11/2012)**

Figure 5-10 shows the locations that the three images above were taken against the TWI map. Point 'a' is the improved grassland in Figure 5-7, point 'b' is the degraded soil, which is shown as potentially well connected to the river network and point 'c' is that of the wheelings, in which sediment rich overland flow was connected to the river network.

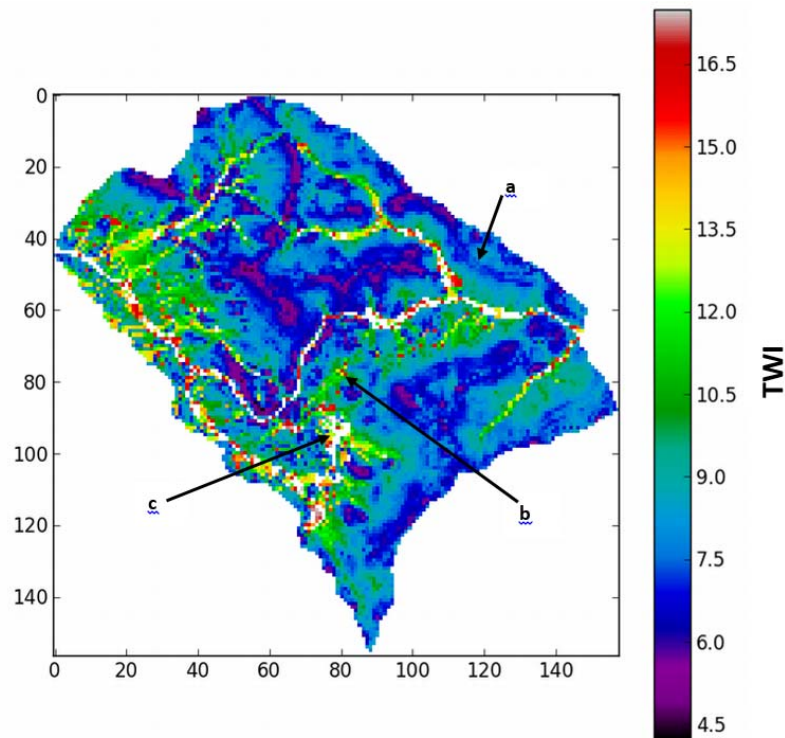


**Figure 5-10 Topographic wetness index map showing the locations of the photographic evidence of degradation**

## 5.4 Hydrological characterisation

This section provides an overview of the hydro-meteorological instrumentation used in the Great Ayton catchment and an assessment of the collected data. The characteristics of rainfall during large storm events are examined to provide an understanding of the processes and causes of flooding. This will provide an insight in to what mitigation methods may be best suited for reducing the flood hazard in the Great Ayton catchment.

### 5.4.1 Rating curve development

As has previously been discussed a rating curve is required to convert water level values to discharge. I have established rating curves for four of the sites monitored by Newcastle University and are summarised in Table 5-4. The rating curves were developed using the VARE modelling methodology (see Chapter 3). The VARE procedure converts the stages to flows to a volume over the duration of the record (Ewen *et al.*, 2010; Geris, 2012). This volume is then used to evaluate the catchment storage-discharge relationship i.e. whether a reasonable water balance has been achieved for a given time period, normally a hydrological year. If the water balance is not reasonable the parameters controlling the velocity-stage relationship are modified; constrained by the manual gauging observations. The monitored flows are reasonably well contained within the gauged range, especially for Little Ayton and the Farm ditch, which are in the lower parts of the catchment. However, flooding of some roads makes access to sites in the upper reaches of the catchment impossible.

The rating curves for the two EA gauges were taken from the National Flood Forecasting System (NFFS) and were developed using hydrodynamic modelling calibrated to fit observed stream gaugings.

Table 5-4 Great Ayton flow record information

Site	No. of Gaugings	Min. gauged Flow (m <sup>3</sup> /s)	Max. gauged Flow (m <sup>3</sup> /s)	In gauged range (%)	Max. rated Flow (m <sup>3</sup> /s)
Lt. Ayton	12	0.095	5.6	96 %	14.42
Lonsdale	10	0.014	0.75	64 %	5.14
Leven vale	9	0.039	1.53	53 %	4.69
Farm ditch	6	0.0002	0.006	80 %	0.57

Exceedance curves for the four Newcastle University sites and two EA gauges are displayed in Figure 5-11. Each location has very similar high flow values in the top 20 % of flows but there are some differences in the mid- and low-flow sections of the curves. The two sites from the upper part of the catchment, Lonsdale and Leven Vale, drain predominantly peaty moorland; their respective flow duration curves are quite similar but differ to other regions of the catchment, especially for the flows exceeded 40 % or more of the time. The Farm Ditch site is an artificial field boundary drain that connects sub-surface agricultural drains to the main stream network; this is the likely reason for greater flow values for 95 % of the time.

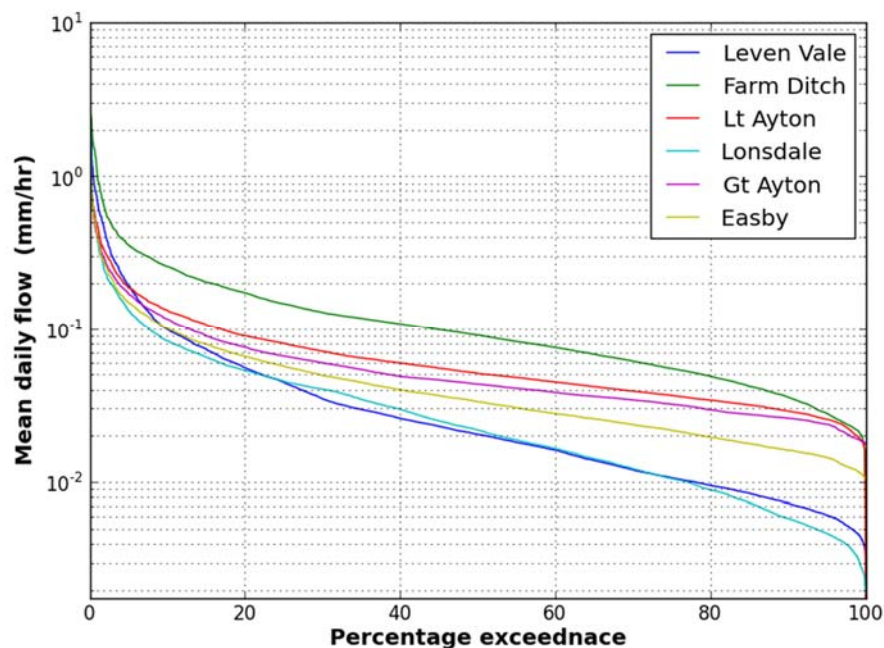


Figure 5-11 Flow exceedance curves for both the EA and Newcastle gauges in Great Ayton

#### 5.4.2 Flood frequency

The Great Ayton gauge has been in place since August 2003, which provides a limited amount of information for producing a meaningful flood frequency curve. The Easby gauge, however, has been in operation since April 1971, with 37 Annual Maximum Flows (AMAX) values compared to the ten for Great Ayton. Of the ten Great Ayton AMAX values shown in Table 5-5, five appear in the top ten ranked events for Easby, including the second ranked event, which would indicate a reasonable level of synchronisation, which isn't surprising given the flows to Easby drain 50 % of the total catchment area.

**Table 5-5 Relative ranking of events at Great Ayton and Easby**

<b>Great Ayton rank</b>	<b>Great Ayton Peak (m<sup>3</sup>/s)</b>	<b>Date of flood peak</b>	<b>Easby rank</b>	<b>Easby Peak (m<sup>3</sup>/s)</b>
1	25.86	16/04/2005	2	18.88
2	17.05	29/11/2009	5	10.32
3	15.5	27/11/2012	6	9.93
4	14.07	25/06/2007	7	9.41
5	11.85	19/04/2004	12	7.45
6	11.64	17/07/2009	9	8.7
7	9.93	06/09/2008	22	4.88
8	8.28	27/04/2012	23	4.86
9	8.01	22/05/2006	21	4.92
10	7.12	16/12/2010	30	3.84

The Flood Frequency Curve (FFC) derived for Great Ayton using the FEH pooled analysis method is shown in Figure 5-12. The FFC development is carried out using the WINFAP-FEH software, which is an UK industry standard method of flood defence design. Pooled analysis involves using the AMAX series for the site of interest which are ‘pooled’ with the AMAX values for catchments with similar FEH catchment descriptors. To create a flood frequency curve of ‘N’ years it is recommended in the FEH methodology that a pooled AMAX set of at least ‘5N’ is used. In this analysis 520 years have been used and assessed using a Generalised Logistics L-moments (GL-LMOM) statistics. The largest event observed at Great Ayton is classified as having a 26 year return interval.

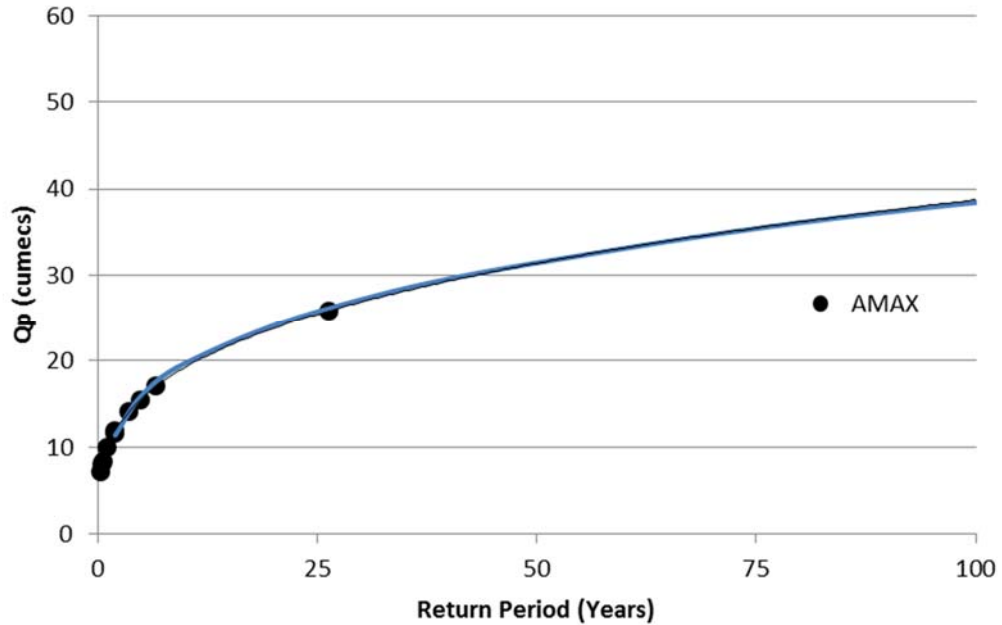


Figure 5-12 Flood frequency curve developed using FEH pooled analysis

### 5.4.3 Rainfall runoff

This section will discuss some of the rainfall-runoff dynamics observed within the Great Ayton catchment as well as presenting some analysis to illustrate the impact of spatial scale on flood flows.

#### *Rainfall characteristics*

Figure 5-13 illustrates how rainfall characteristics affect the magnitude of flood peaks ( $Q_p$ ) over  $0.5 \text{ m}^3/\text{s}$ ; the red dots represent summer events (April to September), blue are winter. It illustrates that the total rainfall is a key controlling factor over  $Q_p$ , with more rainfall leading to larger events (top left panel); the scatter within plot illustrates the importance of antecedent conditions, e.g. with rainfall events ranging from 20 mm to 30 mm in total rainfall, producing flood peaks producing a significant range of the observed peaks at 0.1 mm to 3 mm, in the top left panel. Although not unsurprising, it is the temporal distribution of rainfall that is the most insightful, as it suggests that the larger events are often caused by long duration medium to low intensity storms.

There is some distinction between the summer and winter events, where winter events are those classified as occurring between October and March (Blue) and summer events between April and September (Red). The largest flow event observed occurred in April 2005. The summer events tend to have the greatest amount of rainfall relative to similar sized winter peaks (e.g. peaks between 0.1 and 1mm, top left panel); this could largely



be attributed to the drier antecedent conditions, see Figure 5-14 where two events of similar magnitude but in different seasons are plotted. On average, the summer rainfall events have a higher mean intensity (top right panel) with higher maximum intensities within (bottom left panel), which are indicative of convective rainfall events that are more prevalent in the summer. The winter events are of a lower intensity and of a longer duration, typical of the weather patterns for this time of year.

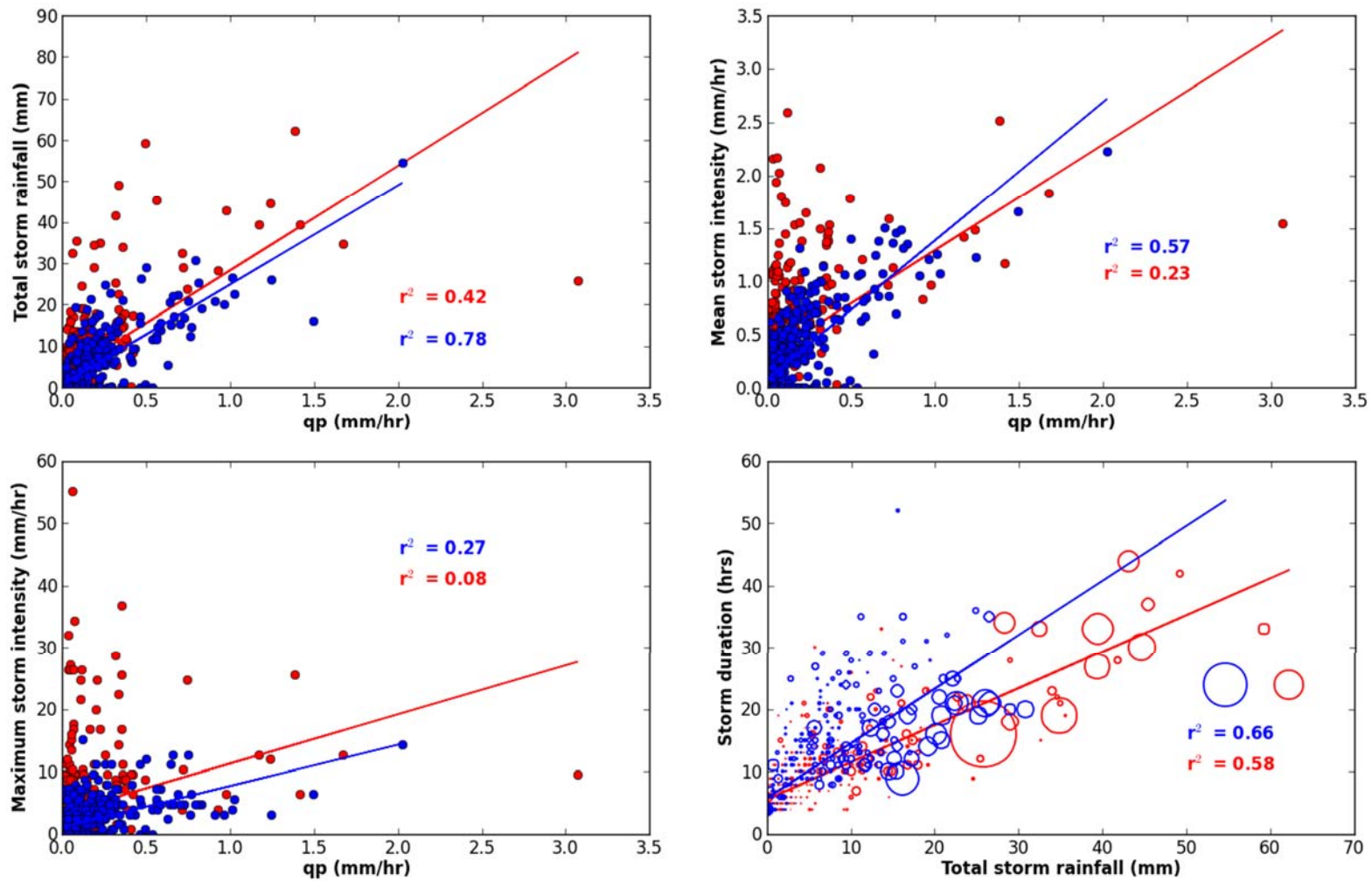


Figure 5-13 Analysis of flood peaks and the rainfall that generates them for Great Ayton; circle size (bottom right), indicates qp magnitude. Red = summer event (April to September), Blue = winter (October to March)

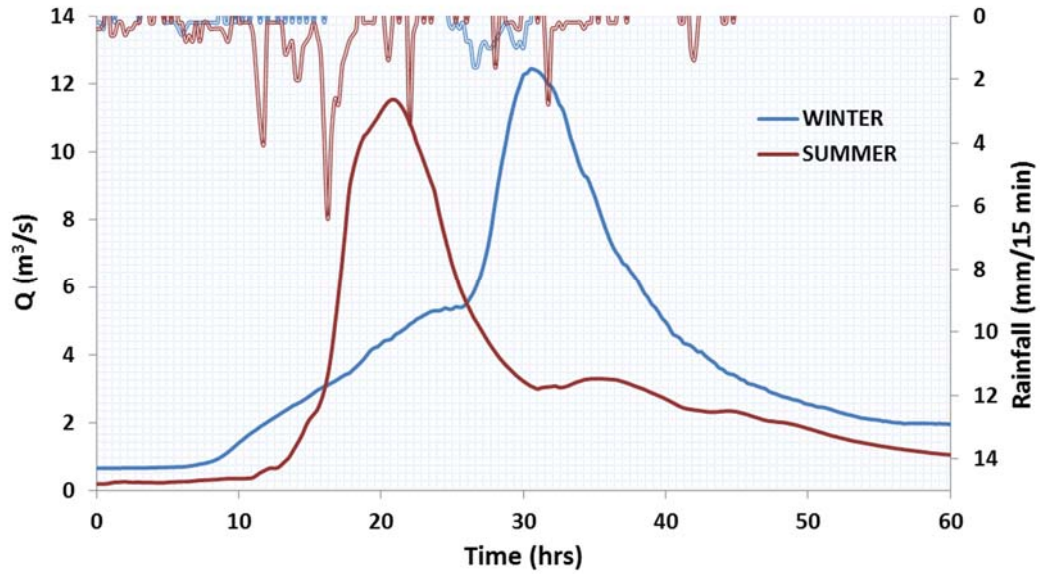


Figure 5-14 Hydrographs and corresponding event rainfall for a summer (17/07/2009) and a winter event (16/01/2010)

The relationship between runoff as percentage of rainfall volume and flood peaks is shown in Figure 5-15 for a range of events. There is significant scatter in the winter events. This may be due to rainfall falling on a saturated catchment or potentially due to under-estimation of the rainfall totals for those events.

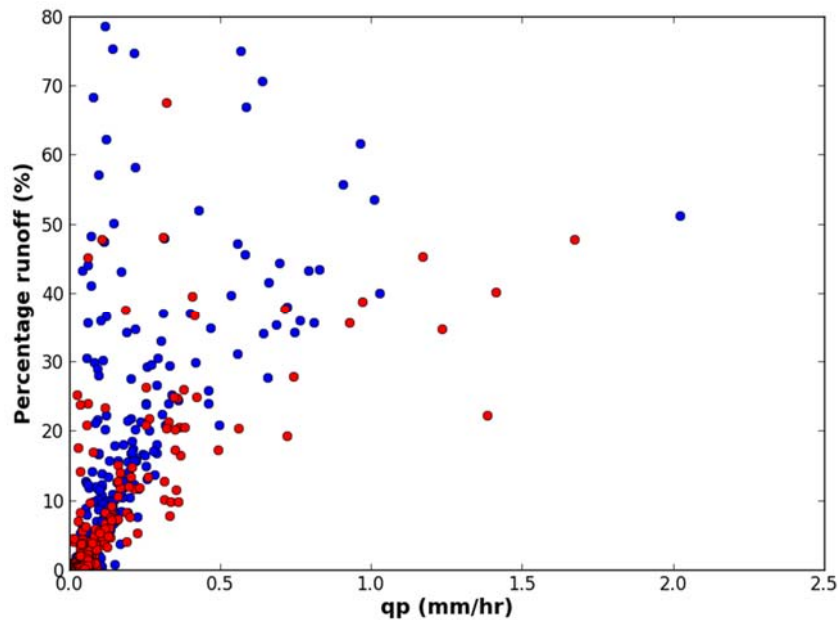
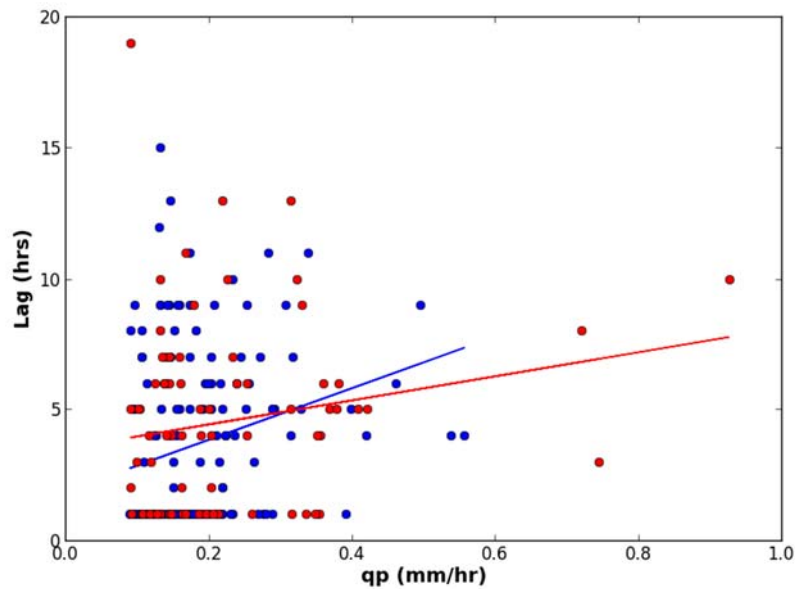


Figure 5-15 Runoff as a percentage of rainfall for a range of flood peaks. Red = summer event (April to September), Blue = winter (October to March Timing and celerity)

The lumped catchment response to rainfall can be calculated through analysing the catchment lag (the time between rain centroid and  $Q_p$ ; Figure 5-16). This lag can then

be used to calculate the time to peak of the unit hydrograph in the FEH rainfall-runoff model as it will be in Chapter 6.



**Figure 5-16 Lag time analysis for the Great Ayton catchment. Red = summer event (April to September), Blue = winter (October to March)**

Examination of the relative timings of sub-catchment flood peaks, compared with the timing of the flood peak at the catchment outlet, provides a useful insight into how flood waves propagate through the system. The relative timings can be used to produce an indicative celerity by dividing the travel time by the distance between the two gauges. The distances between each of the nested gauges and the outlets are provided in Table 5-6. This type of analysis is useful as an understanding of the different rates of response from different parts of the catchment is built up, which prove useful for identifying suitable sub catchments to target for mitigation.

**Table 5-6 Relative distance of the Great Ayton sub-catchment gauges to the outlet**

<b>Location</b>	<b>Distance to Great Ayton (km)</b>
Easby	5.3
Lonsdale	11.2
Leven Vale	10.0
Woodhouse	1.6
Dikes Beck	1.1
Pilly Hall	5.0

Figure 5-17 provides the travel times for a number of events for three sub-catchments to the outlet. The travel time can be converted to celerity by dividing the distance from each of the monitoring points by the travel time to give the wave speed. The calculation of celerity in this way assumes that the peaks observed at the sub-catchment outlets are well synchronised with the outlet at Great Ayton. There is a lot of scatter within Figure 5-17, which has been produced for the catchments from Easby to the headwaters. The catchments with the farthest travel distance, Lonsdale and Leven Vale, have the greatest travel times. The scatter within Figure 5-17 is likely due to the spatial and temporal variability of the rainfall leading to the catchment response not being synchronised.

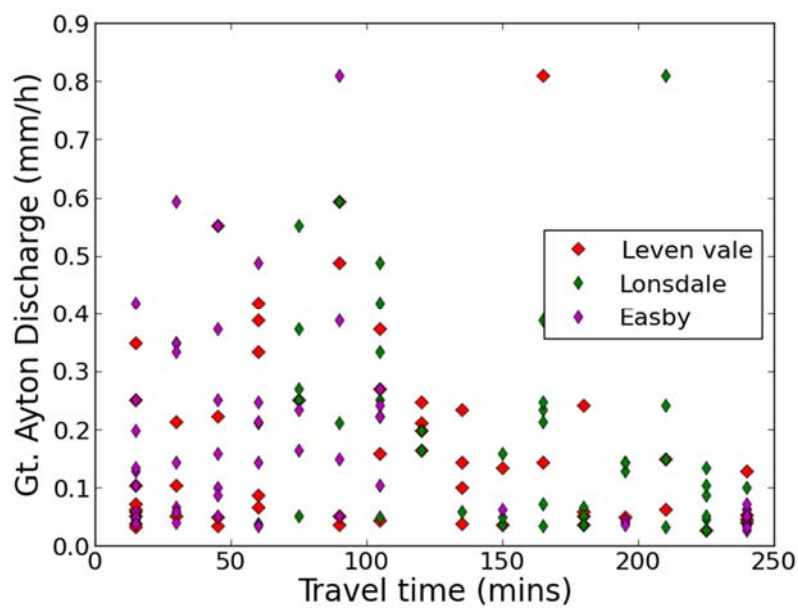


Figure 5-17 Travel time plot the catchments upstream of Easby to Great Ayton

It is clear, however, from Figure 5-18 that the peaks are not very well synchronised, especially during the smaller events. The overall trend is that celerity increases with increasing scale and there is less scatter, illustrating that celerity is a function of discharge.

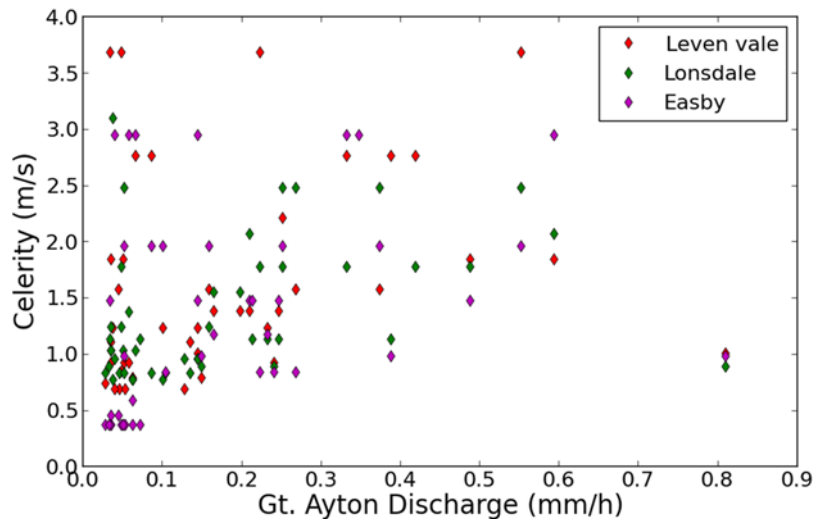


Figure 5-18 Celerity plot for the catchments upstream of Easby to Great Ayton

The celerity-discharge relationships for the remaining catchments in the lower part of the catchment are shown in Figure 5-19. The trend shown in Figure 5-19 is similar to that shown in Figure 5-18, that with increasing discharge there is an increased celerity; again celerity demonstrated as a function of discharge. However, celerity values for the least distal sub-catchment to the outlet, Dikes Beck, are consistently lower than the other, more distal locations in the catchment.

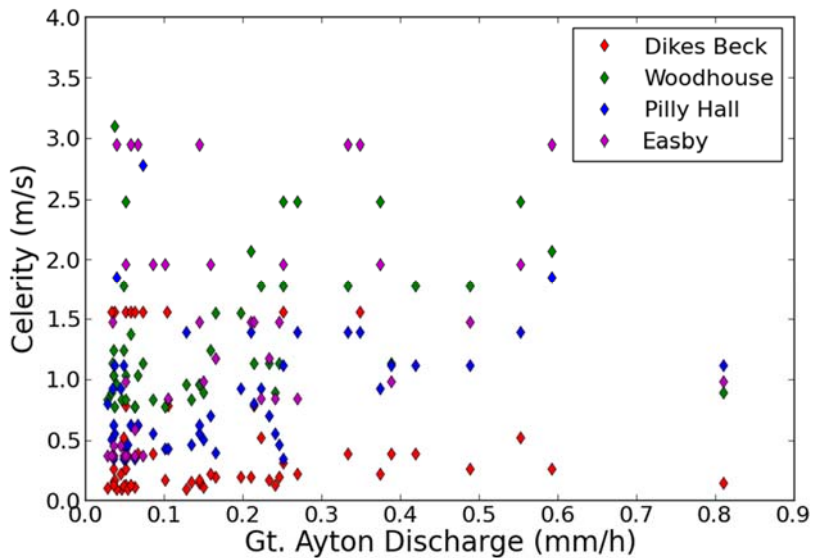


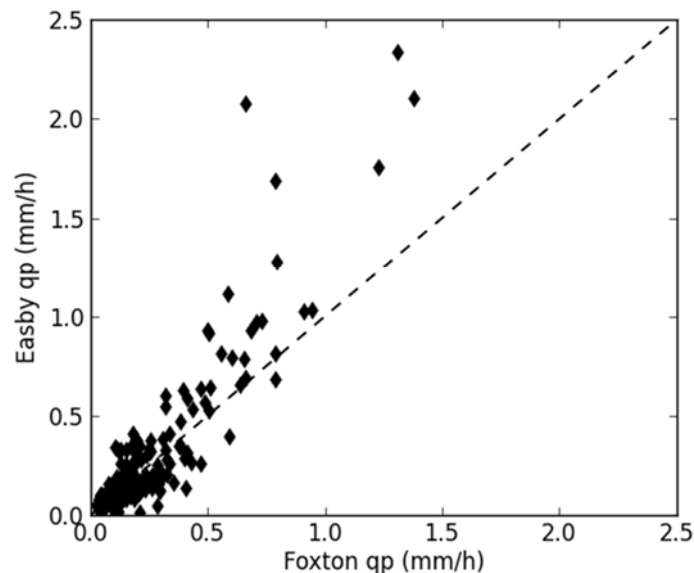
Figure 5-19 Celerity plot the catchments downstream of Easby to Great Ayton

### ***Scale effects to Foxton***

To further investigate the effects of flood propagation to larger scales flow data from the downstream Foxton (168 km<sup>2</sup>) are used to examine the effects on flood magnitude and hydrograph shape. Peaks were selected from the Foxton Bridge flow series over a

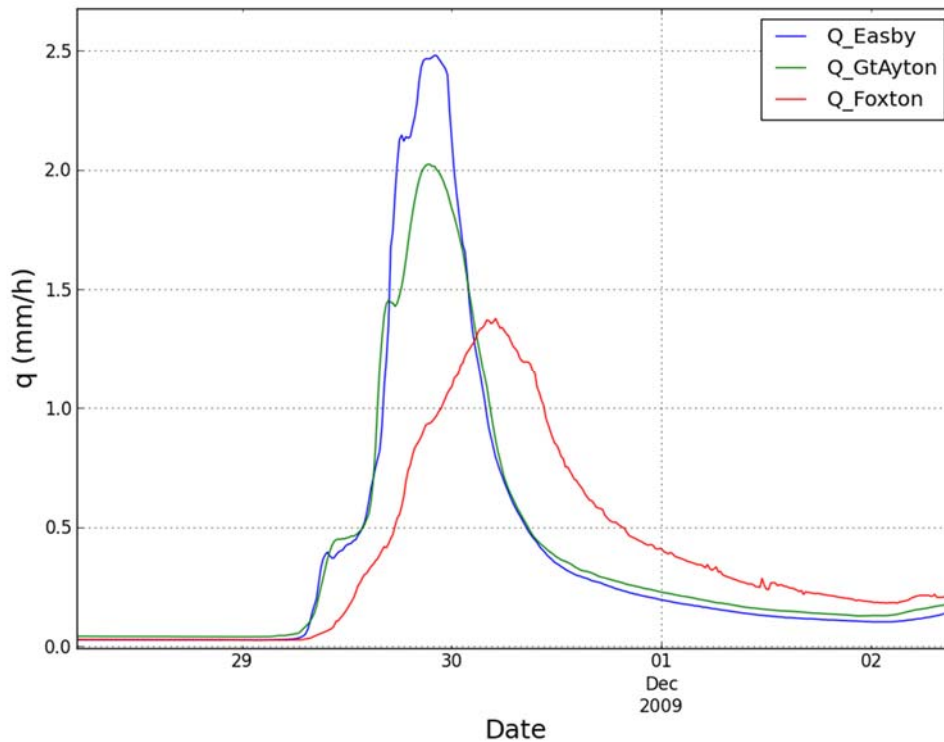
threshold of  $1.5 \text{ m}^3/\text{s}$  for the period 01/12/2005 to 03/07/2013. This provided 266 peaks at a range of flows from  $1.5 \text{ m}^3/\text{s}$  to  $64.5 \text{ m}^3/\text{s}$ . For each of these peaks the corresponding upstream peaks at Great Ayton and Easby were selected.

Figure 5-20 shows the relationship between peak flows at Foxton Bridge and Easby as specific discharges (flow per unit area). It shows that for the larger events specific discharges are greatest at the smaller catchment scale than they are at the larger scale. This is due to a number of factors, including the temporal and spatial variability of rainfall and also the effects of geomorphological and hydrodynamic dispersion within the network, whereby the flood response is dampened as the catchment scale increases due to attenuation of the flood wave (Wolff and Burges, 1994).



**Figure 5-20 Comparison of peak discharges at Foxton Bridge and Easby as specific discharges (mm/hr)**

It is evident from Figure 5-21 that at the smaller scale the hydrographs for Easby and Great Ayton rise and falls much more rapidly than those at the larger-scale, Foxton Bridge site. The event at the end of November 2009 (Figure 5-17) is the largest observed flood event to have occurred at Foxton Bridge. The attenuation of the wave is evident from Easby to Great Ayton but less dramatically so. How this attenuation affects the mitigation impacts as they are routed to the larger catchment scale will be of interest during the modelling.



**Figure 5-21** Leven event of November 2009. Foxton at 168 km<sup>2</sup>, Great Ayton at 30 km<sup>2</sup> and Easby at 15 km<sup>2</sup>

It was discussed in Chapter 4 how spatial and temporal rainfall heterogeneity can create relatively different magnitude peaks, for the outlet versus sub-catchment, depending on where rainfall is highest concentrated. The flood peaks have been selected for Foxton, the location at the greatest scale, along with the corresponding peaks at Easby and Great Ayton. The flood peaks are then ranked from zero, the smallest, to the largest at 258 for this sample. The downstream locations of Foxton or Great Ayton are plotted against an upstream location. For the largest events the relative magnitude of the peaks in the sub-catchments and the outlets become more closely correlated, as illustrated in Figure 5-22.



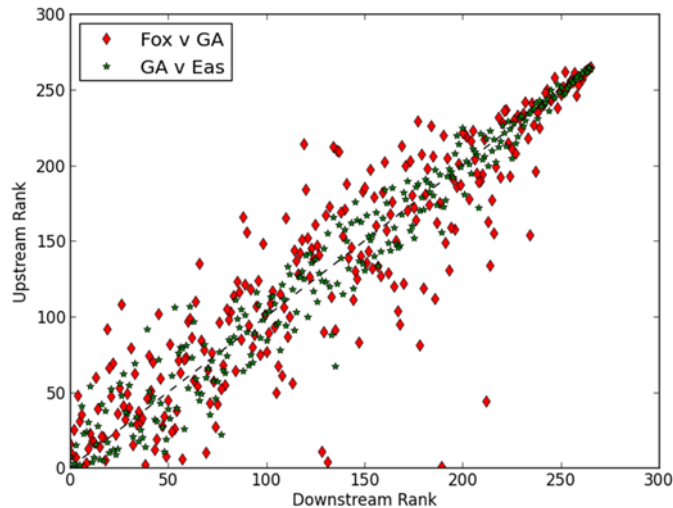


**Figure 5-22 Peak event rankings for Foxton and Great Ayton (RED) and Great Ayton and Easby (GREEN) (High rank equals high flow)**

It is evident from Figure 5-22 that the events of the two locations with the shortest travel distance between them and most similar catchment areas, Great Ayton and Easby (Green) are better correlated ( $R^2 = 0.94$ ) than those with a greatest travel distance Great Ayton to Foxton (Red;  $R^2 = 0.78$ ). However, the relationships between the magnitude of events become increasingly well correlated with increasing event rank, hence magnitude. As was shown in Figure 5-13, the larger events tend to be of a longer duration, with the largest rainfall totals; it is clear from Figure 5-22 that these events must be catchment wide as the events are equally ranked at all scales.

### 5.5 Flood mitigation approaches

This section provides an overview of the flood mitigation approaches adopted in the Great Ayton flood mitigation scheme and the locations in which they have been installed. A discussion of how the mitigation could be enhanced and what forms of mitigation may be best suited to the catchment based upon the analysis of the rainfall runoff records is discussed. The mitigation approaches are categorised as either spatially diffuse or concentrated, based on the classification discussed in the UK governments POST note as was highlighted in Chapter 2 (Pescott and Wentworth, 2011), and the relationship between these mitigation approaches and the expectant catchment-scale level of mitigation is discussed.

The flood mitigation scheme has involved a combination of property level flood proofing and the construction of attenuation features upstream. The upstream features fall in to two categories of online and offline attenuation features. Online features are

designed to impede the in channel and increase interaction with the floodplain; offline features attenuate overland flows to increase the time taken for flow to reach the channel. The seven locations in which features have been installed are shown in Figure 5-23.

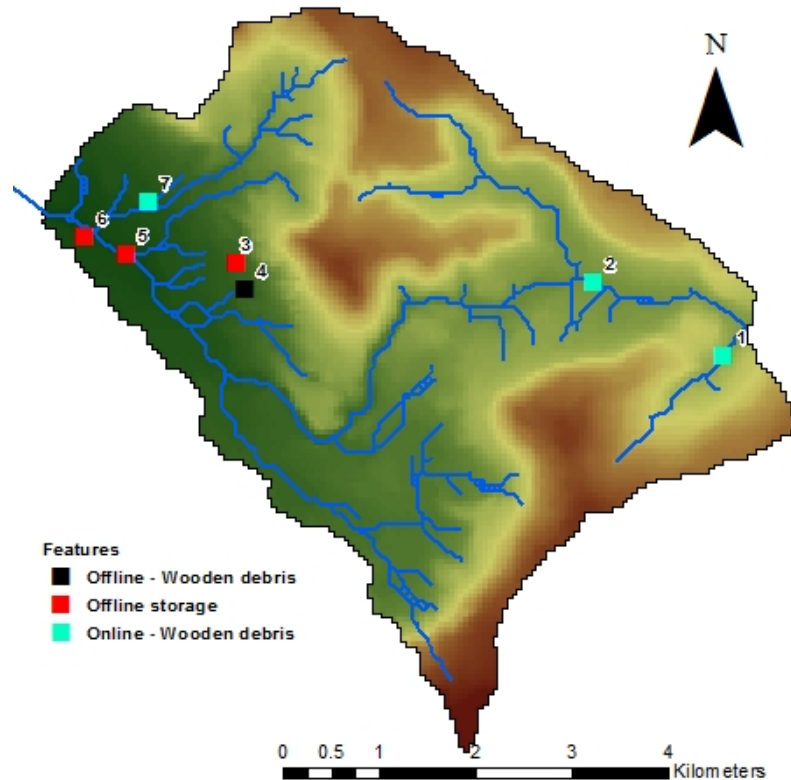


Figure 5-23 Catchment map and mitigation features are numbered for the following discussion (© Crown Copyright/database right 2016. An Ordnance Survey/EDINA supplied service)

### ***5.5.1 Property level protection***

Property level protection work was carried out in conjunction with Redcar and Cleveland council with £90,000 spent installing flood gates and flood proof air bricks to approximately 70 properties. Properties at three locations around the village have been targeted for flood proofing as identified in Figure 5-24 by the red squares. This type of mitigation is categorised as spatially concentrated as it is at the downstream point of impact and is designed to provide a certain level of protection with a high level of confidence in its ability. Property level protection offers a comparatively cheap option, when compared to traditional defences.

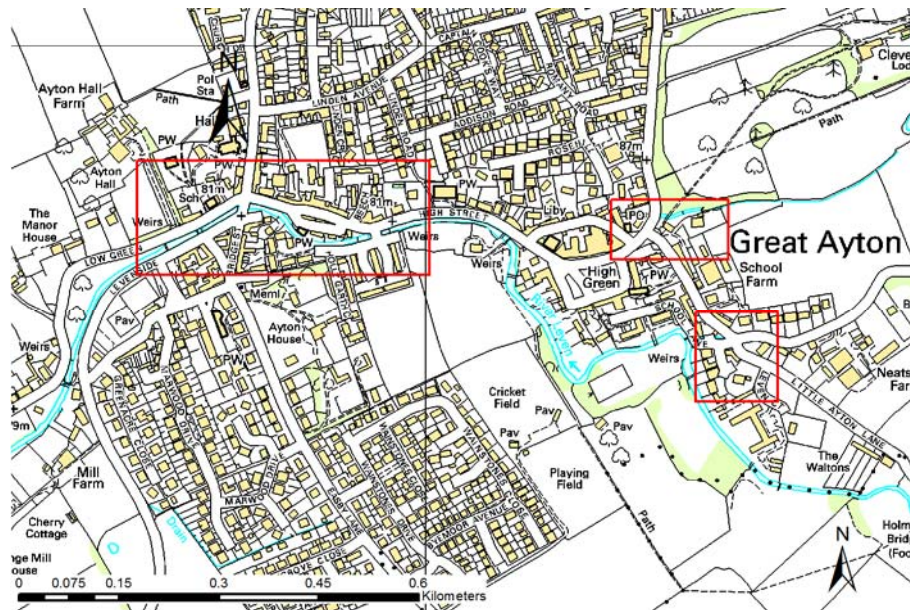


Figure 5-24 Flood proofing locations within Great Ayton highlighted by red squares (© Crown Copyright/database right 2016. An Ordnance Survey/EDINA supplied service)

### 5.5.2 Online - Woody debris features

The features 1, 2 and 7 (Figure 5-23) are constructed of felled trees lain across and in the channel. These features are operational in medium to high flows with lower, residual flows passing without hindrance. Two of the five in-stream features at location 1, in the headwaters of the Leven Vale sub-catchment, are shown in Figure 5-25. These wooden features are designed to attenuate the flows within the channel and spill higher flows on to the flood plain. The use of floodplains, especially where there is riparian woodland, offers increased storage and roughness on the floodplain.



Figure 5-25 Woody debris features in Leven Vale (Site 1)

The wooden features at locations 2 and 7 are quite similar to those at Leven Vale shown in Figure 5-25, however, the channel is not as well incised. At site 2, live Willow has been used to stabilise banks and reduce erosion, as well as being used to roughen the

river bed downstream to reduce velocities both for erosion reduction and flood attenuation purposes. At site 7 there are a sequence of three woody features for attenuating flows in stream, and deflecting a portion of higher flows on to the floodplain.

### **5.5.3 Offline – Wooden attenuation features**

The features at location 3 (Figure 5-23) have been placed on an ephemeral channel, so have been designed to attenuated rapid overland flow when it has been generated. These features are designed to operate only in the largest events when the sub-surface is saturated. Visual inspection of these features show a significant build-up of soil and debris on the upstream side, thus suggesting that they do operate to intercept and temporarily store flood flows



**Figure 5-26 Looking upslope at a wooden barrier feature at site 4 for attenuating overland flows**

These attenuation features are categorised as spatially diffuse as they distributed in the headwaters of the catchment, furthest from the point of impact. There is very little in the literature regarding the catchment scale impact of these types of features, however the local scale impact in increasing  $T_p$  has been modelled (Odoni and Lane, 2010; Thomas and Nisbet, 2012). The impact of these features at a larger catchment scale requires further investigation.

### **5.5.4 Offline storage feature**

The features in Figure 5-23 numbered 3, 5 and 6 are offline and designed to operate in the largest of events. Feature 5 is shown in Figure 5-27 is constructed a short distance upstream of the Little Ayton level gauge (25 km<sup>2</sup>). It is designed to be operational during high flows when the river level reaches an inlet pipe. A large concrete pipe has

been placed in the river bank to reduce the erosion and pressure placed on the river embankment. The inlet pipe to the offline storage feature is shown in Figure 5-27 along with the bund and willow outlet, designed to release the flow at a slower rate than it enters. The storage volume at 350 m<sup>3</sup>, relative to the upstream catchment area of 25 km<sup>2</sup> provides a relative storage volume of 0.0126 mm.



**Figure 5-27 Little Ayton offline storage pond and oxbow feature; a. concrete inlet pipe to the offline storage pond; b. view of offline storage pond and oxbow in the background**

The feature located at location 3 is a duck pond that has been modified with the addition of an embankment constructed on the downslope side to increase storage capacity. The feature at site 3 is maintained by the water table and by capturing overland flows.

A large feature has been constructed at location 6 (Figure 5-28), with an estimated storage capacity of 5000-6000 m<sup>3</sup>; based on an aerial coverage of 6000 m<sup>2</sup> calculated from GIS, and an approximate water depth of one metre. An inlet has been cut in the levy to allow water to enter the playing field during high flows; in addition there is a pair of pipes through the levy allowing water to leave the river. At the end of the playing field a bund has been constructed to store the water and there are a series of pipes to drain the field as the river level recedes.

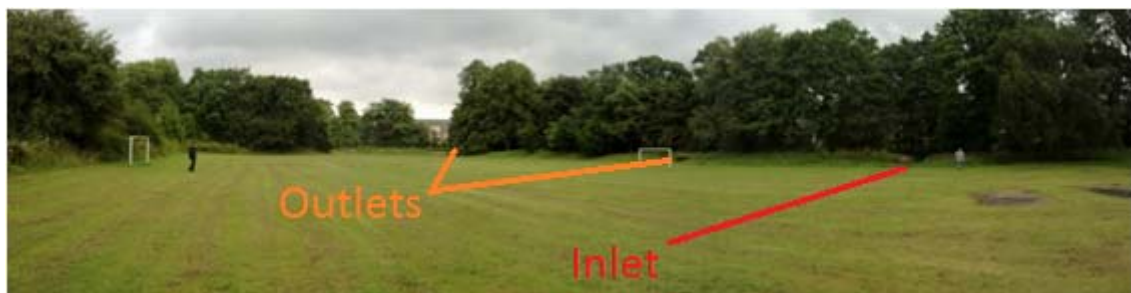


**Figure 5-28 Old Mill pond playing field feature upstream of Great Ayton**

The offline features discussed above fall into both the spatially diffuse and spatially concentrated categories due to the location, scale of the features and potential impact. The features at locations 3 and 5 are spatially diffuse as they are a distance from the downstream point of impact. The feature at location 6 is close to the point of impact and has the potential to take a large volume of water, equivalent to 14.5 times the storage of the features at location 5. This based upon a storage volume of 5500 m<sup>3</sup>, equivalent to 0.18mm catchment wide rainfall held in storage. The inlet height at feature 6 can also be modified if it is thought to operate too frequently, i.e. for events that would not cause flooding regardless of the feature. The closer a feature is built to the point of impact and as long as it is scale appropriate, the more confidence can be had in its effectiveness. Of course, knowing if a feature is scale appropriate will depend on the magnitude of the flood peak and require analysis of the rainfall-runoff records.

#### ***5.5.5 Potential additional features***

There may be scope for increasing the number of both ‘on’ and ‘offline’ attenuation features. The features located on ephemeral overland flow pathways would seem a type of option that has not been overly exploited in this project. These features would appear to be beneficial in a number of ways as they will only operate during the largest events in which overland flows are generated and the disconnect flow paths and add attenuation which has been shown to reduce the flood peak. The main limiting factor on the possible number of features is a financial one. Newcastle recommended that many sites were available and that many more RAFs would be needed if there was to be confidence in reducing the flooding at Great Ayton.

## **5.6 Discussion**

This section summarises the characterisation outputs in this chapter.

### ***5.6.1 Catchment characteristics and data***

The Great Ayton catchment has been shown to have a number of different soil types and underlying geology, which have been shown to affect the rainfall-runoff response from different parts of the catchment. The higher SPR soils are the organic peats found underlying the heather moorland/grassland used for sheep and game rearing.

The instrumentation network to Great Ayton has been described, which comprises of a number of level gauges maintained by the EA and Newcastle University. Analysis of the flow duration curves for all sites have shown that for the largest events the flow

duration curves are relatively similar for the flows exceeded 20 % of the time. However, for flows exceeded 20 to 100 % of the time, and especially during the drier periods the two Newcastle University sites in the headwaters above Easby have much lower flows. This is likely due to the local soil and geology as they are draining the majority of the peaty soils and may be losing water to the sandstone beneath. During large runoff events

### ***5.6.2 Rainfall-runoff response and flood risk***

During the largest events comparatively similar volumes of runoff are being generated by all parts of the catchment. Figure 5-13 showed that the largest events coincide with the greatest rainfall volumes, as would be expected; however, there is significant scatter in the plot, which demonstrates the importance of antecedent conditions in determining  $Q_p$  with similar rainfall volume producing significantly different flood peaks. It is particularly clear from Figure 5-13 that the large summer events require the greatest rainfall volumes falling over a long period to overcome the soil moisture deficit. The summer rainfall events seem to typically be of a greater intensity but this, however, is not a major driver of the largest flood peaks. The largest floods events typically have a mean rainfall intensity of 1 mm/hr and are 10 to 30 hour in length.

### ***5.6.3 Mitigating flood hazard***

The attenuation and diffusion of flood waves was shown to have a considerable impact on the flood peak by broadening the flood wavelength (Figure 5-21), so increasing flood wave attenuation, therefore reducing flood wave celerity with mitigation features would intuitively be a positive approach for flood hazard reduction. To what spatial scale land use management and NFM features are effective at reducing flood hazard needs to be considered. The fact that the flood wave becomes attenuated as it travels downstream means that any flood reduction noticed locally from mitigation, will also potentially be attenuated and have a reduced impact with increasing catchment scale.

### ***5.6.4 What next?***

The next three chapters will use the understanding gained from rainfall runoff analysis to explore a number of land use management and NFM options for mitigating flood flows. The FEH rainfall runoff modelling in Chapter 6 makes use of the lag time analysis, whilst the celerity analysis is used in Chapter 6 by the FEH-FIM tool and Chapters 7 and 8 in the Juke modelling. The analysis has shown that the largest flood peaks tend to be driven by long duration rainfall events that likely cause saturation

excess runoff. The most suitable mitigation for these types of events will increase the amount of temporary storage and attenuation of flood flows, both overland and in riparian areas where possible.

Questions regarding the spatial scale at which different forms of mitigation are adopted and the scale at which impact is felt will need to be addressed with modelling. Distributed modelling is likely to be best suited in order to gain an understating of the flood reduction impacts brought about by the scale of mitigation and the scale at which mitigation is adopted. As was illustrated in the activity diagram (Figure 5-22), all parts of the catchment are not equally active and generating large volumes of water in all events. Only by modelling the distributed mitigation interventions, including the travel distance to the point of impact, will it be possible to understand the cumulative effect of these approaches.

Key data and results from this chapter that are used in the following chapters for model calibration and parametrisation are:

- Calculated time to peak value used to parameterise the FEH rainfall-runoff model in Chapter 6.
- Observed flow series for Great Ayton and Easby to be used in the calibration and parameterisation of the celerity function within the Juke rainfall-runoff model (Chapters 8).



## Chapter 6. Lumped Conceptual Modelling - FEH

### 6.1 Introduction

This chapter investigates the suitability of the Flood Estimation Handbook (FEH) rainfall-runoff model for use in modelling land use management (LUM) change scenarios. Its use for LUM change modelling has been considered in a number of research projects as a means for developing a methodology for practitioners and catchment managers; most notably the Modelling and Decision Support Framework (MDSF) and the DEFRA funded FD2114 (Packman *et al.*, 2004). These methodologies will be explored for the Great Ayton and Morland catchments in the north of England and the results used to populate a decision support risk matrix. The risk matrix helps depict the potential impacts of LUM change and management decisions on flood peaks ( $Q_p$ ).

The FEH was designed for generating design storm events for any catchment, regardless of data availability using regionalised statistics, rather than impact assessments. The FEH has been used in the creation of Catchment Flood Management Plans (CFMPs) and has been described as a screening method for testing a catchment's sensitivity to change. Where sensitivity is identified a more detailed approach should be considered (CIRIA, 2013). A number of scenarios and tests are carried out using the model to investigate the flood mitigation impacts.

An alternative approach to the FEH modelling is demonstrated through the Flood Impact Modelling tool (FIM). It uses a more spatially distributed approach by allowing users to manipulate the hydrographs of sub-catchments, with simple routing rules and superposition of their hydrographs, to potentially identify the sub-catchments most suitable for targeting mitigation efforts.

### 6.2 Modelling approaches

The FEH model was originally developed as the Flood Studies Report (FSR) rainfall-runoff model, as described in Volume 4 of the Flood Estimation Handbook Houghton-Carr (1999). It was developed as a means of estimating flood hydrographs for any catchment, gauged or ungauged, in the UK using regionalised statistics. The FEH model and its updated 'Revitalised Flood Hydrograph' (ReFH) version are described below and then tested to identify any differences in outputs between the two.

### **6.2.1 FEH**

The FEH model is based upon a unit hydrograph and has two key model parameters, Time to peak and ( $T_p$ ) and Standard Percentage Runoff (SPR). The  $T_p$  is the lag between the centroid of the rainfall and the peak of the flow hydrograph; within the FEH the  $T_p$  is used to calculate the unit hydrograph time-to-peak. The typical percentage of rainfall that leaves the catchment as fast runoff is captured by the SPR statistic; i.e. it reflects the response hydrograph rather than the slower sub-surface component that makes up the baseflow.

### **6.2.2 ReFH modelling**

The FEH rainfall-runoff model has been updated and launched as the ReFH (Kjeldsen, 2007). It was developed to '*improve the way that observed flood events are modelled and has a number of advantages over the FSR/FEH unit hydrograph and losses model*' (Kjeldsen, 2007). The key differences between the two models as noted by Kjeldsen (2007) include:

- *a loss model based on the uniform Probability Distributed Model (PDM) model of Moore (1985);*
- *a more flexible unit hydrograph shape; and*
- *improved handling of antecedent soil moisture conditions.*

The 100-year, 12 hour design unit-hydrograph and resultant hydrographs, generated using the FEH and ReFH are shown in Figure 6-1. The ReFH unit-hydrograph has a lower peak but longer recession, there is also an additional baseflow component to the ReFH model.

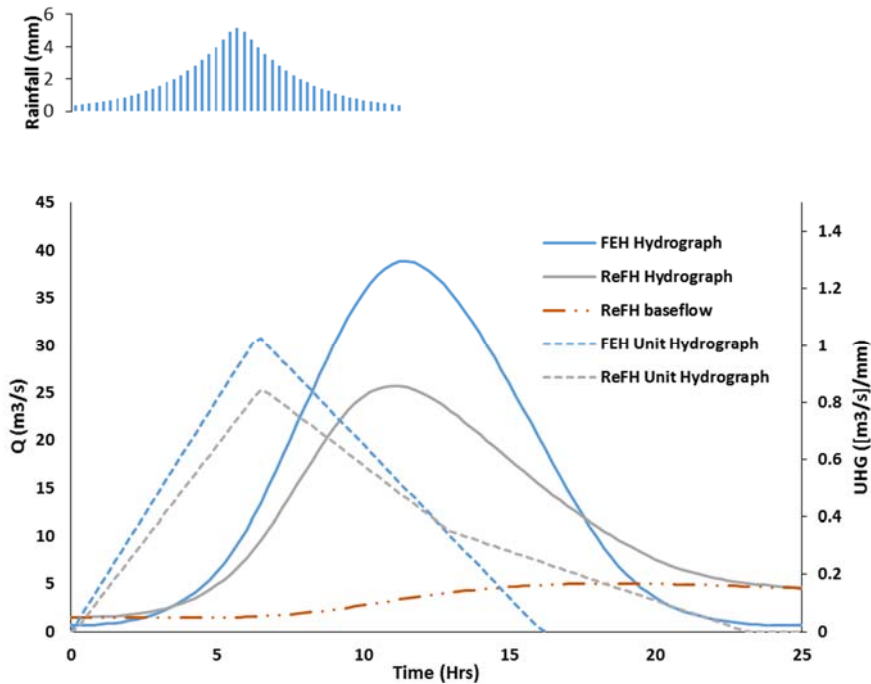


Figure 6-1 FEH and ReFH for the 100-year, 12 hour design storm to Great Ayton

The differences in the unit hydrograph are clear, with the ReFH having a lower magnitude peak and a two-step recession rate. The FEH has a constant Baseflow value, whilst the ReFH is more dynamic.

### 6.2.3 Model parameterisation- Great Ayton

All FEH model parameters can be calculated from FEH catchment descriptors using a number of methods as set out in volume 4 of the FEH. The  $T_p$ , BFI and SPR parameters can be obtained from regionalised datasets, however, it is preferable to analyse observed data when available to get the parameter values. The sections below describe the approaches adopted within the FEH and compares the parameters as calculated from descriptors and from observed data.

#### SPR

The SPRHOST (henceforth referred to as SPR) value for the Great Ayton catchment as provided by the FEH catchment descriptors is 40.68. This comparable to Figure 5-14, Chapter 5.

#### Unit hydrograph time-to-peak

Where records are available, the  $T_p$  of the Instantaneous Unit Hydrograph (IUH),  $T_p(0)$ , is estimated from the catchment lag (time from the centroid of rain to runoff peak), using Equation 6-1. Where observed data are not available  $T_p(0)$  can be

calculated using FEH catchment descriptors as obtained from the FEH volume 3 CD-ROM.

**Equation 6-1**

$$T_p(0) = 0.879 \text{ lag}^{0.951}$$

Analysis of the 28 largest single peaked events (Chapter 5, Figure 5-13) to Great Ayton gave a mean  $T_p$  of 6.41 hours, which compares to the  $T_p$  calculated using catchment descriptors at 5.08 hours. The observed time-to-peaks ranged from 3.3 hours to 12.3 hours with a standard deviation of 2.3 hours.

### ***Storm duration***

The critical design storm duration (i.e. the rainfall event duration that generates the largest flood peak) is estimated from the catchment  $T_p$  and the catchment Standard Average Annual Rainfall (SAAR), which is a 30 year annual average rainfall described by FEH statistics, using Equation 6-2. The critical design storm duration provides a storm profile to give the largest  $Q_p$ . Using the observed  $T_p$  of 6.4 produces a design storm duration of 11.6 hours.

**Equation 6-2**

$$D = T_p \left( 1 + \frac{\text{SAAR}}{1000} \right)$$

### ***6.2.4 FARM decision support tool***

The FARM tool was developed to support decision makers and to help communicate ideas to wider stakeholders (refer to Chapter 2 for details). Land use and catchment management scenarios can be mapped on to the risk matrix to better understand the effect of land management scenarios on flood risk. The matrix axes are designed to be as intuitive as possible and convey the ideas of soil storage and conveyance of water. The management of soil is linked to the SPR axis, with overuse of the land through increasing stocking densities or year round cropping seen to degrade the soil structure and increase fast runoff. The  $T_p$  axis is linked to the attenuation within the catchment and can be affected by the implementation of field drainage for example, which would reduce the  $T_p$ . The removal or addition of natural buffers or ‘roughness’, such as hedgerows or riparian woodland, can also affect the  $T_p$ . The results from the FEH

modelling in this chapter will be mapped to the FARM matrix as depicted in Figure 6-2, in which the values are percentage change from the base value.

### **6.2.1 Land use change**

A number of studies have looked at ways of incorporating the effects of LUM into models to study the likely impacts. The Modelling and Decision Support Framework (MDSF - HR.Wallingford *et al.* (2002) was developed for use in Catchment Flood Management Plans (CFMPs), as a requirement of the EU Floods Directive (2007). One objective of CFMPs is to assess the impact of long-term future LUM plans on flood hydrology. The MDSF study and its recommendations were then used within a Defra funded study which reviewed the impacts of rural LUM on flood generation. Within the report (FD2114, 2004) a methodology was developed for using the FEH rainfall-runoff model for LUM change impact assessment. The key recommendations were that the Tp and SPR parameters within the FEH rainfall-runoff model could be manipulated to reflect the impact of LUM change on the hydrograph.

#### **FD2114-FEH recommendations**

Within the FD2114 project, short-term improvements to the FEH study (hereafter referred to FD2114-FEH) were made, including the impact of soil degradation due to agricultural practices on runoff generation. The impact of soil degradation is thought of in terms of the increase in fast runoff, and to make this applicable to the FEH the impact on the HOST classification were considered (Boorman *et al.*, 1995). The HOST classification provides the SPR values necessary for parameterising the FEH model. The method of reclassifying HOST categories was discussed in Chapter 2.

Likely changes to SPR using the FD2114 approach are shown in Table 6-1. There is a 14 % increase in SPR by moving from the baseline catchment to a degraded catchment. Table 6-1 is populated from GIS analysis of the national soil dataset for the Leven catchment (Packman *et al.*, 2004).

**Table 6-1 Changes in SPR suggested by Packman et.al (2004) for the soil types found in the Leven catchment**

<b>Original HOST class</b>	<b>Alternate HOST class</b>	<b>Original SPR</b>	<b>Alternate SPR</b>
0	-	-	-
5	7	15	27
15	15	48	48
20	20	60	60
24	25	40	49
26	26	59	59
<b>Weighted catchment SPR:</b>		<b>42.46</b>	<b>48.34</b>

Packman *et al.* (2004) modelled four catchments, making changes to parameters as described above. The  $T_p$  and SPR scenarios tested for two catchments, chosen for the difference in the magnitude of SPR manipulation, can be seen in Table 6-2 with the results shown for a number return interval storms in Table 6-3. The impact on SPR is only considered for a worsening scenario, in which it is increased, whilst  $T_p$  is manipulated to become shorter (worsening) and longer (improving).

**Table 6-2  $T_p$  and SPR values modelled by Packman *et al.* (2004)**

<b>Catchment</b>	<b><math>T_{p0}</math>= FEH eqn (base case)</b>	<b><math>T_{p1}</math>= <math>T_{p0} - 1h</math></b>	<b><math>T_{p2}</math>= <math>T_{p0} + 1h</math></b>	<b><math>SPR_0</math>= SPRHOST (base case)</b>	<b><math>SPR_1</math>= Alternate</b>
W. Glen (4.4 km <sup>2</sup> )	5.14	4.14	6.14	41.3	45.9 (+11 %)
Tud (72 km <sup>2</sup> )	13.40	12.40	11.40	32.6	38.3(+17.5 %)

It is clear from Table 6-3 that the scenario in which only the SPR is altered ( $T_{p0}$  and  $SPR_1$ ) that the magnitude increase in  $Q_p$  is very close to the percentage increase in SPR shown in Table 6-2, especially for the larger, higher return interval events.

Table 6-3 Percentage change in Qp taken from Packman *et al.* (2004) for a range of different return interval events

<b>Tp option SPR option</b>	<b>Tp<sub>0</sub> SPR<sub>0</sub> (base case)</b>	<b>Tp<sub>0</sub> SPR<sub>1</sub></b>	<b>Tp<sub>1</sub> SPR<sub>0</sub></b>	<b>Tp<sub>1</sub> SPR<sub>1</sub></b>	<b>Tp<sub>2</sub> SPR<sub>0</sub></b>	<b>Tp<sub>2</sub> SPR<sub>1</sub></b>
<b>Catchment</b>	<b>(Percentage increase in flood peak relative to base case)</b>					
<b>W. Glen</b>						
T=2	1.33	14 %	13 %	29 %	-10 %	2 %
T=10	2.62	13 %	13 %	28 %	-10 %	2 %
T=25	3.47	12 %	14 %	28 %	-10 %	1 %
T=100	5.05	11 %	15 %	28 %	-11 %	-1 %
<b>Tud</b>						
T=2	7.99	21 %	5 %	26 %	-4 %	15 %
T=10	15.49	19 %	5 %	25 %	-4 %	14 %
T=25	20.22	18 %	5 %	24 %	-5 %	13 %
T=100	28.94	17 %	5 %	23 %	-5 %	11 %

The results of the FD2114 modelling indicate that changes to both Tp and SPR can have significant impacts on the outlet Qp. The scenario in which Tp is reduced (Tp<sub>2</sub>) and SPR remains the same (SPR<sub>0</sub>) would indicate that the addition of attenuation to a catchment could potentially prove a means by which Qp could be reduced. No methodologies are offered for increasing Tp, however, this could be done through planting riparian woodland, hedgerows or implementing Runoff Attenuation Features (RAFs) - anything that essentially reduces the connectivity within the landscape and impedes the propagation of the flood wave. As shown above (Figure 6-3) the Tp change should result in a proportional change in Qp.

The analysis of Tp has highlighted the differences in the values obtained from the FEH regionalised approach and those obtained from observed data. The SPRHOST values also differ when obtained from the FEH catchment descriptors (40.68; Section 6.2.3) and derived from GIS analysis (42.46; Table 6-1) of the soil map, due to the differing type and resolution of data used. These differences indicate that there are uncertainties in model parameterisation and therefore modelled outputs and impacts.

This section suggests that the FEH, HOST and likely changes to Qp and Tp from LUMC and NFM are a reasonable starting position for flood impact management and may be useful screening and understanding tool for catchment and flood managers.

### 6.2.2 FEH or ReFH

The FEH rainfall runoff model has been updated and is now known as the ReFH model, as discussed above. Packman *et al.* (2004) used the FEH model, as the ReFH was still under development, when the FD2114 project was undertaken. It was acknowledged that the ReFH model was under development and that the FD2114 methods would apply equally to the ReFH procedure. The purpose of this section is to perform a sensitivity analysis for Great Ayton using both models to identify any difference in the model outputs and what this would mean for impact assessment.

The time base of both models is controlled in much the same way through the calculation of  $T_p$ . The magnitude of the unit hydrograph, however, is calculated in slightly different ways. The FEH model requires that an observed SPR or SPRHOST are given to dictate the fast response of the catchment. The ReFH model requires that an observed Baseflow Index (BFI) or BFIHOST are used to parameterise the baseflow model and calculate an SPR through Equation 6-3:

Equation 6-3

$$SPR = 72.0 - 66.5BFI$$

Both models were used to populate the decision support matrix to examine what impact the differing structures would have for practitioners using these models for catchment planning. The values plotted within the matrix represent the percentage change in  $Q_p$  for a given SPR/ $T_p$  scenario. Packman *et al.* (2004) considered a change in SPR of  $\pm 20\%$  and a  $T_p$  adjustment of  $\pm 2$  hours as extreme, and provide the practical limits on any future potential impacts from LUM and NFM. The bottom left corners of the matrices (Figure 6-2) represent the most improved scenario, where SPR is reduced by 20% and  $T_p$  increased by 2 hours, give similar reductions in  $Q_p$  of 32% (FEH) and 38% (ReFH) for the 100-year, 12 hour event. The differences are likely to be associated with the additional losses incorporated in the ReFH model. The degraded catchment scenarios give significantly less comparable results, with the FEH model indicating a 48% increase in  $Q_p$  and the ReFH an increase of 59%. They do, however, give different  $Q_p$  values for the baseline, i.e. current catchment values, 100-year event; the FEH peak is 33.88 m<sup>3</sup>/s, whilst the ReFH model is 19.31 m<sup>3</sup>/s. A pooled flood frequency analysis using the 10 years of available flow series provide a  $Q_p$  of 40 m<sup>3</sup>/s for the 100-year flood event.



The modelled impacts of manipulating SPR/BFI and Tp on flood peaks for both models are similar. It is only at the most extreme degraded catchment scenario that there is a large difference between the impacts.

a.		Tp						
		8.32	7.68	7.04	6.4	5.76	5.12	4.48
SPR	49 (+20%)	-3.67	2.51	9.58	17.46	26.59	36.71	48.34
	47 (+15%)	-7.24	-1.29	5.51	13.10	21.88	31.61	42.80
	45 (+10%)	-10.81	-5.09	1.44	8.73	17.17	26.52	37.27
	43 (+5%)	-14.38	-8.89	-2.63	4.37	12.46	21.43	31.74
	41(Baseline)	-17.94	-12.69	-6.69	0.00	7.75	16.34	26.20
	39 (-5%)	-21.51	-16.50	-10.76	-4.37	3.04	11.24	20.67
	37 (-10%)	-25.08	-20.30	-14.83	-8.73	-1.68	6.15	15.14
	35 (-15%)	-28.65	-24.10	-18.90	-13.10	-6.39	1.06	9.61
	33 (-20%)	-32.21	-27.90	-22.97	-17.46	-11.10	-4.04	4.07

b.		Tp							
		8.32	7.68	7.04	6.4	5.76	5.12	4.48	
SPR	49 (+20%)	5.33	11.59	18.66	26.76	36.04	46.71	59.18	0.349
	47 (+15%)	-0.60	5.24	11.85	19.40	28.05	38.02	49.65	0.379
	45 (+10%)	-5.93	-0.47	5.74	12.82	20.92	30.28	41.17	0.410
	43 (+5%)	-11.07	-5.95	-0.12	6.51	14.09	22.88	33.08	0.440
	41(Baseline)	-16.39	-11.60	-6.16	0.00	7.07	15.28	32.27	0.471
	39 (-5%)	-21.73	-17.27	-12.23	-6.50	0.06	7.70	16.52	0.502
	37 (-10%)	-26.95	-22.81	-18.15	-12.84	-6.74	0.35	8.51	0.532
	35 (-15%)	-32.40	-28.60	-24.32	-19.44	-13.81	-7.30	0.21	0.563
	33 (-20%)	-37.76	-34.29	-30.36	-25.89	-20.71	-14.75	-7.87	0.593

Figure 6-2 Matrices produced for Great Ayton using the (a) FEH and (b) ReFH models for the 100-year, 12 hour event

The similarity of the modelled output is illustrated in Figure 6-3. The top, middle and bottom rows of the matrices in Figure 6-2 are plotted in Figure 6-3, but instead of the percentage differences in Qp, the actual Qp values are plotted. Each coloured line

represents a different SPR scenario; the solid lines being the output from the FEH model and the broken lines being the output from the ReFH model. The middle blue lines in Figure 6-3 represent the SPR value ascribed to the Great Ayton catchment in the FEH. Although the  $Q_p$  values differ between each of the models, the shape and magnitude difference between the lines is similar.

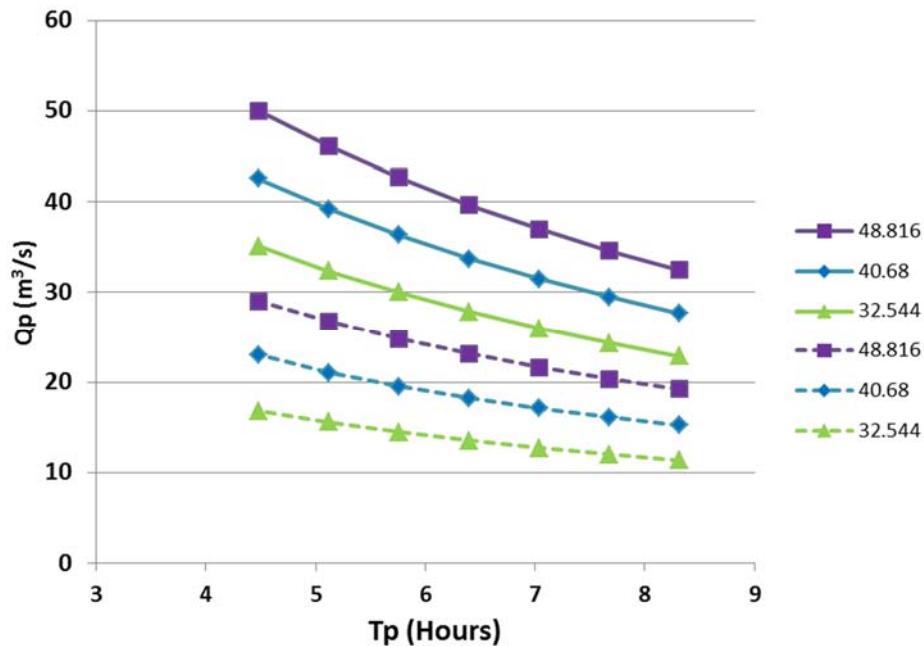


Figure 6-3 Peak discharge values for the 100-year flood for multiple SPR and  $T_p$  scenarios as modelled with FEH (Solid line) and ReFH (Broken line)

The FEH baseline scenario gives a  $Q_p$  for the 100-year event in Great Ayton, closer to the value estimated in the flood frequency analysis than the ReFH. It is for these reasons that the model taken forward for the following study is the FSR FEH rainfall-runoff model.

### 6.3 FEH modelling to Great Ayton

The FEH model will now be used to test a number of LUM scenarios to investigate the potential impacts on  $Q_p$  and the results will be shown using the FARM tool. The scenarios will show what effect the design storm characteristics have on the modelled outputs and therefore impacts; including modelling different return interval events and different storm durations. All modelling is done using a 15 minute data interval.

#### 6.3.1 Impact of change on different return interval floods

Impacts of changes in SPR and  $T_p$  on the 100 and 25 year return interval, 12 hour duration flood events are displayed in Table 6-4 and the matrices for these events

shown in Figure 6-2(a) and Figure 6-4. The matrices show similar percentage increases and decreases for both events with the impact on Qp being almost uniform regardless of return interval.

**Table 6-4 Flood peak discharges for different magnitude storms under different catchment conditions**

<b>Flood Return Interval</b>	<b>Qp Catchment improved (m<sup>3</sup>/s)</b>	<b>Qp Catchment baseline (m<sup>3</sup>/s)</b>	<b>Qp Catchment degraded (m<sup>3</sup>/s)</b>
<b>100-year</b>	22.87 (-32 %)	33.73	50.04 (+48 %)
<b>50-year</b>	19.62 (-32 %)	29.05	43.20 (+49 %)
<b>25-year</b>	16.40 (-33 %)	24.38	36.36 (+49 %)

		<b> Tp</b>						
		8.32	7.68	7.04	<b>6.4</b>	5.76	5.12	4.48
<b> SPR</b>	49 (+20%)	-2.89	3.30	10.37	18.26	27.39	37.51	49.14
	47 (+15%)	-6.62	-0.68	6.11	13.69	22.46	32.19	43.36
	45 (+10%)	-10.35	-4.65	1.86	9.13	17.54	26.86	37.58
	43 (+5%)	-14.08	-8.62	-2.39	4.57	12.61	21.54	31.79
	41(Baseline)	-17.81	-12.60	-6.65	0.00	7.69	16.21	26.01
	39 (-5%)	-21.54	-16.57	-10.90	-4.56	2.77	10.89	20.22
	37 (-10%)	-25.27	-20.54	-15.15	-9.13	-2.16	5.56	14.44
	35 (-15%)	-29.00	-24.52	-19.40	-13.69	-7.08	0.24	8.66
	33 (-20%)	-32.72	-28.49	-23.65	-18.26	-12.01	-5.08	2.88

**Figure 6-4 Risk matrix for the 25-year, 12 hour FEH model run to Great Ayton**

The implications of these patterns are that regardless of the event magnitude, the modelled Qp change is the same. Whether this is realistic is debateable as with increasing event size the percentage of runoff is likely to increase as catchment storage is exhausted, therefore the level of impact is likely to be different but this is not captured by the model.

### **6.3.2 Impact of storm duration**

To investigate the impacts of manipulating Tp and SPR on different storm durations, the matrices have been populated for the 100-year flood event with different rainfall storm durations (Figure 6-5). The duration and intensity of a rainfall event were demonstrated as being influential characteristics in determining Qp (Chapter 5, Figure

5-12. This is an important consideration as the types of mitigation suited to certain storms may differ. Table 6-5 shows that changing the rainfall storm duration leads to a difference in peak rainfall intensity and total rainfall depth for a given return interval flood.

Qp for the current SPRHOST value differ for each of the storm durations, with the most significant difference being between the short duration storm (2.75 hours) and the critical storm duration event (11.25 hours). It is interesting to note that the maximum rainfall intensity is 59 % greater for the short duration storm but the total design storm depth is 59 % less.

**Table 6-5 Rainfall characteristics for different duration storms that produce a 1-in100-year flood**

<b>Storm Duration (hrs)</b>	<b>Max rainfall intensity (mm/hr)</b>	<b>Design storm depth (mm/hr)</b>	<b>Qp for current SPR value (m<sup>3</sup>/s)</b>
2.75	12.81	55.85	23.58
11.25	5.31	88.89	33.73
23.75	3.37	118.76	35.03

The patterns of the matrices (Figure 6-5) show that changing SPR and Tp have a greater impact on the shorter, higher intensity storms (a) than they do on the longer, less intense storms (b).

a.		Tp						
		8.32	7.68	7.04	6.4	5.76	5.12	4.48
SPR	49 (+20%)	-6.82	0.41	8.80	18.86	30.92	45.86	64.75
	47 (+15%)	-10.49	-3.56	4.50	14.14	25.72	40.05	58.16
	45 (+10%)	-14.16	-7.53	0.19	9.43	20.52	34.24	51.59
	43 (+5%)	-17.83	-11.49	-4.12	4.71	15.31	28.43	45.01
	41(Baseline)	-21.51	-15.46	-8.43	0.00	10.11	22.62	38.43
	39 (-5%)	-25.18	-19.42	-12.73	-4.72	4.90	16.80	31.85
	37 (-10%)	-28.85	-23.39	-17.04	-9.43	-0.31	10.99	25.28
	35 (-15%)	-32.52	-27.35	-21.34	-14.15	-5.51	5.18	18.70
	33 (-20%)	-36.20	-31.32	-25.65	-18.86	-10.71	-0.63	12.12
b.		Tp						
		8.32	7.68	7.04	6.4	5.76	5.12	4.48
SPR	49 (+20%)	2.64	6.94	11.57	16.50	21.83	27.52	33.72
	47 (+15%)	-0.99	3.16	7.62	12.37	17.51	23.00	28.98
	45 (+10%)	-4.61	-0.62	3.67	8.25	13.20	18.48	24.24
	43 (+5%)	-8.24	-4.40	-0.27	4.12	8.88	13.96	19.49
	41(Baseline)	-11.87	-8.18	-4.22	0.00	4.56	9.44	14.75
	39 (-5%)	-15.49	-11.96	-8.17	-4.13	0.25	4.92	10.00
	37 (-10%)	-19.12	-15.74	-12.11	-8.25	-4.07	0.40	5.26
	35 (-15%)	-22.74	-19.52	-16.06	-12.37	-8.38	-4.12	0.52
	33 (-20%)	-26.37	-23.30	-20.01	-16.50	-12.70	-8.64	-4.23

Figure 6-5 Risk matrices for FEH model runs to Great Ayton using different storm durations. a) 2.75hrs, b) 23.75hrs

These results suggest that the impacts of LUMC on Qp are more significant during short duration, high intensity rainfall events (indicative of convective events in the summer months), than they are during longer duration storms. Once storm duration is greater than or equal to the critical storm duration (as calculated from the FEH) the modelled Qp and impacts are very similar. The critical storm duration is intended to provide the largest flood peak. It is shown in Table 6-5 that longer duration storms will lead to limited increases in Qp and therefore insignificant changes to the modelled scenarios and matrices produced.

### 6.3.3 Spatial scale and LUM scenario impacts

As a simple test to investigate the impacts of SPR manipulation on catchments of different scales and average SPRs, two sub-catchments within the Great Ayton catchment have been modelled separately. The sub-catchments modelled are Dikes

Beck, with an area of 3 km<sup>2</sup> and a SPRHOST value of 43.89; and Lonsdale, with upstream area of 4 km<sup>2</sup> and a SPRHOST value of 45.09 (Figure 6-8). Each catchment has been modelled using critical storm durations as calculated from FEH catchment descriptors.

Table 6-6 shows that regardless of the catchment size, the resultant Qp change (+/- %) similar for any catchment scenario or change in SPR, which is due to the linearity of the unit hydrograph.

**Table 6-6 The impact on QP for each of the sub catchments of applying the degradation and improved catchment scenarios outlined in the FEH improvements study.**

<b>Catchment (Area)</b>	<b>Qp Improved Catchment (m3/s)</b>	<b>Qp Baseline Catchment (m3/s)</b>	<b>Qp Degraded Catchment (m3/s)</b>
<b>Dikes beck (3 km<sup>2</sup>)</b>	3.7 (-34 %)	5.61	8.42 (+50 %)
<b>Lonsdale (4 km<sup>2</sup>)</b>	5.82 (-33 %)	8.69	13.00 (+50 %)
<b>Great Ayton (30 km<sup>2</sup>)</b>	22.87 (-32 %)	33.73	50.04 (+50 %)

#### ***6.3.4 Knowledge gained from Great Ayton and application to Morland***

Taking the knowledge and understanding gained from the various scenarios modelled for Great Ayton, this section will attempt to populate a FARM matrix for the Morland catchment using a limited number of modelled runs.

The patterns in each of the matrices above indicate a linear relationship with changes in SPR and Tp. The individual rows of the matrix are plotted in Figure 6-6, but instead of the percentage differences in Qp, the Qp values are plotted. Each coloured line represents a certain SPR scenario, with the middle blue line representing the SPRHOST value ascribed to the Great Ayton catchment in the FEH. The x-axis is the Tp multiplier applied to the original, which for Great Ayton is 6.4 hours.

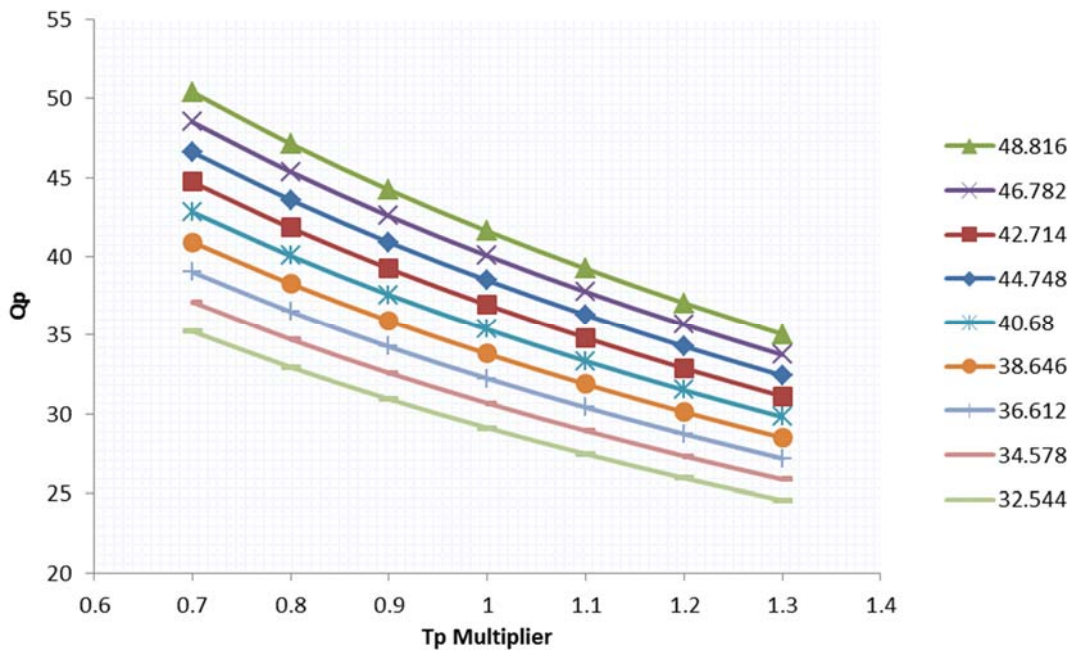


Figure 6-6 Peak discharge values for the 100-year flood for multiple SPR (colour of line) and Tp scenarios (x-axis).

The difference between each of the SPR scenarios, as reflected in the colour of their lines (Figure 6-6), is a 5 % increment from the catchment original of 40.68. The difference between each of the SPR lines is equal for a given Tp value which indicates a purely linear scalar effect of changing SPR and Qp magnitude and can be linked to the underlying assumptions of linearity in the Unit Hydrograph (UH) approach. The effect of changing Tp is, however, not so linear with slight differences in the shape of the lines. Yet by modelling any two rows on the matrix it is possible to complete the matrix, as is demonstrated below for the Morland catchment in Cumbria.

### ***FEH modelling of Morland***

The FEH model has been parameterised using the FEH descriptors, which give a Tp of 2.9 hours and the catchment SPRHOST is 35.72. The two rows in bold shown in Figure 6-7 were populated completely with Qp values generated by the FEH model. Any two rows could have been populated but it was decided that populating the top and bottom rows, with SPR values of plus or minus 20 % would make it clearer how the rest of the matrix was populated. For each alternative Tp scenarios, i.e. the different columns the incremental change from row to row was calculated by subtracting the bottom row from the top row and dividing by the number of empty rows plus one.

The Qp matrix completed using the simple formulation described above is shown in Figure 6-7. The numbers in red are those that have been verified with the FEH model to ensure that the formulation worked in all instances.

		Original Time to Peak						
	SPR	1.3	1.2	1.1	2.9	0.9	0.8	0.7
SPR +20%	42.864	19.6	20.7	21.9	23.2	24.7	26.4	28.2
SPR +15%	41.078	18.8	19.9	21.1	22.4	23.8	25.4	27.2
SPR +10%	39.292	18.1	19.2	20.3	21.5	22.9	24.4	26.1
SPR +5%	37.506	17.4	18.4	19.5	20.7	22.0	23.4	25.1
<b>Original</b>	<b>35.72</b>	16.7	17.7	18.7	19.8	21.1	22.5	24.1
SPR -5%	33.934	16.0	16.9	17.9	19.0	20.1	21.5	23.0
SPR -10%	32.148	15.3	16.1	17.1	18.1	19.2	20.5	22.0
SPR -15%	30.362	14.5	15.4	16.3	17.3	18.3	19.6	20.9
SPR -20%	28.576	13.8	14.6	15.5	16.4	17.4	18.6	19.9

Figure 6-7 Completed Qp matrix using interpolation and verified values in red, for the 100-year, 8 hour event to Morland

The implications of this result are that the modelling FEH-FARM procedure is by no means a way of carrying out a detailed flood mitigation study. It can certainly be useful as a thinking tool for the likely implications of land management decisions within a catchment. The matrices produced, however, do not change a great deal in terms of percentage Qp impact and the pattern of change is the same.

A more bespoke methodology is required that takes into consideration the distributed nature of catchment characteristics, such as soils and the channel network, as well as the way in which LUMC is applied. Such a methodology is described and developed below.

#### 6.4 Flood Impact Modelling tool (FIM)

The location within a catchment that undergoes flood hazard mitigation is likely to play an import role in the level of impact that is experienced at the outlet. The reasons for this are twofold; (1) different regions of the catchment generate different amounts of runoff, and (2) there are travel time and synchronicity effects as flood waves propagate the system and combine with additional sub-catchment contributions. These types of



effects cannot be considered with the lumped FEH rainfall-runoff model, the changes applied are an effective catchment averaged effect.

In order to begin to investigate the effects of travel time and location of mitigation with the FEH rainfall-runoff model the Flood Impact Model tool (FIM) was created. The tool has been developed within Microsoft Excel and is designed to be simple and intuitive.

#### **6.4.1 FIM description**

For the catchment outlet at Great Ayton and 5 key sub-catchments the FEH 100-year flood events have been created using the critical storm durations specific to each of the individual catchments (Figure 6-8). The outlet hydrograph has then been disaggregated using the sub-catchment hydrographs. A constant wave celerity of 1 m/s has been used to route each of the sub-catchment contributions to the outlet (Figure 6-8). The wave celerity is based on the average speed observed in the analysis in Chapter 5, section 5.4.3, Figure 5-17. The contributions of each sub-catchment are summed as in superposition. The sub-catchment contributions are not sufficient to create the outlet hydrograph so unaccounted for flow is added to ensure the outlet hydrograph equals the modelled 1 in 100-year event. This missing flow is kept at a constant as changes are made to the sub-catchments. The model user can then manipulate the sub-catchment  $Q_p$  and  $T_p$  to investigate the impact at the outlet.

The tool has been used as a teaching aid both on the MSc course at Newcastle University and externally at Natural Flood Management (NFM) workshops. There is interest from the Environment Agency (EA) and the Scottish Environment Protection Agency (SEPA) to develop the tool for other catchments to aid engagement and understanding and consultancies are now beginning to develop similar models for catchments where NFM is being considered.

The assumptions listed below are thought to be acceptable for modelling in a simple, semi-lumped manner, the sub-catchments and network to Great Ayton. However, it is thought that as the catchment scale increases it is likely that they will become less acceptable due to the spatial and temporal variation in rainfall, and what this means for the relative rates of activity and timing of peaks in the sub-catchments as was discussed in section 5.5 of Chapter 5. The key assumptions are:

- The 1 in 100-year flood event at the catchment outlet can be disaggregated by assuming that it is made up of the 1 in 100-year events in the sub-catchments
- The catchment outlet hydrograph can be re-created through superposition of the constituent sub-catchment hydrographs having been routed to the outlet.
- No channel and floodplain attenuation effects on the flood wave as it moves through the network
- A fixed wave speed or celerity of 1 m/s is used as a representative speed for a large event in which all sub-catchments are active, based on the analysis of the observed hydrographs in Chapter 5 section 5.4.3, page 123, Figure 5-17.
- $T_p$  adjustment, shifts the full hydrograph by the resultant adjustment value
- $Q_p$  changes affect the full hydrograph not just the peak and there is no reallocation of mass.

#### **6.4.2 Scenarios of changes modelled**

To investigate the potential role that the proximity of mitigation to the outlet has in the overall  $Q_p$  reduction and the relative role of SPR and  $T_p$  manipulation have on outlet the following scenarios will be tested:

1. Impact of reducing  $Q_p$  by 20 % and increasing  $T_p$  by 1.5 hours for the Dyke's Beck sub-catchment in closest proximity to the outlet (Figure 6-9)
2. Impact of reducing  $Q_p$  by 20 % and increasing  $T_p$  by 1.5 hours for the Lonsdale sub-catchment with longest travel distance to the outlet.
3. Impact of changing both the near and distal sub-catchments, as above (1 and 2), on the outlet hydrographs (Figure 6-10)
4. Repeat scenario 3 but manipulate  $Q_p$  (4a) and  $T_p$  (4b) separately to investigate their relative role on the outlet  $Q_p$  impact.

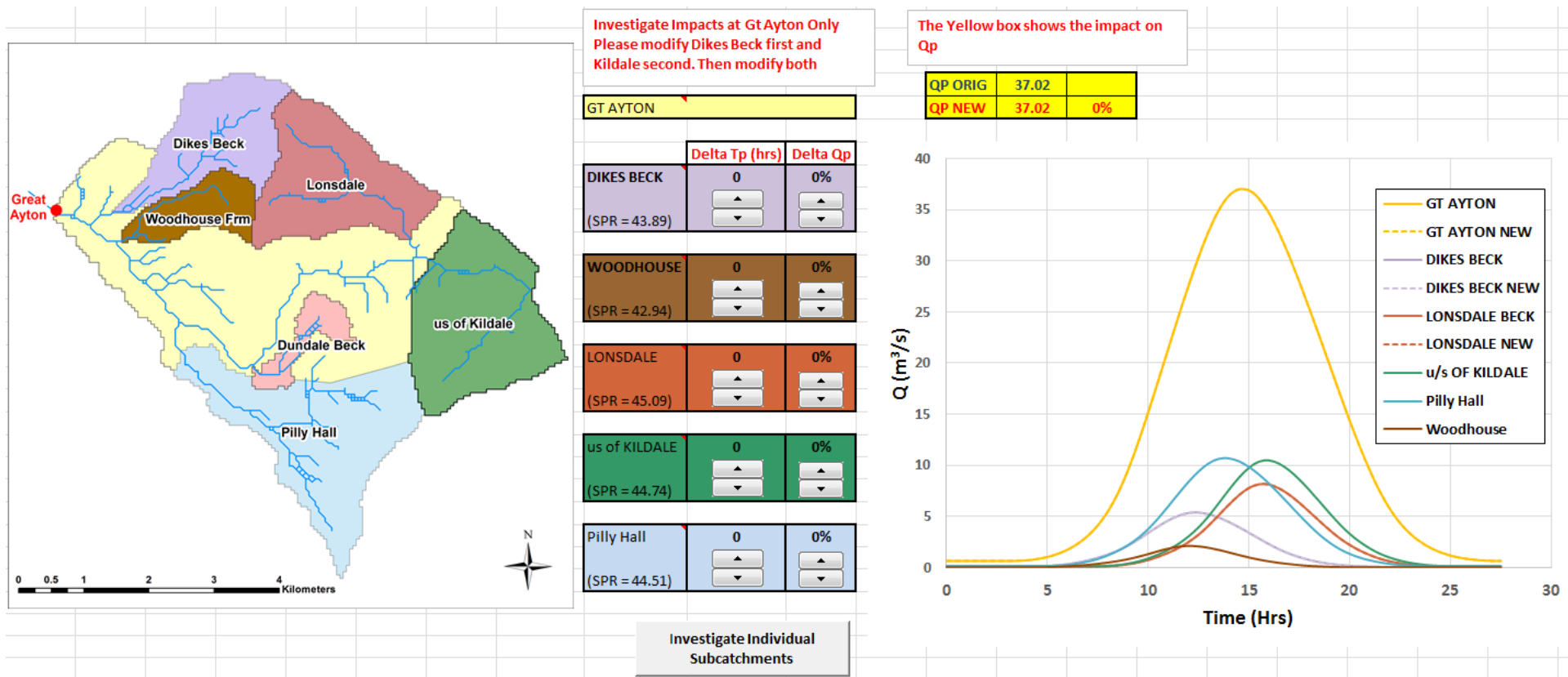


Figure 6-8 The FIM tool interface for the Great Ayton Catchment (parameter manipulations can be made to sub-catchments and the impact at the outlet immediately observed).

Investigate Impacts at Gt Ayton Only  
Please modify Dikes Beck first and  
Kildale second. Then modify both

The Yellow box shows the impact on  
Qp

QP ORIG	37.02	
QP NEW	37.42	1%

GT AYTON	Delta Tp (hrs)	Delta Qp
DIKES BECK (SPR = 43.89)	1.5 ▲ ▼	-20% ▲ ▼
WOODHOUSE (SPR = 42.94)	0 ▲ ▼	0% ▲ ▼
LONSDALE (SPR = 45.09)	0 ▲ ▼	0% ▲ ▼
us of KILDALE (SPR = 44.74)	0 ▲ ▼	0% ▲ ▼
Pilly Hall (SPR = 44.51)	0 ▲ ▼	0% ▲ ▼

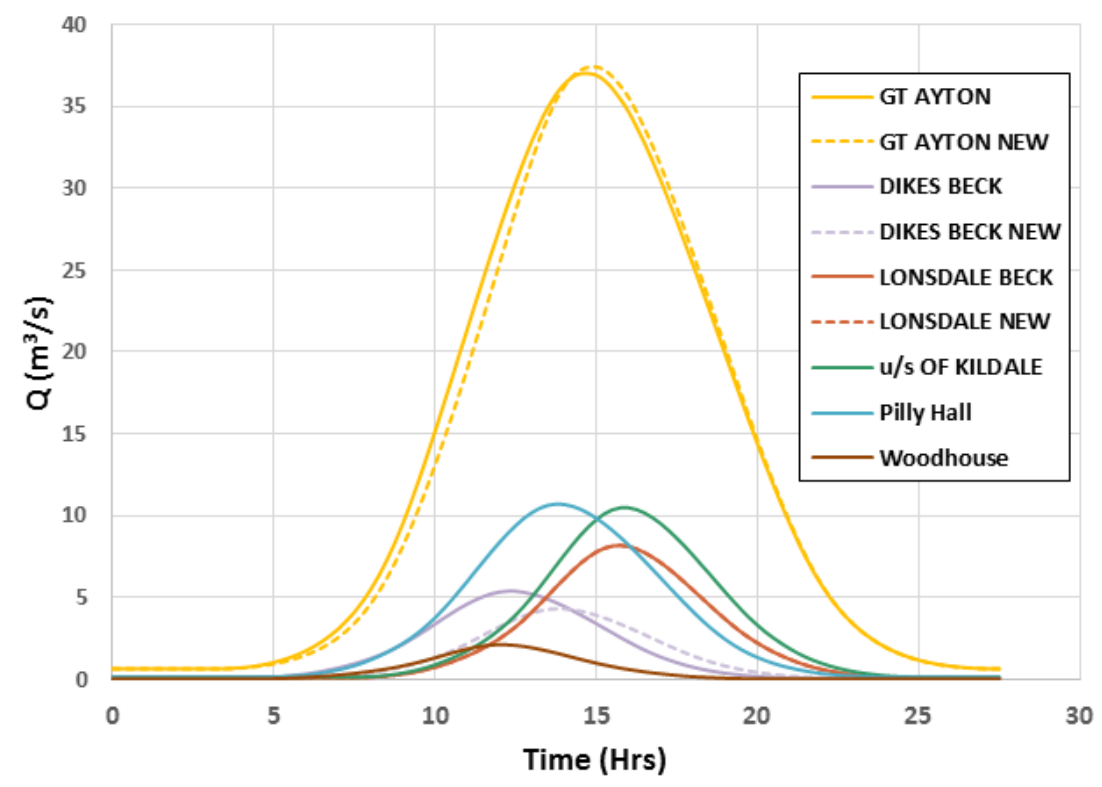


Figure 6-9 Results of increasing the TP and reducing the runoff (through Qp) for the Dikes Beck catchment within the FIM tool.

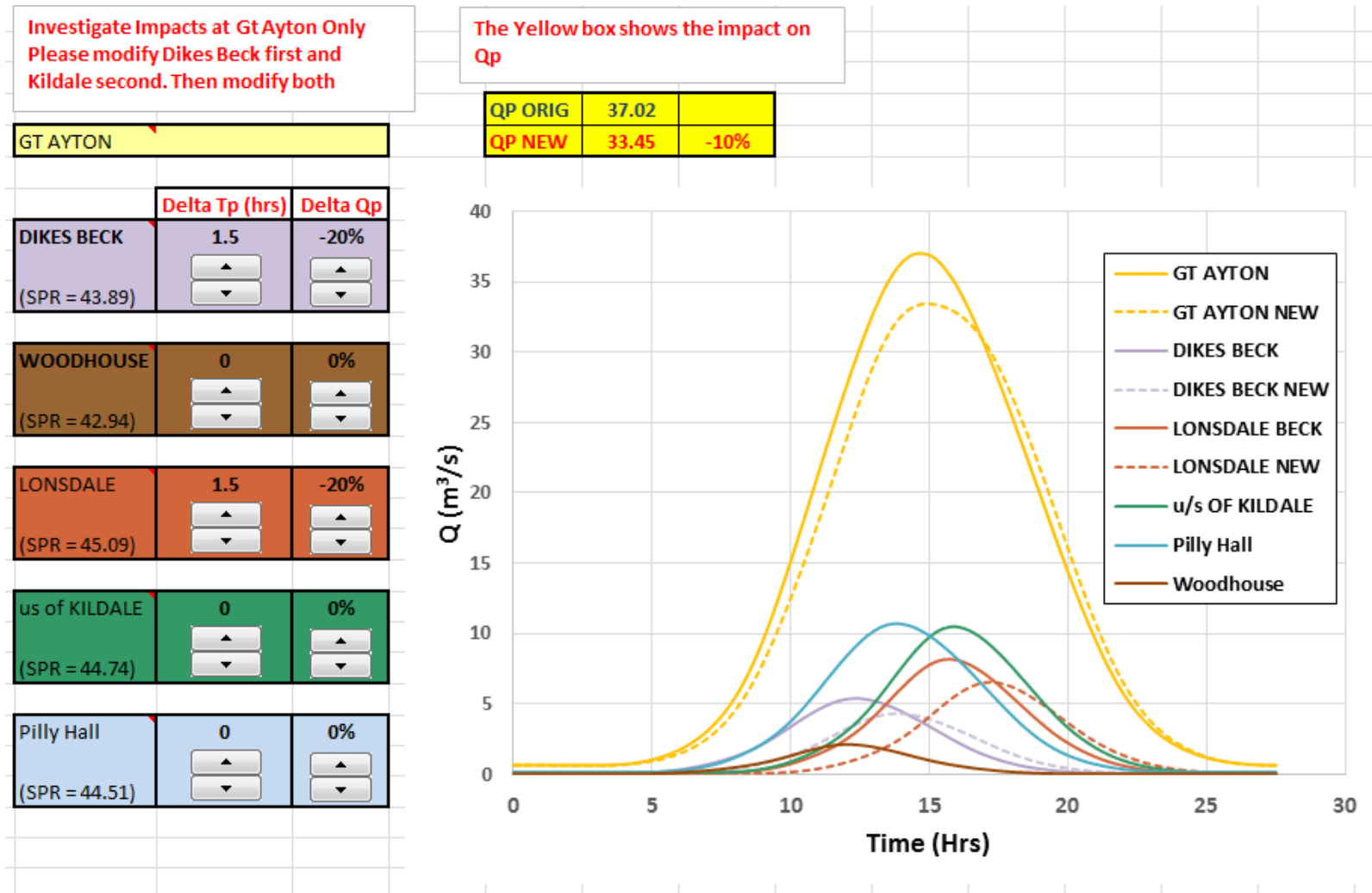


Figure 6-10 Results of increasing the TP and reducing the runoff (through Qp) for the Dikes Beck and Kildale catchments within the FIM tool.

Intuitively, it would be assumed that reducing  $Q_p$  and increasing  $T_p$  of any of the sub-catchments would have a beneficial impact in reducing the outlet peak. However, targeting the sub-catchment closest to the outlet, Dikes Beck, is shown to increase the outlet hydrograph due to the way in which the sub-catchments are synchronised (Figure 6-9, Table 6-7 scenario 1). However, targeting multiple sub-catchments has a beneficial impact (Figure 6-10, Table 6-7 scenario 3).

**Table 6-7 FIM scenario results**

<b>Scenario</b>	<b>Outlet <math>Q_p</math> Impact (% change)</b>
1 – Dyke Beck ( $Q_p$ -20 %, $T_p$ +1.5 hrs)	+1 %
2 – Lonsdale ( $Q_p$ -20 %, $T_p$ +1.5 hrs)	-11 %
3 – Both Dyke Beck and Lonsdale	-10 %
4a – As scenario 3 with only $Q_p$ -20 %	-6 %
4b – As scenario 3 with only $T_p$ +1.5 hrs	-4 %

The modelling of the scenarios with FIM has highlighted the importance of understanding how the catchment and its constituent sub-catchments behave. Mitigating different sub-catchments will have different impacts at the outlet due to the relative travel times and therefore synchronicities with the outlet peak, meaning they potentially have different levels of impact on the outlet peak. The overall concept of flow generation and propagation allows a number of scenarios to be considered, despite the assumptions made. Questions about synchronisation and the degree of intervention can be evaluated and a flood mitigation plan that is relevant to the catchment can be made, which in turn could encourage a more strategic investment. Through the scenarios modelled here, investment in flood mitigation infrastructure such as RAFs would have the greatest impact at reducing catchment flood hazard if implemented in the catchments with the furthest travel distance to the outlet. The coincidence of the of the sub-catchment peaks with the outlet peak is greatest for the upstream Lonsdale catchment, therefore any change in the synchronization of this catchment has a more significant impact than for the other sub-catchments’.

## **6.5 Discussion**

This section summarises the finding from the modelling outputs in this chapter.

### **6.5.1 FEH rainfall-runoff**

The FEH and ReFH models were setup and used to populate a FARM matrix in order to identify if there were any differences between the modelled outputs and hence impacts for Great Ayton. There were differences in the  $Q_p$  results from each of the models, however, the trend and differences between each of the SPR and  $T_p$  scenarios was shown to be similar (Figure 6-3). The resulting impact matrices for Great Ayton using either model are therefore likely to be very similar and any conclusions drawn equally comparable. The FEH rainfall-runoff model was used as it modelled the  $Q_p$  of the 100-year return interval event closest to that obtained from the flood frequency analysis. As the FEH rainfall-runoff model is lumped it is not possible to consider the spatial aspects of mitigation in a clear way, which require a more distributed approach.

#### ***Event magnitude (return interval)***

There was very little difference in the impact of adjusting  $T_p$  and SPR on the modelled  $Q_p$  regardless of return interval. The similarities in modelled impacts are likely due to each return interval events being modelled with a 12 hour duration event, which is slightly larger than the critical storm duration of 11.6 hours. The critical storm duration (as calculated from the FEH methodology) is described as being the duration that will produce the greatest flood peaks, therefore increasing the return interval does not significantly increase the peak discharge.

#### ***Event duration***

The design storm duration was found to have the greatest impact on the modelled  $Q_p$  results and hence the impact of changing SPR and  $T_p$ . The model indicated that short duration, high intensity rainfall will be impacted to a greater extent by LUMC than the longer duration storms. In reality what this means that moving mass within a flashy short duration event has the greater impact than longer duration less intensive events. Two hydrographs and the corresponding hyetographs are illustrated in Figure 6-11. A percentage decrease in the amount of effective rainfall will have the greatest impact in terms of volume of runoff on the shorter duration, higher intensity event. Once the storm duration is greater than or equal to the critical storm duration, the modelled impacts are very similar as the critical storm duration is intended to provide the largest flood peak.

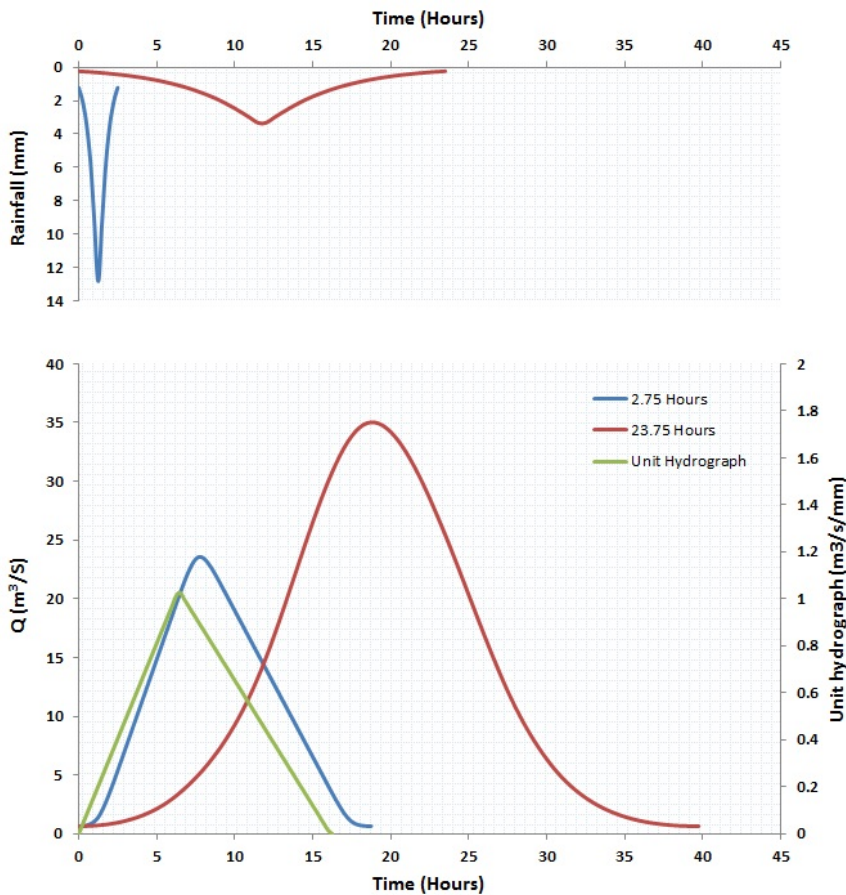


Figure 6-11 The 2.75 hours and 23.75 hours hydrograph and hyetographs generated using the FEH model

This effect was illustrated in the scenarios that investigated the effects of SPR and  $T_p$  manipulation on different magnitude events and different spatial scales. As these scenarios were all modelled using the critical storm duration, specific to each of the catchments and the linear nature of the impact in adjusting SPR and  $T_p$ , the modelled results and impacts were all very similar (as shown in Table 6-6).

***FARM tool***

The FEH modelling procedure offers a way of investigating the likely impacts of LUM decisions in a semi-physical and transparent way. Presenting the modelling results within the FARM tool offers a tangible means of conveying the potential LUMC impacts to non-hydrologists, such as farmers and land managers. Such groups often understand the impact of their decisions at the local scale but may not have considered the implications at the wider catchment scale.

The results in terms of  $Q_p$  adjustments are likely to be very uncertain due to the ambiguity of the initial parametrisation (SPRHOST and  $T_p$ ). It is also difficult to put a



value on SPR reduction or  $T_p$  increase for a given form of mitigation. The FD2114-FEH procedure offers recommendations based on expert knowledge as to the worst possible case of soil degradation (Packman *et al.*, 2004). The HOST reclassification is relatively uncomplicated and applicable at all scales, however, no spatial scale is provided for the adjustment of  $T_p$  by 2-3 hours, however it is unlikely to be valid at multiple scales from 2 km<sup>2</sup> to 30 km<sup>2</sup> and bigger.

#### **6.5.1 What has Morland shown?**

The modelling of Morland demonstrated that the FEH rainfall-runoff is likely to produce very similar impact responses for all catchments (Table 6-6). The matrix produced to demonstrate the potential LUMC impacts was similar in terms of percentage  $Q_p$  impact and the pattern of as that produced for the Great Ayton catchment.

It highlights the need for a modelling methodology that accounts for the distributed nature of catchment characteristics. These include the soils, the channel network and size and shape of the catchment, as well the location in which LUMC is applied. These complexities cannot be captured by a lumped model and led to the development of the semi-lumped FIM tool.

#### **6.5.2 FIM tool**

An alternative use of the FEH has been demonstrated through the FIM tool which proposes a more distributed approach to the way in which LUMC scenarios are applied and routed to the outlet. This was done by disaggregating the outlet hydrograph, through superposition of the waves, to five sub-catchments with a fixed wave speed of 1 m/s. The impact of manipulating individual sub-catchments was then tested and a simple sensitivity carried out.

This process highlighted that the catchment scale impact of mitigation may be sensitive to the location within a catchment that undergoes mitigation. It was found that delaying the peak of the sub-catchment in closest proximity to the outlet, Dykes Beck, could potentially increase flood peaks, even if the volume of runoff was reduced. The increase in outlet  $Q_p$  was due to the increased synchronisation of the sub-catchment peaks. Mitigating the sub-catchment with the greatest travel distance, Lonsdale, was found to have the greatest positive impact on reducing downstream peaks as this reduced the

synchronicity of the component sub-catchments and effectively flattening the outlet peak.

Although mitigating the Lonsdale catchment alone has a greater impact on the outlet  $Q_p$  than combined with Dykes Beck, the Dykes Beck catchment causes flooding locally and is therefore in need of mitigation.

### **6.5.3 What next?**

The modelled outcomes are indicative of the likely impacts of LUM and attempts to be transparent about the residual uncertainty via clearly stated assumptions. However, the model in its current form is too simple to perform detailed LUM change analyses. The most important conclusions that can be drawn from this modelling are that LUMC and NFM have the greatest chance of impacting short duration, high intensity events, and that with increasing duration it becomes more difficult to have a mitigating effect. This is due to any additional storage gained being exhausted before the arrival of the main peak.

As the FEH is widely used by consultants and in the establishment of the Catchment flood management plans (CFMP) it has been demonstrated as a method that is useful for thinking about potential implications. However, it cannot be used to give a definitive level of hazard reduction due to the significant uncertainties in the model inputs as well a lack of understanding and knowledge of how the local impacts of LUMC and NFM manifest at the catchment scale. The tool could be useful for basic flood management plans and its performance can be improved by understanding the catchment response through instrumentation of the network.

Land use change and NFM uptake are always carried out in a distributed fashion and it is unlikely that the whole of the catchment will be mitigated. The way and location in which the distributed changes to runoff are made, and the way in which they synchronise with other parts of the catchment, is unlikely to be captured by a lumped change to  $T_p$ , and certainly unlikely to be as linear as the results shown in this chapter. It is not simply the distributed nature of catchment change that cannot be captured with this model; it is the physical characteristics such as the soil type and topography across the catchment.

As the shortcomings of using the FEH method have been identified in this chapter, it is important to investigate LUMC modelling in a distributed way in order to account for the distributed characteristics of the catchment as well as the distributed nature of change. This is the most appropriate way in which known local-scale LUM change impacts can be propagated to the larger catchment scale. The analysis has shown that the manipulation of travel times ( $T_p$ ) of the distal parts of the catchments need to be captured as they have the most significant impact on catchment outlet  $Q_p$ .

The two subsequent chapters will introduce and use a novel model, Juke, that has been specifically designed to model LUMC and NFM impacts. It is a spatially distributed physically-based model that allows changes to be made to the runoff volume and speed (celerity) at the small-scale (50 m x 50 m), in order to investigate how that manifests at the larger catchment scale.

## Chapter 7. Introduction to Juke

### 7.1 Introduction

The aim of this chapter is to demonstrate Juke as a suitable emulator of the FEH rainfall-runoff model; this will mean the expert knowledge regarding runoff (SPRHOST) and land use impacts that underpin the FEH rainfall-runoff model can be used to investigate flood mitigation in a distributed model structure and is consistent with the FEH. A series of FEH ‘design hydrographs and hyetographs’ generated using the FEH rainfall-runoff model (Chapter 6) are setup within the distributed Juke model. Juke – a distributed, GIS-based, rainfall-runoff model is being used, firstly to show it as a suitable emulator, consistent with the lumped catchment models shown earlier and then to demonstrate the importance of distributed physical information for impact modelling. Demonstrating Juke to be a suitable emulator is important as it is also consistent with the multi-regression analysis that was used to underpin the FEH analysis.

Juke is shown to be a suitable emulator of the FEH using a simple test of reducing SPR for an area of the catchment in order to show that it produces the expected level of reduction in discharge (i.e. agrees with the previously discussed expert knowledge). Three celerity parameters are sensitivity tested to investigate the impact on the hydrograph to understand their potential for use in LUM and NFM scenarios.

The importance of using a distributed model will also be demonstrated through the use of SPRHOST (henceforth referred to as SPR) data for describing the propensity of different soils to generate different amounts of runoff. It will be shown that the impact of changes made to SPR is non-linear and should be considered.

There are a number of assumptions made; primarily, that the FEH events can be disaggregated and that the spatial pattern of SPR is important. From a physical perspective these assumptions seem valid. Whilst there is some uncertainty in the SPR values calculated, the study will demonstrate the potential of the new approach to flood impact modelling.

## 7.2 Juke parameterisation and testing

This section sets out the data requirements and approach taken for parameterising and calibrating Juke to model a series of different return interval FEH hydrographs, generated for a range of storm durations. To calibrate Juke, the required data sets are:

- **Hydrometric data** – At least two flow gauges and a rain gauge are required to develop scaling relationships regarding the celerity of the flood wave.
- **Topography** – A Digital Elevation Model (DEM) for stream network delineation and calculating the upstream areas of each grid cell for the scale relationships. The Juke modelling for the Great Ayton catchment will use a 50m grid resolution.
- **Baseflow threshold** – The value of 2 m<sup>3</sup>/s was selected for the Great Ayton outlet based on analysis of the flow duration curve.
- **Pattern equations** – A set of pattern equations is required to describe how the runoff generation element ( $\gamma$ ) and *celerity* functions are to be parameterised and calculated.

Many different data sets can be used to create the spatial patterns that describe the distributed properties of the catchment. For example soil maps that incorporate the HOST information can be provided to identify areas of the catchment that have a propensity to generate more runoff than others. HOST is possibly the most widely used dataset within hydrological models in the UK, both in industry and in academia (Bulygina *et al.*, 2009; CIRIA, 2013). It is based on observations that provides a direct link between the rainfall-runoff relationships of soils. They can also be used in the development of patterns of change that identify the areas undergoing LUMC. Data sets that are useful for the development of patterns include but is not limited to:

- **HOST** – To describe the relative runoff contributions of soil types or classes
- **Land cover** – National-scale maps can be used to manipulate parameter values for certain soil and land use combinations by using them as a mask to which changes can be made.
- **Topographic wetness index** – Topographic wetness index (TWI) is produced during calibration and can be used to identify potentially the wet and dry regions of the catchment (Beven and Kirkby, 1979). It is calculated for every cell in the

model domain grid, using Equation 7-1, from a combination of the upstream area (a) of the cell and the local slope (b).

- **Topographic wetness ranking** – Ranking based on the topographic index (1 for the wettest cell).

Equation 7-1

$$TWI = \ln \frac{a}{\tan b}$$

### 7.2.1 FEH input data

Design storm hydrographs have been generated using the FEH rainfall-runoff model for Great Ayton and Easby. A number of events of different return intervals (100, 50, 25 and 5 years) and four different storm durations (4, 8, 12 and 24 hours) were generated to reflect rain storms with different rainfall totals and intensities (Table 7-1), to investigate what impact the type of rainfall event has on the magnitude of change in hydrograph peaks (Qp) when the model parametrisation is changed to reflect flood mitigation.

Table 7-1 Summary table of the FEH rainfall event characteristics used to generate the design hydrographs

Storm		Flood Return Interval (years)			
		100	50	25	5
Duration					
24 Hr	Total rain (mm)	118.76	105.34	91.43	62.79
	Max intensity (mm/hr)	13.48	11.96	10.37	7.13
12 Hr	Total rain (mm)	90.14	79.32	68.18	45.65
	Max intensity (mm/hr)	20.66	18.17	15.62	10.46
8 Hr	Total rain (mm)	78.78	69.99	58.96	38.89
	Max intensity (mm/hr)	27.168	23.79	20.33	13.41
4Hr	Total rain (mm)	62.01	53.84	45.57	29.27
	Max intensity (mm/hr)	42.81	37.18	31.46	20.21

The generated storms and storm hydrographs differ significantly from the observed hyetograph and hydrographs but are being used for emulating the FEH. It can be seen from the example storms in Figure 7-1, that the hyetographs are a triangular pulse of rainfall which is then routed through a triangular unit-hydrograph, this results in simple hydrographs.

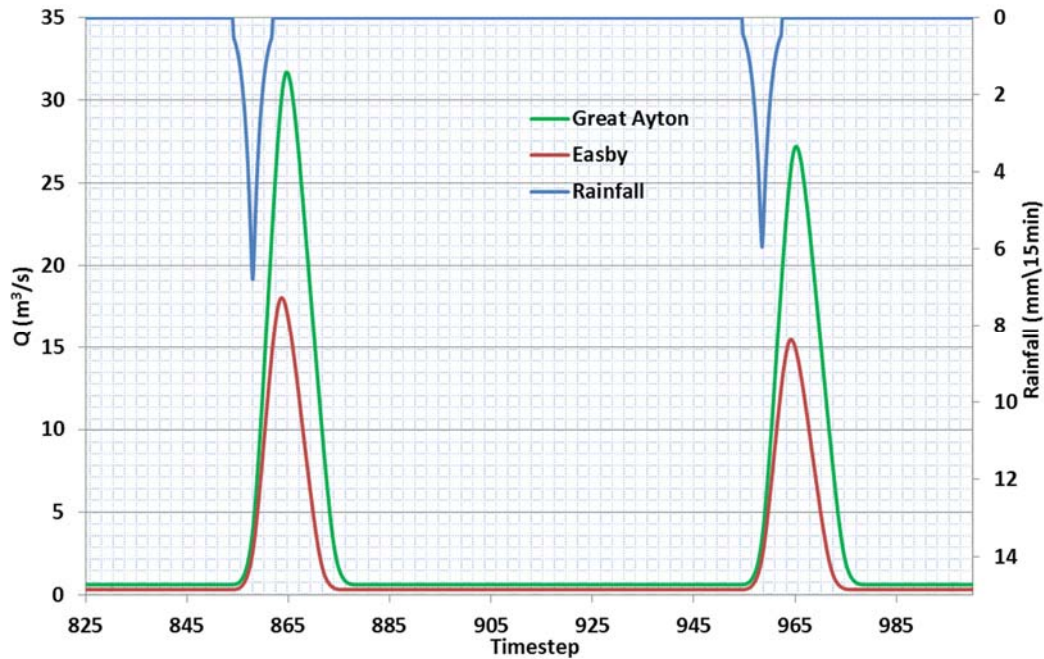


Figure 7-1 The 8 hour, 100 and 50 year return interval events for Great Ayton and Easby

The flood frequency curves associated with different storm durations can be seen in Figure 7-2. The critical storm duration, as calculated by the FEH for Great Ayton is 11.5 hours. The critical storm duration provides a storm profile to give the largest  $Q_p$ ; any storm greater in duration than this does not have a significantly greater peak, but does have a greater volume leading to a longer recession.

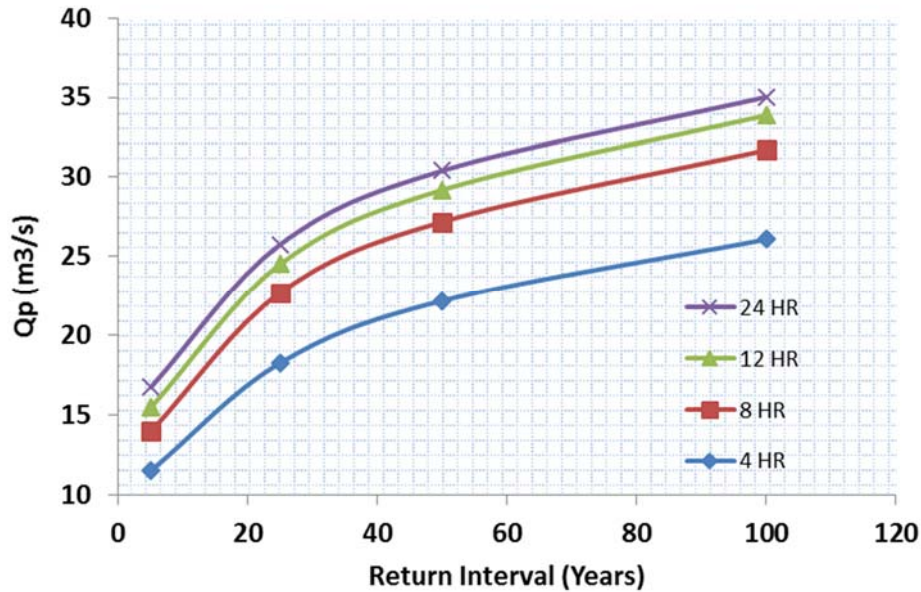


Figure 7-2 Flood frequency curves for Great Ayton generated from the flood peaks for different storm durations by the FEH rainfall-runoff model

## 7.2.2 Runoff generation

### *Uniform rainfall runoff pattern*

This section will investigate the impacts of manipulating the partitioning factor ( $\gamma$ ) of the runoff generation element within JUKE. This parameter is a multiplier applied to the rainfall to convert the total rainfall to an effective amount for routing; it is a distributed element. When the modelling moves to the detailed scenario testing, the model will be given the SPR information to provide the indicative propensities of different soils to generate runoff at different rates. However, in the first simple tests it is assumed that  $\gamma$  is uniform across the catchment, to replicate the lumped structure of the FEH rainfall-runoff model and will be calculated as the catchment average rainfall-runoff ratio required to produce the outlet hydrograph. An analogue for the catchment average rainfall runoff ratio is the matching gain (Lgam) calculated by the matching element in order to achieve the perfect calibration. The matching element calculates a time series of the ratio of distributed modelled flows reaching the matching element and the observed discharge at that time. The Lgam series is simply a multiplier applied to the integrated, distributed, flows arriving at the matching element. The matching gain time series (Lgam) is illustrated in Figure 7-3 against the corresponding hydrograph.



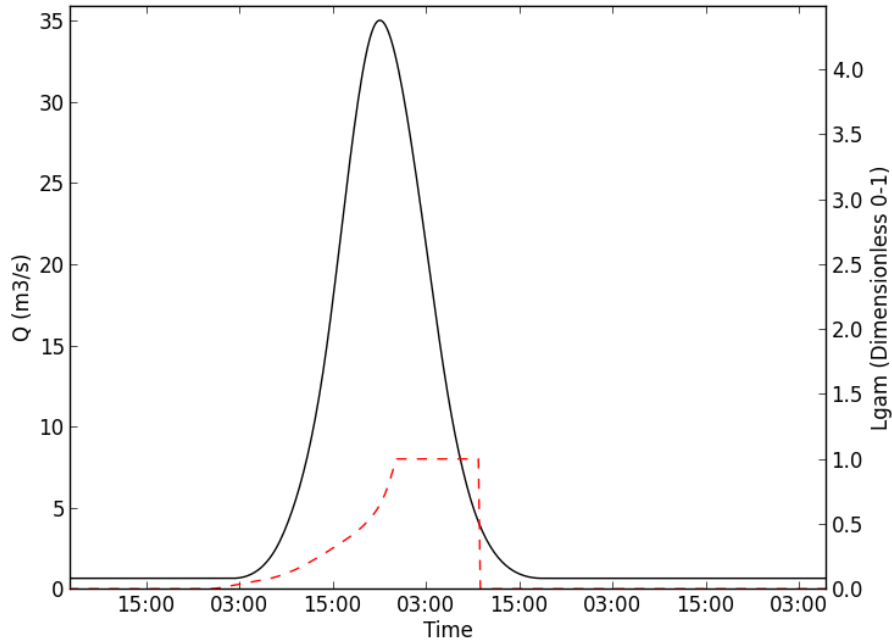


**Figure 7-3 Illustration of the behaviour of the matching gain (Lgam; red) for an FEH 100 year calibrated event (black)**

It is assumed that once the partitioning factor ( $\gamma$ ) has been calculated to achieve the perfect calibration, it can be manipulated to reflect potential changes to runoff volumes; the volume of the simulated hydrographs should change simply in relation to the area modified and the degree of change in the  $\gamma$  parameter values. Given the simplicity of these representations, it would be possible to obtain an approximate solution using a simple calculation, whereby any reduction or increase in  $Q_p$  is proportional to the area affected and the magnitude of SPR manipulation.

So for 20 % reduction in  $\gamma$  across the whole of the catchment we would expect close to a 20 % reduction in  $Q_p$ . For a 20 % reduction in  $\gamma$  over 40 % of the catchment, it would be expected approximately an 8 % ( $0.2 \times 0.4$ ) reduction in  $Q_p$ .

**Table 7-2 Percentage change in  $Q_p$  for range of design storms modelled with Juke and the FEH**

<b>SPR Change</b>	<b>Juke 100yr 8hr</b>	<b>FEH 100yr 8hr</b>	<b>Juke 100yr 24hr</b>	<b>FEH 100yr 24hr</b>	<b>Juke 25yr 8hr</b>	<b>FEH 25yr 8hr</b>
<b>+20 %</b>	18.74	17.84	18.86	16.50	18.24	18.67
<b>+10 %</b>	9.37	8.92	9.43	8.25	9.12	9.33
<b>-10 %</b>	-9.37	-8.92	-9.43	-8.25	-9.12	-9.32
<b>-20 %</b>	-18.74	-17.84	-18.86	-16.50	-18.24	-18.65

The change in  $Q_p$  is consistent for each of the scenarios shown in Table 7-2. There isn't exactly a 1 % reduction in  $Q_p$  for a 1 % reduction in SPR, however, it is very close and the relationship is consistent with a uniform change in  $Q_p$  for a change in SPR. This is also consistent between Juke and the FEH, although the percentage change in  $Q_p$  are not identical, they are similar in magnitude and the relationships are linear; the matching element within Juke is similar to the losses model in the FEH rainfall-runoff model. The differences are likely linked to the distributed nature of Juke with the travel time effects included. The implication of the routing impacts will be discussed in more detail later in this chapter.

The studies with SPR, although simple, do perform a form of model verification, i.e. the model does what is intended, and the sensitivities match what are anticipated. Thus, the expert knowledge has been adequately represented. There will be some uncertainty in the source SPR data, but perhaps a greater degree of uncertainty is understanding how, when this study moves on to scenario modelling, land use change impacts on runoff generation.

### ***Distributed rainfall runoff pattern - HOST***

This section will demonstrate the distributed runoff generation element and why it is considered important to use distributed models for impact modelling over a lumped approach. It has been illustrated that Juke responds in a way that demonstrates it is a suitable emulator of the lumped FEH rainfall runoff model. Juke is here provided with additional distributed information regarding runoff generation through the incorporation of SPR data. The dataset is derived from the 1:250,000 national soil map held by Cranfield University and is shown for the Great Ayton catchment in Figure 7-4 below.

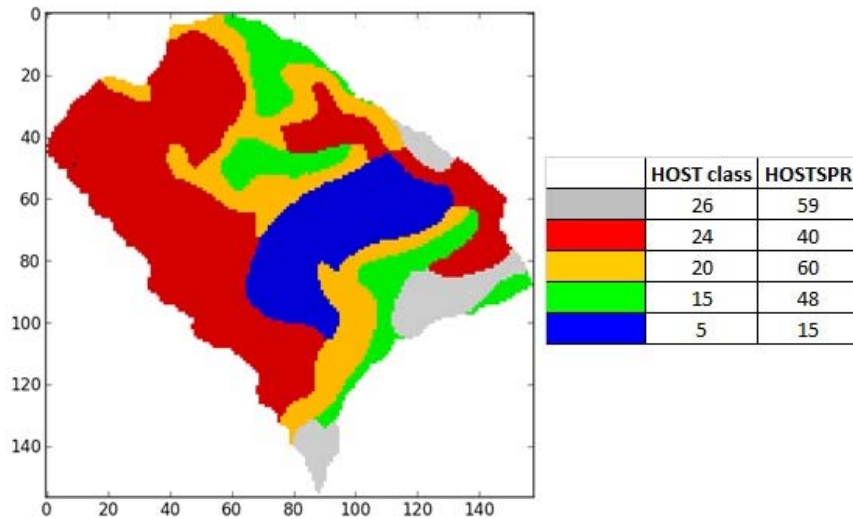


**Figure 7-4 Soils map for Great Ayton showing the HOST attributes (Soil data © Cranfield University (NSRI) and for the Controller of HMSO 2015)**

These data do not provide a fixed SPR but provide the model with information regarding the relative propensities of different soils to generate varying levels of runoff for the same rainfall input. For example, a soil with a SPR of 0.4 will generate twice the amount of runoff compared with a soil of 0.2, for the same rainfall (runoff is limited to 100 % of rainfall). It is a form of distribution function based on the HOST pattern. Having the partitioning factor based on SPR makes the manipulation of it to reflect land use scenarios transparent.

Some results for manipulating SPR are shown in Figure 7-5. This figure shows the change in  $Q_p$  for catchment wide changes to the distributed partitioning factor ( $\gamma$ ) for the uniform and SPR calibration of  $\gamma$ . As the HOST pattern provides a non-uniform distribution of SPR values, when a modification to the pattern values is made as a percentage increase or decrease, different parts of the catchment will change by a different amount. This leads to a non-linear response in the impact on hydrograph peaks (Figure 7-5), as was demonstrated with the FEH-FIM tool in chapter 6.

The magnitude of  $Q_p$  changes are not as great for variable SPR version of the  $\gamma$  pattern as they are for the uniform  $\gamma$  (Figure 7-5). The response is also non-linear and different for different return interval and duration events, where the response from the uniform  $\gamma$  pattern is almost the same and linear; this is the same result that was demonstrated from the lumped FEH rainfall-runoff model in Chapter 6. The non-linear response in the changes to  $Q_p$  for the smaller changes in  $\gamma$  is attributed to the celerity function and will be discussed in more detail later in this chapter. The shorter duration events, using the

variable SPR pattern, produces a greater increase and decrease to the flood peaks than for the longer duration events (Compare the Variable  $\gamma$  24hr and 8hr lines).

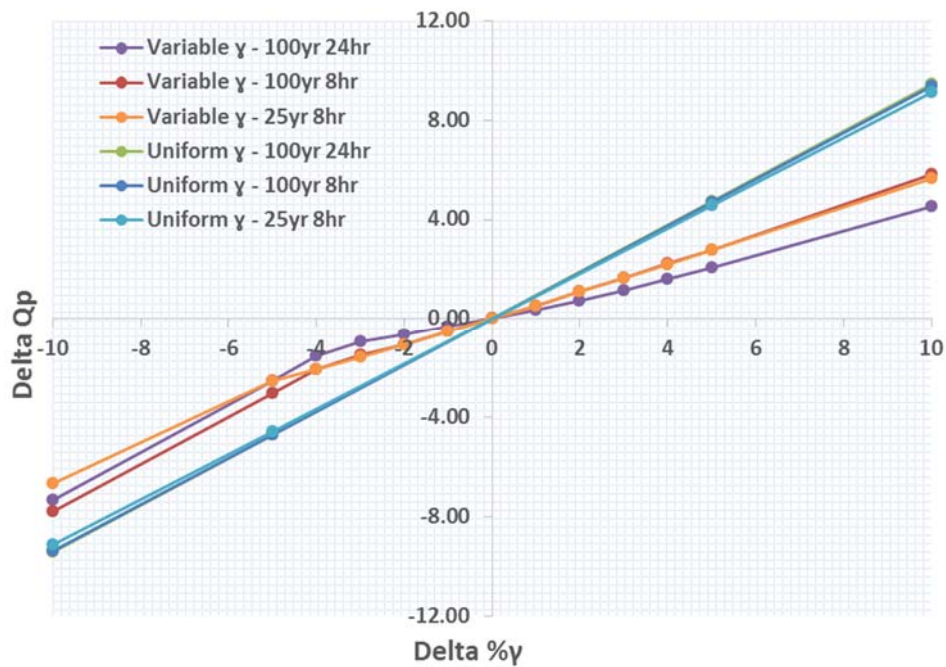


Figure 7-5 Results illustrating the changes in Qp when manipulating uniform and distributed patterns of  $\gamma$

### 7.3 Celerity – flow routing

This section describes the celerity function and the way in which it is parametrised. The parameters within the function are sensitivity tested to demonstrate their potential for use within land use change and flood mitigation scenarios.

Every cell in the catchment has a celerity function, which is assumed to be a function of the hydrograph and the cell's spatial scale (defined as the upstream area of a cell as a fraction of the catchment total). A single cell at the head of the catchment has a scale of  $1/N$ , where  $N$  is the number of cells in the catchment, the outlet cell therefore has a scale of 1.

Peak rates of flow for an event tend to increase systematically with scale. Therefore it was assumed Equation 7-2 was a valid representation of flow scaling.

Equation 7-2

$$q = baq^*$$

Where  $q$  is the peak flow at all locations with scale  $a$ , and  $q^*$  is the corresponding catchment outlet peak discharge. The value of  $b$  is calibrated against the full set of peaks in the flow and rainfall records. It is assumed that a value for  $b$  can be calculated for any scale between the calibrated values using linear interpolation. The calibrated values for  $b$  can be seen in Table 7-3.

**Table 7-3 Peak scaling parameters**

	a	b
Cell	$8.533 \times 10^{-4}$	24.795
Sub-catchment	0.475	1.046
Outlet	1	1

The celerity of the flow network is governed by Equation 7-3. There are three parameters that can be changed to alter the celerity for a given flow at a given scale. The  $q_p$  parameter is the expected local flow rate ( $m^3/s$ ) that corresponds to the current peak discharge at the outlet. Delta ( $\delta$ ) is associated with the larger scales and higher celerity (e.g. flood plains); eta ( $\eta$ ) is associated with small scales and lower celerity (e.g. for subsurface drainage) and is the limit for celerity as scale goes to zero; and phi ( $\phi$ ) controls how the celerity varies with scale.

**Equation 7-3**

$$|c| = \delta - \frac{\phi}{|q_p| + \frac{\phi}{\delta}} + \eta$$

The celerity function is plotted for three different scales in Figure 7-6. It shows that as scale increases celerity increases, as expected. The plot has three lines representing the different scales used in the model calibration. There are many cells at the single scale cell whilst there is only a single cell (i.e. with no upstream contributing area) at the outlet scale, illustrated in Figure 7-7. Cells between the headwaters and the outlet will have celerity relationship somewhere in-between e.g. the sub-catchment scale (Figure 7-6).

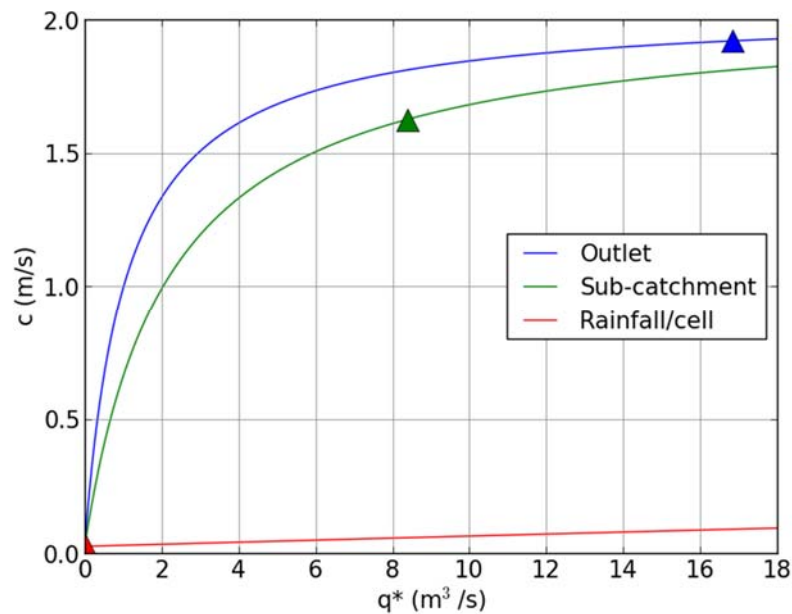


Figure 7-6 Celerity function plotted for three different scales, where  $q^*$  is the flow at a particular scale

The peak discharge observed at Great Ayton outlet is  $16.85\text{m}^3/\text{s}$  on 30/11/2009, and is plotted as a blue triangle in Figure 7-6, with a celerity of  $1.92\text{m/s}$ . The calculated peak flow, as calculated by Equation 7-2, at the sub-catchment scale is  $8.38\text{ m}^3/\text{s}$ , with a celerity of  $1.63\text{m/s}$  and plotted as the green triangle in Figure 7-6. The higher celerity's will never be reached at the single pixel scale ( $50 \times 50\text{m}$ ,  $0.0025\text{ km}^2$ ); these values will only ever be very small and therefore have comparatively low celerity. Relationships of this type and form have been observed in the field and are found to asymptote to constant velocity with increasing discharge (Beven, 1979; Bates and Pilgrim, 1983). A plot of the distribution of the number cells with a given upstream area is provided in Figure 7-7.

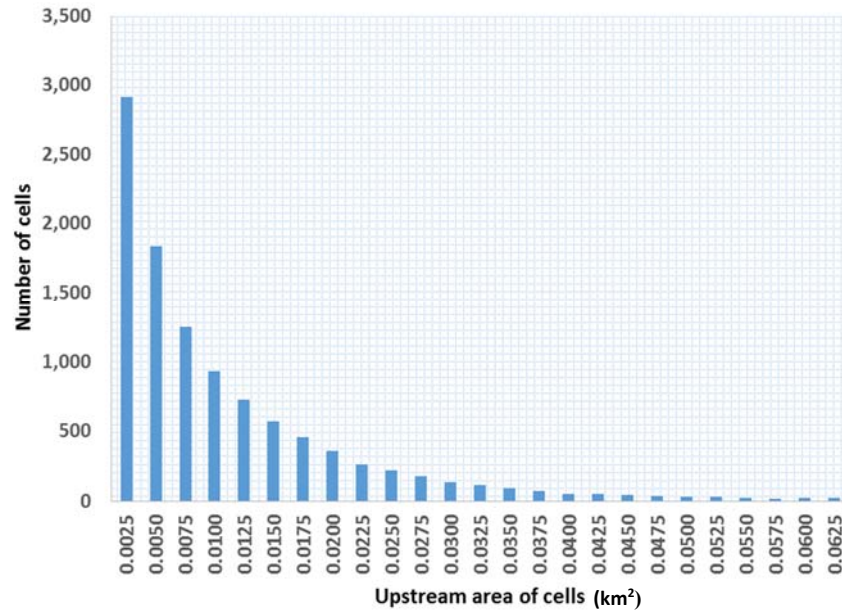


Figure 7-7 Illustration of the number of cells with a given upstream area

Sensitivity analysis of the parameters that make up the function have shown that  $\delta$  and  $\emptyset$  are the most sensitive parameters. The maximum celerity to which the function asymptotes is controlled by  $\delta$ , and  $\emptyset$  controls the shape of the function.  $\eta$  is only sensitive at the small scale, with increasing scale the impact becomes less but does marginally change the peak celerity to which the function asymptotes.

In the following sections sensitivity tests of the celerity function parameters are performed to demonstrate their potential for flood mitigation scenarios in which attenuation features are incorporated. The results plotted in each of the following graphs are for impact to the flood peaks, for the range of return interval events (100, 50, 25 and 5 years) with an 8 hour duration.

### ***Delta ( $\delta$ )***

A decrease in  $\delta$ , reduces the celerity, therefore increasing the  $T_p$  of the outlet hydrograph, as can be seen in Figure 7-8 (a). It also reduces  $Q_p$  by shifting the mass within the hydrograph from the peak and rising limb to the recession (Figure 7-9). When only small reductions are made to  $\delta$  the change in  $T_p$  is greatest for the smaller events, whilst the opposite happens when it is halved.

The impact of reducing  $\delta$  for the 8 hour, 100-year event is shown in Figure 7-9. Reducing  $\delta$  leads to slower rate of rise towards the peak and slower recession. The  $\delta$  parameter is identified as that representing the high scales of celerity, e.g. for floodplains, and will therefore be used in the modelling of a number of potential LUMC scenarios in which floodplains are modified e.g. through riparian woodland.

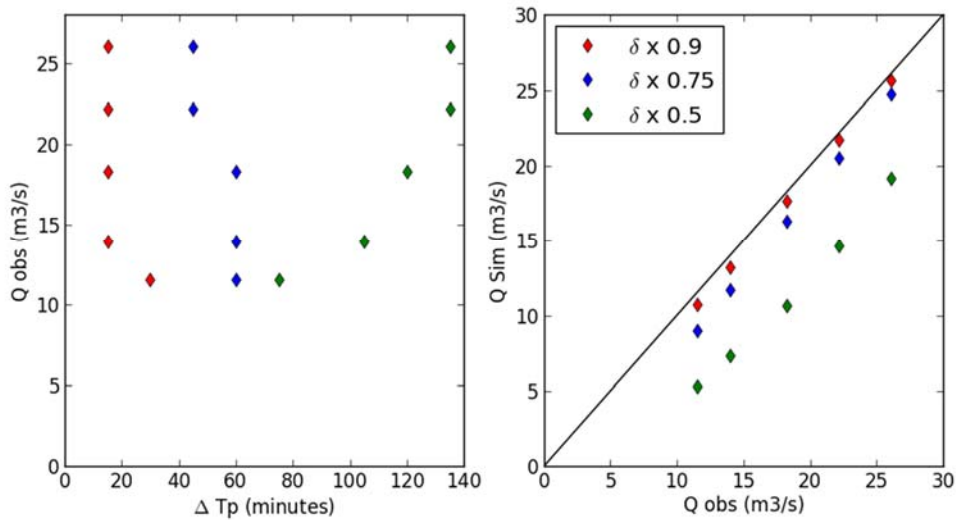


Figure 7-8 Impact of manipulating  $\delta$  plots; a. Change in  $T_p$  (positive  $t$  = increase) b. Change in  $Q_p$  from the modelled FEH hydrographs

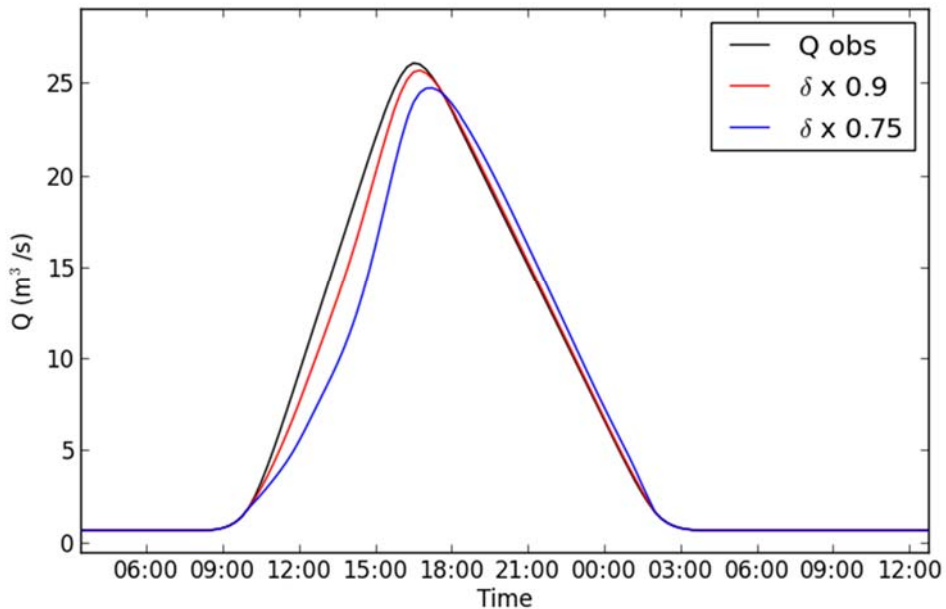


Figure 7-9 Impact of changing  $\delta$  on the FEH 100-year, 8 hours duration event



### Phi ( $\phi$ )

The impact of changing  $\phi$  is much the same as for  $\delta$ , however, it is an increase in  $\phi$  that leads to a reduction in celerity and thus an increase in  $T_p$ .

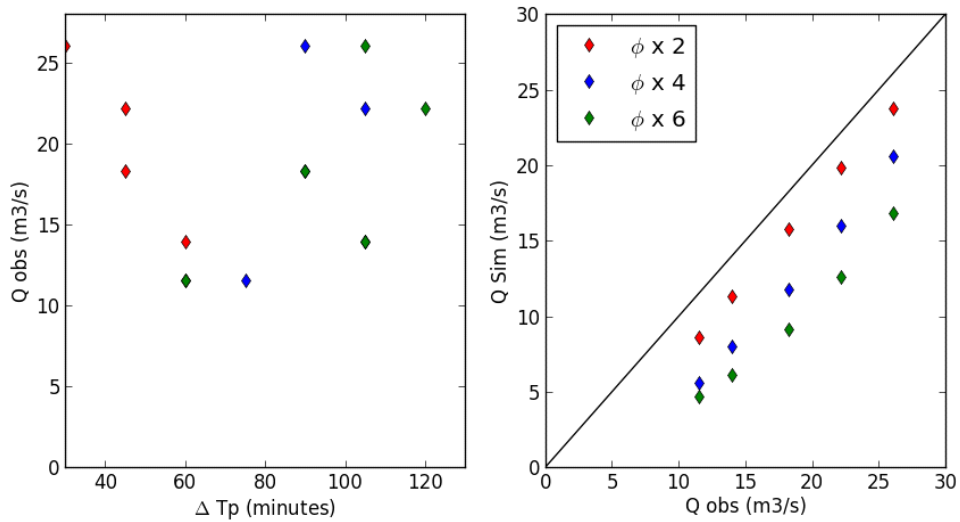


Figure 7-10 Impact of manipulating  $\phi$  plots; a. Change in  $T_p$  (positive  $t$  = increase) b. Change in  $Q_p$  from the modelled FEH hydrographs

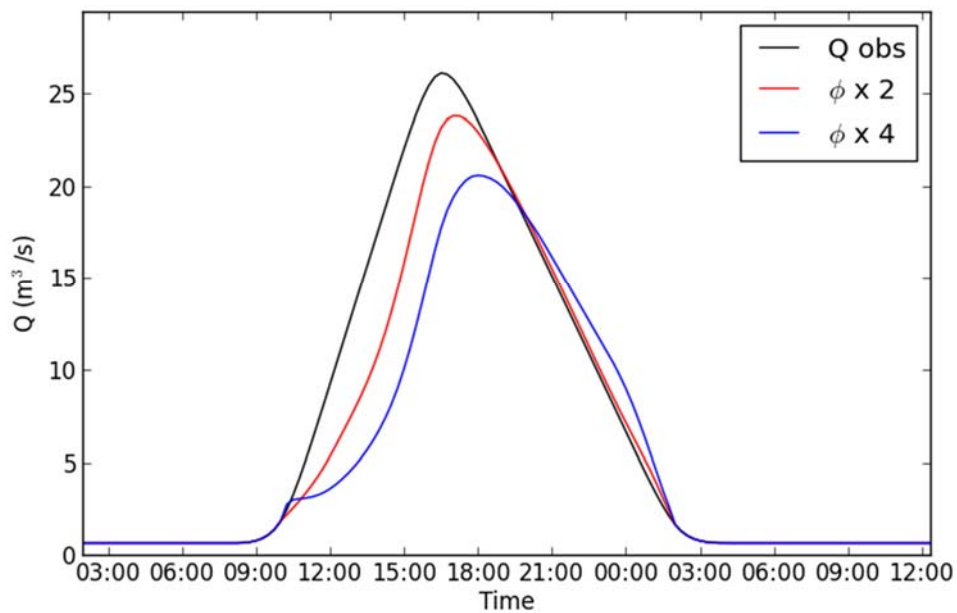
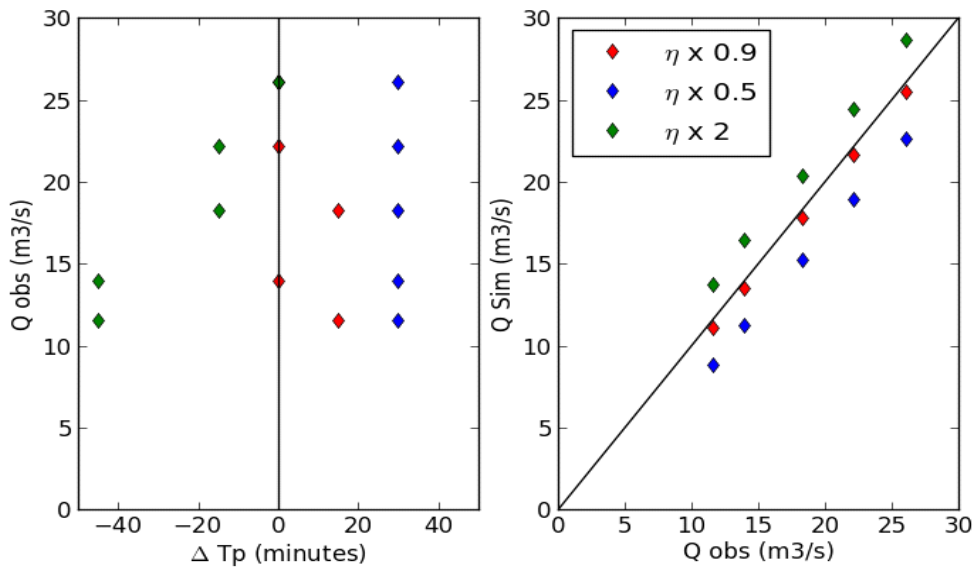


Figure 7-11 Impact of changing  $\phi$  on the FEH 100-year, 8 hours duration event

### ***Eta* ( $\eta$ )**

This parameter is associated with the small scales of celerity and is the minimum limit for celerity as the scale tends to zero. This parameter will not be used in the land management scenarios as the celerity function (through qp) itself takes care of land management scenarios that affect the small scale, such as reduced SPR through improved soil condition. A reduction in SPR leads to reduced runoff and therefore discharge, which leads to a reduction in celerity as it is a function of discharge.



**Figure 7-12 Impact of manipulating  $\eta$  plots; a. Change in  $T_p$  (positive  $t$  = increase) b. Change in  $Q_p$  form observed**

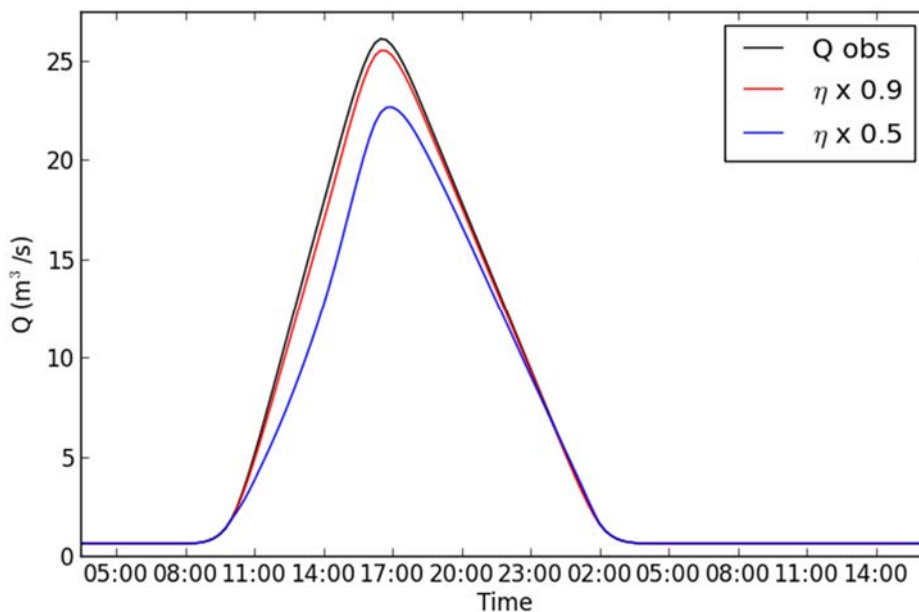


**Figure 7-13 Impact of changing  $\eta$  on the FEH 100-year, 8 hours duration event**

## 7.4 Conclusions

Juke has been shown to be more advanced for impact assessment over the lumped FEH rainfall runoff model; primarily the travel time and runoff patterns create nonlinear responses in the reduction of  $Q_p$ . This becomes especially true when spatially distributed HOST data is included in the runoff parametrisation. As different areas of the catchment generate different volumes of water throughout an event, a percentage increase or decrease will have different impacts on different areas of the catchment depending on the location of change.

An interesting and notable characteristic of the Juke model is that as the celerity at any scale is a function of discharge, as flow is reduced though a reduction in SPR the celerity changes accordingly to match the change in discharge, as is illustrated in Figure 7-14.

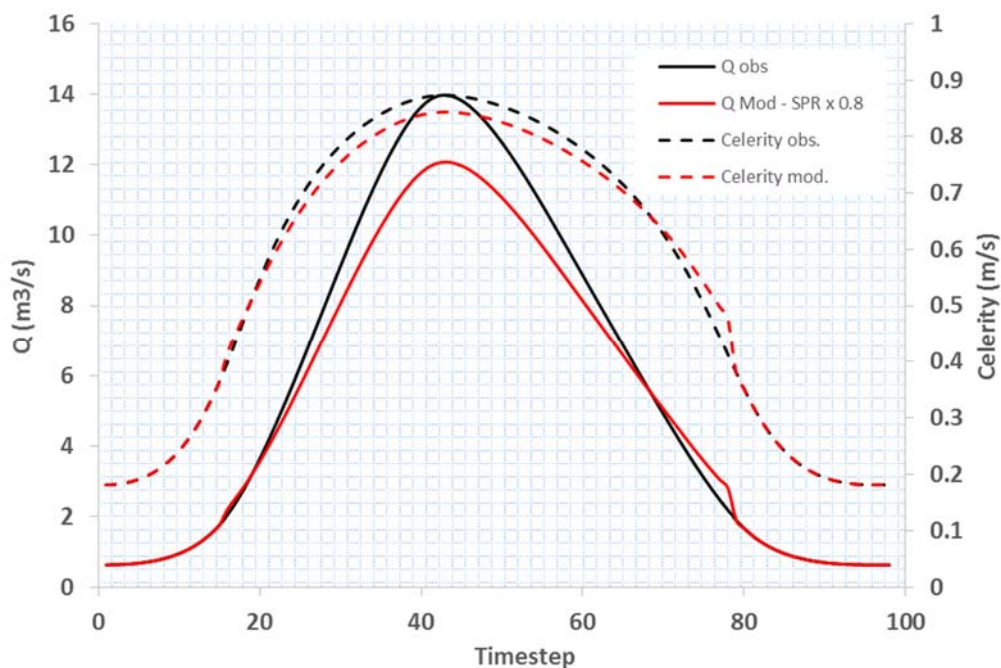


Figure 7-14 Observed and modified hydrographs with their corresponding outlet celerity plots

It has been demonstrated that the celerity parameters can be used in the modelling of attenuation type features, which physically restrict the movement of water. For this,  $\delta$ , has been identified as the most appropriate parameter.

It should be noted that the modelling in this Chapter has been carried out using FEH design hydrographs, which have been shown to be different to observed hydrographs (Chapter 4), with each storm having the same uniform shape. Observed storms vary in

multiple ways, including the spatial and temporal variations in the rainfall. These differences mean that the hydrographs have different shapes and rates of response and that in turn alters the celerity parameters and therefore the sensitivity.

The next chapter will use the Juke model that incorporates the distributed HOST data to simulate a series of scenarios. These scenarios investigate the potential for LUMC and NFM as a means of reducing flood hazard for observed rainfall and runoff records.

## **Chapter 8. Juke: Impact Scenarios**

### **8.1 Introduction**

This chapter explores the impact, using the Juke hydrological model of different management scenarios on flood peaks for the Leven catchment to Great Ayton. A similar set of scenarios are performed for the Morland catchment to provide a contrast in terms of catchment scale and hydrological response. The changes reflect expert knowledge regarding the impacts of land use management change (LUMC) and Natural Flood Management (NFM) on flood generation, as embedded within the mathematical structure of Juke rainfall runoff model. The use of LUMC and NFM as flood mitigation options will be considered, with an investigation of which approaches are most beneficial as well as where they are best located in the landscape and what proportion of the catchment is likely to need to undergo change to have discernible flood hazard reduction.

The scenarios aim to make best use of the GIS capabilities embedded in the Juke model, in that the scenarios target different land uses through the inclusion of land cover maps. Specific sub-catchments can also be targeted to investigate their impact, taking in to account the relative travel time and hence contribution to flood formation. Different regions of the landscape can be targeted through for example the use of the topographic wetness index (TWI), which is calculated by Juke. This can be used to identify the wetter and drier parts of the catchment which can be used to identify hillslopes, riparian areas and floodplains, and appropriate mitigation options.

### **8.2 Flood mitigation scenarios**

This section describes the scenarios to be modelled, why they were chosen and the way in which they will be implemented.

#### **8.2.1 Scenarios**

Table 7-1 provides an overview of the LUMC and NFM scenarios to be investigated. They have been designed to consider the portioning of the catchment for flood mitigation in two ways: (1) as a network with sub-catchments and (2) as a landscape, with hillslopes, riparian area and floodplains. This is with the aim of potentially identifying the most effective way of targeting runoff; whether it would be more beneficial to implement a lumped approach in certain sub-catchments or a more targeted, landscape based form of mitigation. The first, baseline scenario is not a LUMC scenario but the calibration and

parameterisation run which represents the ‘as now’ scenario. This scenario will provide the starting parameterisation which will be altered to reflect the LUMC impacts being modelled.

The quantity of fast runoff generated, i.e. the effective rainfall that contributes directly to the response hydrograph, will be manipulated through changes to the distributed partitioning factor ( $\gamma$ ), as described in Chapter 7, is parameterised to reflect the propensity of different soils to generate different amounts of runoff through the SPRHOST pattern. The partitioning factor can then be manipulated to account for expert knowledge of land use impacts on runoff generation. Any form of mitigation that involves physical attenuation of flood waters can be implemented by manipulating the asymptotic limit ( $\delta$ ) of the celerity function. This effect was demonstrated in the previous chapter and is associated with the larger scale features such as floodplains.

As the model is distributed, it can be provided with any gridded GIS data deemed useful for parameterising the runoff components or specifying the spatial extent of LUMC scenarios. Each grid square in the data set is referred to as a cell. These gridded data can be used to create the ‘patterns’ within Juke. Patterns reflect the natural landscape elements such soil distribution or land cover. Patterns are also used as way of applying specific LUMC scenarios. A binary pattern of locations can be used to identify the cells that will undergo change and can be established from a number of base GIS layers e.g. TWI, land covers or specific sub-catchments. The manipulation of the parameters for the cells within it can be changed through a ‘*pattern equation.*’

The scale at which mitigation is implemented in proportion to the overall catchment will have an important bearing on overall flood reduction impact. As was illustrated in the characterisation of the Great Ayton catchment, Chapter 5, the shape and ‘*flashiness*’ of the hydrograph changes as the wave propagates downstream. As discussed in Chapter 3 (Section 3.7.2), the changes to the hydrograph are caused by both hydrodynamic and geomorphological dispersion; hydrodynamic dispersion being the effects of the travel path length; geomorphological being the addition of other sub-catchments and how they synchronise at confluences and eventually at the outlet (Rinaldo *et al.*, 1991). The hydrograph becomes more spread out, with a reduced peak when examined as a normalised, specific discharge, and reduced rate of rise and recession.

The Morland catchment will be parameterised and have a similar but less extensive series of scenarios run to compare the relative modelled impact of LUMC and NFM. The results are of interest as the catchments are of different spatial scales with Morland, 12.5 km<sup>2</sup> compared to Great Ayton at 30 km<sup>2</sup>. As will be discussed below, the Morland peaks are generally caused by shorter, higher intensity rainfall events.

**Table 7-1 Overview of LUMC and NFM scenarios**

<b>SCENARIO</b>	<b>COMMENT</b>
Baseline scenario (Scenario 0)	The ‘as now’ scenario, calibration run which parameterise the model to represent our best understanding of runoff generation and celerity for current land use and cover.
Degraded catchment (100 % degradation) (Scenario 1)	The future ‘worst case’ scenario in which the maximum level of soil degradation is applied for comparison. Uses the Hollis (Packman <i>et al.</i> , 2004) recommendations for SPR manipulation.
Riparian woodland (Scenario 2)	Previous modelling studies have shown the potential for significant attenuation of flood flows on floodplains with riparian tree planting e.g. Thomas and Nisbet (2007). A series of scenarios explore the potential for wet woodland through the manipulation of celerity.
NFM (Scenario 3)	Field evidence and modelling has demonstrated the potential for leaky bund features to attenuate flood flows at the local scale (Nicholson <i>et al.</i> , 2012; Nicholson, 2014).
Sub-catchment sensitivity (Scenario 4)	To investigate if individual sub catchments may be more suitable for targeting interventions. This could be an important consideration for catchment managers with limited funds for mitigation.
Catchment scale effects on mitigation impact. (Scenario 5)	This scenario investigates how flood mitigation impacts propagate and change with increasing scale.

The local impact of riparian woodland and more engineered features is illustrated in Figure 7-1. An NFM feature that completely obstructs the flow path, but drains through an outlet pipe, potentially offers the greatest attenuation through temporary storage. The riparian woodland offers increased floodplain roughness that will reduce flow speed and increase flow depth when compared to a grassed, less rough, floodplain.

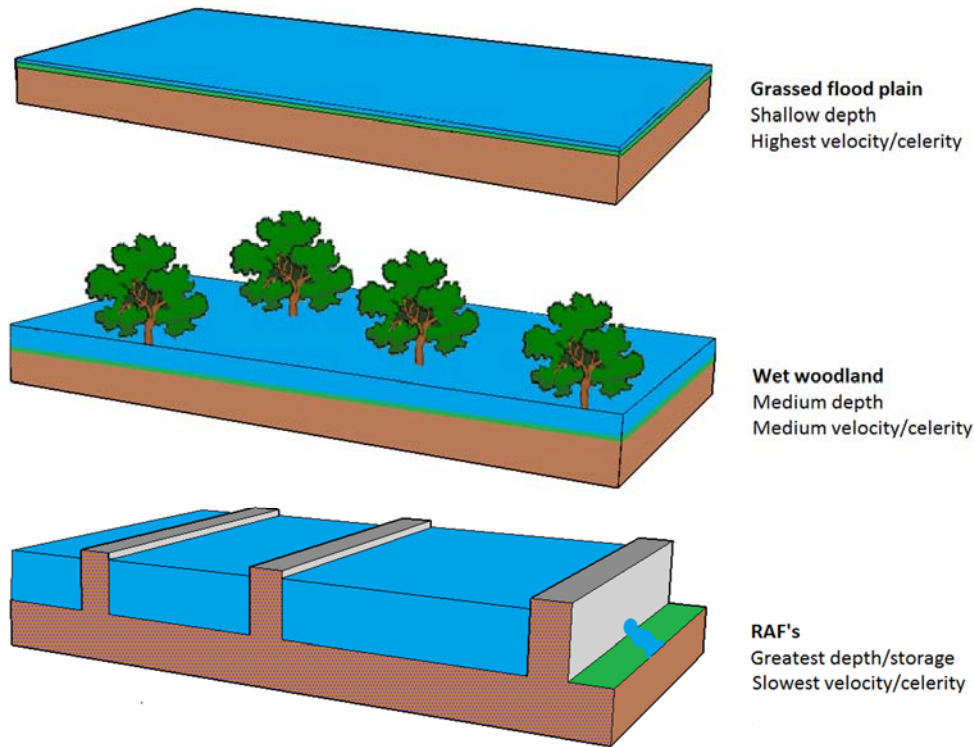


**Figure 7-1 Relative effects of LUM and NFM on flood flows**

Scenarios that require the effect of reduced flow velocity will be performed the manipulation of celerity. As has previously been discussed the flood wave celerity does not equal the bulk instream velocity of the water, it is the speed of the pressure wave as it propagates through system and cannot be measured in-situ at a single site. The Manning’s equations provide an approximation for converting celerity to velocity and vice-versa (Equation 7-1). The relationship is linear, with celerity calculated using Manning’s equation as being two-thirds greater than velocity; therefore, halving the celerity theoretically halves the velocity. As stated, the relationship is an approximation as they represent different things; celerity is the speed of the pressure wave, whilst the velocity represents the speed of water particles as they move along the channel reach (Equation 7-1).



**Equation 7-1**

$$c = \frac{5}{3} v$$

The results will concentrate on the scenario impacts for events greater than the median annual flood, defined as QMED in the FEH and is taken to be the 2 year return interval flow from the Flood Frequency Curve (FFC), which is 11.4 m<sup>3</sup>/s as calculated in Chapter 5. The 2 year interval flood is also widely accepted as being indicative of the bank full flow, therefore important for identifying out of bank flows (Dunne and Leopold, 1978). Using this threshold, 4 peaks are selected within the modelled period as list in Table 7-2; the results from the rainfall event characterisation (Chapter 5, Figure 5-12) are also listed.

**Table 7-2 Hydrological characteristics of the four largest flood peaks modelled to Great Ayton**

<b>Rank</b>	<b>Qp (m<sup>3</sup>/s)</b>	<b>Date</b>	<b>Qp Return interval (years)</b>	<b>Total event rain (mm)</b>	<b>Mean intensity (mm/hr)</b>	<b>Max intensity (mm/hr)</b>	<b>Duration (hours)</b>
1	16.86	29/11/2009	6	61.40	1.95	14.40	31.50
2	15.23	27/11/2012	5	76.80	1.15	6.40	66.50
3	12.44	16/01/2010	4	16.40	1.53	6.40	10.75
4	11.54	17/07/2009	3	79.00	1.87	25.60	42.25

The three largest events are winter events, with a single summer event also selected (Table 7-2). The summer event has the greatest rainfall total as well as the greatest maximum storm intensity embedded within, typical of convective summer events. All four events have comparatively high mean rainfall intensity when compared to the analysis in Figure 5-12, Chapter 5. The second largest peak has the greatest rainfall but is the longest duration at 76 hours (over 3 days of continuous rain) which is over 24 hours longer than any other event. The third largest event in January 2010, is the shortest duration but comes after a prolonged wet period as can be seen in Figure 7-2.

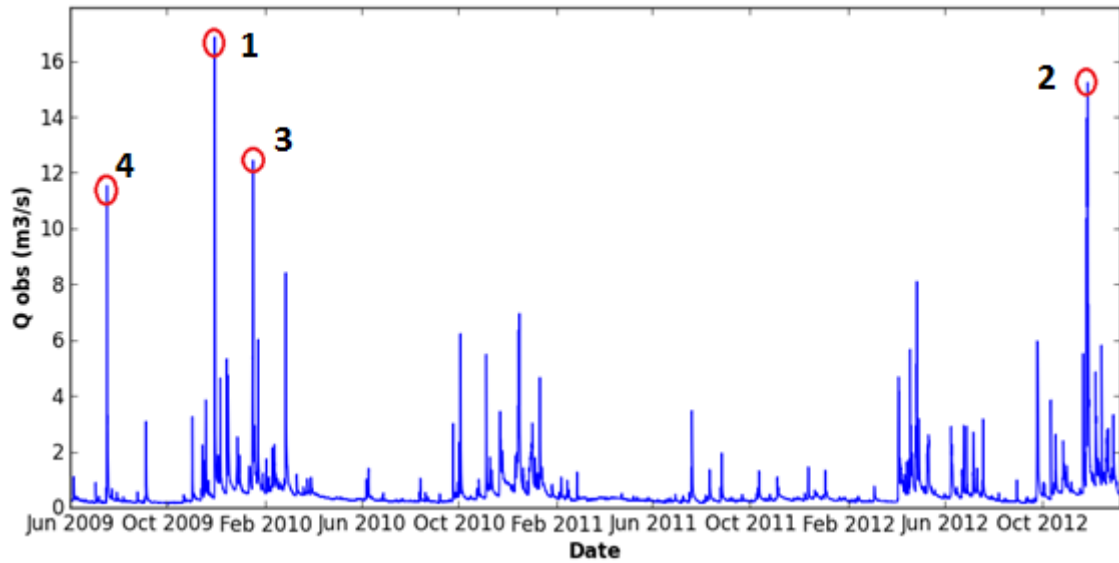


Figure 7-2 Great Ayton observed hydrograph, highlighting the four largest modelled events

### 8.3 Great Ayton scenario results

#### 8.3.1 Scenario 0 – Baseline Parameterisation

To parameterise both the celerity and partitioning factor ( $\gamma$ ), Juke requires observed time series for flow and rainfall and physical characteristics from a DEM; the distributed runoff dynamics (i.e.  $\gamma$ ) are provided by the HOST classification.

The routing of rainfall to the outlet is controlled by the hillslope bucket (local storage), which is controlled by  $tix$  (linear out flow parameter) and the channel routing (celerity; Chapter 3, Figure 3 14). If the hillslope is too sluggish, the routing parameters will compensate, leading to unrealistically high values (and *vice versa*). Also the effects will be seen in the matching element, through the time series of  $Lgam$ .  $Lgam$  will have high values at the onset of storms to compensate for the fact there is insufficient runoff being generated.

The model was calibrated for a number of different  $tix$  values assessing whether the routing celerity parameters and the matching gain ( $Lgam$ ), analogous for the catchment average rainfall runoff ratio, were physically reasonable. Physically reasonable was deemed as the outlet celerity asymptotes towards a value between 1.5 and 2 m/s, which is based on the literature, e.g. Beven *et al.* (1988) and the peak to peak analysis in Chapter 5 and the lumped catchment,  $Lgam$ , not reaching 1, i.e. 100 % runoff too readily. There is interplay between  $tix$  and celerity as the higher the  $tix$  value the greater the maximum celerity. Increasing  $Tix$  dampens the response of the storage outflow.

For the Great Ayton catchment a *tix* value of 8 hours was found to be suitable. This provided the celerity parameters listed in Table 7-3. Delta ( $\delta$ ) is associated with the large scales and celerity (e.g. floodplains); eta ( $\eta$ ) is associated with small scales and celerity (e.g. for subsurface drainage) and is the limit for celerity as scale goes to the single cell; and phi ( $\phi$ ) controls how the celerity varies with scale, i.e. the shape of the relationship.

**Table 7-3 Celerity parameters for the Leven to Great Ayton**

<b>Delta (<math>\delta</math>)</b>	<b>Phi (<math>\phi</math>)</b>	<b>Eta (<math>\eta</math>)</b>
2.017	2.191	0.026

As was discussed in Chapter 7, the celerity function is scale dependant, with the upstream area of an individual cell being a parameter in the calculation of the celerity (Chapter 7, Equation 7-2). The maximum celerity, based on the largest event in the modelled period, for three different spatial scales, full catchment, sub-catchment and individual cell are plotted as triangles in Figure 7-7 (originally shown in Chapter 7, Figure 7-7). It is likely that the values plotted represent the largest that will be experienced due to the asymptotic nature of the relationship; the red triangle can therefore represents the effective speed of sheet wash on a hillslope.

The matching gain series (Lgam) is plotted in Figure 7-3 and illustrates that it behaves in a natural way, increasing as the event progresses, reflecting the increased level of saturation. The matching element calculates Lgam to create the perfect calibration and it is clear from Figure 7-3 that element is not simply a black box that cancels out noise in the modelled output, as the trace is smooth and reflects the rainfall input.

The runoff generation element is distributed with each cell having its own value ( $\gamma$ ). The  $\gamma$  values can be based on known information such as the different rates at which different soils tend to generate runoff, i.e. the combination of soil maps and the HOST classification system. The  $\gamma$  value is multiplier applied to the rainfall, it can be best thought of as a partitioning factor applied to the rainfall and is calculated so that the catchment average is 1 (Chapter 3, Equation 3-4).

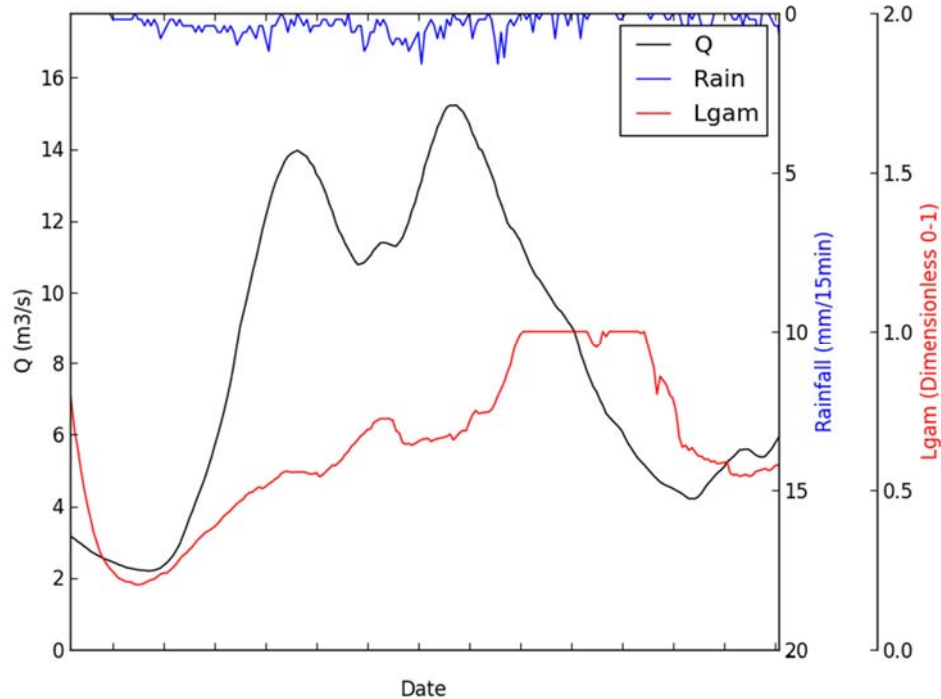


Figure 7-3 Hydrograph for a large event in November 2012 and the corresponding Lgam

### **Implementation**

The model was setup with a 50 metre grid resolution running with a data resolution of 15 minutes. The DEM resolution of 50 meter was chosen as it gave the best delineation of the river network and sub-catchments, compared to higher resolution data sets (5 m, 10 m) during GIS analysis. It was also identified by O’Connell *et al.* (2007) as an appropriate scale for tracking the development of floods from source to point of impact. The DEM data provided by Edina and the National Soil Resource Institute (NSRI), NATMAP vector, data at a scale of 1:250,000 for the soil and SPRHOST classification.

### **8.3.2 Scenario 1 – Degraded catchment**

This is the “worst case” scenario, where there is severe degradation to mineral soils from intense agriculture. The parameterisation of SPR is based upon the expert knowledge provide by Packman *et al.* (2004).

### **Details and Evidence**

As described in the Chapter 2, recommendations were made in FD2114 regarding the reclassification of HOST classes to an alternate class to reflect potential future worst case scenario of degradation. A map of the HOST classifications was shown in chapter 7 and the ‘current’ (pre degradation) and ‘alternate’ (post degradation) SPRs for Great Ayton are provided in Table 7-4. This scenario represents a future in which all environmental

considerations are ignored to maximise the short term economic potential of the land through greater stocking densities of animals and year round cropping. The scenario involves an increase of 7 % to SPR, fast runoff, for two HOST classes that account for 61 % of the catchment area (Figure 7-4).

**Table 7-4 HOST classification and alternate SPRs as recommended by (Packman *et al.*, 2004)**

<b>HOST Class</b>	<b>Fractional area (-)</b>	<b>SPR (%)</b>	<b>Alternate SPR (%)</b>	<b>ΔSPR (%)</b>
5	0.16	15	22	+7
15	0.13	48	48	-
20	0.19	60	60	-
24	0.45	40	47	+7
26	0.08	59	59	-
Weighted catchment SPR		42.76	47.03	+4.27

### ***Overview of scenario implementation***

The partitioning function ( $\gamma$ ) can be changed by is manipulating the pattern equation as shown in Equation 7-2. The SPR layer is manipulated using values from Table 7-4in Equation 7-2 (where n is the total number of cells).

**Equation 7-2**

$$\gamma_i = \frac{spr_i \pm \Delta spr_i}{1/n \sum_i^n spr_i}$$

This scenario represents a change in management; therefore, there is no explicit change in land cover that requires a manipulation of celerity to be calculated; if overland resistance was envisaged as changing this could be implemented by manipulating the celerity parameters. Celerity is not explicitly changed in the scenario, but celerity is a function of runoff, hence increased runoff will implicitly lead to greater celerity. It is clear in Figure 7-7 that as discharge decreases the celerity does likewise; initially the changes will only be small for the largest event due to the asymptotic relationship but significant reductions in flow could potentially impact significantly on celerity.

The areas where HOST will change are illustrated in grey in Figure 7-4 and closely correspond to the areas in which superficial glacial deposits are found (Chapter 5, Figure

5-4). These areas are located in the valley sides and bottoms and coincide with the mineral soils, as was discussed in the characterisations. The organic peat soils, which have relatively high SPR (60 %), are not envisaged as generating any extra fast runoff through degradation due to the fact that during the largest events these soils will be saturated and generating close to 100 % runoff (Holden and Burt, 2003).

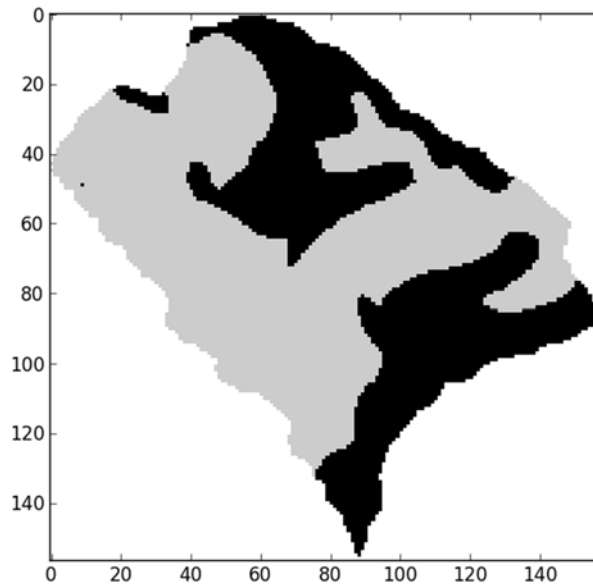


Figure 7-4 Map of the areas where SPRs are changed to an alternate, grey, and remain the same, black

### Results

The results of the degradation scenario are shown in Figure 7-5. The figure shows the difference between the observed peaks and those modelled with the alternate HOSTSPR values.

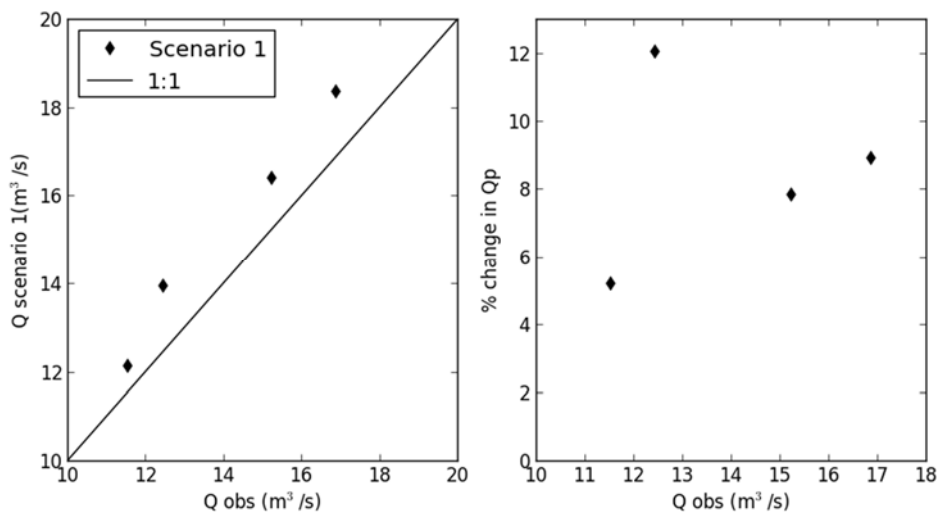


Figure 7-5 Result for worst-case scenario showing change in peak magnitude

In Figure 7-5 the general trend is that there is a greater percentage change in  $Q_p$  for the larger flood peaks. However, the third largest event does not fit this trend; this is the shortest duration (Table 7-2), i.e. the flashiest. It is clear that the peak has increased as has the rate of recession (Figure 7-6).

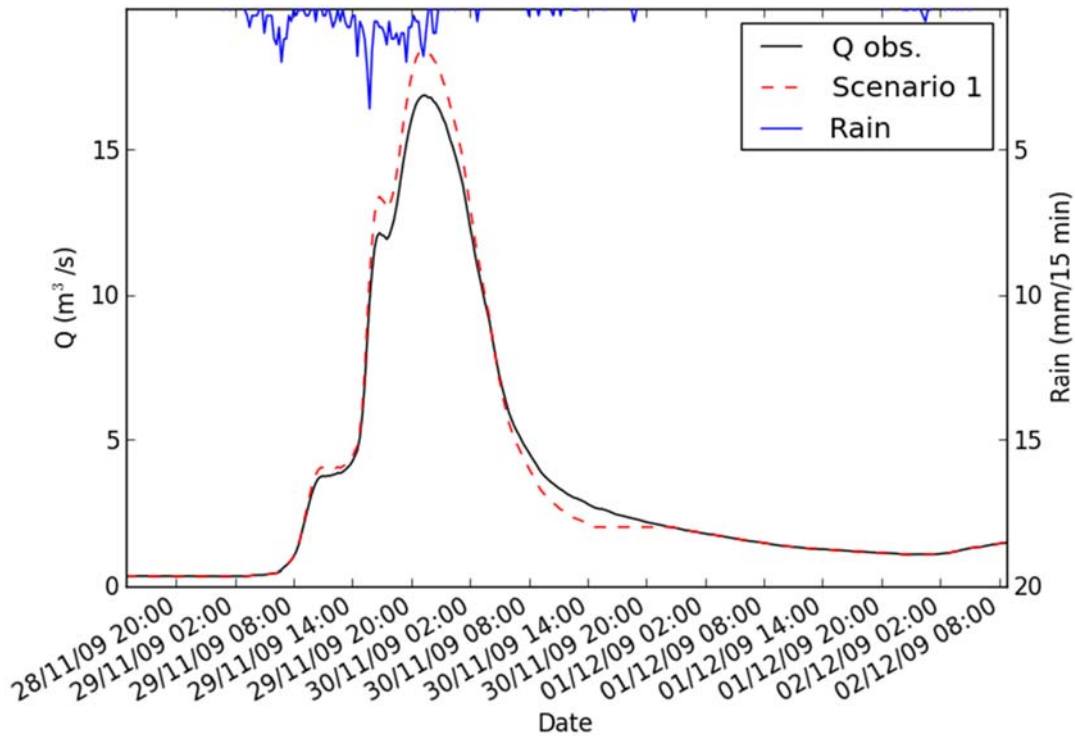


Figure 7-6 Plots of the observed versus the modelled hydrograph for scenario 1 for the rank 3 event

### 8.3.3 Scenario 2 - Riparian woodland

This scenario investigates the potential for flood peak reduction through woodland planting in the riparian areas of targeted sub-catchments.

#### Details and Evidence

The establishment of woodland on floodplains and riparian areas can be beneficial for mitigating flood flows in a number of ways. Firstly, infiltration rates are greater under wooded areas than pasture on the same soil type, as observed on hill slopes in the Pontbren research catchment (Wheater *et al.*, 2008; Marshall *et al.*, 2009). Secondly, two UK based modelling projects have shown the potential for attenuating flood waves using riparian woodland and wooden debris dams, in contrasting catchments as described below.

Thomas and Nisbet (2007) used a coupled 1D-2D hydraulic model to investigate the impact of the addition of riparian woodland to a 2.2 km reach by increasing the floodplain roughness of the adjacent banks. The 2.2 km reach was approximately 300 m upstream of the catchment outlet at Somerton on the River Cary, a tributary of the River Parrett, with an upstream catchment area of 82.4 km<sup>2</sup>. The gradient of the channel is very low with a drop of 1 m along the 2.2 km reach. The celerity along the reach is low when compared to the values obtained for the analysis of Great Ayton; the unmitigated model run had a celerity of 0.204 m/s (Q<sub>p</sub> travel time of 3 hours along the reach) for the 1 in 100 year event of 15 m<sup>3</sup>/s; where the addition of the 2.2 km of riparian woodland reduced the celerity to 0.114 m/s, a reduction of 44 % (Q<sub>p</sub> travel time of 5 hours 20 minutes along the reach; Thomas and Nisbet (2007)). When compared to the Great Ayton celerity function, Figure 7-7, these celerity values are very low and would be expected at much smaller spatial scales.

Modelling carried out to identifying the most suitable locations for riparian woodland and wooden debris dams on Pickering Beck (69 km<sup>2</sup>), had mixed results (Odoni and Lane, 2010). The modelling suggested that features in certain locations may exacerbate the flooding problem due to the synchronicity of the catchment flows as a whole. The modelling results also suggest that mitigating on the main stream had greater impact, reducing the flood peak by 9.5 %, compared to 3.4 % when only mitigating on the than smaller streams (Odoni and Lane, 2010). No return interval was provided for the event being modelled, but it did cause flooding to properties.

A methodology proposed for identifying potential wet woodland locations was developed by the Forest Habitat Networks Scotland (FHNS; (Moseley and Ray, 2007)). The methodology proposes identifying areas that have TWI that ranks them in the wettest 50 % and have a local slope of less than 0.5°. The TWI is calculated through a GIS analysis that includes the upstream area and the local slope of a cell (Beven and Kirkby, 1979). Cells with larger upstream areas and lower local slope have higher wetness index values. These higher values tend to coincide with valley bottoms, i.e. riparian areas.

### ***Overview of implementation***

For this scenario potential wet woodland areas were identified through a number of GIS layers. The TWI is used to identify the wettest 25 % of the catchment; the FHNS methodology described above selects the wettest 50 % of cells, however, this identified



too many cells away from the channel. As local slope is accounted for within the calculation of the TWI, it was not additionally factored in here. It was decided that the riparian woodland would only be placed in sub-catchments and not on or adjacent to the main channel due to the increasing stream power and energy that may potentially provide an increased risk of trees being uprooted and transported downstream where they may increase flood hazard due to being trapped behind structures such as culverts or bridges. Only cells with an upstream area of less than 4 km<sup>2</sup> were included. A binary pattern was created with a 1 for areas deemed suitable and 0 for areas not.

The binary pattern layer can then be used as multiplier for reducing celerity through the upper asymptotic limit ( $\delta$ ) for all upstream cells. In Chapter 7, the asymptotic limit of celerity ( $\delta$ ) was described as the celerity parameter associated with larger scales and can be manipulated to represent the impact of attenuation on flood mitigation features on the floodplains. The impact of reducing  $\delta$  by half on the celerity function, at three spatial scales is shown in Figure 7-7, the blue lines represent the celerity functions at the outlet and the triangles represent the maximum modelled celerity achieved in the largest event as described in Chapter 7. The broken blue line effectively represents the celerity function for the outlet if the whole of the catchment were planted with trees and it is assumed that all regions were impacted equally. The green line in Figure 7-7 represents the celerity function for the Easby sub-catchment with an upstream area of 15 km<sup>2</sup>, 50 % of the total catchment area; within this catchment lie the Lonsdale and Leven Vale sub-catchments which will be affected in this scenario. The celerity functions for the Lonsdale and Leven vale sub-catchments lie somewhere between the green and red lines.

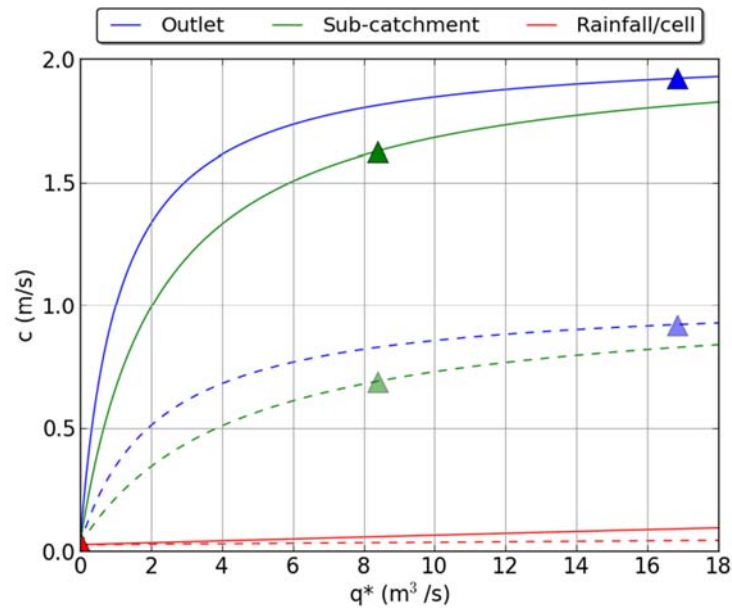


Figure 7-7 The effect of reducing  $\delta$  by half on the celerity function; broken line modified

### ***Versions of scenario 2***

Due to uncertainty in the hydrological and hydraulic impacts of riparian woodland a number of versions of the scenario were conducted to explore the potential outcomes. These include:

2.1 Use the modelling outcomes of Thomas and Nisbet (2007) and reduce the asymptotic upper limit ( $\delta$ ) of celerity by 50 % and also model a 25 % reduction as personal judgement being that the likely impact will lie between 50 and 25 %.

2.2 A scenario that includes an increase in infiltration expected under woodland, represented as a 20 % reduction in SPR and with a reduction of 50 % to upper asymptotic upper limit ( $\delta$ ) of celerity for all cells that flow through the riparian area.

2.3 A hypothetical extreme scenario in which the asymptotic upper limit of celerity ( $\delta$ ) is reduced by 50 and 75 % for all cells to represent riparian woodland on the wettest 25 % of the catchment as identified from the TWI including the main channel.

### ***Pattern***

The pattern shown in Figure 7-8 is derived using the following GIS rules:

### **GIS rule base for establishing mitigation pattern**

1. Select the wettest 25 % of cells as identified by the TWI
2. From 1 select cells with an upstream area of 4 km<sup>2</sup> or less and that lie within one of four sub-catchments; Lonsdale, Leven vale, Pilly Hall or Dyke Beck (Figure 7-16).

The grey areas within Figure 7-8 are those identified as being suitable for wet woodland and have a value of 1, whilst the black, unsuitable, areas have a value of 0. This means the pattern can be applied as a multiplier in a pattern equation to modify only the areas valued 1. The total area identified as suitable is 3.56 km<sup>2</sup>, approximately 12 % of the catchment.

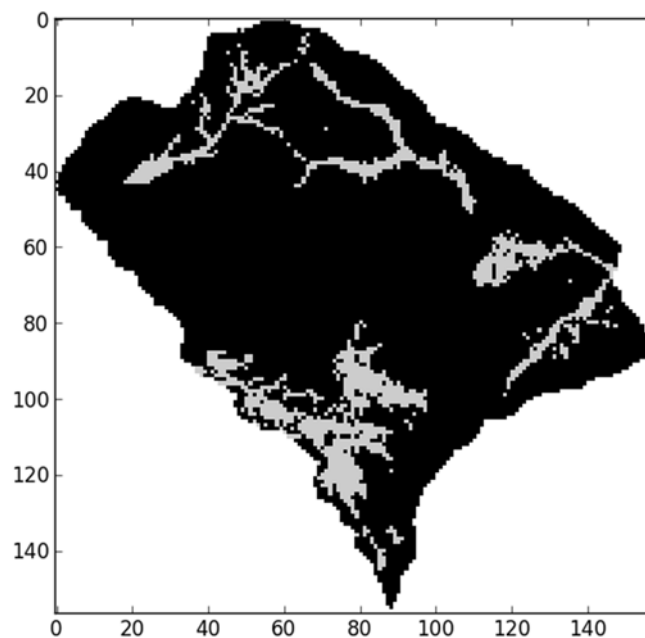


Figure 7-8 Pattern showing areas suitable for wet woodland identified in grey

### ***Results***

The results for the two wet woodland scenarios are shown in Figure 7-9, the red diamonds represent the results for the 25 % reduction in the asymptotic limit of celerity ( $\delta$ ) parameter so the upper celerity for flood flows is equivalent to 75 % of the original. The blue diamonds are for the 50 % reduction results. There is a higher increase in  $T_p$  for the large flood peaks, i.e. the larger flows are being slowed the most.

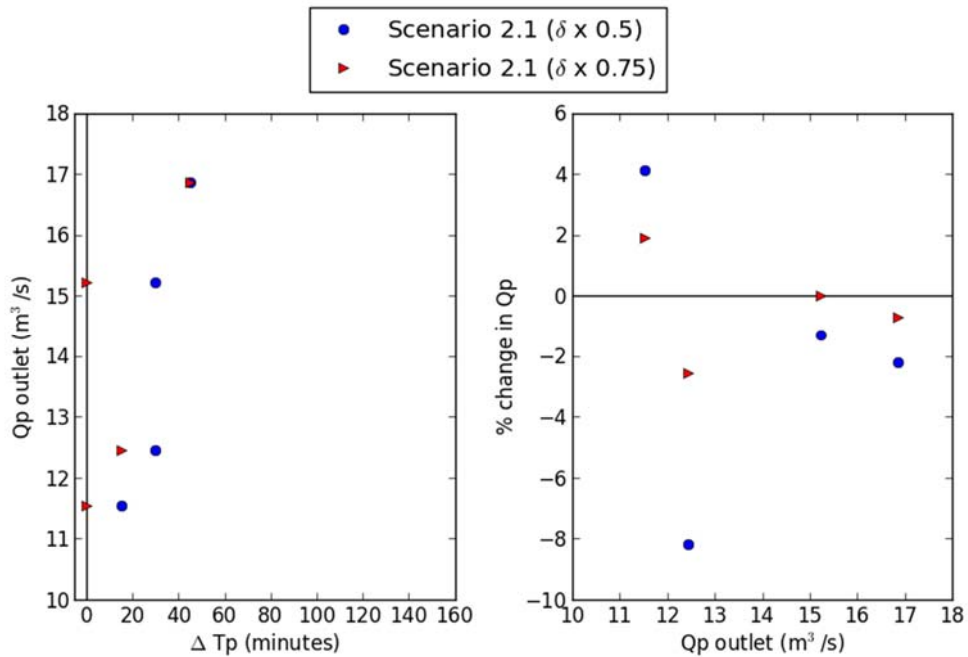
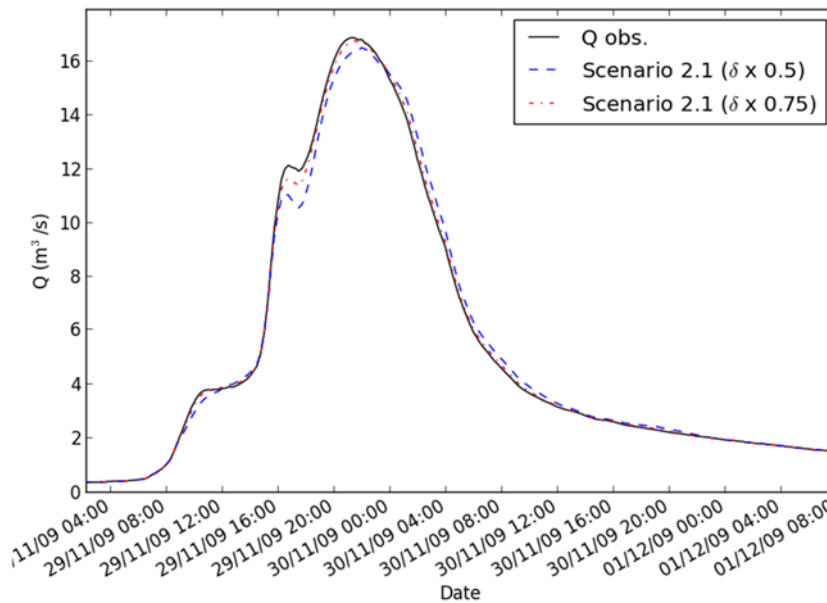


Figure 7-9 Riparian woodland results; change in Tp and % change in Qp

The changes in Tp are not as high as those presented by Thomas and Nisbet (2007); however the two catchments are very different with the River Parrett having very low relief. The modelled impact of celerity reducing by 50 % was estimated immediately after the stand of trees, where in this study the mitigation is more dispersed and there is a sizeable amount of catchment downstream that has not been mitigated.

The model outputs are shown against the observed flow hydrographs for two versions of the scenario in Figure 7-10 for an event in November 2009. The flows have been attenuated with the hydrograph rate of rise having reduced along with the flood peaks and the reduced rate of recession.



**Figure 7-10 Hydrographs of wet woodland having beneficial impact on the downstream hydrograph**

The fourth largest event modelled was negatively impacted (i.e. the peak increased) and is plotted in Figure 7-11 to show the effect on the hydrograph. The rate of rise of the hydrograph has been decreased in both scenarios; however, the mass has not been moved to the recession as would be hoped, some now coincides with the peak causing an increase in  $Q_p$ .

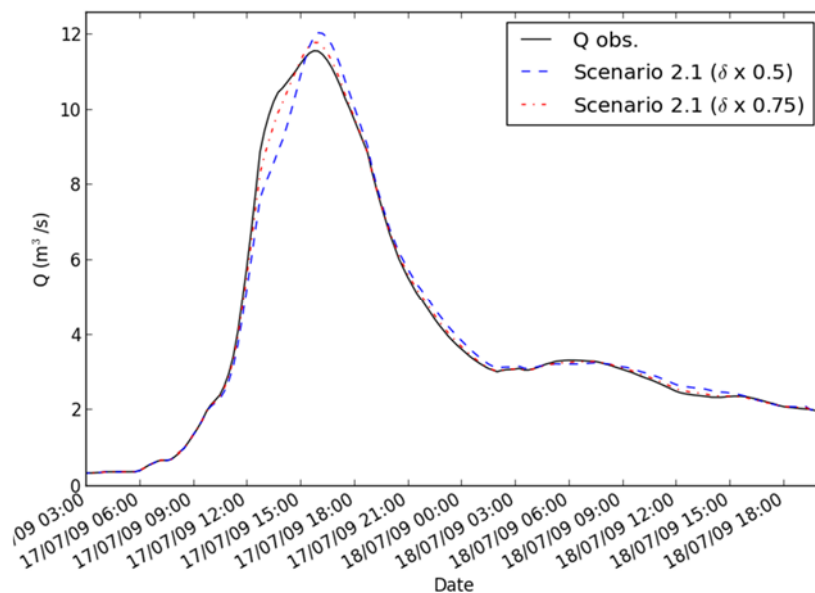


**Figure 7-11 Hydrographs of riparian woodland having a negative impact on the downstream hydrograph**

It has been noted that the soil beneath trees have an increased infiltration rate when compared to adjacent pasture (Wheater *et al.*, 2008; Marshall *et al.*, 2014). An increase in infiltration will reduce the catchment SPR, by how much is unclear however, as we

have no field evidence. A scenario has been modelled in which the celerity has been reduced by 50 % for all cells within and upstream of the wet woodland and the SPR has been reduced by 20 % for the cells within the wet woodland pattern. The results for the effect on Qp are shown in Figure 7-12, the modelled results show that the 20 % reduction in SPR has provided an additional 0.5-1 % of Qp reduction.

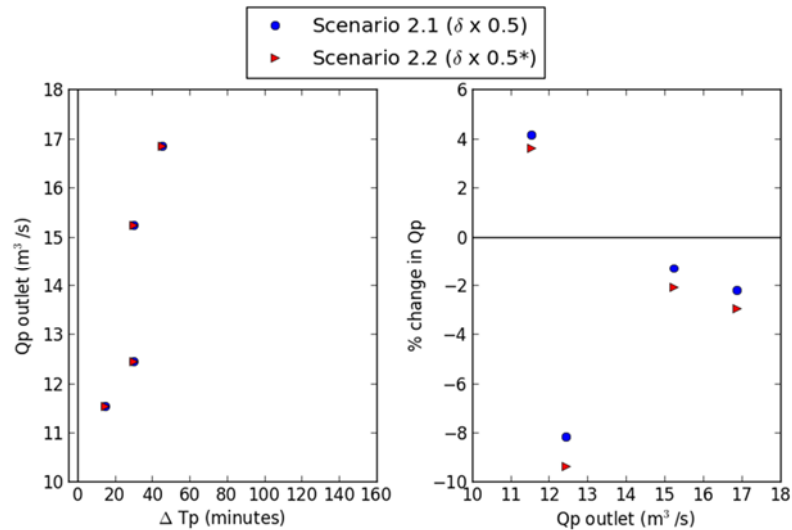


Figure 7-12 Riparian woodland scenarios; δ reduced by 50 %, \* indicates SPR reduced by 20 %

The two examples provided in the evidence for this scenario implemented riparian woodland at the larger scale main rivers and therefore impacting larger flows originating from a considerably larger area of the catchment. A further scenario was run in which the wettest 25 % of cells in the Great Ayton catchment, including the main channel, were identified and all upstream cells impacted by running both the 25 % and 50 % reduction in the asymptotic limit of celerity (δ) scenarios. The results are shown in Figure 7-13 and are plotted against the original scenario in which only the sub-catchments were impacted (triangles; 25 % δ reduction, red and 50 % δ reduction blue).

The fourth largest event, in Figure 7-13, is made worse in both versions of the scenario. This event is comparatively long; it has the greatest volume of rainfall as well as having a very high intensity peak embedded within it. Due to length of the event and the significant rainfall intensity within the event there are likely complicated timing issues which increase the flood peak. Generally, the results suggest that this form of mitigation works best for higher intensity ‘flashier’ events.

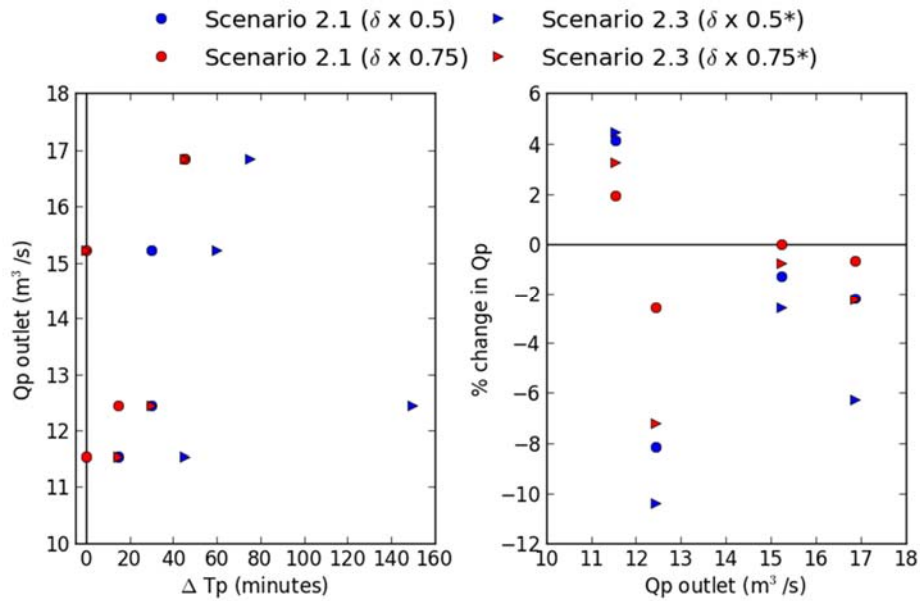


Figure 7-13 Riparian woodland results for sub catchment mitigation (Scenario 2.1; triangles) and main channel sub catchment mitigation (Scenario 2.3; circle; \*)

### 8.3.4 Scenario 3 – NFM

This scenario investigates the potential for flood peak reduction through significant attenuation of flood flows through the implementation of RAF features.

#### **Details and Evidence**

To reflect significant attenuation of flows behind RAFs the asymptotic limit of celerity ( $\delta$ ) is reduced by 75 % for cells within and upstream of the NFM feature locations. No transparent way of implementing the observed attenuation from the field monitoring studies discussed in Chapter 2; the rationale for this scenario is that RAF features offer the most considerable form of attenuation as illustrated in Figure 7-1; a sensitivity approach is therefore adopted to reduce celerity by a greater amount than in Scenario 2. As the routing in Juke is directly from the cell to the outlet, all upstream cells must be impacted.

#### **Pattern**

The pattern used is the same as that for Scenario 2 in which the wettest 25 % of cells within the target sub-catchments were identified from the TWI (Figure 7-8). This pattern is being used as RAFs are typically constructed in headwater catchments where the energy regime of flows is typically smaller than the main channel at larger scales; the features are therefore less likely to be washed away.

## Results

The resultant modelled hydrographs are shown in Figure 7-14 for the same December 2009 events shown in Figure 7-11. Significantly more mass is removed from the rising limb in this scenario and redistributed to the recession. However, the reduction of celerity to this magnitude is not thought physically reasonable without a significant form of storage being introduced.

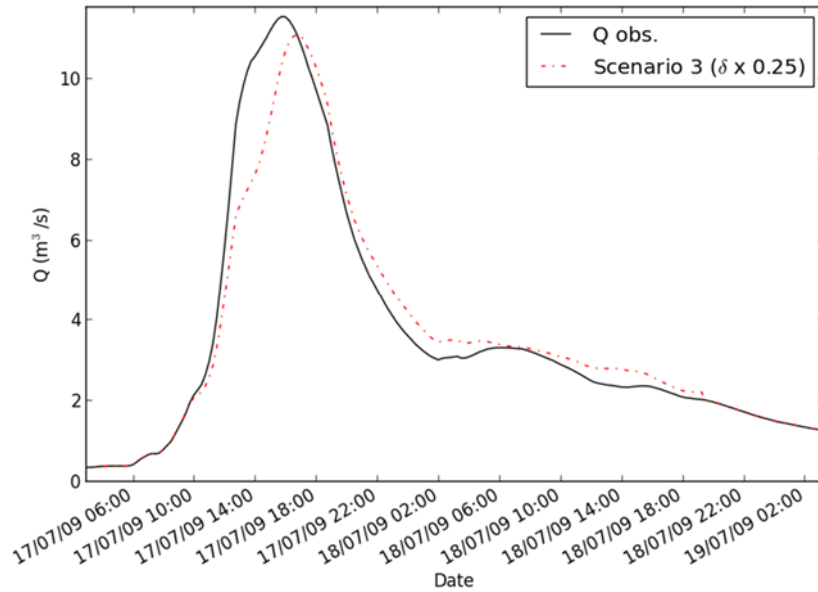


Figure 7-14 Hydrographs of NFM scenario where  $\delta$  is reduced by 75 %

The results for the effects on timing and magnitude on the flood peaks for scenario 3 are shown in Figure 7-15. There is a significant increase in the time to peak for most events, with all events having shifted by at least 15 minutes. The peak discharges have also been significantly impacted, however, two of the smaller events see an increase in  $Q_p$ . An interesting observation for the two events in which  $Q_p$  increases is that reducing the asymptotic limit of celerity ( $\delta$ ) by 75 % causes a significant increase in  $Q_p$  for one of the events but has a reduced impact for the other when compared to the 50 % reduction scenario. These different responses highlight the complexity of timing and synchronicity in catchments.



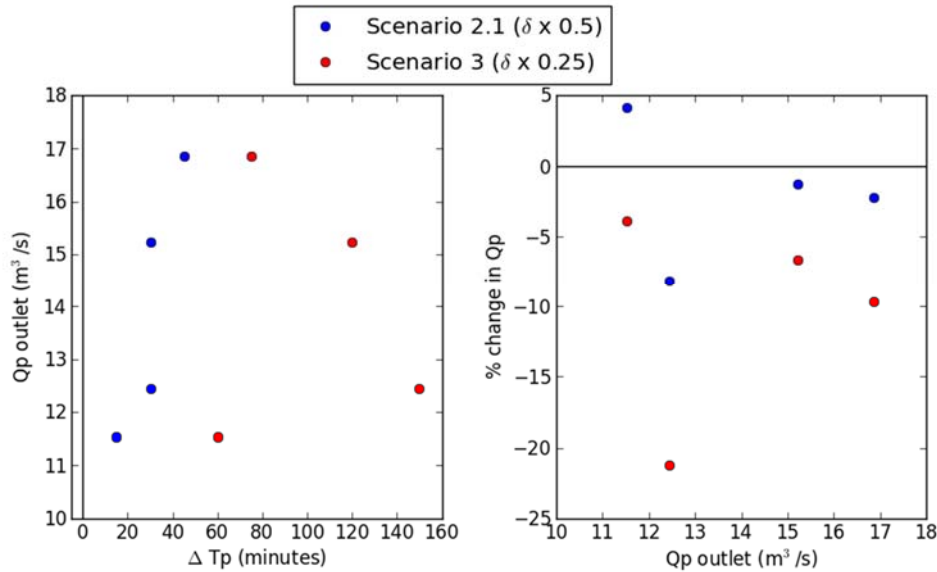


Figure 7-15 Wet woodland scenarios;  $\delta$  reduced by 50 % and 75 %

### 8.3.5 Scenario 4 - Sub catchment suitability

This scenario will take a sensitivity analysis approach to investigate the impact of changing runoff production and celerity rates of different sub catchments. The aim of this scenario is to determine if certain sub catchments may be better suited to mitigation due local factors such as soil and travel distance to the outlet.

#### Details

This scenario is being considered in attempt to identify whether certain sub-catchments may have a greater impact on the reduction of the outlet Qp due to the local HOST classes as well as the relative travel time and superposition of flows. It was demonstrated in chapter 7 with the FIM tool that attenuating the flows of sub-catchments with the shortest routing distance to the outlet may exacerbate flooding through delaying the flows and increasing synchronicity. The FIM tool was very simple in that the contributions of each sub-catchment were added together through superposition to produce the outlet hydrograph; any change to the timing of flows through manipulation of the time-to-peak (Tp) caused the translation of the hydrograph by the same amount, not just a gradual response as would be expected in a natural system with added attenuation. Reproducing this scenario with Juke should prove more robust as the manipulation of the wave speed through celerity will have a more gradual impact, becoming larger as the flow increases, as illustrated in Figure 7-7. Juke is also distributed so the effects have to be routed and combined with flows from other parts of the catchment not undergoing mitigation.

No particular mitigation options are offered as suitable for achieving the desired runoff reductions and increases in  $T_p$ . These simulations can be seen as a form of spatial sensitivity analysis, with the potential to identify where mitigation may be most beneficial, for example if given a limited financial resource.

### ***Implementation***

For four sub-catchments (Leven Vale, Lonsdale, Pilly Hall and Dikes Beck; Figure 7-16) an SPR reduction of 20 % was applied as a 20 % reduction to the baseline  $\gamma$  parameter and a reduction of the asymptotic limit of the celerity function ( $\delta$ ) of 50 %. These magnitudes of reduction to runoff and celerity may potentially be achieved by a combination of land use management, such as reduced stocking densities, and the construction of RAFs. To ensure that any differences modelled between the sub-catchments are due to travel distance and not the total of the mitigated area, a rule will be applied that  $\sim 3 \text{ km}^2$ , 10 % of the total catchment, will be modified.

### ***Patterns***

#### ***GIS rule base for establishing mitigation pattern***

- To be included in the pattern, cells must lie within one of the respective sub catchments (Leven Vale, Lonsdale, Pilly Hall and Dikes Beck).
- Cells included in the pattern must drain less than 1200 upstream cells ( $3 \text{ km}^2$ , determined by the smallest catchment Dyke Beck;  $400 \text{ cells} = 1 \text{ km}^2$ ) to ensure that mitigated areas are equal.

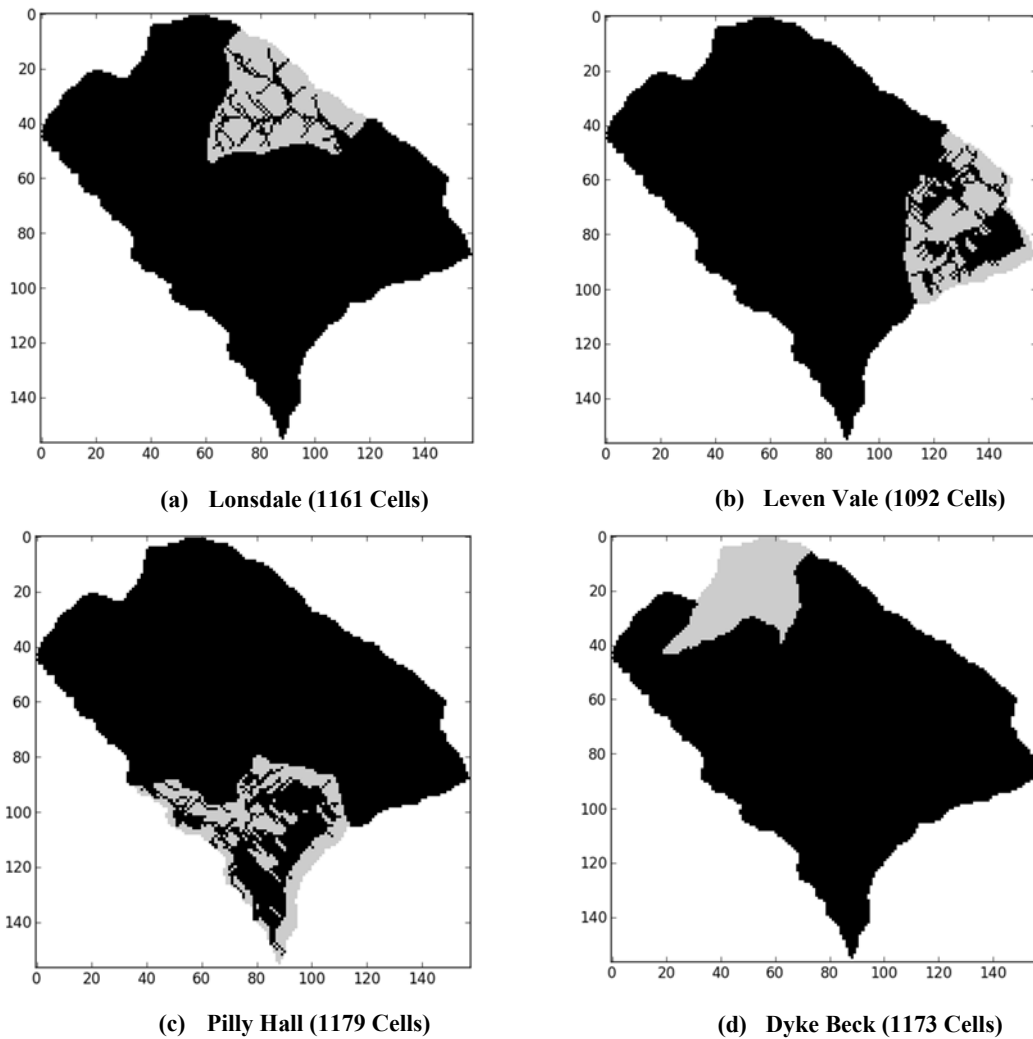


Figure 7-16 Patterns used in Scenario 4; Grey indicate cells within the pattern, Black are not.

### ***Results***

The modelling indicates that generally the changes made to the two catchments with longest travel distance but also higher SPR soils, Lonsdale and Leven Vale, marginally have the greatest impacts in reducing  $Q_p$ , Figure 7-17. Although the greatest percentage  $Q_p$  reduction is seen for the shortest duration event (Rank 3) in which mitigating the catchment with the shortest travel distance to the outlet. Only 10 % of the catchment has been modelled as undergoing change in each version of the scenario, so a significant area of the catchment remains unchanged. It is the relative timing of the contributions from the changed and unchanged parts of the catchment combined with the temporal patterns of the rain, embedded within the disparate contributions that produce the scatter.

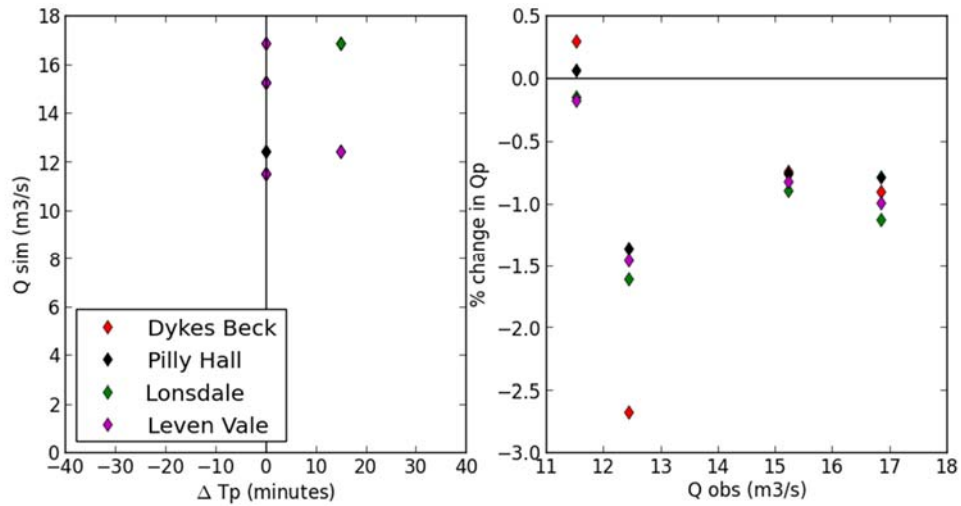


Figure 7-17 Sub-catchment investigation results; change in  $T_p$  and percentage  $Q_p$  change

The Rank 3 (Table 7-2) event which has the greatest modelled percentage reduction in  $Q_p$  is shown in Figure 7-18. All four versions of the scenario reduce  $Q_p$  to some extent. The red hydrograph in Figure 7-18 represents the scenario in which the Dikes Beck sub-catchment is mitigated; Dikes Beck is the sub catchment with the shortest travel distance to the outlet (Figure 7-16). Mitigating the Dikes Beck sub catchment has the greatest impact on the rate of rise as the delay in its contribution has the most significant effect in the synchronicity of the flows.

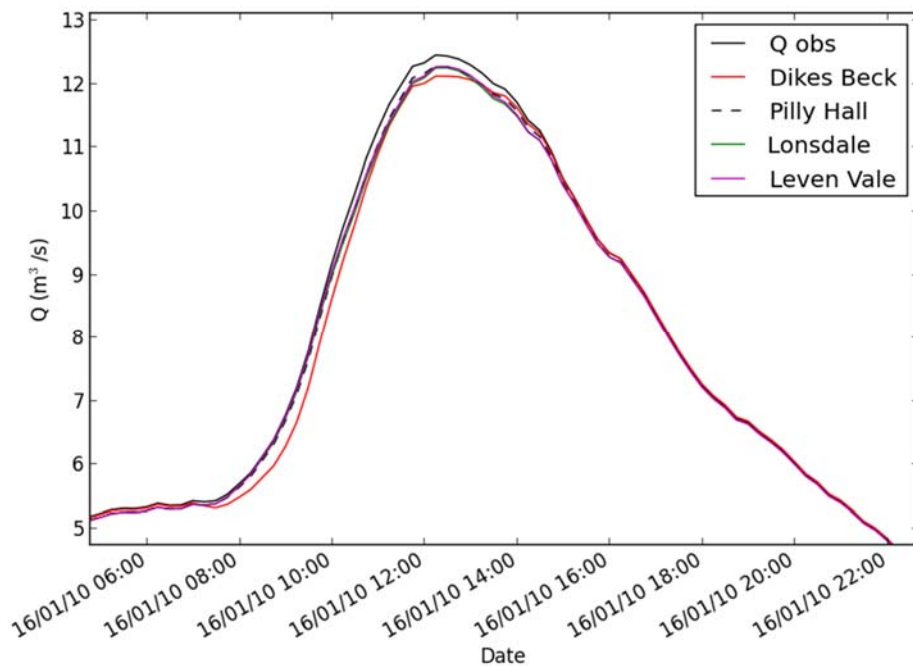


Figure 7-18 Event with the greatest reduction in  $Q_p$  for each version of the scenario

To understand the relative impact of the SPR and celerity manipulations, Juke has been re-run twice carrying out the respective manipulations to celerity and then SPR in turn (Figure 7-19). The overall reductions in  $Q_p$  are greatest for the SPR scenario and all peaks are reduced. Where affecting the timing and synchronicity through the celerity is again shown to make the fourth largest event worse.

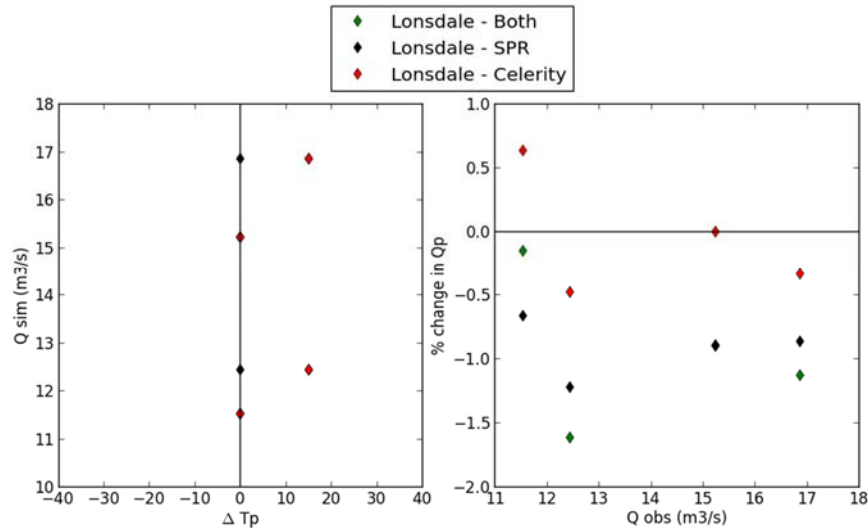


Figure 7-19 Results of changing SPR and Celerity independently and together (both) for Lonsdale

### 8.3.6 Scenario 5 – Scale effects

The aim of this scenario is to understand how changes made at one scale propagate through the system and manifest with increasing catchment scale.

#### Details

For this scenario two of the sub-catchments, Lonsdale and Leven Vale, both upstream of Easby have had their SPR data reduced by 10 % and 20 %, for both of the catchments together and separately. It possible to get model results for Easby, the nested flow location provided for the parameterisation of the celerity function. Easby represents nearly half the total catchment area to the outlet at Great Ayton. The areas of the component catchments to Great Ayton are provided in Table 7-5; the areas listed in are as they are delineated in Juke and differ slightly to those described in the characterisation chapter due to the resolution of the DEM from which they are derived. The ‘Proportion of catchment to’ column in Table 7-5 is the proportion of the total catchment area undergoing change at those respective locations.

**Table 7-5 Areas of the component catchments and the proportion of total catchment they represent undergoing modification**

	Area (km <sup>2</sup> )	Proportion of catchment to	
		Easby	Gt. Ayton
Leven vale	4.8	0.34	0.16
Lonsdale	3.9	0.28	0.13
Leven and Lonsdale	8.7	0.58	0.30
Easby	13.9	1.00	0.47
Gt. Ayton	29.3	-	1.00

***Implementation***

A total of six results are produced from this scenario, two for each of the sub-catchments individually and then together, with SPR reductions of 10 and 20 %.

***Pattern***

Three patterns to be used, one for each of the sub catchments individually and a third that contains both the Lonsdale and Leven Vale catchments together.

**GIS rule base for establishing mitigation pattern**

- Mitigate areas that lie in either or both of the sub-catchments, Leven Vale and Lonsdale, depending on the scenario being run (Figure 7-20)

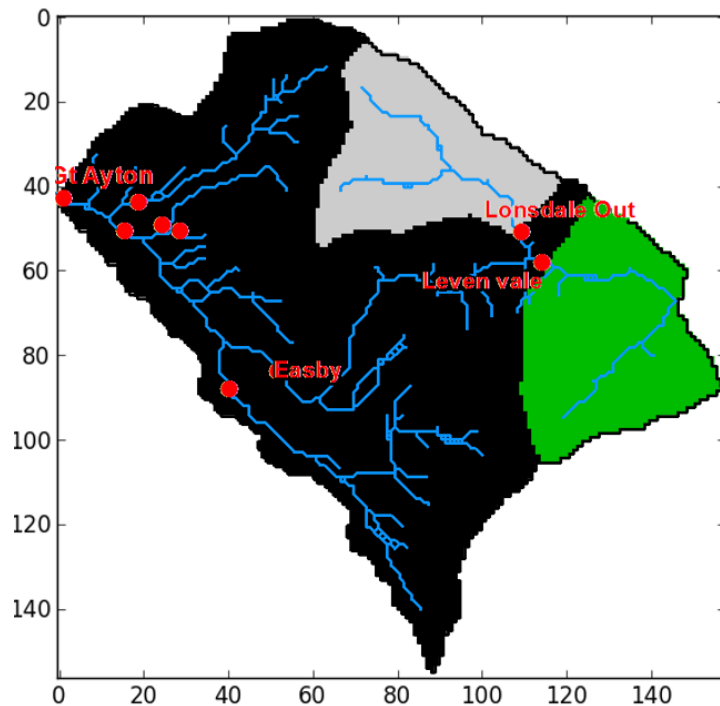


**Figure 7-20 Pattern of the two sub-catchments being used in this scenario, Leven Vale (green) and Lonsdale (grey)**

## Results

The results showing the impact on  $Q_p$  and the timing of the peak to both Easby and Great Ayton, where both sub-catchments are modified by a reduction in SPR by 10 and 20 % are shown in Figure 7-21. There is clear difference in the level of impact distinguished with less percentage  $Q_p$  reduction at the outlet where there is a greater proportion of unmitigated flows.

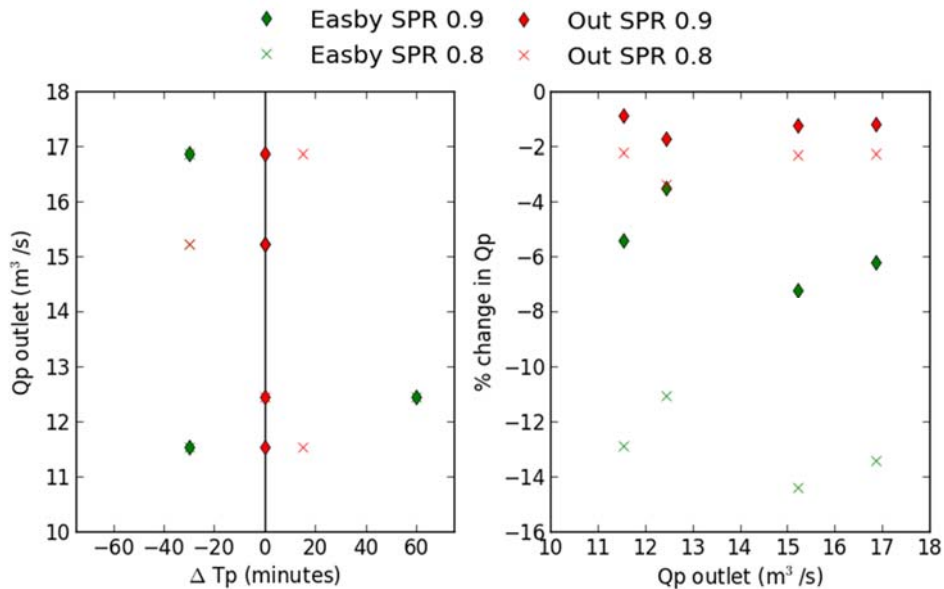


Figure 7-21 Impact of reducing SPR in both Leven Vale and Lonsdale at Easby and Great Ayton

The average percentage reduction for each of the six scenarios is plotted in Figure 7-22, against the proportion of the catchment having undergone mitigation. The different colours in Figure 7-22 represent the level of mitigation implemented, red being a 20 % reduction in SPR and blue 10 %; the broken line represents the impact as measured at Great Ayton and the solid line is the impact measured at Easby. It is clear from these results that, as would be expected, as the amount of mitigation increases both as a proportion of catchment area and SPR reduction, the impact increases. The interesting observation to note in Figure 7-22 is where the scale of the mitigation as a proportion of total catchment area overlap, roughly 0.3, they do not intersect; this again is due to the geomorphological dispersion effect, where the impact is greatest, closest to the mitigation area.

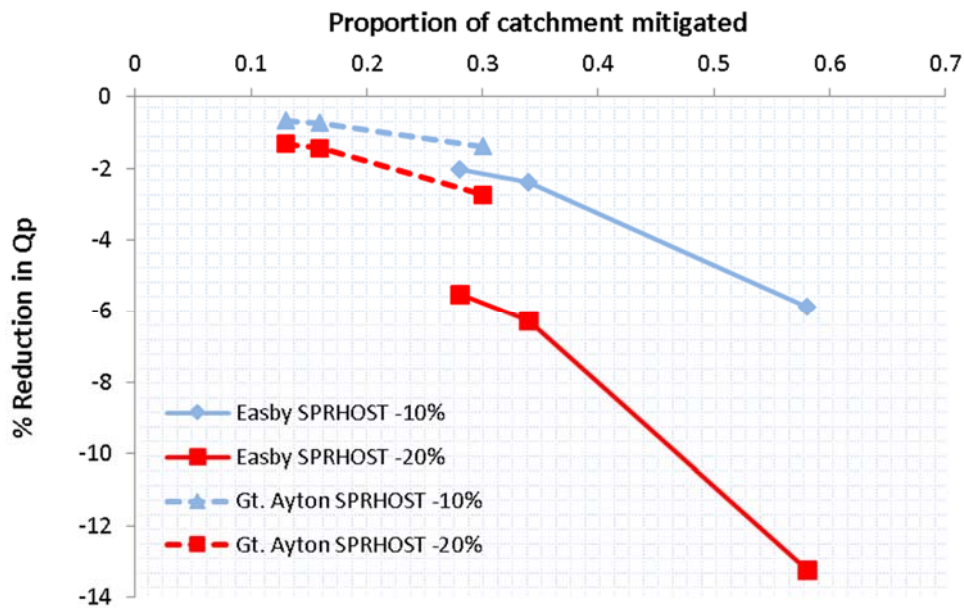


Figure 7-22 Impact as the average percentage reduction on local Qp, at Great Ayton (broken line) and Easby (Solid line) for the two SPR reduction scenarios of 10 % (blue) and 20 % (red)

### 8.3.7 Morland

Two scenarios are modelled for the Morland catchment to investigate the potential impact of the mitigation work being carried out under the DTC project and secondly a riparian woodland scenario for comparison with Great Ayton.

#### Scenarios

Table 7-6 Scenarios modelled for Morland

SCENARIO	COMMENT
NFM in the mitigation catchment (Scenario 1)	Identify the channel and riparian areas in the mitigation catchment using the TWI. For cells that flow those identified reduce the asymptotic limit of celerity by 75 % to reflect a series of RAFs designed for the attenuation of flood flows and the removal sediment.
Riparian woodland throughout the catchment (Scenario 2)	Identify the channel and riparian areas using the TWI. For cells that flow those identified reduce the asymptotic limit of celerity by 50 %. These results can be compared to the same scenario for the Great Ayton catchment.

The largest four events in Morland each have return interval of between 3 to 4 years and will be used for comparison to the Great Ayton peaks (Table 7-7). Generally the Morland



rainfall events are of a higher mean intensity (1.9 mm/hr compared to 1.6 mm/hr for Great Ayton) and shorter in duration on average 17 hours compared to 37 hours at Great Ayton. The contrasting rainfall characteristics for the largest flood peaks in each of the catchments provide a useful comparison of mitigation options.

**Table 7-7 Rainfall characteristic of the four largest flood peaks modelled to Morland**

<b>Rank</b>	<b>Qp (m<sup>3</sup>/s)</b>	<b>Date</b>	<b>Total rain (mm)</b>	<b>Mean intensity (mm/hr)</b>	<b>Max intensity (mm/hr)</b>	<b>Duration (hours)</b>
1	8.37	22/11/2012	40.03	1.70	15.89	23.00
2	8.04	28/06/2012	27.63	2.35	38.73	11.00
3	7.54	20/12/2013	34.93	1.72	7.29	20.00
4	7.38	23/12/2013	29.15	1.98	8.08	14.00

***Pattern***

Two patterns are used, one for each of the scenarios. The first pattern identifies the channel and riparian areas within the mitigation sub-catchment using the wettest 25 % of cells from the TWI.

***GIS rule base for establishing mitigation pattern***

Scenario 1: Cells selected if they are within the wettest 25 % of cells as identified by the TWI and in the mitigation catchment.

Scenario 2: Cells selected if they are within the wettest 25 % of the catchment as identified from the TWI.

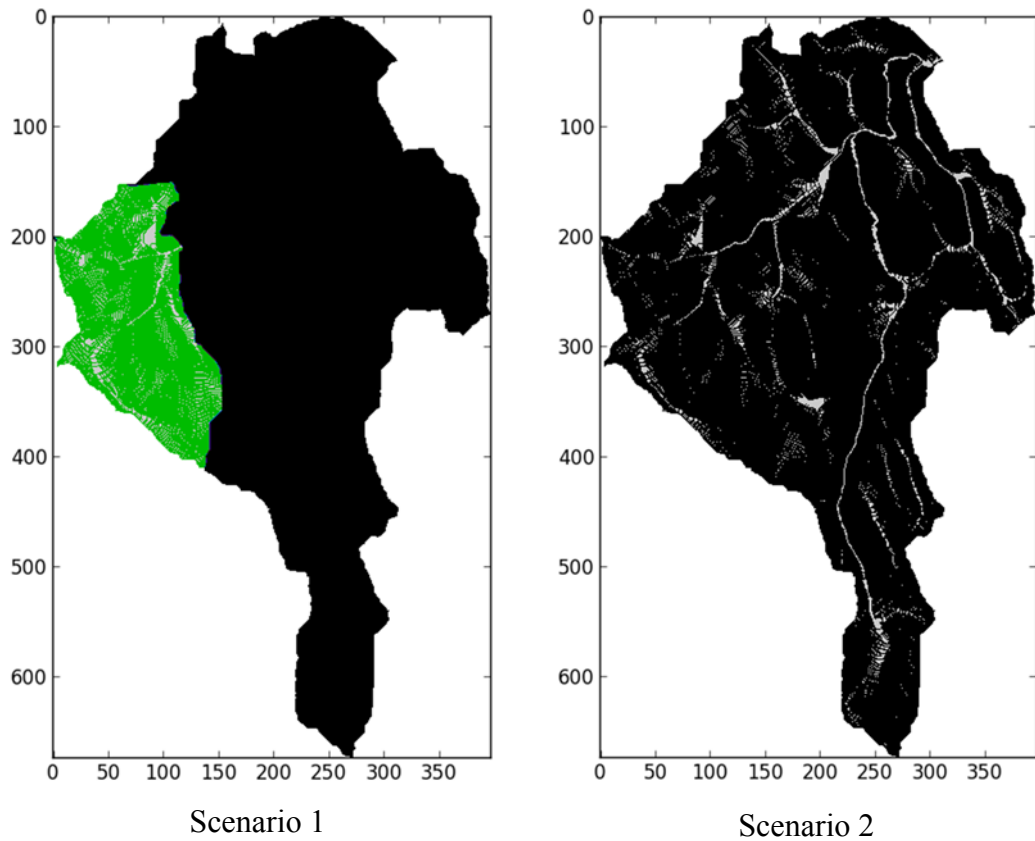


Figure 7-23 Patterns used for the Morland scenarios (Scenario 1: Grey area in the mitigation pattern, black and green not in the pattern, green indicates the mitigation catchment. Scenario 2: Grey area in the mitigation pattern, black excluded)

### Results - Scenario 1

The impact on Qp from this scenario is minimal and the signal is mixed, as shown in Figure 7-24

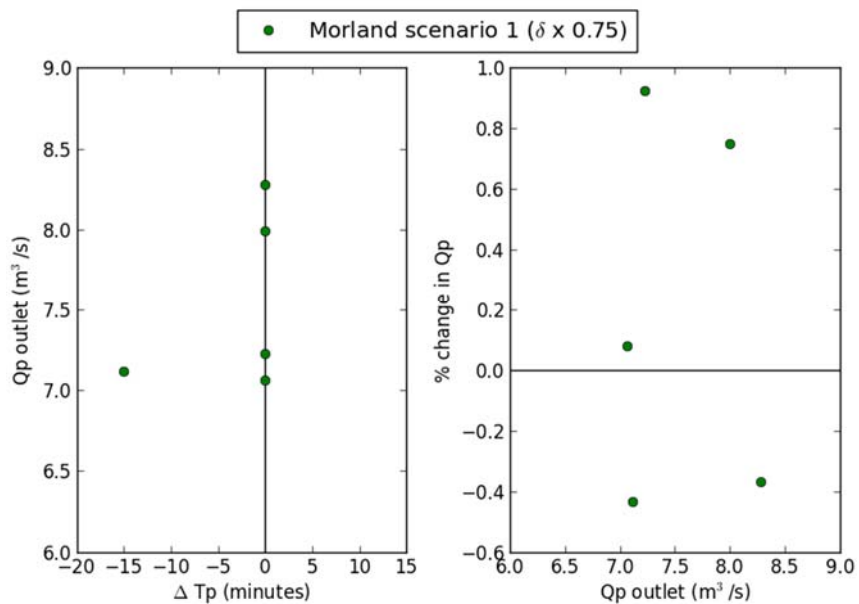
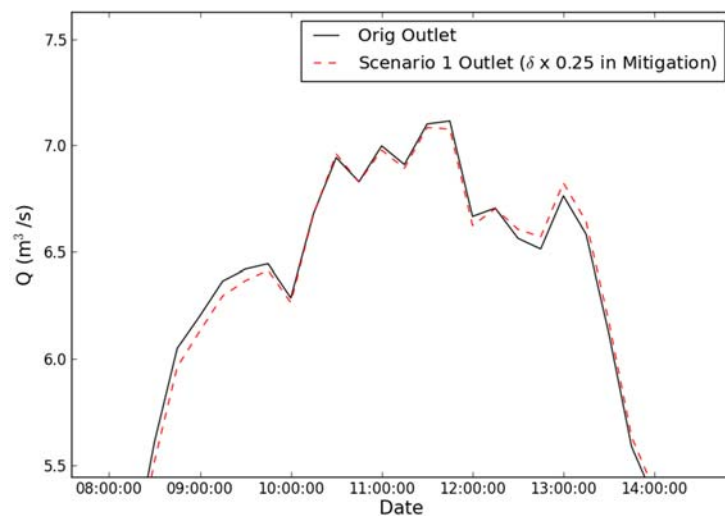


Figure 7-24 Morland Scenario 1 results showing change to Tp and Qp

For the fourth ranked event the  $T_p$  appears to have been reduced, which is counterintuitive as reducing celerity would be expected to increase the  $T_p$ . However, on examining the peak it is evident that the result is due to noise within the hydrograph peak, as shown in Figure 7-25. The peak has been reduced by a greater amount than the point previous in the hydrograph so that the earlier point is larger in the mitigated hydrograph, which causes the reduction in  $T_p$ . The hydrograph shows that the mitigation scenario is doing as is hoped by removing mass from the peak and rising limb and displacing it to the recession



**Figure 7-25 Noisy in the hydrograph peak (Rank 4 event) makes it appear the that  $T_p$  has been reduced under mitigation**

Although impact is minimal in Figure 7-26, the peak has been increased, with mass being move from the rising limb but now coinciding with the peak to increase it marginally.

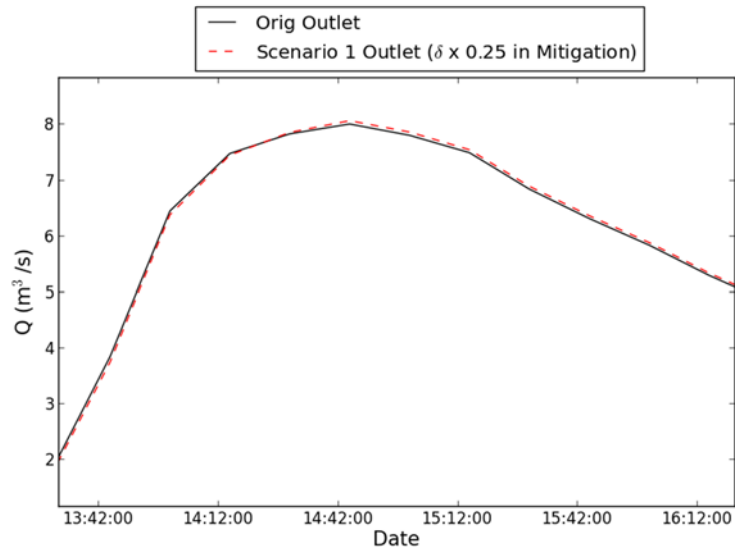


Figure 7-26 Increased Qp due to attenuation of flows but cause coincidence with the peak (Rank 2)

**Results - Scenario 2**

The results for the modelled impact of riparian woodland uptake in both the Morland and Great Ayton catchments are similar, as illustrated in Figure 7-27. There is mixed impact modelled in both catchments with some improvement as well as some increases of the peaks.

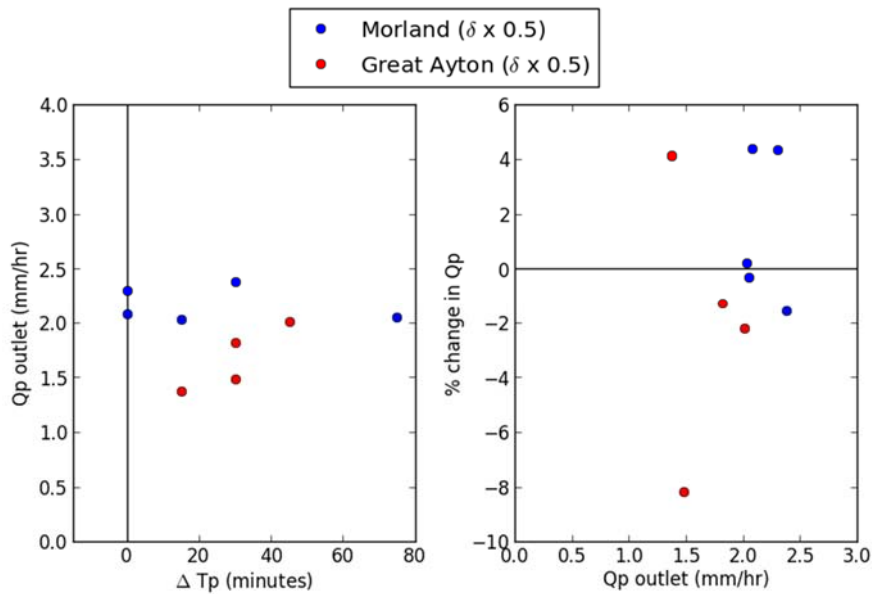


Figure 7-27 Impact on flood peaks for the Morland and Great Ayton catchments with catchment wide riparian woodland implemented

## 8.4 Measurement errors and model parametrisation uncertainty on Qp impacts

As an investigation in to the effects of data measurement errors and model parametrisation uncertainty on Qp impacts, a series of scenarios have been run for the Morland catchment.

### *Uncertainty in rating curves*

Two alternative rating curves have been calibrated using the VARE model, with the observed rainfall increased and decreased by 10 %, respectively. Note that a given error in the rainfall series must be applied to both Juke and the VARE model, which calibrates a rating curve constrained by the mass balance given by the resultant flow series, rainfall and evaporation.

The changes in runoff and evaporation for a +/- 10 % change in rainfall calculated using VARE are shown in Table 7-8, noting that it is assumed that the change in catchment storage over the 2 year period is zero (i.e. rainfall – evaporation – runoff = 0). Due to the effects of changes in rainfall on evaporation (calculated by VARE using the FAO Penman equation) a +/- 10 % change in rainfall is not associated with a +/- 10 % change in runoff. For example, during the winter period when evaporation is energy limited it is not expected that increased rainfall will be associated with increased evaporation losses.

**Table 7-8 Rainfall-runoff totals for the three derivations of the Morland outlet rating curves (The values in brackets are the percentage equivalent of the original, two year period.**

	Rain (mm)	Evap (mm)	Q (mm)
Increases (10 % up)	4223 (110 %)	1061 (107 %)	3161 (111 %)
Original	3847	992	2855
Increases (10 % down)	3476 (90 %)	869 (88 %)	2606 (91 %)

To investigate the QP impact for each of the rating curves, Juke was recalibrated for the baseline case (Scenario 0) twice using the new flow series and the corresponding rainfall series. Simulations were then performed for Scenario 1, which reflects a worst case, future state, of the catchment.

Figure 7-28 shows the percentage change in Qp for the five largest events for the two new flow series plus the original model run. The average Qp impact of degrading the catchment from the original model was an average increase of 18.5 % with a standard

deviation of 2.9 %. The decreased and increased rainfall models have mean Qp increases of 17.1% and 19.4 %, respectively. These correspond to average absolute differences of -1.4 % and +1 % compared to the original Scenario 1 flood peaks for differences of +/- 10 % in the rainfall, respectively.

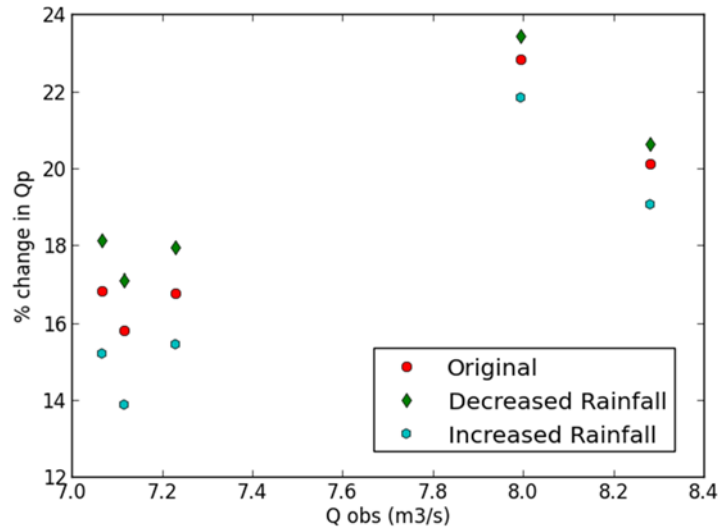


Figure 7-28 Rating curve uncertainty impact on the modelled flood peaks for the degradation scenario

### ***Juke parameter uncertainty and uncertainty in rating curves***

This set of scenarios considers both uncertainty in the rating curves and in the current state of the catchment with regard to soil condition. To reflect the uncertainty in soil condition, the HOST values used in the parameterisation of the partitioning factor ( $\gamma$ ) used to generate runoff, a set of scenarios have been performed in which the catchment was assumed to be in an initially partially degraded state. Using the three rating curves from the above, a revised baseline current state was calibrated in which the HOST values were assigned 50 % of the SPR increases suggested by Packman *et al.* (2004) to represent an initial level of degradation. Scenario 1 (fully degraded catchment) was then performed, with the impact results provided in Figure 7-29. As expected, the resultant impacts from a partially to fully degraded catchment on Qp are less than were shown previously for an initially undegraded catchment in Figure 7-28. Taking the five modelled peaks for the three rating curves, there is a mean increase in Qp of 7.9 % (Std. dev. 1.2 %) if it is assumed the catchment is already partially degraded versus 18.3 % (Std. dev. 2.9 %) for the undegraded HOST values.

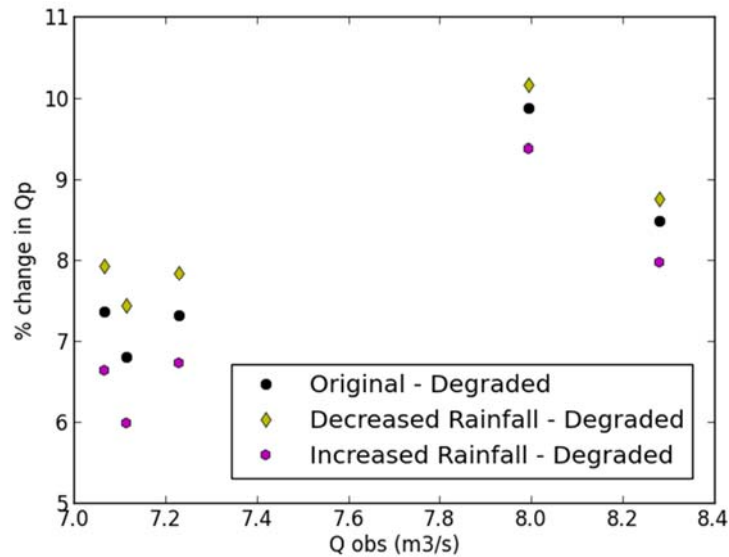


Figure 7-29 Modelling results for the experiment to investigate the uncertainties associated with the rating curves and runoff parameterisation.

### 8.5 FARM tool

Key modelling components of Juke are those that generate runoff and the rate at which the runoff propagates through the system, making it straightforward to map the scenarios to a FARM matrix. The runoff generation element within Juke has been parameterised using the SPRHOST patterns, therefore any changes to this element to reflect greater or less runoff can easily be mapped to the y-axis; the y-axis on the FARM matrix reflects soil condition, which in the FEH modelling (Chapter 6) was reflected in scenarios by manipulating SPR, which is also being performed with Juke. The x-axis of the FARM matrix represents connectivity, which in the FEH modelling (Chapter 6) was linked to the  $T_p$  parameter, which is not manipulated in such a direct way using Juke. The propagation of runoff in Juke has been manipulated through the celerity function which affects  $T_p$  indirectly.

The ‘as now’ scenario (0) is mapped to the middle of the matrix. There is an acceptance that there is already some level of degradation, although uncertain of the extent, but it is accepted that there are both better and worse scenarios. All scenarios are mapped and identified as higher or lower risk against the as now situation. Three matrices are plotted to reflect the different types of scenarios modelled and to convey important messages regarding the type and scaler of intervention required and also a simple message regarding the uncertainty in the impact.

### 8.5.1 Catchment wide - $\gamma$ (SPR) modification

To provide a comparison with matrices produced in Chapter 6, a series of scenarios have been modelled where the partitioning factors ( $\gamma$ ) for the whole catchment have undergone incremental changes of 5 %, both as an increase and decrease. These changes reflect the percentage change in SPR as per the FEH in Chapter 6 and relate to soil condition. Results for the changes to  $T_p$  and  $Q_p$  for the top four ranked events (Table 7-2) are plotted in Figure 7-30. The results show consistent increases or decrease that reflects the manipulation of  $\gamma$ .

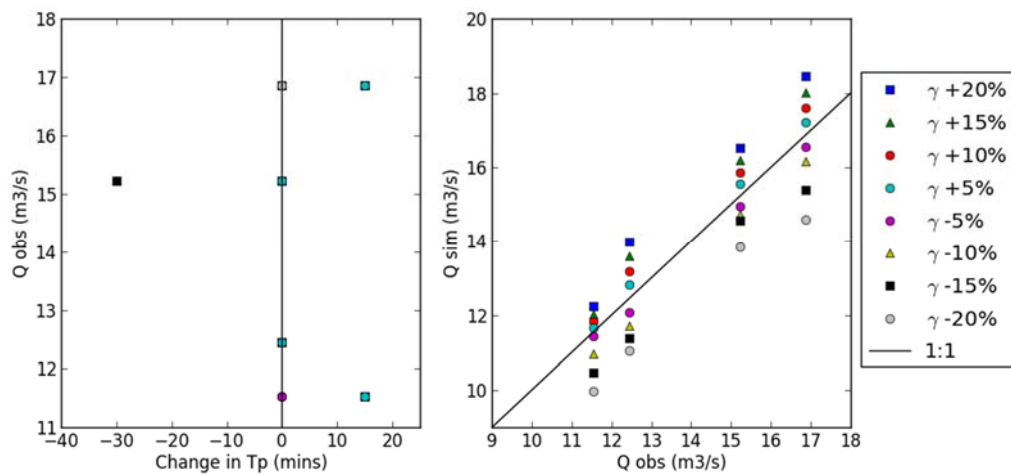


Figure 7-30 Modelling results showing the changes in  $Q_p$  and  $T_p$  for a range of  $\gamma$  manipulation scenarios

Results are shown in Figure 7-31 for the rank 1 event, where the values plotted on the matrix are the percentage change in  $Q_p$  compared to Scenario 0 ('as now'  $\gamma$  and  $T_p$  [celerity] values). This matrix highlights the advantage of Juke over the FEH for modelling impact – there are nonlinear changes in  $Q_p$  due to the spatial patterns of SPR and the variability in travel path lengths.

No explicit changes were made to the travel times/celerity parameterisation; this however, again highlights the advantage Juke provides over the FEH and FEH-FIM for impact assessment as celerity is a function of discharge, it therefore changes accordingly to alterations in runoff production (Figure 7-31). A limitation of the original FARM tool is also demonstrated as the catchment response is not as simple as illustrated in Chapter 6, impact differs from event to event and changes to SPR should not be made independently of  $T_p$ /connectivity.



		Connectivity (Reflects Tp)			
		+15 mins	Original		
γ /SPR (Soil condition)	+20%			9.47	
	+15%			6.91	
	+10%			4.36	
	+5%			2.04	
	Original			0.00	
	-5%		-1.76		
	-10%		-4.07		
	-15%		-8.74		
	-20%		-13.41		

Figure 7-31 A farm matrix showing the percentage change in Qp and change in Tp for the rank 1 event

It should be noted that the change in Tp does not necessarily move in the direction intuitively expected. The rank 2 event, which is the longest by 24 hours, shows a reduction of 30 minute in Tp for two of the scenarios in which  $\gamma$  is reduced. However, as shown in Figure 7-32 this event has multiple peaks and the reduction in Tp is a related to the synchronicity of the impacted flows.

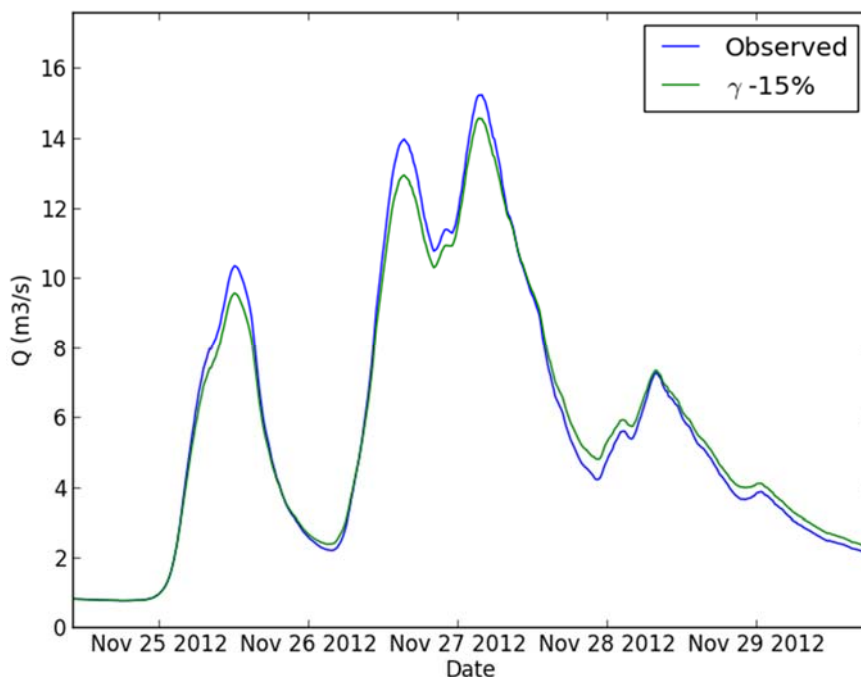


Figure 7-32 Multiple peaked, rank 2 event, with a reduced Tp for less runoff

### 8.5.2 LUM and NFM scenarios

An extension of the existing FARM tool is to provide a storyboard with specific land use scenarios mapped onto the matrix, with an indication of potential impact, Figure 7-33. This should instill greater confidence of the potential of NFM and LUM as historical events, experienced by the community, have been simulated to identify opportunities for the reduction of flood peaks.

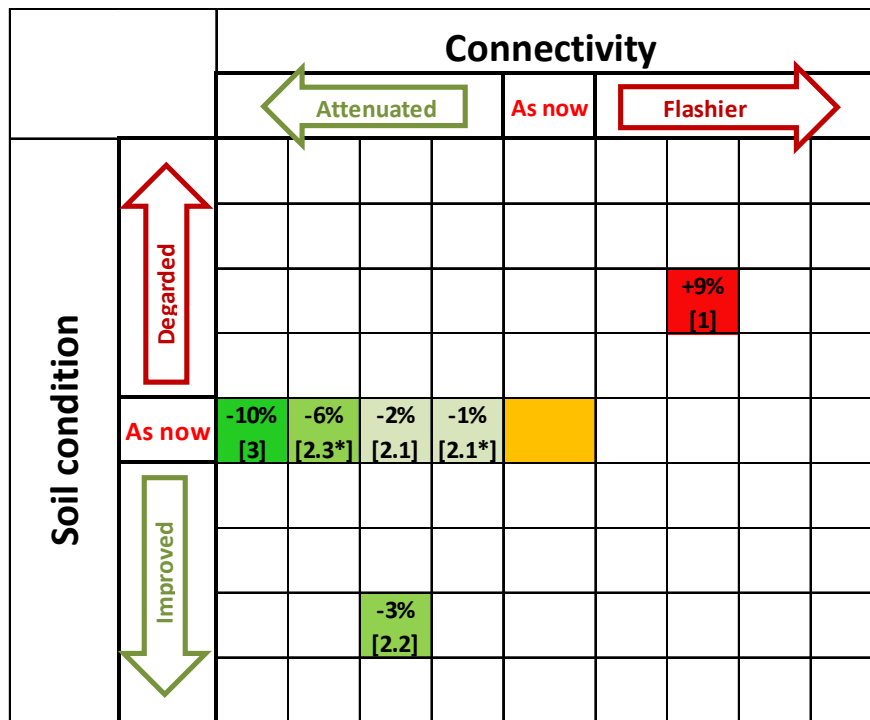


Figure 7-33 FARM matrix showing the results for the rank 1 event for the scenarios modelled

Table 7-9 provides a summary of the scenarios mapped in Figure 7-33 with the associated parameter manipulations and the percentage of the catchment affected.

Scenario	Name	Celerity change ( $\delta$ )	Change to Fast runoff ( $\gamma$ )	Percentage of catchment affected
1	Worst case	0	Approx. +5 %	61 %
2.1	Riparian wood - 1	-50 %	0	53 %
2.1*	Riparian wood - 2	-25 %	0	53 %
2.2	Riparian wood - 3	-50 %	-20 %	53 %
2.3*	Riparian wood - 4	-50 %	0	100 %
3.0	NFM	-75 %	0	53 %

Table 7-9 Summary of the scenarios, parameter manipulation made and the percentage of catchment affected

### 8.5.3 Scale effects

The results from Scenario 5 in which the  $\gamma$  parameter was reduced by 20 % for two headwater catchments, representing a mitigated area of 8.7 km<sup>2</sup>, are illustrated in Figure 7-34. Each points represents one of the ranked events (Table 7-2) and the size of the enclosing circle reflects the variability in the impact on the event peaks, hence potential uncertainty. At Easby (13.9 km<sup>2</sup>), the reduction in peak flows are 11 to 15 %, but downstream at Great Ayton (29.3 km<sup>2</sup>) the corresponding reductions are 2 to 3 %. This reflects the relative proportion of the area upstream of the gauge under going change, but also geomorphological dispersion due to the relative timings of contributions.

The points with the largest percentage reductions in Qp are at the nested Easby gauge, whilst the points closer to the centre ('as now') represent the same events and scenarios, but illustrating the level of impact detected at Great Ayton.

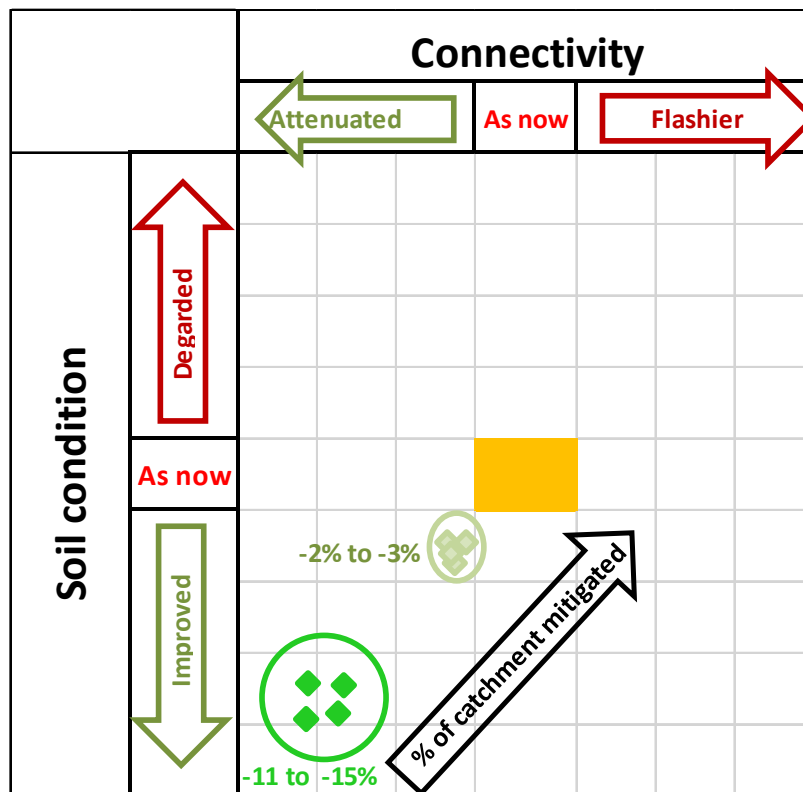


Figure 7-34 FARM matrix illustrating the effects of the spatial extent of mitigation and the scatter/uncertainty in the magnitude of reduction magnitude

## 8.6 Discussion and conclusions

This section summarises the findings from the modelling of scenarios using Juke.

### **8.6.1 Degradation impacts**

Using the Packman *et al.* (2004) recommendations for representing a deteriorated catchment through the reclassification of HOST classes demonstrated that an increase of 7 % in SPR and therefore fast runoff to 61 % of the catchment could potentially result in up a 12 % increase in flood peaks. The trend in the percentage increase in  $Q_p$  has shown that the impact may increase with increasing event magnitude.

### **8.6.2 Flood mitigation**

The investigation into which parts off the catchment may have a greater impact on outlet flood peaks showed that it may be more beneficial to work in the sub-catchments with the greatest travel distance to the outlet. This may not be the case for other catchments, it may be due to these catchments having higher SPR organic soils, where a percentage reduction will have greater impact than for lower SPR soils. However, if we were to consider the contributions of each sub-catchments and the way they are likely to synchronize as was demonstrated with the FIM too, the distal sub-catchments contributions were shown to synchronize closely with the outlet peak. There is potentially greater dispersion of the outlet hydrograph, especially the peak when affecting the catchments further way, where the closer sub-catchments will to a lesser extent.

It was also found that changing just the SPR had a greater impact than just affecting the travel time through celerity as shown in Figure 7-19. Reducing the amount of fast runoff is beneficial in two ways; firstly there is less water available to contribute to the flood peak; secondly, as the discharge is reduced so is the celerity as they are intrinsically linked, although the results shown in this Chapter demonstrate only small shifts in  $T_p$ .

The result of mitigating the sub-catchments most distal from the outlet having the greatest impact was partially contradicted by the final analysis which looked at the scale of mitigation relative to the overall catchment area. The analysis showed for two monitoring points at different scales, 29 km<sup>2</sup> and 14 km<sup>2</sup>, that had the same proportional area mitigated, the impact was greatest where the travel distance from point of mitigation to point of impact was least. This is put down to the level of attenuation caused by the dispersion of the flood wave and hence the impact as it propagates the network.

Although mitigating runoff through manipulating SPR in Juke has shown to be a positive means for mitigating flood flows, how achievable this is in reality is likely to be a harder proposition. Field measurements have shown that infiltration rates can be increased

through reduced compaction brought about by reduced stocking densities and alternative land covers such as woodland, no clear link as to what this means in changes to catchment runoff rates could be found. This does not mean however, that catchment scale impacts did not and do not occur. There is also the consideration of how the observed effects of increased infiltration scale with magnitude of event as the modeling results show, the relative  $Q_p$  reductions reduce with increasing event magnitude. It is highly likely that significant parts of the catchment will be producing close to 100 % runoff regardless of the SPR and infiltration, purely because they will be saturated.

Although attenuating the flows through manipulating celerity were shown to have lesser impact than SPR, it is likely that this will be more achievable means of mitigation. It can also be designed to target and become operational during the very largest events. This was demonstrated in the Belford catchment where inlets to offline storage features were raised as it was thought they operated too regularly and therefore for too low a flow, meaning there was less storage for bigger events (Nicholson *et al.*, 2012).

Obviously this type of modeling cannot take into consideration all factors that contribute to flooding. For example hydraulic controls such as bridges and culverts. These factors are known to exacerbate if not cause flooding locally, for example the Dyke Beck tributary causes flooding locally when a culvert surcharges and spills on to the road.

### **8.6.3 FARM tool**

Three versions of the FARM tool are demonstrated to illustrate a number of points regarding the strengths and weaknesses of both Juke and the Farm tool; and the way in which they can potentially be used to convey complicated ideas regarding scale and uncertainty of NFM and LUM schemes, whilst at the same time provide confidence of the flood mitigating potential. The first matrix in Figure 7-31 demonstrated the strengths of Juke over the FEH rainfall runoff and FEH-FIM models as celerity is a function of discharge, the reduction in flow, feeds back to reduce celerity. A limitation of the original FARM tool is also demonstrated as the catchment response is not as straightforward as illustrated in Chapter 6, it differs from event to event to event and changes to SPR should not be made independently of  $T_p$ /connectivity.

Two further examples of the FARM were illustrated to demonstrate the potential building confidence in stakeholders that LUM and NFM are viable flood mitigation methods; additionally they can be used for conveying more complex messages such as; (1)

uncertainty in the mitigation of different types of events as well as the data and model uncertainty if known and it is being conveyed to a suitable audience; (2) scale effects.

#### **8.6.4 Model and data uncertainty**

Section 8.4 has demonstrated the effect that data errors have on the modelled impact. The greatest uncertainty lies in the runoff (HOST) parameterisation regarding the current state of the soil in the catchment. For the scenarios modelled, the uncertainty associated with the partitioning factor ( $\gamma$ ) parameterisation, was twice that of the rating curve uncertainty. Local data, for example obtained by walk over surveys, should be performed to reduce this type of uncertainty.

#### **8.6.5 Juke - Flood Impact Modelling**

This modelling has highlighted the importance of routing and especially the importance of the location of the mitigation and how that the impact at the local scale will be different to that at the larger catchment scale. This suggests that the FEH-FIM procedure described in Chapter 6 may be improved through the incorporation of a simple kinematic wave, routing component.

The modelling in this chapter has shown that NFM and land use management are potentially viable options for mitigation flood flows; allowing the modeler to consider how much intervention is likely required and what location may potentially offer the greatest impact. Table 7-10 shows the mean impact of each of the scenarios on Qp and Tp. The NFM scenario (Scenario 3) has been shown to have the greatest flood hazard reducing impact, when compared to against the wet woodland scenarios (2.1, 2.2, 2.3).

**Table 7-10 Summary statistics of the scenario impacts on Qp and Tp**

<b>Scenario</b>	<b>Qp</b>		<b>Tp</b>	
	<b>Mean % change</b>	<b>Std. Dev.</b>	<b>Mean change (mins)</b>	<b>Std. Dev.</b>
1	8.5	2.8	0.0	0.0
2.1	-1.9	5.0	22.5	17.9
2.2	-2.7	5.3	30.0	12.2
2.3	-2.7	5.1	52.5	46.1
3	-10.4	7.6	101.3	41.3

A key finding of the Juke scenarios has been to demonstrate that the synchronicity of different sub-catchments and the mitigated and non-mitigated flows within a catchment can have an impact on the level of  $Q_p$  change. Through strategic planning and understanding what causes the largest events in catchments, mitigation schemes can be tailored to catchments to have the greatest impacts.

## Chapter 9. Conclusions and recommendations

### 9.1 Introduction

This chapter will summarise the findings of this thesis and evaluate how successfully the objectives were met. Recommendations and suggestions for further work are provided. Finally, considerations as to whether the findings of this thesis have helped to address key policy making issues relating to the potential of NFM are provided, e.g.; where should NFM be deployed and how can local synchronisation issues be addressed; and do the tools developed help build confidence in NFM approaches at this scale ( $\leq 30 \text{ km}^2$ )?

### 9.2 Research summary

The aim of the study as stated in Chapter 1 was *‘to demonstrate the potential effectiveness of NFM interventions in reducing flood hazard at the small catchment scale ( $\leq 30 \text{ km}^2$ ) using modelling techniques of increasing complexity supported by field observations.’*

The thesis has provided an insight into the potential for land use management (LUM) and Natural Flood Management (NFM) through data collection and modelling. Two catchments in Northern England were monitored with hydrological instrumentation to understand the rainfall runoff dynamics, including the generation and propagation. The analysis of these hydrological data was used to inform and parameterise the rainfall-runoff models. The modelling contributes evidence that LUM and NFM can reduce flood hazard within the catchments modelled. There is, however, uncertainty as to the extent of the likely impact and a number of complicating factors were highlighted, such as the importance of antecedent conditions and type of rainfall event in determining the magnitude of the flood hazard reduction.

The outcomes of the thesis suggest the need for a set of tools that help flood managers understand and mitigate the flood hazard within their catchment. Firstly, there is a need to understand the flooding issue within a given catchment which is best done through field measurements at multiple scales to understand catchment functioning. Secondly, a set of modelling tools are required of differing complexity depending on the level detail required; from a broad-brush of appraisal of different catchments to a more detailed study of where in a catchment to put the features. As will be discussed below, the more detailed and novel the modelling, the greater the technical expertise required to conduct it; however, the development of the FEH-Flood Impact Modelling Tool (FIM) provides a



comparatively simple approach that can be setup for any catchment in the UK, due to the use of national datasets.

Several objectives were set for achieving the thesis aim; these are listed below with a summary of the conclusions drawn against each.

### **9.3 Conclusions**

The conclusions of this thesis relevant to the objectives listed in Chapter 1 are:

*1. Carry out a comprehensive literature review of the current understanding and quantification of the impacts of NFM interventions and agricultural practices on flood generation.*

A review of the literature was carried out in Chapter 2. Good examples of field studies that demonstrated the potential for LUM and NFM for mitigating flood generation and propagation have been found. However, generally the impacts have only been demonstrated at the local scale, with the impact at larger scales difficult to attribute or detect due to a number of factors such as climate variability, data errors and the limited length of data records for statistically significant results. These factors are also what make attributing any increase in flood frequency within historical data records specifically to land use impacts difficult if not impossible.

One approach to relate change to impact is to use a mathematical model. When using a model for LUM or NFM impact assessment a number of considerations as to the type and structure of model used need to be made. The model structure and parameterisation affect the transparency, sensitivity and uncertainty of the modelled output. Lumped models offer a relatively simple option with few parameters, where physically based distributed models offer a more complex and potentially more detailed method but with a large number of parameters. A key benefit of lumped models is that they are comparatively quick to run and can be used to rapidly build up an idea as to the potential LUM and NFM flood mitigation impacts. The weakness with the lumped models, however, is that the parameter manipulations are lumped and there is no transparent way of accounting for the travel time effects and synchronicity of the mitigated and unmitigated flows. Distributed models offer this capability of testing distributed LUM and NFM flood reduction schemes. A significant contributor to the uncertainty in physically based, distributed models (PBDM) is the large number of parameters. There is a potential for

multiple parameter sets to offer equally adequate performance during calibration of PBDM. This uncertainty in parameter sets then affects the confidence of modelled impact results in NFM and LUM scenario testing.

The outcome of this objective is that the onus is on the modeller to understand the local impacts of LUM and NFM how these may be incorporated within a model. The type and complexity of the model may depend on the question being asked; a broad brush appraisal of the potential of LUM and NFM may require a simple and lumped approach, whilst a detailed study, with interest in where to locate features or have LUM restrictions within catchment, may use a more distributed model.

*2. Collect high quality hydrological data from two catchments in which NFM interventions are either planned or have been implemented. Great Ayton (River Leven) and Morland (Newby Beck) have been chosen as the study catchments, as these provide a good contrast in term of spatial scale and interventions proposed.*

I have collected data for the Great Ayton and Morland catchments in northern England. The stream network in the Morland catchment, Cumbria, was instrumented at three locations with upstream areas from 1.5 km<sup>2</sup> to 12.5 km<sup>2</sup>. The Great Ayton catchment, North Yorkshire, is larger than Morland and is instrumented at seven locations at spatial scales from 0.5 km<sup>2</sup> to 30 km<sup>2</sup>. Both catchments were instrumented in a nested design to collect data at multiple spatial scales; this was done as understanding the spatial and temporal development of flood events was deemed important to this study. The value of local data for an individual catchment is paramount as all catchments differ in biogeophysical characteristics and have local issues (Uniqueness of place; (Beven, 1999)). The data, although subject to some uncertainty, was invaluable for understanding the flow rates and travel times. Equally the cost of the instruments are low enough to suggest that future flood studies would benefit from this type of data.

*3. Characterise the study catchments to understand how floods develop and along which hydrological pathways the water is being transferred.*

The physical and hydrological characteristics of the two catchments were examined to analyse what causes the largest flood peaks. Generally, the summer rainfall events (April to September) were found to be of shorter duration and higher intensity than the winter. In the Great Ayton catchment in particular, the rainfall totals for summer events were

comparatively higher than winter events that produced similar sized flood peaks; this is due to a storage deficit needing to be satisfied before the onset of rapid runoff.

The Morland catchment is underlain by limestone and this has a significant impact in one of the monitored sub-catchments during low flows. For approximately 18 % of the time little if not zero flow passes the monitoring station of the catchment undergoing mitigation. However, a geological appraisal of the catchment stated that it was unlikely there were losses to regional aquifers, the flow therefore re-emerging in the catchment.

Activity diagrams for both the Morland and Great Ayton catchments illustrate that for the largest events all sub-catchments are equally active, i.e. are similarly contributing to the flood peak. This was found to be true for the mitigation catchment in Morland, which means that the groundwater component is not as important for the largest events; near surface processes are.

Analysis of catchment response times through lag time analysis and flood wave travel times has shown that there can be considerable scatter in the response, particularly during the small and medium events. This is largely due to the antecedent conditions and the characteristics of the rainfall event. However, the scatter reduces with increasing event magnitude which again can be linked to the catchment activity. Studying local GIS and hydrological time series data is important for understanding the local catchment issues. Furthermore, it is important to gain local insight to the problems through frequent site visits and meeting local regulators and farmers. Hence readily available data, supported by campaigns to collect data and visits to site are fundamental to characterising sites that need to be managed.

*4. Develop suitable scenarios for potential LUMC and NFM adoption, designed to reduce flood hazard within catchments, based on expert knowledge and field data.*

A number of potential LUM and NFM scenarios were drawn up and modelled in different ways using lumped and distributed approaches. The FEH model was used to populate a number of FARM risk matrices with a series of scenarios in which the SPR and Tp parameters were manipulated to reflect both degraded and improved catchment flood response. Degradation was implemented as an increase in the SPR (Standard Percentage Runoff; an event based hydrological statistic that describes the typical percentage of rainfall that leaves the catchment as fast runoff) and a reduction in Tp (Time-to-peak;

event based statistic that describes the typical time from the centroid of rainfall event to flood peak). The impacts of these scenarios for events of different return intervals and durations were investigated.

The Flood Impact Modelling (FIM) tool was proposed to use the FEH rainfall-runoff model in a more distributed way. A series of scenarios were implemented to investigate the impact of changing  $Q_p$  and  $T_p$  within different sub-catchments and assess downstream impacts. The scenarios investigated as a sensitivity test the impact of mitigating flows within catchments with varying travel times (distances) to the outlet. This helped in the understanding of catchment synchronicity and the possible effects of mitigating in certain parts of the catchment which can be used for strategic planning of schemes within the Great Ayton catchment.

The Juke modelling considered five scenarios, including one representing a degraded catchment, parameterised using the expert opinion of Packman *et al.* (2004) that specified alternative HOST classes to reflect a worst possible case of soil degradation from agriculture. Two of the scenarios incorporated the effects of riparian wood land and attenuation ponds. The final two scenarios involved a spatial sensitivity test in which the location and scale/area of the mitigation was investigated to establish whether certain sub-catchments are more suited to interventions. Also considered was the extent of mitigation required for a meaningful reduction in flood hazard.

The process of relating field information to changes in model parameters is difficult. The impact assessment focussed on the key parameters of  $Q_p$  and  $T_p$ . Conversations with local flood impacted communities and Environment Agency (EA) flood managers during catchment walk over surveys, were useful for identifying possible scenarios that needed to be addressed. The chosen scenarios cover a broad range of possible interventions as it was important to demonstrate hazard reduction impacts both locally and at the larger catchment scale.

*5. Explore the limitations of a widely used 'traditional' modelling approach. The FEH method, which is widely used by practitioners.*

The FEH rainfall-runoff model was run for several different scenarios that involved manipulating the SPR and  $T_p$  parameters. Results were used to populate the FARM risk matrix with percentage changes to flood peaks. The response, as expected given the

assumptions of the unit hydrograph, was shown to be linear for changes made to both the SPR and  $T_p$  parameters. Knowing only a few modelled results, one would have enough information to predict any scenario required, in terms of changes to SPR and  $T_p$ . An important result that the FEH modelling did show was that mitigation was most effective for short duration, high intensity rainfall events.

A key limiting factor of the FEH rainfall runoff model for LUM and NFM impact assessment is that it is not distributed. The location within a catchment that mitigation takes place is of importance due to the way in which flows from various parts of the catchment are synchronised. The FIM methodology was proposed using the FEH rainfall-runoff model to generate sub-catchment contributions separately and route these to the outlet using superposition. Manipulations of the  $Q_p$  and  $T_p$  of sub-catchments can then be made to investigate the impact when routed to the outlet and combined with the flows from the non-mitigated catchments. A key result from the FIM modelling was to show that mitigating catchments in closest proximity to the outlet by delaying their contribution may potentially exacerbate the flooding problem due to the synchronicity of the contributions. It was also shown that these effects could be offset by introducing attenuation elsewhere in the catchment. Even though the assumptions of the FIM approaches and the FEH are relatively simple, it is still possible to use the tool to explore realistic flood management issues. Moreover, the tool is readily usable by flood management professionals who are competent using the tools and methods presented here. The FIM tool has been used to train a number of consultants and representatives of Non-Governmental Organisations [NGO] as part of a Continuing Professional Development [CPD] course. The model does lack detail and hence the simplifying assumptions need to be backed up by more detailed studies such as the Juke study (Simplifying assumptions include fixed wave speed/celerity and simple scaling of the hydrograph to reflect reduced runoff volume.).

*6. Use a novel modelling (Juke) technique to test potential catchment management scenarios including land use change and NFM on the catchment flood response.*

The scenario representing a ‘fully’ degraded Great Ayton catchment indicates that poor soil condition could potentially increase flood peaks up to 12 %. Section 8.4 in Chapter 8 showed that with considerable uncertainty in the rating curve and model parameterisation the soil degradation may lead to  $Q_p$  increases between 6 and 12 %.

The trend in the percentage increase in  $Q_p$  showed that the impact would increase with increasing event magnitude.

As there is uncertainty as to what level of impact NFM and LUM will have, a range of scenarios were tested as a form sensitivity analysis. It is thought that the scenarios will envelope the potential impact. The riparian woodland scenario showed that a riparian zone accounting for 25 % of the total catchment area has the potential for  $Q_p$  reductions of up to 11 %. There is, however, variability in the modelled impact, with  $Q_p$  increasing for some events and decreasing for others. This is linked to the temporal patterns within the rainfall and the way the runoff generated is synchronised for disparate parts of the catchment.

NFM in the form of Runoff Attenuation Features (RAF's) was found to have a significant impact on the flood hydrograph, reducing flood peaks for all four largest events. For one event the flood peak was reduced by 22 % but for the three other large events the reductions were 5 to 10 %.

The outcomes from all the scenarios modelled with Juke demonstrated how complicated an issue flood mitigation through distributed LUM and NFM measures is. There were mixed results in terms of the level of reduction achieved and this was linked to the rainfall characteristics of individual events. Generally, it has been demonstrated that NFM and LUM can reduce flood peaks and this impact will be greatest for the shorter duration higher intensity events.

Juke enables a modeller to investigate what level of intervention and how much NFM and LUM is needed and where in a catchment it could be placed to get the most significant impact. As was shown in the scenario that represented the current level of intervention in the Morland catchment, it was demonstrated that targeting a specific sub catchment was less effective than implementing distributed measures across the catchment.

Juke may not be readily deployable in its current form to flood risk management professionals, but the results have shown a number of key phenomena that help build our knowledge of flood generation, NFM modification and flow propagation across scale. It underpins many of the assumptions made in the FEH-FIM models, for example, that NFM has a local impact and that the local NFM needs to have a significant impact on local flow before downstream benefits accrue.

The uncertainty associated with some of the scenarios and the demonstration that in some instances  $Q_p$  can occasionally increase should not be dismissed. These findings suggest that flood managers need to substantially intervene in order to be confident of not exacerbating the flood problem. Users of the FEH-FIM can reflect the uncertainties in the level of intervention and parameterisation by allowing a greater range in the  $Q_p$  and  $T_p$  change parameters. As a sensitivity approach has been employed in the RAF scenario (based on literature), the exact number of features required is not known.

*7. The outcomes of 5 and 6 will be used to populate a series of risk matrices based on the Floods and Agriculture Risk Matrix (FARM) tool (Wilkinson et al., 2013). The tool helps to synthesise and convey both the limitations of traditional modelling structures for land use change scenario modelling and the implications of land use management decisions on flood risk. The results will provide guidance to practitioners, the scientific community and others with an interest in NFM and land use management as a means of reducing flood risk.*

A series of FARM risk matrices were populated with results from the both the FEH and Juke model scenarios. The FARM tool provides a clear and simple visualisation to understand ways of conveying the principles of LUM and NFM and the potential impacts on flood peaks.

The matrices populated with result from the FEH model help to illustrate the principle weakness of the FEH model for impact assessment as the results were linear and the matrices did not differ significantly from catchment to catchment or for the type of event being modelled. This is due to the underlying assumptions of linearity in the Unit Hydrograph (UH) approach.

A FARM matrix was populated with results from the Juke modelling to show the potential impact on the largest observed event. Putting numbers for  $Q_p$  reduction on the matrix that represents potential real scenarios tailored and tested for a catchment provides more confidence in LUM and NFM to stakeholders and flood managers.

#### **9.4 Recommendations and future work**

There is still a need to produce the evidence of the efficacy of LUM and NFM in reducing flood hazard at scales larger than the field. The evidence base is increasing, but currently limited to an unsatisfactorily small number of studies.

#### **9.4.1 Catchment observations**

There is certainly still a need to build upon the field evidence of LUM and NFM impacts at both the local and point/feature/field scale and the larger catchment scale (>10 km<sup>2</sup>). To fully understand the forms of intervention best suited to a given catchment, examples need to be found or implemented in catchments of different types, i.e. different soils, topography and land use. This will strengthen the arguments for their uptake and build a portfolio of potential options for different catchment types.

#### **9.4.2 Modelling**

The Juke model has been demonstrated as a novel form of distributed rainfall-runoff model capable of testing a range of LUM and NFM scenarios in a transparent manner. The link between the observations of change in infiltration and runoff volumes (SPR) and propagation have been difficult to quantify. Progress is needed to relate changes in soil condition and field scale runoff.

Hydrodynamic modelling may be an option that has been under used in examining LUM/NFM impacts. The Pond Model developed for a reach of the Belford Burn catchment demonstrated the potential local impact of attenuation ponds (Nicholson *et al.*, 2012; Nicholson, 2014). However, it should be possible to run models for larger spatial scales and longer river reaches that include detailed representation of these types of feature. The impact of riparian or wet woodland could be investigated using 1-D or more detailed 2-D models that can investigate floodplain flows. The limiting factor of these models is the need for detailed, accurate surveyed data. One such study was highlighted for the River Parrett and showed the potential for significant attenuation of the flood wave. However, the Parrett catchment is not representative of most catchments due to low velocities, typically less than 0.2 m/s (Thomas and Nisbet, 2007).

There is potential for the FEH-FIM modelling approach developed in this thesis to be further developed to include a more robust and transparent method of reducing  $Q_p$  in the sub-catchment contributions. At present the model simply scales the whole sub-catchment hydrograph, meaning there is no conservation of mass. The  $T_p$  adjustment also shifts the whole hydrograph in a lumped linear way rather than a more transitional, nonlinear and physical response. This could be performed by running the FEH for a range of SPR and  $T_p$  values to provide a lookup library of hydrographs. The routing of the sub-catchment flows could be done in a more realistic and sophisticated manner rather than a fixed wave speed that doesn't consider the nonlinear relationship between flow volume



and wave celerity. One method for nonlinear routing is a Muskingham approach which can also make use of the analysed travel time/celerity values, which underpin the Juke parameterisation.

#### **9.4.3 What next for policy?**

This thesis has addressed questions commonly asked by policy makers and other stakeholders regarding the potential for NFM and LUM in catchments. The combination of field observations, the FEH-FIM tool and Juke have been demonstrated as a method for investigating these types of questions and could help underpin investment strategies in catchments. The FEH-FIM tool has been used in local studies by the EA and SEPA in recent months where NFM approaches have been proposed; it has helped users to think about synchronisation issues and the spatial location of features. The users were guided to explore a range of  $Q_p$  and  $T_p$  change scenarios, studying as many sub catchments as possible.

During the winter of 2015/16 there were a series of large events, including Storm Desmond in Cumbria. During storm Desmond traditional engineered defences were overtopped. There is a growing appreciation that formal defences cannot continue getting larger and catchment management and more novel methods may have a role to play. Irrespective of the measurement and modelling uncertainty, we know that we can manage runoff volumes and timing at the local scale from existing examples in the literature. Juke has demonstrated that it may be feasible at larger scales also, but a better understanding of the way field observations of the impacts can be incorporated in to models is needed. Although the tools shown here do not provide conclusive evidence for the benefits of NFM compared to other management strategies, they enable the user to explore the degree of impact needed at local and wider catchment scales for NFM schemes to be successful. The models use enough physical process representation and key observed data, to hopefully provide enough confidence to policy makers that positive benefits can be achieved through NFM at scales up to 30 km<sup>2</sup>.

It is suggested that policy makers continue to invest in combined field and modelling research to increase the number of catchments in which NFM and LUM are studied, improving the evidence base. There is also a need for alternative and novel modelling approaches, designed specifically for impact assessment. It is hoped that new research studies, such as the EA Working with Natural Processes project, will allow larger

catchments to be instrumented and modelled across scale and include large scale trials of LUMC and NFM.

## References

- ABI (2010) *Massive rise in Britains flood damage bill highlights the need for more help for flood vulnerable communities says the ABI* Available at: <https://www.abi.org.uk/News/News-releases/2010/11/massive-rise-in-britains-flood-damage-bill-highlights-the-need-for-more-help-for-flood-vulnerable-communities-says-the-abi.aspx> (Accessed: 24/07/2013).
- Allen, D.J., Newell, A.J. and Butcher, A.S. (2010) '*Preliminary review of the geology and hydrogeology of the Eden DTC sub-catchments*'. Available at: <http://nora.nerc.ac.uk/12788/1/OR10063.pdf> (Accessed: 12/10/2012).
- Allen, R.G., Pereira, L.S., Raes, D. and Smith, M. (1998) '*Crop evapotranspiration-Guidelines for computing crop water requirements-FAO Irrigation and drainage paper 56*', FAO, Rome, 300(9), p.
- Archer, D., Climent-Soler, D. and Holman, I. (2010) 'Changes in discharge rise and fall rates applied to impact assessment of catchment land use', *Hydrology Research*, 41(1), pp. 13-26.
- Armstrong, A.C. and Garwood, E.A. (1991) 'Hydrological consequences of artificial drainage of grassland', *Hydrological Processes*, 5(2), pp. 157-174.
- Ballard, C.E., McIntyre, N., Wheeler, H.S., Holden, J. and Wallage, Z.E. (2011) 'Hydrological modelling of drained blanket peatland', *Journal of Hydrology*, 407(1-4), pp. 81-93.
- Barber, N.J. and Quinn, P.F. (2012) 'Mitigating diffuse water pollution from agriculture using soft-engineered runoff attenuation features', *Area*, 44(4), pp. 454-462.
- Barredo, J. (2007) 'Major flood disasters in Europe: 1950-2005', *Natural Hazards*, 42(1), pp. 125-148.
- Barredo, J.I. (2009) 'Normalised flood losses in Europe: 1970-2006', *Natural Hazards & Earth System Sciences*, 9(1).
- Barton, R., R. (1998) '*Simulation metamodels*', Proceedings of the 30th conference on Winter simulation. Washington, D.C., USA. IEEE Computer Society Press.
- Bates, B. and Pilgrim, D.H. (1983) 'Investigation of storage-discharge relations for river reaches and runoff routing models' *Civil Engineering Trans, Instn Engrs, Australasia.*, (3), pp. 153-161.
- BBC (2014) *Back-to-nature flood schemes need 'government leadership'*. Available at: <http://www.bbc.co.uk/news/uk-politics-25752320> (Accessed: 02/01/2016).
- BBC (2015) *North Yorkshire flood defences scheme finished*. Available at: <http://www.bbc.co.uk/news/uk-england-york-north-yorkshire-34137466> (Accessed: 02/01/2016).
- Beven, K. (1979) 'On the generalized kinematic routing method', *Water Resources Research*, 15(5), pp. 1238-1242.

- Beven, K.J. and Kirkby, M.J. (1979) 'A physically based, variable contributing area model of basin hydrology / Un modèle à base physique de zone d'appel variable de l'hydrologie du bassin versant', *Hydrological Sciences Bulletin*, 24(1), pp. 43-69.
- Beven, K.J., Wood, E.F. and Sivapalan, M. (1988) 'On hydrological heterogeneity — Catchment morphology and catchment response', *Journal of Hydrology*, 100(1–3), pp. 353-375.
- Beven, K., Young, P., Romanowicz, R., O'Connell, E., Ewen, J., O'Donnell, G., Homan, I., Posthumus, H., Morris, J. and Hollis, J. (2008) 'Analysis of historical data sets to look for impacts of land use and management change on flood generation', *Defra R&D Final Report FD2120*. Defra, London.
- Beven, K.J. (1999) 'Uniqueness of place and process representations in hydrological modelling', *Hydrol. Hydrology and Earth System Sciences.*, 4(2), pp. 203-213.
- Beven, K.J. (2001) *Rainfall-runoff modelling: the primer*. 1st edn. Hoboken : Wiley.
- Beven, K.J. (2011) *Rainfall-runoff modelling: the primer*. 2nd edn. Hoboken : Wiley.
- Bilotta, G.S., Brazier, R.E. and Haygarth, P.M. (2007) 'The Impacts of Grazing Animals on the Quality of Soils, Vegetation, and Surface Waters in Intensively Managed Grasslands', in Donald, L.S. (ed.) *Advances in Agronomy*. Academic Press, pp. 237-280.
- Bilotta, G.S., Brazier, R.E., Haygarth, P.M., Macleod, C.J.A., Butler, P., Granger, S., Krueger, T., Freer, J. and Quinton, J. (2008) 'Rethinking the Contribution of Drained and Undrained Grasslands to Sediment-Related Water Quality Problems All rights reserved. *Journal of Environmental Quality*, 37(3), pp. 906-914.
- Birkinshaw, S.J., Bathurst, J.C. and Robinson, M. (2014) '45 years of non-stationary hydrology over a forest plantation growth cycle, Coalburn catchment, Northern England', *Journal of Hydrology*, 519, Part A, pp. 559-573.
- Blackburn, M., Methven, J. and Roberts, N. (2008) 'Large - scale context for the UK floods in summer 2007', *Weather*, 63(9), pp. 280-288.
- Blöschl, G., Ardoin-Bardin, S., Bonell, M., Dorninger, M., Goodrich, D., Gutknecht, D., Matamoros, D., Merz, B., Shand, P. and Szolgay, J. (2007) 'At what scales do climate variability and land cover change impact on flooding and low flows?', *Hydrological Processes*, 21(9), pp. 1241-1247.
- Bloschl, G., Grayson, R.B. and Sivapalan, M. (1995) 'On the representative elementary area (REA) concept and its utility for distributed rainfall-runoff modelling', *Hydrological processes*, 9(3), pp. 313-330.
- Boardman, J. (1995) 'Damage to Property by Runoff from Agricultural Land, South Downs, Southern England, 1976-93', *The Geographical Journal*, 161(2), pp. 177-191.
- Boardman, J., Ligneau, L., de Roo, A. and Vandaele, K. (1994) 'Flooding of property by runoff from agricultural land in northwestern Europe', *Geomorphology*, 10(1–4), pp. 183-196.

- Boorman, D.B., Hollis, J.M. and Lilly, A. (1995) Hydrology of soil types: a hydrologically-based classification of the soils of United Kingdom. (IH Report 126). Wallingford: Hydrology, I.o. [Online]. Available at: <http://nora.nerc.ac.uk/7369/>.
- Bosch, J.M. and Hewlett, J.D. (1982) 'A review of catchment experiments to determine the effect of vegetation changes on water yield and evapotranspiration', *Journal of Hydrology*, 55(1-4), pp. 3-23.
- Bracken, L.J. and Croke, J. (2007) 'The concept of hydrological connectivity and its contribution to understanding runoff - dominated geomorphic systems', *Hydrological processes*, 21(13), pp. 1749-1763.
- Brazier, R.E., Beven, K.J., Freer, J. and Rowan, J.S. (2000) 'Equifinality and uncertainty in physically based soil erosion models: application of the GLUE methodology to WEPP—the Water Erosion Prediction Project—for sites in the UK and USA', *Earth Surface Processes and Landforms*, 25(8), pp. 825-845.
- Brazier, R.E., Rowan, J.S., Anthony, S.G. and Quinn, P.F. (2001) "“MIRSED” towards an MIR approach to modelling hillslope soil erosion at the national scale', *CATENA*, 42(1), pp. 59-79.
- Brown, A.E., Zhang, L., McMahon, T.A., Western, A.W. and Vertessy, R.A. (2005) 'A review of paired catchment studies for determining changes in water yield resulting from alterations in vegetation', *Journal of Hydrology*, 310(1-4), pp. 28-61.
- Bulygina, N., Ballard, C., McIntyre, N., O'Donnell, G. and Wheeler, H. (2012) 'Integrating different types of information into hydrological model parameter estimation: Application to ungauged catchments and land use scenario analysis', *Water Resources Research*, 48(6), p. W06519.
- Bulygina, N., McIntyre, N. and Wheeler, H. (2009) 'Conditioning rainfall-runoff model parameters for ungauged catchments and land management impacts analysis', *Hydrol. Earth Syst. Sci.*, 13(6), pp. 893-904.
- Bulygina, N., McIntyre, N. and Wheeler, H. (2011) 'Bayesian conditioning of a rainfall-runoff model for predicting flows in ungauged catchments and under land use changes', *Water Resources Research*, 47(2), p. W02503.
- Burgess, C.P., Chapman, R., Singleton, P.L. and Thom, E.R. (2000) 'Shallow mechanical loosening of a soil under dairy cattle grazing: Effects on soil and pasture', *New Zealand Journal of Agricultural Research*, 43(2), pp. 279-290.
- Burt, T.P. and Slattery, M.C. (1996) Time-dependent changes in soil properties and surface runoff generation. *Advances in Hillslope Processes* edn. New York: J. Wiley.
- Cabus, P. (2008) 'River flow prediction through rainfall-runoff modelling with a probability-distributed model (PDM) in Flanders, Belgium', *Agricultural Water Management*, 95(7), pp. 859-868.
- Calder, I.R. (1990) *Evaporation in the Uplands*. Wiley Chichester.
- Carroll, Z.L., Bird, S.B., Emmett, B.A., Reynolds, B. and Sinclair, F.L. (2004) 'Can tree shelterbelts on agricultural land reduce flood risk?' *Soil Use and Management*, 20(3), pp. 357-359.

- Centre for Ecology and Hydrology, C. (2007) *Land Cover Map 2007*. Available at: <http://www.ceh.ac.uk/landcovermap2007.html> (Accessed: 12/10/2012).
- Choi, W. and Deal, B.M. (2008) 'Assessing hydrological impact of potential land use change through hydrological and land use change modeling for the Kishwaukee River basin (USA)', *Journal of Environmental Management*, 88(4), pp. 1119-1130.
- CIRIA (2013) *Land use management effects on flood flows and sediments - guidance on prediction*. London: CIRIA.
- Conway, V.M. and Millar, A. (1960) 'The hydrology of some small peat-covered catchments in the northern Pennines', *Journal of the Institute of Water Engineers*, 14, pp. 415-424.
- Crooks, S. and Davies, H. (2001) 'Assessment of land use change in the Thames catchment and its effect on the flood regime of the river', *Physics and Chemistry of the Earth, Part B: Hydrology, Oceans and Atmosphere*, 26(7-8), pp. 583-591.
- De Roo, A., Odiijk, M., Schmuck, G., Koster, E. and Lucieer, A. (2001) 'Assessing the effects of land use changes on floods in the Meuse and Oder catchment', *Physics and Chemistry of the Earth, Part B: Hydrology, Oceans and Atmosphere*, 26(7-8), pp. 593-599.
- Deasy, C., Quinton, J.N., Silgram, M., Bailey, A.P., Jackson, B. and Stevens, C.J. (2010) 'Contributing understanding of mitigation options for phosphorus and sediment to a review of the efficacy of contemporary agricultural stewardship measures', *Agricultural Systems*, 103(2), pp. 105-109.
- Defra (2013) *Agriculture in the United Kingdom 2012*. Available at: [https://www.gov.uk/government/uploads/system/uploads/attachment\\_data/file/183200/defra-stats-foodfarm-landuselivestock-farmingstats-june-statsrelease-june12finaluk-121220.pdf](https://www.gov.uk/government/uploads/system/uploads/attachment_data/file/183200/defra-stats-foodfarm-landuselivestock-farmingstats-june-statsrelease-june12finaluk-121220.pdf) (Accessed: 24/07/2013).
- Dexter, A.R. (1991) 'Amelioration of soil by natural processes', *Soil and Tillage Research*, 20(1), pp. 87-100.
- Drewry, J.J. (2006) 'Natural recovery of soil physical properties from treading damage of pastoral soils in New Zealand and Australia: A review', *Agriculture, Ecosystems & Environment*, 114(2-4), pp. 159-169.
- Drewry, J.J., Littlejohn, R.P. and Paton, R.J. (2000) 'A survey of soil physical properties on sheep and dairy farms in southern New Zealand', *New Zealand Journal of Agricultural Research*, 43(2), pp. 251-258.
- Drewry, J.J. and Paton, R.J. (2000) 'Effects of cattle treading and natural amelioration on soil physical properties and pasture under dairy farming in Southland, New Zealand', *New Zealand Journal of Agricultural Research*, 43(3), pp. 377-386.
- Dunne, T. and Black, R.D. (1970) 'An experimental investigation of runoff production in permeable soils', *Water Resources Research*, 6, pp. 478-490.
- Dunne, T. and Leopold, L.B. (1978) *Water in environmental planning*. Macmillan. W.H. Freeman & Co Ltd.

- Dunkerley, D. (2008) 'Identifying individual rain events from pluviograph records: a review with analysis of data from an Australian dryland site', *Hydrological Processes*, 22(26), pp. 5024-5036.
- EA, E.A. (2014) *Risk of Flooding from Rivers and Sea maps*. Available at: [http://watermaps.environment-agency.gov.uk/wiyby/wiyby.aspx?topic=floodmap&scale=11&ep=map&layerGroups=default&lang=\\_e&y=521121&x=359870#x=359842&y=521187&scale=11](http://watermaps.environment-agency.gov.uk/wiyby/wiyby.aspx?topic=floodmap&scale=11&ep=map&layerGroups=default&lang=_e&y=521121&x=359870#x=359842&y=521187&scale=11) (Accessed: 02/12/2014).
- Ewen, J., Geris, J., O'Donnell, G., Mayes, W. and O'Connell, E. (2010) Multiscale Experimentation, Monitoring and Analysis of Long-term Land Use Changes and Flood Risk - SC060092: Final Science Report (SC06009).
- Ewen, J., O'Donnell, G., Burton, A. and O'Connell, E. (2006) 'Errors and uncertainty in physically-based rainfall-runoff modelling of catchment change effects', *Journal of Hydrology*, 330(3-4), pp. 641-650.
- Ewen, J., O'Donnell, G., Bulygina, N., Ballard, C. and O'Connell, E. (2013) 'Towards understanding links between rural land management and the catchment flood hydrograph', *Quarterly Journal of the Royal Meteorological Society*, 139(671), pp. 350-357.
- Ewen, J. and Parkin, G. (1996) 'Validation of catchment models for predicting land-use and climate change impacts. 1. Method', *Journal of Hydrology*, 175(1-4), pp. 583-594.
- Ewen, J., Parkin, G. and O'Connell, P. (2000) 'SHETRAN: Distributed River Basin Flow and Transport Modeling System', *Journal of Hydrologic Engineering*, 5(3), pp. 250-258.
- Feyen, L., Dankers, R., Bódis, K., Salamon, P. and Barredo, J. (2012) 'Fluvial flood risk in Europe in present and future climates', *Climatic Change*, 112(1), pp. 47-62.
- Fohrer, N., Haverkamp, S., Eckhardt, K. and Frede, H.G. (2001) 'Hydrologic Response to land use changes on the catchment scale', *Physics and Chemistry of the Earth, Part B: Hydrology, Oceans and Atmosphere*, 26(7-8), pp. 577-582.
- Fraser, C.E., McIntyre, N., Jackson, B.M. and Wheeler, H.S. (2013) 'Upscaling hydrological processes and land management change impacts using a metamodeling procedure', *Water Resources Research*, 49(9), pp. 5817-5833.
- Geris, J.R.C. (2012) *Multiscale impacts of land use/management changes on flood response in the river Hodder catchment, North-West England*. PhD thesis. University of Newcastle Upon Tyne.
- Greig, S.M., Sear, D.A. and Carling, P.A. (2005) 'The impact of fine sediment accumulation on the survival of incubating salmon progeny: Implications for sediment management', *Science of The Total Environment*, 344(1-3), pp. 241-258.
- Gustard, A., Bullock, A. and Dixon, J. (1992) *Low flow estimation in the United Kingdom*. Institute of Hydrology.
- Gustard, A. and Wesselink, A.J. (1993) 'Impact of land-use change on water resources: Balquhiddy catchments', *Journal of Hydrology*, 145(3-4), pp. 389-401.

- Hall, J., Sayers, P. and Dawson, R. (2005) 'National-scale Assessment of Current and Future Flood Risk in England and Wales', *Natural Hazards*, 36(1-2), pp. 147-164.
- Hall, J. and Solomatine, D. (2008) 'A framework for uncertainty analysis in flood risk management decisions', *International Journal of River Basin Management*, 6(2), pp. 85-98.
- Hamza, M.A. and Anderson, W.K. (2005) 'Soil compaction in cropping systems: A review of the nature, causes and possible solutions', *Soil and Tillage Research*, 82(2), pp. 121-145.
- Hannaford, J. and Marsh, T.J. (2008) 'High-flow and flood trends in a network of undisturbed catchments in the UK', *International Journal of Climatology*, 28(10), pp. 1325-1338.
- Heathwaite, A.L. and Dils, R.M. (2000) 'Characterising phosphorus loss in surface and subsurface hydrological pathways', *Science of The Total Environment*, 251–252(0), pp. 523-538.
- Hewett, C.J.M., Quinn, P.F., Whitehead, P.G., Heathwaite, A.L. and Flynn, N.J. (2004) 'Towards a nutrient export risk matrix approach to managing agricultural pollution at source', *Hydrology and Earth System Science*, 8(4), pp. 834-845.
- Holden, J. and Burt, T.P. (2003) 'Runoff production in blanket peat covered catchments', *Water Resources Research*, 39(7), p. 1191.
- Holden, J., Chapman, P.J. and Labadz, J.C. (2004) 'Artificial drainage of peatlands: Hydrological and hydrochemical process and wetland restoration', *Progress in Physical Geography*, 28(1), pp. 95-123.
- Holden, J., Evans, M.G., Burt, T.P. and Horton, M. (2006) 'Impact of land drainage on peatland hydrology', *Journal of Environmental Quality*, 35(5), pp. 1764-1778.
- Holman, I.P., Hollis, J.M., Bramley, M.E. and Thompson, T.R.E. (2003) 'The contribution of soil structural degradation to catchment flooding: a preliminary investigation of the 2000 floods in England and Wales', *Hydrology and Earth System Science*, 7(5), pp. 755-766.
- Holman, I.P., Hollis, J.M. and Thompson, T.R.E. (2002) 'Impact of agricultural soil conditions on floods–Autumn 2000', R&D Project W5C (00), 4.
- Horn, R., Way, T. and Rostek, J. (2003) 'Effect of repeated tractor wheeling on stress/strain properties and consequences on physical properties in structured arable soils', *Soil and Tillage Research*, 73(1–2), pp. 101-106.
- Horton, R.E. (1933) 'The role of infiltration in the hydrologic cycle', *Transactions, American Geophysical Union*, 14, pp. 446-460.
- Houghton-Carr, H. (1999) 'Flood Estimation Handbook, Vol. 4' Restatement and application of the Flood Studies Report rainfall-runoff method. Wallingford, UK: Institute of Hydrology.



- Houlbrooke, D.J., Paton, R.J., Littlejohn, R.P. and Morton, J.D. (2011) 'Land-use intensification in New Zealand: effects on soil properties and pasture production', *Journal of Agricultural Science-London*, 149(3), p. 337.
- HR.Wallingford, Halcrow, Centre, F.H.R., Wallingford, C., Consultants, R.E.E. and University, C. (2002) *Catchment Flood Management Plans, Development of a Modelling and Decision Support Framework (MDSF)* (HR Report EX4495).
- Isodaq, T. (2015a) 'Casella tipping bucket raingauge specifications', *Casella Tipping Bucket Raingauge*. Available at: <http://www.isodaq.co.uk/log2net-solutions/rain-gauges/casella-tipping-bucket-raingauge.html> (Accessed: 12/02/2015).
- Isodaq, T. (2015b) 'Frog logger specifications', *Frog RX data logger*. Available at: <http://www.isodaq.co.uk/data-logging-systems/isodaq-loggers/frog-rx-data-logger.html> (Accessed: 12/02/2015).
- Lipiec, J. and Stpniewski, W. (1995) 'Effects of soil compaction and tillage systems on uptake and losses of nutrients', *Soil and Tillage Research*, 35(1–2), pp. 37-52.
- Jackson, B.M., Wheeler, H.S., McIntyre, N.R., Chell, J., Francis, O.J., Frogbrook, Z., Marshall, M., Reynolds, B. and Solloway, I. (2008) 'The impact of upland land management on flooding: insights from a multiscale experimental and modelling programme', *Journal of Flood Risk Management*, 1(2), pp. 71-80.
- Jakeman, A.J., Littlewood, I.G. and Whitehead, P.G. (1993) 'An assessment of the dynamic response characteristics of streamflow in the Balquhiddar catchments', *Journal of Hydrology*, 145(3–4), pp. 337-355.
- Jones, H.K., Morris, B.L., Cheney, C.S., Brewerton, L.J., Merrin, P.D., Lewis, M.A., MacDonald, A.M., Coleby, L.M., Talbot, J.C. and McKenzie, A.A. (2000) 'The physical properties of minor aquifers in England and Wales', *British Geological Survey Technical Report*, WD/00/04, Environment Agency R&D Publication 68.
- Keep, M. (2009) 'Agriculture: historical statistics', House of Commons library standard note SN/SG/3339.
- Kendon, E.J., Roberts, N.M., Fowler, H.J., Roberts, M.J., Chan, S.C. and Senior, C.A. (2014) 'Heavier summer downpours with climate change revealed by weather forecast resolution model', *Nature Climate Change*, 4, 570–576.
- Kirby, C., Newson, M.D. and Gilman, K. (1991) *Plynlimon research: the first two decades (109)*. Wallingford.
- Kjeldsen, T.R. (2007) *The revitalised FSR/FEH rainfall-runoff method. Flood Estimation Handbook Supplementary Report No. 1*. Centre for Ecology and Hydrology.
- Klemes, V. (1986) 'Operational testing of hydrological simulation models', *Hydrological Sciences Journal*, 31(1), pp. 13-24.
- Kundzewicz, Z.W. and Robson, A.J. (2004) 'Change detection in hydrological records—a review of the methodology / Revue méthodologique de la détection de changements dans les chroniques hydrologiques', *Hydrological Sciences Journal*, 49(1), pp. 7-19.

- Kurz, I., O'Reilly, C.D. and Tunney, H. (2006) 'Impact of cattle on soil physical properties and nutrient concentrations in overland flow from pasture in Ireland', *Agriculture, Ecosystems & Environment*, 113(1–4), pp. 378-390.
- Lamb, R., Beven, K. and Myrabø, S. (1998) 'Use of spatially distributed water table observations to constrain uncertainty in a rainfall–runoff model', *Advances in Water Resources*, 22(4), pp. 305-317.
- Lane, S.N. and Milledge, D.G. (2013) 'Impacts of upland open drains upon runoff generation: A numerical assessment of catchment-scale impacts', *Hydrological Processes*, 27(12), pp. 1701-1726.
- Lipiec, J. and Stpniewski, W. (1995) 'Effects of soil compaction and tillage systems on uptake and losses of nutrients', *Soil and Tillage Research*, 35(1–2), pp. 37-52.
- Lukey, B.T., Sheffield, J., Bathurst, J.C., Hiley, R.A. and Mathys, N. (2000) 'Test of the SHETRAN technology for modelling the impact of reforestation on badlands runoff and sediment yield at Draix, France', *Journal of Hydrology*, 235(1–2), pp. 44-62.
- Marsh, T.J. (2001) 'The 2000/01 floods in the UK — a brief overview', *Weather*, 56(10), pp. 343-345.
- Marshall, M.R., Ballard, C.E., Frogbrook, Z.L., Solloway, I., McIntyre, N., Reynolds, B. and Wheeler, H.S. (2014) 'The impact of rural land management changes on soil hydraulic properties and runoff processes: results from experimental plots in upland UK', *Hydrological Processes*, 28(4), pp. 2617-2629
- Marshall, M.R., Francis, O.J., Frogbrook, Z.L., Jackson, B.M., McIntyre, N., Reynolds, B., Solloway, I., Wheeler, H.S. and Chell, J. (2009) 'The impact of upland land management on flooding: results from an improved pasture hillslope', *Hydrological Processes*, 23(3), pp. 464-475.
- Mayes, W.M., Walsh, C.L., Bathurst, J.C., Kilsby, C.G., Quinn, P.F., Wilkinson, M.E., Daugherty, A.J. and O'Connell, P.E. (2006) 'Monitoring a flood event in a densely instrumented catchment, the Upper Eden, Cumbria, UK', *Water and Environment Journal*, 20(4), pp. 217-226.
- McCulloch, J.S.G. and Robinson, M. (1993) 'History of forest hydrology', *Journal of Hydrology*, 150(2–4), pp. 189-216.
- McIntyre, N. and Marshall, M. (2010) 'Identification of rural land management signals in runoff response', *Hydrological Processes*, 24(24), pp. 3521-3534.
- Mesa, O.J. and Mifflin, E.R. (1986) 'On the Relative Role of Hillslope and Network Geometry in Hydrologic Response', in Gupta, V.K., Rodríguez-Iturbe, I. and Wood, E.F. (eds.) *Scale Problems in Hydrology: Runoff Generation and Basin Response*. Dordrecht: Springer Netherlands, pp. 1-17.
- Monbiot, G. (2015a) *Do little, hide the evidence: the official neglect that caused these deadly floods.* Available at: <http://www.theguardian.com/commentisfree/2015/dec/07/hide-evidence-storm-desmond-floods-paris-talks> (Accessed: 02/01/2016).

- Monbiot, G. (2015b) *Our government's big green idea: let's subsidise natural disasters*. Available at: <http://www.theguardian.com/commentisfree/2015/feb/25/green-natural-disasters-britain-farming-damage> (Accessed: 02/01/2016).
- Monbiot, G. (2015c) *This flood was not only foretold – it was publicly subsidised*. Available at: [http://www.theguardian.com/commentisfree/2015/dec/29/deluge-farmers-flood-grouse-moor-drain-land?CMP=share\\_btn\\_tw](http://www.theguardian.com/commentisfree/2015/dec/29/deluge-farmers-flood-grouse-moor-drain-land?CMP=share_btn_tw) (Accessed: 02/01/2016).
- Moore, R. (2007) 'The PDM rainfall-runoff model', *Hydrology and Earth System Sciences Discussions*, 11(1), pp. 483-499.
- Moseley, D.G. and Ray, D. (2007) 'Forest Habitat Networks Scotland Grampian Report February 2007', *Ecology Division Forest Research*, UK.
- Mualem, Y. (1976) 'A new model for predicting the hydraulic conductivity of unsaturated porous media', *Water Resour. Res.*, 12(3), pp. 513-522.
- Nicholson, A.R. (2014) *Quantifying and simulating the impact of flood mitigation features in a small rural catchment*. Newcastle University, PhD thesis [Online]. Available at: <http://hdl.handle.net/10443/2382>.
- Nicholson, A.R., Wilkinson, M.E., O'Donnell, G.M. and Quinn, P.F. (2012) 'Runoff attenuation features: a sustainable flood mitigation strategy in the Belford catchment, UK', *Area*, 44(4), pp.463-469.
- O'Connell, P.E., Beven, K.J., Carney, J.N., Clements, R.O., Ewen, J., Fowler, H., Harris, G.L., Hollis, J., Morris, J., O'Donnell, G.M., Packman, J.C., Parkin, A., Quinn, P.F., Rose, S.C., Shepherd, M. and Tellier, S. (2004) *Review of Impacts of Rural Land Use and Management on Flood Generation, Report A: Impact Study Report*. London: DEFRA.
- O'Connell, P.E., Ewen, J., O'Donnell, G. and Quinn, P. (2007) 'Is there a link between agricultural land-use management and flooding?', *Hydrology and Earth System Sciences*, 11(1), pp. 96-107.
- Ockenden, M.C., Deasy, C., Quinton, J.N., Surridge, B. and Stoate, C. (2014) 'Keeping agricultural soil out of rivers: Evidence of sediment and nutrient accumulation within field wetlands in the UK', *Journal of Environmental Management*, 135(0), pp. 54-62.
- Odoni, N. and Lane, S. (2010) *Assessment of the impact of upstream land management measures on flood flows in Pickering Beck using Overflow*. [Online]. Available at: [http://www.forestry.gov.uk/pdf/Pickering\\_crim\\_report\\_April\\_2010.pdf/\\$FILE/Pickering\\_crim\\_report\\_April\\_2010.pdf](http://www.forestry.gov.uk/pdf/Pickering_crim_report_April_2010.pdf/$FILE/Pickering_crim_report_April_2010.pdf) (Accessed: 08/08/2013).
- Oreskes, N., Shrader-Frechette, K. and Belitz, K. (1994) 'Verification, validation, and confirmation of numerical models in the earth sciences', *Science*, 263(5147), pp. 641-646.
- Owen, G.J., Perks, M.T., Benskin, C.M.H., Wilkinson, M.E., Jonczyk, J. and Quinn, P.F. (2012) 'Monitoring agricultural diffuse pollution through a dense monitoring network in the River Eden Demonstration Test Catchment, Cumbria, UK', *Area*, 44(4), pp. 443-453.

Packman, J.C., Quinn, P.F., Hollis, J. and O'Connell, P.E. (2004) *Short term improvement to the FEH rainfall-runoff model: technical background*. (Defra R&D Project Record FD2114/PR3).

Penman, H.L. (1948) 'Natural Evaporation from Open Water, Bare Soil and Grass', *Proceedings of the Royal Society of London A: Mathematical, Physical and Engineering Sciences*, 193(1032), pp. 120-145.

Schlumbereger (2014) Mini Diver information. Available at: <http://www.swstechnology.com/groundwater-monitoring/groundwater-dataloggers/mini-diver> (Accessed: 12/02/2015).

Penning-Rowsell, E., Johnson, C. and Tunstall, S. (2006) 'Signals' from pre-crisis discourse: Lessons from UK flooding for global environmental policy change?', *Global Environmental Change*, 16(4), pp. 323-339.

Pereira, J.O., Défossez, P. and Richard, G. (2007) 'Soil susceptibility to compaction by wheeling as a function of some properties of a silty soil as affected by the tillage system', *European Journal of Soil Science*, 58(1), pp. 34-44.

Pescott, O. and Wentworth, J. (2011) *Natural flood management*. The Parliamentary Office of Science and Technology, POSTNOTE 396. [Online]. Available at: <https://www.google.co.uk/url?sa=t&rct=j&q=&esrc=s&source=web&cd=1&cad=rja&uact=8&ved=0ahUKEwi8qOzb5vrLAhVI1RoKHXJLBXsQFggcMAA&url=http%3A%2F%2Fwww.parliament.uk%2Fbriefing-papers%2FPOST-PN-396.pdf&usg=AFQjCNEMbd50JohStFs6G24FD3iuL7E75g>, (Accessed: 20/08/2012).

Pietola, L., Horn, R. and Yli-Halla, M. (2005) 'Effects of trampling by cattle on the hydraulic and mechanical properties of soil', *Soil and Tillage Research*, 82(1), pp. 99-108.

Poelmans, L., Rompaey, A.V., Ntegeka, V. and Willems, P. (2011) 'The relative impact of climate change and urban expansion on peak flows: a case study in central Belgium', *Hydrological Processes*, 25(18), pp. 2846-2858.

Poesen, J., Nachtergaele, J., Verstraeten, G. and Valentin, C. (2003) 'Gully erosion and environmental change: Importance and research needs', *Catena*, 50(2-4), pp. 91-133.

Quinn, P., O'Donnell, G., Nicholson, A., Wilkinson, M., Owen, G., Jonczyk, J., Barber, N., Hardwick, M. and Davies, G. (2013) *Potential Use of Runoff Attenuation Features in Small Rural Catchments for Flood Mitigation*. <http://research.ncl.ac.uk/proactive/belford/newcastlenfmrafreport/reportpdf/June%20NFM%20RAF%20Report.pdf>.

Rinaldo, A., Marani, A. and Rigon, R. (1991) 'Geomorphological dispersion', *Water Resources Research*, 27(4), pp. 513-525.

Roberts, N.M., Cole, S.J., Forbes, R.M., Moore, R.J. and Boswell, D. (2009) 'Use of high-resolution NWP rainfall and river flow forecasts for advance warning of the Carlisle flood, north-west England', *Meteorological Applications*, 16(1), pp. 23-34.

Robinson, M. (1985) 'Hydrological effects of moorland gripping: a re-appraisal of the Moor House research', *Journal Environmental Management*, 21(3), pp. 205-211.

- Robinson, M. (1986) 'Changes in catchment runoff following drainage and afforestation', *Journal of Hydrology*, 86(1-2), pp. 71-84.
- Robinson, M. (1990) *Impact of improved land drainage on river flows* (IH Report No. 113). Wallingford.
- Robinson, M. (1998) '30 years of forest hydrology changes at Coalburn: water balance and extreme flows', *Hydrology and Earth System Science.*, 2(2/3), pp. 233-238.
- Robinson, M. and Armstrong, A., C (1988) 'The extent of agricultural field drainage in England and Wales, 1971- 80', *Transactions - Institute of British Geographers*, 13(1), pp. 19-28.
- Robinson, M., Rodda, J.C. and Sutcliffe, J.V. (2013) 'Long-term environmental monitoring in the UK: origins and achievements of the Plynlimon catchment study', *Transactions of the Institute of British Geographers*, 38(3), pp. 451-463.
- Robinson, R.A. and Sutherland, W.J. (2002) 'Post - war changes in arable farming and biodiversity in Great Britain', *Journal of Applied Ecology*, 39(1), pp. 157-176.
- Robson, A.J., Jones, T.K., Reed, D.W. and Bayliss, A.C. (1998) 'A study of national trend and variation in UK floods', *International Journal of Climatology*, 18(2), pp. 165-182.
- Rose, S., Rosolova, Z., Lamb, R., Worrall, P., Hammond, G. and Hester, N. (2011) *Holnicote Multi-Objective Flood Management Demonstration Project: An Analysis of the Impacts of Rural Land Management Change on Flooding and Flood Risk*. [Online]. Available at: <http://ccmhub.net/wp-content/uploads/2013/01/Holnicote-Position-Paper-v9.pdf>.
- Rose, S., Worrall, P., Hammond, G., Hester, N. and Rosolova, Z. (No date) *Holnicote Multi-Objective Flood Demonstration Project*. Available at: <http://www.crew.ac.uk/sites/www.crew.ac.uk/files/documents/Steve%20Rose%20-%20JBA.pdf> (Accessed: 01/12/2015).
- Rose, S., Worrall, P., Rosolova, Z. and Hammond, G. (2010) EGU General Assembly Conference Abstracts.
- Sansom, A.L. (1999) 'Upland vegetation management: The impacts of overstocking', *Water Science and Technology*, 39(12), pp. 85-92.
- Seibert, J. and McDonnell, J.J. (2002) 'On the dialog between experimentalist and modeler in catchment hydrology: Use of soft data for multicriteria model calibration', *Water Resources Research*, 38(11), pp. 23-1-23-14.
- Soilscapes (2015) *Soilscapes - soil types viewer - Cranfield University*. Available at: <http://www.landis.org.uk/soilscapes/> (Accessed: 02/03/2015).
- Z., Solloway, I., Francis, O. and Chell, J. (2008) 'Impacts of upland land management on flood risk: Multi-scale modelling methodology and results from the Pontbren experiment'.

Sweeney, J.C. and O'Hare, G.P. (1992) 'Geographical Variations in Precipitation Yields and Circulation Types in Britain and Ireland', *Transactions of the Institute of British Geographers*, 17(4), pp. 448-463.

Teledyne (2013) *StreamPro ADCP*. Available at: <http://www.rdinstruments.com/streampro.aspx> (Accessed: 21/04/2015).

Thomas, H. and Nisbet, T.R. (2007) 'An assessment of the impact of floodplain woodland on flood flows', *Water and Environment Journal*, 21(2), pp. 114-126.

Tunstall, S.M., Johnson, C.L. and Penning-Rowsell, E.C. (2004) *World Congress on Natural Disaster Mitigation*, New Delhi.

USDA (1986) '*Urban Hydrology for Small Watersheds*', United States Department of Agriculture, (TR55), pp. 1-164.

Valeport (2011) *MODEL 801 Electromagnetic Flow Meter - Data sheet*. Available at: [http://www.valeport.co.uk/Portals/0/Docs/Datasheets/Valeport\\_Model801\\_v2a.pdf](http://www.valeport.co.uk/Portals/0/Docs/Datasheets/Valeport_Model801_v2a.pdf).

Van Genuchten, M.T. (1980) 'A closed-form equation for predicting the hydraulic conductivity of unsaturated soils', *Soil science society of America journal*, 44(5), pp. 892-898.

Vázquez, R.F., Beven, K. and Feyen, J. (2008) 'GLUE Based Assessment on the Overall Predictions of a MIKE SHE Application', *Water Resources Management*, 23(7), pp. 1325-1349.

Vázquez, R.F., Feyen, L., Feyen, J. and Refsgaard, J.C. (2002) 'Effect of grid size on effective parameters and model performance of the MIKE-SHE code', *Hydrological Processes*, 16(2), pp. 355-372.

Verstraeten, G. and Poesen, J. (1999) 'The nature of small-scale flooding, muddy floods and retention pond sedimentation in central Belgium', *Geomorphology*, 29(3-4), pp. 275-292.

Walling, D.E. (1999) 'Linking land use, erosion and sediment yields in river basins', *Hydrobiologia*, 410(0), pp. 223-240.

Whalley, W.R., Dumitru, E. and Dexter, A.R. (1995) 'Biological effects of soil compaction', *Soil and Tillage Research*, 35(1-2), pp. 53-68.

Wheater, H., Reynolds, B., McIntyre, N., Marshall, M., Jackson, B., Frogbrook, Z., Solloway, I., Francis, O. and Chell, J. (2008) '*Impacts of upland land management on flood risk: Multi-scale modeling methodology and results from the Pontbren experiment*'. Available at: [https://web.sbe.hw.ac.uk/frmrc/downloads/ur16\\_impacts\\_upland\\_land\\_management\\_wp2\\_2\\_v1\\_0.pdf](https://web.sbe.hw.ac.uk/frmrc/downloads/ur16_impacts_upland_land_management_wp2_2_v1_0.pdf)

Wheater, H.S., Ballard, C., Bulygina, N., McIntyre, N. and Jackson, B.M., 2012. Modelling environmental change: quantification of impacts of land use and land management change on UK flood risk. In *System Identification, Environmental Modelling, and Control System Design* (pp. 449-481). Springer London.

Wilkinson, M.E., Mackay, E., Quinn, P.F., Stutter, M., Beven, K.J., MacLeod, C.J.A., Macklin, M.G., Elkhatab, Y., Percy, B., Vitolo, C. and Haygarth, P.M. (2015) 'A cloud based tool for knowledge exchange on local scale flood risk', *Journal of Environmental Management*, 161, pp. 38-50.

Wilkinson, M.E. and Quinn, P.F. (2010). *Runoff management: Mitigation measures for disconnecting flow pathways in the Belford Burn catchment to reduce flood risk*. Proceedings of the SAC and SEPA Biennial Conference.

Wilkinson, M.E., Quinn, P.F. and Hewett, C.J.M. (2013) 'The Floods and Agriculture Risk Matrix: a decision support tool for effectively communicating flood risk from farmed landscapes', *International Journal of River Basin Management*, pp. 1-16.

Wilkinson, M.E., Quinn, P.F. and Welton, P. (2010) 'Runoff management during the September 2008 floods in the Belford catchment, Northumberland', *Journal of Flood Risk Management*, 3(4), pp. 285-295.

Wolff, C.G. and Burges, S.J. (1994) 'An analysis of the influence of river channel properties on flood frequency', *Journal of Hydrology*, 153(1), pp. 317-337.

## **Appendix a – Published journal papers**

Owen, G.J., Perks, M.T., Benskin, C.M.H., Wilkinson, M.E., Jonczyk, J. and Quinn, P.F. (2012) 'Monitoring agricultural diffuse pollution through a dense monitoring network in the River Eden Demonstration Test Catchment, Cumbria, UK', *Area*, 44(4), pp. 443-453.

Perks, M.T., Owen, G.J., Benskin, C.M.H., Jonczyk, J., Deasy, C., Burke, S., Reaney, S.M. and Haygarth, P.M. (2015) 'Dominant mechanisms for the delivery of fine sediment and phosphorus to fluvial networks draining grassland dominated headwater catchments', *Science of The Total Environment*, 523, pp. 178-190.

Snell, M., Barker, P., Surridge, B., Large, A., Haygarth, P., Jonczyk, J., Reaney, S., Benskin, C., Perks, M., Owen, G., Cleasby, W., Deasey, C. and Burke, S. (2014) 'The role of 'real time ecology' in understanding the nutrient and community dynamics of headwater streams', *Environmental Science: Processes & Impacts*, 16, 1629-1636.

Adams, R., Quinn, P.F., Perks, M., Barber, N.J., Jonczyk, J. and Owen, G.J. (2016) 'Simulating high frequency water quality monitoring data using a catchment runoff attenuation flux tool (CRAFT)', *Science of The Total Environment*, <http://dx.doi.org/10.1016/j.scitotenv.2016.01.045>.



# Monitoring agricultural diffuse pollution through a dense monitoring network in the River Eden Demonstration Test Catchment, Cumbria, UK

G J Owen\*, M T Perks\*\*, C McW H Benskin†, M E Wilkinson\*, J Jonczyk\* and P F Quinn\*

\*School of Civil Engineering and Geosciences, Newcastle University, Newcastle NE1 7RU

\*\*Department of Geography, Durham University, Durham DH1 3LE

†Lancaster Environment Centre, Lancaster University, Lancaster LA1 4YQ

Email: g.j.owen@newcastle.ac.uk

Revised manuscript received 20 April 2012

*The water quality of our rivers and lakes is a reflection of the landscape over and through which it travels. The UK government, along with all European Union member states, are obliged under the Water Framework Directive (WFD) to aim for good ecological status of fresh water bodies by 2015. In order to evaluate the effectiveness of potential mitigation measures in reducing diffuse water pollution from agriculture at the catchment scale, the Demonstration Test Catchment (DTC) project was developed. The project is jointly funded by Defra, the Environment Agency (EA) and the Welsh Assembly Government (WAG). There are three DTCs across the country: the Eden catchment, Cumbria; the Wensum catchment, Norfolk and the Hampshire Avon catchment. The Eden DTC has established three ~10 km<sup>2</sup> focus catchments, chosen to reflect different farming practices, geologies, elevations and hydrological characteristics. Within each focus catchment, two sub-catchments have been selected, one control and one mitigated, in which numerous existing and novel mitigation measures will be tested. It is hoped that the mitigation features will be multi-purpose, having positive effects on pollutant retention, flooding, carbon sequestration, habitat creation and biodiversity. The effectiveness of these measures is assessed through networks of hydro-meteorological and water-quality instrumentation, most of which will provide data in near real time, with sub-hourly time steps.*

**Key words:** River Eden, diffuse pollution, hydrological monitoring, water quality

## Introduction

Agricultural activity is a major source of nitrogen (N), phosphorous (P), fine sediment and organic wastes in watercourses throughout the UK. In rural areas, the majority of N and P transfer occurs as a result of mobilisation of N- and P-based fertilisers and manure. Although current application rates are lower than during the previous century, rates remain high, averaging 128 kg ha a<sup>-1</sup> and 36 kg ha a<sup>-1</sup>, respectively (Petry *et al.* 2002). It has also been observed that significant contributions of fine sediment (<2 mm) in rivers may be derived from agricultural land, such as topsoil from pasture, cultivated land and land drains (Walling and Woodward 1992; Foster *et al.* 2002; Walling *et al.* 2006). The quality of the mobilised sediment

is also of paramount importance, given that agricultural pollutants and contaminants may be readily adsorbed to its surface and transferred through the river system (Barling and Moore 1994; Nguyen and Sukias 2002).

Many rivers across the UK are showing evidence of increasingly high concentrations of nutrients and fine suspended sediment, often exceeding the established guidelines on nutrient status and sediment quality (Owens *et al.* 2005). These elevated concentrations must be reduced in order to meet the requirements of the European Union Water Framework Directive (WFD, Directive 2000/60/EC). In some cases, reductions may need to be as much as 50–80% by 2015 if good chemical status is to be achieved (Defra 2004). However, these demands are contradicted by the requirement of increasing farming intensity due to

demand for food security in the coming years, which may cause an increase in the application of fertilisers as well as manure from livestock (Tilman et al. 2002). Future climate change may also exacerbate water quality problems (IPCC 2007).

The Demonstration Test Catchments (DTC) programme aims to achieve a better understanding of the way in which farming activity affects the quality of the aquatic environment. The DTC is a research initiative jointly funded by the Department for Environment, Food and Rural Affairs (Defra), the Environment Agency (EA) and the Welsh Assembly Government (WAG). The scope of the project is to gather evidence to test the hypothesis proposed by Defra that

It is possible to cost-effectively reduce the impact of agricultural diffuse water pollution on ecological function, while maintaining food security through the implementation of multiple on-farm mitigation measures. (Demonstrating Catchment Management 2012)

There are three national DTCs across England: the Wensum (Norfolk; Wensum 2011), the Avon (Hampshire; Avon 2011) and the Eden (Cumbria; Eden 2011). The catchments were selected because of their variable geographical, geological, climatic and land use features (Figure 1). This paper focuses on the ways in which the Eden DTC is testing this hypothesis.

### Study area

The area drained by the River Eden contains a wide variety of landscapes, land uses and farming types. It covers an area of 2288 km<sup>2</sup>, draining the uplands of the Pennines and Lake District into the Irish Sea, via the Solway Firth. Annual rainfall totals range from less than 650 mm in the lowland valley to more than 2000 mm in the uplands (Mayes et al. 2006). The Eden catchment has previously been studied through the Catchment Hydrology and Sustainable Management (CHASM) project (O’Connell et al. 2007). In this project, parts of the catchment were densely monitored with rain-gauges and water-level gauges, many of which are still in operation. CHASM and numerous other localised studies provide a strong insight into the hydrological characteristics to be expected.

### Experimental design

The approach taken by the Eden DTC has been to establish three ~10 km<sup>2</sup> focus catchments at Pow, Dacre and Morland, chosen to reflect the different farming practices and geologies observed across the Eden (Figure 1). There is a fourth demonstration catchment, which has a contributing area of 1 km<sup>2</sup> and is located at Sewborwens Farm, at the Newton Rigg campus of Askham Bryan College, Penrith. This catchment has been instrumented

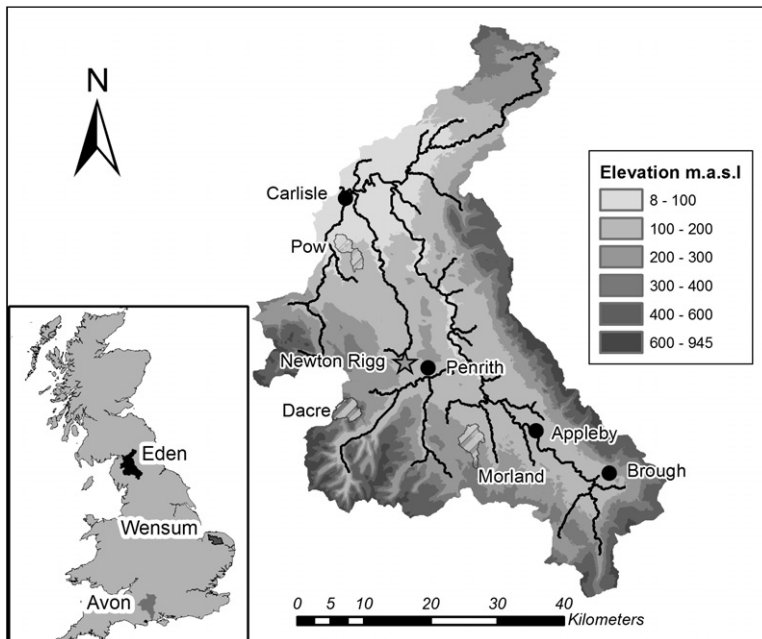


**Figure 1** Location of the DTC research areas and the location of the Pow, Dacre and Morland focus catchments within the Eden DTC catchment

Source: © Crown Copyright/database rights 2011. An Ordnance Survey/EDINA supplied service

to demonstrate the types of data that are freely available to stakeholders and other interested parties.

In the west of the Eden catchment, less than 5 km from Ullswater, lies the Dacre catchment, which was selected to represent the uplands, and is the only upland-dominated catchment represented across all three national DTCs (Figure 1). This is a hardrock catchment dominated by the volcanic andesite sheets of the Borrowdale Volcanic Group (Allen *et al.* 2010). The main farming land types are improved grassland (41%), which is grazed by both sheep and cattle, and unimproved grassland/rough grazing (46%), which is predominantly grazed by sheep. Key diffuse pollution pressures in this catchment have been identified as fine sediment and phosphorus.

The Pow catchment, located approximately 4 km south of Carlisle, is underlain by complex geology consisting of sandstone, siltstone and mudstone bedrock units. It is the most intensively farmed of the three catchments with a patchwork of intensive dairy, beef, sheep, pig and poultry farming, in a landscape made up of 71 per cent improved grassland, 14 per cent arable land and just 4 per cent rough grazing. The catchment also contains a waste recycling facility and landfill site. It is hypothesised that the key diffuse pollution elements are fine sediment, nitrates and phosphorus, making this catchment one of the most polluted water courses in the Eden, where the water quality is defined as poor.

The Morland catchment contains a large proportion of improved grassland (83%), with just 10 per cent rough grazing and 3 per cent arable land. The predominant farming types encompass a mixture of dairy and meat production, and the dominant pollution pressure is from

sediment and phosphorus. Over 99 per cent of the catchment area is underlain by carboniferous limestone, shales and sandstones. This means there is likely to be a significant groundwater component to the diffuse pollution issue. Data have been collected through borehole exploration and geophysical studies to better understand the intricacies of the groundwater movement.

Within each of the 10 km<sup>2</sup> focus catchments, two sub-catchments have been selected – one control and one mitigated – in which a number of existing and novel mitigation measures will be tested. This catchment instrumentation is illustrated in Figure 2.

The mitigated catchments are to have waste management plans produced to mitigate against diffuse water pollution from agriculture (DWPA) at all stages within the farming landscape. An example of an adopted waste management strategy is the collection and storage of dirty water in runoff attenuation features (RAFs; cf. Barber and Quinn forthcoming). These features provide an area of deposition where pollutants such as fine sediment and phosphorus may be stored. A specific example of RAFs is the Mitigation Options for Phosphorus and Sediment (MOPS) ponds (Deasy *et al.* 2009), which collect and filter overland flow. The sediments and associated nutrients can then be recycled back to the land by the farmer. These types of features are dual purpose, with benefits for both mitigating diffuse pollution and reducing flood risk. By disrupting and attenuating the overland flow, the time taken for the water to reach the channel is increased, potentially reducing the flood peak (Wilkinson *et al.* 2010). Positive impacts should also include carbon sequestration, habitat creation and improved biodiversity (Wilkinson and Quinn 2010).

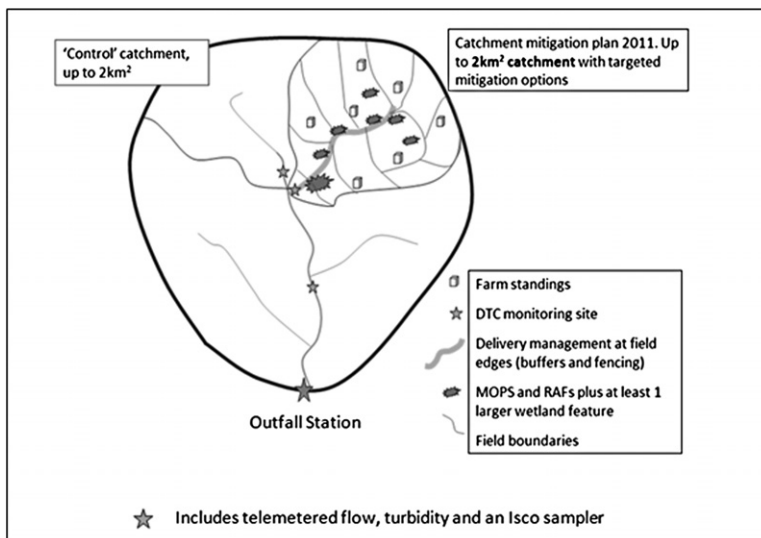


Figure 2 Schematic of the experimental design

## Hydro-meteorological monitoring

Each catchment has been installed with an Automatic Weather Station (AWS), which logs rainfall, air temperature, radiation, wind speed and wind direction every 15 minutes. Two additional 0.2-mm tipping bucket rain-gauges log on an event basis. Additional EA and Met Office rain-gauges and weather stations are present within the focus catchments, which complement the dense monitoring network. Using the data collected, the calculation of evapo-transpirational losses is possible (Penman 1948), which is particularly important for calculating water balances, and will be used in catchment rainfall runoff models. Each water-quality monitoring station is equipped with a pressure transducer to record the water level. The water-level series is then converted into a flow hydrograph through the establishment of a rating curve based on spot measurements of flow. Flow, velocity and water level are also continuously monitored at the outfall stations using Sontek Argonaut-SW Doppler instruments. Level and velocity are measured to within  $\pm 0.03$  cm and  $\pm 0.5$  cm s<sup>-1</sup> respectively.

## Water quality monitoring

Each of the focus catchments has an outfall station, of which there are two types. The Dacre focus catchment is equipped with a YSI 6600 V2 sonde, enabling the simultaneous measurement of conductivity (0–100 mS cm<sup>-1</sup>  $\pm$  0.5%), temperature ( $-5$  to  $+50^\circ\text{C}$   $\pm$  0.15°C), pH (0–14 units  $\pm$  0.2 units), dissolved oxygen (0–500%  $\pm$  2%), turbidity (0–1000 nephelometric turbidity units (NTU)  $\pm$  2%) and chlorophyll-a (0–400  $\mu\text{g L}^{-1}$ ). The YSI optical probes are equipped with self-cleaning sensors in order to minimise bio-fouling, which is further reduced by housing the sonde in a flow-through cell.

The Pow and Morland outfall stations have the same model YSI sonde as described above, and are in addition equipped with an ammonium (NH<sub>4</sub>) and nitrate (NO<sub>3</sub>) probe, and wet chemistry analysers that test for soluble reactive phosphorus (SRP) and total phosphorus (TP) content. The ammonium sensor uses an ion-selective electrode with automatic potassium compensation to detect ammonium ions (NH<sub>4</sub><sup>+</sup>) directly as ammonium nitrogen and has an operating range of 0.2–1000 mg L<sup>-1</sup> ( $\pm$ 5%) (NH<sub>4</sub>-N; Hach Lange 2011a). The nitrate measurements are collected by a Hach Lange Nitratex SC 1000 sensor. This probe provides an immediate measurement of nitrate (NO<sub>3</sub>-N) in water, which is turbidity compensated through reference measurement, and has an operating range of 0.1–100 mg L<sup>-1</sup> ( $\pm$ 3%; Hach Lange 2011b). The operating range for both TP and SRP (measured as PO<sub>4</sub>-P) is 0.01–5.0 mg L<sup>-1</sup> (Hach Lange 2011c), and analysis is based on the DIN-equivalent molybdenum blue method.

At the 2–5 km<sup>2</sup> scale in each focus catchment there are two or three sub-stations, which provide a continuous record of turbidity and water level. Turbidity is a measure of the decrease in the transparency of a solution due to the presence of sediment particles, coloured organic matter and the water itself, which causes incident light to be scattered, reflected and attenuated (Ziegler 2002). The McVan Analite 390 series probes used measure the degree of scattering at an angle of 90° to the incident light beam, operating in the range of 0–1000 NTUs, with  $\pm$ 1% precision.

Turbidity is the most widely used surrogate for measuring suspended sediment concentrations (SSCs; Gray and Gartner 2009; Pruitt 2002). Relationships between turbidity and SSC are established through spot samples and storm event sampling, whereby lab results of SSC are cross referenced with the turbidity reading taken *in situ* (Minella et al. 2007; Pavanelli and Bigi 2005; Teixeira and Caliarì 2005). Turbidity has also been demonstrated to be a predictor of TP content (Nairn and Mitsch 1999), especially in environments where the most significant P losses are in particulate form (Haygarth et al. 2000). These stations may therefore have the dual benefit of quantifying both the fine suspended sediment and TP flux (Jones et al. 2011).

All data are collected and stored using state of the art hydro-meteorological logging systems. Most parameters are collected at a frequency of 15 minutes, providing more detailed information than traditional spot-sampling and/or storm-event based sampling regimes. This is imperative given that spot sampling can lead to underestimation of up to 60% for annual P loads, when compared with hourly or sub-hourly time series (Cassidy and Jordan 2011). Infrequent sampling may fail to capture temporal variability in constituent export behaviour, resulting in poor precision of load estimates (Johnes 2007). Only near continuous monitoring can capture rapid temporal changes in constituent concentrations (Cassidy and Jordan 2011).

## Communication technology

The data collected from the Eden DTC are open access: near real-time data are freely available on the internet from the majority of the stations at [www.edendtc.org.uk](http://www.edendtc.org.uk). GPRS mobile phone technologies have been adopted as the means for telemetry. This allows for near real-time connection to the instruments, and also provides the capability for setting alarms on sensors. For example, a rain-gauge can alert interested users (via text message or e-mail) when a certain rain intensity threshold has been crossed. The ISCO automatic water samplers can also be triggered remotely using these technologies, providing flexibility in sampling campaigns. It is, however, important to note that these are raw data with a time delay

before the quality-assured data are realised. The live data on the Eden DTC website allows stakeholders to engage interactively with the project. For example, the farming community has shown great interest in the near live rainfall data from across the catchment.

### Example of monitoring outputs

This section demonstrates some of the early data from a range of instruments installed in the Morland focus catchment and highlights its potential applications. The spatial distribution of the instrumentation in this catchment is demonstrated in Figure 3.

The YSI sonde installed at the 10 km<sup>2</sup> outfall station produces raw data in the format shown in Figure 4. This time series spans 10 days from 6 to 16 October. Two storm events were observed on 9 and 12 October, which led to the simultaneous rise in TP, SRP, NO<sub>3</sub>, NH<sub>4</sub> (Figure 4b), turbidity and chlorophyll (Figure 4c), with a drop in conductivity and pH (Figure 4d).

Nested within the Morland 10 km<sup>2</sup> catchment are the control and mitigation catchments, which have contributing areas of 3.63 km<sup>2</sup> and 1.55 km<sup>2</sup> respectively. Figure 5 presents the rainfall, water level and turbidity measurements during an event between 17 and 18 October 2011 measured in the mitigation catchment. There is a clear

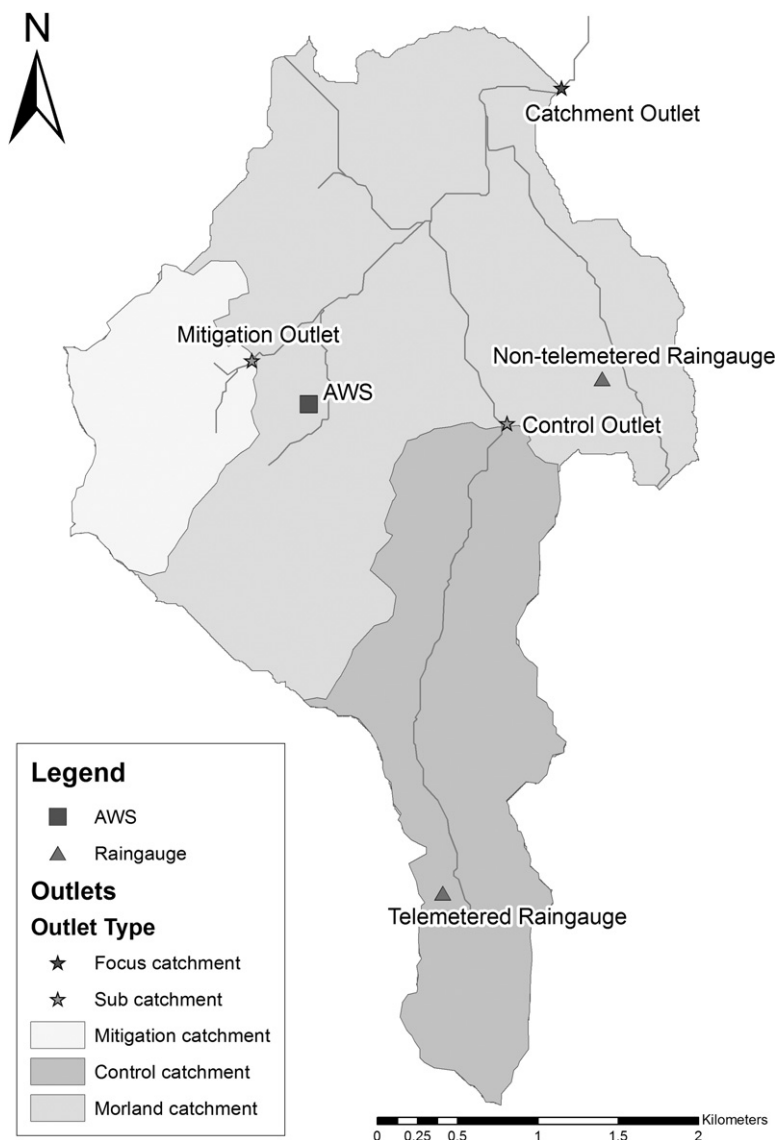


Figure 3 Diagram providing detail of the catchment layout and locations of instrumentation in the Morland catchment

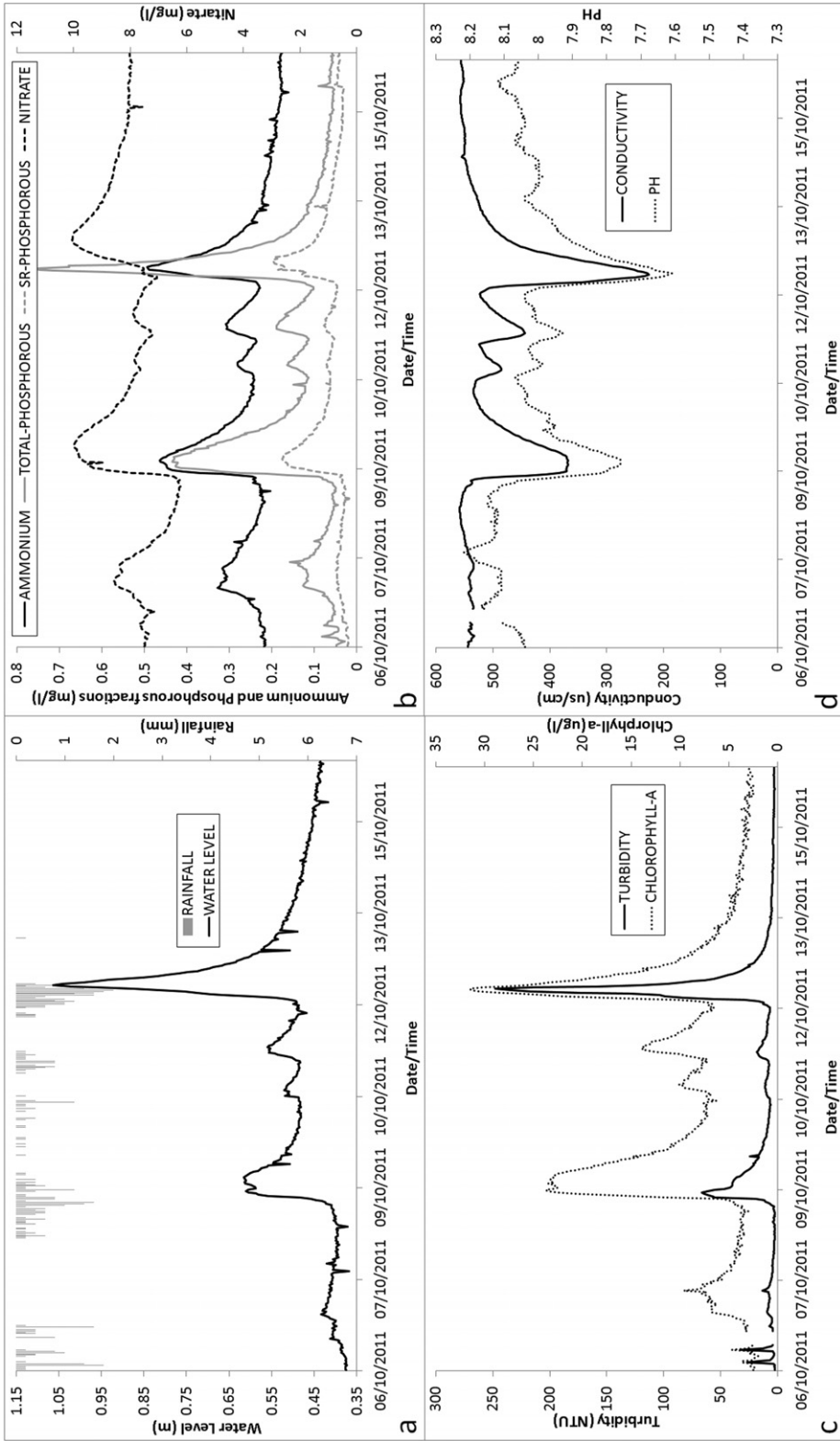


Figure 4 Example data collected over a 10-day period at the Morland outfall station, describing (a) rainfall and water-level response; (b) ammonium, total phosphorous, soluble reactive phosphorous and nitrate response; (c) turbidity and chlorophyll-a response and (d) conductivity and pH response

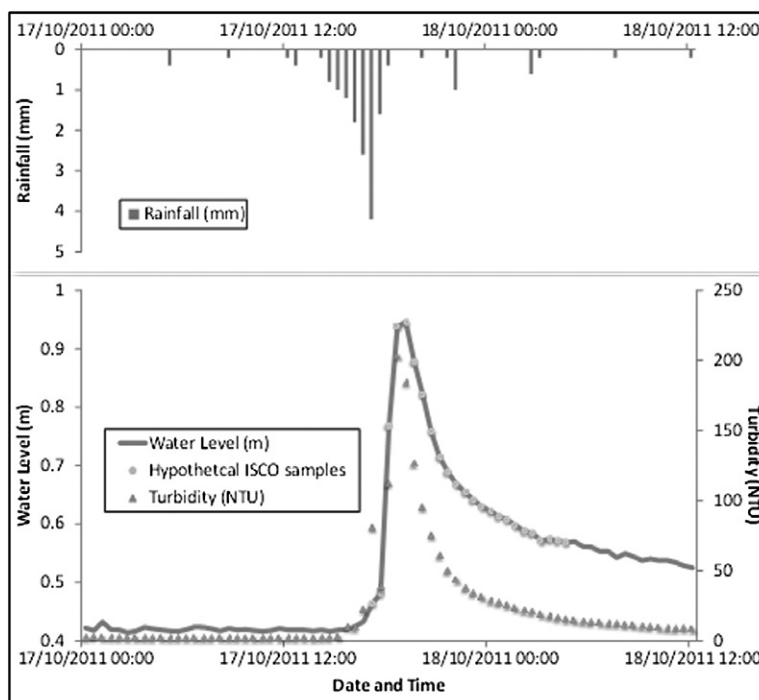


Figure 5 Half-hourly rainfall data from the Morland AWS plotted against the water level measured at the Morland outfall station, along with points representing a hypothetical ISCO sampling regime based on a trigger level of 0.45 m and sampling interval of 30 minutes

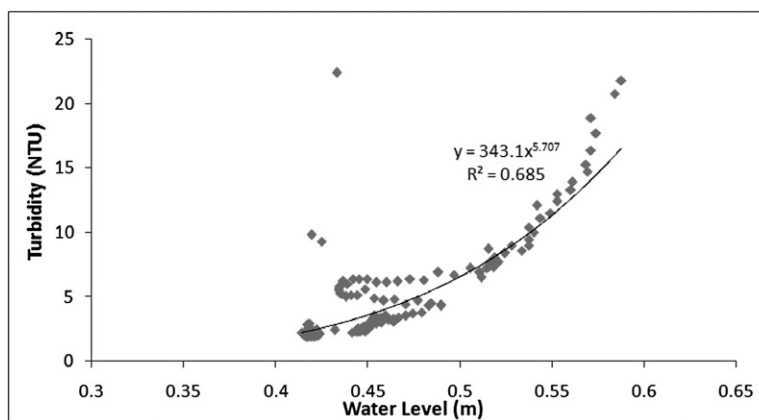


Figure 6 Relationship between water level (m) and turbidity (NTU) during an event on 16–17 October 2011 in the Morland mitigation catchment

response in the observed water level to rainfall inputs, with a lag time of 120 minutes between peak precipitation intensity and peak flow. There is also an advanced response of 30 minutes in turbidity in relation to the maximum flow, resulting in clockwise hysteresis (Williams 1989).

Using the data presented in Figure 5, regression analysis between the two series can be carried out to describe the relationship mathematically, as a power function

(Figure 6). Although these are raw data which are yet to undergo quality control, there is relatively strong correlation between increasing water level and increasing turbidity.

During this event, the effects of the storm are transmitted downstream and measured at the Morland outfall station. This is demonstrated by the time-series of turbidity data in Figure 7. There is a clear increase in turbidity, the

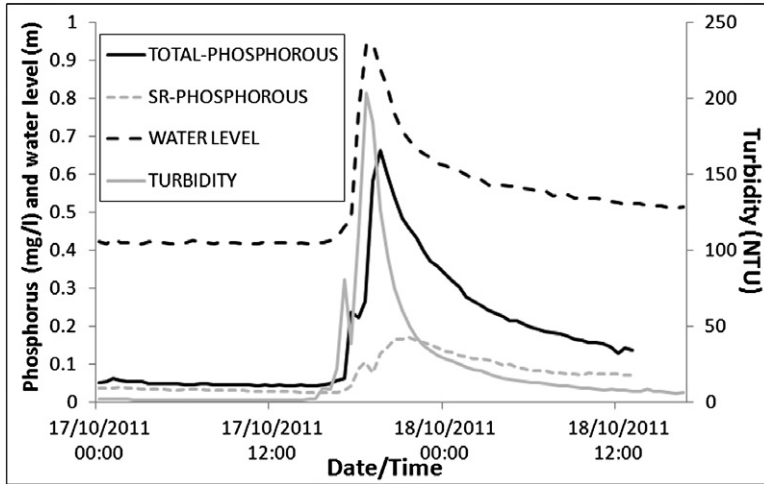


Figure 7 Observed turbidity and phosphorous response during a storm event captured at the Morland outfall station between 17 and 18 October 2011

maximum of which precedes the maximum river level by 30 minutes, which is comparable to that documented in the mitigation catchment. TP and SRP concentrations are also elevated during this storm, peaking at  $0.67 \text{ mg L}^{-1}$  and  $0.17 \text{ mg L}^{-1}$  respectively, compared with the pre-event concentrations of  $0.06 \text{ mg L}^{-1}$  and  $0.04 \text{ mg L}^{-1}$ . A decline in the TP concentration occurs following reductions in turbidity; this can be attributed to a drop in particulate P, which is mobilised with sediments (Gburek *et al.* 2005). The SRP peak occurs after both turbidity and TP, due to the pathway/transport mechanism being slower, as it is leaching from the soil in solution (Gburek *et al.* 2005).

Empirical relationships between river flow, turbidity and a range of determinants (e.g. SSC and TP) will be developed at the outfall and sub-stations through sampling campaigns using the ISCO automatic water samplers. The Eden DTC samplers are triggered once a predefined water-level threshold has been crossed, and samples are delivered within 24 hours of the end of the event to EA Laboratories for analysis. A total of 17 parameters are analysed, including SSC, SRP, TP, metals and boron, the latter being an indicator of leaking or overflowing septic tanks, which requires separate mitigation. The empirical relationship can then be applied to the full time series, which in turn can be used to estimate annual loadings. By collecting turbidity data at each site, it will be possible to quantify the changes to SS and TP loadings within the stream, across scales.

As the project progresses and sufficient data accumulate, it will become possible to establish further relationships and strengthen those that are illustrated here. Figure 8 illustrates some of these additional relationships and data types.

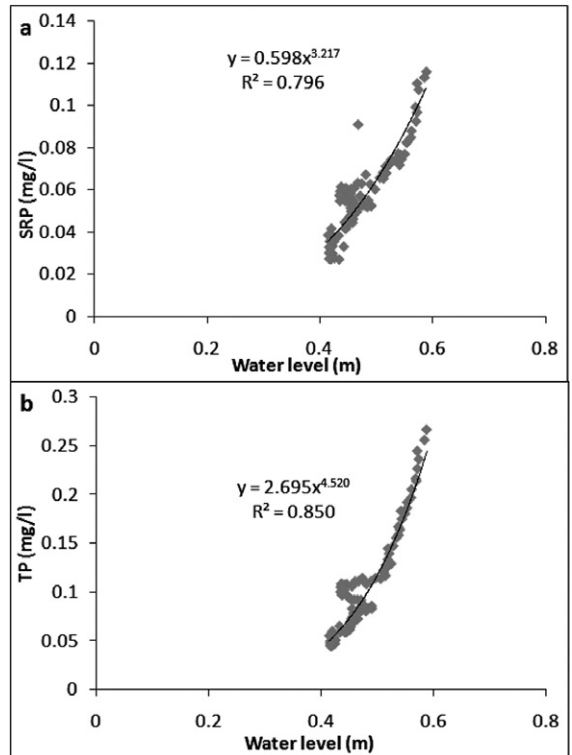


Figure 8 Example analysis demonstrating (a) the relationship between river level and soluble reactive phosphorous and (b) river level and total phosphorous



## Further monitoring

ISCO samplers are also to be used to bracket mitigation features, e.g. there will be one upstream and one downstream of any mitigation feature. Both will be triggered from a simple float switch that will initiate the sampling, making it straightforward to quantify the direct effect of the mitigation feature on the various parameters, but most importantly SS and TP. This type of sampling was used in the RAFs and MOPS research projects (Barber and Quinn this issue).

Time Integrated Mass-flux samplers (TIMs), designed by Phillips *et al.* (2000), are distributed throughout the river networks of the research catchment. The TIMs are subject to the full range of flow conditions and sediment fluxes over the sampling period, providing a continuous record of fine sediment flux that may be representative of all events (Walling 2005). The fine suspended samples obtained from this device may be used for sediment fingerprinting (e.g. Fox and Papanicolaou 2007; Collins *et al.* 2010; Fukuyama *et al.* 2010; Martínez-Carreras *et al.* 2010) and estimating the relative suspended sediment yield of the river (e.g. Bolland *et al.* 2010).

In addition to the water-quality sampling stations, different types of camera have been deployed. Cameras located at the catchment outlets provide qualitative information on flow dynamics as well as the river level and water colour. These outlet cameras take an image every 10 minutes and post it to an ftp site via a GPRS mobile phone SIM card. Motion sensor cameras are to be used at strategic locations to capture in-stream activity of livestock, in order to assess their impact on turbidity levels in the water course.

An Unmanned Aerial Vehicle (UAV) is also being used for capturing land cover change, management practices and other seasonal activity that may affect mobilisation of pollutants. This is being done by regularly flying the same routes within the catchment and monitoring any changes.

## Conclusions

The aim of this research is to produce an abundance of high-quality, multi-scale continuous data provided in near real time, which is readily accessible to the public. Initial measurements have produced high-quality, high-frequency data that have the potential for developing more accurate assessments of nutrient loadings than traditional monitoring schemes. The project faces a number of potential challenges related to the size, scale and potential implications of the project. The wealth of information being gathered at a number of different scales will enhance knowledge and improve the effectiveness and efficiency of waste management and mitigation methods. Most importantly, concepts can be tested, models can be made more robust and ultimately policy will be better informed.

## Acknowledgements

The authors would like to acknowledge Defra (especially Dan McGonigle, project lead), the Environment Agency and the Welsh Assembly Government for commissioning the DTC programme and the rest of the Eden DTC consortia (led by Phil Haygarth, Lancaster University). We would like to thank the reviewers for their helpful and constructive comments.

## References

- Allen D J, Newell A J and Butcher A S 2010 *Preliminary review of the geology and hydrogeology of the Eden DTC sub-catchments* British Geological Survey, Keyworth
- Avon D T C 2011 Homepage (<http://www.avondtc.org.uk>) Accessed 1 November 2011
- Barber N J and Quinn P F forthcoming Mitigating diffuse water pollution from agriculture using soft-engineered runoff attenuation features *Area* doi: 10.1111/j.1475-4762.2012.01118.x
- Barling R and Moore I 1994 Role of buffer strips in management of waterway pollution: a review *Environmental Management* 18 543–58
- Bolland J D, Bracken L J, Martin R and Lucas M C 2010 A protocol for stocking hatchery reared freshwater Pearl Mussel (*margaritifera margaritifera*) *Aquatic Conservation: Marine and Freshwater Ecosystems* 20 695–704
- Cassidy R and Jordan P 2011 Limitations of instantaneous water quality sampling in surface water catchments: comparison with near-continuous phosphorus time-series data *Journal of Hydrology* 405 182–93
- Collins A L, Walling D E, Stroud R W, Robson M and Peet L M 2010 Assessing damaged road verges as a suspended sediment source in the Hampshire Avon catchment, southern United Kingdom *Hydrological Processes* 24 1106–22
- Deasy C, Quinton J N, Silgram M, Bailey A P, Jackson B and Stevens C J 2009 Mitigation options for sediment phosphorus loss from winter-sown arable crops *Journal of Environmental Quality* 38 2121–30
- Defra 2004 Impacts of CAP reform agreement on diffuse water pollution from agriculture – executive summary Reference GRP-P-175 (<http://archive.defra.gov.uk/foodfarm/landmanage/water/csf/documents/gfa-race-execsumm.pdf>) Accessed 21 October 2011
- Demonstrating Catchment Management 2012 Homepage (<http://www.demonstratingcatchmentmanagement.net>) Accessed 21 May 2012
- Eden D T C 2011 Homepage (<http://www.edendtc.org.uk>) Accessed 21 October 2011
- Foster I D L, Lees J A, Jones A R, Chapman A S and Turner S E 2002 The possible role of agricultural land drains in sediment delivery to a small reservoir, Worcestershire, UK: a multiparameter fingerprint study in Dyer F J, Thoms M C and Olley J M eds *The structure, function and management implications of fluvial sedimentary systems* (Proceedings of an international symposium held at Alice Springs, Australia, September 2002) IAHS publication 276
- Fox J F and Papanicolaou A N 2007 The use of carbon and nitrogen isotopes to study watershed erosion processes *Journal of the American Water Resources Association* 43 1047–64

- Fukuyama T, Onda Y, Gomi T, Yamamoto K, Kondo N, Miyata S, Kosugi K I, Mizugaki S and Tsubonuma N** 2010 Quantifying the impact of forest management practice on the runoff of the surface-derived suspended sediment using fallout radionuclides *Hydrological Processes* 24 596–607
- Gburek W J, Barberis W J, Haygarth P M, Kronvang B and Stamm C** 2005 Phosphorus mobility in the landscape in **Sims J T and Sharpley A N** eds *Phosphorus: agriculture and the environment* American Society of Agronomy, Madison WI 941–79
- Gray J R and Gartner J W** 2009 Technological advances in suspended-sediment surrogate monitoring *Water Resource Research* 45 W00D29 doi: 10.1029/2008WR007063
- Hach Lange** 2011a Ammonium sensor page (<http://www.hach.com/asset-get.download-en.jsa?id=7639982041>) Accessed 21 October 2011
- Hach Lange** 2011b Nitrate sensor page ([http://www.hach-lange.es/shop/action\\_q/download%3Bdocument/DOK\\_ID/10808/type/pdf/lkz/GB/spkz/en/TOKEN/Yfrq8B70k4CgTD-AG8RBgW2dRbk/M2ZQeOQ](http://www.hach-lange.es/shop/action_q/download%3Bdocument/DOK_ID/10808/type/pdf/lkz/GB/spkz/en/TOKEN/Yfrq8B70k4CgTD-AG8RBgW2dRbk/M2ZQeOQ)) Accessed 21 October 2011
- Hach Lange** 2011c Phosphax sigma page ([http://www.hach-lange.es/shop/action\\_q/download%3Bdocument/DOK\\_ID/6553/type/pdf/lkz/GB/spkz/en/TOKEN/zl-XhQe-y\)XUWuHBpKJWzySoibo/M/PEvDwQ/DOC023\\_52\\_03113\\_MAI02.pdf](http://www.hach-lange.es/shop/action_q/download%3Bdocument/DOK_ID/6553/type/pdf/lkz/GB/spkz/en/TOKEN/zl-XhQe-y)XUWuHBpKJWzySoibo/M/PEvDwQ/DOC023_52_03113_MAI02.pdf)) Accessed 21 October 2011
- Haygarth P M, Heathwaite A L, Jarvis S C and Harrod T R** 2000 Hydrological factors for phosphorus transfer from agricultural soils *Advances in Agronomy* 69 153–78
- IPCC** 2007 *Climate change 2007: impacts, adaptation and vulnerability* Working group II contribution to the Intergovernmental Panel on Climate Change fourth assessment report: summary for policymakers ([http://www.meteotrentino.it/clima/pdf/rapporti\\_meteo/IPCC\\_Impacts\\_Adaptation\\_and\\_Vulnerability.pdf](http://www.meteotrentino.it/clima/pdf/rapporti_meteo/IPCC_Impacts_Adaptation_and_Vulnerability.pdf)) Accessed 21 October 2011
- Johnes P J** 2007 Uncertainties in annual riverine phosphorus load estimation: impact of load estimation methodology, sampling frequency, baseflow index and catchment population density *Journal of Hydrology* 332 241–58
- Jones A S, Stevens D K, Horsburgh J S and Mesner N O** 2011 Surrogate measures for providing high frequency estimates of total suspended solids and total phosphorus concentrations *JAWRA Journal of the American Water Resources Association* 47 239–53
- Martínez-Carreras N, Krein A, Udelhoven T, Gallart F, Iffly J, Hoffmann L, Pfister L and Walling D E** 2010 A rapid spectral-reflectance-based fingerprinting approach for documenting suspended sediment sources during storm runoff events *Journal of Soils and Sediments* 10 400–13
- Mayes W M, Walsh C L, Bathurst J C, Kilsby C G, Quinn P, Wilkinson M E, Daugherty A J and O'Connell P E** 2006 Monitoring a flood event in a densely instrumented catchment, the Upper Eden, Cumbria, UK *Water and the Environment Journal: CIWEM* 20 217–26
- Minella J P G, Merten G H, Reichert J M and Clarke R T** 2007 Estimating suspended sediment concentrations from turbidity measurements and the calibration problem *Hydrological Processes* 22 1819–30
- Nairn R W and Mitsch W J** 1999 Phosphorus removal in created wetland ponds receiving river overflow *Ecological Engineering* 14 107–26
- Nguyen L and Sukias J** 2002 Phosphorus fractions and retention in drainage ditch sediments receiving surface runoff and subsurface drainage from agricultural catchments in the north island, New Zealand *Agriculture, Ecosystems and Environment* 92 49–69
- O'Connell P E, Quinn P F, Bathurst J C, Parkin G, Kilsby C, Beven K J, Burt T P, Kirkby M J, Pickering A, Robinson M, Soulsby C, Werritty A and Wilcock D** 2007 Catchment hydrology and sustainable management (CHASM): an integrating methodological framework for prediction in **Schertzer D, Hubert P, Koide S and Takeuchi K** eds *Predictions in ungauged basins: PUB kick-off* Brasilia 20–22 November 2002 IAHS publication 309
- Owens P N, Batalla R J, Collins A J, Gomez B, Hicks D M, Horowitz A J, Kondolf G M, Marden M, Page M J, Peacock D H, Petticrew E L, Salomons W and Trustrum N A** 2005 Fine-grained sediment in river systems: environmental significance and management issues *River Research and Applications* 21 693–717
- Pavanelli D and Bigi A** 2005 A new indirect method to estimate suspended sediment concentration in a river monitoring programme *Biosystems Engineering* 92 513–20
- Penman H L** 1948 Natural evaporation from open water, bare soil and grass *Proceedings of the Royal Society London* 193 120–45
- Petry J, Soulsby C, Malcolm I A and Youngson A F** 2002 Hydrological controls on nutrient concentrations and fluxes in agricultural catchments *Science of the Total Environment* 294 95–110
- Phillips J M, Russell M A and Walling D E** 2000 Time-integrated sampling of fluvial suspended sediment: a simple methodology for small catchments *Hydrological Processes* 14 2589–602
- Pruitt B A** 2002 Use of turbidity by state agencies *Turbidity and other sediment surrogates workshop* 30 April–2 May Reno NV
- Teixeira E C and Caliani P C** 2005 Estimation of the concentration of suspended solids in rivers from turbidity measurement: error assessment in **Walling D E and Horowitz A J** eds *Sediment budgets* IAHS publication 291 International Association of Hydrological Sciences, Wallingford 151–60
- Tilman D, Cassman K G, Matson P A, Naylor R and Polasky S** 2002 Agricultural sustainability and intensive production practices *Nature* 418 671–7
- Walling D E** 2005 Tracing suspended sediment sources in catchments and river systems *Science of the Total Environment* 344 159–84
- Walling D E and Woodward J C** 1992 Use of radiometric fingerprints to derive information on suspended sediment sources in **Bogen J, Walling D E and Day T J** eds *Erosion and sediment transport monitoring programmes in river basins (Proceedings of the Oslo Symposium, August 1992)* IAHS publication 210
- Walling D E, Collins A L, Jones P A, Leeks G J L and Old G** 2006 Establishing fine-grained sediment budgets for the Pang and Lambourn LOCAR catchments UK *Journal of Hydrology* 330 126–41
- Wensum D T C** 2011 Homepage (<http://www.wensumalliance.org.uk>) Accessed 1 November 2011
- Wilkinson M E and Quinn P F** 2010 Belford catchment proactive flood solutions: a toolkit for managing runoff in the rural land-

- scape *Proceedings of the SAC and SEPA Biennial Conference* Edinburgh
- Wilkinson M E, Quinn P F and Welton P** 2010 Runoff management during the September 2008 floods in the Belford catchment, Northumberland *Journal of Flood Risk Management* 3 285–95
- Williams G P** 1989 Sediment concentration versus water discharge during single hydrologic events in rivers *Journal of Hydrology* 111 89–106
- Ziegler A C** 2002 Issues related to the use of turbidity measurements as a surrogate for suspended sediment *Turbidity and other sediment surrogates workshop* 30 April–2 May Reno NV



# Dominant mechanisms for the delivery of fine sediment and phosphorus to fluvial networks draining grassland dominated headwater catchments



M.T. Perks<sup>a,\*</sup>, G.J. Owen<sup>b</sup>, C.McW.H. Benskin<sup>c</sup>, J. Jonczyk<sup>b</sup>, C. Deasy<sup>c,d,e</sup>, S. Burke<sup>f</sup>, S.M. Reaney<sup>d</sup>, P.M. Haygarth<sup>c</sup>

<sup>a</sup> School of Geography Politics and Sociology, Newcastle University, Newcastle upon Tyne NE1 7RU, United Kingdom

<sup>b</sup> School of Civil Engineering and Geosciences, Newcastle University, Newcastle upon Tyne NE1 7RU, United Kingdom

<sup>c</sup> Lancaster Environment Centre, Lancaster University, Lancaster LA1 4YQ, United Kingdom

<sup>d</sup> Department of Geography, Durham University, Durham DH1 3LE, United Kingdom

<sup>e</sup> Northumbrian Water Ltd., Boldon House, Wheatlands Way, Pity Me, Durham DH1 5FA, United Kingdom

<sup>f</sup> British Geological Survey, Environmental Science Centre, Nicker Hill, Keyworth, Nottingham NG12 5GG, United Kingdom

## HIGHLIGHTS

- We assess how sediment and phosphorus is transported in an agricultural catchment
- Multiple pathways are observed for particulate and soluble constituents
- Delivery is complicated by dominance & variability of erosive processes & pathways
- Large challenges faced in mitigating delivery of contaminants to headwater rivers

## ARTICLE INFO

### Article history:

Received 12 January 2015

Received in revised form 2 March 2015

Accepted 2 March 2015

Available online 10 April 2015

Editor: D. Barcelo

### Keywords:

Fluvial  
Suspended sediment  
Phosphorus  
Diffuse pollution  
Water quality  
Headwater  
Connectivity  
Grassland

## ABSTRACT

Recent advances in monitoring technology have enabled high frequency, in-situ measurements of total phosphorus and total reactive phosphorus to be undertaken with high precision, whilst turbidity can provide an excellent surrogate for suspended sediment. Despite these measurements being fundamental to understanding the mechanisms and flow paths that deliver these constituents to river networks, there is a paucity of such data for headwater agricultural catchments. The aim of this paper is to deduce the dominant mechanisms for the delivery of fine sediment and phosphorus to an upland river network in the UK through characterisation of the temporal variability of hydrological fluxes, and associated soluble and particulate concentrations for the period spanning March 2012–February 2013. An assessment of the factors producing constituent hysteresis is undertaken following factor analysis (FA) on a suite of measured environmental variables representing the fluvial and wider catchment conditions prior to, and during catchment-wide hydrological events. Analysis indicates that suspended sediment is delivered to the fluvial system predominantly via rapidly responding pathways driven by event hydrology. However, evidence of complex, figure-of-eight hysteresis is observed following periods of hydrological quiescence, highlighting the importance of preparatory processes. Sediment delivery via a slow moving, probably sub-surface pathway does occur, albeit infrequently and during low magnitude events at the catchment outlet. Phosphorus is revealed to have a distinct hysteretic response to that of suspended sediment, with sub-surface pathways dominating. However, high magnitude events were observed to exhibit threshold-like behaviour, whereby activation and connection of usually disconnected depositional zones to the fluvial networks results in the movement of vast phosphorus fluxes. Multiple pathways are observed for particulate and soluble constituents, highlighting the challenges faced in mitigating the delivery of contaminant fluxes to headwater river systems.

Crown Copyright © 2015 Published by Elsevier B.V. All rights reserved.

## 1. Introduction

Understanding the hydrological and pollutant dynamics of headwater catchments, and the implicit connections between the land and the river is of great importance (Bishop et al., 2008). These rivers account for 60 to 80% of the entire river network (Benda et al., 2005), providing

\* Corresponding author.

E-mail address: [matthew.perks@ncl.ac.uk](mailto:matthew.perks@ncl.ac.uk) (M.T. Perks).

potable drinking water (Sturdee et al., 2007), buffering capacity for flood risk (Posthumus et al., 2008), dilution of nutrient rich waters downstream (Bowes et al., 2003) and ecological habitats fundamental to the health of the aquatic ecosystems (Meyer et al., 2007). Maintaining the quality of headwater resources is thus essential for the sustainability of the water environment (Soulsby et al., 2002). A significant risk to the systems' functional integrity is the presence of surface sediment sources that are enriched with phosphorus (P) following years of excessive fertiliser inputs (Heathwaite et al., 2006; Withers et al., 2001, 2007), which may be exacerbated by land-use conflicts (Pacheco et al., 2014; Valle Junior et al., 2014) and accelerating rates of terrestrial erosion (Mainstone et al., 2008; McHugh, 2007). The delivery of these materials to hydrological networks is augmented by the relatively low filter resistance and restricted potential for temporary storage in these small catchments. Resultantly, the catchment export of sediment and P may be closely related to the magnitude of erosion and land degradation (Kovacs et al., 2012), with adverse impacts on the aquatic habitats ensuing (Collins and Walling, 2004; Haygarth et al., 2005a,b; Holden et al., 2007; Valle Junior et al., 2015).

To moderate the number of watercourses failing to produce ecologically sustainable habitats as a result of enhanced erosion and delivery of pollutants to sensitive headwater fluvial networks, identification of the fine sediment and nutrient sources, and the pathways of delivery is firstly required (Jarvie et al., 2008), with management efforts subsequently focussing on restoring natural attenuation within catchments and disconnecting the identified Critical Source Areas (CSAs), or hot-spots from the fluvial networks (Heathwaite et al., 2005; Kovacs et al., 2012; Newson, 2010; Pionke et al., 1996). Many well established factors act to define the CSAs of fine sediment and P, however, our understanding of how and when these areas are connected to the fluvial networks is limited by the heterogeneity of factors governing process rates (Dean et al., 2009). These factors include antecedent moisture conditions, runoff mechanisms, spatial variation of rainfall intensity, and land management operations. These process controls influence the mechanisms of mobilisation, pathways of transfer, and the complex biogeochemical processes occurring along the land–water continuum, yet, they are diffuse, difficult to quantify at the catchment-scale, and vary on an event basis. Understanding of how pollutant transmission varies in response to temporal and spatial constraints may however provide key information about connectivity of pollutant sources, pathways of delivery and pollutant transfer in a catchment (Lexartza-Artza and Wainwright, 2009).

A large amount of research has been conducted to improve our understanding of the timing and mechanisms responsible for the transport of aquatic pollutants in surface and sub-surface runoff from agricultural land, with investigations into the fluvial export of suspended sediment from small agricultural catchments enabling exploration of the processes responsible for its delivery (e.g., Glendell and Brazier, 2014; Steegen et al., 2000; Thompson et al., 2013). Likewise, studies have sought to characterise the nature of P losses from headwater agricultural catchments (e.g., Haygarth et al., 2005b; Hodgkinson and Withers, 2007; Pionke et al., 1996; Soulsby et al., 2002; Stutter et al., 2008). However, there is currently a dearth of continuous, high-temporal resolution hydro-chemical and suspended sediment monitoring datasets available for rivers draining sensitive headwater catchments. Such high-frequency datasets of discharge, suspended sediment (SS), total phosphorous (TP) and total reactive phosphorus (TRP) enable characterisation of the complex non-linear responses of the monitored determinands at sub-hourly timescales.

Non-linear concentration–discharge relationships have been widely acknowledged for many contaminants, with assessment of this hysteresis being used as a means of interpreting probable pollutant pathways and origins (e.g., Lefrançois et al., 2007; Naden, 2010; Outram et al., 2014; Smith and Dragovich, 2009). Small scale experiments, in which the pollutant transport processes are controlled,

have successfully produced the expected hysteresis dynamics, offering support for this indirect approach (e.g., Chanat et al., 2002; Eder et al., 2014). Analysis of the process dynamics of multiple contaminants using this hysteresis framework enables commonalities in transport systems to be assessed, and maximum information to be extracted about pollutant and catchment response to hydrological events (e.g., Halliday et al., 2014; Mellander et al., 2012; Outram et al., 2014; Owen et al., 2012; Wade et al., 2012). Specifically, this framework enables an assessment of the complicating factors and influences on SS and P transfer at multiple scales (e.g., Haygarth et al., 2012); and, the interaction between catchment structure, connectivity, and pathway dominance under varying environmental conditions (Bilotta et al., 2007, 2010; Bracken et al., 2014).

Such information is valuable and necessary to inform mitigation strategies for reducing diffuse water pollution from agriculture (DWPA) in the UK (McGonigle et al., 2014). The development of a solid evidence base prior to the implementation of mitigation measures is required to: a) determine the effectiveness of control measures (e.g., Wilkinson et al., 2014); b) assess the cost-effectiveness of resource allocation (e.g., Posthumus et al., 2013); and c) enable reliable and transparent decisions to be made about future catchment operations (Collins et al., 2012).

In this present study, high resolution hydro-meteorological, SS and P data collected during a range of low and moderate magnitude runoff events over one year are analysed to determine the intra-storm hysteresis dynamics of SS, TP and TRP concentrations. Analysis of the environmental factors associated with observed pollutant dynamics is conducted using factor analysis (FA) which incorporates a suite of environmental variables representing the event storm conditions and antecedent hydro-meteorological conditions. The aim of this analysis is to extract fundamental information describing the transport pathways and pollutant dynamics of the system, providing the basis for examining the key components driving the transfer of SS and P at multiple scales across a small agricultural catchment in the UK.

## 2. Materials and methods

### 2.1. Study area

This research was conducted in the upper reaches of the Newby Beck sub-catchment of the River Eden, NW England, UK (Fig. 1). Newby Beck is a predominantly upland catchment with moderate slopes (7.4%) and a mean elevation of 234 m. The catchment is underlain by steeply dipping, fractured limestone and sandstone units with interbedded siliciclastic argillaceous rock of the Carboniferous period. The soils draining the headwaters in the south of the catchment are well drained, locally deep, fine loamy soils with slowly permeable and seasonally wet acid loamy and clayey soils through the middle reaches, moving towards slowly permeable, seasonally waterlogged reddish fine and coarse loamy soils in the north of the catchment (Cranfield University, 2014). The catchment was designated as a priority under the England Catchment Sensitive Farming Delivery Initiative (ECSFDI) to reduce diffuse water pollution resulting from farming activity. Improved grassland dominates the catchment (76% by area), along with acid grassland (10%) and arable land (6%), with 2.88 livestock units (LU) ha<sup>-1</sup> (cattle and sheep). The average Olsen P concentration from across 38 fields (14% of catchment) is 23.6 mg kg<sup>-1</sup> ( $\sigma = 9.9$  mg kg<sup>-1</sup>) with a range of 8–46 mg kg<sup>-1</sup>. The climate of this region is cool temperate maritime with a long-term average rainfall of 1187 mm ( $\sigma = 184$  mm) (Met Office, 2009). The catchment responds relatively rapidly with a time-to-peak of 3 h (Houghton-Carr, 1999) and the standard percentage runoff (SPR) is estimated to be 35% based on the Hydrology of Soil Types (HOST) classification.

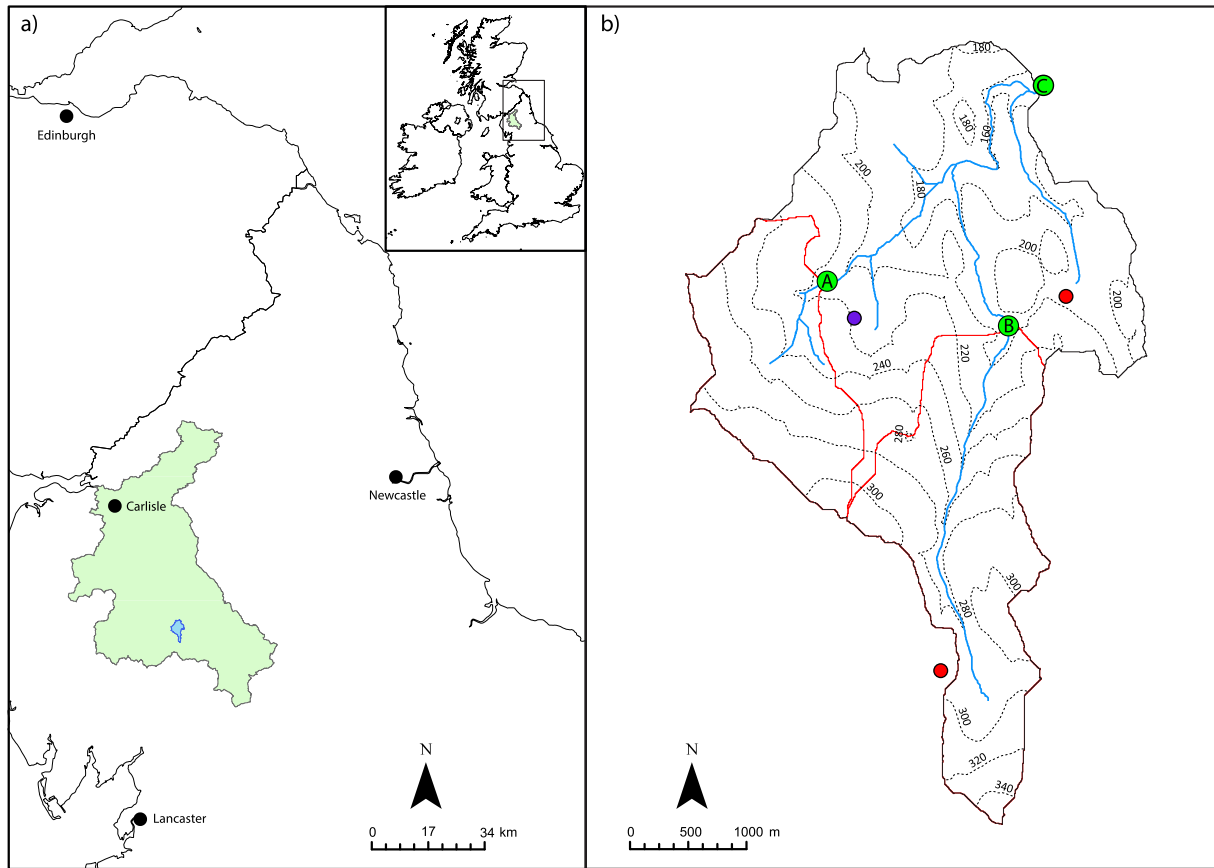


**Fig. 1.** a) Regional map showing the location of the Eden and Newby Beck catchments, coloured green and blue respectively. b) Detailed map of the Newby Beck catchment. Locations of rain gauges are represented by red points, the weather station is coloured purple and in-stream water quality stations are coloured green. Contour intervals are 20 m. © Crown Copyright/database right 2014. An Ordnance Survey/EDINA supplied service.

## 2.2. Research design

This study utilises the River Eden Demonstration Test Catchment (DTC) research platform (cf. Owen et al., 2012). The DTC programme was implemented to inform policy and practical approaches for the

reduction of DWPA and the improvement of ecological status in freshwaters, whilst maintaining economically viable food production (McGonigle et al., 2014). The Newby Beck catchment consists of three hydro-meteorological monitoring stations distributed across the catchment (Table 1), with in-stream monitoring stations located at strategic

**Table 1**  
Description of the characteristics for each of the monitored sub-catchments of the Newby Beck catchment.

	Sub-catchment A	Sub-catchment B	Outlet (C)
Monitoring location (WGS 1984)	54°34'13.5"N 2°38'54.2"W	54°34'00.2"N 2°37'29.0"W	54°35'07.3"N 2°37'12.2"W
Catchment area (km <sup>2</sup> )	2.2	3.8	12.5
Mean elevation (m AOD)	261.03	275.49	234.22
Catchment average slope (m m <sup>-1</sup> )	0.0600	0.0825	0.0746
Geology (as % of area)			
Limestone	51.43	54.15	50.80
Limestone + shales	48.47	45.85	49.00
Sandstone + shales	0.00	0.00	0.20
Soil drainage (as % of area)			
Well drained	25.47	69.02	20.12
Seasonally wet	74.53	30.98	65.69
Seasonally waterlogged	0.00	0.00	14.19
Major land-use units (as % of area)			
Improved grassland	65.35	82.89	76.42
Acid grassland	17.88	12.53	9.84
Arable	9.66	1.25	6.16
Woodland	4.69	2.70	2.36
Other	2.42	0.63	5.22
Average Olsen P (mg kg <sup>-1</sup> )	–	–	23.6
Standard percent runoff (%)	–	–	35
Time to peak (hours)	–	–	3

points to effectively partition the catchment into two sub-catchments: (A) 2.2 km<sup>2</sup>, and (B) 3.8 km<sup>2</sup>, with the outlet monitoring station (C) draining an area of 12.5 km<sup>2</sup>.

### 2.3. Instrumentation and sampling

#### 2.3.1. Hydrometeorology

The catchment was equipped with an Environmental Measurement Limited (EML) Automatic Weather Station (AWS), logging rainfall (mm), air temperature (°C) and net radiation ( $W m^{-2}$ ) every 15 min. Two additional Casella 0.2 mm tipping bucket rain gauges log on an event basis (Fig. 1). Each in-stream monitoring station was equipped with a non-vented SWS Mini-Diver, which when corrected for atmospheric pressure, record water level ( $\pm 0.005$  m; i.e., <0.5% of maximum gauged level) at 5 minute intervals. Site specific rating-curves were produced using river level data and the collection of flow measurements. Velocity measurements were taken using a Valeport electromagnetic current meter at low flows and a Teledyne RD Instruments StreamPro ADCP during high-flows. Discharge values were calculated using the Area–Velocity method. At peak flows, extrapolation of the rating curves beyond the maximum gauged discharge was necessary for 2.96, 0.67 and 0.61% of the time for Stations A, B and C, respectively. This was achieved using the Velocity Area Rating Extension (VARE) approach (Ewen et al., 2010).

#### 2.3.2. Water quality parameters

Turbidity probes were deployed at all three in-stream monitoring stations to provide high-frequency surrogate measurements of suspended sediment concentrations. Measurements were made at fifteen minute intervals using McVan Analite 395 nephelometers (Stations A and B) and a YSI 6600 multi-parameter sonde (Station C). These probes were equipped with wipers, programmed to clean the sensor at sub-hourly intervals. At Station C, P concentrations were measured using a Hach Lange combined Sigmatax sampling module and Phosphax Sigma analyser. The system was subjected to a weekly cleaning cycle, with automatic calibration with a 2 mg L<sup>-1</sup> standard solution being performed daily. TP is determined colourimetrically following heating of the sample to 140 °C under pressure and being subjected to persulfate digestion, whilst molybdate-reactive phosphorus (TRP) concentrations are determined colourimetrically on an unfiltered sample (Elisenreich et al., 1975; Wade et al., 2012). TRP is an operationally defined measurement predominantly comprised of orthophosphate (PO<sub>4</sub>; SRP), although readily hydrolysable P species in the sample may also be present within this TRP fraction (Halliday et al., 2014). TP and TRP measurements were made alternately every 15 min.

### 2.4. Quality control & data treatment

#### 2.4.1. Hydrometeorology

Data from the three rain gauges across the catchment were visually compared to detect events that were not registered by individual stations due to malfunction. Following assurance of the data quality, precipitation from the available stations was interpolated using an Inverse Distance Weighting function (Ahrens, 2006). River level was visually inspected for artificial anomalies. For short-lived erroneous events, anomalies were removed through linear interpolation of adjacent values (cf. Horsburgh et al., 2010).

#### 2.4.2. Water quality

The limits of detection of the Hach Lange Sigmatax/Phosphax systems were assessed by analysing replicate blank samples consisting of deionised water. These ‘blanks’ were pumped through the entire system and analysed by the Phosphax analyser. Average concentrations of 0.009 mg L<sup>-1</sup> for TRP and 0.02 mg L<sup>-1</sup> for TP were observed. These concentrations were assigned as the limits of detection for the method, with measurements below these values being removed from the dataset. In-situ measurements of turbidity, TP and TRP were regularly compared with laboratory derived reference measurements (as defined in Table 2). River samples were obtained for these tests using an ISCO 3700 automatic sampler. Suspended sediment concentration (SSC) was determined using the gravimetric method (American Society for Testing and Materials, 2000). SRP and TP concentrations were analysed by a Konelab Discrete and a Skalar Continuous Flow analyser respectively at the UKAS accredited National Laboratory Service. This laboratory follows standard methodology and both instruments have a limit of detection of 0.001 mg L<sup>-1</sup>. Preparation of the sample for SRP analysis involved passing the sample through a 0.45 µm cellulose acetate membrane filter to remove solids.

A linear regression model was adopted to best describe the fit between the in-situ and reference measurements for all determinants. A condition specifically imposed for the turbidity-SSC model was that the intercept had to pass through the origin. This was chosen to prevent negative prediction of SSC values at very low turbidity levels (Perks et al., 2014). For each of the developed linear models, the uncertainty of the regression coefficients was evaluated by bootstrapping the residuals 10,000 times, replacing the original sample and providing detailed information about the characteristics of the population.

### 2.5. Event classification and extraction

The initiation of a hydrologically significant event was defined following partitioning of the hydrograph into base and storm flow components based on the Hydrograph Separation Program (HYSEP) local minimum method (Sloto and Crouse, 1996). Initial classification of events was undertaken at the outlet, Station C. Only high flows that were observed at both the sub-catchments were selected for analysis. This resulted in a total of 55 events being retained, which occurred between the 10th of May 2012 and the 14th of February 2013 (Fig. 2). At each site, and for events with available data, an assessment of the TP/TRP/SSC hysteresis dynamics was conducted based on the comprehensive account of hysteresis patterns provided by Williams (1989).

### 2.6. Factor analysis

The compilation of hydrochemistry and meteorology for periods immediately prior to and during the storm events, collected across three water quality and three meteorology monitoring stations, resulted in the production of a complex, multi-dimensional dataset, parameters, units and measurement intervals of which are provided in Table 3. Multivariate statistical treatment of the data was used to extract the underlying information (Singh et al., 2004). Factor analysis (FA) was chosen to provide a structured and transparent method of analysing the complex dataset. To examine the suitability of the data for FA, the Kaiser–Meyer–Olkin (KMO) and Bartlett’s sphericity

**Table 2**

Comparisons made between the in-situ measurements and the laboratory derived reference samples for each monitoring station. X indicates that a test between the two parameters was conducted.

	Turbidity versus SSC	In-situ TP versus lab TP	In-situ TRP versus lab SRP
Station A	X		
Station B	X		
Station C	X	X	X

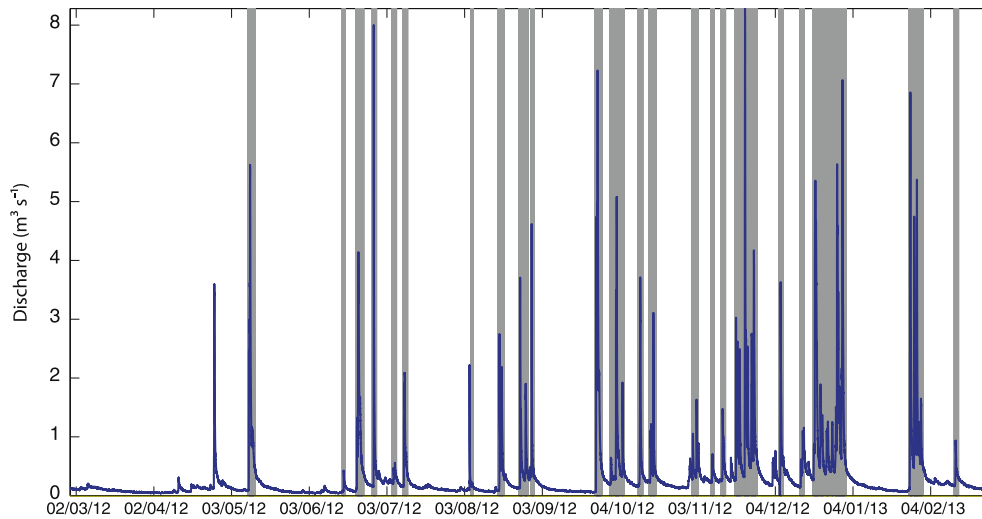


**Fig. 2.** Discharge data generated from during the monitoring period (March 2012 to March 2013) at the catchment outlet (Station C). Hydrologically significant events selected for analysis with suspended sediment and phosphorus data available are highlighted.

tests were performed. Following calculation of the KMO measure of sampling adequacy (MSA), individual variables with unacceptable MSA values ( $<0.60$ ) were removed following the recommendations of Kaiser (1974). Bartlett's test of sphericity on each of the three z-scale transformed experimental datasets produced a significance level of zero, indicating significant relationships amongst variables. This indicates an adequate degree of common variance, indicating that the matrixes are factorable (Shrestha and Kazama, 2007). A varimax rotation scheme was employed and a three-factor model determined (Kaiser, 1958).

### 3. Results

#### 3.1. Performance of in-situ and surrogate measurements

The performance metrics of each of the in-situ (TRP/TP) and surrogate (turbidity) measurements used in this study are provided in Table 4. These include the uncertainty of the regression coefficients for each developed model, along with the number of calibration samples ( $n$ ) and summary statistics. It is demonstrated that turbidity is an excellent surrogate for SSC, with each of the developed linear models being

**Table 3**  
Abbreviations, names and units for the variables entered into the factor analysis.

Variables	Description	Units
<i>Antecedent conditions</i>		
P1d	Precipitation total for 1 day prior to the event	mm
P5d	Precipitation total for the 5 days prior to the event	mm
P7d	Precipitation total for the 7 days prior to the event	mm
P21d	Precipitation total for the 21 days prior to the event	mm
Q1d	Median discharge for the 1 day prior to the event	$\text{m}^3 \text{s}^{-1}$
Q5d	Median discharge for the 5 days prior to the event	$\text{m}^3 \text{s}^{-1}$
Q7d	Median discharge for the 7 days prior to the event	$\text{m}^3 \text{s}^{-1}$
Q21d	Median discharge for the 21 days prior to the event	$\text{m}^3 \text{s}^{-1}$
Qb	Base-flow discharge immediately before the event	$\text{m}^3 \text{s}^{-1}$
T1d	Median air temperature for 1 day prior to the event	$^{\circ}\text{C}$
T5d	Median air temperature for 5 days prior to the event	$^{\circ}\text{C}$
T7d	Median air temperature for 7 days prior to the event	$^{\circ}\text{C}$
T21d	Median air temperature for 21 days prior to the event	$^{\circ}\text{C}$
<i>Event hydrology</i>		
Pt	Event precipitation total	mm
$I_{\text{max}}$	Maximum precipitation intensity	$\text{mm } 15 \text{ min}^{-1}$
$Q_{\text{max}}$	Maximum event discharge	$\text{m}^3 \text{s}^{-1}$
$Q_{\text{mean}}$	Mean event discharge	$\text{m}^3 \text{s}^{-1}$
$QR_{\text{max}}$	Maximum rise in discharge	$\text{m}^3$
$QR_{\text{mean}}$	Mean rise in discharge	$\text{m}^3$
Wt	Water yield	$\text{hm}^3$
<i>Soluble and particulate transport</i>		
$SSC_{\text{max}}$	Maximum suspended sediment concentration	$\text{mg L}^{-1}$
$SSC_{\text{median}}$	Median suspended sediment concentration	$\text{mg L}^{-1}$
Sediment flux	Suspended sediment flux	tonnes
TP flux	Total phosphorus flux	kg
$TP_{\text{max}}$	Maximum total phosphorus concentration	$\text{mg L}^{-1}$
$TP_{\text{median}}$	Median total phosphorus concentration	$\text{mg L}^{-1}$
TRP flux	Total reactive phosphorus flux	kg
$TRP_{\text{max}}$	Maximum total reactive phosphorus concentration	$\text{mg L}^{-1}$
$TRP_{\text{median}}$	Median total reactive phosphorus concentration	$\text{mg L}^{-1}$



**Table 4**

Summary statistics of field calibrations for measurements made by turbidity probes and Phosphax analyser. Confidence intervals (CI) of the model coefficients (a and b) are provided following bootstrapping of the residuals, where  $n = 10,000$ . Relationships that are significant at the 99.9% level are italicised.

	Regression equation ( $y = ax$ or $y = a + bx$ )	Range ( $\text{mg L}^{-1}$ )	a [95% CI]	b [95% CI]	R <sup>2</sup>
<i>Station A</i>					
Turbidity versus SSC ( $n = 76$ )	$y = 1.5386x$	4.9–815.0	1.448–1.629	–	0.92
<i>Station B</i>					
Turbidity versus SSC ( $n = 89$ )	$y = 1.1645x$	3.0–778.0	0.991–1.254	–	0.72
<i>Station C</i>					
Turbidity versus SSC ( $n = 108$ )	$y = 1.5655x$	3.0–386.0	1.418–1.625	–	0.83
In-situ TP versus lab TP ( $n = 128$ )	$y = -0.0103 + 0.8649x$	0.02–0.51	–0.017 to –0.004	0.838–0.89	0.97
In-situ TRP versus lab SRP ( $n = 129$ )	$y = -0.0055 + 0.8629x$	0.07–0.20	–0.013–0.002	0.783–0.934	0.80

highly statistically significant ( $P < 0.001$ ). These site specific models were used for calibration, with turbidity being converted to SSC. The relationship between the in-situ and laboratory derived TP concentrations is also highly significant ( $R^2 = 0.97$ ;  $P < 0.001$ ) although the field measurements typically overestimate the reference (laboratory derived) concentrations. This is likely an artefact of different analytical procedures and the reagents used during the in-situ analysis. However, this does provide assurance that the Hach Lange apparatus is operating in a stable and precise manner. An additional comparison was made between the in-situ TRP and lab-based orthophosphate (SRP) concentrations. Although these are essentially different determinands, a relationship between the two may be expected given that TRP includes SRP plus any easily hydrolysable P species. Linear regression between the two results in a statistically significant relationship ( $R^2 = 0.80$ ;  $P < 0.001$ ), with the field measurements of TRP exceeding orthophosphate concentration as expected. Interpretation of the model coefficients suggests that the vast majority of TRP found within this headwater catchment is of soluble reactive form (Table 4).

### 3.2. Factor analysis

Taking samples and variables into account, three factors explained 82.75%, 72.61%, and 74.71% of the variance for monitoring Stations A, B and C, respectively. In order to determine the dominant variables of each factor, loadings were computed. ‘Strong’, ‘moderate’ and ‘weak’ loadings are defined as  $>0.75$ ,  $0.75$ – $0.50$  and  $0.50$ – $0.30$ , respectively (Shrestha and Kazama, 2007). For each of the stations, the factor which explains the greatest variance in the dataset (i.e., factor one) is characterised by high positive factor loadings ( $>0.75$ ) for the event storm conditions. These include variables such as the mean and maximum discharge, rate of discharge rise, precipitation total and the mass of suspended sediment transported during the event (Table 5). Factor two is characterised by high positive factor loadings for variables describing the antecedent hydrological conditions prior to the commencement of the storm event. These include the amount of precipitation over the preceding 1/5/7/21 days and the discharge associated with these antecedent periods. The third

**Table 5**

Summary of factor loadings for all variables accepted for use in FA for Newby Beck monitoring Stations A, B and C. Only factor loadings  $\geq 0.5$  are provided, with values  $\geq 0.75$  presented in bold.

Variables	Factor loadings for Station A			Factor loadings for Station B			Factor loadings for Station C		
	Factor 1	Factor 2	Factor 3	Factor 1	Factor 2	Factor 3	Factor 1	Factor 2	Factor 3
P1d					0.58			0.59	
P5d		<b>0.92</b>			<b>0.91</b>			<b>0.92</b>	
P7d		<b>0.94</b>			<b>0.87</b>			<b>0.87</b>	
Q1d		0.58			0.64			0.71	
Q5d		<b>0.99</b>			<b>0.91</b>			<b>0.93</b>	
Q7d		<b>0.99</b>			<b>0.90</b>			<b>0.90</b>	
Q21d		0.57							
Qb								0.56	
Pt	0.71						<b>0.82</b>		
Q <sub>max</sub>	<b>0.97</b>			<b>1.00</b>			<b>0.96</b>		
Q <sub>mean</sub>				<b>0.83</b>			<b>0.82</b>		
QR <sub>max</sub>	<b>0.82</b>			<b>0.88</b>			0.73		
QR <sub>mean</sub>	<b>0.88</b>			<b>0.92</b>			<b>0.87</b>		
SSC <sub>max</sub>	0.74			0.68			<b>0.87</b>		
I <sub>max</sub>	0.74						0.72		
Wt				0.64					
Sediment flux	<b>0.95</b>			<b>0.93</b>			<b>0.95</b>		
TP flux							<b>0.86</b>		
TRP <sub>max</sub>							0.56		
TRP <sub>median</sub>									
T1d			<b>0.94</b>			<b>0.91</b>			<b>0.90</b>
T5d			<b>0.99</b>			<b>0.99</b>			<b>0.93</b>
T7d			<b>0.99</b>			<b>0.99</b>			<b>0.98</b>
T21d			<b>0.94</b>			<b>0.93</b>			<b>0.99</b>
Explained variance (%)	39.62	23.23	19.90	30.18	25.03	17.40	34.80	25.42	14.48
Cumulative explained variance (%)	39.62	62.85	82.75	30.18	55.21	72.61	34.80	60.23	74.71

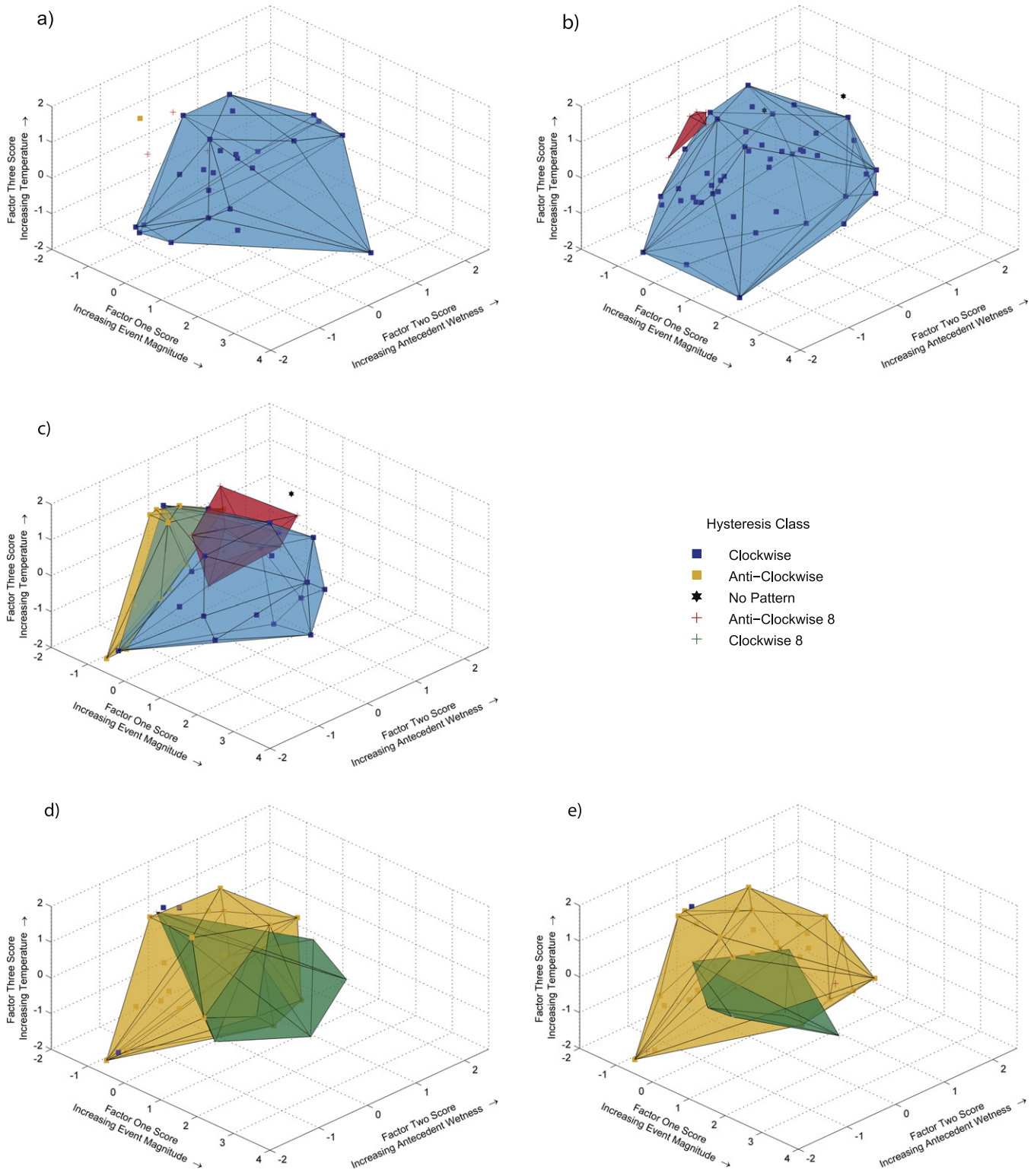


**Fig. 3.** Distribution of events in the I–III factorial plane according to hysteresis classification for a) suspended sediment at Station A ( $n = 29$ ); b) suspended sediment at Station B ( $n = 53$ ); c) suspended sediment at Station C ( $n = 45$ ); d) total reactive phosphorus at Station C ( $n = 42$ ); and e) total phosphorus at Station C ( $n = 45$ ).

factor is characterised by high positive factor loadings for variables describing the ambient temperature over the preceding 1/5/7/21 days. These three factors which were retained for varimax rotational analysis and utilised to understand the necessary conditions for the production of distinct hysteresis loops therefore represent: 1) event magnitude; 2) antecedent wetness; and 3) temperature.

### 3.3. Suspended sediment

At monitoring Station A, hysteresis patterns are almost entirely dominated by clockwise hysteresis (86.2%; Fig. 3a). These events are the dominant behaviour of the system and occur across the full range of factor conditions, represented by the large standard

deviation ( $\sigma$ ) of factor (F) scores ( $s$ ) ( $F1 \bar{s} = 0.11, \sigma = 1.03$ ;  $F2 \bar{s} = 0.10, \sigma = 1.04$ ;  $F3 \bar{s} = -0.15, \sigma = 0.99$ ). For 10.4% of events, figure-of-eight with an anti-clockwise loop (A8) hysteresis is observed. These events are characterised by negative factor one and factor two scores ( $F1 \bar{s} = -0.55, \sigma = 0.51$ ;  $F2 \bar{s} = -0.53, \sigma = 0.37$ ), and high factor three scores ( $F3 \bar{s} = 0.89, \sigma = 0.38$ ), demonstrating their predisposition to occur following warm, dry periods during low magnitude events. Anti-clockwise events are also observed (3.4% of events) under similar conditions to that of A8 events ( $F1 \bar{s} = -1.20, F2 \bar{s} = -0.79$ ;  $F3 \bar{s} = 1.29$ ).

At monitoring Station B, within-storm sediment dynamics are again dominated by clockwise hysteresis (86.8%; Fig. 3b), occurring across the full range of factor score conditions ( $F1 \bar{s} = 0.10, \sigma = 1.04$ ;  $F2 \bar{s} = 0.01, \sigma = 1.01$ ;  $F3 \bar{s} = -0.16, \sigma = 0.96$ ). A8 events are again found to occur infrequently (9.4%). These occur under similar conditions to those observed at monitoring Station A; i.e., low factor one scores ( $F1 \bar{s} = -0.71, \sigma = 0.24$ ), low factor two scores ( $F2 \bar{s} = -0.66, \sigma = 0.29$ ) and high factor three scores ( $F3 \bar{s} = 1.26, \sigma = 0.41$ ). The remaining events (3.8%) are described as having no discernible hysteresis pattern and are characterised as having low factor one scores ( $F1 \bar{s} = -0.51, \sigma = 0.16$ ), high factor two scores ( $F2 \bar{s} = 1.46, \sigma = 1.03$ ) and high factor three scores ( $F3 \bar{s} = 0.61, \sigma = 0.29$ ).

At monitoring Station C, hysteresis patterns are varied despite clockwise hysteresis events being most prominent (Fig. 3c). 42.2% of events can be described as exhibiting clockwise hysteresis, which occurs across the spectrum of factor score conditions ( $F1 \bar{s} = 0.59, \sigma = 1.10$ ;  $F2 \bar{s} = 0.04, \sigma = 1.01$ ;  $F3 \bar{s} = -0.14, \sigma = 0.98$ ). Both A8 and anti-clockwise events also occur in significant numbers at the outlet station, contributing to 20% and 22.2% of the total, respectively. Similarly to monitoring Stations A and B, A8 events occur when factor one scores are negative ( $\bar{s} = -0.25, \sigma = 0.45$ ) i.e., during low-moderate magnitude events. However, these are also characterised by high factor three and low factor two scores, or the inverse ( $F2 \bar{s} = 0.54, \sigma = 0.92$ ;  $F3 \bar{s} = 0.29, \sigma = 0.94$ ). Anti-clockwise events predominately occur during events characterised as having highly negative factor one and factor two scores ( $F1 \bar{s} = -0.75, \sigma = 0.19$ ;  $F2 \bar{s} = -0.64, \sigma = 0.70$ ). The remaining events may be characterised as exhibiting figure-of-eight with a clockwise loop (C8) hysteresis (4.4%) and no discernible hysteresis pattern (11.1%).

### 3.4. Total reactive phosphorus

At monitoring Station C, the within-storm dynamics associated with TRP are dominated by anti-clockwise hysteresis (62.2%; Fig. 3d). These events occur across the full range of varifactor conditions with the exception of events that are characterised by a combination of high VF1 and VF2 conditions ( $VF1 \bar{s} = -0.20, \sigma = 0.66$ ;  $VF2 \bar{s} = -0.02, \sigma = 0.99$ ;  $VF3 \bar{s} = -0.13, \sigma = 1.01$ ). C8 events are also frequently observed (17.8%) and these events are characterised by high VF1 scores, although they do occur across the full range of VF conditions ( $VF1 \bar{s} = 0.68, \sigma = 1.42$ ;  $VF2 \bar{s} = 0.17, \sigma = 1.07$ ;  $VF3 \bar{s} = 0.19, \sigma = 0.90$ ). The remaining events are characterised as exhibiting clockwise (6.7%) or no discernible hysteresis (13.3%).

### 3.5. Total phosphorus

At monitoring Station C, the within-storm dynamics associated with TP are almost entirely dominated by anti-clockwise hysteresis (73.3%; Fig. 3e). This is the dominant behaviour of the system and occurs across the full range of varifactor conditions with the exception of events which are characterised by a combination of high VF1 scores and negative VF3 scores ( $VF1 \bar{s} = -0.18, \sigma = 0.80$ ;  $VF2 \bar{s} = 0.14, \sigma = 0.99$ ;  $VF3 \bar{s} = -0.01, \sigma = 1.03$ ). C8 type events account for a further 13.3%, which are also not limited to specific conditions, although they do dominate when VF1 is high ( $\bar{s} = 0.80, \sigma = 1.19$ ) and when VF3 is low ( $\bar{s} = -0.26, \sigma = 0.53$ ) i.e., moderate-high magnitude events periods of low ambient temperature. Remaining events may be

characterised as exhibiting A8 (4.4%), clockwise (2.2%), and no discernible hysteresis (6.7%).

## 4. Discussion

### 4.1. Suspended sediment transfer in response to temporal and spatial constraints

Clockwise hysteresis events dominate, accounting for 86% and 89% of events and for 96% and 99% of the sediment flux generated during storm periods at Stations A and B, respectively. The incidence of these events is consistent between sub-catchments, with comparable hysteresis responses occurring on 93% of occasions. The rapid response of SSC to hydrological forcing implies that the SS sources are readily accessible with the majority of SS being generated from areas proximal to the channel (Bača, 2008; Lefrançois et al., 2007; Rodríguez-Blanco et al., 2013). These sediment sources include: bed material (Arnborg et al., 1967; Bogen, 1980), bank material (Langlois et al., 2005; Seeger et al., 2004; Smith and Dragovich, 2009) and hydrologically connected areas close to the channel which respond rapidly at the onset of a storm (Mano et al., 2009; Reid et al., 2007). Factor analysis has illustrated that these event dynamics have no threshold of initiation and may occur across the full range of environmental conditions observed.

A secondary response at the sub-catchment scale, which is infrequently observed, is figure-of-eight hysteresis with an anti-clockwise loop (A8). This is a result of temporary elevated SSCs on the rising limb, followed by a period of enhanced transfer following peak discharge. The processes producing A8 events are difficult to decipher, although the enhanced SSC at low discharges on the rising limb of the hydrograph is likely a result of event water prominence and more specifically, within-channel sediment sources that are readily mobilised during the initial stages of the event (Eder et al., 2014). Such event characteristics are likely a result of rapid remobilisation of material deposited during the recession period of the previous event (Bull, 1997; Eder et al., 2014). Factor analysis has indicated that the occurrence of these events at Stations A and B is preceded by a combination of fluvial quiescence and relatively high air temperatures. These antecedent hydro-meteorological characteristics will be a principal control of the preparatory processes operating during the relaxation period between events, and they may govern the rate of sediment generation and condition the system response (Bracken et al., 2014; Lexartza-Artza and Wainwright, 2009). For example, an extended recession period may result in the relative abundance of easily accessible within-channel sources being present due to a lack of depletive flows (Carling, 1983; Stutter et al., 2008; VanSickle and Beschta, 1983). Meanwhile, elevated temperatures and high net radiation would enhance the presence of in-stream vegetation producing a stabilising effect and efficiently trapping fine grained material within the channel at base-flow (Cotton et al., 2006). These characteristics may act to increase the within-channel availability of fine sediment throughout the relaxation period, with the subsequent storm mobilising this accumulated and easily accessible sediment stock, triggering the initial elevated SSCs; the initial phase of the A8 hysteresis pattern. The continued transfer of sediment through the system on the falling limb of the hydrograph is however indicative of a delayed contribution from an additional significant sediment source (Eder et al., 2010).

At the catchment scale (Station C), clockwise hysteresis is still highly important in the export of SS from the Newby Beck catchment. Despite accounting for only 42% of events, they account for 75% of total flux generated during storms. Events classified as clockwise at Stations A and B are, however, only replicated at the outlet on 47% and 56% of occasions respectively, with an increased incidence of A8 and anti-clockwise hysteresis at this catchment-scale. This lack of uniformity between sub-catchments and the catchment outlet reflects between-scale variations in dominant processes and may reflect inconsistencies in sediment sources (Smith and Dragovich,

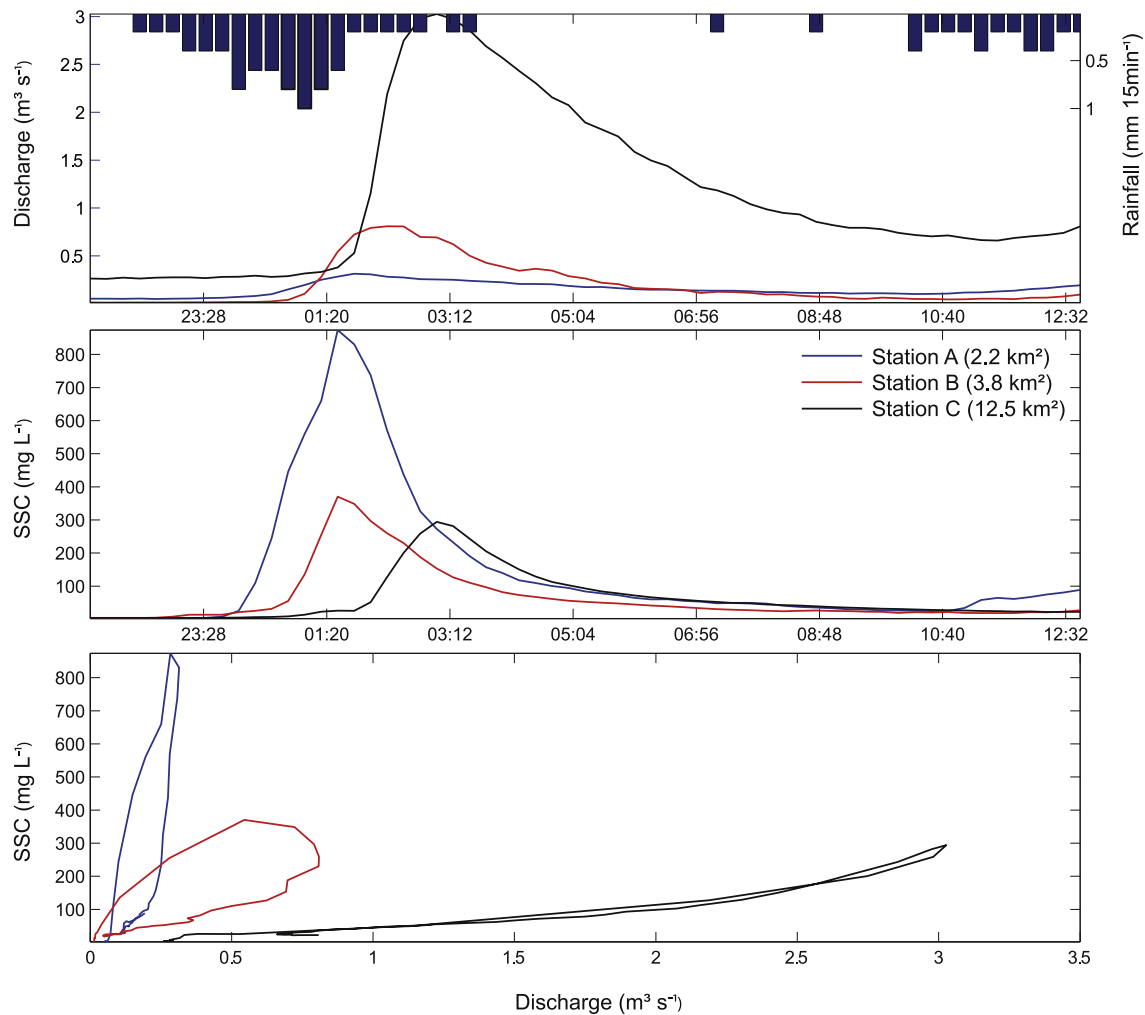


Fig. 4. An example of the divergent suspended sediment hysteresis dynamics with increasing scale over the course of a catchment-wide storm beginning on the 18th of November 2012.

2009). An example of the between scale divergent response is provided in Fig. 4. In this instance, a storm producing 11.8 mm of rainfall results in a catchment-wide hydrological response and the creation of broad, clockwise SS hysteresis loops at both Stations A and B. However, at Station C, these dynamics are not replicated, and an A8 loop is produced. This is a commonly observed variant response throughout the time-series, representing 20% of events at the outlet and producing 9% of the storm generated flux. Similar to Stations A and B, these events occur during low–moderate magnitude run-off events with their occurrence across a gradient of antecedent conditions and ambient temperature (Fig. 3c).

More striking inconsistencies in the SS hysteresis patterns between scales are observed when the occurrence of anti-clockwise hysteresis is examined. These event dynamics are extremely infrequently reported at Stations A and B. However, at Station C these account for 22% of the events, and 2% of the storm generated sediment flux. The generation of these sediment dynamics is likely the result of the dominant sediment delivery pathway being a) extensive with a source distal to the main channel (Eder et al., 2010; Marttila and Kløve, 2010), or b) slow-moving (Sadeghi et al., 2008). Given that these dynamics are observed at the outlet station only, during low magnitude events and following relatively dry antecedent conditions, it is highly unlikely that contributing area expansion, the capturing of headwater zones and widespread hydrological connectivity would result in significant contributions from distal sources (Bača, 2008; Giménez et al., 2012; Marttila and Kløve, 2010; Webb and Walling, 1982). Rather, given the event characteristics, sub-surface

flow is anticipated to be a significant contributor to both the storm-water discharge and, potentially, the material flux (e.g., Deasy et al., 2009; Russell et al., 2001). Sub-surface particulate fluxes are likely to occur following soil pipe erosion (Verachtert et al., 2011), or detachment at the surface by raindrop impact which is subsequently delivered through soil macro-pores or sub-surface drains (Pilgrim and Huff, 1983). Although these sub-surface processes may be important during low magnitude events, as storm intensity increases, additional pathways of sediment movement become progressively important (Sayer et al., 2006), limiting the occurrence of anti-clockwise hysteresis events to low magnitude runoff events.

These findings highlight the importance of spatial constraints on controlling the dynamics of sediment transfer. As scale increases, SS transmission is complicated by the dominance and variability of erosive processes and connected pathways in the catchment (de Vente and Poesen, 2005; Lextarza-Artza and Wainwright, 2011). In Newby Beck, this spatial dependency is likely a consequence of the transition from the relatively freely draining soils of the elevated sub-catchments to the lower-lying, slowly permeable soils of the wider catchment, which necessitates the increased presence of under-drainage for sustainable agricultural production (cf. Table 1). The manifestation of this is a small reduction in surface driven sediment transfer at the catchment scale, and conversely, a greater incidence of slow-moving pathways, as a result of disconnection between the surface supply–delivery system. Furthermore, although surface pathways dominate in terms of SS delivery at each spatial scale, there is a temporal dependency that influences the dominance of a particular pathway, especially at increasing

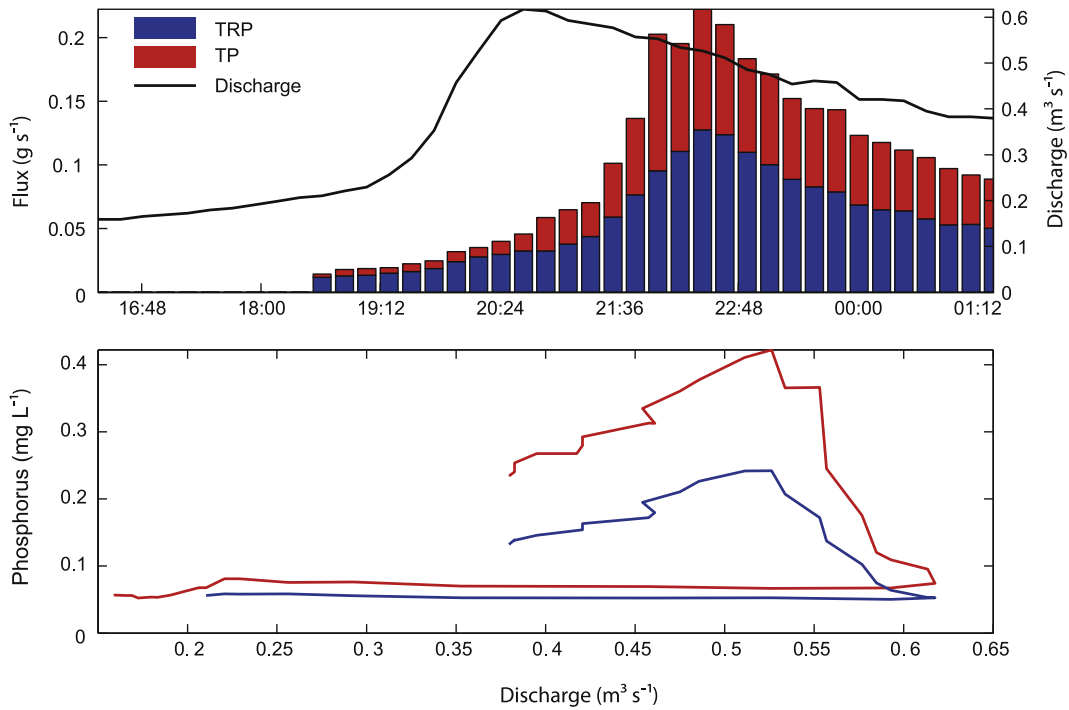


**Fig. 5.** An example of the anti-clockwise hysteresis dynamics exhibited for total phosphorus (TP) and total reactive phosphorus (TRP) at Station C. Fig. 5a illustrates the delay in both TP and TRP fluxes in the catchment, with TRP becoming less dominant during times of peak flux. Fig. 5b illustrates the magnitude of anti-clockwise hysteresis observed for TP and TRP concentrations.

spatial scales where catchment linkages become more complex. It is clear that key environmental drivers alter the distribution of pollutant pathways, with delivery of SS through shallow sub-surface pathways during low magnitude events becoming increasingly frequent despite transferring relatively little in terms of total flux.

4.2. Dominant pathways of phosphorus transfer

Monitoring of TRP and TP at Newby Beck has provided new insights into the processes responsible for their delivery in a headwater agricultural catchment. In catchments dominated by ‘natural sources’, P is

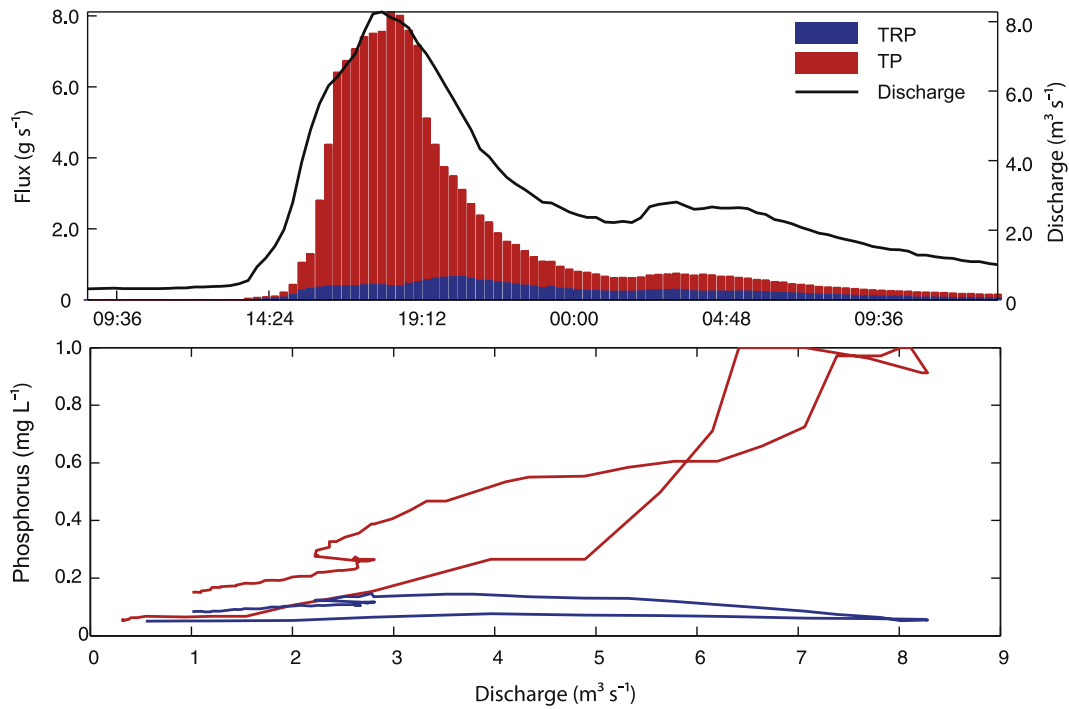


**Fig. 6.** An example of the figure-of-eight (clockwise loop) hysteresis dynamics exhibited for total phosphorus (TP) and total reactive phosphorus (TRP) during infrequent but high magnitude events. Fig. 6a illustrates the synchronicity of both TP and TRP fluxes in the catchment, with TRP becoming less dominant as runoff increases rapidly. Fig. 6b illustrates the timing of concentration pulses which lead to the production of the figure-of-eight (clockwise loop) hysteresis.

mobilised by physical processes of erosion, with the majority of transfer typically taking place in particulate form (Jarvie et al., 2008; Withers and Jarvie, 2008). In Newby Beck, this particulate contribution is secondary to the predominantly soluble TRP fraction, with a median event ratio between TRP and TP of 0.57:1. This suggests the importance of anthropogenically derived sources, with excess fertiliser application possibly leading to a potential surplus of nutrient stock that is not exhausted (Römer, 2009).

This analysis has revealed that the dominant pathways of P delivery to the fluvial system are largely distinct to the pathways responsible for delivering SS, with anti-clockwise hysteresis dominating both the TRP and TP time-series of events (Fig. 3). Previous studies have inferred these dynamics to be a consequence of point sources such as septic tanks and dairy shed retention ponds, which continue to contribute following the hydrograph peak (McKee et al., 2000). However, in this instance, the positive relationship between discharge and P concentrations on a seasonal and event-basis and the lack of dilution-effects does not support this interpretation (Jarvie et al., 2008). Rather, the dominance of anti-clockwise hysteresis provides support for a non-channel source, with soil water being the dominant pathway (Bowes et al., 2005; Chanut et al., 2002; Hatch et al., 1999). Although this may not be typical of agricultural catchments (e.g., Harrington and Harrington, 2014; Sharpley et al., 1992; Siwek et al., 2013), near-surface runoff as a conduit for effective P transfer has been highlighted in other headwater catchments, with the presence of field drains producing preferential hydrological pathways (Dils and Heathwaite, 1999; Hatch et al., 1999; Heathwaite et al., 2006; Heathwaite and Dils, 2000; Rhea et al., 1996; Sims et al., 1998). This sub-surface pathway will not only enable the movement of soluble P within the soil matrix, but also very fine colloidal material, which may contribute significantly to the export of TP and TRP (Foster et al., 2003; Heathwaite and Dils, 2000). Given the potential for both particulate and soluble fractions to be effectively transported by these sub-surface connections, a great deal of synchronicity in TP and TRP hysteresis dynamics is observed, with 82% of the events producing anti-clockwise hysteresis for TRP resulting in a comparable TP response (e.g., Fig. 5). It is this shallow sub-surface component that is dominant in over 73% of the events analysed for TP and 62% for TRP. These pathways are also responsible for a significant proportion of the event P flux, with anti-clockwise hysteresis events accounting for 49% of the storm driven P flux.

The alternate C8 hysteresis dynamics may only account for 13% of events but they represent 25% of the storm driven P flux. The C8 pattern is the result of P concentrations responding moderately at the beginning of the event, prior to a surge in concentrations towards peak discharge on the rising limb of the hydrograph (e.g., Fig. 6). These dynamics are mainly observed during moderate and high magnitude events for both TRP and TP. The threshold type behaviour observed during the rising-limb is indicative that the factor(s) constraining the transfer of mobilised particulate material have been overcome. In this instance, usually disconnected depositional zones may become linked to the fluvial networks as a result of intense rainfall across the catchment. In these usually disconnected depositional zones, sediment can be an important source of P (Quinton et al., 2010), which, when activated and connected to the wider catchment can result in the transfer of vast fluxes of P in surface water (cf. Haygarth et al., 1999). Upon rainfall subsiding, concentrations rapidly decline as surface runoff ceases (Siwek et al., 2013), with a secondary pulse being observed on the falling limb of the hydrograph as P enters the river via shallow through-flow pathways.

#### 4.3. Implications for catchment management

This analysis provides a behavioural understanding that has important implications for reducing P and fine sediment exports within predominantly grassland headwater catchments, with divergent delivery mechanisms being identified between contaminants and

across the catchment-unit. The dominant clockwise hysteresis dynamics for suspended sediment highlights fast, surface-water driven delivery from areas proximal to the channel. In these agricultural catchments, transfer of pollutants as a result of infiltration-excess flow should be rare, however, land management practices commonly used in food production increase compaction and soil degradation, enhancing its occurrence (Heathwaite et al., 2005). Where soil structure is compromised, soil resistance and function could be restored through the use of soil aeration and sward lifters to improve soil infiltration. Where surface runoff pathways are driven by topographic, or man-made features such as tracks and tractor wheelings, physical interception is required to prevent potential sediment source areas becoming CSAs. Decoupling of the hillslope-channel system may be achieved by proactively disconnecting these linkages through the creation of within field, or field edge detention areas through the use of soil bunds, woodland buffer zones, or offline storage ponds. These features slow and temporarily store runoff, enabling mobilised sediment to be recaptured in strategic locations (Burt, 2001; Jordan et al., 2003; Wilkinson et al., 2014). Accessible sediment and P sources from the channel networks could also be further reduced by fencing channels to reduce livestock access. The slow-moving, near surface dominant pathway identified for TP and TRP can only be addressed through a combination of improving soil condition and structure to reduce the occurrence of dry cracked soils and macro-pores; fertiliser management to reduce the source and; proactive interception of land-drains at their outfall within the farm ditch system. The issue of disconnecting depositional zones that become active during infrequent high magnitude events is somewhat more troublesome and requires whole-farm planning and careful nutrient budgeting.

## 5. Conclusion

Assessment of the intra-event hysteresis dynamics and factor analysis of hydro-chemical and suspended sediment datasets for a small agricultural catchment has provided indirect evidence of the dominant mechanisms and pathways of SS and P transfer. At both the sub-catchment (2.2–3.8 km<sup>2</sup>) and catchment scale (12.5 km<sup>2</sup>) and across the complete range of antecedent and hydrological conditions observed, SS is delivered to the fluvial systems predominantly via a rapidly responding pathway close to the drainage network. At the sub-catchment scale, figure-of-eight hysteresis with an anti-clockwise loop is infrequently evidenced; however these are not controlled by the event hydrology, but rather the antecedent conditions and ambient temperature. This highlights the importance of preparatory processes during the relaxation period. SS is also observed to be delivered via a slow moving pathway during 22% of events at the catchment outlet. These are low magnitude events, during which SS is delivered to the fluvial network predominantly via sub-surface pathways. Remarkably, P has been revealed to exhibit a distinct hysteresis response to that of SS. Anti-clockwise hysteresis dominates, accounting for 73% and 62% of events for TP and TRP. This slow moving pathway may be atypical of agricultural catchments, but represents the importance of near-surface runoff as a conduit for P transfer. During high magnitude events however, figure-of-eight hysteresis with a clockwise loop is observed. This threshold-like behaviour is likely the result of the activation and connection of usually disconnected depositional zones to the fluvial networks which results in the transfer of vast P fluxes. The divergent dynamics observed between contaminants across this small agricultural catchment exemplifies the complexity and variability of fine sediment and P transfer processes, highlighting the need to understand dominant pollutant pathways and for the development of contaminant specific management plans to ensure that control measures are most effective at the catchment scale.

## Acknowledgements

The Eden Demonstration Test Catchment (Eden DTC) research platform is funded by the Department for Environment, Food and Rural Affairs (Defra) (project WQ0210) and is further supported by the Welsh Assembly Government and the Environment Agency. The Eden DTC ([www.edendtc.org.uk](http://www.edendtc.org.uk)) includes Lancaster University, University of Durham, Newcastle University, Eden Rivers Trust, Centre for Ecology and Hydrology, British Geological Survey and Newton Rigg College. We are grateful for the assistance of farmers and land owners in the Newby Beck catchment and would also like to thank Paul Quinn, Greg O'Donnell, Mary Ockenden, Nick Barber and three anonymous reviewers for their suggestions and comments, which improved the manuscript.

## Appendix A. Supplementary data

Supplementary data to this article can be found online at <http://dx.doi.org/10.1016/j.scitotenv.2015.03.008>.

## References

- Ahrens, B., 2006. Distance in spatial interpolation of daily rain gauge data. *Hydrol. Earth Syst. Sci.* 10, 197–208.
- American Society for Testing and Materials, 2000. Standard Test Methods for Determining Sediment Concentration in Water Samples: D 3977-97 11.02 pp. 395–400.
- Arnborg, L., Walker, H.J., Peippo, J., 1967. Suspended load in the Colville River, Alaska, 1962. *Geogr. Ann. Ser. A Phys. Geogr.* 49, 131–144.
- Bača, P., 2008. Hysteresis effect in suspended sediment concentration in the Rybárik basin, Slovakia. *Hydrol. Sci.* 53, 224–235.
- Benda, L., Hassan, M.A., Church, M., May, C.L., 2005. Geomorphology of steepland headwaters: the transition from hillslopes to channels. *J. Am. Water Resour. Assoc.* 41, 835–851.
- Bilotta, G.S., Brazier, R.E., Haygarth, P.M., 2007. Processes affecting transfer of sediment and colloids, with associated phosphorus, from intensively farmed grasslands: erosion. *Hydrol. Process.* 21, 135–139.
- Bilotta, G.S., Krueger, T., Brazier, R.E., Butler, P., Freer, J., Hawkins, J.M.B., et al., 2010. Assessing catchment-scale erosion and yields of suspended solids from improved temperate grassland. *J. Environ. Monit.* 12, 731–739.
- Bishop, K., Buffam, I., Erlandsson, M., Fölster, J., Laudon, H., Seibert, J., et al., 2008. *Aqua Incognita: the unknown headwaters*. *Hydrol. Process.* 22 (8), 1239–1242.
- Bogen, J., 1980. The hysteresis effect of sediment transport (river) systems. *Nor. Geogr. Tidsskr.* 34, 45–54.
- Bowes, M.J., House, W.A., Hodgkinson, R.A., 2003. Phosphorus dynamics along a river continuum. *Sci. Total Environ.* 313, 199–212.
- Bowes, M.J., House, W.A., Hodgkinson, R.A., Leach, D.V., 2005. Phosphorus-discharge hysteresis during storm events along a river catchment: the River Swale, UK. *Water Res.* 39, 751–762.
- Bracken, L.J., Turnbull, L., Wainwright, J., Bogaart, P., 2014. Sediment connectivity: a framework for understanding sediment transfer at multiple scales. *Earth Surf. Process. Landf.* 40 (2), 177–188.
- Bull, L.J., 1997. Magnitude and variation in the contribution of bank erosion to the suspended sediment load of the River Severn, UK. *Earth Surf. Process. Landf.* 22, 1109–1123.
- Burt, T.P., 2001. Integrated management of sensitive catchment systems. *Catena* 42, 275–290.
- Carling, P.A., 1983. Particulate dynamics, dissolved and total load, in two small basins, northern Pennines, UK. *Hydrol. Sci.* 28, 355–375.
- Chanat, J.G., Rice, K.C., Hornberger, G.M., 2002. Consistency of patterns in concentration–discharge plots. *Water Resour. Res.* 38, 22-1–22-10.
- Collins, A.L., Walling, D.E., 2004. Documenting catchment suspended sediment sources: problems, approaches and prospects. *Prog. Phys. Geogr.* 28, 159–196.
- Collins, A.L., Ohandja, D.G., Hoare, D., Voulvoulis, N., 2012. Implementing the Water Framework Directive: a transition from established monitoring networks in England and Wales. *Environ. Sci. Pol.* 17, 49–61.
- Cotton, J.A., Wharton, G., Bass, J.A.B., Heppell, C.M., Wotton, R.S., 2006. The effects of seasonal changes to in-stream vegetation cover on patterns of flow and accumulation of sediment. *Geomorphology* 77, 320–334.
- Cranfield University, 2014. *The Soils Guide*. Cranfield University.
- de Vente, J., Poesen, J., 2005. Predicting soil erosion and sediment yield at the basin scale: scale issues and semi-quantitative models. *Earth Sci. Rev.* 71, 95–125.
- Dean, S., Freer, J., Beven, K., Wade, A., Butterfield, D., 2009. Uncertainty assessment of a process-based integrated catchment model of phosphorus. *Stoch. Environ. Res. Risk Assess.* 23, 991–1010.
- Deasy, C., Brazier, R.E., Heathwaite, A.L., Hodgkinson, R., 2009. Pathways of runoff and sediment transfer in small agricultural catchments. *Hydrol. Process.* 23, 1349–1358.
- Dils, R.M., Heathwaite, A.L., 1999. The controversial role of tile drainage in phosphorus export from agricultural land. *Water Sci. Technol.* 39, 55–61.
- Eder, A., Strauss, P., Krueger, T., Quinton, J.N., 2010. Comparative calculation of suspended sediment loads with respect to hysteresis effects (in the Petzenkirchen catchment, Austria). *J. Hydrol.* 389, 168–176.
- Eder, A., Exner-Kittridge, M., Strauss, P., Blöschl, G., 2014. Re-suspension of bed sediment in a small stream – results from two flushing experiments. *Hydrol. Earth Syst. Sci.* 18, 1043–1052.
- Eisenreich, S.J., Bannerman, R.T., Armstrong, D.E., 1975. A simplified phosphorus analysis technique. *Environ. Lett.* 9, 43–53.
- Ewen, J., Geris, J., O'Donnell, G., Mayes, Q., O'Connell, E., 2010. *Multiscale Experimentation, Monitoring and Analysis of Long-term Land Use Changes and Flood Risk – SC060092: Final Science Report*. Newcastle University, Newcastle-Upon-Tyne.
- Foster, I.D.L., Chapman, A.S., Hodgkinson, R.M., Jones, A.R., Lees, J.A., Turner, S.E., et al., 2003. Changing suspended sediment and particulate phosphorus loads and pathways in underdrained lowland agricultural catchments; Herefordshire and Worcestershire, U.K. In: Kronvang, B. (Ed.), *The Interactions Between Sediments and Water* 169. Springer, Netherlands, pp. 119–126.
- Giménez, R., Casali, J., Grande, I., Díez, J., Campo, M.A., Álvarez-Mozos, J., et al., 2012. Factors controlling sediment export in a small agricultural watershed in Navarre (Spain). *Agric. Water Manag.* 110, 1–8.
- Glendell, M., Brazier, R.E., 2014. Accelerated export of sediment and carbon from a landscape under intensive agriculture. *Sci. Total Environ.* 476–477, 643–656.
- Halliday, S., Skeffington, R., Bowes, M., Gozzard, E., Newman, J., Loewenthal, M., et al., 2014. The water quality of the River Enborne, UK: observations from high-frequency monitoring in a rural, lowland river system. *Water* 6, 150–180.
- Harrington, S.T., Harrington, J.R., 2014. Dissolved and particulate nutrient transport dynamics of a small Irish catchment: the River Owenabue. *Hydrol. Earth Syst. Sci.* 18, 2191–2200.
- Hatch, L.K., Reuter, J.E., Goldman, C.R., 1999. Daily phosphorus variation in a mountain stream. *Water Resour. Res.* 35, 3783–3791.
- Haygarth, P.M., Heathwaite, A.L., Jarvis, S.C., Harrod, T.R., 1999. Hydrological factors for phosphorus transfer from agricultural soils. In: Sparks, D.L. (Ed.), *Advances in Agronomy* volume 69. Academic Press, pp. 153–178.
- Haygarth, P.M., Condon, L.M., Heathwaite, A.L., Turner, B.L., Harris, G.P., 2005a. The phosphorus transfer continuum: linking source to impact with an interdisciplinary and multi-scaled approach. *Sci. Total Environ.* 344, 5–14.
- Haygarth, P.M., Wood, F.L., Heathwaite, A.L., Butler, P.J., 2005b. Phosphorus dynamics observed through increasing scales in a nested headwater-to-river channel study. *Sci. Total Environ.* 344, 83–106.
- Haygarth, P.M., Page, T.J.C., Beven, K.J., Freer, J., Joynes, A., Butler, P., et al., 2012. Scaling up the phosphorus signal from soil hillslopes to headwater catchments. *Freshw. Biol.* 57, 7–25.
- Heathwaite, A.L., Dils, R.M., 2000. Characterising phosphorus loss in surface and subsurface hydrological pathways. *Sci. Total Environ.* 251–252, 523–538.
- Heathwaite, A.L., Quinn, P.F., Hewett, C.J.M., 2005. Modelling and managing critical source areas of diffuse pollution from agricultural land using flow connectivity simulation. *J. Hydrol.* 304, 446–461.
- Heathwaite, A.L., Burke, S.P., Bolton, L., 2006. Field drains as a route of rapid nutrient export from agricultural land receiving biosolids. *Sci. Total Environ.* 365, 33–46.
- Hodgkinson, R.A., Withers, P.J.A., 2007. Sourcing, transport and control of phosphorus loss in two English headwater catchments. *Soil Use Manag.* 23, 92–103.
- Holden, J., Shotbolt, L., Bonn, A., Burt, T.P., Chapman, P.J., Dougill, A.J., et al., 2007. Environmental change in moorland landscapes. *Earth Sci. Rev.* 82, 75–100.
- Horsburgh, J.S., Spackman Jones, A., Stevens, D.K., Tarboton, D.G., Mesner, N.O., 2010. A sensor network for high frequency estimation of water quality constituent fluxes using surrogates. *Environ. Model. Softw.* 25, 1031–1044.
- Houghton-Carr, H., 1999. Restatement and application of the Flood Studies Report rainfall-runoff method. *Flood Estimation Handbook* vol. 4. Institute of Hydrology, Wallingford, UK.
- Jarvie, H.P., Withers, P.J.A., Hodgkinson, R., Bates, A., Neal, M., Wickham, H.D., et al., 2008. Influence of rural land use on streamwater nutrients and their ecological significance. *J. Hydrol.* 350, 166–186.
- Jordan, T.E., Whigham, D.F., Hofmocker, K.H., Pittek, M.A., 2003. Nutrient and sediment removal by a restored wetland receiving agricultural runoff. *J. Environ. Qual.* 32, 1534–1547.
- Kaiser, H., 1958. The varimax criterion for analytic rotation in factor analysis. *Psychometrika* 23, 187–200.
- Kaiser, H., 1974. An index of factorial simplicity. *Psychometrika* 39, 31–36.
- Kovacs, A., Honti, M., Zessner, M., Eder, A., Clement, A., Blöschl, G., 2012. Identification of phosphorus emission hotspots in agricultural catchments. *Sci. Total Environ.* 433, 74–88.
- Langlois, J.L., Johnson, D.W., Mehuys, G.R., 2005. Suspended sediment dynamics associated with snowmelt runoff in a small mountain stream of Lake Tahoe (Nevada). *Hydrol. Process.* 19, 3569–3580.
- Lefrançois, J., Grimaldi, C., Gascuel-Oudoux, C., Gillet, N., 2007. Suspended sediment and discharge relationships to identify bank degradation as a main sediment source on small agricultural catchments. *Hydrol. Process.* 21, 2923–2933.
- Lexartza-Artza, I., Wainwright, J., 2009. Hydrological connectivity: linking concepts with practical implications. *Catena* 79, 146–152.
- Lexartza-Artza, I., Wainwright, J., 2011. Making connections: changing sediment sources and sinks in an upland catchment. *Earth Surf. Process. Landf.* 36, 1090–1104.
- Mainstone, C.P., Dils, R.M., Withers, P.J.A., 2008. Controlling sediment and phosphorus transfer to receiving waters – a strategic management perspective for England and Wales. *J. Hydrol.* 350, 131–143.
- Mano, V., Nemery, J., Belleudy, P., Poirel, A., 2009. Assessment of suspended sediment transport in four alpine watersheds (France): influence of the climatic regime. *Hydrol. Process.* 23, 777–792.

- Marttila, H., Kløve, B., 2010. Dynamics of erosion and suspended sediment transport from drained peatland forestry. *J. Hydrol.* 388, 414–425.
- McGonigle, D.F., Burke, S.P., Collins, A.L., Gartner, R., Haft, M.R., Harris, R.C., et al., 2014. Developing Demonstration Test Catchments as a platform for transdisciplinary land management research in England and Wales. *Environ. Sci. Process. Impacts* 16, 1618–1628.
- McHugh, M., 2007. Short-term changes in upland soil erosion in England and Wales: 1999 to 2002. *Geomorphology* 86, 204–213.
- McKee, L., Eyre, B., Hossain, S., 2000. Intra- and interannual export of nitrogen and phosphorus in the subtropical Richmond River catchment, Australia. *Hydrol. Process.* 14, 1787–1809.
- Mellander, P.-E., Melland, A.R., Jordan, P., Wall, D.P., Murphy, P.N.C., Shortle, G., 2012. Quantifying nutrient transfer pathways in agricultural catchments using high temporal resolution data. *Environ. Sci. Pol.* 24, 44–57.
- Met Office, 2009. UKCP09: Average Annual Rainfall Dataset.
- Meyer, J.L., Strayer, D.L., Wallance, J.B., Eggert, S.L., Helfman, G.S., Leonard, N.E., 2007. The contribution of headwater streams to biodiversity in river networks. *J. Am. Water Resour. Assoc.* 43, 86–103.
- Naden, P., 2010. The fine-sediment cascade. In: Burt, T.P., Allison, R. (Eds.), *Sediment Cascades: An Integrated Approach*. Wiley & Sons, Chichester, UK, p. 471.
- Newson, M., 2010. Understanding 'hot-spot' problems in catchments: the need for scale-sensitive measures and mechanisms to secure effective solutions for river management and conservation. *Aquat. Conserv. Mar. Freshwat. Ecosyst.* 20, S62–S72.
- Outram, F.N., Lloyd, C.E.M., Jonczyk, J., Benskin, C.M.H., Grant, F., Perks, M.T., et al., 2014. High-frequency monitoring of nitrogen and phosphorus response in three rural catchments to the end of the 2011–2012 drought in England. *Hydrol. Earth Syst. Sci.* 18, 3429–3448.
- Owen, G.J., Perks, M.T., Benskin, C.M.H., Wilkinson, M.E., Jonczyk, J., Quinn, P.F., 2012. Monitoring agricultural diffuse pollution through a dense monitoring network in the River Eden Demonstration Test Catchment, Cumbria, UK. *Area* 44, 443–453.
- Pacheco, F.A.L., Varandas, S.G.P., Sanches Fernandes, L.F., Valle Junior, R.F., 2014. Soil losses in rural watersheds with environmental land use conflicts. *Sci. Total Environ.* 485–486, 110–120.
- Perks, M.T., Warburton, J., Bracken, L., 2014. Critical assessment and validation of a time-integrating fluvial suspended sediment sampler. *Hydrol. Process.* 28, 4795–4807.
- Pilgrim, D.H., Huff, D.D., 1983. Suspended sediment in rapid subsurface stormflow on a large field plot. *Earth Surf. Process. Landf.* 8, 451–463.
- Pionke, H.B., Gburek, W.J., Sharpley, A.N., Schnabel, R.R., 1996. Flow and nutrient export patterns for an agricultural hill-land watershed. *Water Resour. Res.* 32, 1795–1804.
- Posthumus, H., Hewett, C.J.M., Morris, J., Quinn, P.F., 2008. Agricultural land use and flood risk management: engaging with stakeholders in North Yorkshire. *Agric. Water Manag.* 95, 787–798.
- Posthumus, H., Deeks, L.K., Rickson, R.J., Quinton, J.N., 2013. Costs and benefits of erosion control measures in the UK. *Soil Use Manag.*
- Quinton, J.N., Govers, G., Van Oost, K., Bardgett, R.D., 2010. The impact of agricultural soil erosion on biogeochemical cycling. *Nat. Geosci.* 3, 311–314.
- Reid, S.C., Lane, S.N., Montgomery, D.R., Brookes, C.J., 2007. Does hydrological connectivity improve modelling of coarse sediment delivery in upland environments? *Geomorphology* 90, 263–282.
- Rhea, S.A., Miller, W.W., Blank, R.R., Palmquist, D.E., 1996. Presence and behavior of colloidal nitrogen and phosphorus in a Sierra Nevada watershed soil. *J. Environ. Qual.* 25, 1449–1451.
- Rodríguez-Blanco, M.L., Taboada-Castro, M.M., Taboada-Castro, M.T., 2013. Linking the field to the stream: soil erosion and sediment yield in a rural catchment, NW Spain. *Catena* 102, 74–81.
- Römer, W., 2009. Concepts for a more efficient use of phosphorus based on experimental observations. *Ber. Landwirtschaft.* 87, 5–30.
- Russell, M.A., Walling, D.E., Hodgkinson, R.A., 2001. Suspended sediment sources in two small lowland agricultural catchments in the UK. *J. Hydrol.* 252, 1–24.
- Sadeghi, S.H.R., Mizuyama, T., Miyata, S., Gomi, T., Kosugi, K., Fukushima, T., et al., 2008. Determinant factors of sediment graphs and rating loops in a reforested watershed. *J. Hydrol.* 356, 271–282.
- Sayer, A.M., Walsh, R.P.D., Bidin, K., 2006. Pipeflow suspended sediment dynamics and their contribution to stream sediment budgets in small rainforest catchments, Sabah, Malaysia. *For. Ecol. Manag.* 224, 119–130.
- Seeger, M., Errea, M.-P., Beguería, S., Arnáez, J., Martí, C., García-Ruiz, J.M., 2004. Catchment soil moisture and rainfall characteristics as determinant factors for discharge/suspended sediment hysteretic loops in a small headwater catchment in the Spanish Pyrenees. *J. Hydrol.* 288, 299–311.
- Sharpley, A.N., Smith, S.J., Jones, O.R., Berg, W.A., Coleman, G.A., 1992. The transport of bioavailable phosphorus in agricultural runoff. *J. Environ. Qual.* 21, 30–35.
- Shrestha, S., Kazama, F., 2007. Assessment of surface water quality using multivariate statistical techniques: a case study of the Fuji River basin, Japan. *Environ. Model. Softw.* 22, 464–475.
- Sims, J.T., Simard, R.R., Joern, B.C., 1998. Phosphorus loss in agricultural drainage: historical perspective and current research. *J. Environ. Qual.* 27, 277–293.
- Singh, K.P., Malik, A., Mohan, D., Sinha, S., 2004. Multivariate statistical techniques for the evaluation of spatial and temporal variations in water quality of Gomti River (India)—a case study. *Water Res.* 38, 3980–3992.
- Siwiek, J., Siwiek, J.P., Zelazny, M., 2013. Environmental and land use factors affecting phosphate hysteresis patterns of stream water during flood events (Carpathian Foothills, Poland). *Hydrol. Process.* 27, 3674–3684.
- Sloto, R.A., Crouse, M.Y., 1996. HYSEP: A Computer Program for Streamflow Hydrograph Separation and Analysis. U.S. Geological Survey, p. 46.
- Smith, H.G., Dragovich, D., 2009. Interpreting sediment delivery processes using suspended sediment-discharge hysteresis patterns from nested upland catchments, south-eastern Australia. *Hydrol. Process.* 23, 2415–2426.
- Soulsby, C., Gibbins, C., Wade, A.J., Smart, R., Helliwell, R., 2002. Water quality in the Scottish uplands: a hydrological perspective on catchment hydrochemistry. *Sci. Total Environ.* 294, 73–94.
- Steegen, A., Govers, G., Nachtergaele, J., Takken, I., Beuselinck, L., Poesen, J., 2000. Sediment export by water from an agricultural catchment in the Loam Belt of central Belgium. *Geomorphology* 33, 25–36.
- Sturdee, A., Foster, I., Bodley-Tickell, A.T., Archer, A., 2007. Water quality and *Cryptosporidium* distribution in an upland water supply catchment, Cumbria, UK. *Hydrol. Process.* 21, 873–885.
- Stutter, M.I., Langan, S.J., Cooper, R.J., 2008. Spatial contributions of diffuse inputs and within-channel processes to the form of stream water phosphorus over storm events. *J. Hydrol.* 350, 203–214.
- Thompson, J., Cassidy, R., Doody, D.G., Flynn, R., 2013. Predicting critical source areas of sediment in headwater catchments. *Agric. Ecosyst. Environ.* 179, 41–52.
- Valle Junior, R.F., Varandas, S.G.P., Sanches Fernandes, L.F., Pacheco, F.A.L., 2014. Environmental land use conflicts: a threat to soil conservation. *Land Use Policy* 41, 172–185.
- Valle Junior, R.F., Varandas, S.G.P., Pacheco, F.A.L., Pereira, V.R., Santos, C.F., Cortes, R.M.V., et al., 2015. Impacts of land use conflicts on riverine ecosystems. *Land Use Policy* 43, 48–62.
- VanSickle, J., Beschta, R.L., 1983. Supply-based models of suspended sediment transport in streams. *Water Resour. Res.* 19, 768–778.
- Verachtert, E., Maetens, W., Van Den Eckhaut, M., Poesen, J., Deckers, J., 2011. Soil loss rates due to piping erosion. *Earth Surf. Process. Landf.* 36, 1715–1725.
- Wade, A.J., Palmer-Felgate, E.J., Halliday, S.J., Skeffington, R.A., Loewenthal, M., Jarvie, H.P., et al., 2012. Hydrochemical processes in lowland rivers: insights from in situ, high-resolution monitoring. *Hydrol. Earth Syst. Sci.* 16, 4323–4342.
- Webb, B.W., Walling, D.E., 1982. The magnitude and frequency characteristics of fluvial transport in a Devon drainage basin and some geomorphological implications. *Catena* 9, 9–23.
- Wilkinson, M.E., Quinn, P.F., Barber, N.J., Jonczyk, J., 2014. A framework for managing runoff and pollution in the rural landscape using a Catchment Systems Engineering approach. *Sci. Total Environ.* 468–469, 1245–1254.
- Williams, G.P., 1989. Sediment concentration versus water discharge during single hydrologic events in rivers. *J. Hydrol.* 111, 89–106.
- Withers, P.J.A., Jarvie, H.P., 2008. Delivery and cycling of phosphorus in rivers: a review. *Sci. Total Environ.* 400, 379–395.
- Withers, P.J.A., Edwards, A.C., Foy, R.H., 2001. Phosphorus cycling in UK agriculture and implications for phosphorus loss from soil. *Soil Use Manag.* 17, 139–149.
- Withers, P.J.A., Hodgkinson, R.H., Adamson, H., Green, G., 2007. The impact of pasture improvement on phosphorus concentrations in soils and streams in an upland catchment in Northern England. *Agric. Ecosyst. Environ.* 122, 220–232.



# High frequency variability of environmental drivers determining benthic community dynamics in headwater streams

Cite this: *Environ. Sci.: Processes Impacts*, 2014, 16, 1629

M. A. Snell,<sup>\*a</sup> P. A. Barker,<sup>a</sup> B. W. J. Surridge,<sup>a</sup> A. R. G. Large,<sup>b</sup> J. Jonczyk,<sup>c</sup> C. McW. H. Benskin,<sup>a</sup> S. Reaney,<sup>d</sup> M. T. Perks,<sup>b</sup> G. J. Owen,<sup>d</sup> W. Cleasby,<sup>e</sup> C. Deasy,<sup>ad</sup> S. Burke<sup>f</sup> and P. M. Haygarth<sup>a</sup>

Headwater streams are an important feature of the landscape, with their diversity in structure and associated ecological function providing a potential natural buffer against downstream nutrient export. Phytobenthic communities, dominated in many headwaters by diatoms, must respond to physical and chemical parameters that can vary in magnitude within hours, whereas the ecological regeneration times are much longer. How diatom communities develop in the fluctuating, dynamic environments characteristic of headwaters is poorly understood. Deployment of near-continuous monitoring technology in sub-catchments of the River Eden, NW England, provides the opportunity for measurement of temporal variability in stream discharge and nutrient resource supply to benthic communities, as represented by monthly diatom samples collected over two years. Our data suggest that the diatom communities and the derived Trophic Diatom Index, best reflect stream discharge conditions over the preceding 18–21 days and Total Phosphorus concentrations over a wider antecedent window of 7–21 days. This is one of the first quantitative assessments of long-term diatom community development in response to continuously-measured stream nutrient concentration and discharge fluctuations. The data reveal the sensitivity of these headwater communities to mean conditions prior to sampling, with flow as the dominant variable. With sufficient understanding of the role of antecedent conditions, these methods can be used to inform interpretation of monitoring data, including those collected under the European Water Framework Directive and related mitigation efforts.

Received 13th December 2013  
Accepted 7th March 2014

DOI: 10.1039/c3em00680h

rsc.li/process-impacts

## Environmental impact

Headwater streams are a central feature of the landscape, with their diversity in structure and associated ecological function providing a potential natural buffer against downstream nutrient export. Assessment of these systems through their dominant biota, the phytobenthos, is critical given the key role of headwaters within catchments. By understanding the responses of benthic diatoms to antecedent conditions we can begin to determine key physical and chemical drivers of these communities, which could then be used to inform stream and wider catchment mitigation and monitoring efforts.

## Introduction

Headwater streams, of first and second order, drain up to 80% of catchments yet pose daunting challenges to the assessment of ecological status using indicator organisms,<sup>1–3</sup> necessary for

meeting the objectives of the European Water Framework Directive (WFD).<sup>4</sup> The dynamic nature of discharge in many headwater catchments is attributed to their small catchment areas and therefore short residence times of precipitation. This results in frequent disturbance and resetting of community structure by high discharge events and episodic nutrient fluxes.<sup>5</sup> To understand the biodiversity and ecology of headwater systems it is important to recognise that the natural flow regime of headwaters is dynamic<sup>6</sup> and that this dynamism plays a central role in determining and maintaining ecosystem integrity.<sup>7–11</sup> Traditional biomonitoring approaches are typically based on single season sampling of relatively long-lived organisms such as fish or macrophytes, or multi-season sampling of invertebrates,<sup>12–15</sup> providing only snap-shots of a community and not capturing the natural variability that defines headwaters.

<sup>a</sup>Lancaster Environment Centre, Lancaster University, Lancaster, LA1 4YQ, UK. E-mail: m.snell@lancaster.ac.uk

<sup>b</sup>School of Geography, Politics and Sociology, Newcastle University, Newcastle upon Tyne, NE1 7RU, UK

<sup>c</sup>School of Civil Engineering and Geosciences, Cassie Building, Newcastle University, Newcastle upon Tyne NE1 7RU, UK

<sup>d</sup>Department of Geography, Durham University, Durham DH1 3LE, UK

<sup>e</sup>Eden Rivers Trust, Dunmail Building, Newton Rigg Campus, Penrith, CA11 0AH, UK

<sup>f</sup>British Geological Survey, Environmental Science Centre, Nicker Hill, Keyworth, Nottingham, NG12 5GG, UK

Headwater ecosystems are often dominated by benthic communities<sup>16</sup> forming biofilms comprising a mixture of algae and microbial components.<sup>17,18</sup> Foremost amongst the algae in terms of biomass are diatoms; siliceous unicellular algae with strong environmental affinities, which are widely used in monitoring.<sup>19–23</sup> Benthic diatoms have the most rapid turnover of organisms used in stream monitoring and readily respond to changes in discharge and nutrient availability,<sup>24–27</sup> making them useful proxies of temporally-rapid ecosystem change and one of the few that can capture the dynamics of headwaters. Understanding ecological sensitivities is important if adequate baselines are to be established from which to assess attempts to mitigate diffuse pollution, in headwaters specifically and within wider river systems more generally.

The dynamic hydrological environment of headwaters ensures that nutrient resources are also highly temporally variable.<sup>28,29</sup> In small headwater catchments, nutrients enter streams through varied hydrological pathways,<sup>30–32</sup> where event-driven processes predominate, rather than the damped, baseflow-influenced hydrological regime within larger, lowland catchments.<sup>33</sup> This generates considerable variability across diverse temporal scales in nutrient concentration and nutrient availability to the benthic community in these systems.<sup>34,35</sup> Community structural variability can be captured using nutrient-sensitive metrics such as the Trophic Diatom Index (TDI).<sup>36</sup> The TDI is an index used for classifying ecological status in the UK<sup>37</sup> based on the ecological sensitivity of diatoms to water quality, and especially to total phosphorus (TP) concentration.<sup>36,38</sup> Therefore, event-driven discharge patterns and nutrient delivery processes are particularly important in understanding benthic diatom community dynamics,<sup>39</sup> which are in a continuous mode of re-set and response. It has long been established through temporal studies that benthic diatom communities are a function of not only the nutrient loading on the system but also the hydrological regime.<sup>40</sup> Further studies<sup>41</sup> conducted over 15 months in 12 New Zealand gravel-bed streams have demonstrated through monthly sampling that diatom taxonomic richness is influenced by interaction between annual flood frequency and nutrient concentrations. Despite these observations, understanding of the temporal impacts of flow-nutrient transfer relationships on community dynamics in headwaters over an extended period of time remains limited. However, advances in monitoring technology have led to the opportunity for near-continuous measurements of environmental variables such as water chemistry and discharge<sup>42–47</sup> to better determine the salient drivers of ecological communities and crucially their response period.

This paper aims to evaluate the influence of temporal variability in discharge and TP concentration on benthic headwater communities, and therefore the reliability of ecological status assessments based on infrequent sampling of these organisms. Twenty five months of diatom community data from two headwater streams in the River Eden catchment, England, were investigated to address the hypothesis that, at any given point in time, the benthic diatom community will reflect the accumulated effect of a critical period of antecedent temporal dynamics in discharge and nutrient conditions. Hence, the calculated metrics used in ecological assessments will be skewed toward

these antecedent conditions, rather than reflecting the spot water samples often collected as part of monitoring. For the first time, we attempt to define the duration of diatom community representivity and response periods in headwater streams. This evaluation will contribute to the interpretation of the ecological monitoring of water quality in headwater ecosystems, and give greater insights into diversity and species interactions that condition the resilience and dynamics of headwater phyto-benthos and, ultimately, down-stream function.<sup>48–50</sup>

## Methods

### Study area

Data were collected from two small rivers, Newby Beck (54°35'N, 02°962'W) which drains the headwaters of the Morland catchment, and Pow Beck (54°50'N, 02°57'W) which drains the Pow catchment, with areas of 12.5 and 10.5 km<sup>2</sup> respectively, within the wider River Eden catchment, NW England. These sub-catchments (Fig. 1) form part of the Defra (Department for the Environment and Rural Affairs)-funded Demonstration Test Catchments (DTC) programme, a catchment-scale research platform testing measures for addressing the effects of diffuse pollution from agriculture on stream ecosystems.<sup>42,43,47,51–54</sup>

Automatic weather stations in each catchment measure rainfall at intervals of 15 minutes.<sup>45</sup> Fixed monitoring stations, designed by NWQIS and built by AT Engineering,<sup>55</sup> are located no more than 3 m from stream channels, adjacent to biological

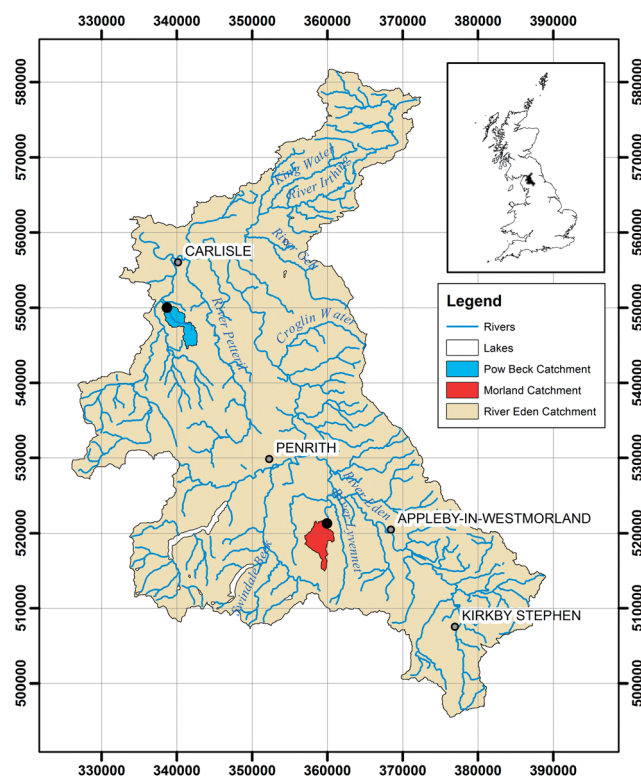


Fig. 1 Morland (Newby Beck) and Pow Beck catchments of the River Eden, NW England. Black circles indicate sampling locations for discharge, water quality and diatom communities. ©Crown Copyright/database right 2014. An Ordnance Survey/EDINA supplied service.

sampling areas providing *in situ* water quality measurements. A Hach Lange combined Sigmatax SC sampling and homogenisation unit and Phosphax Sigma wet chemistry analyser, is used to measure phosphorus concentration. A sample is taken from the watercourse using an intake pipe located mid-stream, *via* a peristaltic pump, which fills a flow cell located inside the monitoring station. The pump runs for five minutes every 30 minutes, allowing the flow cell to overflow with stream water. The Sigmatax draws a sample from the flow cell into a glass chamber, where it is homogenised by ultrasonication for 3 minutes. A 10 ml aliquot of the homogenised sample is delivered to a glass cuvette inside the Phosphax Sigma. Therefore, within the 30 minute sampling time, a single measurement of TP is made before the flow cell is re-filled. Due to asynchrony between pump timing and Sigmatax sampling frequency, the Hach Lange data is reported at hourly frequency.<sup>42,44,47</sup>

Discharge measurements are derived by applying stage–discharge relationship to 15 minute water level readings recorded by a pressure transducer. The stage–discharge relationship was developed through the collection of manual current metering measurements and extrapolated beyond the gauged range using assumptions for the stage–velocity relationship and the hydrological water balance.<sup>56</sup> To identify major errors in the high-resolution rainfall, discharge and TP time series, each dataset was visually assessed to identify anomalies. Evident outliers for periods where the readings clearly demonstrated instrument drift were removed. Missing value replacement, based on averaging of neighbouring values, was undertaken when three days or less of missing data were observed, gaps greater than three days were left blank.

From March 2011 to March 2013 mid-monthly diatom samples were taken from submerged stones in riffle areas (10–15 cm water depth).<sup>57</sup> Clean frustule suspensions were obtained by oxidizing organic matter with hot hydrogen peroxide (30% v/v). Permanent slides were then prepared using Naphrax high resolution diatom mountant. Three hundred diatom valves were identified and counted along transects at 1000× magnification, under oil immersion, with a Zeiss Axioskop microscope. Valves were identified using standard floras (primarily Krammer and Lange-Bertalot, 1986, 1988 and 1991).<sup>58</sup> Margalef Index of community diversity was calculated for each monthly diatom assemblage. Calculation and interpretation of TDI v3 and Ecological Quality Ratio (EQR) followed the WFD protocol under the classification tool DARLEQ (Diatom Assessment of River and Lake Ecological Status).<sup>59,60</sup> The TDI developed by Kelly and Whitton<sup>36</sup> and subsequently revised,<sup>61</sup> is based on the weighted average equation:

$$\frac{\sum_{j=1}^n a_j \times s_j}{\sum_{j=1}^n a_j}$$

where  $a_j$  = abundance of valves of species  $j$  in sample,  $s_j$  = pollution sensitivity of species  $j$ . Values of diatom sensitivity range from 1 (indicating low nutrient conditions) to 5 (indicating very high nutrient conditions). This equation provides

the weighted mean sensitivity (WMS) of taxa present in a given sample. TDI is the WMS expressed on a scale of 0–100, with 0 indicating low nutrient condition and 100 indicating high nutrient condition. TDI is calculated as  $(WMS \times 25) - 25$ . EQR is calculated based on the observed TDI value for a particular river system and that expected under reference conditions (see WFD UK TAG (2008) for specific details).<sup>59</sup>

Daily average rainfall, discharge and TP data were used to explore relationships with TDI and chlorophyll-a. Monthly TDI values are based on scrapes from 5 cobbles taken from riffles which are pooled to form a composite sample. Benthic chlorophyll-a measurements were taken using *in situ* fluorometry (ISF), through a hand-held probe, the BenthosTorch®.<sup>62</sup> Three cobbles were taken at random from the same riffle zones and benthic chlorophyll-a of each was measured. Results were then averaged. Calculations of antecedent forcing periods of TDI and ISF chlorophyll-a to rainfall were based on daily averaged data over 18 months for Pow, and 25 months for Newby Beck. Daily averages for discharge and TP for Newby Beck are based over 23 and 16 months, and for Pow 18 and 10 months, respectively. Pearson's  $r$  statistic was calculated between monthly TDI and chlorophyll-a against mean discharge for Pow Beck and Newby Beck, and TP for Newby Beck. The quasi-continuously sampled discharge and TP data were averaged over periods from zero to 21 days.

## Results

High temporal variability in the benthic communities of the two River Eden sub-catchments was anticipated as an ecological response to rainfall and associated discharge characteristics (Table 1) and nutrient transfer processes. The flashy hydrological regime is clearly revealed by the tight coupling between daily precipitation and discharge over a 24 month period for Newby Beck, and over a 20 month period for Pow Beck (Fig. 3). Correlations between rainfall and discharge are significantly positively correlated (Newby Beck:  $r = 0.74$ ,  $p < 0.01$ ; Pow Beck:  $r = 0.63$ ,  $p < 0.01$ ). TP concentrations are also significantly positively correlated with discharge (Newby Beck:  $r = 0.74$ ,  $p < 0.01$ ; Pow Beck:  $r = 0.54$ ,  $p < 0.01$ ). In Pow Beck, high TDI and low biomass periods are generally associated with high discharge events and corresponding peaks in TP concentration (Fig. 3). During these periods fast growing pioneer diatom species, such as *Achnanthydium minutissimum* and *Amphora pediculus*, which have optimal colonisation rates on the scoured cobble substrate, are seen to dominate up to 68% of the diatom assemblage (Fig. 2). In spring of both years *Achnanthydium minutissimum* is particularly dominant comprising more than

**Table 1** Rainfall and discharge characteristics for Morland and Pow catchments over the hydrological years 2011–12 and 2012–13

Catchment	Morland	Pow	Morland	Pow
Hydrological year	2011–2012	2011–2012	2012–2013	2012–2013
Rainfall (mm)	1205	1014	1190	801
Discharge (mm)	707	498	708	500
Rainfall : runoff ratio	0.59	0.49	0.59	0.62

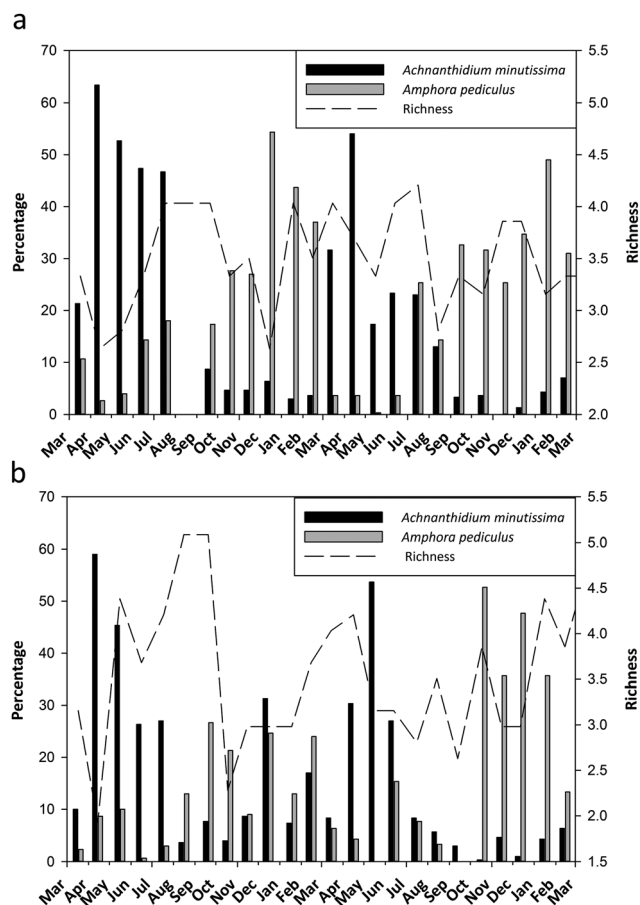


Fig. 2 Percentage assemblage dominance for (a) Morland (Newby Beck) and (b) Pow Beck of *Achnanthydium minutissimum* and *Amphora pediculus* and assemblage richness as calculated by Margalef species richness. Values calculated from March 2011 to March 2013.

50% of the diatom assemblage. *Amphora pediculus* becomes dominant throughout autumn and winter. In 2011 *Amphora pediculus* reaches a maximum of 27% in September, while in 2012 a maximum of 48% is reached in December (Fig. 2b).

Periods of higher biomass are generally associated with an increase in abundance of *Achnanthydium minutissimum*, as observed in May 2012, and *Cocconeis placentula var euglypta*, as typified in October 2011 and September 2012. In Newby Beck, key pioneer species also dominate community structure on an annual cycle with *Achnanthydium minutissimum* dominating the species assemblage in spring and early summer. *Amphora pediculus* becomes dominant from September to February, reaching maximum percentage abundance in December of both years (Fig. 2a). In Pow Beck, values of Margalef species richness demonstrated greater variation in species and assemblage heterogeneity, ranging from 1.92 to 5.08, than Newby Beck which ranged from 2.63 to 4.2 (Fig. 2).

Fig. 3 illustrates the monthly development of two measures related to the headwater diatom communities, namely the calculated TDI water quality measure and the ISF benthic chlorophyll-a. For Newby Beck (Fig. 3a), two distinct quasi-cyclic periods can be distinguished in the diatom community structure. TDI values, used here as a proxy for community structure,

are higher between September and February than March to August ( $t(10df) = -16.07, p < 0.05$ ), with a peak in December in both years, indicating a higher level of nutrient-tolerant taxa and thus, more nutrient-enriched conditions. This is supported by generally higher TP concentrations during these months. These patterns in TDI are partly tracked by benthic chlorophyll-a, which is used as a surrogate for benthic productivity. Within relatively quiescent hydrological periods, e.g. January to May 2012, broadly positive relationships between benthic productivity and community structure are observed, where lower TP concentrations and improved water quality, as inferred from the TDI, is matched by an increase in benthic chlorophyll-a. However, Fig. 3a demonstrates near anti-phasing of chlorophyll-a with TDI during high discharge episodes, such as December 2012 and January 2013. Considerable resilience of these diatom communities is highlighted by the stability of the inter-monthly TDI scores against the highly variable hydrological regime, and even the benthic chlorophyll-a. However, the annual range of TDI values is high, spanning 'high' to 'poor' EQR status and chlorophyll-a values from 1.73 to 10.35  $\mu\text{g cm}^{-2}$ .

Similar quasi-cyclic periods are observed in the Pow catchment for TDI (Fig. 3b) with TDI values indicative of poorer water conditions from September to March in both years. While monthly values of TDI across both Morland and Pow catchments are correlated over the study periods ( $r = 0.72, p < 0.05$ ), the range of TDI values in Pow (41 to 79) is less than that observed in Morland (32 to 83). Inter-monthly variations are again relatively small in Pow, but as in Newby Beck, the range is significant in terms of classification, spanning 'high' to 'poor' EQR classes. However, chlorophyll-a values range from 0.14 to 7.92  $\mu\text{g cm}^{-2}$  in Pow Beck, which is generally lower than in Newby Beck. Unlike in Newby Beck, there is usually an inverse relationship between the TDI and benthic chlorophyll-a. When values of TDI are high in Pow from October to March in both years, benthic chlorophyll-a was seen to be less than 1  $\mu\text{g cm}^{-2}$ , which is lower than chlorophyll-a in the Morland catchment. Similar to Newby Beck, there is a non-significant relationship between water temperature and chlorophyll-a (Newby Beck:  $r = 0.24, p > 0.05$ ; Pow Beck:  $r = 0.18, p > 0.05$ ). Clusters of high rainfall events and associated high stream discharges correlate with high TDI values and low chlorophyll-a, suggesting that unlike in Newby Beck, physical rather than nutrient factors dominate. Extreme examples of this inverse response in the ecological community structure and function to high discharge occurred in December 2011 and October 2012. Similarly to the case study at Newby Beck in the Morland catchment, the resilience of the communities in the Pow is evidenced by their overall stability in key species *Achnanthydium minutissimum*, *Amphora pediculus* and *Cocconeis placentula var euglypta*, and associated productivity.

## Discussion

Increases in discharge in these study catchments can occur rapidly with timescales of hours to days, and recovery from peaks to baseline conditions also occurs quickly (Fig. 3). Within the Morland catchment, these flashy hydrographs are due to the

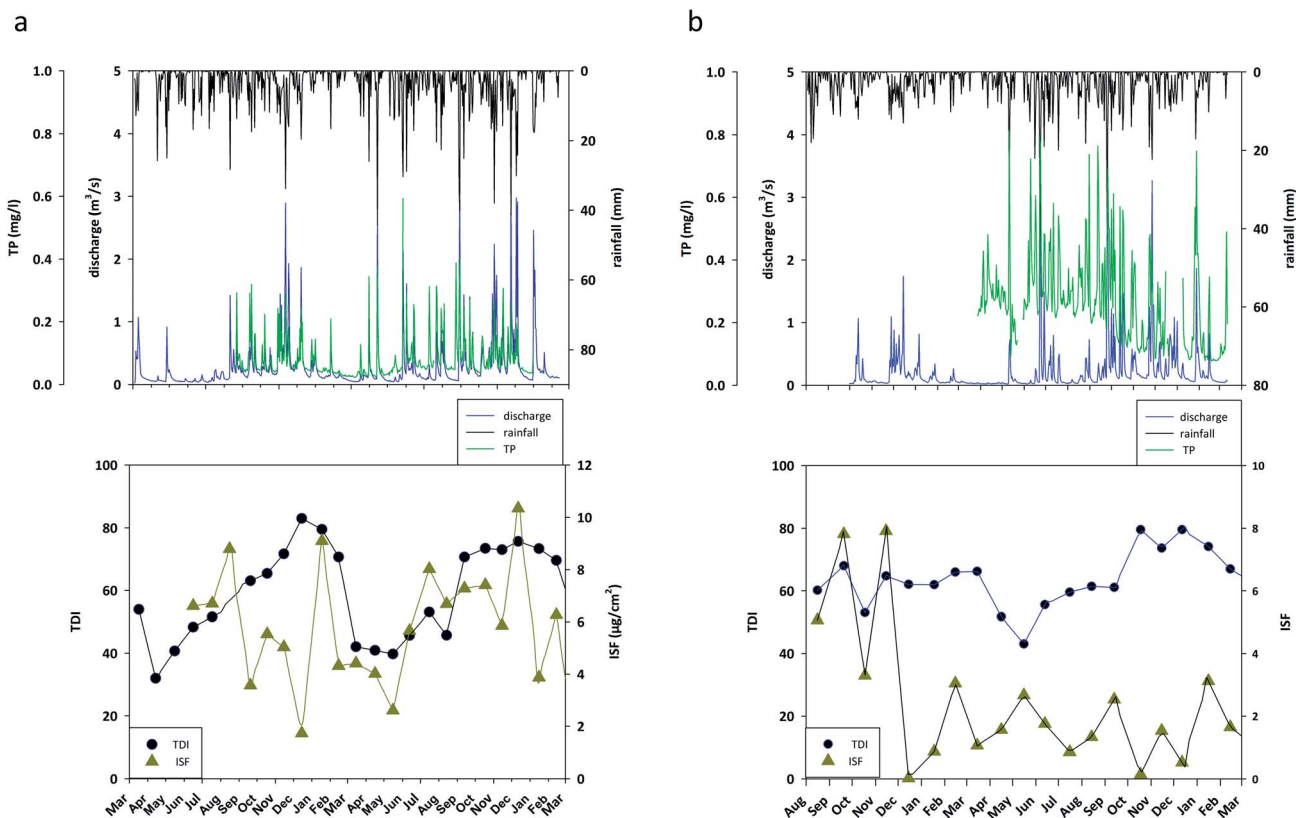


Fig. 3 Monitoring data from River Eden Demonstration Test Catchment outflow stations (a) Morland (Newby Beck) (b) Pow Beck for the period 2011–2013. Precipitation, discharge and TP values presented as daily averages. Monthly ecological sampling has been used to calculate the trophic diatom index (TDI) and *in situ* fluorometric chlorophyll-*a* (and fitted with spline curve).

steepness of the terrain and shallow soils overlying bedrock. As clay-rich glacial till is widespread in the Pow catchment, surface runoff can quickly be generated following rainfall. Similarly in other catchments this flashy hydrological response has been shown to contribute to extremely variable nutrient concentrations,<sup>46,63,64</sup> which benthic communities, with longer regeneration times, must respond to. Key questions in in-stream ecological assessment are how these benthic communities respond and recover from event-driven disturbances, and how sensitive they are to antecedent nutrient and discharge conditions.

Despite the dynamic nature of the physical environment, strong similarities in the overall structural and functional benthic ecosystem changes in these two headwater streams are observed. The primary control appears to be rainfall and associated discharge, which is coherent between these geographically related sites. For both Newby Beck and Pow Beck, TDI increases as discharge increases, indicating delivery of nutrients to the streams during high rainfall and associated discharge events. Conversely, chlorophyll-*a* values tend to be lower during high discharge events. This is most likely a combination of high bed shear stress scouring the biofilms, probably enhanced by sediment abrasion, and lower light levels restricting photosynthesis under deep water with high turbidity levels.<sup>65–67</sup> Our data suggest that yearly biomass of the community can change 10-fold, whereas month-on-month community composition

remains relatively stable within the annual cycle. The TDI does mask some internal variation in assemblage diversity of more specialist species, but the value is largely controlled by the ratio of aforementioned key pioneer species that are both present and abundant all year round in the benthic assemblage, and have the ability to withstand changes in their habitat associated with discharge including shear stress, light and nutrient concentration. From a community perspective, these flow related habitat characteristics can be significant in terms of succession stage,<sup>68–70</sup> with successional state having a direct result on metric scores and WFD classification.<sup>71</sup>

This lends to the hypothesis that at any point in time the benthic diatom community will represent a critical time period which reflects the cumulative impact of antecedent temporal dynamics in discharge–nutrient conditions. The continuous water chemistry, rainfall, and discharge data collected by the EdenDTC project enables the critical antecedent period determining the diatom community structure (using TDI as a surrogate) and biomass (ISF benthic chlorophyll-*a*) to be investigated. Fig. 4 shows that the TDI is positively correlated with mean discharge and the strength of the correlation increases according to the antecedent period. For Newby Beck an initial correlation is found between TDI and mean discharge on the day of diatom sampling ( $p < 0.05$ ,  $r = 0.54$ ), which strengthens to a maximum after 18 days ( $p < 0.05$ ,  $r = 0.7$ ). Significant correlations are also observed between TDI and TP

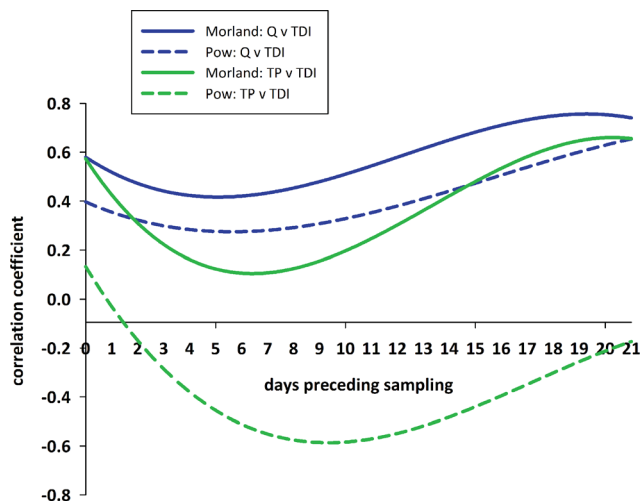


Fig. 4 Antecedent forcing periods of TDI. Pearson's  $r$  is calculated between TDI and mean discharge and TP for Pow and Newby Beck. The continuously sampled environmental data is averaged over periods from zero to 21 days. Curves are 3rd order polynomial regressions. The TDI data are collected monthly over 25 months for Newby Beck ( $n = 25$ ) and 18 months for Pow Beck ( $n = 18$ ).

after 15 days ( $p < 0.05$ ,  $r = 0.53$ ), but this increases further to a maximum after 21 days ( $p < 0.05$ ,  $r = 0.66$ ). A similar correlation with discharge is observed in Pow Beck, although with lower coefficients and a maximum is reached later (21 days;  $p < 0.05$ ;  $r = 0.63$ ). For Pow Beck, significant correlations are observed between TDI and TP between 7 and 12 days ( $p < 0.05$ ,  $r = -0.6$ ). Overall, this indicates that at-a-point community composition is a product of factors related to discharge over the preceding 15–21 days. Given the positive relationship between discharge and TP in the Morland catchment, it is possible the relationship between TDI and discharge is partly mediated by nutrient concentration.

In Newby Beck and Pow Beck, a non-significant relationship is found between benthic chlorophyll-*a* and antecedent discharge–TP conditions, thus indicating that antecedent conditions over the preceding 21 days are not key determinands of benthic productivity, which may be due to disturbance frequency.<sup>5</sup> While non-significant relationships are observed between benthic productivity and antecedent discharge–TP conditions, a clear response to high discharge conditions is evident in Fig. 3. This is consistent with community structure being defined by nutrient supply and retention within benthic biofilms,<sup>72</sup> whereas physical controls on productivity, especially damage to biofilms through scouring, may be expected to have a more immediate influence.<sup>40</sup> This analysis demonstrates that aspects of community structure and ecological functional processes, such as chlorophyll-*a* production, respond differently to antecedent discharge and nutrient conditions, and that this may be dependent on catchment specific factors such as geology and land use which may be equally important determinands of these benthic communities as climate.<sup>73–75</sup>

Our results confirm temporal coupling between benthic algal biomass and nutrient concentrations in the two streams through the monthly sampling period, although the relationship between

these variables differs in its strength and direction. The near-cyclical patterns observed in the two years of ecological data from both Eden sub-catchments suggest that variability linked to rainfall patterns on an almost seasonal basis is an inherent part of these systems. Note, these are not true seasonal cycles, but rather are linked to clusters in the incidence of precipitation and nutrient delivery. The ability of the community to recover from event-driven disturbances to their underlying equilibrium with water quality implies considerable resilience.<sup>76</sup> Moreover, sustained differences in the magnitude of the TDI and chlorophyll-*a* levels between Newby Beck and Pow Beck highlights the importance of catchment specific factors, as well as temporal changes in physical and chemical variables. The two similarly sized catchments have comparable rainfall and discharge characteristics, yet local influences on the stream ecology are likely, including geology, water flow paths, residence times and most importantly, farming practices.<sup>77–80</sup>

Due to the inherent variability of headwater streams it is important that ecological monitoring is conducted at an appropriate temporal resolution, and employs appropriate community measures.<sup>81</sup> These data imply that a single season monitoring frequency, such as those suggested under the WFD, is inadequate and is unlikely to give results representative of the full annual cycle. At the other extreme, the benthic diatom community structure will not reflect single events, but rather an accumulated average of the preceding two to three weeks of stream physical and chemical condition. This finding is beneficial to studies of baseline water quality conditions and highlights the time-integrating property of water quality assessments based on benthic community structure.<sup>82</sup>

## Conclusion

The opportunities provided by near-continuous environmental measurements within the DTC programme, have revealed the time-scale of response and sensitivities of benthic ecosystems in headwaters. The data indicate that assessment tools and metrics developed under the WFD for lower order rivers can be applied to headwater streams despite their dynamic nature, and that they can discriminate nutrient pressures between catchments. Nevertheless, it is essential to understand the importance of the impact of precipitation on these streams, and therefore both climate change<sup>83</sup> and land use management<sup>84</sup> have to be considered in parallel when planning for the future. Both of these factors can only be evaluated against long term data sets and an understanding of catchment processes across all seasons for several years. An appropriate temporal approach of multi-annual duration that encompasses both short term events and seasonal variability would provide particular value in terms of informing mitigation efforts to reduce diffuse pollution. Future research should be focused on improving understanding of benthic community composition and productivity in appropriate temporal frameworks, and environmental decision-making must accommodate event-driven physical and chemical processes, as only by understanding the real-time dynamics of headwaters can we fully understand the ecology of these streams.

## Acknowledgements

We thank our funding project: Defra FFG0909 – Design and implementation of monitoring approach at catchment scale, and development of the catchment conceptual (WQ0210). We would also like to thank other EdenDTC team members: D. Bellaby, L. Dugdale, B. Harris, M. Holloway, S. Johnson, T. Marsh, D. McGonigle, G. O'Donnell, M. Ockenden, P. Quinn, J. Quinton, and M. Wilkinson.

## References

- 1 K. Tockner and J. A. Stanford, *Environ. Conserv.*, 2002, **29**, 308–330.
- 2 L. Benda, M. A. Hassan, M. Church and C. L. May, *J. Am. Water Resour. Assoc.*, 2005, **41**, 835–851.
- 3 J. L. Meyer, D. L. Strayer, J. B. Wallace, S. L. Eggert, G. S. Helfman and N. E. Leonard, *J. Am. Water Resour. Assoc.*, 2007, **43**, 86–103.
- 4 W. Directive, *Off. J. Eur. Communities: Inf. Not.*, 2000, **22**, 2000.
- 5 K. Lohman, J. R. Jones and B. D. Perkins, *Can. J. Fish. Aquat. Sci.*, 1992, **49**, 1198–1205.
- 6 N. L. Poff, J. D. Allan, M. B. Bain, J. R. Karr, K. L. Prestegard, B. D. Richter, R. E. Sparks and J. C. Stromberg, *Bioscience*, 1997, **47**, 769–784.
- 7 V. H. Resh, A. V. Brown, A. P. Covich, M. E. Gurtz, H. W. Li, G. W. Minshall, S. R. Reice, A. L. Sheldon, J. B. Wallace and R. C. Wissmar, *Journal of the North American Benthological Society*, 1988, **7**, 433–455.
- 8 S. E. Bunn and A. H. Arthington, *Environ. Manage.*, 2002, **30**, 492–507.
- 9 N. L. Poff, *Journal of the North American Benthological Society*, 1992, **11**, 86–92.
- 10 A. H. Arthington, S. E. Bunn, N. L. Poff and R. J. Naiman, *Ecol. Appl.*, 2006, **16**, 1311–1318.
- 11 W. A. Monk, P. J. Wood, D. M. Hannah and D. A. Wilson, *River Res. Appl.*, 2008, **24**, 988–1001.
- 12 N. T. H. Holmes, P. J. Boon and T. A. Rowell, *Aquat. Conservat. Mar. Freshwat. Ecosyst.*, 1998, **8**, 555–578.
- 13 H. A. Hawkes, *Water Res.*, 1998, **32**, 964–968.
- 14 K. D. Fausch, J. R. Karr and P. R. Yant, *Trans. Am. Fish. Soc.*, 1984, **113**, 39–55.
- 15 M. K. Joy and R. G. Death, *Freshwater Biol.*, 2002, **47**, 2261–2275.
- 16 L. Kupe, F. Schanz and R. Bachofen, *Clean: Soil, Air, Water*, 2008, **36**, 84–91.
- 17 G. G. Geesey, R. Mutch, J. W. Costerton and R. B. Green, *Limnol. Oceanogr.*, 1978, **23**, 1214–1223.
- 18 Y. Hodoki, *Hydrobiologia*, 2005, **539**, 27–34.
- 19 M. G. Kelly, A. Cazaubon, E. Coring, A. Dell' Uomo, L. Ector, B. Goldsmith, H. Guasch, J. Hurlimann, A. Jarlman, B. Kawecka, J. Kwandrans, R. Laugaste, E. A. Lindstrom, M. Leitao, P. Marvan, J. Padisak, E. Pipp, J. Prygiel, E. Rott, S. Sabater, H. van Dam and J. Vizinet, *J. Appl. Phycol.*, 1998, **10**, 215–224.
- 20 N. J. Smucker and M. L. Vis, *Journal of the North American Benthological Society*, 2009, **28**, 659–675.
- 21 M. Feio, S. Almeida, S. Craveiro and A. Calado, *Ecol. Indic.*, 2009, **9**, 497–507.
- 22 S. Blanco, C. Cejudo-Figueiras, L. Tudesque, E. Becares, L. Hoffmann and L. Ector, *Hydrobiologia*, 2012, **695**, 199–206.
- 23 Y. D. Pan, R. J. Stevenson, B. H. Hill, A. T. Herlihy and G. B. Collins, *Journal of the North American Benthological Society*, 1996, **15**, 481–495.
- 24 C. Tien, W. Wu, T. Chuang and C. Chen, *Chemosphere*, 2009, **76**, 1288–1295.
- 25 F. Rimet, H. M. Cauchie, L. Hoffmann and L. Ector, *J. Appl. Phycol.*, 2005, **17**, 119–128.
- 26 J. McGrady-Steed and P. J. Morin, *Ecology*, 2000, **81**, 361–373.
- 27 A. Burns and D. S. Ryder, *Ecol. Manag. Restor.*, 2001, **2**, 53–64.
- 28 J. L. Meyer, W. H. McDowell, T. L. Bott, J. W. Elwood, C. Ishizaki, J. M. Melack, B. L. Peckarsky, B. J. Peterson and P. A. Rublee, *Journal of the North American Benthological Society*, 1988, **7**, 410–432.
- 29 C. L. Dent and N. B. Grimm, *Ecology*, 1999, **80**, 2283–2298.
- 30 A. C. Edwards and P. J. A. Withers, *J. Hydrol.*, 2008, **350**, 144–153.
- 31 L. Heathwaite, P. Haygarth, R. Matthews, N. Preedy and P. Butler, *J. Environ. Qual.*, 2005, **34**, 287–298.
- 32 D. W. Meals, S. A. Dressing and T. E. Davenport, *J. Environ. Qual.*, 2010, **39**, 85–96.
- 33 P. M. Haygarth, F. L. Wood, A. L. Heathwaite and P. J. Butler, *Sci. Total Environ.*, 2005, **344**, 83–106.
- 34 D. D. Hart and C. M. Finelli, *Annu. Rev. Ecol. Syst.*, 1999, **30**, 363–395.
- 35 I. Lavoie, S. Campeau, F. Darchambeau, G. Cabana and P. J. Dillon, *Freshwater Biol.*, 2008, **53**, 827–841.
- 36 M. G. Kelly and B. A. Whitton, *J. Appl. Phycol.*, 1995, **7**, 433–444.
- 37 M. Kelly, S. Juggins, R. Guthrie, S. Pritchard, J. Jamieson, B. Rippey, H. Hirst and M. Yallop, *Freshwater Biol.*, 2008, **53**, 403–422.
- 38 J. G. Winter and H. C. Duthie, *Journal of the North American Benthological Society*, 2000, **19**, 32–49.
- 39 J. M. Davies and M. L. Bothwell, *Freshwater Biol.*, 2012, **57**, 2602–2612.
- 40 B. Biggs and M. Close, *Freshwater Biol.*, 1989, **22**, 209–231.
- 41 B. J. F. Biggs and R. A. Smith, *Limnol. Oceanogr.*, 2002, **47**, 1175–1186.
- 42 A. J. Wade, E. J. Palmer-Felgate, S. J. Halliday, R. A. Skeffington, M. Loewenthal, H. P. Jarvie, M. J. Bowes, G. M. Greenway, S. J. Haswell, I. M. Bell, E. Joly, A. Fallatah, C. Neal, R. J. Williams, E. Gozzard and J. R. Newman, *Hydrol. Earth Syst. Sci.*, 2012, **16**, 4323–4342.
- 43 M. J. Bowes, E. J. Palmer-Felgate, H. P. Jarvie, M. Loewenthal, H. D. Wickham, S. A. Harman and E. Carr, *J. Environ. Monit.*, 2012, **14**, 3137–3145.
- 44 P. Jordan, J. Arnscheidt, H. McGrogan and S. McCormick, *Hydrol. Earth Syst. Sci.*, 2005, **9**, 685–691.
- 45 G. J. Owen, M. T. Perks, C. M. H. Benskin, M. E. Wilkinson, J. Jonezyk and P. F. Quinn, *Area*, 2012, **44**, 443–453.

- 46 R. Cassidy and P. Jordan, *J. Hydrol.*, 2011, **405**, 182–193.
- 47 P. Jordan, A. Arnscheidt, H. McGrogan and S. McCormick, *Hydrol. Earth Syst. Sci.*, 2007, **11**, 372–381.
- 48 R. L. Vannote, G. W. Minshall, K. W. Cummins, J. R. Sedell and C. E. Cushing, *Can. J. Fish. Aquat. Sci.*, 1980, **37**, 130–137.
- 49 R. B. Alexander, E. W. Boyer, R. A. Smith, G. E. Schwarz and R. B. Moore, *J. Am. Water Resour. Assoc.*, 2007, **43**, 41–59.
- 50 T. Gomi, R. C. Sidle and J. S. Richardson, *Bioscience*, 2002, **52**, 905–916.
- 51 ADAS, *Hampshire Avon Demonstration Test Catchment (DTC) Project*, <http://www.avondtc.org.uk/>, accessed 05/12, 2013.
- 52 UEA, *River Wensum Demonstration Test Catchment Project*, <http://www.wensumalliance.org.uk/>, accessed 05/12, 2013.
- 53 EdenDTC, *EdenDTC – A DEFRA Demonstration Test Catchment*, accessed 21/11/2013, 2013.
- 54 NDTCN, *Demonstrating Catchment Management: Learning from the Demonstration Test Catchment Projects*, <http://www.demonstratingcatchmentmanagement.net/>, accessed 05/2013.
- 55 TEng, Tadley Engineering Ltd, accessed 15, 2014.
- 56 J. Ewen, J. Geris, G. O'Donnell, J. Meyes and O. C. E. O'Connell, *Multiscale Experimentation, Monitoring and Analysis of Long-term Land Use Changes and Flood Risk*, Newcastle University, 2010.
- 57 CEN, *Water Quality – Guidance Standard for the Routine Sampling and Pretreatment of Benthic Diatoms from Rivers*, EN 13946:2003, Geneva, 2003.
- 58 CEN, *Water Quality – Guidance Standard for the Identification, Enumeration and Interpretation of Benthic Diatom Samples from Running Waters*, EN 14407:2004, Geneva, 2004.
- 59 WFD U.K. TAG, *Phytobenthos - Diatom Assessment for River Ecological Status (DARES)*, SNIFFER, Edinburgh, 2008.
- 60 DARES, *Diatom Assessment of River Ecological Status*, <http://craticula.ncl.ac.uk/DARES/>, accessed 17/11, 2013.
- 61 M. G. Kelly, C. Adams, J. Jamieson, J. Krokowski, E. B. Lycett, J. Murray-Bligh, S. Pritchard, and C. Wilkins, *The Trophic Diatom Index: A User's Manual Revised Edition*, Environment Agency, Bristol, 2001.
- 62 C. Carpentier, A. Dahlhaus, N. van de Giesen and B. Marsalek, *Environ. Sci.: Processes Impacts*, 2013, **15**, 783–793.
- 63 N. M. Johnson, G. E. Likens, F. H. Bormann, D. W. Fisher and R. S. Pierce, *Water Resour. Res.*, 1969, **5**, 1353–1363.
- 64 M. J. Hinton, S. L. Schiff and M. C. English, *Biogeochemistry*, 1997, **36**, 67–88.
- 65 K. Lange, A. Liess, J. J. Piggott, C. R. Townsend and C. D. Matthaei, *Freshwater Biol.*, 2011, **56**, 264–278.
- 66 B. P. G. Smith, P. S. Naden, G. J. L. Leeks and P. D. Wass, *Sci. Total Environ.*, 2003, **314**, 451–474.
- 67 K. Besemer, G. Singer, I. Hodl and T. J. Battin, *Appl. Environ. Microbiol.*, 2009, **75**, 7189–7195.
- 68 C. G. Peterson and R. J. Stevenson, *Ecology*, 1992, **73**, 1445–1461.
- 69 B. J. F. Biggs and H. A. Thomsen, *J. Phycol.*, 1995, **31**, 233–241.
- 70 M. R. Luttenton and C. Baisden, *Hydrobiologia*, 2006, **561**, 111–117.
- 71 H. Mykra, T. Saarinen, M. Tolkkinen, B. McFarland, H. Hamalainen, K. Martinmaki and B. Klove, *Ecol. Indic.*, 2012, **18**, 208–216.
- 72 S. Findlay and R. L. Sinsabaugh, *Microb. Ecol.*, 2006, **52**, 491–500.
- 73 F. Rimet, L. Ector, H. M. Cauchie and L. Hoffmann, *Hydrobiologia*, 2004, **520**, 105–117.
- 74 J. N. Houser, P. J. Mulholland and K. O. Maloney, *J. Environ. Qual.*, 2006, **35**, 352–365.
- 75 S. Sabater, A. Elosegi, V. Acuna, A. Basaguren, I. Munoz and J. Pozo, *Sci. Total Environ.*, 2008, **390**, 475–484.
- 76 J. H. Connell and W. P. Sousa, *Am. Nat.*, 1983, **121**, 789–824.
- 77 J. Soinenen and J. Weckstrom, *Fundam. Appl. Limnol.*, 2009, **174**, 205–213.
- 78 B. L. Brown, C. M. Swan, D. A. Auerbach, E. H. C. Grant, N. P. Hitt, K. O. Maloney and C. Patrick, *Journal of the North American Benthological Society*, 2011, **30**, 310–327.
- 79 J. Heino, *Biol. Rev.*, 2013, **88**, 166–178.
- 80 N. J. Smucker and M. L. Vis, *Ecol. Indic.*, 2011, **11**, 1191–1203.
- 81 K. Irvine, *Aquat. Conservat. Mar. Freshwat. Ecosyst.*, 2004, **14**, 107–112.
- 82 M. G. Kelly, *Environ. Pollut.*, 2003, **125**, 117–122.
- 83 I. Durance and S. J. Ormerod, *Global Change Biol.*, 2007, **13**, 942–957.
- 84 I. Donohue, D. Styles, C. Coxon and K. Irvine, *J. Hydrol.*, 2005, **304**, 183–192.





Contents lists available at ScienceDirect

Science of the Total Environment

journal homepage: [www.elsevier.com/locate/scitotenv](http://www.elsevier.com/locate/scitotenv)

## Simulating high frequency water quality monitoring data using a catchment runoff attenuation flux tool (CRAFT)

Russell Adams<sup>a,\*</sup>, Paul F. Quinn<sup>a</sup>, Matthew Perks<sup>b</sup>, Nicholas J. Barber<sup>c</sup>, Jennine Jonczyk<sup>a</sup>, Gareth J. Owen<sup>a</sup>

<sup>a</sup> School of Civil Engineering and Geosciences, Newcastle University, Newcastle Upon Tyne NE1 7RU, UK

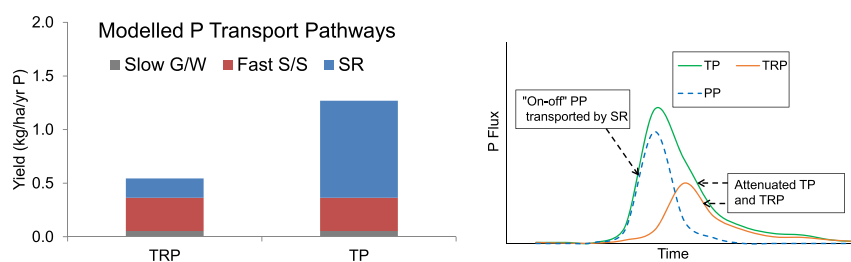
<sup>b</sup> School of Geography, Politics and Sociology, Newcastle University, Newcastle Upon Tyne NE1 7RU, UK

<sup>c</sup> Dept. of Geography, Science Laboratories, Durham University, South Rd, Durham DH1 3LE, UK

### HIGHLIGHTS

- The Catchment Runoff Attenuation Flux tool (CRAFT) model has been used to model sediment and phosphorus export.
- The model was applied to the Newby Beck catchment in NW England.
- Model performance was highly satisfactory in reproducing the observed runoff and high resolution water quality data.
- The results indicated that surface runoff is the major flow pathway for phosphorus and sediment export.

### GRAPHICAL ABSTRACT



### ARTICLE INFO

#### Article history:

Received 19 November 2015

Received in revised form 8 January 2016

Accepted 8 January 2016

Available online xxx

Editor: D. Barcelo

#### Keywords:

Catchment modelling

Diffuse pollution

Nutrient pollution

Phosphorus

Sediment transport

High resolution data

### ABSTRACT

High resolution water quality data has recently become widely available from numerous catchment based monitoring schemes. However, the models that can reproduce time series of concentrations or fluxes have not kept pace with the advances in monitoring data. Model performance at predicting phosphorus (P) and sediment concentrations has frequently been poor with models not fit for purpose except for predicting annual losses. Here, the data from the Eden Demonstration Test Catchments (DTC) project have been used to calibrate the Catchment Runoff Attenuation Flux Tool (CRAFT), a new, parsimonious model developed with the aim of modelling both the generation and attenuation of nutrients and sediments in small to medium sized catchments. The CRAFT has the ability to run on an hourly timestep and can calculate the mass of sediments and nutrients transported by three flow pathways representing rapid surface runoff, fast subsurface drainage and slow groundwater flow (baseflow). The attenuation feature of the model is introduced here; this enables surface runoff and contaminants transported via this pathway to be delayed in reaching the catchment outlet. It was used to investigate some hypotheses of nutrient and sediment transport in the Newby Beck Catchment (NBC) Model performance was assessed using a suite of metrics including visual best fit and the Nash-Sutcliffe efficiency. It was found that this approach for water quality models may be the best assessment method as opposed to using a single metric. Furthermore, it was found that, when the aim of the simulations was to reproduce the time series of total P (TP) or total reactive P (TRP) to get the best visual fit, that attenuation was required. The model will be used in the future to explore the impacts on water quality of different mitigation options in the catchment; these will include attenuation of surface runoff.

© 2016 Elsevier B.V. All rights reserved.

### 1. Introduction

Much research has been carried out at the field scale particularly to investigate the cycling of phosphorus (P) and fine sediments during

\* Corresponding author.

E-mail address: [russelladams68@gmail.com](mailto:russelladams68@gmail.com) (R. Adams).

storm events and to identify generation and transformation processes that can be deduced from observations (e.g. hysteresis patterns and the connectivity of the riparian zone to the hillslope during runoff events) (e.g. Halliday et al., 2014; Mellander et al., 2012; Outram et al., 2014; Perks et al., 2015). These have been studied at different scales from plot to catchment (<1 ha to 100+ km<sup>2</sup>) (e.g. Haygarth et al., 2005; Bowes et al., 2003) and in different climatic conditions to attempt to identify the transient, yet important drivers for high fluxes (e.g. antecedent conditions) without using models (e.g. Bilotta et al., 2007, 2010). Models are however necessary where predictions of the effects of land use and climate change on water quality are required (Wellen et al., 2015).

Water quality models however, have not kept pace with the proliferation of high resolution water quality monitoring networks in the past decade. The most widely used such as INCA, AGNPS/AnnAGNPS and SWAT (Wade et al., 2002; Binger et al., 2011; Gassman et al., 2007) operate on a daily or monthly timestep whereas observations of nutrient concentrations are now available at intervals as short as 30 min. Physically-based models such as SHETRAN and complex, lumped models like HSPF (Bicknell et al., 1996) are capable of simulating sub-daily fluxes of nutrients (e.g. from SHETRAN the Slapton nitrate study of Birkinshaw and Ewen, 2000; and the P modelling study in Ireland of Nasr et al., 2007) but their data requirements are onerous in terms of parameterizing both the physical catchment (e.g. gridded elevation and soil property data) and the nutrient cycle (e.g. a complete representation of the nitrogen (N) and P cycles). Wellen et al. (2015) have reviewed the performance of all the models listed above at predicting nutrients and sediments, emphasising poor performance both in terms of inaccurate predictions of concentrations and/or loads and sub-standard modelling practices (e.g. not performing a sensitivity analysis) even when running at a daily timestep. Jackson-Blake et al. (2015) have critiqued both the performance of the INCA-P model and the methods commonly used to assess performance (e.g. the Nash–Sutcliffe efficiency NSE) as being inadequate for water quality models. Beven (2009) has also critiqued the methods commonly used to evaluate hydrological models as not being appropriate in many cases and has encouraged a full evaluation of model uncertainties to be made, using the limits of acceptability as pre-defined by the modeller (e.g. Hollaway et al., this issue).

In the European Union the Water Framework Directive (WFD) (2000/60/EC) has prioritised the reduction of diffuse pollution of freshwaters from agricultural catchments (McGonigle et al., 2014). Barber and Quinn (2012) have suggested that tackling ‘incidental’ sources of N and P should be a priority in order to prevent high loads and concentrations of these agricultural pollutants entering surface water courses unchecked. In the Eden catchment, the 2012 WFD classification data (<http://data.gov.uk/dataset/wfd-surface-water-classification-status-and-objectives>) identified that 46% of the area had achieved this status, 41% was classified as “good” and 13% as “poor” or “bad”.

Several mitigation options have been studied in detail in terms of either spatially targeted (engineered) features (e.g. Barber and Quinn, 2012; Wilkinson et al., 2014) to remediate hotspots and Contributing Source Areas (CSAs; as identified by Heathwaite et al., 2005; Pionke et al., 2000), or policies such as seasonally-implemented management measures including winter breaks in slurry and fertiliser applications (e.g. the closed winter periods implemented under the Nutrients Action Programme (NAP) in Ireland, Jordan et al., 2012). An assessment has been made of the improvements caused by these options. In terms of the NAP this was made by soil P status testing and measuring of in-stream water quality using bankside analysers (Jordan et al., 2012). However, one conclusion of their study was that the “flashiness” of the hydrology was a better predictor of the P loss during the closed periods than other more traditional measures such as soil P status and fertiliser application rates. In terms of engineered features, preliminary studies have identified that concentrations of NO<sub>3</sub>, P and SS have been reduced based on observations of concentrations by constructed runoff

attenuation features: e.g. the Lady’s Well feature at Belford (Barber and Quinn, 2012; Wilkinson et al., 2014). However, further research is urgently required to quantify the benefits of mitigation projects in terms of reducing loads and fluxes at the catchment scale, although obtaining flow measurements and pollutant concentrations can be problematic in the field (Lloyd et al., 2015).

More information from models is required in order to assess their impacts on different nutrient fluxes and pathways and to better target mitigation strategies for nutrient and sediment reduction in the UK/EU and elsewhere in the world. If newly developed models are capable of successfully predicting changes to pollutant dynamics, modelling could add value to these studies and assist in their design and implementation by predicting the number and density of mitigation features that need to be constructed. It should then be possible to quantify the benefits of these improvements in terms of specific land management practices, required in order to meet specific water quality improvements (e.g. WFD) at the catchment scale by reducing diffuse pollution (McGonigle et al., 2014).

Jackson-Blake et al. (2015) have questioned how models lacking parameter values relating to different land uses (i.e. spatially lumped) can be applied to mitigation measures, especially given a lack of additional spatial monitoring data to assess model performance at a sub-catchment level. The Catchment Runoff Attenuation Flux Tool (CRAFT model; Adams et al., 2015) can explore the key concept of attenuation (and thus buffering rates) and its impact on water quality dynamics. Therefore, it can be used to assess the importance of attenuation on firstly catchment fluxes, then secondly potential management options, a feature not incorporated into the models reviewed above. The model can then be run to test different runoff hypotheses and management scenarios. Hypotheses testing against the robustness of time series of data can help to indicate both the dynamics and reproducibility of processes by a model (Jakeman et al., 2006). The model can also help to test the data information content, perhaps leading on to further improvements in order to incorporate management options such as mitigation measures (e.g. Runoff Attenuation Features – RAFs). Lastly, the model can indicate how these observations and impacts may be scaled up from the plot scale (where features are installed) to the catchment scale.

This study aims to model the delivery of fine/suspended sediment and phosphorus concentrations in a small, intensively monitored headwater catchment over a period of one year. This will enable: (i) the identification of pathway(s) that contribute the major sources of TRP, TP and SS exported from the catchment; and (ii) an examination of the potential for land management or mitigation to reduce fine sediment and nutrient exports through pollution-swapping (cf. Adams et al., 2015). The CRAFT model has been used in this study since: (i) its use allows hypotheses surrounding the major flow pathways in the catchment to be investigated; (ii) it can run on an hourly timestep thereby capturing within-storm processes (unlike INCA-P and SWAT which can only run on a daily timestep); and (iii) it enables the catchment exports of nutrients and sediments to be disaggregated into the amounts exported through each flow pathway (Adams et al., 2015). Modelling flow, nutrients and sediment is a challenge at this high frequency and many questions may arise from a detailed analysis of the data. Having a model that can simulate all the flux processes simultaneously, using a common set of soil and hydrological parameters, is also revealing in terms of model accuracy and structure. Both calibration and validation were performed using the continuous monitoring dataset. The modelling will be discussed in more detail in Section 2.2.

## 2. Methodology

### 2.1. Description of case study

We used data collected from the Newby Beck catchment in Cumbria, NW England (the NBC) as described by Perks et al. (2015). The NBC

forms a subcatchment of the much larger Eden catchment. The 2012 WFD classification data indicated that the NBC catchment had achieved “moderate” ecological status and the intention is for it to achieve “good” ecological status by 2027. It is 125 km<sup>2</sup> in area and has continuous monitoring of flow (Q) and water quality at the catchment outlet since 2011 (Fig. 1). In addition there are two tipping bucket raingauges and one weather station in the catchment also shown on Fig. 1 and the rainfall data used in the study is the average of the three values from these.

Firstly in terms of land use, the catchment is 90% improved grassland supporting intensive grazing by livestock, a mixture of dairy and beef cattle (Outram et al., 2014), see Fig. 1. There are also areas of farmland that are being reseeded or with feed (fodder) crops. The NBC consists of three categories of soils. In the headwaters to the south of the catchment are locally deep and well drained fine loamy soils. In the middle reaches of the catchment there are slowly permeable and seasonally waterlogged acid loamy to clay soils, exhibiting some degradation in

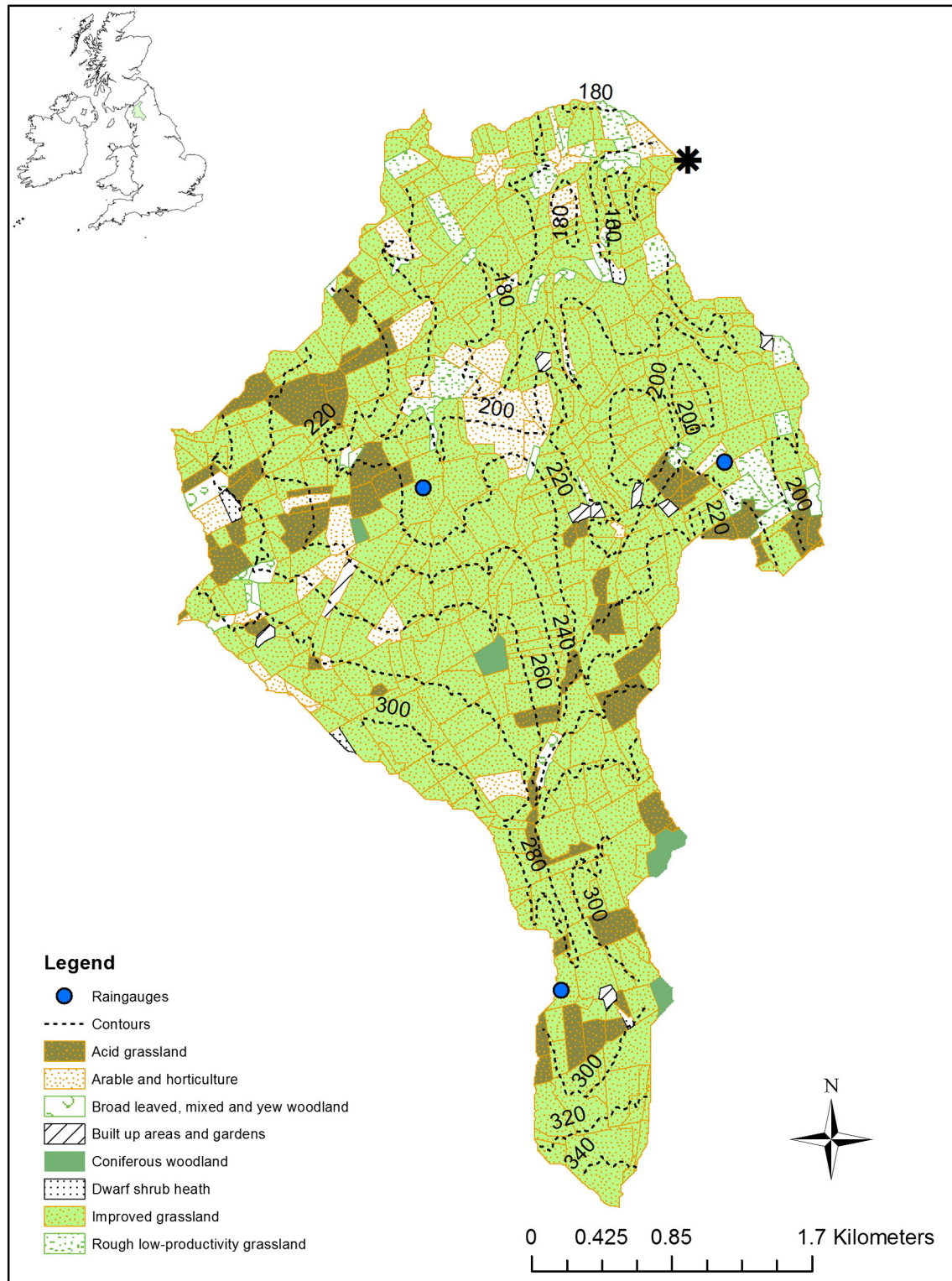


Fig. 1. Base map of Newby Beck catchment showing land use, raingauges and contours (m AOD). Catchment outlet indicated by black star. Inset shows Eden catchment (shaded).

structure. Finally, in the north of the catchment near the outlet there are reddish fine and coarse loamy soils (Cranfield University, 2014). Bedrock consists of a mixture of steeply dipping fractured limestone and sandstone units of the Carboniferous Yoredale group interbedded with argillaceous rocks (shales and mudstones) of lower permeability (Allen et al., 2010). This is overlain over most of the NBC by glacial till deposits. The long term average annual rainfall recorded in the NBC is 1187 mm (Met Office, 2009), and the regional climate is described as cool temperate maritime.

The continuous monitoring station at the catchment outlet measured TRP (total reactive phosphorus) and TP (total phosphorus) using Hach Lange combined Sigmatax sampling module and Phosphax Sigma analyser analysers at 30-min intervals (Owen et al., 2012; Perks et al., 2015). TP incorporates all phosphorus species, whilst TRP is an operationally defined measurement predominantly comprising of orthophosphate ( $\text{PO}_4$ ; SRP) in the NBC catchment (Perks et al., 2015), although readily hydrolysable P species in the sample may also be present within this TRP fraction (Halliday et al., 2014).

Turbidity was measured at 15-min intervals using a YSI 6600 multi-parameter sonde. A strong relationship (from regression analysis) between turbidity and SS (suspended sediments; collected by an autosampler at the NBC outlet during events) was identified by Perks et al. (2015), enabling turbidity to act as a proxy for SSCs. These data are used for the calculation of an “observed” yield from the catchment for modelling purposes. Loads and yields for the NBC were also calculated from the observed TRP and TP data and are shown in Table 1. During 2011–2 the mean annual TRP concentration was  $0.041 \text{ mg L}^{-1} \text{ P}$  and the mean TP concentration  $0.076 \text{ mg L}^{-1} \text{ P}$ . The mean annual SS concentration calculated through regression of SS against turbidity data was  $10.1 \text{ mg L}^{-1}$ . Perks et al. (2015) also regressed TRP against SRP concentrations (obtained from manual and automatic sampling) and estimated SRP to constitute 89% of the observed TRP concentrations. Inspection of the observed hourly time series of TRP and TP indicated that many peaks in concentration coincided with peaks in flow, and these events will subsequently be termed “Type 1” and “behavioural”. Perks et al. (2015) indicated that near stream mobilisation of P would have generated these high concentrations of P during events. The information from the hourly data will be lost if aggregated to daily mean values.

### 2.1.1. Hydrology

The first year of the continuous monitoring dataset commencing on 1st October 2011 was chosen over which to calibrate and run model simulations. Analysis of the observed flows identified both dry and wet periods during the twelve months, including runoff events in all four seasons. Runoff (specific discharge)  $Q$  was calculated by dividing the hourly flows by the catchment area. The total precipitation for 2011–2 was 1207 mm generating 709.5 mm of runoff (a runoff coefficient of 0.59). During the winter of 2011–2 most of this precipitation fell as rainfall and snow was uncommon and the winter and early spring were unusually dry (see Table 1 for the water balance), so subsequently it is referred to as “rain”. A second period of data was available for validating the model from late 2012 to early 2013. Unfortunately due to gaps in the continuous monitoring dataset it was not possible to validate the model using a year of P concentration data. Table 1 also shows the observed rainfall and runoff over this period which was also fairly wet with a high runoff coefficient.

**Table 1**  
Rainfall, flows and yields from observed data and default model (calibration and validation periods), NBC 2011–3.

Dataset	Time period	Rain (mm)	Q (mm)	TP yield ( $\text{kg ha}^{-1} \text{ year}^{-1}$ )	TRP yield ( $\text{kg ha}^{-1} \text{ year}^{-1}$ )	SS yield <sup>a</sup> ( $\text{t km}^{-2} \text{ year}^{-1}$ )
Observed (2011–2)	1/10/2011–30/9/2012	1207	709.5	1.41	0.52	38.2
Observed (2012–3)	1/11/2012–25/2/2013 <sup>b</sup>	517.1	412.0	Annual data	Not	Available
Modelled (default – calibration)	1/10/2011–30/9/2012	1207	717.8	1.27	0.54	34.9
Modelled (default – validation)	1/11/2012–25/2/2013 <sup>b</sup>	517.1	432.0	Annual data	Not	Available

<sup>a</sup> SS analysis ended on 24/5/2012 due to a period of questionable observed turbidity data in summer 2012.

<sup>b</sup> Phosphorus analysis and modelling commenced on 1/12/2012 due to missing data in November 2012.

### 2.2. Description of CRAFT model and scenarios

The CRAFT model is used in this study to simulate three different runoff pathways and the associated export of sediment and nutrients (N and P) via each. The model has been developed with the concept of runoff attenuation (pollution mitigation) in mind enabling the effects of altering one or multiple water/pollutant pathways on the export of sediment and nutrients (N and P) to be determined. A schematic diagram of the model is shown in Fig. 2. There are three stores each associated with a flow pathway (see Section 2.2.1 and Fig. 2). Rainfall is the principal factor generating surface runoff from the Dynamic Surface store when the drainage capacity of this store ( $S_{\text{DMAX}}$ ) is exceeded by the rainfall rate. Therefore, (i) selecting an appropriate value for this parameter and (ii) the choice of timestep (daily vs. hourly) are very important as both of these will influence the model's performance in terms of generating surface runoff.

Readers are directed to Adams et al. (2015) for a more detailed overview of the CRAFT model including equations for the runoff component. A full description of the model with equations has also been included in Appendix A1 in the Supplementary material and a description of the parameters can be found in Table 3. In this application, observed TRP (C) data were available for comparison with the model results. Loads are summed at the catchment outlet according to Eq. (1a), firstly for TRP ( $L_{\text{TRP}}$ )

$$L_{\text{TRP}} = Q_{\text{SS}} \times C_{\text{SS}}(\text{TRP}) + Q_{\text{GW}} \times C_{\text{GW}}(\text{TRP}) + K_{\text{SR}}(\text{TRP}) \times Q_{\text{SR}} \quad (1a)$$

Secondly, the TP load ( $L_{\text{TP}}$ ) is calculated using Eq. (1b), where the particulate P (PP) load transported by surface runoff is added to the TRP load calculated above (here the assumption is made that the PP is unreactive, insoluble P)

$$L_{\text{TP}} = L_{\text{TRP}} + K_{\text{SR}}(\text{PP}) \times Q_{\text{SR}} \quad (1b)$$

where  $Q_{\text{SS}}$  and  $C_{\text{SS}}(\text{TRP})$  are the flow and concentration of TRP in the fast subsurface pathway respectively and  $Q_{\text{GW}}$  and  $C_{\text{GW}}(\text{TRP})$  are the flow and concentration of TRP in the slow groundwater pathway respectively.

$K_{\text{SR}}(\text{PP})$  and  $K_{\text{SR}}(\text{TRP})$  are coefficients relating the concentration of PP and TRP respectively in surface runoff to the instantaneous surface runoff ( $Q_{\text{SR}}$ ) assuming that a linear concentration vs. discharge relationship applies. Suspended sediment (SS) loads are also calculated using Eq. (1a) but in this case with the  $K_{\text{SR}}$  coefficient and the concentrations in the deep groundwater  $C_{\text{GW}}$  and fast subsurface  $C_{\text{SS}}$  taking calibrated values for SS rather than P.

The CRAFT runs within a MS Excel™ interface (allowing the user to calibrate the model manually and investigate different model structures; i.e. an “Expert” mode). The NBC was not delineated into smaller units e.g. sub-catchments for modelling purposes, since the land use was dominated by improved grassland (Fig. 1) and it was assumed that a spatially lumped representation would be adequate, as has been the case in previous applications of this model to the Frome catchment. In the Frome application the model simulated runoff and pollutant concentrations at a daily time-step, thereby precluding the need to employ a delay function with it being assumed that the flood peaks reached the outlet (where the gauging station was located) within one day (Adams

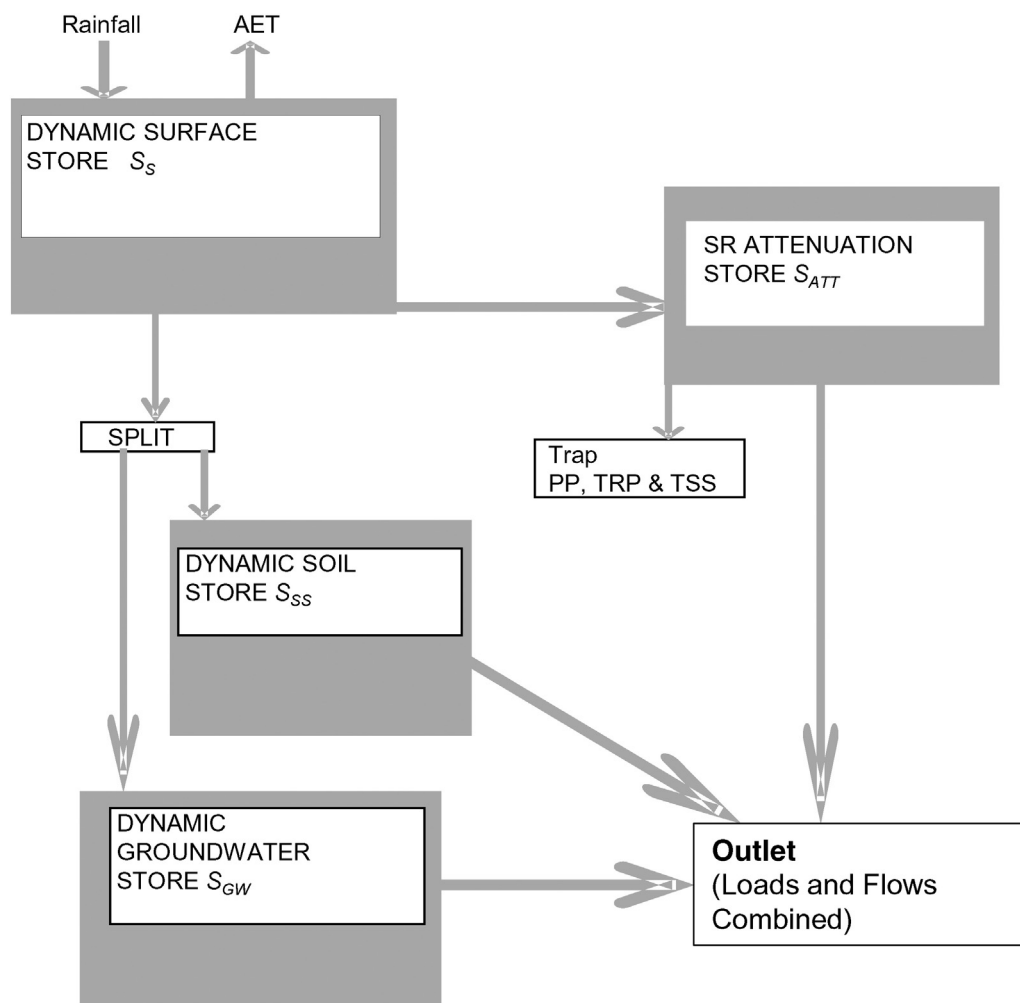


Fig. 2. Schematic diagram of CRAFT model with SR attenuation store added.

et al., 2015). For this application however, pollutants are measured at 30-min intervals and the model was run on an hourly time step (the interval of the rainfall and flow data) therefore channel routing effects could not be ignored even in this small 12.5 km<sup>2</sup> catchment.

### 2.2.1. Attenuation features of the CRAFT model

The attenuation features of the model are associated with each of the three flow pathways and are key to the performance of CRAFT. Attenuation can be adjusted by the modeller in the three flow pathways by the following:

- (i) Surface Runoff – Increasing the maximum drainage rate from the surface store  $S_{DMAX}$  to permit more drainage to the two subsurface stores, and decreasing  $K_{SURF}$  to reduce the magnitude of the peak flows. This can represent better management of the cultivated layer of the soil.
- (ii) Fast Subsurface flow – Decreasing the time constant  $K_{SS}$  to reduce the peak value of this flow. This can represent adding attenuation to the field drainage network.
- (iii) Slow Groundwater flow – Decreasing the time constant  $K_{GW}$  to lengthen recession periods in order to store water in the subsurface for a longer period of time.

It was imperative that the issue associated with routing flow through the drainage network was appropriately tackled, due to the

potential for an incorrect choice of timestep introducing timing errors depending on the speed of propagation of the flood wave down the river system. It was necessary therefore to introduce an additional component that could attenuate surface runoff (as this was identified as the most important of the three flow pathways in terms of controlling the runoff dynamics during events and floods).

### 2.2.2. Surface runoff attenuation component

Surface runoff (SR) attenuation has been achieved through the addition of a SR attenuation store, which uses a simple linear storage function to delay the surface runoff in reaching the catchment outlet based on that used by the AWBM model (Boughton, 2004). Nutrients and sediments that travel via the surface runoff pathway are also subject to attenuation, and here the assumption is made that the same delay (i.e. time lag) applies. The lagged surface runoff  $Q_{SRLAG}$  is calculated from the storage in the SR attenuation store ( $S_{ATT}$ ) by Eq. (2)

$$Q_{SRLAG} = S_{ATT} \times (1 - K_{LAG}) \quad (2)$$

where  $K_{LAG}$  is the time coefficient, representing the fraction of the SR attenuation store that drains at each timestep. Clearly, a value of unity will never permit any surface runoff, whereas a value of zero will not generate any lag (by draining the attenuation store in one timestep which is the model's default mode for a daily timestep e.g. Adams et al., 2015). The store is assumed to have infinite capacity and is empty at the start

of the simulation. A mass balance updates the value of  $S_{ATT}$  at the current times ( $t$ ) from the value at the previous one ( $t - 1$ )

$$S_{ATT}(t) = S_{ATT}(t-1) + Q_{SR} - Q_{SRLAG}. \quad (3)$$

To simulate the attenuation of sediments and nutrients the same procedure is adopted where flows are replaced by loads, e.g.  $L_{SR}(PP)$  representing the load of particulate P transported by surface runoff which is defined by Eqs (1a) and (1b) (see above). The attenuation parameter  $K_{LAG}$  can either be calibrated using the same method (e.g. using a criteria such as maximising the Nash–Sutcliffe efficiency (NSE)) as the other runoff parameters, or alternatively by visually comparing the shapes of peaks in the observed and modelled water quality concentration time series (i.e. “chemigraphs” and “sedigraphs”) and their timing, as  $K_{LAG}$  has a negligible effect on total runoff volumes or nutrient loads. The hypotheses that firstly a lag is required and secondly that different lags may apply to runoff and the different water quality variables will be explored further through a series of hypothetical model simulations.

### 2.2.3. Runoff attenuation features

The attenuation capability of CRAFT can also be used to simulate runoff attenuation features (e.g. swales and wetlands) that are constructed in the catchment as part of mitigation schemes (e.g. Wilkinson et al., 2014; Barber, 2013; Barber and Quinn, 2012; Ockenden et al., 2012). In this case a removal (or trapping) efficiency  $e$  (for surface runoff) has to be specified by the user based on data collected in the field from monitoring flow and transport through mitigation features (Barber, 2013; Ockenden et al., 2012). Fast subsurface flow can be attenuated by decreasing the value of the  $K_{SS}$  parameter to reduce the flashiness of the flow, and the flow rate can be reduced by decreasing  $K_{SPLIT}$ , to represent improved soil management and potentially pollution swapping. It is assumed for modelling purposes that the surface runoff attenuation factor  $K_{LAG}$  is the same for flow and the modelled sediments and nutrients, however the efficiency may vary (e.g. be higher for particulate nutrients than dissolved nutrients) if the user has sufficient information for this. The basic form of the removal rate equation where  $L_{SR(ATT)}$  is the load of sediment or nutrient transported by the surface runoff pathway into the attenuation store is thus written as

$$L_{SR(ATT)} = L_{SR} \times (1 - e). \quad (4)$$

A further publication will investigate how the field data can be used to parameterize the values of efficiencies for N, P and sediment removal from different types of mitigation features based on data collected from field studies (e.g. Ockenden et al., 2012; Barber, 2013).

### 2.2.4. Model calibration and validation

For the manual calibration procedure used here there are 6 parameters (described in Table 3) for the runoff component that require calibrating plus  $K_{LAG}$ . These 6 are  $K_{SURF}$ ,  $S_{DMAX}$ ,  $S_{RMAX}$ ,  $K_{SPLIT}$ ,  $K_{GW}$  and  $K_{SS}$  (cf. Adams et al., 2015). The water quality component uses Eqs. (1a) and (1b) with the related parameters for P and SS described above and in Table 3 to calculate loads, then concentrations are simply calculated by dividing the loads by the total flow. To simplify the model calibration process the ratios between  $K_{SR}(TRP)$ ,  $K_{SR}(PP)$  and  $K_{SR}(SS)$  were assumed to be fixed, thus reducing by two the number that require calibration. Evidence from the observed concentration time series at Newby Beck outlet of TRP, TP and SS was used to verify that this interdependence was plausible ( $R^2$  values between these time series  $>0.7$  were calculated). Perks et al. (2015) observed that peak event concentrations of TP were generally double that of TRP as measured at the catchment outlet.

The performance metrics used to assess the simulations were as follows: (i) for runoff: mass balance error (MBE) and Nash–Sutcliffe efficiency (NSE); (ii) for water quality: load error (LE), NSE (SS only); normalised 1/RMSE; (iii) visual fit (by eye) for runoff and water quality. These metrics were calculated on each model time series of flow and

concentration by the MS Excel™ interface, and the multi-criteria approach proposed by Jackson-Blake et al. (2015) was used rather than merely depending on a single metric to discriminate between different model runs.

Model validation was carried out using the observed data (see Section 2.1.1). The same suite of performance metrics was used to evaluate the model as were used in the calibration procedure but the model parameters themselves were not adjusted.

### 2.2.5. Alternative model structure hypotheses

The CRAFT model was developed using the Minimum Information Required (MIR) philosophy (Quinn et al., 2008). In principle MIR models are based on the amount of information which is obtained from localised and experimental studies on nutrient and sediment losses, so that the most pertinent process components can be retained in the model. A series of simulations were first carried out to determine single, optimal parameter sets for the default structure plus each of the options discussed below. These structures were:

- (1) The default with no SR attenuation component, i.e.  $K_{LAG}$  was set to zero. The parameter values were optimised to give the best fit visually to flows whilst achieving the maximum possible NSE and smallest MBE values for flows.
- (2) Using the SR attenuation component to apply a lag to the default model simulation, and calibrating an optimum value of the parameter  $K_{LAG}$  for predicting runoff and concentration. This is referred to as the “lagged” model structure and the resulting simulation as the “lagged” simulation. A sensitivity analysis on the effects of varying  $K_{LAG}$  on the NSE for each model output (flow and concentrations) was carried out as part of the calibration procedure.
- (3) Testing the lagged model with the  $K_{SURF}$ ,  $K_{SR}(PP)$  and  $K_{SR}(TRP)$  parameter values set to values intended to maximise the generation of PP and TRP in surface runoff, with the performance assessment being primarily made visually by inspecting the time series plots for goodness of fit (possibly at the expense of poorer NSE and MBE/LEs). Employing the SR attenuation component was considered to be important here to “lump and route” P to the outlet, hence this model simulation will be referred to as “LR”.

The 1/RMSE metric was used in this study following the findings of a full uncertainty analysis of the INCA-P model by Dean et al. (2009). They found it difficult to obtain positive NSE values for TP when simulating the Lugg catchment, leading to the requirement for an alternative method to the NSE metric to assess water quality model performance. This metric has a positive value for all simulations, and its value increases as the model error decreases (i.e. for a “best fit” a high value is desirable). Here it is normalised by first dividing the RMSE by the observed mean concentration of the nutrient or sediment. Wellen et al. (2015) also noted, from a review of several hundred modelling studies, that the NSEs were usually lower for water quality simulations than for runoff alone, and furthermore that the 25<sup>th</sup> percentile NSE values were lower for TP simulations than for phosphate (SRP).

The loads of SS, TRP and TP were also broken down by flow pathway (surface runoff, fast subsurface and deep groundwater) to enable the different model structures to be compared to see if there were any differences between the flow pathways and for comparison against the observed load.

## 3. Results

### 3.1. Different model structures

#### 3.1.1. Calibration of default model

The results obtained using the default model are shown firstly for the entire 2011–12 calibration period in Fig. 3 as time series plots of

modelled and observed runoff with rainfall also shown by the blue line. Secondly, in Fig. 4a–d the runoff ( $Q$  – 4a) and modelled and observed concentrations (TRP – 4b, TP – 4c and SS – 4d) at the NBC outlet are shown for August 2012 only (since this month had some interesting events which will be further discussed below). In Fig. 3, the time series plot of modelled and observed runoff indicates a good model fit over most of the year with a NSE value of 0.82 (Table 2). At higher flows, some of the peaks were under or over estimated by the model and this can be seen more readily in Fig. 4a along with a timing error of 1–2 h between the modelled and observed flow peaks, which generally occur shortly after rainfall events. There was also a tendency for the model to generate runoff after every rainfall event, where peaks were not necessarily observed, particularly in the summer months. Perks et al. (2015) reported that a time-to-peak of three hours had been estimated from the observed runoff. Surface runoff (SR) accounted for 16% of the total runoff over the year according to the default model. The baseflow index (BFI) according to the gauged flow record was 0.39 according to Ockenden et al. (this issue) which is in broad agreement with the partitioning of flows by the model (deep groundwater accounted for 50% of the total runoff). Fig. 4 also shows daily mean flows and concentrations for comparison with the hourly observed data, at a daily interval most of the information is lost from the dataset by averaging.

### 3.1.2. Validation of default model

The model results for the validation period are summarised in Table 2. Additional time series plots of the modelled and observed  $Q$ , TRP, TP and SS concentrations can be found in the Supplementary material (Fig. 9). In summary, the results for the validation period for runoff were almost as good as for the calibration period with only a small decrease in the NSE (to 0.78) and an increase in the MBE indicating that the model was overpredicting runoff depth by nearly 5%. The performance in terms of reproducing the observed nutrient and SS concentrations (the NRMSE and NSE metrics for TRP and SS) was still acceptable, although the load errors (for TP and SS) were higher than desirable. The NSE values for both TRP and SS concentrations did not reduce significantly either from those obtained during the calibration period. Interestingly the NRMSE metric indicated (for  $Q$  and P) a slightly better fit over the validation period than over the calibration period.

### 3.1.3. Results from alternative model structures

In order to assess visually the results obtained from the different model structures, some additional results from these runs are shown in Fig. 4a–d for  $Q$ , TRP, TP and SS. The parameter values, determined by manual calibration (evaluating both the default and the alternative model structures) are listed in Table 3. In the “LR” simulation the  $K_{SURF}$  parameter was increased so that SR accounted for 20% of the total runoff. However, it was not possible to distinguish any major differences in the runoff predictions compared to the default structure

over a 1 year period by using a graphical method alone, although there were clear differences in the timing of the runoff peaks in the lagged and “LR” simulations (later than in the default simulation) which can be seen in Fig. 4a. Therefore, the performances of these alternative model structures (at predicting runoff) were compared against the default CRAFT model using the metrics MBE and NSE, which are also shown in Table 2.

The time series plots of flows, nutrient and sediment concentrations covering August 2012 illustrate several issues with the observed data and the different model structures. The plots in Fig. 4b and c show that most of peaks in TRP and TP coincided with the peaks in surface runoff (in Fig. 4a) and are thus classed as Type 1 (“behavioural”) events. This finding supports the hypothesis that surface runoff is the major flow pathway for P export in the NBC also proposed by Perks et al. (2015). Visually, the simulations with a lag term applied have fitted the observed time series of TRP and TP better than the default with no lag, although there was still a tendency to underpredict or overpredict some of the observed event concentrations.

In summer 2012 in particular some peaks were observed in TRP and TP concentrations that were outside the predictive range of the calibrated model, thus these can be termed “non-behavioural” Type 2 events. One Type 2 event in particular is highlighted by a red circle (in early August 2012) in Fig. 4b and c. In this period the observed peaks in TRP and TP concentrations were not associated with correspondingly high observed runoff (and also the modelled runoff from the SR component in the CRAFT). The “LR” simulation, which in Fig. 4b and c is shown to generate higher concentrations of both TRP and TP, was not able to reproduce this observed peak either. These results may also have implications for modelling the catchment in general terms and identifying the significant flow and transport pathways. This will be discussed further below in Section 4.2.

### 3.2. Load breakdown

In order to evaluate the modelled flow pathways the loads transported by each pathway were calculated (i.e. from the time series of flow and concentrations). These are converted to annual exports (i.e. loads per unit area per year) to enable comparison to be made with other studies and the observed values (shown in the top left pane of Fig. 5 by the green bars). The observed SRP load was estimated to be 89% of the TRP load based on data analysed by Perks et al. (2015), and the dashed black line indicates this value. The observed total exports of TP, TRP and SS and the modelled exports from the default simulation over the calibration period are shown in Table 1. The yields of TRP and TP exported via the three model pathways are shown in Fig. 5 by bar charts, one from each of the different model structures. Note that the yields from the lagged and default models were identical so only two panes of results are shown. The modelled PP yields exported by the surface runoff (SR) pathway were the largest of the three flow

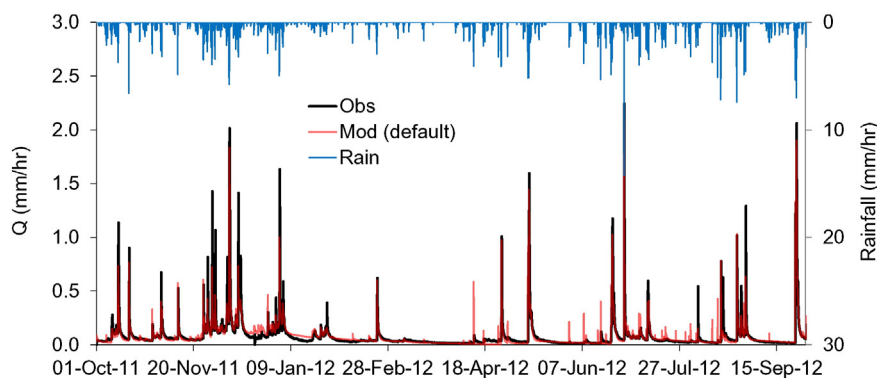
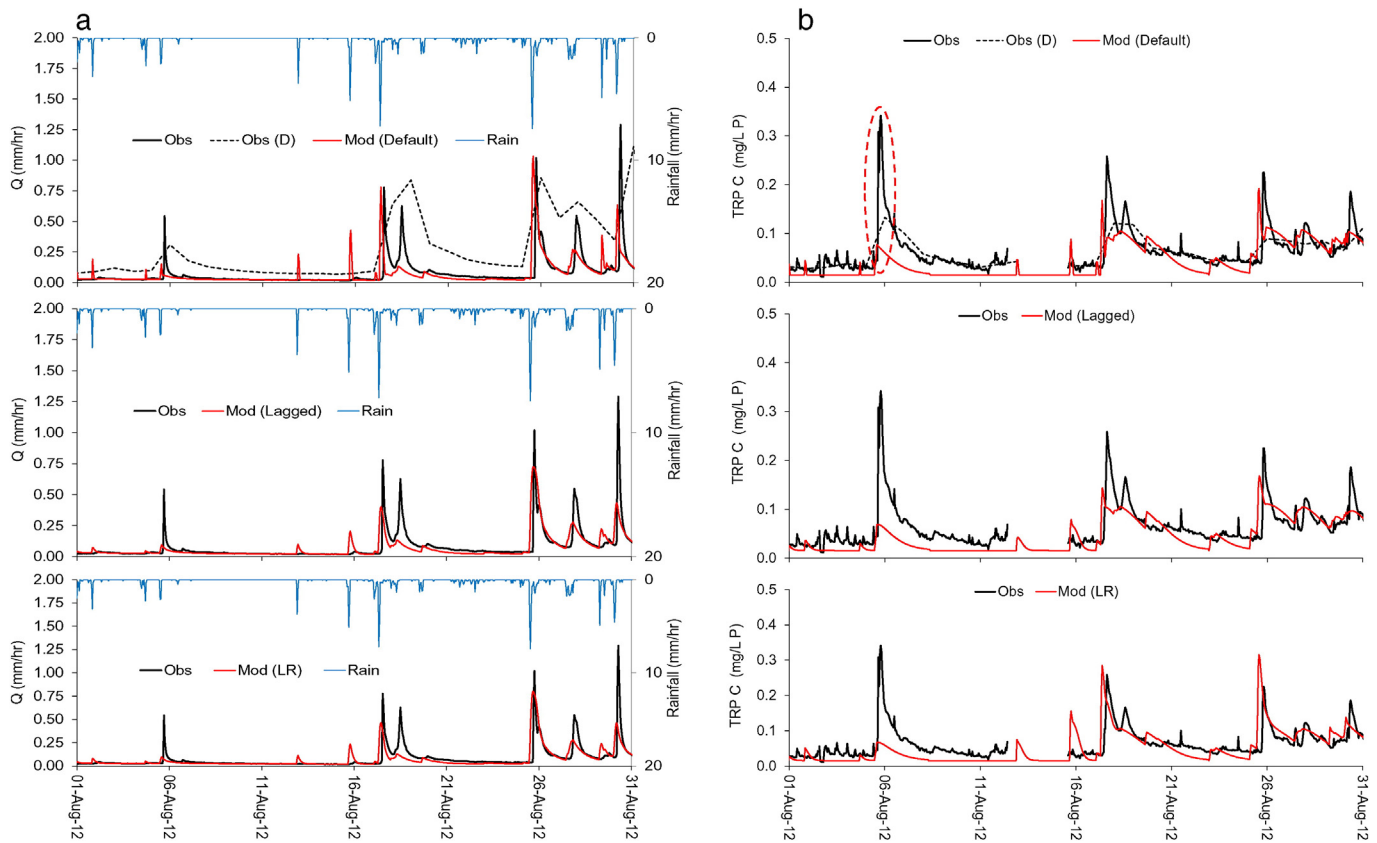


Fig. 3. Time series plot of hourly modelled and observed runoff ( $Q$ ) and rainfall (Rain) for entire modelled period 1/10/2011–30/9/2012, default model simulation. (For interpretation of the references to colour in this figure, the reader is referred to the web version of this article.)



**Fig. 4.** Time series plots of Q (4a), TRP (4b), TP (4c) and SS (4d) during August 2012 indicating model predictions (red line) and observed hourly values (solid black line) from different model structures/simulations. Red ovals on TP and TRP panes indicate Type 2, i.e. “non-behavioural” events. Hourly rainfall is also shown in subplot a by the blue line. The dashed black lines indicate observed daily mean data (denoted by the suffix “D” in the legends). (For interpretation of the references to colour in this figure legend, the reader is referred to the web version of this article).

pathways transporting P (at around 60–70% in all three simulations), with the “LR” having the largest of all the simulations. The modelled SS yields broken down by flow pathway from all three simulations are not shown graphically, since the fraction transported by the SR pathway accounted for around 70–75% of the total export from all three of the simulations.

#### 4. Discussion

The choice of the CRAFT model to simulate runoff, sediment and nutrient generation in the NBC has been justified by the model results after calibration, in this case using an hourly timestep. The MBEs of less than  $\pm 2\%$  and NSE values of at least 0.7 in terms of predicting runoff, indicated that the performance of the model was satisfactory. In terms of predicting P and SS concentrations, positive NSE values and LEs of less than  $\pm 10\%$  were also obtained from the default model structure for SS, TP and TRP. The model is therefore suitable for assessing future scenarios relating to the effects of mitigation measures in the NBC catchment. The model performance compares favourably with other distributed and physically based models widely used by the nutrient and sediment modelling community (Wellen et al., 2015). Jackson-Blake et al. (2015) have discussed the issue of assessing water quality model performance (specifically INCA-P) and suggested that a “weight of evidence” approach is used that includes a visual comparison of modelled and observed time series. They have also pointed out that performance that is considered acceptable in terms of predicting flows (e.g. a NSE  $> 0.65$  being considered as “good”) may be difficult to achieve when predicting P concentrations from agricultural catchments where a much lower NSE may suffice. This study has achieved NSE values of

$> 0.2$  for TRP and TP,  $> 0.3$  for SS vs. a NSE value of circa 0.8 for runoff, which fits neatly into their evaluation of model performance at simulating flow, nutrients and sediments.

In terms of model validation, over a short period in winter 2012–3 the model results were evaluated and model predictions were still very good for runoff and acceptable for P and SS. It must be stressed that there may be unknown issues with using such a short time period to validate the water quality component of the model. Also, there may have been step changes in the concentration and turbidity data obtained by the bankside analysers which have not been picked up by the QA/QC procedure. Therefore, both the observed P concentrations and turbidity values (used to obtain the observed SS timeseries) may have shifted upwards and downwards respectively. In general, validation must be viewed cautiously when used with high-frequency water quality monitoring data due to these limitations and issues.

In terms of resolving the uncertainty issue, it is assumed here that expert judgement on what constitutes a “best fit” model is more important when simulating sediments and nutrients than attempting to quantify uncertainty directly as was attempted by Hollaway et al. (this issue) using SWAT without fully resolving the issue.

##### 4.1. Comparison of different model structures

In terms of predicting runoff, Table 2 shows that there was little difference in the NSE and MBE values from the lagged and default model structures and that these metrics alone do not really discriminate between these. This reflected that it was relatively straightforward to calibrate the CRAFT model to the hourly flow data and achieve NSE values circa 0.75–0.8 both with and without a lag term. Higher NSE values were



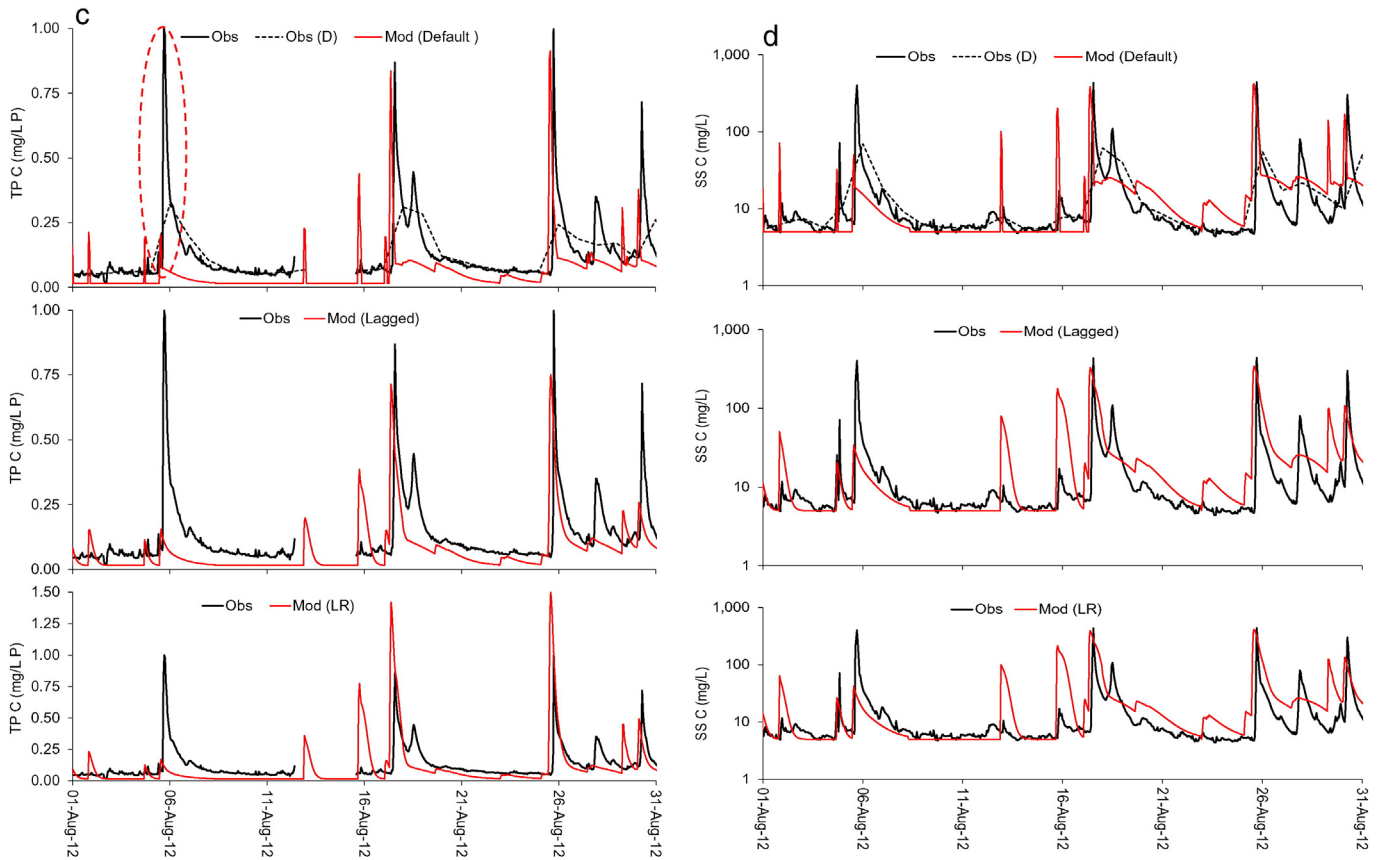


Fig. 4 (continued).

achievable in the default simulation (up to 0.83) at the expense of a poorer visual fit to the hydrographs, with a tendency to underpredict the peak runoff during events. In terms of the modelled outputs (P and SS), Fig. 6 shows that the default model structure generally performed the best out of all the model structures in terms of achieving the best NSE and LE values with one or two exceptions that will be discussed in Section 4.1.1.

4.1.1. Introduction of SR attenuation component

The introduction of a SR attenuation (lag) component in the CRAFT has improved (according to the NSE values shown in Fig. 6) the prediction of flow and P but has had a detrimental effect on the model's prediction of SS (the NSE decreased from 0.37 to 0.3 as shown in Fig. 6). Fig. 7 explores the attenuation feature of the model further by varying

$K_{LAG}$  between 0.25 and 0.8 for each modelled variable in turn and calculating the increase or decrease in the NSE (an increase resulting in a positive y-axis value) relative to the default simulation with a zero lag. It can be seen through the shape of the 4 different curves that each of these variables would benefit from different optimal values of  $K_{LAG}$  and that TP benefitted most from a high value of  $K_{LAG}$  with an optimal value of 0.75 (the value chosen for the lagged model simulation). Perks et al. (2015) analysed a series of events over 2012–3 that included the second half of the twelve month period analysed in our study. They found that there were different hysteresis patterns in the observed event SS and P dynamics SS was mobilised by events with clockwise hysteresis indicating that there were near-stream sources of sediment that were readily mobilised by surface runoff during storms. The evidence from both Fig. 4d, which shows that visually the peaks in late-August 2012 were in fact best predicted by the default model (compared to both the lagged and “LR” models), and Fig. 7, which shows that setting  $K_{LAG}$  to less than 0.25 produced the highest NSE value for SS, supports this finding and is in agreement with the findings of Perks et al. (2015).

Visually, (Fig. 4b and c respectively) the results from the “LR” simulation also indicated that the transport of TP and TRP by the SR pathway can be better modelled using this method of lumping a large load of P into this pathway, then attenuating its transport to the outlet, rather than restricting the routing of both TP and TRP to the outlet to take place over a single hour. The purpose of examining the “LR” version of the lagged model structure has also been to illustrate that the model can better reproduce some of the “Type 1 behavioural” peaks of P exhibited by the NBC using this technique. In terms of the visual fit to the TP and TRP observed concentrations during events in summer 2012, the “LR” simulation performed the best of the three Fig. 4b and c shows that in August 2012 this model was able to fit the observations reasonably well except for one “non-behavioural” Type 2 event at the start of the month. These results were however obtained at the expense of a

Table 2 Performance metrics achieved by different CRAFT simulations.

Metric	Modelled variable	Modelled (default – calibration)	Modelled (default – validation)	Modelled (lagged)	Modelled (LR)
NSE (–)	Q	0.82	0.78	0.79	0.81
	TP	0.19	0.09	0.25	–1.4
	TRP	0.25	0.20	0.28	–0.12
	SS	0.42	0.20	0.26	0.13
NRMSE (–)	TP	0.95	1.0	0.99	0.56
	TRP	1.5	1.6	1.5	1.2
	SS	0.44	0.43	0.39	0.36
MBE (%)	Q	–1.1	–4.9	–1.1	–3.8
	TP	9.7	32.7	9.7	–56
LE (%)	TRP	–3.8	10.4	–3.8	–38
	SS	6.5	–53.1	6.5	–10

**Table 3**

Parameter values from each CRAFT simulation “LR” denotes lumped and route model simulation.

Parameter (units)	Description	Default	Lagged	LR
$S_{DMAX}$ (mm $h^{-1}$ )	Maximum drainage rate from dynamic surface store (DSS)	1.4	1.4	1.4
$S_{RMAX}$ (mm)	Maximum storage in root zone of DSS	55	55	55
$K_{SURF}$ ( $h^{-1}$ )	Time constant of surface runoff from DSS	0.092	0.092	0.11
$K_{SPLIT}$ (–)	Partitioning coefficient to determine recharge to the two subsurface stores (fraction draining from dynamic soil store)	0.4	0.4	0.4
$K_{GW}$ ( $h^{-1}$ )	Time constant of discharge from dynamic groundwater store	$14 \times 10^{-4}$	$14 \times 10^{-4}$	$14 \times 10^{-4}$
$K_{SS}$ ( $h^{-1}$ )	Time constant of discharge from dynamic soil store	0.06	0.06	0.06
$K_{LAG}$ ( $h^{-1}$ )	Time constant of discharge from surface attenuation store	0	0.75	0.75
$K_{SR}(TRP)^a$	Slope of TRP C vs. $Q_{SR}$ relationship used to determine $C_{SR}$ (TRP)	0.22	0.22	0.37
$C_{SS}(TRP)$ ( $mg L^{-1} P$ )	Concentration of TRP in dynamic subsurface store	0.125	0.125	0.125
$C_{GW}(TRP)$ ( $mg L^{-1} P$ )	Concentration of TRP in dynamic GW store	0.015	0.015	0.015
$K_{SR}(PP)^a$	Slope of PP C vs. $Q_{SR}$ relationship used to determine $C_{SR}$ (PP)	0.9	0.9	1.5
$K_{SR}(SS)^a$	Slope of SS C vs. $Q_{SR}$ relationship used to determine $C_{SR}$ (SS)	520	520	520
$C_{SS}(SS)$ ( $mg L^{-1}$ )	Concentration of SS in dynamic subsurface store	30	30	30
$C_{GW}(SS)$ ( $mg L^{-1}$ )	Concentration of SS in dynamic GW store	5	5	5

<sup>a</sup> Units ( $mg h mm^{-4}$ ).

higher LE (i.e. model overprediction) compared to the default model structure. There may be an issue here in terms of the “fitness for purpose” of the model, and the best way of obtaining a “good fit” to the observed data.

Both simulations incorporating attenuation (lagged and “LR”) generated a significant delay in the time to peak (of the time series shown in Fig. 4b–d) of several hours compared to the default simulation (where runoff and nutrient peak concentrations were predicted to occur 1 h after the rainfall peak). The importance of this behaviour may be that

without any attenuation the modelled peaks in concentration are simply too “spiky” and also have been predicted to occur several hours before the observed peaks. Again, Fig. 7 shows that using the attenuation term with  $K_{LAG} > 0.25$  improved the goodness of fit compared to the “default” simulation for both TP and TRP. This delay may be due to the anti-clockwise hysteresis patterns identified by Perks et al. (2015) from the observed flow and concentration patterns, which was attributed to soil water being the dominant flow pathway (equivalent to the fast subsurface flow pathway in the CRAFT).

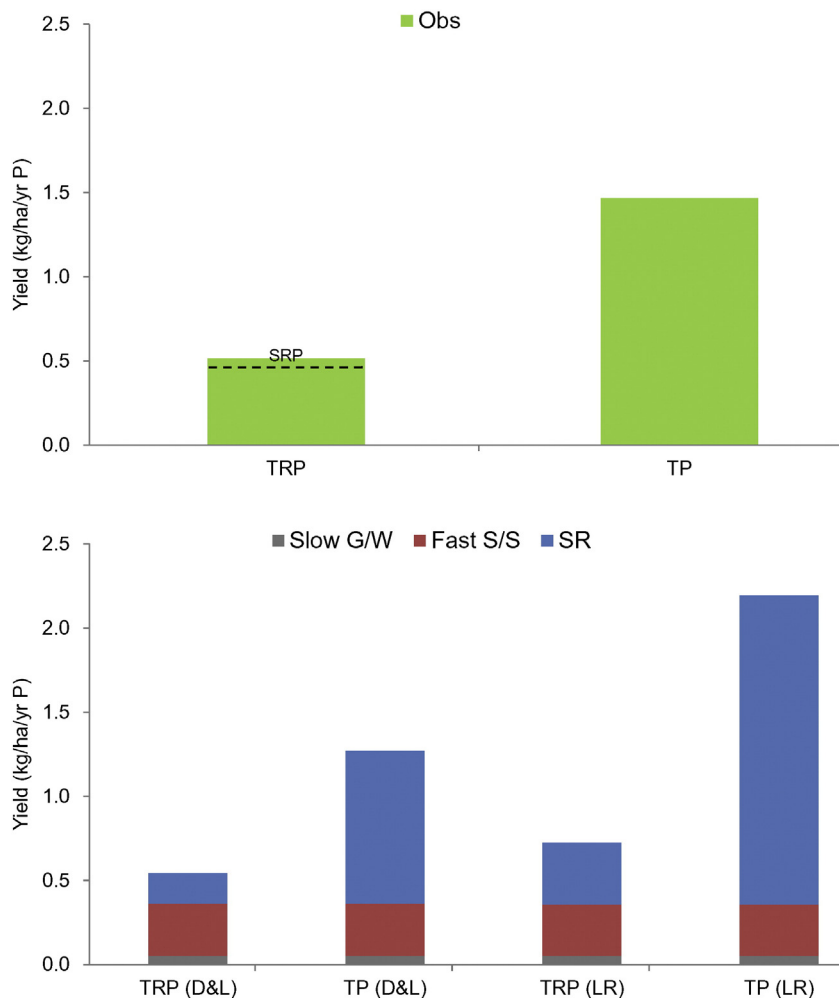


**Fig. 5.** Breakdown of modelled TRP and TP yields from 2011 to 2 by different flow and transport pathways for each model structure/simulation (bottom pane), and observed TRP, SRP and TP yields (top pane) for comparison. (For interpretation of the references to colour in this figure, the reader is referred to the web version of this article).

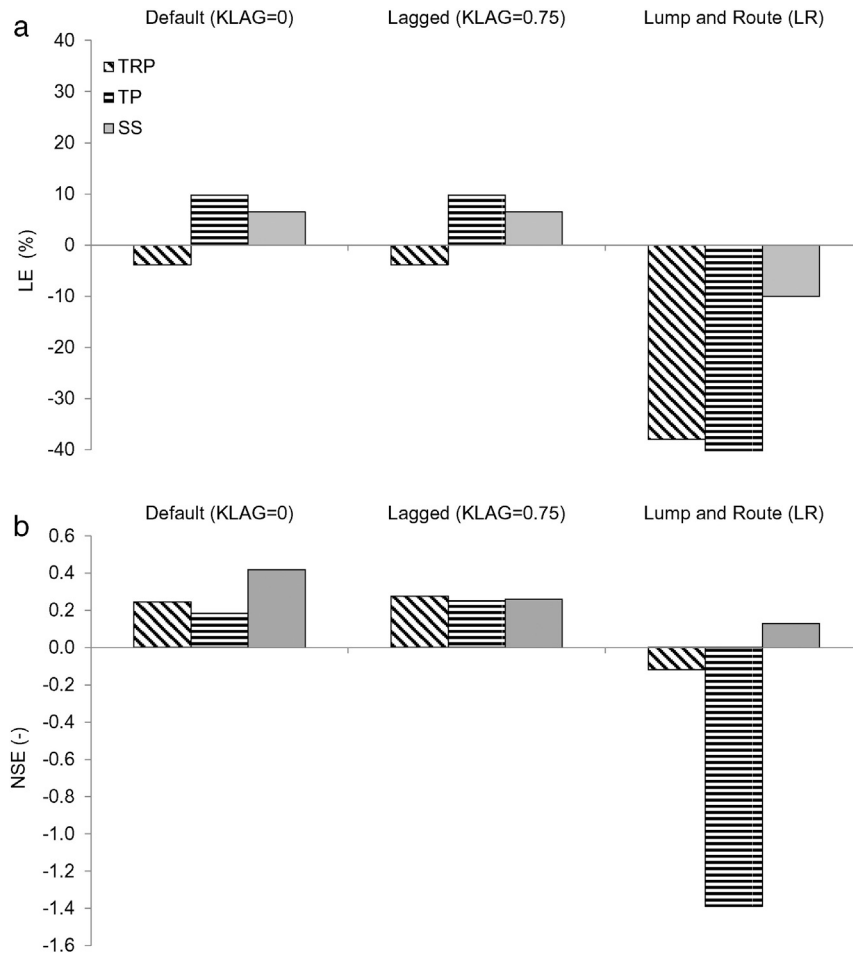


Fig. 6. Results of comparing different model structures as assessed by (a top) load error LE (b bottom) NSE performance metrics for TRP, TP and SS predictions.

The SR attenuation component does lower the concentrations but does not affect the load exported. The observed SS concentrations do not demonstrate the influence of attenuation and hence the predicted SS concentrations do not benefit from the SR attenuation component. The SS appears to be more dominated by 'on-off' dynamics that are very sensitive to the rainfall and surface runoff rates. Suspended sediment concentrations may well be reducing in surface runoff whilst P

concentrations are still high in the near surface of the soil and in land drains, as stated by Perks et al. (2015).

#### 4.1.2. Conceptual model of P and SS dynamics

It is postulated here that surface runoff also entrains high concentrations of P through runoff entering and leaving the upper soil layers that are heavily disturbed and compacted by agricultural activities (i.e.

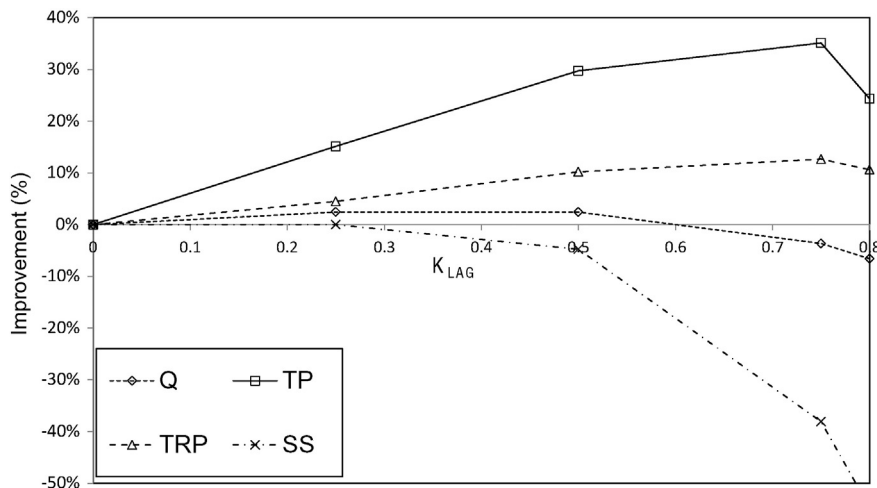


Fig. 7. Graph showing the effect of varying the degree of SR attenuation ( $K_{LAG}$ ) for flow (Q), TP, TRP and SS. Positive values indicate an improvement in the NSE relative to the value achieved by the default simulation with  $K_{LAG} = 0$ .

intensive grazing and ploughing). The overall impact on catchment load or yield of these different patterns and the model's ability to capture them is probably less important, so calibrating the model to fit the peak concentrations is probably the key here if it is to be a useful tool for examining mitigation options.

Fig. 8 below shows a conceptual sketch of fluxes (flow, P and SS) observed at the NBC outlet during an event. Evidence from the observed data (TP and TRP flux time series) suggests that a peak in TRP is observed after a peak in TP at the catchment outlet and it is assumed that the flow pathways that transport TRP and SRP are identical given no evidence to support a more complex mechanism (TRP flux is shown by the red line). The flux timeseries of PP is also shown by the dashed blue line and this peak is coincident with the peaks in both surface runoff ( $Q_{SR}$ ) (top pane) and suspended sediment (bottom pane). The TP flux (green line) is thus the sum of the PP and TRP fluxes.

We are thus implying (in Fig. 8) that the SS dynamics are sensitive to short bursts of fully connected surface runoff, however the P dynamics

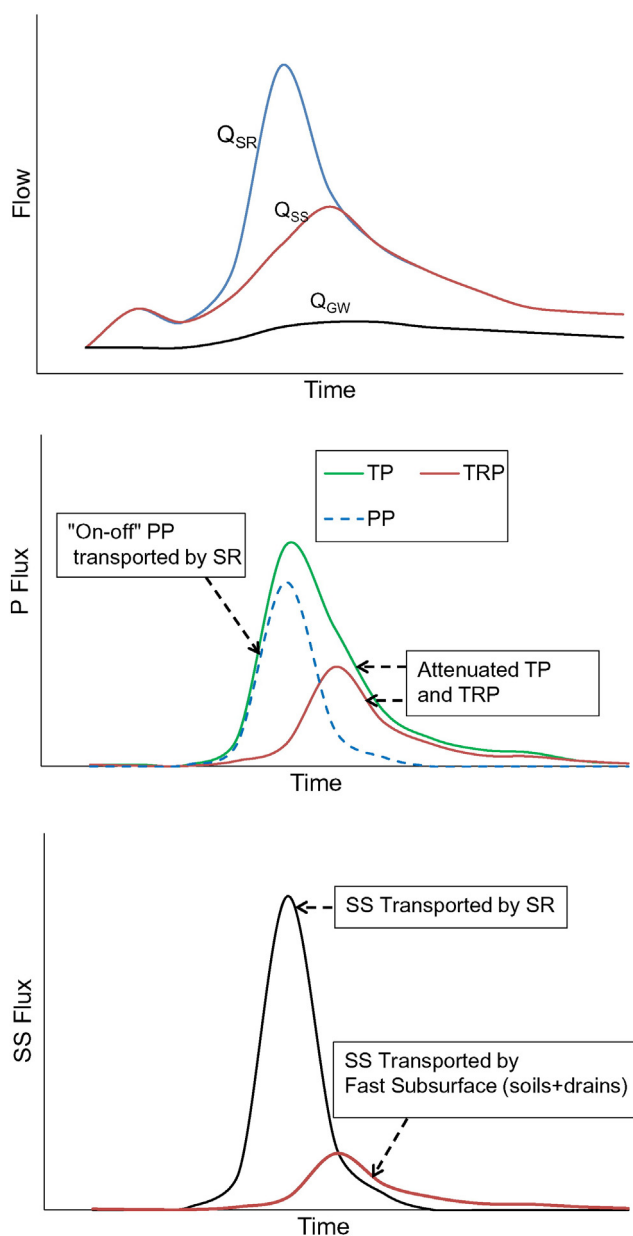


Fig. 8. Conceptual sketch showing fluxes during an event in NBC (top: flow; middle: P; bottom: SS). (For interpretation of the references to colour in this figure, the reader is referred to the web version of this article).

are not dominated by this flow pathway alone and a fast subsurface flow pathway including land drains or grips could account for the attenuation shown in the TRP time series (Dils and Heathwaite, 1999) apparent both in Fig. 8 and in the observed time series of concentration in Fig. 4 from which the conceptual model shown in Fig. 8 is derived. This “on-off” effect, generating and transporting PP and SS via surface runoff, is sensitive to rainfall rates and generates rapid, connected surface runoff (often termed “overland flow”) that may switch off and re-infiltrate when the rainfall rate declines, hence the surface runoff becomes rapidly disconnected from the watercourses. Conversely should the rainfall rates increase, near-surface flow could lead to surface runoff restabilising and generating increased SS losses. There is assumed to be a secondary peak in suspended sediment flux from the fast subsurface pathway (i.e. in conjunction with  $Q_{SS}$ ) which may be due to rapid drainage of SS through the field drainage network. Suspended sediment fluxes via the slow groundwater pathway are assumed to be negligible.

Hence a model is needed that can capture both the “on-off” spiky nature of surface runoff and the more attenuated subsurface pathways for P. The data information content and current analysis do not reveal if the P losses are occurring in the near surface of the soil or through interactions with the land drains (or both). However, the soils in the area are prone to water logging and land drains are installed to alleviate this problem (see Dils and Heathwaite (1999) for an overview of the role of drains in transporting P in agricultural catchment) so the two processes are probably closely linked. The attenuation term is useful and the impact on attenuation on flow concentration is strong, and may be relevant to policy makers.

#### 4.1.3. Using a suite of metrics to assess model performance

In comparing the two different metrics NSE and normalised 1/RMSE to assess model performance, it was clear that in this study that the use of a NSE was able to distinguish reasonably well between the performance of the different model structures at predicting both P and SS. The normalised 1/RMSE metric, as used by Dean et al. (2009), was less discriminatory for TRP than the NSE metric (values were within  $\pm 16\%$  for TRP from the three simulations). The normalised 1/RMSE metric could be useful though where the NSE values from all runs are negative (as was reported by Dean et al. (2009)), however any model predictions made (using these parameter sets with NSE values below zero) will be worse than using the observed mean as the predictor of flow or concentration. Visual methods of assessing model performance at predicting concentrations of P were also deemed acceptable alongside using metrics such as NSE, correlation and bias by Jackson-Blake et al. (2015), and evidence from the results of this study suggests that using a suite of model assessment metrics may be the best method in the NBC as well.

#### 4.2. Load breakdown by pathway

The default model can generate high fluxes of P immediately following events via the SS component (by employing high values of  $C_{SS}$  (TRP)) and high concentrations and fluxes during events in surface runoff (by employing high values of  $K_{SR}$  (PP)). In “behavioural” events it is assumed that peak Cs were positively correlated with peak flows and occurred at approximately the same time, as was observed in the other Eden subcatchments by Barber (2013), Mills and Bathurst (2015) and Ockenden et al. (this issue). Both mechanisms have a plausible physical basis in representing the wet areas of the catchment that become connected to the stream channel network during and after runoff events and have a readily mobilised source of TRP and PP (e.g. from farmyards and hardstandings) (Outram et al., 2014). A second source of P includes the drainage of enriched soil water via a subsurface field drain system (i.e. a fast subsurface pathway) (Perks et al., 2015) and the entrainment of particulate and colloidal sources of P from the degraded soil surface and tracks (Outram et al., 2014), which is classified as a surface runoff pathway.

The modelled load breakdown (in the default simulation) of P shown in Fig. 5 also indicated that the surface runoff pathway accounted for 64% of the modelled TP export and 72% of the modelled SS export. Perks et al. (2015) suggested that physical runoff interception would be the best method of targeting the surface runoff pathway that is by far the largest source of SS according to the model. Observed TRP and TP yields (Fig. 5 top pane) indicated that reactive P only constituted approximately 40% of the TP yield from the NBC. This indicates that there must be a large source of unreactive P, e.g. organic P being mobilised in the catchment which may be either particulate or soluble. Moreover, the lag observed in the observed TRP concentration due to attenuation could have implications when selecting mitigation options for this catchment.

#### 4.3. Seasonality and non-behavioural events

Rainfall and runoff were fairly uniformly distributed during the 12 months in 2011–2 except for a dry spell in late winter and early spring, with the runoff coefficient for the entire period being high (0.59). Any seasonality in the year analysed (2011–2) was not especially pronounced in terms of runoff generation. The dry spell in between these periods may have reduced the runoff ratio somewhat in late spring–early summer as later on during summer 2012 it was above 0.7 due to the wet conditions. There were also at least two Type 2 non-behavioural events observed during summer 2012. These events were not significant in terms of TRP and TP export as the flows during the events were fairly low. The relatively high observed P concentrations (TP:  $1.0 \text{ mg L}^{-1}$  P, TRP:  $0.35 \text{ mg L}^{-1}$  P) were likely a result of random agricultural activities in the catchment, which could be either point sources e.g. wash-down operations at dairy farms and piggeries, or diffuse sources such as badly-timed applications of slurry to the fields, and as such are almost impossible to model. Suspended sediment also exhibited a correspondingly high C peak in early August (Fig. 4d) that was not reproduced by the model, which supports the hypothesis that slurry applications may have been the cause (Ockenden et al., this issue).

#### 4.4. Comparison with other studies

A previous study of sediment export in the Eden catchment by Mills and Bathurst (2015) found that the subcatchments monitored by the CHASM project exported between 4 and  $73 \text{ t km}^{-2} \text{ y}^{-1}$  of SS with no clear relationship between size and yield. In comparison with their findings, the SS export of  $38.2 \text{ t km}^{-2} \text{ y}^{-1}$  (for the entire 12 month period) from the NBC (calculated from this study) was similar, when compared to a subcatchment of a similar size to Newby Beck (Helm Beck;  $18 \text{ km}^2$ ;  $46 \text{ t km}^{-2} \text{ y}^{-1}$ ), but higher than the export from Swindale Beck ( $16 \text{ km}^2$ ;  $26 \text{ t km}^{-2} \text{ y}^{-1}$ ). The authors suggested that sediment yield varied considerably between the smaller subcatchments in the Eden due to heterogeneity in the rates of both sediment supply and transport.

Barber (2013) analysed a dataset comprising both TP and SRP samples collected by grab and automatic sampling (autosamplers) from the same Eden subcatchments monitored by the CHASM project. The mean export of TP from the upper Eden catchment was  $42.4 \text{ kg km}^{-2} \text{ y}^{-1}$ , and the export of SRP was  $14.5 \text{ kg km}^{-2} \text{ y}^{-1}$ . These totals were calculated for the period 2010–2011. The export rates from the  $9 \text{ km}^2$  Blind Beck subcatchment were the highest out of all the subcatchments, with the 2011 totals being higher than 2010 (precipitation was higher at 1429 mm versus 779 mm in 2010). The NBC was not included within the nested CHASM subcatchments, however it has exported similar amounts of TP, TRP and SS for the period analysed here (Table 1) probably due to having similar land uses, soils and climate.

## 5. Conclusions

The NBC catchment in the upper Eden, NW England has been intensively monitored since 2011 with the objective of understanding nutrient and sediment pathways and transfer, with the ultimate aim of developing and field testing strategies to reduce diffuse pollution via mitigation. Export rates of P and sediments (SS) over the 12 months from October 2011 were not especially high compared to previous studies in the upper Eden catchment, where land use and climate are similar to this one, a dry spell in late winter may have contributed to this.

Modelling of this dataset is important in order to assess the impact of future mitigation plans on sediment and nutrient export. For this purpose the CRAFT model has been evaluated. The hypothesis testing reported above indicated that the default CRAFT model structure is appropriate at simulating both flow and water quality in the NBC for most applications, but with some drawbacks in terms of phosphorus (P) simulation in particular due to in-stream routing effects. Water quality models are often assessed in terms of their performance at predicting loads, and also over a daily or even longer time period rather than by using hourly concentration data. In this study we showed that concentration data could also be acceptably reproduced by the CRAFT model using an hourly timestep, which has rarely been reported elsewhere by modelling studies.

Any seasonality over the 12 month period assessed in the NBC was not particularly evident as runoff was generated at all times of the year. The continuous monitoring of nutrients using bankside analysers has identified that there was probably more than one occasion (in summer 2012) when farming activities may have generated peak P concentrations that appear to be outside the predictive range of the default CRAFT model structure. This assumes that high concentrations of P and SS are generated from high surface runoff rates using a linear relationship between Q and C which may not always hold true, and this could be enhanced in future versions of the model if the observations support a more complex relationship.

We assessed a revised version of the CRAFT model structure incorporating a surface runoff attenuation component (i.e. lag) to delay the peaks in flow and concentrations (of P and SS) in reaching the outlet. These results were interesting. The revised model structure produced better results for flow than the default model in terms of the visual fit to the data (assessed via time series plots) since timing errors were addressed, however the NSE reduced slightly. In terms of modelling both TP and TRP, a better fit was achieved by adding attenuation to the model. A further model simulation, including attenuation, termed LR (standing for “lump and route”) generated much higher concentrations of both PP and TRP during runoff events and then routed these to the outlet using the attenuation component. The results obtained from this simulation were acceptable in terms of matching the peak TP and TRP concentrations visually, but as a result overpredicted the TP export from the NBC by 56%.

For simulating the future effects of mitigation features however, the attenuation capabilities of the CRAFT model will be highly useful and should be tested with a wide range of model parameter values including those obtained from the LR simulation. The attenuation of both surface runoff and fast subsurface flow should be considered as a result of these features introducing a lag to the system and also if improved farming practices have resulted in a decrease in surface runoff due to improved soil conditions. These measures will be required if the catchment is to achieve “Good” ecological status by 2027 as targeted. A conceptual understanding of both hydrology and diffuse pollution (sources and pathways) points towards improved management regimes. It is important that water quality models are transparent to end users and can be applied to the assessment of mitigation measures and the effect of pollution swapping (changing the dominant flow pathways) in the catchment. The breakdown by (modelled) load pathways in the NBC indicated that surface runoff will transport up to 90% of SS and 60% of P making this the key pathway that needs to be targeted by mitigation.

measures in this particular catchment. A further study will examine the use of the extended attenuation capabilities of the CRAFT model to simulate the behaviour of these mitigation features in the NBC.

### Acknowledgements

This study was carried out using field data supplied by the Eden Demonstration Test Catchment (Eden DTC) research platform. The Eden DTC is funded by the Department for Environment, Food and Rural Affairs (DEFRA), project WQ0210, although the lead author was not funded by or involved directly with this project.

### Appendix A. Supplementary data

Supplementary data to this article can be found online at <http://dx.doi.org/10.1016/j.scitotenv.2016.01.045>.

### References

- Adams, R., Quinn, P.F., Bowes, M.J., 2015. The catchment runoff attenuation flux tool, a minimum information requirement nutrient pollution model. *Hydrol. Earth Syst. Sci.* 19 (4), 1641–1657.
- Allen, D.J., Newell, A.J., Butcher, A.S., 2010. Preliminary review of the geology and hydrogeology of the Eden DTC sub-catchments. BGS Groundwater Science Programme, Open Report OR/10/063 45 pp.
- Barber, N.J., Quinn, P.F., 2012. Mitigating diffuse water pollution from agriculture using soft-engineered runoff attenuation features. *Area* 44 (4), 454–462.
- Barber, N., 2013. Sediment, nutrient and runoff management and mitigation in rural catchments. Unpubl PhD Thesis. Newcastle University, School of Civil Engineering and Geosciences 447 pp.
- Beven, K., 2009. *Environmental Modelling: An Uncertain Future? An Introduction to Techniques for Uncertainty Estimation in Environmental Prediction*. Routledge, Abingdon, Oxon (UK).
- Bicknell, B.R., Imhoff, J.C., Kittle Jr., J.L., Donigan Jr., A.S., Johanson, R.C., 1996. Hydrologic Simulation Program – FORTAN (HSPF): User's Manual for Release 11. US EPA Environmental Research Lab, Athens, GA, USA.
- Bilotta, G.S., Brazier, R.E., Haygarth, P.M., 2007. Processes affecting transfer of sediment and colloids, with associated phosphorus, from intensively farmed grasslands: erosion. *Hydrol. Process.* 21, 135–139.
- Bilotta, G.S., Krueger, T., Brazier, R.E., Butler, P., Freer, J., Hawkins, J.M.B., et al., 2010. Assessing catchment-scale erosion and yields of suspended solids from improved temperate grassland. *J. Environ. Monit.* 12, 731–739.
- Binger, R L; Theurer, F D; and Yuan, Y, 2011 AnnAGNPS Technical Processes. Version 52, <http://www.ars.usda.gov/research/docs.htm?docid=5222>. Last accessed 17/11/15.
- Birkinshaw, S.J., Ewen, J., 2000. Modelling nitrate transport in the Slapton Wood catchment using SHETRAN. *J. Hydrodyn.* 230 (1), 18–33.
- Boughton, W., 2004. The Australian water balance model. *Environ. Model. Softw.* 19, 943–956.
- Bowes, M.J., House, W.A., Hodgkinson, R.A., 2003. Phosphorus dynamics along a river continuum. *Sci. Total Environ.* 313, 199–212.
- Cranfield University, 2014. *The Soils Guide*. Cranfield University.
- Dean, S., Freer, J., Beven, K., Wade, A.J., Butterfield, D., 2009. Uncertainty assessment of a process-based integrated catchment model of phosphorus. *Stoch. Environ. Res. Risk Assess.* 23, 991–1010.
- Dils, R.M., Heathwaite, A.L., 1999. The controversial role of tile drainage in phosphorus export from agricultural land. *Water Sci. Technol.* 39, 55–61.
- Gassman, P., Reyes, M., Green, C., Arnold, J., 2007. The soil and water assessment tool: historical development, applications, and future research directions. *Trans. ASABE* 50 (4), 1211–1250.
- Halliday, S., Skeffington, R., Bowes, M., Gozzard, E., Newman, J., Loewenthal, M., et al., 2014. The water quality of the River Enborne, UK: observations from high frequency monitoring in a rural, lowland river system. *Water* 6, 150–180.
- Haygarth, P.M., Wood, F.L., Heathwaite, A.L., Butler, P.J., 2005. Phosphorus dynamics observed through increasing scales in a nested headwater-to-river channel study. *Sci. Total Environ.* 344, 83–106. <http://dx.doi.org/10.1016/j.scitotenv.2005.02.007>.
- Heathwaite, A.L., Quinn, P.F., Hewett, C.J.M., 2005. Modelling and managing critical source areas of diffuse pollution from agricultural land using flow connectivity simulation. *J. Hydrodyn.* 304, 446–461. <http://dx.doi.org/10.1016/j.jhydrol.2004.07.043>.
- Hollaway, M.J., 2016. Evaluating a water quality model on a small UK headwater catchment: defining limits of acceptability. *Sci. Total Environ.* (This issue).
- Jackson-Blake, L.A., Dunn, S.M., Helliwell, R.C., Skeffington, R.A., Stutter, M.I., Wade, A.J., 2015. How well can we model stream phosphorus concentrations in agricultural catchments? *Environ. Model. Softw.* 64, 31–46.
- Jakeman, A.J., Letcher, R.A., Norton, J.P., 2006. Ten iterative steps in development and evaluation of environmental models. *Environ. Model. Softw.* 21 (5), 602–614.
- Jordan, P., Melland, A.R., Mellander, P.E., Shortle, G., Wall, D., 2012. The seasonality of phosphorus transfers from land to water: implications for trophic impacts and policy evaluation. *Sci. Total Environ.* 434, 101–109.
- Lloyd, C.E.M., Freer, J.E., Johns, P.J., Coxon, G., Collins, A.L., 2015. Discharge and nutrient uncertainty: implications for nutrient flux estimation in small streams. *Hydrological Processes*.
- McGonigle, D.F., Burke, S.P., Collins, A.L., Gartner, R., Haft, M.R., Harris, R.C., et al., 2014. Developing demonstration test catchments as a platform for transdisciplinary land management research in England and Wales. *Environ. Sci. Process. Impacts* 16, 1618–1628.
- Mellander, P.-E., Melland, A.R., Jordan, P., Wall, D.P., Murphy, P.N.C., Shortle, G., 2012. Quantifying nutrient transfer pathways in agricultural catchments using high temporal resolution data. *Environ. Sci. Pol.* 24, 44–57.
- Met Office, 2009. UKCP09: Average Annual Rainfall Dataset.
- Mills, C.F., Bathurst, J.C., 2015. Spatial variability of suspended sediment yield in a gravel-bed river across four orders of magnitude of catchment area. *Catena* 133, 14–24.
- Nasr, A., Bruen, M., Jordan, P., Moles, R., Kiely, G., Byrne, P., 2007. A comparison of SWAT, HSPF and SHETRAN/GOPC for modelling phosphorus export from three catchments in Ireland. *Water Res.* 41 (5), 1065–1073.
- Ockenden et al. Potential effects of changing climate on catchment processes and nutrient transfers: evidence from high temporal concentration-flow dynamics in headwater catchments. *Sci. Total Environ.* (This issue).
- Ockenden, M.C., Deasy, C., Quinton, J.N., Bailey, A.P., Surridge, B., Stoate, C., 2012. Evaluation of field wetlands for mitigation of diffuse pollution from agriculture: sediment retention, cost and effectiveness. *Environ. Sci. Pol.* 24, 110–119.
- Outram, F.N., Lloyd, C.E.M., Jonczyk, J., Benskin, C.M.H., Grant, F., Perks, M.T., et al., 2014. High-frequency monitoring of nitrogen and phosphorus response in three rural catchments to the end of the 2011–2012 drought in England. *Hydrol. Earth Syst. Sci.* 18, 3429–3448.
- Owen, G.J., Perks, M.T., Benskin, C.M.H., Wilkinson, M.E., Jonczyk, J., Quinn, P.F., 2012. Monitoring agricultural diffuse pollution through a dense monitoring network in the River Eden Demonstration Test Catchment, Cumbria, UK. *Area* 44 (4), 443–453.
- Perks MT, Owen GJ, Benskin CMH, Jonczyk J, Deasy C, Burke S, Reaney SM and Haygarth PM, 2015 Dominant mechanisms for the delivery of fine sediment and phosphorus to fluvial networks draining grassland dominated headwater catchments. *Sci. Total Environ.* 523(0): 178–190.
- Pionke, H.B., Gburek, W.J., Sharpley, A.N., 2000. Critical source area controls on water quality in an agricultural watershed located in the Chesapeake Basin. *Ecol. Eng.* 14, 325–335. [http://dx.doi.org/10.1016/S0925-8574\(99\)00059-2](http://dx.doi.org/10.1016/S0925-8574(99)00059-2).
- Quinn, P., Hewitt, C.J.M., Dayawansa, N.D.K., 2008. TOPCAT-NP: a minimum information requirement model for simulation of flow and nutrient transport from agricultural systems. *Hydrol. Process.* 22 (14), 2565–2580.
- Wade, A.J., Durand, P., Beaujouan, V., Wessel, W.W., Raat, K.J., Whitehead, P.G., Butterfield, D., Rankinen, K., Lepisto, A., 2002. A nitrogen model for European catchments: INCA, new model structure and equations. *Hydrol. Earth Syst. Sci.* 6 (3), 559–582. <http://dx.doi.org/10.5194/hess-6-559-2002>.
- Wellen, C., Kamran-Disfani, A.R., Arhonditsis, G.B., 2015. Evaluation of the current state of distributed watershed nutrient water quality modeling. *Environ. Sci. Technol.* 49 (6), 3278–3290.
- Wilkinson, M.E., Quinn, P.F., Barber, N.J., Jonczyk, J., 2014. A framework for managing runoff and pollution in the rural landscape using a Catchment Systems Engineering approach. *Sci. Total Environ.* 468–469, 1245–1254.